ASSESSING THE IMPACT OF IONISING RADIATION IN TEMPERATE COASTAL SAND DUNE ECOSYSTEMS:

MEASUREMENT AND MODELLING

Thesis submitted in accordance with the requirements of the
University of Liverpool for the degree of Doctor in Philosophy

by

Michael David Wood

January 2010

ABSTRACT

Assessing the impact of ionising radiation in temperate coastal sand dune ecosystems: measurement and modelling

Michael D. Wood*

This thesis presents the results of a 6-year research project to investigate the radioecology of temperate coastal sand dunes. Samples (n = 617) of soil, water and biota were collected from the Drigg coastal sand dunes (West Cumbria, UK) between February 2005 and October 2007. Biota groups sampled included amphibians, birds, invertebrates, mammals, reptiles, plants (including lichens and mosses) and fungi. All samples were analysed for ^{40}K, ^{137}Cs and ^{241}Am. A sub-set of samples (n = 26) was analysed for ^{90}Sr, ^{99}Tc, ^{238}Pu and $^{239+240}$Pu. Additional soil analyses included soil moisture, bulk density, pH, organic matter content, carbonate content and cation concentrations (Ca^{2+}, K^{+}, Na^{+} & Mg^{2+}).

The application of three publicly-available environmental radiation protection models (ERICA, R&D128/Sp1a & RESRAD-BIOTA) to an assessment of ionising radiation impacts at the Drigg coastal sand dunes site was evaluated. Soil activity concentration data were used as input data and model results compared with measured activity concentrations in sand dune biota. Radionuclide concentration ratios (CRs) were identified as an important source of variation in model predictions. For sand dune small mammals, Am, Cs and Pu CRs were found to be 1 – 2 orders of magnitude lower than those for small mammals in other terrestrial ecosystems. For reptiles, the variability could be attributed to the paucity of data on transfer to this vertebrate group.

Through literature review, mining of unpublished data sets and analysis of samples collected from the Drigg coastal sand dunes, CR databases were developed for reptiles (across a range of ecosystem types) and for sand dune biota. Analysis of sand dune soil data suggested that both sea-to-land transfer and the transport of sand grains in saltation influence the soil activity concentrations in coastal sand dunes. The low CRs for sand dune biota may be due to low bioavailability of particulate-bound radionuclides.

* University of Liverpool, UK; E-mail address: mwood@liv.ac.uk

(This page is left blank intentionally)

ACKNOWLEDGMENTS

I wish to thank Dr David Copplestone (Environment Agency, UK), Dr Rick Leah and Professor Alan McCarthy (both from the University of Liverpool, UK) for their supervision and support during the development of this thesis. I am indebted to all three of them. Special thanks are expressed to David for his ongoing support and friendship and to Alan for taking on the role of primary supervisor following Rick's sudden death in February 2009.

I would like to acknowledge the additional support of Dr Nicholas Beresford (Centre for Ecology and Hydrology (CEH), UK) for his comments and advice on various sections of the manuscript.

I am also grateful to my internal assessors at the University of Liverpool (Professor Alan McCarthy and Professor Andrew Plater) for their feedback on the early design and development of my research programme.

For their excellent technical support at the University of Liverpool, I am grateful to Mr Mike O'Connor, Mr Leslie Connor and Mr Keith Hatton. Mike endured many weeks of fieldwork with me on the Drigg coastal sand dunes. Without his patience and willingness to work both long days and during night-time amphibian surveys, the sampling would have been significantly less productive. Mike also took some of the photographs that are presented in Chapter 2 of this thesis.

Mike, Les and Keith provided technical support for the soil property determinations and gamma spectrometry analysis. In addition, Les provided technical support for the cation analyses.

I am also grateful to Ms Phillipa Hall, Ms Jessica Smallcombe and Ms Sally Wittrick from the University of Liverpool for their assistance with sample preparation.

I would like to acknowledge Ms Catherine Barnett (CEH) and Dr Richard Wilson (Westlakes Scientific Consulting, UK) for their support in analysing biota samples and water samples respectively.

For their help in accessing international data sets to support the reptile transfer database development presented in Chapter 7 of this thesis, I wish to acknowledge Dr John Ferris,

Dr Matthew Johansen and Dr John Twining (all from the Australian Nuclear Science and Technology Organisation (ANSTO)), Dr Dmitry Semanov (A.N. Severtsov Institute of Ecology and Evolution, Russia) and Dr Tamara Yankovich (AREVA Resources Canada Inc., Canada).

In addition to the people already acknowledged, I am grateful to Dr Brenda Howard (CEH), Professor Steve Jones, Professor Paul McDonald and Dr Jordi Vives-i-Battle (all from Westlakes Scientific Consulting Ltd) for advice received during the preparation of peer-reviewed publications from this thesis.

Although the research for this part-time Ph.D. was 'self-funded', I would like to acknowledge the financial contributions from the EC 6th Framework Programme, the Environment Agency and English Nature (now Natural England, UK) for research project funding which has, in part, helped to cover some of the sampling and analysis costs associated with the development of this thesis. I also acknowledge the Hereptological Conservation Trust (for licensing and facilitating herptile sample collection), the British Association of Shooting and Conservation (BASC) and the Egremont and District Wildfowlers Association (for the provision of bird samples) and the Lake District National Parks Authority, the Muncaster Estate and Mr Ireland (for permitting site access and sampling).

Finally I wish to thank my family for supporting me in undertaking this part-time Ph.D. research. In particular, I wish to thank my wife, Mrs Helen Wood, for her encouragement and patience throughout the many evenings, weekends and holidays that I have spent working on this thesis.

This thesis is dedicated to Helen and Abigail with love

(This page is left blank intentionally)

CONTENTS

(This page is left blank intentionally)

LIST OF FIGURES

Figure *Page*

LIST OF TABLES

Table *Page*

LIST OF ABBREVIATIONS

α	Alpha particle
A-bomb	Atomic bomb or atom bomb
AD	Anno Domini
AF	Area factor
AGR	Advanced gas-cooled reactors
amu	Atomic mass unit
ANOVA	Analysis of Variance
β	Beta particle
BASC	British Association for Shooting and Conservation
BIOMASS	Biosphere Modelling and Assessment
BIOMOVS	Biospheric Model Validation Study
BiV	Bioaccumulation factor (equivalent to CR)
BNFL	British Nuclear Fuel Ltd
Bq	Unit of activity (1 Bq = 1 decay event per second)
B_T	Fraction of the total body burden of the radionuclide in tissue *T*
CEH	Centre for Ecology & Hydrology
CF	Concentration factor (equivalent to CR)
COGER	Coordinating Group on Environmental Radioactivity
CR	Concentration Ratio

DCC	Dose conversion coefficient
DCF	Dose conversion factor (equivalent to DCC)
D-ERICA	Guidance document for the ERICA Integrated Approach
DNA	Deoxyribonucleic acid
DPUC	Dose per unit concentration (equivalent to DCC)
dwt	Dry weight
EARP	Enhanced Actinide Removal Plant
EC	European Commission
EDR_{10}	The dose rate representing a 10% effect in the exposed group in comparison to the control group
EF	Enrichment factor
EMCL	Environmental Media Concentration Limit
EMRAS	IAEA programme on 'Environmental Modelling for Radiation Safety'
ERA	Ecological risk assessment
ERICA	EC EURATOM-funded project 'Environmental Risk from Ionising Contaminants: Assessment and Management' which developed the ERICA Integrated Approach
ERICA Tool	The computer model that was developed to support the application of the ERICA Integrated Approach
EURATOM	The European Atomic Energy Community
FAAS	Flame atomic absorption spectrophotometer
FASSET	EC 5^{th} Framework Programme project 'Framework for Assessment of Environmental Impact'

FMI	Fresh matter intake rate
FM_T	Fractional fresh weight mass of tissue *T* relative to the whole-body mass
FREDERICA	Radiation effects database developed from the FASSET Radiation Effects Database (FRED) within the ERICA project
fwt	Fresh weight
γ	Gamma photon
GF	Geometry factor
GIT	Gastrointestinal tract
G-M	Geiger-Muller
GPS	Global Positioning System
GUI	Graphical User Interface
Gy	Unit of absorbed dose (1 Gy is equal to the absorption of 1 joule of energy by 1 kg of matter)
H-bomb	Hydrogen bomb
HCT	Herpetological Conservation Trust
HDPE	High-density polyethylene
HPGe	High-purity germanium
HTML	Hyper Text Markup Language
IAEA	International Atomic Energy Agency
IC	Ion Chromatograph
ICRP	International Commission for Radiological Protection
IEEM	Institute of Ecology and Environmental Management

INES	International Nuclear Event Scale
IRD	Inter-refuge distance
IRSN	Institut de Radioprotection et du Sûreté Nucléaire
K_d	Distribution coefficient
LDNPA	Lake District National Parks Authority
LET	Linear energy transfer
LLWR	Low-level radioactive waste repository
LNR	Local Nature Reserve
LOD	Limit of detection
LOI	Loss on ignition
LSD	Least Significant Difference
LWR	Light water reactor
M	Molar
MAC	Medium active concentrate
MHW	Mean high water
MLW	Mean low water
MOX	Mixed oxide
$M_{REF.T}$	Ratio between the fractional mass of tissue *T* and the fractional mass of the reference tissue
NATURA 2000	European network of SACs and SPAs
NDA	Nuclear Decommissioning Authority
NERC	Natural Environment Research Council

OF	Occupancy factor
OM	Organic matter
pH	A measure of the acidity or alkalinity of a solution
PNEDR	Predicted no-effect dose rate
PROTECT	EC-funded project on Protection of the Environment in a Regulatory Context
PSA	Particle size analysis
R&D128/SP1a	Computer model developed for use by the Environment Agency England & Wales for use in assessing the impact of ionising radiation on wildlife
RAP	Reference animal and plant
RBE	Relative Biological Effectiveness
RESRAD-BIOTA	Computer model for implementing the USDoE graded approach
ROF	Royal Ordnance Factory
RQ	Risk quotient
$R_{REF.T}$	Fresh weight ratio between the contaminant burden in tissue *T* and the concentration in the reference tissue
SAC	Special Area of Conservation
SD	Standard deviation
SG	Specific gravity
SI	'le Système international d'unités' (International System of Unit)
SIXEP	Sellafield Ion Exchange Effluent Plant

SMP	Sellafield MOX Plant
SPA	Special Protection Area
SSD	Species sensitivity distribution
SSSI	Site of Special Scientific Interest
Sv	Unit of *dose equivalent* that provides a measure of the joules of energy deposited per kilogram of material and incorporates a dimensionless 'quality factor' that accounts for factors such as the type of radiation (α, β, γ) and the radiosensitivity of the exposed tissue
$T_{1/2}$	Half-life
THORP	Thermal Oxide Reprocessing Plant
TNT	Trinitrotoluene
UF	Uncertainty factor
UK	United Kingdom
UNSCEAR	United Nations Scientific Committee on the Effects of Atomic Radiation
USA	United States of America
USDoE	United States Department of Energy
USSR	Union of Soviet Socialist Republics
VAMP	Validation of Environmental Model Predictions
WAGR	Windscale advanced gas-cooled reactor

CHAPTER 1 - INTRODUCTION

1.1. Environmental radioactivity

1.1.1. Rejuvenation in the nuclear industry

A history of misunderstanding and mismanagement has led to a widespread negative view of all things nuclear and an ongoing perception that nuclear power generation is a dangerous and unsustainable strategy for helping to meet the global community's future energy needs (e.g. Kaygusuz, 2008). Events such as the bombing of Hiroshima and Nagasaki in the summer of 1945 (Key, 1971), the Windscale, Three Mile Island and Chernobyl accidents in 1957, 1979 and 1986 respectively (Miller, 1994; Nenot, 1990; Norman & Dickson, 1986), the publicised compensation claims from those involved in nuclear weapons testing (Roff, 2004) and the poisoning of Alexander Litvinenko (Ham, 2009) have increased public awareness of the risks and potential health impacts of ionising radiation. Despite efforts to put the relative risk of radiation incidents into context, for example by contrasting the risks with those from air pollution, passive smoking and obesity (Smith, 2007), risk perception continues to be a fundamental reason for the public opposition to the nuclear industry (Whitfield et al., 2009).

However, attitudes towards nuclear power generation are highly politically motivated (Costa-Font et al., 2008) and are mediated by familiarity with nuclear issues (Greenberg, 2009). Perhaps the most striking example is the public support for nuclear power generation in Japan following campaigns by pro-nuclear politicians in the 1950s, even though less than a decade earlier Japan had become the only country in history to suffer a nuclear attack (Kondoh, 2009). In response to the conflicting pressures of increasing energy demand, dwindling economically-viable fossil fuel supplies, the need to reduce green house gas emissions in an attempt to reduce the rate of climate change and a heightened awareness of the need for energy security (Milstein & Cherp, 2007; Pielke, 2009), nuclear power is playing an increasing role in national energy strategies (e.g. Adlys et al., 2008; Kashiwagi & Oda, 2008; Lee & Jung, 2008; Yi-Chong, 2008) and policies for trans-boundary energy exchange (Ochoa & van Ackere, 2009). Therefore, it would appear that the global community is on the verge of a nuclear renaissance and public acceptance is increasing in parallel (Whitfield et al., 2009).

Although policy analysts have suggested that reliance on nuclear power to achieve targets set out in current climate change policy, such as the United Kingdom (UK) Climate Change Act 2008, is unlikely to be successful due to the extent of decarbonisation that the policy calls for (an annual decarbonisation rate in the UK > 4%) (e.g. Pielke, 2009), the UK Government has initiated a Strategic Siting Assessment process to identify candidate sites for the construction of new reactors (DTI, 2007). Similar assessments are underway for the siting of a new repository to store radioactive waste. This repository would be expected to handle both legacy wastes and wastes generated as a result of new nuclear build. Regulatory compliance, at a generic level, of various reactor designs is being assessed (HSE & EA, 2009; IAEA, 2008) and the new nuclear-build component of the UK energy strategy is gaining momentum. Therefore, radionuclide discharges to the environment, both nationally and internationally, may be expected to continue for the foreseeable future and, in conjunction with the need to manage the global nuclear legacy, will result in an ongoing need to assess the risks to both humans and the environment from these discharges.

1.1.2. Impacts of ionising radiation

1.1.2.1. Ionising radiation and dose

Radionuclides are unstable nuclides that emit ionising radiation (radiation that causes ionisation of atoms in the absorbing medium). They are a consequence of a nuclear reaction, the origin of which may be either anthropogenic (man-made), such as the reactions taking place within a nuclear reactor, or natural, such as the reactions that took place during the formation of the universe (Eisberg & Resnick, 1985). Atomic nuclei in an unstable state will undergo nuclear decay, the rate of this exponential decay process being described by the half-life ($T_{1/2}$) of the radionuclide (Table 1.1). Half-lives are radionuclide-specific and can differ by many orders of magnitude, ranging from 10^{-7} s (^{212}Po) to 10^{10} y (^{232}Th) for the radionuclides presented in Table 1.1. Whilst it is not possible to state the exact amount of time until a decay event occurs in an *individual* unstable nucleus, the half-life describes the time required for 50% of the unstable nuclei that are present to undergo nuclear decay. The quantity of a given radionuclide that is present is described by the activity concentration. Measured in SI[1] units of Becquerel (Bq) per unit mass or volume (e.g. Bq kg^{-1} for soil and sediment, Bq m^{-3} for air and Bq l^{-1} for water), it describes the number of decay events per second for a given radionuclide in a given mass or volume of medium (1 Bq = 1 decay event per second).

[1] The abbreviation SI comes from 'le Système international d'unités' meaning International System of Units

Through the nuclear decay process, an unstable nucleus reaches the lowest possible energy state for the number of nucleons (protons and neutrons) that it contains. Nuclear decay can be divided into three main categories: alpha (α), beta (β) and gamma (γ) decay. Each decay mode releases energy in the form of ionising radiation and the absorption of that energy in matter is described by its linear energy transfer (LET), which is a function of the mass, charge and energy of the radiation.

The properties of these different categories of nuclear decay are described in various texts and reports (e.g. Copplestone et al., 2001a; Eisberg & Resnick, 1985; Kelly & Thorne, 2003; Whitten et al., 1988) and are summarised below.

Alpha particles have the highest mass, 4.0026 atomic mass units (amu), consisting of two protons and two neutrons and hence carrying a 2+ charge. These particles have the highest LET of the three nuclear decay categories, their energy being absorbed in 0.04mm depth of biological tissue.

Beta particles are electrons with either a negative (1–) or positive (1+) charge, the latter being referred to as positrons, and have a mass of 0.00055 amu. Absorption of beta particle energy takes place within 5 mm depth of biological tissue.

Gamma rays are pulses of electromagnetic energy (photons) rather than particles. They do not have a charge and their mass is negligible (≈ 0 amu). Gamma photons have the lowest LET and may completely penetrate biological tissue.

The quantity of ionising radiation energy absorbed in a given organ, tissue or whole organism is termed the absorbed dose and is measured in Gray (Gy), where 1 Gy is equal to the absorption of 1 joule of energy by 1 kg of matter. There is a fundamental difference between ionising and non-ionising contaminants, namely that exposure to ionising radiation, and hence the receipt of a radiation dose, does not require direct physical contact between the receptor and the contaminant. The total dose that an organism receives is the sum of the absorbed dose from radionuclides external to the organism (external dose) and radionuclides within the organism's tissues (internal dose). In the context of environmental radiation protection under chronic exposure scenarios, it is normally the dose rate (e.g. μGy h^{-1}) rather than the absolute dose that is evaluated.

Table 1.1. Properties of some natural and anthropogenic radionuclides (data from Kelly & Thorne, 2003)

Radionuclide	Half-life	Radiation(s)
Natural radionuclides		
^{40}K	1.3 x 10^{9} y	β,γ
^{210}Bi	5 d	α,β,γ
^{210}Pb	19 y	β,γ
^{210}Po	138 d	α,γ
^{212}Bi	61 min	α,β,γ
^{212}Pb	11 h	β, γ
^{212}Po	3.0 x 10^{-7} s	α
^{214}Bi	20 min	α,β,γ
^{214}Pb	27 min	β,γ
^{214}Po	1.6 x 10^{-4} s	α
^{216}Po	0.16 s	α,β
^{218}Po	3.1 min	α,β
^{220}Rn	55 s	α,γ
^{222}Rn	3.8 d	α,γ
^{224}Ra	3.6 d	α,γ
^{226}Ra	1.6 x 10^{3} y	α,γ
^{228}Ac	6.1 h	β,γ
^{228}Ra	6.7 y	β,γ
^{228}Th	1.9 y	α,γ
^{230}Th	8.0 x 10^{4} y	α,γ
^{232}Th	1.4 x 10^{10} y	α,γ
^{234}Pa	1.2 min	β,γ
^{234}Th	24 d	β,γ
^{234}U	2.5 x 10^{5} y	α,γ
^{238}U	4.5 x 10^{9} y	α,γ
Anthropogenic radionuclides		
^{60}Co	5.27 y	β,γ
^{90}Sr	29.1 y	β
^{99}Tc	2.1 x 10^{5} y	β
^{134}Cs	2.06 y	β,γ
^{137}Cs	30 y	β,γ
^{238}Pu	87.7 y	α,β,γ
^{239}Pu	2.4 x 10^{4} y	α,β,γ
^{240}Pu	6.5 x 10^{3} y	α,β,γ
^{241}Am	432 y	α,γ

1.1.2.1. Effects of ionising radiation on non-human biota

Although radiation effects may be observed at various levels of biological organisation, from the sub-cellular to the ecosystem level, the direct damage caused by radiation is at the molecular level when ionisation of atoms in the absorbing medium occurs (Kelly & Thorne, 2003). If these ionisation events occur in a cell's deoxyribonucleic acid (DNA), the result

can be a dissociation of molecules in the DNA structure. Such breaks in single DNA strands can readily be repaired by cellular repair mechanisms but double strand breaks are more difficult for cells to repair effectively. Therefore, there are three possible outcomes of an ionisation event in a cell's DNA (Copplestone et al., 2001a):

1. Cellular repair mechanisms restore normal functionality and the cell survives
2. Cellular repair is incomplete and the residual damage may be expressed in the cell or its progeny
3. The radiation damage may kill the cell directly or induce apoptosis (cell death)

If residual damage occurs in somatic cells then this may lead to macroscopic radiation effects in the exposed individual. However, damage in germ cells can be inherited by an offspring and may result in effects at the population level over subsequent generations.

There have been many studies on radiation effects in biota and the most comprehensive source of compiled radiation effects data to date is the FREDERICA radiation effects database (Copplestone et al., 2008). Various attempts have been made to summarise data on radiation effects (e.g. Real et al., 2004; UNSCEAR, 1996). The relative manifestation of effects in different biota groups at a particular dose rate (radiosensitivity) appears to be a function of the degree of biological complexity, with viruses being the least radiosensitive organisms and mammals the most radiosensitive (UNSCEAR, 1996).

Human radiation protection aims to limit the risk of harm to individuals whereas the focus of environmental radiation protection is normally to limit the risk of harm to populations (Andersson et al., 2009; Brechignac & Doi, 2009; Copplestone et al., 2009; UNSCEAR, 1996). Another difference between human and environmental radiation protection is that the focus of environmental radiation protection is deterministic effects for which a threshold dose exists below which no observable effects occur, whereas human radiation protection considers stochastic effects, such as cancer induction, for which radiation protection theory assumes no dose threshold. Therefore, whilst biota radiation effects data have been collated in the FREDERICA database on a range of biological endpoints (Table 1.2), it is deterministic effects on endpoints linked to population sustainability that are of greatest relevance to environmental radiation protection.

To facilitate assessments of radiation impact on biota, effects data have been used to develop values against which absorbed dose rates for biota can be compared (e.g. Copplestone et al., 2009). Values currently used by regulators are shown in Table 1.3, but

the derivation of these values has not always been transparent. The recent EC-funded project on Protection of the Environment in a Regulatory Context (PROTECT) has taken a more transparent approach, analysing data from the FREDERICA radiation effects database using a species sensitivity distribution (SSD) approach (Garnier-Laplace et al., 2006; Garnier-Laplace et al., 2008) to derive benchmark values (Andersson et al., 2009). The effects data used in the development of the SSD were EDR_{10} data, the dose rate representing a 10% effect in the exposed group in comparison to the control group. The generic predicted no-effect dose rate (PNEDR) calculated in the PROTECT project and recommended for use in assessments to screen out situations that are not of concern is 10 µGy h^{-1} (Andersson et al., 2009). However, due to the application of various quality control criteria (Andersson et al., 2009; Copplestone et al., 2008) fewer than 30 studies in the FREDERICA database were found to be suitable for use in the derivation of this benchmark value and only one study reported an EDR_{10} below 10 µGy h^{-1}. There is a need for further research into the effects of chronic radiation exposure, but this must follow rigorous scientific protocols (see Wood et al., 2003) to ensure that the outputs are of a standard suitable for inclusion in the derivation PNEDRs.

1.2. Environmental radiation protection

Radiation protection has historically focussed on protection of man. On the basis that man is the most radiosensitive organism and that comprehensive assessments are required of the potential impacts of regulated release of ionising radiation on humans, the International Commission for Radiological Protection (ICRP) proposed the following in their 1977 recommendations:

'Although the principal objective of radiation protection is the achievement and maintenance of appropriately safe conditions for activities involving human exposure, the level of safety required for the protection of all human individuals is thought likely to be adequate to protect other species, although not necessarily individual members of these species. The Commission therefore believes that if man is adequately protected then other living things are also likely to be sufficiently protected.' (ICRP, 1977)

Table 1.2. Definitions for the umbrella endpoints used to group radiation effects data within the FREDERICA database (reproduced from Copplestone et al., 2008).

Endpoint	Definition
Adaptation	Changes in an organism's physiology, biochemistry or DNA that allows them to survive in conditions/environments that they previously would not.
Ecological	Non-direct ecological effects of radiation due to interactive relationships between populations, including competition, predator-prey interaction and mutualism. The radiation responses of individual populations cause indirect changes in the ecological balance between species in the ecosystem.
Morbidity	A loss of functional capacities generally manifested as reduced fitness, which may render organisms less competitive and more susceptible to other stressors, thus reducing their life span.
Mortality	Death; the death rate; ratio of number of deaths to a given population.
Mutation	A change in the chromosome or genes of a cell which may affect the structure and development of the resultant offspring.
Reproductive capacity	The ability of organisms to reproduce over their lifespan. This is related to fecundity (the survival of offspring) and fertility (the ability to produce offspring).
Stimulation	Activation of defence mechanisms in organisms that lead to an increase in, for example, survival rates, number of offspring and growth.

Table 1.3. Dose rates used by regulatory agencies to demonstrate that biota are adequately protected from the effects of ionising radiation (data from Copplestone et al., 2009).

Country	Value used for regulatory purposes
Canada	20 μGy h^{-1} – screening value for fish 110 μGy h^{-1} – screening value for other freshwater organisms 220 μGy h^{-1} – screening value for terrestrial organisms
England & Wales	5 μGy h^{-1} – screening value for all biota groups 40 μGy h^{-1} – management action level for all biota groups
United States	40 μGy h^{-1} – benchmark values for terrestrial animals 400 μGy h^{-1} – benchmark values for terrestrial plants 400 μGy h^{-1} – dose limit for aquatic animals

However, a number of publications since the 1977 recommendations have highlighted the need to demonstrate that the environment *per se* is adequately protected from the effects of ionising radiation (Pentreath, 1998; Thompson, 1988) and the ICRP is also beginning to consider environmental radiation protection specifically (ICRP, 2007a). Radioecology has responded to the need for environmental radiation protection with the development of models, frameworks and approaches, hereafter referred to collectively as models, for use in assessing the impacts of ionising radiation on wildlife (e.g. Beresford et al., 2008b).

1.2.1. Radioecology and the development of environmental radiation protection models

The discipline of radioecology evolved during the last century, responding to the global community's need to understand the consequences of radionuclide releases in terms of their behaviour and fate in the environment and the effects of ionising radiation on biota. From issues of large scale trans-boundary radionuclide contamination due to weapons testing and nuclear accidents (Alexakhin, 2009), the emphasis of radioecological research has shifted towards issues associated with nuclear power generation and, in particular, the management of radioactive waste (Alexakhin & Prister, 2008). Over the last decade, there has been an increasing focus on the development of models for assessing the impacts of ionising radiation on wildlife.

The extent of resource allocation for development of these models is not universally supported. Well-justified arguments have been made against the need for complex systems of protection for wildlife (Smith, 2005). However, model development is now being driven by environmental legislation (EC, 1979; EC, 1992) that some countries have interpreted as imposing a legislative requirement to demonstrate that the environment is adequately protected (e.g. Copplestone et al., 2005b). Whilst model development and application is more a regulatory response to these legislative requirements than a reflection of any expectation that exposure to radionuclides from regulated discharges will result in significant environmental impacts (Higley & Alexakhin, 2004)[2], there is a need to ensure that modelling approaches are fit-for-purpose, justifiable to stakeholders and that the results can be easily communicated to stakeholders. It is on these aspects of model development and application that research needs to be focussed.

[2] There is no evidence that significant environmental impacts at the population level have occurred due to regulated discharges and only limited evidence that such effects have occurred following accidental releases (Smith, 2005).

1.2.2. Models and model testing

Many of the environmental radiation protection models currently available (see Beresford et al., 2008a; Beresford et al., 2008b; Vives i Batlle et al., 2007) follow the same generic structure (Figure 1.1), using activity concentration data for radionuclides in environmental media (sediment/soil, water and air) as the modelling input. In conjunction with parameters to describe the physical dimensions (geometry), residence time (time spent at the site under assessment), habitat utilisation (time spent in different areas of the site) and trophic transfer of radionuclides for each organism being modelled, these media activity concentration data are used to estimate the internal and external dose rates for each organism. The estimated dose rates are compared to guideline values or radiation effects data to determine whether the organisms are adequately protected.

Three models that are publicly available for download and use by third parties are ERICA, R&D128/SP1a and RESRAD-BIOTA. The ERICA Tool (Brown et al., 2008) was developed during the EC EURATOM funded project 'Environmental Risks from Ionising Contaminants: Assessment and Management' (ERICA) to support the application of the 'ERICA Integrated Approach' to assessing the impact of ionising radiation on ecosystems (Larsson, 2008). Building on the outputs of the Framework for Assessment of Environmental Impact (FASSET) project, which was funded by the EC 5th Framework Programme (Larsson, 2004), the ERICA Tool was developed specifically to meet the needs of users in EC Member States. This was achieved through direct interaction with the end-user community from the outset of the Tool development process and at regular intervals throughout the 3-year project (Zinger et al., 2008b).

R&D128/Sp1a (Copplestone et al., 2001a; Copplestone et al., 2003) was developed for the Environment Agency of England and Wales to assist them in fulfilling their regulatory obligations under European and national legislation (EC, 1979; EC, 1992; UK Parliament, 1981; UK Parliament, 1994). The development time for the model was less than 6 months and the scope of the model (in terms of the radionuclides and organisms for which parameters are provided) is therefore more limited than ERICA. It should also be noted that, although the model is publicly available, it was developed for a specific user (the Environment Agency) rather than the broad range of intended users that ERICA was developed for.

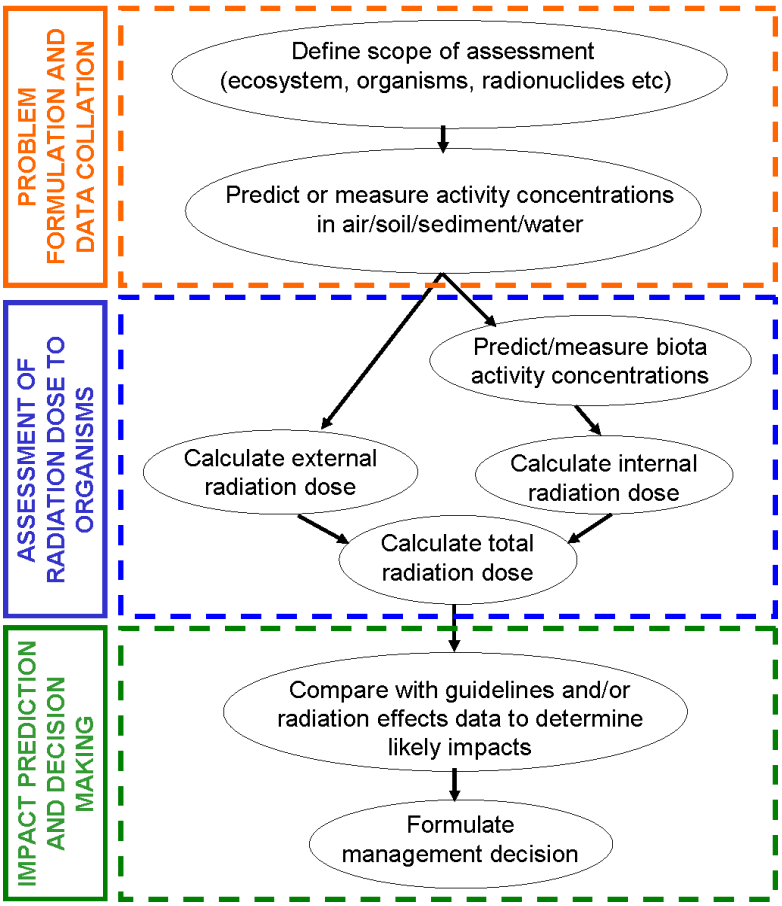

Figure 1.1. Generic structure of models for assessing the environmental impact of ionising radiation.

RESRAD-BIOTA is part of the RESRAD family of model codes developed by Argonne National Laboratory in the United States. It implements the United States Department of Energy (USDoE) graded approach for evaluating radiation doses to aquatic and terrestrial biota (USDoE, 2004). As with R&D128/SP1a, the model was developed for a specific user (the USDoE) and has subsequently been made publicly available, with training courses being offered to those wishing to use the model for undertaking assessments.

ERICA, R&D128/SP1 and RESRAD-BIOTA are already being applied in a decision-making context (Beresford et al., 2008b) and may thus have economic implications. Given that all three models are publicly available and that the current nuclear renaissance is likely to lead to an increasing demand for application of these models, there is a need to understand their effectiveness in different assessment situations. Some evaluation of the models has been undertaken as part of the International Atomic Energy Agency (IAEA)

Environmental Modelling for Radiation Safety (EMRAS) programme (Beresford et al., 2008c). This model testing has been limited to comparison of model parameters related to transfer (Beresford et al., 2008a) and dosimetry (Batlle et al., 2007) and the application of models to a freshwater and terrestrial scenario (Beresford et al., 2008c; Yankovich et al., in press). To increase stakeholder confidence in model outcomes, this model testing needs to be extended to cover a wider range of radionuclides and other ecosystem types. In particular, the effectiveness of models when faced with the challenge of assessing interface ecosystems, such as coastal sand dunes, requires assessment.

1.3. Objectives

This thesis presents the results of a 6-year investigation into the radioecology of temperate coastal sand dune ecosystems. The overall aim of the project was to critically evaluate, and where necessary provide parameters to improve, the predictive capability of environmental radiation protection models when they are applied to coastal sand dune ecosystems. The objectives of the project were divided into two groups: measurement and modelling.

1.3.1. Measurement

1. Develop a baseline dataset of ^{90}Sr, ^{99}Tc, ^{137}Cs, ^{238}Pu, $^{239+240}$Pu and ^{241}Am activity concentrations in soils and a range of biota (including species of amphibian, bird, invertebrate, mammal, reptile, plant, lichen and fungus) from the Drigg coastal sand dunes, which could be used to test the application of environmental radiation models to a coastal sand dune ecosystem. The radionuclides selected were anthropogenic radionuclides known to have been released into the environment from the nearby nuclear fuel reprocessing site at Sellafield and are radionuclides that commonly require assessment in reactor effluent discharges (see Chapters 3 and 8).

2. Quantify natural radionuclide activity concentrations in sand dune soil to determine the relative natural and anthropogenic radionuclide contributions to the total external gamma dose rates at the site (see Chapters 3 and 8).

3. Quantify the activity concentrations of gamma-emitting radionuclides in water and sediment samples from dune slack pools to determine the extent to which this aquatic environment may be an important contributor to the radiation exposure of amphibians at the site (see Chapters 3 and 8)

4. Quantify ^{137}Cs and ^{241}Am depth profiles in soil with increasing distance inland from the mean high water position to investigate the influence of sea-to-land transfer on the inventories of these anthropogenic radionuclides in the coastal sand dune soil and to assess their contribution to external dose rates (see Chapters 3 and 8).

5. Quantify the activity concentrations of gamma-emitting radionuclides in total deposition samples collected from the seaward and landward margins of the coastal sand dunes to investigate the extent to which the sea-to-land transfer of radionuclides is detectable in contemporary total deposition (see Chapters 3 and 8).

6. Quantify external gamma dose rates in air with increasing distance inland from the mean high water position to provide measurement data against which calculated external dose rates could be compared (see Chapters 3, 5 and 8).

7. Determine variability in soil properties (pH and bulk density) with increasing distance inland from the mean high water position to provide an indication of the extent to which the soil has weathered (see Chapters 3 and 8).

8. Quantify the chemical concentration of stable element cations (Ca^{2+}, K^{+}, Mg^{2+} and Na^{+}) with increasing distance inland from the mean high water position to investigate the influence of sea-to-land transfer and sand dune stabilisation on the concentrations of these stable elements and to provide data on cations that may influence the mobility of radionuclides within the sand dunes (see Chapters 3 and 8).

9. Evaluate the influence of sea-to-land transfer of radionuclides on radionuclide distribution and trophic-level transfer in coastal sand dune ecosystems (see Chapters 3, 6 and 8).

1.3.2. Modelling

10. Critically evaluate the suitability of three publically available models (ERICA, R&D128/Sp1a and RESRAD-BIOTA) for undertaking assessments of radiation impacts on wildlife inhabiting a coastal sand dune ecosystem (see Chapters 4 and 5).

11. Identify major sources of uncertainty in the modelling process when applying the models to coastal sand dune sites (see Chapters 4 and 5).

12. Analyse unpublished data from the coastal sand dune complex adjacent to Sellafield to develop a transfer parameter database for radionuclide transfer to invertebrates and small mammals in coastal sand dunes (see Chapter 6).

13. Quantify differences in observed radionuclide transfer to invertebrates and small mammals between coastal sand dunes and other terrestrial sites (see Chapter 6 and Chapter 8).

14. Mine published and unpublished data sources to develop a database of transfer parameters for reptiles, one of the least studied organism groups in radioecology, against which the coastal sand dune data on transfer to reptiles could be compared (see Chapter 7).

15. Use the activity concentration data from the Drigg coastal sand dunes to expand the transfer database for sand dune biota to include amphibians, birds, reptiles, plants, lichens and fungi (see Chapter 8).

16. Estimate absorbed dose rates for specific organisms inhabiting the Drigg coastal sand dunes and compare these dose rates to guideline values to assess whether ionising radiation from regulated discharges may be significantly impacting sand dune biota at the population level (see Chapters 4 and 5).

(This page is left blank intentionally)

CHAPTER 2 – THE DRIGG COASTAL SAND DUNES

This chapter provides an introduction to coastal sand dunes. Topics covered include the processes that influence dune growth and morphology, the development and characteristics of sand dune soil, sand dune hydrology and the ecological characteristics of temperate coastal sand dunes. Subsequent sections introduce the study site (the Drigg coastal sand dunes), explain the rationale for selecting this site and describe the range of sources that may have contributed to the anthropogenic radionuclide contamination at the site. The information presented in this chapter is referenced in later chapters to support discussion of radionuclide transport processes and the trophic transfer of radionuclides.

2.1. Coastal sand dunes

Coastal dunes are amongst the most dynamic landscapes on earth and their evolution is mediated by both climatic and environmental conditions (Jungerius, 2008). Given that fluctuations in these conditions can significantly influence the form and stability of sand dune complexes (Nield & Baas, 2008), sand dunes provide insights into the way in which climate and land use has changed over time. For example, historical human activity in coastal areas, such as settlement development and livestock grazing, is reflected in the dune forms seen today (Gilbertson et al., 1999). Present day coastal dune landscapes are therefore an outcome of the interaction of geomorphological, climatic and ecological processes and anthropogenic pressures.

Coastal dunes have an extensive global distribution (Martinez et al., 2004b; Viles & Spencer, 1995). The coastal dunes of Europe cover a total land area in excess of 5300 km^2 (Delbaere, 1998) of which more than 10% (> 563 km^2) are found in Great Britain (Doody, 1989). Most of the North-West European dune systems developed in the early Holocene period and it has been suggested that the oldest UK sand dunes date to between 5000 and 6000 y before present (Viles & Spencer, 1995). European coastal dunes can be categorised into five main geographic regions: the Atlantic, Baltic, Black Sea, Mediterranean and North Sea regions (Helsenfeld et al., 2004). The dunes in all regions provide a range of ecosystem services, *sensu* the Millenium Ecosystem Assessment (MA, 2003; MA, 2005). These include provisioning services, such as agricultural products and material for mining, regulating services, such as storm protection through coastal defence and purification of river water, and cultural services, such as tourism and education (Jones et al., 2006;

Martinez et al., 2004b; Van der Meulen et al., 2004). Dune systems are rich in biodiversity. For example, coastal dunes in the Netherlands cover up to 1% of the country's land area yet support > 50% of all higher plant species found in the Netherlands (Helsenfeld et al., 2004). Due to their ecological value and dynamic nature, dunes have long been a focus for research, with pioneering work on ecological succession having been undertaken on the vegetation of the Lake Michigan sand dunes by Henry Chandler Cowles in the late 19th century (Cowles, 1899). Sand dunes can thus be viewed as having considerable value from an anthropocentric perspective. These highly complex systems should be protected for the benefit of future generations but they are increasingly under threat from pressures such as climate change induced sea-level rise, pollution, urban expansion and overuse in the form of mining, recreation and agriculture (Martinez et al., 2004a).

2.1.1. Sand transport, dune growth and morphology

Sand dunes are formed when aeolian (wind-blown) sand is intercepted by an obstacle, sometimes termed a sand binder (Jungerius, 2008), around which sand can accumulate. These embryonic foredunes develop at the back of beaches, in or above the litter zone. The obstacle that initiates sand accumulation may be either biotic, such as *Agropyron junceiforme* (sand couch grass) or another halophytic species, or abiotic, such as a pebble or item of beach litter (Ranwell, 1972).

The primary source of sand supply for aeolian transport is the marine environment. Four sandy shore zones have been identified which contribute to the sand transport process (Krumbein & Slack, 1956), the zones being delineated by their proximity to the sea (Table 2.1). Sustained sand dune growth is dependent on a continuous supply of sand in all four zones but the majority of the direct sand supply for dune growth is derived from the backshore zone (Ranwell, 1972).

The growth rate and morphology of dune systems is a function of various complex ecogeomorphic interactions (Nield & Baas, 2008), with feed-back effects introduced by the dune formation process. For example, although the primary determinant of dune morphology is the wind rose (Andreotti et al., 2009), dune topography itself influences the localised wind pattern so the development of sand dune complexes is not an easy process to predict (Jungerius, 2008). However, the physics of initial dune growth and dune development are well documented.

Table 2.1. Sandy shore zones involved in the supply of sand for dune development (adapted from Krumbein & Slack, 1956).

	Zone			
	Nearshore bottom	**Foreshore**	**Backshore**	**Dunes**
Spatial delineation	Mean low water (MLW) to minus 9m below MLW	MLW to high tide line	High tide line to dunes	Above highest tide limit
Degree of tidal inundation	Nearly always submerged	Alternately submerged and exposed	Nearly always exposed (only occasional submersion during storms or exceptionally high water)	Always exposed
Cause(s) of sand movement	Currents and breaking waves	Currents, breaking waves and occasional wind action	Breaking waves and wind action	Wind action

The kinetics of aeolian sand movement are determined by particle size and wind velocity. As a general rule, particles < 0.05 µm can be lifted by wind action and transported inland in suspension but, for particles > 0.05 µm, the sand grains move in saltation (Bagnold, 1954). In the process of saltation, these > 0.05 µm sand grains are lifted by sufficiently strong wind action (see below) and transported in laminar flow (air flow just above the sand surface). These sand grains fall back to the sand surface under gravity and then rebound into the moving air stream. The energy from the impact of sand grains falling onto the sand surface causes other sand particles to be lifted into the air stream, propagating sand movement in the direction of air flow (Ranwell, 1972).

Initiation of saltation is dependent on wind velocity, turbulence and surface erodibility, which is affected by factors such as grain size and moisture content (van Boxel et al., 1999). When studying the fluid mechanics of sand in dune formation, these three parameters are expressed within a single parameter, the friction velocity (u^*), which is defined by the following equation (Gualtieri & Mihailovic, 2008):

$$u^* = \frac{V_s \times \kappa}{\ln(Z_s/Z_0) - \psi_m \times (Z_s/L)}$$

where V_s is the wind speed at the midpoint (Z_s) of the surface layer, κ is the von Karman constant (which in the case of sand dunes describes the logarithmic velocity profile of turbulent air flow near the sand-air boundary), Z_0 is the surface roughness (a value of Z_0 = 0.01 is used for desert systems), ψ_m is the stability parameter for momentum and L is the Monin-Obukhov length (which is the height at which turbulence is generated more by buoyancy than by wind shear). For neutral conditions $\psi_m = 0$ and $Z_s / L = 0$.

The wind speed required to generate a friction velocity in excess of the threshold friction velocity for sand movement in coastal sand dunes has been calculated as 4.5 m s^{-1} at 1 cm above the sand surface (Bagnold, 1954) and 6 m s^{-1} at 2 m above the sand surface (van Boxel et al., 1999)[3]. Obstructions to air movement can cause localised acceleration and deceleration of wind, with corresponding increases in the uplift and deposition of sand grains (Ranwell, 1972). A study of more than 4000 hourly wind profiles on three foredunes of differing topography has demonstrated that topographic changes cause accelerations in air movement and surface roughness causes decelerations (Arens et al., 1995). As wind travels up the seaward slope of a foredune its friction velocity increases, the acceleration effect being greater than the drag-induced deceleration due to surface roughness (Arens et al., 1995). There may therefore be some erosion of the seaward face of the foredune as the wind passes over the dune. However, at the crest of the foredune the friction velocity reduces rapidly and sand grains are deposited either on the crest or on the landward slope of dune (van Boxel et al., 1999). If deposition is on the landward slope, it is rarely more than 100 m from the crest (Jungerius, 2008). The process of sand transfer to the dune zone from the nearshore bottom, foreshore and backshore, coupled with erosion of the seaward face of foredunes due to the wind acceleration effect, leads to a continuous building of the foredunes and a gradual transfer of sand further inland, forming other dunes to the landward side of the foredunes. These landward dunes become progressively more stabilised due to colonisation by vegetation, the cohesive effect of the resultant increase in organic matter in the upper soil horizon and the binding action of plant roots (Jungerius & Vandermeulen, 1988; Ranwell, 1972).

In addition to erosion and remobilisation of sand from the seaward face of foredunes, there are two other important erosion processes that facilitate a wind-driven landward migration of sand particles. These are the formation of blowouts by wind action and the generation of splash drift and overland flow (slope wash) by rainfall.

[3] The mean wind speed at the Drigg coastal sand dunes is between 4.75 m s^{-1} (summer) and 6.59 m s^{-1} (winter). The maximum summer wind speed is 14.92 m s^{-1} and the maximum winter wind speed is19.03 m s^{-1} (George, 2006). This is discussed further in Chapter 8.

The term ‘blowout’ is used to describe an erosional hollow, depression, trough or swale that develops in the surface of the sand dune landscape (Carter et al., 1990). Blowouts are formed by wind erosion of the landward face of partially vegetated dunes. However, their occurrence is not directly related to increasing wind speed. A study of dunes on the Dutch coast demonstrated that the optimum wind velocity for blowouts was 11.25 m s^{-1} (Jungerius, 2008). At lower wind speeds the friction velocity generated was insufficient to cause a blowout whereas at higher wind speeds the blowouts became areas of sand accretion rather than erosion.

Susceptibility of sand to wind erosion is strongly influenced by the presence of organic matter (Jungerius & Vandermeulen, 1988). Sand with an organic material coating (‘grey’ sand) is resistant to wind erosion due to the cohesive properties of the organic matter film on the sand particles. Sand with little or no organic matter (‘yellow’ sand) lacks these cohesive properties and is highly susceptible to wind erosion as a result. Where vegetation has colonised (see Section 2.1.3), the vegetation helps to bind the sand and minimise the likelihood of a blowout occurring. However, disturbance to the vegetation cover and upper soil horizons that exposes the underlying yellow sand, whether due to the grazing and burrowing activities of animals or due to human activities, can destabilise these dunes and make them susceptible to blowouts.

The influence of rainfall on sand movement is related to the type of dune under consideration.

Foredunes that are largely unvegetated have high water infiltration rates, due to the lack of organic material in the sand, so there is little opportunity for the generation of surface run-off leading to overland flow. However, the impact of raindrops on the sand surface during periods of heavy rain can act in a similar way to the sand grains that fall due to gravity during the process of saltation. The rain droplet impact dislodges aggregates of sand and lifts them into the laminar air flow which transports these aggregates in the direction of the wind, predominantly landward. The process is known as splash drift (Jungerius, 2008).

Grey sand on more stabilised dunes has a higher concentration of organic matter in the upper soil horizon. The sand strongly repels water leading to very low infiltration rates, particularly following dry summer periods when the surface sand has dried out. In these circumstances, heavy rainfall can result in surface run-off creating slope wash which transports dislodged sand along a trajectory that follows the surface contours of the dune

(Jungerius & Vandermeulen, 1988). The material transported by this overland flow is deposited at the base of the dune slope.

2.1.2. Soil development

The parent material for coastal sand dune soil is a mixture of particles eroded from local rock formations, glacial deposits and the remains of marine organisms, particularly shell fragments (Ranwell, 1972). These shell fragments result in high carbonate, especially calcium carbonate ($Ca^{2+}CO_3^{2-}$), concentrations in the sand dune soil. Therefore, the yellow sand of young dunes, which has not been exposed to extended periods of weathering, is alkaline (high pH) (Salisbury, 1922). However, in older more stabilised dunes where grey sand is found, the progressive weathering of the sand and the release of humic acids from the accumulated organic matter results in a leaching of carbonate as soluble bicarbonate (HCO_3^-) (Ranwell, 1972; Wilson, 1960). Estimates of carbonate leaching rates suggest that, in dunes with an initial carbonate load of < 5% by weight, most free carbonate is leached from the upper 10 cm of stabilised sand dune soil within 300 – 400 y and, based on data from the sand dunes of Indiana, leaching from the top 2 m of soil occurs within 1000 y (Olson, 1958; Ranwell, 1972). The resulting decalcified dunes have an acidic soil (low pH) (Salisbury, 1922). For example, the pH of yellow sand in the Newburgh dunes, Scotland, was 6.68 whereas the pH of stabilised and weathered soil of the dune heath was 4.27 (Webley et al., 1952). Similar differences in soil pH have been recorded in the dunes of the South Haven Peninsula, England (Wilson, 1960).

Thus, as sand dune soils age, their organic matter content increases, their pH and calcium carbonate concentrations decrease and a soil profile begins to develop (Jungerius & Vandermeulen, 1988; Rezk, 1970). Eventually this leads to the classical pedological soil profile described by the O, A, B, C horizon sequence (Table 2.2), but only in stable dune areas (Jungerius & Vandermeulen, 1988). Many dunes have a profile which reflects the dynamic nature of the system (Jones et al., 2008), with A horizons being sequentially buried by aeolian sand transport (Jungerius & Vandermeulen, 1988). The rate of soil development is highest in stabilised dune habitats that are wet and under dense vegetation cover (Jones et al., 2008).

The chemical composition of sand dune soils is strongly influenced by the composition of the parent material, the proximity of sand dunes to the marine environment and the stage of soil development. There are significant differences in the concentrations of soluble ions between yellow sand areas that are close to the sea and the more developed grey sand areas

that are found further inland. For example, Ca^{2+}, Cl^{-}, HCO_3^{-}, Mg^{2+}, Na^{+} and NO_3^{-} concentrations are higher in yellow sand and K^{+}, NH_4^{+}, PO_4^{3-} and SO_4^{2-} concentrations are higher in grey sand (Gorham, 1958). To illustrate these differences and provide some typical concentrations, Table 2.3 presents concentration data for soluble ions in yellow sand and grey sand areas of the sand dunes at Blakeney Point in Norfolk.

Table 2.2. Classification of soil horizons (based on information from Lutgens & Tarbuck, 1989)

Horizon	Description
O	Organic matter (leaf litter and humus) layer at top of soil profile.
A	Surface soil which is largely mineral matter but with high biological activity and humus generally present.
B	Sub-soil which is generally finer grained than the A-horizon, containing an accumulation of clay particles that result from eluviations (washing out) in the A horizon. Biological activity is lower than in the A horizon.
C	Weathered bedrock dominates this horizon and there is little or no organic matter.

Table 2.3. Soluble ion concentrations (mg kg^{-1}) in surface soil (to 3 cm depth) from the sand dunes at Blakeney Point, Norfolk (Gorham, 1958)

Ion	Yellow sand (*n* = 10)	Grey sand (*n* = 10)
Na^+	52.88	8.05
K^+	9.77	21.50
Ca^{2+}	49.10	8.02
Mg^{2+}	10.33	4.86
NH_4^+	0.54	9.02
HCO_3^-	149.49	45.76
Cl^-	74.45	14.18
SO_4^{2-}	50.43	40.83
PO_4^{3-}	0.63	17.41
NO_3^-	3.41	0.31

2.1.3. Zonation and succession

The classical description of sand dune zonation identifies four distinct zones based on their ecological and geomorphological characteristics (Jungerius, 2008).

Zone 1 encompasses the beach and embryo dunes. It is in this zone that the sand dunes begin to develop. The zone is characterised by limited colonisation from halophytic plants, such as *Agropyron junceiforme*, and a dominance of aeolian processes.

Landward of the embryo dunes are the yellow dunes, also known as white dunes (Zone 2). Aeolian processes continue to dominate in this zone but their influence decreases with increasing distance from Zone 1. The Zone 2 dunes (foredunes and the dune forms immediately behind them) are more stabilised than the embryo dunes of Zone 1, this stabilisation often being initiated by algae (van den Ancker et al., 1985) and subsequently by mosses and lichens (Jungerius, 2008). Specialised grasses, like *Ammophila arenaria* (marram grass), which is highly resistant to burial, are commonly found within this zone (Ranwell, 1972).

The vegetation cover of the grey dunes (Zone 3) is dominated by mosses and lichens, although marram grass and *Festuca rubra* (red fescue) are also commonly encountered within this zone. The soil is characterised by increased organic matter content over that of Zones 1 and 2. Pluvial rather than aeolian processes are the dominant geomorphic influence in this zone (Jungerius, 2008) although aeolian processes still have localised impact in the form of blowouts (see Section 2.1.1.).

Brown, or black, dunes (Zone 4) are characterised by the heathland area that develops at the back of the dune system. Grasses like *F. rubra* and various *Erica* (heather) species tend to dominate the vegetation cover. Geomorphic processes no longer induce change in the landform of this zone and the increasing organic matter content and ageing of the stabilised soil leads to the development of a classical soil profile as described in Section 2.1.2.

An important ecological feature of temperate coastal sand dunes is dune slacks, which are often found in Zones 3 and 4. Dune slacks are moist or water-filled depressions that support greater plant species diversity than the remainder of the dune system (Jones et al., 2006; Ranwell, 1972), although *Salix repens* (creeping willow) is often the dominant species (Gorham, 1961). The moisture content of temperate dune slacks varies seasonally, primarily in response to fluctuations in the water table (Jones et al., 2006), resulting in seasonal differences in the dominant contributors to plant and animal biomass within the dune slacks and supporting particular stages in the life-history of biota groups such as amphibians.

The four zones and dune slacks each have a characteristic vegetation cover (Ranwell, 1972) but increasing stabilisation of the dune system provides the opportunity for plant succession (Gorham, 1961), especially in Zones 3 and 4. In highly stabilised systems, such as the dunes at Ainsdale in Lancashire (UK), plant succession extends through to extensive scrub growth and the development of pine forests. The degree of grazing pressure at a dune site, either by livestock or resident wildlife, influences the successional status of the dunes and sand dune stability. For example, livestock grazing on machair grassland (Zone 4) in Ireland has been shown to reduce species diversity in the plant community and destabilise areas of dune by increasing the exposure of bare sand (Cooper et al., 2005). Where grazing pressure is reduced, plant diversity increases and succession can occur. This is reflected in the significant increase in the scrub cover of British dune systems due to the dramatic reduction in *Oryctolagus cuniculus* (European rabbit) population densities following the introduction of myxoma virus in the mid-1950s (Ranwell, 1972).

2.1.4. Hydrology

Coastal sand dunes are an essentially arid environment so the dynamics of water movement and retention within sand dune soils play an important role in determining the plant and animal species that can be sustained, both temporally and spatially, within a dune system. Sand dunes are classically viewed as freshwater systems in hydrological terms (Ranwell, 1972). Although there is growing evidence from stable isotope research that deposition of

sea water (via sea spray) can play an important role in the hydrological regime of embryo dunes and foredunes, the significance of this has only been demonstrated for summer period water dynamics in dunes at a distance of 5 – 12 m from mean high water (MHW) (Greaver & Sternberg, 2007). Additionally, there have been suggestions that intrusion of saline water may occur through the groundwater but, unless groundwater extraction is creating a negative drainage gradient, this is not seen in practice. Even when dunes are surrounded by sea water, freshwater floats on the surface of this sea water so tidal fluctuations change the depth of the surface of the fresh water table rather than introducing sea water into the dune system (Ranwell, 1972). Thus, for the majority of a dune system, the water content of the soil is derived from precipitation and ground water inputs only, the dominant source depending on season, time of day and location within the dune system (Gardner & McLaren, 1999), and it remains appropriate to consider the hydrological components of that system as being freshwater rather than marine.

2.1.4.1. Precipitation

Most sand dune soils are highly permeable and precipitation easily penetrates as a result. However, this permeability is significantly affected by the initial moisture content of the soil. After an extended dry period, sand dune soils, especially in the grey dunes (Zone 3) become increasingly impermeable, leading to the slope wash process described in section 2.1.1. As precipitation begins to penetrate and the moisture content increases, so too does the permeability (Jungerius, 2008). Once this infiltration of water has commenced, the water percolates through the soil, under the influence of gravity and along matric suction and root suction gradients (Gardner & McLaren, 1999). Movement of precipitation-derived water in the sand dune soil can thus be both vertical and horizontal (Gardner & McLaren, 1999). It has also been shown that preferential pathways exist within the soil structure (Dekker & Jungerius, 1990; Gardner & McLaren, 1999; Jungerius, 2008), so infiltration rates can be difficult to predict.

Following a period of precipitation, evaporation of moisture from the soil surface begins to reduce the moisture content of the surface soil. This creates a suction gradient that draws water back towards the surface, although the effect of this evaporation-induced gradient appears to be most significant for the upper 30 cm of the soil profile (Gardner & McLaren, 1999).

Diurnal temperature fluctuations can be as high as 30^{o}C at the surface of the yellow dunes (Salisbury, 1952) and this can lead to a temperature gradient at night between the colder

soil surface and warmer deeper soils with higher moisture content. This gradient drives an upward movement of water vapour which condenses in the surface soil. However, although this diurnal dew formation has been well documented in sand dunes soils (see Ranwell, 1972), this moisture is subject to rapid evaporation (Gardner & McLaren, 1999) so is unlikely to act as a significant daytime water source for dune vegetation.

2.1.4.2. Groundwater

For much of a sand dune system, the groundwater table is many metres below the rooting zone and is not a significant source of water for plant growth (Ranwell, 1972). However, groundwater is an important source of water for low lying features of dune systems such as dune slacks (Malcolm & Soulsby, 2001; van der Hagen et al., 2008). Seasonal variation in groundwater recharge influences the height of the water table and, as a result, the moisture content of the dune slack soil (Jones et al., 2006). In temperate dune systems this often leads to water-logging of surface soils during winter and spring (Pye, 1990). In some instances, standing water occurs and the dune slacks become temporary ponds (Grootjans et al., 2004).

2.2. The study site

2.2.1. Site location

The Drigg coastal sand dune system (Ordnance Survey National Grid Reference: SD065965) is primarily an acidic dune complex supporting large areas of Atlantic decalcified fixed dunes, which is one of the habitat features for which the dunes are protected under conservation legislation (JNCC, 2006). The dunes occupy a spit of land that is bounded by the Irish Sea to the west, the mouth of the Esk Estuary to the south and the River Irt and inner Esk Estuary to the east (Figure 2.1). The nuclear reprocessing plant at Sellafield (Ordnance Survey National Grid Reference: NY028039) is situated 10 km to the north and the dunes are adjacent to the site of the low-level radioactive waste repository (LLWR; Ordnance Survey National Grid Reference: SD055992). The geographic extent of the dunes, approximately 6 km^2, incorporates a local nature reserve (LNR), falls within the Lake District National Park and the Drigg Coast Site of Special Scientific Interest (SSSI) and comprises approximately 40% of the Drigg Coast NATURA 2000 site (JNCC, 2006).

2.2.2. Site description

The parent material for the dunes belongs to the Sandwich soil association[4] with a substrate geology dominated by dune sand and marine shingle (Soil Survey of England & Wales, 1983). The underlying bedrock is sandstone (Parker, 1977). The dunes have developed on a shingle spit and are believed to be approximately 5000 y old (Vincent, 1998). However, the cartographic records of Speed in 1676 and Monk in 1836 suggest that the length of this spit has increased during the last 300 – 400 y and that there have been corresponding changes in the course of the River Irt (Steers, 1946).

All principal phases of dune development are represented within the Drigg coastal sand dunes (embryo dunes, yellow dunes, fixed grey dunes and dune heath, see Figures 2.2 – 2.5); the majority of the area is covered by fixed grey dunes and dune heath with many humid dune slacks also present (Figure 2.6). To the rear of the sand dune spit, where it borders the River Irt, the dune heath transitions into a tidally-inundated beach area (Figure 2.7) and extensive saltmarsh (Figure 2.8). There is public access to all parts of the dunes and signs of direct human disturbance, mainly erosion around footpaths, are apparent, albeit over small geographical areas. The dunes are maintained in a semi-natural state by agricultural livestock grazing (predominantly sheep), which retards the natural plant succession. The combination of these physical attributes and pressures has resulted in a varied flora and fauna and created habitats of importance for a range of protected species.

Vegetation cover is dominated by *A. arenaria* and *F. rubra*. Heather species are present across much of the fixed dune area, with *Calluna vulgaris* (heather) and *Erica cinerea* (bell heather) common in the drier areas of the dune heath and *Erica tetralix* (cross-leaved heather) in the wetter areas. Mosses (e.g. *Racomitrium canescens*) and lichens (e.g. *Cladonia portentosa*) are prevalent on the fixed dunes and throughout the grassland areas of the dune heath. There is some *Ulex europaeus* (gorse) coverage but this is concentrated in small areas of the dunes and is a relatively small contributor to the total vegetation cover. Protected species, such as the rare *Ophioglossum azoricum* (small adder's tongue fern), are also present.

The dune fauna includes both permanent residents and migratory species. Notable resident species include the vulnerable *Cicindela hybrida* (northern dune tiger beetle), *Triturus cristatus* (great crested newt) and *Bufo calamita* (natterjack toad). Many bird species utilise the dunes for breeding and feeding. There is a large *Alauda arvensis* (skylark) population

[4] Deep well-drained sandy soils commonly found in sand dunes and some wetland habitats

and *Anthus pratensis* (meadow pipits) are widespread. In addition to the grazing livestock, mammals present include *Apodemus sylvaticus* (field mouse), *Microtus agrestis* (field vole), *Sorex araneus* (common shrew), *O. cuniculus*, *Vulpes vulpes* (fox) and a few *Capreolus capreolus* (roe deer). The dunes also support strong herptile populations. All six native amphibian species are present (*Bufo bufo* (common toad), *B. calamita*, *Rana temporaria* (common frog), *T. cristatus*, *Triturus helveticus* (palmate newt) and *Triturus vulgaris* (smooth newt)) along with three reptile species, namely *Vipera berus* (European adder), *Lacerta vivipara* (common lizard) and *Anguilis fragilis* (slow worm).

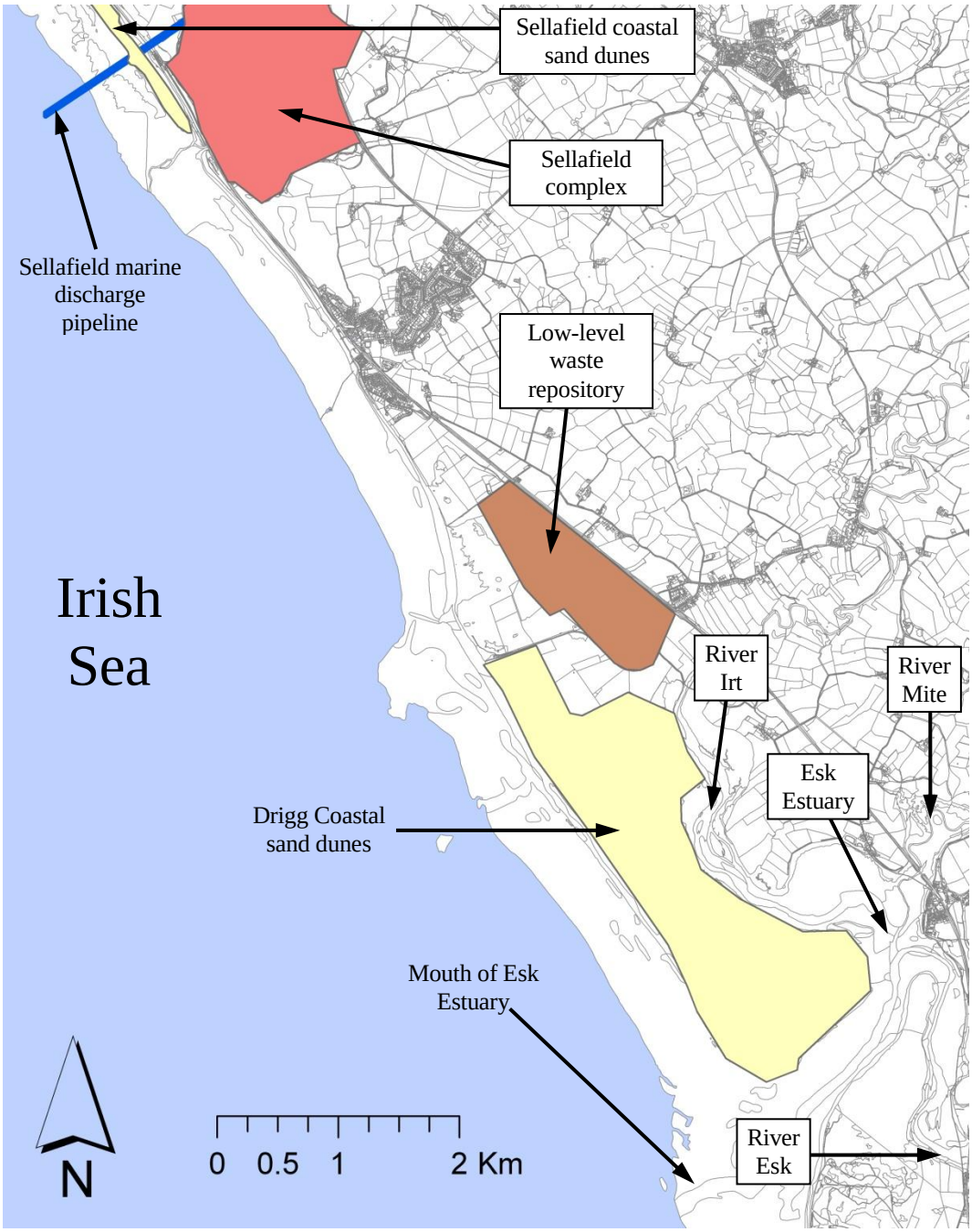

Figure 2.1. Location of the Drigg coastal sand dunes and other features on the west Cumbrian coast. ©Crown Copyright/database right 2009. An Ordnance Survey/EDINA supplied service.

Figure 2.2. Beach at Drigg coastal sand dunes with embryo dunes merging into yellow foredunes.

Figure 2.3. View along the ridgeline of the foredunes at the Drigg coastal sand dunes.

Figure 2.4. Grey dunes within the Drigg coastal sand dunes.

Figure 2.5. Dune heath within the Drigg coastal sand dunes.

Figure 2.6. Dune slack within the Drigg coastal sand dunes.

Figure 2.7. Beach at rear of sand dunes at the interface with the River Irt.

Figure 2.8. Saltmarsh at rear of sand dunes at the interface with the River Irt. Sellafield can be seen in the background.

2.2.3. Site disturbance

Although, as with any dune system, there is a continuous reworking of the dune landscape taking place at the Drigg coastal sand dunes, due to the ecogeomorphological processes described in Section 2.1, there is written and fixed-point photographic evidence to suggest that the grey dune and dune heath areas of this sand dune complex have not been subject to significant macro-level change since the late 1970s (Woolven et al., 1988; Appendix 1). However, prior to the early 1970s there were large areas of bare sand, particularly on the LNR, which were the result of disturbance from war time activities on the dunes (Steers, 1946; Woolven et al., 1988).

During the Second World War, the nearby Holmrook Hall (Ordnance Survey National Grid Reference: NY001081), christened ‘HMS Volcano’ by the Royal Navy, was

commandeered by the Admiralty between 1943 and 1946 as a 'Special bomb training centre' for British and Allied personnel to be trained in demolition and bomb clearance. The Drigg coastal sand dunes were used for bomb disposal training in preparation for D-Day mine clearance[5]. Evidence of this military history can still be seen on the dunes, particularly the remains of observation towers on the ridgeline of the foredunes and re-vegetated bomb craters in the dune slacks.

There are other relics that have been found in the dunes that demonstrate a much longer history of human activity at the site. The earliest archaeological evidence suggests that the dune complex was a site of stone age settlement (Rollinson, 1978). For example, charcoal from a relic fire hearth found within the dunes has been dated to approximately 4000 y before present (Cherry, 1982) and a Neolithic axe has been found at the site (Parker & Collingwood, 1926).

The Drigg area was occupied by the Romans during the early part of the first millennium AD (Parker & Collingwood, 1926). Thereafter, the dunes appear to have been common land until approximately 1800 AD when the land was accepted by Lord Muncaster in lieu of tithes (Parker & Collingwood, 1926) and the dunes are still in the ownership of the Muncaster estate today. Originally used by Lord Muncaster as a rabbit warren (Parker & Collingwood, 1926), the dunes later became an important gullery, supporting one of the largest *Larus ridibundus* (black-headed gull) colonies in Britain (Woolven et al., 1988). Anecdotal accounts from the early 20th century (e.g. Parker & Collingwood, 1926) suggest that this was a highly productive gullery but there was a sharp decline in breeding numbers in the latter part of the 20th century, from more than 10,000 breeding pairs prior to 1975 to approximately 1,500 breeding pairs in 1984 (Lowe, 1991). It was speculated that this decline may be due to radionuclide discharges from the Sellafield complex but available scientific evidence does not support that assertion (Lowe, 1991; Woodhead, 1986). A more plausible explanation for the decline is the combined pressures introduced by high *V. vulpes* (predator) densities, low *O. cuniculus* densities (an alternative prey species for *V. vulpes*) due to myxamotosis and an unusually dry summer, the resultant drought causing a reduction in the availability of *L. ridibundus* prey items, such as earthworms (Lowe, 1991).

In addition to their terrestrial usage, the Drigg dunes and surrounding area have also supported maritime activities. For example, the Esk estuary, which separates the majority

[5] Details from **http://www.users.globalnet.co.uk/~rwbarnes/defence/volcano.htm** and **http://www.users.globalnet.co.uk/~rwbarnes/defence/copeland/holmroo_/beach-.htm**, accessed 3rd September 2009

of the dune spit from the mainland, was the site of a Roman sea port (Parker & Collingwood, 1926). During the industrial revolution, slate from the quarries on Honister Crag was transported by pack horse to the Drigg coast and loaded onto ships for transport (Rollinson, 1978). The Drigg dunes have thus had an extensive history of human disturbance but, as noted previously, they are now used for recreation and grazing alone and the current dune forms have remained largely unchanged since the late 1970s.

2.3. Justification for site selection

There were several reasons for selecting a coastal sand dune site, in particular the Drigg dunes, to test models for assessing the impacts of ionising radiation on biota. The selection reflects the limited radioecological data available for coastal dune systems, the extent to which the Drigg coastal sand dunes are representative of other temperate coastal sand dune systems, the potential for the Drigg dune complex to be impacted by ionising radiation (resulting from exposure to a range of radionuclides), the mechanism by which radionuclides may contaminate the dunes, the level of public interest in the Drigg coastline and the requirement to undertake radiation impact assessments for coastal sites that fall within NATURA 2000 sites in England and Wales (Copplestone et al., 2005b). These points are expounded below.

Little is known of coastal sand dune radioecology, with only one previous study that presented a coherent radionuclide activity concentration data set for a coastal sand dune complex for non-human species (Copplestone, 1996; Copplestone et al., 2001b), so there was an interest in studying coastal sand dunes to improve radioecological understanding of this ecosystem type.

The Drigg coastal sand dunes were an ideal study site to select because the sand dune complex includes all of the main features of temperate coastal sand dunes (see Section 2.2.2). Although highly stabilised in most areas, the foredunes and southern-most dunes of the Drigg coastal sand dune complex are dynamic (see Chapter 8). Therefore, the Drigg coastal sand dunes can be viewed as representative of both the dynamic dune forms and stabilised dune heath areas present in other temperate dune systems. One factor that may make the Drigg coastal sand dunes appear atypical is the separation of the dune spit from other inland areas by the River Irt. However, this does not affect the dunes directly and has been used to provide comparative data for another interface ecosystem, the saltmarsh (see Chapter 8).

With regard to validating the environmental radiation protection models described in Section 1.2.2, it was recognised that the sand dunes presented an opportunity to consider many poorly studied radionuclide – reference organism combinations and to test the assumptions used to derive transfer parameters for these models. For example, where sufficient data are available, default transfer parameters used in the ERICA Integrated Approach and R&D128/SP1a are derived from published data. However, where data are limited, alternative approaches have been used to derive the default transfer parameters (Beresford et al., 2008d; Copplestone et al., 2003). For example, the ERICA default parameter for the transfer of ^{241}Am to reptiles and amphibians is derived from data for mammals and the default parameter for the transfer of ^{99}Tc to shrubs is derived from data for grasses and herbs.

Another reason for choosing to study coastal sand dunes was their transitional nature and ecological characteristics, which provide unusual contamination pathways. Coastal sand dunes are at the interface between the marine and terrestrial environments and those at Drigg may be contaminated through the deposition of radionuclides transferred from sea to land (Bryan et al., 2008; Eakins et al., 1981; Hill et al., 2008; see section 2.4.1.1.3). Dunes are also dynamic, being formed by aeolian sand entrapment and stabilised, to varying degrees, by plant colonisation. In well-developed coastal sand dune complexes, such as the Drigg dunes, humid dune slacks with seasonal ponds can occur, resulting in a dune system that interfaces terrestrial, marine and freshwater environments. The Drigg dunes thus presented a challenging and very different environment to those explored in other case study-based model validation and intercomparison exercises to date (e.g. Beresford et al., 2007f; Beresford et al., 2008a; Vives i Batlle et al., 2007; Yankovich et al., in press).

Stakeholder engagement opportunities added value to the selection of the Drigg dunes as a study site. There has been considerable public interest in the Sellafield site and, to a lesser extent, the LLWR near Drigg, with regard to their potential impacts on humans and the environment in the west Cumbrian region of the UK. The coastline of that region receives particular attention because it supports habitats and species that are protected at local, national and European level. These two aspects of environmental awareness within the region provided the opportunity to explore stakeholder engagement in model application, in particular the ERICA Integrated Approach (see Chapter 4), using well-established stakeholder networks.

The final reason for studying the Drigg coastal sand dunes was the legislative requirement in England and Wales to assess the environmental impact of ionising radiation at European-

designated NATURA 2000 sites in the UK (Copplestone et al., 2005b), including coastal sand dunes. The UK has approximately 560km^2 of sand dunes along its coastline and there are over 20 coastal sand dune complexes that are components of NATURA 2000 sites (UK Biodiversity Group, 1999) and hence protected due to their unique habitat features. Also, these dunes support a range of European and UK protected species including amphibians such as *T. cristatus* and *B. calamita*. European and UK legislation (EC, 1979; EC, 1992; UK Parliament, 1981; UK Parliament, 1994) requires that protection of designated sites and species from hazardous substances be demonstrated and the England & Wales Environment Agency has interpreted this legislation to include ionising radiation (Copplestone et al., 2005b). The Environment Agency has been using the 'R&D Publication 128' methodology (Copplestone et al., 2001a; Copplestone et al., 2003) as an interim approach for the assessment of radiation impact on NATURA 2000 sites, but is likely to be adopting the ERICA Integrated Approach for future assessments (Copplestone et al., 2005b).

2.4. Anthropogenic sources of environmental radioactivity along the Drigg Coast

Since the 1950s, the Drigg coastal sand dunes have received radionuclide inputs from a number of anthropogenic sources. These sources include planned releases of radioactivity to the environment, such as in the case of regulated discharges and weapons testing, and unplanned releases, such as the Windscale and Chernobyl accidents (see Sections 2.4.1 & 2.4.2).

The history of radionuclide deposition at the dunes from these planned and unplanned releases would be expected to be reflected in the soil radionuclide activity concentrations at the site and the radionuclide depth distribution profiles. However, it is known that the Drigg coastal sand dunes have been subject to considerable human disturbance, especially during the 1940s, with subsequent stabilisation of the dunes occurring at the macro-level from the late 1970s (see Section 2.2.2). Therefore, the radionuclide accumulation in dune soils may be characterised by approximately two decades of soil profile disturbance followed by four decades of radionuclide accumulation in a largely stable soil structure.

2.4.1. Planned releases of radioactivity to the environment

2.4.1.1. Sellafield

The Sellafield site has evolved considerably over time in response to changing operational requirements and to regulatory pressures. This has resulted in significant temporal changes in the releases of radionuclides to the environment, both via atmospheric emission and liquid effluent discharge into Irish Sea (Gray et al., 1995). The major developments at the site are outlined below and the resultant changes in atmospheric and marine discharges are presented in sections 2.4.1.1.1 and 2.4.1.1.2 respectively.

During the Second World War, there were two Royal Ordnance Factories (ROFs) on the West Cumbrian coast that produced munitions to support the war effort. One ROF was established at Sellafield and the second near the village of Drigg (see Section 2.4.1.2). In 1945, the UK government transferred ownership of the Sellafield site to the Ministry of Supply to support the nuclear weapons programme (BNG Sellafield Ltd, 2007). In 1947, the move towards nuclear operation commenced with the construction of two nuclear reactors, known as the Windscale Piles, and a reprocessing plant that was principally intended to produce weapons-grade plutonium (Webb et al., 2006). Windscale Pile 1 went critical, reaching the point at which a self-sustaining nuclear chain reaction commenced, in October 1950. Criticality in Pile 2 was achieved in April 1951 and the reprocessing plant commenced operations in 1952 (Gray et al., 1995).

During the 1950s, the Sellafield site expanded its activities to include nuclear power generation with the construction of four graphite-moderated gas-cooled magnox reactors (Gallie, 1996). This part of the site became known as Calder Hall. The first of these magnox reactors commenced operation in 1956, making it the world's first commercial nuclear power station (Gallie, 1996). Calder Hall continued to generate nuclear power until decommissioning commenced in 2003.

The next major development at the site was construction of the Windscale advanced gas-cooled reactor (WAGR), which was completed in 1962. The WAGR was a prototype version of the second generation of nuclear reactors to be built in the UK, the advanced gas-cooled reactors (AGRs). The WAGR was operational from 1963 until 1981.

Recognising the need to reprocess spent fuel from the operation of magnox reactors, such as the four Calder Hall reactors, a magnox reprocessing plant was constructed on the Sellafield site and reprocessing activities commenced in 1964.

Expansion of reprocessing activities began with the 1977-1978 Windscale inquiry into the proposal by British Nuclear Fuel Ltd (BNFL), which took operational control of the site in 1971, to develop a plant to reprocess irradiated oxide nuclear fuel. The thermal oxide reprocessing plant (THORP) was designed to reprocess spent fuel from AGRs and light water reactors (LWRs) (Mulkern, 1995). Although approval for THORP was given in 1978, it wasn't until 1994 that commercial operation of THORP commenced.

Commissioning of the Sellafield Ion Exchange Effluent Plant (SIXEP) in May 1985 improved the capacity for on-site treatment of liquid waste prior to discharge to the marine environment (Gray et al., 1995). This capacity to treat liquid waste was further enhanced by the opening, in 1994, of the Enhanced Actinide Removal Plant (EARP).

The last major development at the Sellafield site was the construction of the Sellafield mixed oxide (MOX) plant (SMP), which was designed to produce MOX fuel for use in LWRs (Edge & Walls, 1997). Although construction was completed in 1997, the SMP only became operational in 2001 and, based on recent statements regarding its long-term viability (e.g. Macalister, 2009), it is likely that this plant will soon close.

2.4.1.1.1. Atmospheric discharges from the Sellafield complex

Atmospheric discharge points for ventilation air from the reactors, fuel storage and reprocessing facilities at the Sellafield site vary in height from 'roof level' up to 120 m (Webb et al., 2006). In order to construct an atmospheric discharge chronology for the site, these discharge points have been grouped into those that can be represented by an effective stack height of 10 m and those that can be represented by an effective stack height of 80 m (Gray et al., 1995). The 10 m effective stack height chronology is presented in Figure 2.9 and the 80 m effective stack height chronology in Figure 2.10.

Radioisotopes of the noble gases argon and krypton are the principal components of the emissions to atmosphere from Sellafield, comprising > 99% of the total activity discharged. Emissions of ^{41}Ar, primarily from the Windscale Piles, dominated the atmospheric emissions from Sellafield during the 1950s (see Figures 2.9. and 2.10). There were also notable emissions of ^{3}H from the 10 m effective stack height discharge points (see Figure 2.9). Following the shutdown of the Windscale Piles in 1957 (see Section 2.4.2.2), there was a marked reduction in emissions from atmospheric discharge points falling within the 80 m effective stack height category (Figure 2.10). Although at a lower total annual discharge activity, ^{85}Kr was the dominant contributor to discharges at the 80 m effective stack height level from 1960 onwards and there was a general increase in emissions of ^{85}Kr

over time. The emissions at the 10 m level continued to be dominated by ^{41}Ar, although this radionuclide contributed < 12% of the total gaseous discharge activity from 1968 onwards whereas ^{85}Kr contributed > 87%.

Whilst total discharges of activity to atmosphere from the Sellafield site have been between 10^2 and 10^3 TBq y^{-1} (1 terabequerel is equal to 10^{12} Bq) since the early 1960s, the prevailing wind direction (south-westerly[6]) makes it unlikely that deposition from these discharges will be a significant contributor to anthropogenic radionuclide inputs to the Drigg dunes.

[6] Wind direction is defined on the basis of the origin so a south-westerly wind travels from the south west towards the north east.

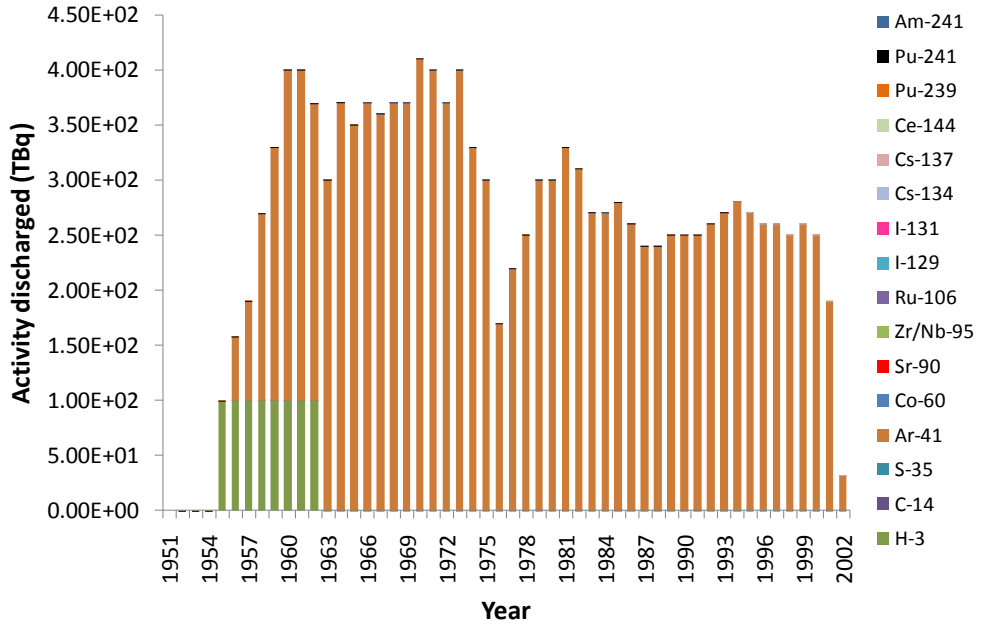

Figure 2.9. Temporal changes in Sellafield atmospheric discharges at an effective stack height of 10 m (data from Gray et al., 1995 and BNFL annual monitoring reports).

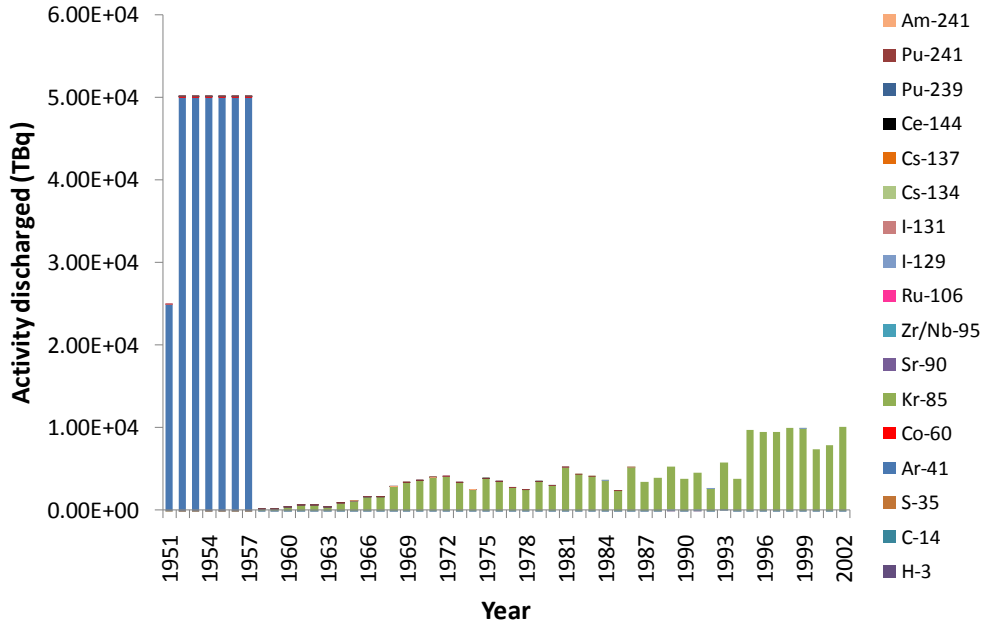

Figure 2.10. Temporal changes in Sellafield atmospheric discharges at an effective stack height of 80 m (data from Gray et al., 1995 and BNFL annual monitoring reports).

2.4.1.1.2. Marine discharges from the Sellafield complex

Liquid radioactive effluent is discharged to the Irish Sea via a discharge pipeline which transects the Sellafield coastal sand dunes (see Chapter 6) and releases the effluent approximately 2.5 km from the shore for subsequent dilution and dispersal. As a result of changing activities at the Sellafield site, the composition of the marine discharge has changed over time (Figure 2.11).

Discharges of radioactivity into the Irish Sea gradually increased from the early 1950s, reflecting the onset and expansion of nuclear reactor operation at the Sellafield site. During the late 1960s, marine discharges increased rapidly, reaching their peak in 1970, with a total annual discharge of 16,600 TBq and then declining gradually until the mid 1980s. The total annual discharge of activity remained fairly constant from the mid 1980s to the mid-1990s, but then increased by approximately 1000 TBq y^{-1}.

Throughout the operating history of Sellafield, ^{3}H accounted for > 10% of the activity discharged and, from 1986 onwards, > 90% of the annual discharge to the marine environment was ^{3}H. Other radionuclides that contributed > 10% of the annual activity discharged o the marine environment between 1952 and 2002 were ^{95}Nb, ^{95}Zr, ^{106}Ru, ^{137}Cs and ^{241}Pu. The discharges of ^{95}Nb, ^{95}Zr and ^{106}Ru were highest prior to the early 1970s. From the early 1970s to the mid 1980s, ^{137}Cs and ^{241}Pu discharges were elevated, ^{137}Cs dominating the discharge between 1974 and 1982 (accounting for 35 – 51% of the total activity discharged per annum). Although the activities discharged reduced for most radionuclides from the mid to late 1970s, there was a notable increase in ^{99}Tc discharges in the mid to late 1990s. This was due to an increase in the treatment of stored effluent but has reduced significantly since 2004 due to the introduction of abatement technology[7] (Bryan et al., 2006).

With the exception of ^{241}Pu, the actinides (^{238}Pu, ^{239}Pu, ^{241}Pu and ^{241}Am) were not major contributors to the total activity discharged. However, the marine discharges of these radionuclides from Sellafield warrant specific consideration because the sea-to-land transfer mechanism is particularly effective at returning actinides to the land (see Section 2.4.1.1.3). The temporal profiles of activity discharged for each of the actinides are shown in Figures 2.12 and 2.13. All four actinides had discharge activity peaks in the early to mid 1970s and the Pu isotopes had a second peak in the late 1970s. In addition to having only one

[7] Historically, magnox medium active concentrate (MAC) was stored to allow decay of short-lived radionuclides and then discharged, via EARP, to the Irish Sea. After 2004, MAC was routed to the High-Level Waste Plant for vitrification instead of using the marine discharge route (Mayall, 2005).

discharge peak, ^{241}Am also differs from the Pu isotopes in that its distribution of discharges is more discrete. By 1977 > 90% of the total ^{241}Am activity discharged from Sellafield up to 2002 had been released into the marine environment. This didn't occur until 1980 for ^{239}Pu, 1981 for ^{241}Pu and 1982 for ^{238}Pu.

Overall, radioactivity discharged to the marine environment from the Sellafield site over the last 30 years has reduced markedly due to improvements in the effluent treatment facilities (Bryan et al., 2006) in response to regulatory pressures and radionuclide activity concentrations in the environment around Sellafield have declined as a result (RIFE, 1996 - 2008).

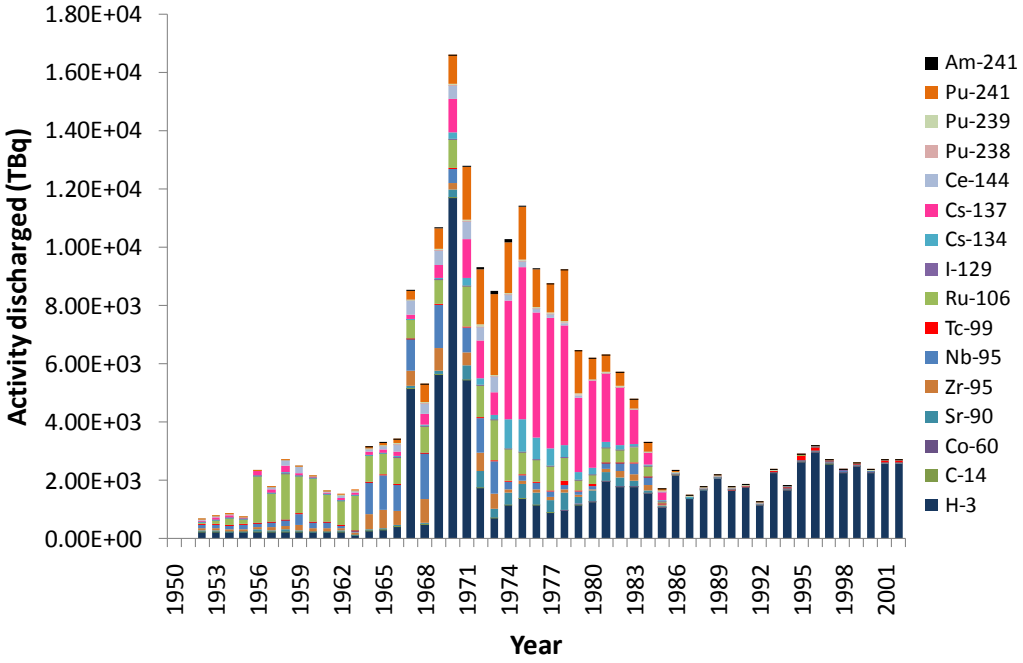

Figure 2.11. Temporal changes in the radionuclide activity profile of the total annual discharge to the marine environment from the Sellafield complex (data from Jackson et al., 2000 and BNFL annual monitoring reports)

(a)

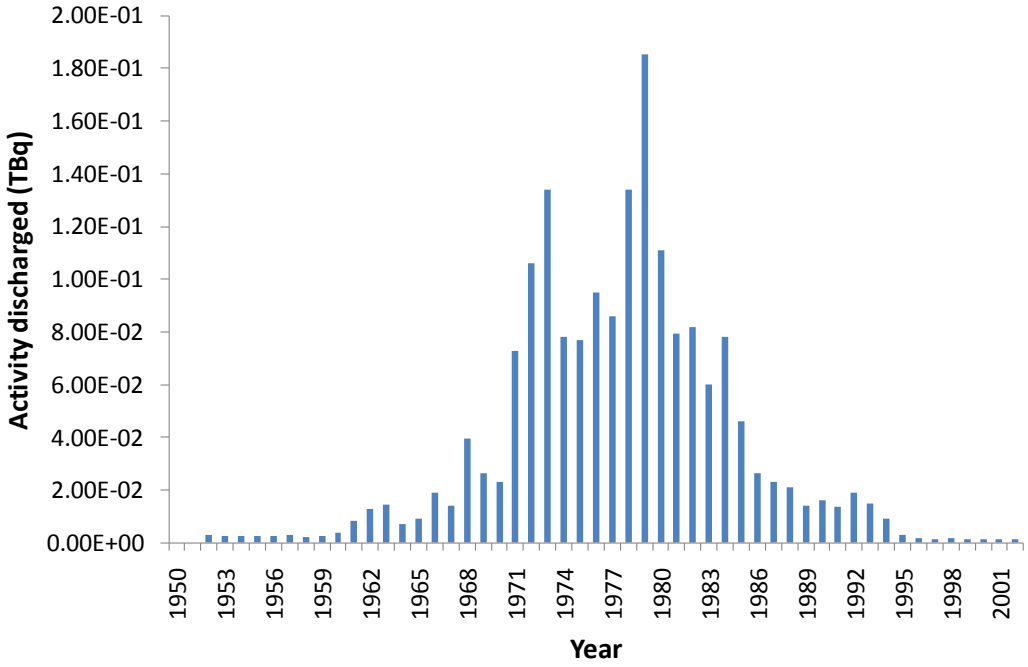

(b)

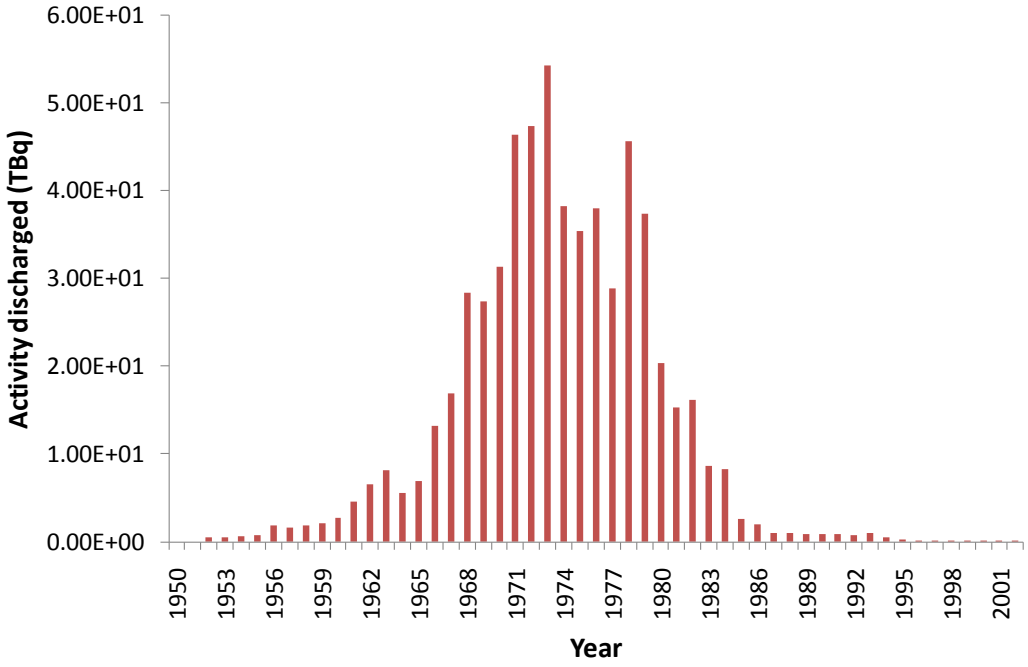

Figure 2.12. Temporal changes in the activity of (a) ^{238}Pu and (b) ^{239}Pu discharged to the Irish Sea from Sellafield (data from Jackson et al., 2000 and BNFL annual monitoring reports).

(a)

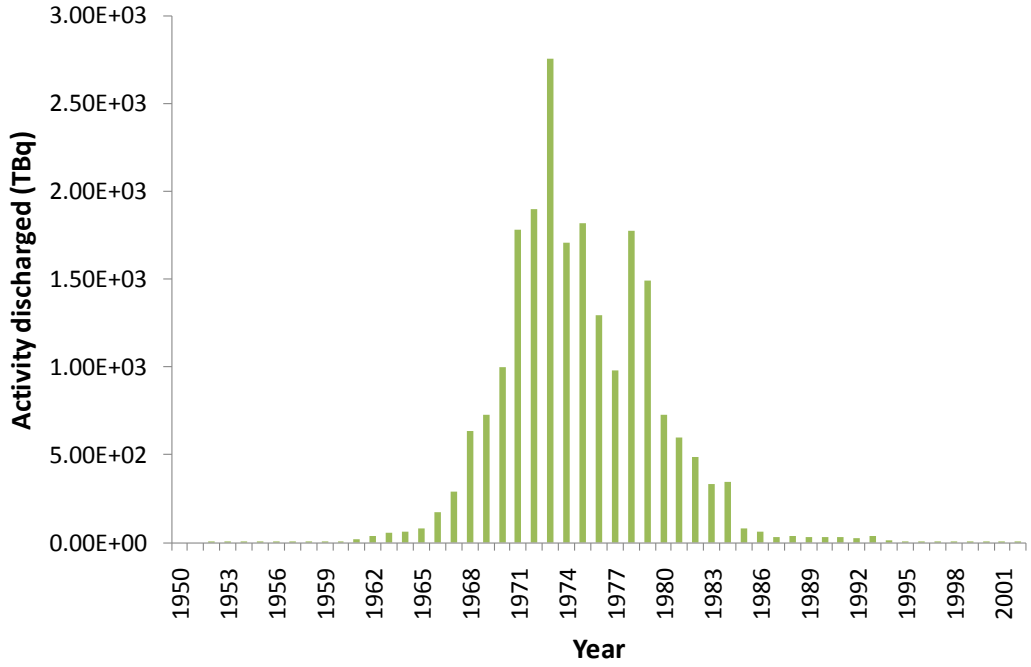

(b)

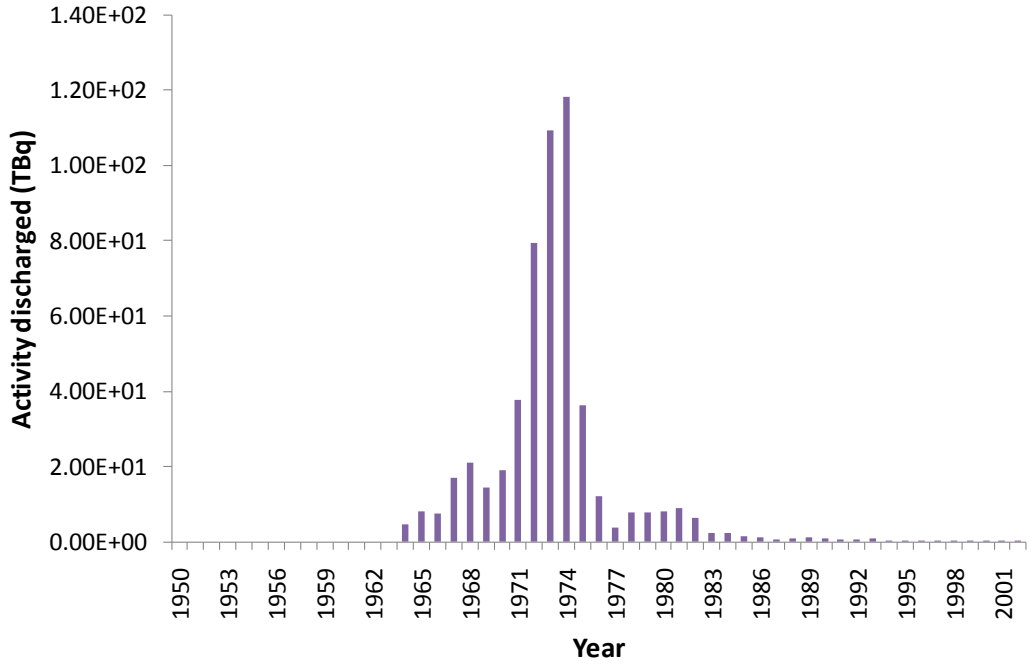

Figure 2.13. Temporal changes in the activity of (a) ^{241}Pu and (b) ^{241}Am discharged to the Irish Sea from Sellafield (data from Jackson et al., 2000 and BNFL annual monitoring reports).

2.4.1.1.3. The sea-to-land transfer mechanism

The process by which radioactivity discharged into the marine environment from the Sellafield site is returned to land warrants specific consideration because this is thought to be the dominant pathway by which Sellafield- derived radionuclides are transported to the Drigg coastal sand dunes (Branford & Nelis, 1996; Nelis, 1990).

Although the direction of sea current movement in the Irish Sea is predominantly to the North (Kershaw et al., 1995), dilution and dispersal of radionuclides within the highly turbulent coastal waters results in detectable activity concentrations of Sellafield-derived radionuclides in sea water and sediments to the South as well as to the North of Sellafield (RIFE, 2008). Activity concentrations of some of these radionuclides are also detectable in coastal soils (Eakins et al., 1981). Differences in the ^{137}Cs activity concentrations in coastal soils do not appear to be strongly correlated with distance from the sea (Eakins et al., 1981; Nelis, 1990), at least at distances > 50 m from the shoreline (Branford & Nelis, 1996). However, there are many studies that demonstrate a clear relationship between actinide activity concentrations in the coastal terrestrial environment and proximity to the coast (Bryan et al., 2006; Bryan et al., 2008; Cambray & Eakins, 1982; Copplestone et al., 2001b; McHugh et al., 1986; Nelis, 1990; Pattenden et al., 1987). The deposition of actinides transferred from sea to land in west Cumbria has been shown to reduce by approximately 2 orders of magnitude between the beach and 8 km inland (Eakins et al., 1982), although the sea-to-land transfer still dominated actinide deposition at 17 km inland from the sea (Pattenden et al., 1987).

In the coastal marine environment, radionuclides partition between water and sediment. The sediment may either be in the form of suspended sediments or benthic sediments (Periáñez et al., 1996). The partitioning of a given radionuclide (*R*) is a function of its particle reactivity, which is indicated by the distribution coefficient (K_d) for that radionuclide:

$$K_d\ (l\ kg^{-1}) = \frac{Activity\ concentration\ of\ R\ in\ sediment\ (Bq\ kg^{-1})}{Activity\ concentration\ of\ R\ in\ filtered\ water\ (Bq\ l^{-1})}$$

Studies on actinide partitioning in the coastal waters of West Cumbria yielded K_d values in the $10^5 – 10^6$ l kg^{-1} range (McKay & Walker, 1990), which is in agreement with the generic marine K_d values recommended by the International Atomic Energy Agency (IAEA, 2004;

Table 2.4)[8]. These K_d values indicate that americium and plutonium are highly particle reactive and are predominantly associated with suspended and benthic sediments as a result. The suspended sediment loadings in the West Cumbrian coastal waters are highest close to the shoreline and the highest total sea water activity concentrations for actinides are therefore found in these near-shore coastal waters. Available evidence suggests that, following their discharge from Sellafield, the residence time of actinides in these coastal waters is in excess of 6 years (McKay & Walker, 1990).

Table 2.4. Distribution coefficient (K_d, l kg^{-1}) values for a selection of elements in the coastal marine environment (IAEA, 2004)

Element	**K_d**
Am	2×10^6
Ca	5×10^2
Cs	4×10^3
H	1×10^0
Na	1×10^{-1}
Pu	1×10^5
Ru	4×10^4
Sr	8×10^0
Tc	1×10^2

Four possible mechanisms by which radionuclides in coastal waters could be transferred to land were originally proposed (Cambray & Eakins, 1982):

1. Direct suspension of the sea surface in the form of spray
2. Conversion of the sea surface material into aerosols by bubble bursting
3. Injection of seawater and suspended sediments into the air by waves breaking in the surf zone
4. Movement of sediment to intertidal regions with subsequent resuspension by wind.

[8] Although this agreement may be expected because the IAEA recommended values for Am and Pu are also derived from Irish Sea data.

Data on ^{137}Cs concentrations in coastal soils do not indicate an enrichment of radiocaesium in sea spray relative to sea water but, for the more particle reactive actinides (K_d for Cs is 2 – 3 orders of magnitude lower than the actinides), the sea spray must be enriched relative to the sea water in order to account for the deposition pattern observed (Cambray & Eakins, 1982). Therefore, the direct suspension of the sea surface in the form of spray (marine aerosols) can explain the marine contribution to ^{137}Cs activity concentrations in the coastal terrestrial environment but not the enhanced actinide activity concentrations.

Marine aerosols are defined as the component of atmospheric aerosols (i.e. the air including solid particles and liquid drops in suspension) whose source is the sea (McKay & Pattenden, 1990). The generation of marine aerosols occurs when bubbles in sea water reach the surface and burst, releasing their contents to atmosphere (Woolf, 1993). Bubble production is mediated by a range of conditions and processes including water temperature (Asher & Farley, 1995), wind speed (Wu, 1988) and wave action, especially the formation of 'whitecaps' on breaking waves (Blanchard & Woodcock, 1957). The resultant bubbles typically range in size from < 200 nm (Sellegri et al., 2006) to 200 μm (Spiel, 1998), with a median bubble size of approximately 100 μm (McKay & Pattenden, 1990).

As bubbles travel through sea water towards the surface they scavenge particulates (Belot et al., 1982) and this results in an enrichment of the microlayer (or surface film) of the bubbles (Blanchard, 1982). Upon reaching the surface of the sea, the upper part of the microlayer breaks through the surface of the water and bursts. The disintegration of this upper section of the microlayer generates droplets, known as film drops (McKay & Pattenden, 1990), which rise to a height of approximately 1 cm above the sea surface (Resch et al., 1986). The remaining bubble cavity collapses, with the lower section of the remaining microlayer being drawn towards the centre of the cavity (McKay & Pattenden, 1990). This results in a rapid upward movement of the lower section of the bubble microlayer and produces a jet which disintegrates into a number of droplets, known as jet drops that attain heights of up to 20 cm above the sea surface (Blanchard, 1955). The marine aerosols (film drops and jet drops) that result from this bubble bursting process are then transported by the wind. The prevailing wind is generally towards the shore in coastal regions, hence sea-to-land transfer occurs.

Calculated enrichment factors (EFs), the concentration ratio between an element in sea water and that element in the marine aerosols, indicate that the particulate scavenging and resultant microlayer enrichment are most effective at scavenging larger particles (> 5.8 μm) (Belot et al., 1982). Actindes tend to be associated with larger particulates in the marine

environment (Eakins et al., 1988) so this explains why the enrichment of marine aerosols is more pronounced for actinides than other radionuclides, such as ^{137}Cs.

Although the sea-to-land transfer associated with bubble bursting is likely to be the dominant transfer process for long distance transport and is in line with observations on the correlation between radionuclide activity concentrations and particulates on dry-cloth monitoring screens (Fry, 1983), for sand dunes in general, and embryo and foredunes in particular, the movement of radionuclide contaminated intertidal sediment via wind may also be important sea-to-land transfer process. It has been demonstrated that actinides in sandy intertidal sediments in West Cumbria are mainly associated with sand rather than silt, 95 % of the activity being present in the sand fraction (Eakins et al., 1988). Therefore, actinide contaminated sand grains moving in saltation (see Section 2.1.1) may account for some of the actinide inventory present within coastal sand dunes.

2.4.1.2. The low-level waste repository

The UK's low-level radioactive waste repository (LLWR) is owned by the Nuclear Decommissioning Authority (NDA) operated by Low-level Waste Repository Ltd under contract from the NDA (NDA, 2008). Located approximately 7 km to the South of the Sellafield site and adjoining the northeast border of the Drigg coastal sand dune spit (see Figure 2.1), the repository is approximately 1 km from the sea. The underlying geology is the same as that of the sand dunes, namely glacial deposits overlying sandstone bedrock (Parker et al., 1989).

The LLWR site was originally the site of ROF Drigg (see Section 2.4.1.1) but has been used for low-level waste disposal since 1959 (Duerden et al., 2003). The LLWR is a 'near surface' disposal facility (Fox et al., 2006) and waste was originally disposed of by loose-tipping into a series of shallow trenches (Duerden et al., 2003). In the late 1980s, BNFL started to package waste into containers prior to disposal and an engineered concrete vault was developed at the LLWR to house these containers. The first container was deposited in the vault in 1988 (Duerden et al., 2003). During the last two decades, further vaults have been constructed and presently there are 9 disposal vaults at the site.

Historically, liquids draining from the disposal trenches and vaults were discharged via the Drigg stream that runs from the site, along the northeast border of the sand dune complex and into the River Irt (Parker et al., 1989). Direct discharges of this leachate to the stream stopped in 1991 (RIFE, 2005). There was also some movement of radioactivity from the trenches via groundwater, although this was principally an eastwards migration (inland

away from the coastal dunes) and, since the early 1990s, has been "reduced to very low levels" (RIFE, 2007). The current route for disposal of leachates is via a marine discharge pipeline which discharges 1 km offshore but the activities discharged are negligible in comparison with the Sellafield discharge and, once in the marine environment, cannot be distinguished from the Sellafield discharges (RIFE, 2005). In addition to the negligible contribution of LLWR marine discharges on anthropogenic environmental radioactivity in west Cumbria, there have been no significant aerial discharges from the LLWR site (RIFE, 1996). Therefore, discharges from the LLWR are not likely to comprise a significant component of the radionuclide contamination of the nearby coastal sand dunes.

2.4.1.3. Weapons testing

The main source of anthropogenic radionuclide contamination of terrestrial and marine ecosystems globally is the testing of nuclear weapons (Aarkrog, 1989; Aoyama et al., 2006; Livingston & Povinec, 2000). The majority of radioactivity releases to the environment as a result of weapons testing occurred between the first detonation of a nuclear weapon (codenamed 'Gadget') on 16th July 1945, at the Trinity Site in New Mexico, and the signing by the USA, USSR and UK of the atmospheric test ban treaty in 1963, although China performed its last atmospheric test in October 1980 (Bergan, 2002). Weapons tests post-1980 have been conducted as underground tests (Figure 2.14.), which result in minimal radionuclide releases to atmosphere (Bennett, 2002; UNSCEAR, 2000).

Nuclear weapons can be divided into two categories, namely fission and fusion devices (UNSCEAR, 2000). In a fission device, energy is released when a nucleus of high atomic number splits, forming two nuclei of intermediate atomic number. Conversely, in a fusion device, energy is released when two nuclei of low mass number combine to form a more stable nucleus of higher mass number (Eisberg & Resnick, 1985).

Fission devices are commonly known as atomic bombs or atom bombs (A-bombs). Within a fission device, fissile material (enriched uranium or plutonium) must reach supercritical mass, the mass at which an exponentially growing self- sustaining nuclear reaction occurs (Meggitt, 2006). The two designs that have been used in A-bombs to create supercritical mass are the implosion-type and the gun-type design (Bunn & Wier, 2006). In implosion-type A-bombs, supercritical mass is achieved through compression of a sub-critical mass of fissile material using conventional chemical explosives, as in the case of early weapons such as 'Gadget' and 'Fat Man' (the bomb dropped on Nagasaki). The gun-type design also uses conventional explosives but in this case the explosives are used to create a

supercritical mass by firing one subcritical mass of fissile material into another subcritical mass of fissile material. The 'Little Boy' bomb that was dropped on Hiroshima utilised this technology.

Fusion devices, known as thermonuclear devices or hydrogen bombs (H-bombs), can produce higher energy yields than fission devices (UNSCEAR, 2000). In a fusion device, a fission bomb is used to compress and heat fusion fuel (tritium and deuterium), causing a fusion reaction. The fusion reaction produces high speed neutrons which can induce fission in material such as depleted uranium. Fusion bombs haven't been used in military attacks to date but the highest yield nuclear explosion recorded, with an energy release equivalent to 50 Mt of trinitrotoluene (TNT), was from the testing of a fusion bomb in the former Soviet Union in 1961 (UNSCEAR, 2000).

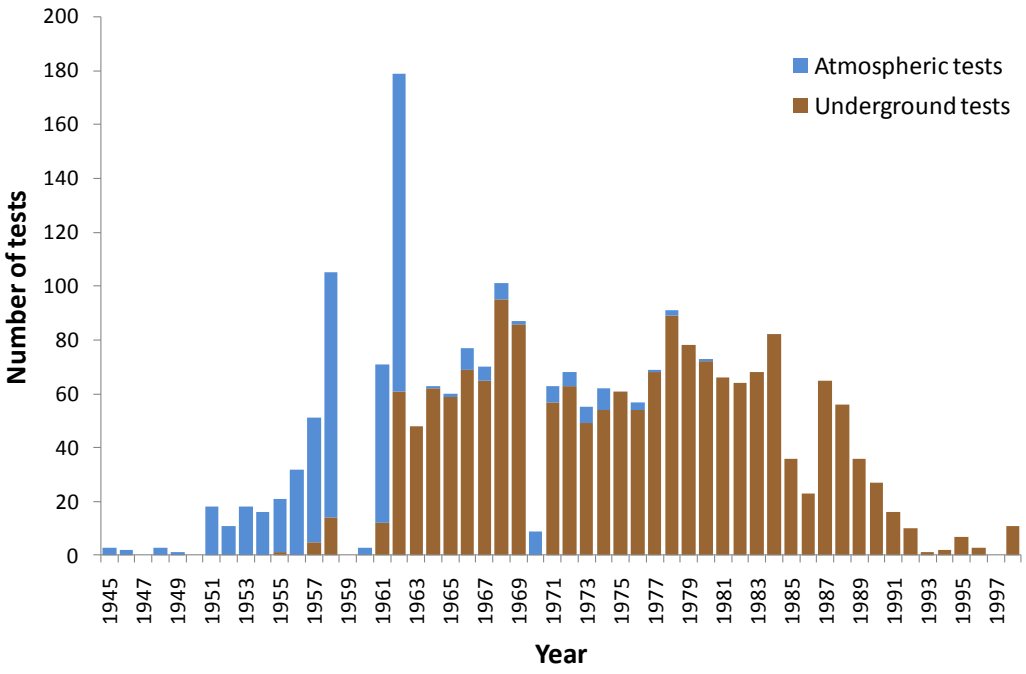

Figure 2.14. Temporal variation in the number of above and below ground tests of nuclear weapons, including two military applications in 1945 (data from UNSCEAR, 2000).

Atmospheric testing of nuclear weapons has resulted in global environmental contamination by fission and fusion products (UNSCEAR, 2000). Early A-bomb tests released radioactive debris into the troposphere whereas H-bomb tests, which began in 1952, caused

debris to be released into the stratosphere. Debris released into the troposphere returns to earth much more quickly than that released into the stratosphere. Residence times for debris in the stratosphere are of the order of 1 – 3 y and this longer residence time prior to deposition results in global circulation and fallout of released activity (Bennett, 2002). Radionuclides released from atmospheric tests include isotopes of Ba, C, Ce, Cs, Fe, H, I, Mn, Pu, Ru, Sb, Sr, Y and Zr (Figure 2.15). The activities released range from 4.35 PBq of ^{240}Pu to 759000 PBq of ^{140}Ba, where 1 petabequerel (PBq) equals 10^{15} Bq. The total activity released as a result of atmospheric weapons testing is approximately 25 ZBq, where 1 zetabequerel (ZBq) equals 10^{21} Bq.

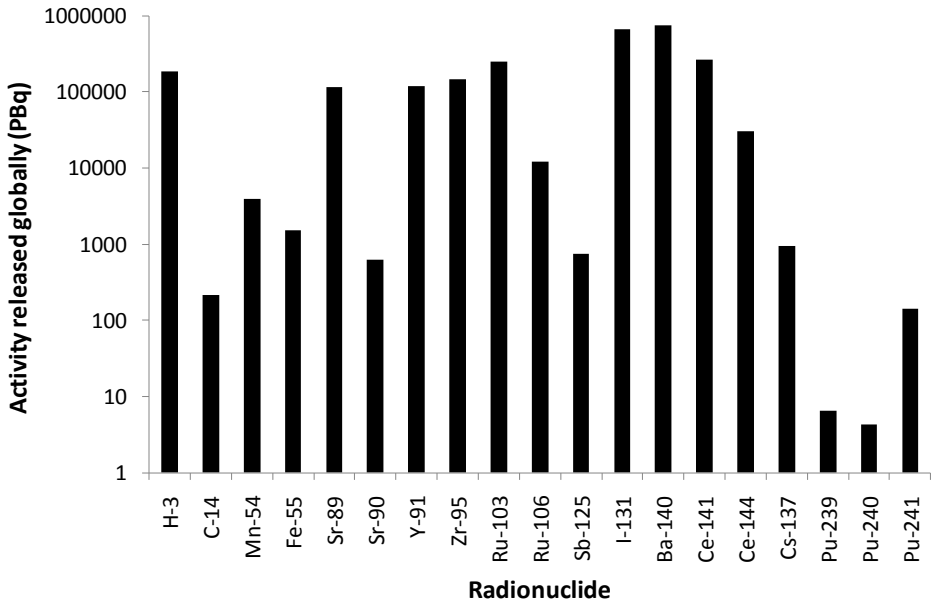

Figure 2.15. Activity of radionuclides produced and dispersed globally as a result of above ground testing of fission and fusion devices (data from UNSCEAR, 2000).

Deposition of fallout from weapons testing is reflected in soil and lake sediment samples from west Cumbria (e.g. Cambray et al., 1989; Michel et al., 2002). Although inputs from global fallout have been declining steadily since weapons testing activities shifted from predominantly above-ground testing to below-ground testing (Cambray et al., 1989),

weapons testing fallout remains an important source of anthropogenic radionuclide contamination and would be expected to contribute to the accumulated radionuclide inventory within the coastal sand dunes of west Cumbria, as has been demonstrated for other coastal grassland sites in the area (e.g. Rudge, 1989)[9].

2.4.2. Nuclear accidents

Of the few major accidents that have taken place during the history of the nuclear industry, two have resulted in notable radionuclide inputs to the environment in West Cumbria. These are the Windscale accident of 1957 and the Chernobyl accident of 1986. The following sections provide a brief overview of these accidents and the resultant radionuclide releases.

2.4.2.1. Windscale

On the 10th and 11th October 1957, a fire occurred in Windscale Pile No. 1 during an annealing procedure to release stored Wigner energy, the result of neutron-induced carbon atom displacement in the crystal lattice, from the graphite core (Dunster et al., 2007; Garland & Wakeford, 2007; Simpson, 1992). This resulted in an unplanned release of radionuclides to the surrounding environment (Figure 2.16). The radionuclides of radiological significance that were released included ^{89}Sr, ^{90}Sr, ^{131}I, ^{137}Cs and ^{210}Po, with a total combined activity of approximately 770 TBq (Alexakhin, 2009). Although undamaged by the fire, Windscale Pile 2 was shut down as a safety precaution and the Piles are currently being decommissioned (Sexton & Asme, 2007).

The Windscale accident has been rated at International Nuclear Event Scale (INES) level 5, an accident resulting in severe damage to the reactor core/radiological barriers and resulting in off-site risk with a need to implement countermeasures (Webb et al., 2006). However, due to the effectiveness of implemented countermeasures, particularly the imposed milk ban in the area following the accident, doses to exposed individuals from this accident have been estimated in the range 1 – 9 mSv[10] (Nenot, 1990; Webb et al., 2006).

[9] Rudge (1989) estimated that the ^{137}Cs deposition (Bq m^{-2}), measured in pre-Chernobyl West Cumbrian soil cores collected to 15 cm depth, consisted of contributions from Sellafield marine discharges (15%), weapons testing (30%) and atmospheric discharge from Sellafield including the 1957 Windscale fire (55%).

[10] The unit Sievert (Sv) is used in human radiation protection. As for absorbed dose (measured in Gy), the Sv is a measure of the joules of energy deposited per kilogram of material. However, Sv is a unit of *dose equivalent*, incorporating a dimensionless 'quality factor' that accounts for factors such as the type of radiation (α, β, γ) and the radiosensitivity of the exposed tissue. (Allisy-Roberts, 2005).

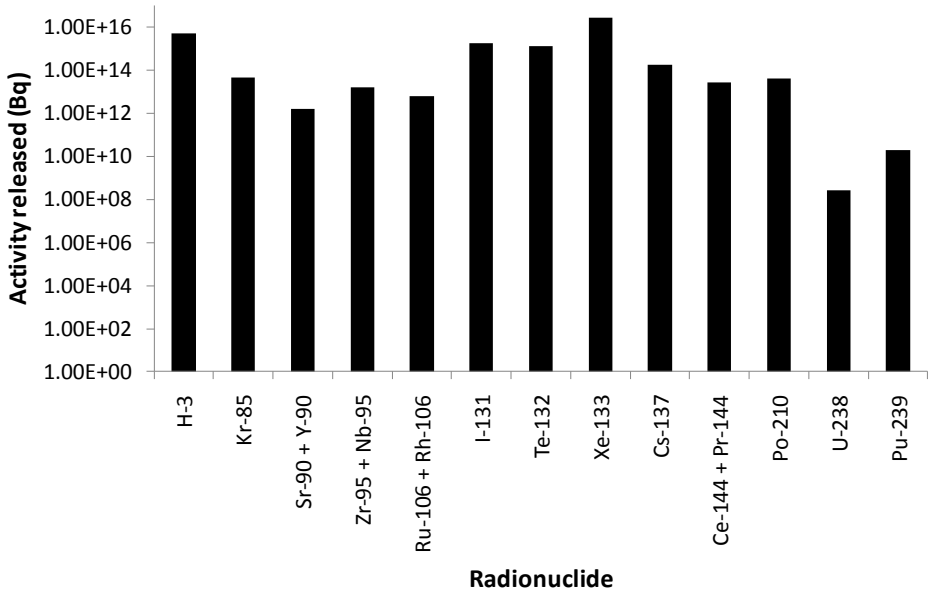

Figure 2.16. Radionuclides released to atmosphere from the 1957 Windscale accident (data from Garland & Wakeford, 2007).

The contaminant plume released from Windscale Pile 1 spread over much of mainland Europe during the days following the accident (Johnson et al., 2007). Deposition in west Cumbria of radionuclides released into the atmosphere as a result if the Windscale fire was largely in the form of dry deposition (Chamberlain, 1996). The deposition plume extended southeast from Sellafield and there was a maximum deposition measured at Drigg (Chamberlain & Dunster, 1958).

2.4.2.2. Chernobyl

The explosion on 26th April 1986 in the Unit 4 RBMK-1000 reactor, a graphite-moderated LWR at the Chernobyl nuclear power plant in the Ukraine, and the subsequent fire that burnt for several days, was a dramatic consequence of human failure in both the design and management of the Chernobyl reactor (Cherkashov et al., 2006; Salge & Milling, 2006; Wakeford, 2006). The accident released approximately 5.3 EBq of activity to the environment (1 exabequerel is equal to 10^{18} Bq), with ^{90}Sr, ^{131}I and ^{137}Cs being the dominant radionuclides emitted (Alexakhin, 2009).

The radioactive plume from the Chernobyl accident reached the UK on 2nd May 1986 (Fry, 1987). Deposition of both ^{131}I and ^{137}Cs occurred as the plume passed over the UK, with average deposition on grass in Cumbria between 3rd and 6th May 1986 calculated as 2246 Bqm^{-2} and 1334 Bqm^{-2} respectively (Clark & Smith, 1988) These two radionuclides showed a different depositional pattern across the UK because ^{137}Cs in the plume was predominantly in the particulate phase whereas ^{131}I was present in both particulate and vapour phases. As a result, ^{131}I deposition occurred as both wet and dry deposition but ^{137}Cs deposition was mainly due to wet deposition (Clark & Smith, 1988; Smith & Clark, 1986). The $T_{1/2}$ for ^{131}I is approximately 8 d whereas the $T_{1/2}$ for ^{137}Cs is 30 y. Therefore, 23 y on from the Chernobyl accident, deposited ^{131}I has decayed but detectable activity concentrations of ^{137}Cs remain and restrictions continue on the movement of sheep from a number of upland farms (Bell & Shaw, 2005).

Cumbria received particularly high deposition of ^{137}Cs (Clark & Smith, 1988). Soil samples collected from the Drigg coastal sand dunes in June 1986 indicate that the Chernobyl-derived ^{137}Cs accounted for 46% of the total ^{137}Cs inventory in the top 0 – 4 cm of the soil profile and 27% in the top 0 – 14 cm (Rudge, 1989). Other more recent studies have also identified Chernobyl as a significant contributor to ^{137}Cs contamination of soils in west Cumbria (e.g. Beresford et al., 2007e; Copplestone, 1996). Therefore, it is likely that radiocaesium from the Chernobyl accident will still be contributing to the ^{137}Cs inventory present in the soil at the Drigg coastal sand dunes.

CHAPTER 3 - METHODS

This chapter provides full details of field sampling (Section 3.1), sample preparation (Section 3.2) and analytical (Section 3.3) methodologies that were used during the project. However, these methods do not necessarily apply to all chapters of this thesis. Therefore, subsequent chapters include a brief overview of the methods that are relevant to that chapter and the reader is referred to this chapter for further details.

3.1. Field study

The field component of this project was undertaken between February 2005 and October 2007, with pilot fieldwork undertaken in February 2005 to establish the locations to be targeted for subsequent sampling and to collect preliminary samples of soil and vegetation. An intensive field campaign was undertaken between March 2006 and October 2007. Samples (n = 617) collected from the Drigg coastal sand dunes included environmental media and various biota samples (Table 3.1). In addition, *in situ* measurements of gamma air kerma rate[11] were made across the dunes. A number of approvals, consents and licences had to be obtained prior to commencing work at the site due to the private ownership of the Drigg coastal sand dunes, the tenancy arrangements in place and the protected nature of both the sand dune habitat and many of the biota present.

3.1.1. Licensing and permissions

3.1.1.1. Site access

The Drigg coastal sand dunes site is owned by the Muncaster Estate (see Section 2.2.3). A project proposal was submitted to the Muncaster Estate in December 2004 and permission to undertake fieldwork on the sand dunes was granted in January 2005.

The Muncaster Estate leases the sand dunes and associated saltmarsh area to a local farmer (Mr Ireland) under a tenancy agreement. During an on-site meeting with Mr Ireland in February 2005, the purpose of the project was described and he gave his permission for necessary sampling equipment (see Sections 3.1.2.2.2 and 3.1.3.2.5.1) to be installed at the site.

[11] A measure of the radiation energy that is absorbed per unit mass of air over a given time period ($\mu Gy\ h^{-1}$) – see Section 3.1.4.

Table 3.1. Samples collected from the Drigg coastal sand dunes between 2005 and 2007.

Sample type	Latin name	Common name / Description	*n*[1]
Soil/Sediment		surface soil samples to 10 cm depth	6
		soil cores to 40 cm depth	77[2]
		soil cores to 100 cm depth	3[2]
Water		pool water	7
		total deposition	20
Amphibian	*Bufo bufo*	common toad	7
	Bufo calamita	natterjack toad	3
	Rana temporaria	common frog	7
	Triturus cristatus	great crested newt	7[4]
	Triturus helveticus	palmate newt	15[4]
	Triturus vulgaris	smooth newt	1
Bird	*Anas platyrhynchos*	mallard	1
	Anas crecca	teal	2
Invertebrate	*Arctiidae spp*	caterpillar	4[4]
	Gastropoda	slugs and snails	5[4]
	Lumbricus terrestris	earthworm	1[4]
Mammal	*Apodemus sylvaticus*	field mouse	15
	Microtus agrestis	field vole	3
	Sorex araneus	common shrew	3
	Talpa europaea	common mole	1
Reptile	*Anguis fragilis*	slow worm	9[4]
	Lacerta vivipara	common lizard	8[4]
	Vipera berus	adder	3
Plants, Lichen & Fungi	*Ammophila arenaria*	marram grass	16[3]
	Festuca rubra	red fescue	7[3]
	Calluna vulgaris	heather	1
	Erica cinerea	bell heather	3
	Erica tetralix	cross-leaved heather	3
	Ulex europaeus	common gorse	3
	Cladonia portentosa	lichen	1
	Racomitrium canescens	moss	1
	Hygrophorus sp	fungus	1
	Lepiota sp	fungus	1
	Lycoperdon sp	fungus	2
	Marasmius sp	fungus	6
	Rhodophyllus sp	fungus	2
	Russula sp	fungus	5

[1] total number of samples (n = 617) included media (n = 468) and biota (n = 149) samples; [2] sectioned cores yielded n = 441 samples; [3] samples of mixed herbage (including *A. arenaria* and *F. Rubra*) were also collected (n = 2); [4] bulk samples.

Part of the Drigg coastal sand dunes site falls within the boundary of the Lake District National Park, which is managed by the Lake District National Parks Authority (LDNPA). It incorporates a local nature reserve (LNR), the Drigg Dunes and Gullery LNR, which is under the joint management of the Muncaster Estate and the LDNPA. Therefore, it was necessary to obtain permission to undertake sampling work from the LDNPA in addition to the permission obtained from the Muncaster Estate. This permission was granted by the LDNPA in January 2005.

The study-site is a Site of Special Scientific Interest (SSSI), part of the Drigg Coast Special Area of Conservation and a European-designated NATURA 2000 site, under the management of English Nature, now Natural England. A project proposal was submitted to English Nature in November 2004 and, following a meeting with English Nature representatives at the area office in Kendal in December 2004, written permission was granted to undertake sampling work at the site.

3.1.1.2. Sampling protected species

Protected species licences from English Nature, and subsequently Natural England, were required because destructive sampling of reptiles and the two protected amphibian species present at the Drigg coastal sand dunes, *T. cristatus* and *B. calamita*, is an offence under Schedule 5 of the Wildlife and Countryside Act 1981.

The licence application for reptile and amphibian (herpetofauna) sampling required evidence of previous experience of working with the target species. This was demonstrable for the amphibians, as a result of previous training through the Institute of Ecology and Environmental Management (IEEM) and relevant project experience, but that was not the case for reptiles. English Nature expressed specific concerns over licensing research work with venomous reptiles (*V. berus* is venomous). Therefore, between June and September 2005, training in the capture and handling of venomous snakes was provided by a herpetologist, Mr Paul Rowley, at the UK Home Office-accredited Alistair Reid Venom Research Unit of the Liverpool School of Tropical Medicine, Liverpool (UK). Working with venomous snakes including *Echis carinatus* (African Carpet Vipers), rattlesnakes (*Crotalus* spp.) and *Vipera ammodytes* (Nose-horned vipers) provided the necessary expertise to support the licence application to English Nature.

Following submission of the licence application and a meeting with a representative of the Herpetological Conservation Trust (HCT) in October 2005, two licences were granted for the study at the Drigg coastal sand dunes. The licences specified the maximum number of

specimens of particular amphibian and reptile species that could be taken from the dunes during the licence period. The first licence (Reference No.: 121257) was granted for the period 6th October 2005 to 6th October 2006 and permitted the collection of *A. fragilis* (*n* = 10), *L. vivipara* (*n* = 10), *V. berus* (*n* = 6), *B. calamita* (*n* = 8) and *T. cristatus* (*n* = 15). The second (Reference No.: 20071434) was granted for the period 4th May 2007 to 4th May 2008 and permitted the collection of up to *A. fragilis* (*n* = 10), *L. vivipara* (*n* = 20), *V. berus* (*n* = 6), *B. calamita* (*n* = 8) and *T. cristatus* (*n* = 15).

In addition to the herpetofauna licence application, a 'general licence' was obtained from English Nature for taking shrews (*Soricidae*) for scientific purposes. Shrews are protected under the Wildlife and Countryside Act 1981. Although they were not a target species for small mammal sampling at the site (see Section 3.1.3), unplanned captures can and did occur so a licence was required to cover this eventuality.

A further licensing consideration was the need for a Home Office licence for euthanising animals collected from the site. However, the Home Office decided that the work did not require a licence because the animals were euthanised in the field rather than being transported back to the laboratory for euthanising.

3.1.2. Collection of environmental media samples

Three shore-normal[12] sampling transects were established at the Drigg coastal sand dunes (Figure 3.1) to provide a good spatial coverage of the entire dune system and reflecting the *a priori* hypothesis that sea-to-land transfer is likely to be the principal route by which Sellafield-derived anthropogenic radionuclides, especially actinides, reach the dunes (see Section 2.4.1.1.3). The transects were positioned to maximise the number of dune habitat types that were covered by each transect. These included the upper beach area above the mean high water position (MHW), the embryo dunes, yellow foredunes, grey dunes and dune heath (see Section 2.1.3). Transects 2 and 3 extended onto beach and saltmarsh areas respectively at the rear of the sand dune spit (see Section 2.2.2) to provide comparative data from these tidally inundated interface zones.

The general path of each transect was identified on an Ordnance Survey map during an initial site visit in December 2004. Subsequently, the final transect paths were decided on site at the start of the first field campaign in February 2005. Beginning at MHW on the foreshore, each transect was orientated in the prevailing wind direction (south-westerly) and

[12] At right-angles to the shoreline

sampling locations established at 100 m intervals. Initially, each transect was laid out using a compass, tape measure and garden canes (to act as a temporary marker for each sampling location along the transect and help maintain transect alignment). Once the transects were established, each sampling location was georeferenced using a handheld Garmin eTrex Global Positioning System (GPS) and the garden canes removed. The georeferences for the sampling locations along transects 1 – 3 are given in Table 3.2. Given that sampling locations were at 100 m intervals along each transect, the GPS reading accuracy of up to ± 7 m were acceptable for use in defining each sampling location. Site photographs were taken to aid future identification of the exact sampling location.

These three transects defined the main locations from which soil and vegetation samples were collected (see Sections 3.1.2.1 & 3.1.3.1 respectively). However, additional soil samples and pool water samples (see Section 3.1.2.2.1) were collected from seven dune slacks that were targeted for amphibian sampling (see Section 3.1.3.2.1). These dune slacks were georeferenced by taking four Ordnance Survey National Grid Reference readings around the perimeter of each slack using a handheld Garmin eTrex GPS (Table 3.3).

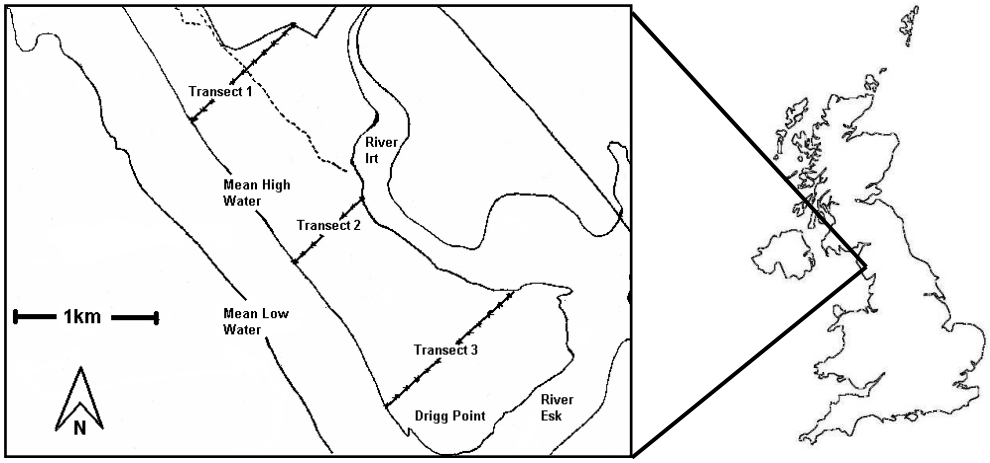

Figure 3.1. Location of the sampling transects at Drigg.

Table 3.2. Sampling locations on Transects 1 – 3.

Transect no.	Position no.[1]	Sampling location[2]	GPS Reading	Accuracy (± m)	Location classification[3]
1	1	1.1	SD 05247 97452	6	Zone 1 (MHW)
1	2	1.2	SD 05327 97557	6	Zone 2
1	3	1.3	SD 05384 97623	6	Zone 3
1	4	1.4	SD 05464 97685	6	Zone 3
1	5	1.5	SD 05525 97770	6	Zone 3
1	6	1.6	SD 05600 97835	6	Zone 4
1	7	1.7	SD 05659 97903	6	Zone 4
1	8	1.8	SD 05746 97958	4	Zone 4
1	9	1.9	SD 05802 98037	5	Zone 4
1	10	1.1	SD 05888 98120	7	Zone 4
1	11	1.11	SD 05963 98183	7	Zone 4
2	1	2.1	SD 05973 96434	6	Zone 1 (MHW)
2	2	2.2	SD 06040 96493	5	Zone 2
2	3	2.3	SD 06093 96562	7	Zone 2
2	4	2.4	SD 06180 96631	6	Zone 2
2	5	2.5	SD 06250 96701	5	Zone 3
2	6	2.6	SD 06322 96776	5	Zone 3
2	7	2.7	SD 06398 96846	6	Zone 4
2	8	2.8	SD 06464 96920	6	Zone 1 (Beach[4])
3	1	3.1	SD 06650 95380	6	Zone 1 (MHW)
3	2	3.2	SD 06700 95420	5	Zone 1
3	3	3.3	SD 06780 95500	5	Zone 2
3	4	3.4	SD 06850 95570	5	Zone 3
3	5	3.5	SD 06930 95640	5	Zone 4
3	6	3.6	SD 07000 95710	5	Zone 4
3	7	3.7	SD 07070 95780	6	Zone 4
3	8	3.8	SD 07150 95870	5	Zone 4
3	9	3.9	SD 07230 95940	5	Zone 4
3	10	3.10	SD 07300 95990	5	Zone 4
3	11	3.11	SD 07380 96070	5	Zone 4 (Blowout[6])
3	12	3.12	SD 07440 96140	5	Zone 1[6,7]
3	13	3.13	SD 07520 96200	5	Saltmarsh[6]

[1] Position number 1 is at MHW. Subsequent position numbers are at intervals of 100 m inland from MHW (e.g. position 10 on transect 1 is at 900 m inland from MHW); [2] Sampling location number is derived from the transect number and the position number; [3] Zone classification as defined in Section 2.1.3; [4] located at landward end of transect 2 on shoreline of River Irt/Esk Estuary; [5] located in revegetated blowout; [6] located at landward end of transect 3 on shoreline of River Irt/Esk Estuary; [7] no tidal inundation

Table 3.3. Dune slack sampling locations

Slack no.	Position no.[1]	GPS Reading	Accuracy (± m)
1	1	SD 06196 96815	7
1	2	SD 06228 96835	7
1	3	SD 06204 96829	7
1	4	SD 06186 96818	7
2	1	SD 06348 97079	6
3	1	SD 06166 97229	7
3	2	SD 06173 97222	7
3	3	SD 06186 97235	7
3	4	SD 06176 97237	7
4	1	SD 05919 97518	6
4	2	SD 05934 97514	6
4	3	SD 05945 97523	6
4	4	SD 05927 97535	6
5	1	SD 05945 97552	5
5	2	SD 05961 97560	5
5	3	SD 05942 97562	5
5	4	SD 05933 97550	5
6	1	SD 05318 98126	5
6	2	SD 05324 98129	5
6	3	SD 05322 98132	5
6	4	SD 05315 98131	5
7	1	SD 05287 98100	6
7	2	SD 05282 98103	6
7	3	SD 05277 98096	6
7	4	SD 05281 98095	6

[1] four Ordnance Survey National Grid Reference readings define the perimeter of each slack with the exception of slack 2 which had a diameter of 2 m so was represented by a reading taken from the centre of the slack.

3.1.2.1. Soil/sediment sampling

3.1.2.1.1. Soil/sediment cores to 10 cm and 40 cm depth

To provide data for the model validation study presented in Chapter 4, soil samples were collected from the foredune and dune heath areas of each of the three transects (6 samples in total) to a depth of 10 cm. For Chapters 5 and 8, soil cores were taken to a depth of 40 cm at all sampling locations along each transect, although only the radionuclide activity concentration data for the top 10 cm of these deep cores were used in the model intercomparison reported in Chapter 5. In addition, for Chapter 8, 40 cm deep sediment cores were taken from each of the sand dune slacks targeted for amphibian sampling.

A stainless-steel split-blade corer of 10 cm diameter was used to extract the soil cores following a standard coring method (Beresford et al., 2007e; Wood et al., 2007). The soil

surface was cleared of vegetation and stones. Any surface litter was removed by gently scraping it away with a spatula. The corer was hammered in to 40 cm depth using a soft-headed mallet (Figure 3.2). The corer was then extracted (Figure 3.3), positioned on the ground and the upper blade retracted to expose the core (Figure 3.4). On some occasions, the lower section of the core was lost during extraction. If repeat attempts failed to yield an intact 40 cm deep core, the maximum core length that could be collected was retained for subsequent processing and analysis.

For the 10 cm depth samples reported in Chapter 4, the 40 cm deep core was cut at 10 cm below the upper surface using a stainless-steel knife and the bottom 30 cm section was returned to the hole from which the core was extracted. For the 40 cm cores, the core was sectioned into six depth intervals using a stainless steel knife: 0 – 5 cm, 5 – 10 cm, 10 – 15 cm, 15 – 20 cm, 20 – 30 cm and 30 – 40 cm. No notable core compression occurred during the coring process so the depth sections were accurate representations of the *in situ* soil at each depth.

During coring it is possible that, as the corer moves down through the soil, material from the soil surface may be smeared down the side of the core. To avoid any potential influence of smearing on subsequent analytical results, the outer surface of each core section was removed using a stainless steel pastry cutter of 9 cm diameter (the pastry cutter was cleaned between core sections). The remaining material from each core section was transferred to a labelled plastic sample bag, double-bagged and retained for analysis. Samples were packed into a Thermos cool-box with ice packs to maintain sample integrity during transport to the analytical laboratory.

3.1.2.1.2. Soil/sediment cores to 1 m depth

At three locations on Transect 1, cores were sampled to 1 m depth to investigate changes in the sub-40 cm distribution of radionuclides in the soil with increasing distance from MHW (see Chapter 8). The coring was undertaken using an Atlas Copco Berema AB Pionjär 130 motor drill fitted with a 1 m core tube. This deep coring was restricted to three locations on Transect 1, the transect closest to the road (Shore Road) where the field vehicle was parked, because transporting and operating the equipment requires three people due to its weight.

Figure 3.2. Sampling soil to 40 cm depth

Figure 3.3. Extracting the 40 cm core

Figure 3.4. Soil core (40 cm) extracted from the dune heath area of the Drigg coastal sand dunes.

The samples were collected following a method similar to that used for the core sampling to 40 cm depth. Loose material was removed from the soil surface and the 1 m core tube positioned on the soil surface in a vertical orientation. With the core tube supported by one person, the other two people started the petrol-driven motor drill and lowered this unit onto the top of the core tube. The entire assembly was maintained in a vertical orientation whilst the motor drill drove the core tube into the soil (Figure 3.5). Once the core tube had penetrated to a depth of 100 cm, the motor drill was stopped and removed from the core tube. A purpose-built 'A-frame' and lifting tackle were used to extract the core tube (Figure 3.6) and the 'window' in the core tube was opened to expose the core (Figure 3.7). The core was sectioned into twelve depth intervals: 0 – 5 cm, 5 – 10 cm, 10 – 15 cm, 15 – 20 cm, 20 – 30 cm, 30 – 40 cm, 40 – 50 cm, 50 – 60 cm, 60 – 70 cm, 70 – 80 cm, 80 – 90 cm and 90 – 100 cm. Each section was passed through the 9 cm stainless steel pastry cutter to remove any potential influence of smearing (see Section 3.1.2.1.1). Samples were double-bagged and transported back to the laboratory in Thermos cool-boxes chilled with ice packs.

Figure 3.5. Steadying the motor drill and core tube assembly during coring

Figure 3.6. Extracting the core tube using A-frame and lifting tackle

Figure 3.7. Core tube with 'window' opened to expose the 1 m soil core

3.1.2.2. Water

3.1.2.2.1. Pool water

During March 2006, water samples were taken from each of the seven dune slack pools that were targeted for amphibian sampling (Table 3.3). Maximum water depths in the slacks at that time were between 40 cm and 70 cm. Each water sample was collected using a 2 litre plastic sample bottle which was slowly immersed in the pool and allowed to fill gradually. Care was taken to avoid disturbing bottom sediments during this process. Once filled, the bottle was lifted from the water and the sample acidified with nitric acid. Each bottle was sealed, labelled and packed into a Thermos cool-box with ice packs for transport to the analytical laboratory.

3.1.2.2.2. Total deposition

Total deposition collectors (Figure 3.8) were installed on the foredune and dune heath areas of each of the three transects (Table 3.4). The locations of these collectors corresponded to the locations from which the soil samples were collected for Chapter 5 (see Section 3.1.2.1.1). Each total deposition collector consisted of a 25 l high-density polyethylene

(HDPE) carboy with a hole drilled through the cap to accept a wide-mouth funnel (295 mm diameter). The funnel was secured to the cap using araldite resin.

The Drigg dunes are grazed by sheep so fenced enclosures were established to house each collector assembly. To minimise any disturbance of deposition processes in the vicinity of the collectors, the enclosures were built to be 2 m x 2 m and the fencing extended to a maximum of 1 m above the ground. Wooden stakes (1.5 m long) were hammered into the ground to a depth of 50 cm at the four corners of the 2 m x 2 m enclosure area. Wire mesh (approximately 10 cm square) was used to create the fencing between the corner posts to further reduce any potential influence on air-flow and hence deposition. This also served to reduce the visual impact of the collector installations.

The collectors were deployed between February and August 2006 and checked at approximately 2-week intervals. When between 2 l and 4 l of water had been collected, the contents of the collector were emptied into a separate plastic sample bottle. The sample bottle was labelled and packed, with ice packs, into a Thermos cool-box for transport to the analytical laboratory. The collector was then cleaned and redeployed.

On some occasions, a total deposition collector was found to have been vandalised. This mainly affected the deposition collectors on the foredune area of transect 1 and the dune heath area of transect 3 because these were both areas commonly accessed by the general public. When vandalism occurred, the collector was, cleaned, repaired and redeployed.

3.1.3. Collection of biota samples

3.1.3.1. Vegetation (including moss, lichen and fungi)

Where possible, vegetation (grass, shrub, moss, lichen and fungi) samples were collected on a species-specific basis from each transect.

The methodology used for the collection of the grass samples was that described in Wood et al. (2007). The grass was clipped to 2 – 3 cm above the soil surface using garden shears. The cut vegetation was transferred to a labelled plastic sample bag. Once approximately 400 g (fresh weight) of material had been collected, the sample bag was sealed and a record made of the area of vegetation cover that had been cut. The labelled plastic bags were packed into a cool-box for transport to the analytical laboratory.

Shrub samples were collected by taking cuttings of shoots using secateurs. Moss lichen and fungi samples were collected by cutting with scissors close to the soil surface and carefully removing any adherent soil particles. Where possible, up to 400 g (fresh weight) of sample was collected and sealed in a labelled plastic sample bag. These bags were then packed into Thermos cool-boxes, chilled with ice packs, to maintain sample integrity during transport to the laboratory.

Figure 3.8. Total deposition collector in fenced enclosure on the dunes at Drigg.

Table 3.4. Total deposition collector locations

Transect	Location	GPS Reading	Accuracy (± m)
1	Foredune	SD 05303 97551	6
1	Dune heath	SD 05963 98183	7
2	Foredune	SD 06041 96508	5
2	Dune heath	SD 06412 96793	5
3	Foredune	SD 06780 95500	5
3	Dune heath	SD 07495 96035	5

3.1.3.2. Animals

Animal sampling was conducted in accordance with the requirements of the Wildlife and Countryside Act 1981 (amended by the Environmental Protection Act 1990), the Conservation (Natural Habitats, & C.) Regulations1994 and the Animals (Scientific Procedures) Act 1986.

3.1.3.2.1. Amphibian sampling

Amphibians spend much of the year in the terrestrial environment but return to water to breed. Therefore, temporary pools in dune slacks have high amphibian activity during the breeding period, which takes place between March and June but peaks in late April/early May. When in the terrestrial environment, amphibians are dispersed and are difficult to locate so the breeding period provides an opportunity for efficient sampling.

Amphibian sampling took place over 5 nights in March 2006, 2 nights in April 2006 and 3 nights in May 2007. The two methodologies that proved effective at the Drigg coastal sand dunes were bottle trapping and torching, with hand capture (Gent & Gibson, 1998). These methodologies are described below.

Amphibians collected for analysis were euthanised immediately using the appropriate humane method specified in Schedule 1 of the Animals (Scientific Procedures) Act 1986. The samples were placed in labelled plastic bags and packed into a Thermos cool-box with ice packs for transport to the analytical laboratory.

3.1.3.2.1.1. Bottle trapping

The construction of a bottle trap is shown in Figure 3.9. The top was cut off a 2 l plastic drinks bottle, inverted and inserted into the body of the bottle to form a funnel. This was secured in place by punching a pair of holes at one side of the bottle and tying a loop of string through these holes to form a hinge. Two similar pairs of holes were punched at the other side of the bottle and a cocktail stick inserted to secure the assembly. This allowed the contents of the bottle trap to be accessed with ease by removing the cocktail stick and lifting the funnel.

The traps were deployed during late afternoon/early evening. The number of traps used was dependent on the size of the pool. The traps were positioned at approximately 2 m intervals around the perimeter of the pool, which resulted in approximately 25 – 30 traps per pool. Each bottle trap was slowly submerged until two thirds of the trap was filled with

water. The trap was then positioned at a 45 degree angle so that the mouth of the trap was lowest and there was an air pocket in the end of the trap. The air pocket ensured that trapped amphibians would have a sufficient oxygen supply until the bottle traps were retrieved. The traps were secured in this position using a garden cane and a length of elastic. Traps were retrieved the morning after deployment and the animals collected.

Bottle trapping proved particularly effective at trapping newts of all species, namely the great crested newt (*T. cristatus*), the palmate newt (*Triturus helveticus*) and the smooth newt (*Triturus vulgaris*). Some common frogs (*Rana temporaria*) and a few common toads (*Bufo bufo*) were also caught in the bottle traps. The bottle trapping technique often caught more individuals than were required for the sampling programme (or than could be taken under the conditions of the herpetofauna licence) so excess individuals were released at the point of capture.

Figure 3.9. Construction of bottle traps for amphibian sampling. On the left is the drinks bottle from which the trap is constructed. In the centre the top section has been removed and the hinge fitted to one side of the inverted top section. On the right is the completed trap with the cocktail stick inserted to act as a lock.

3.1.3.2.1.2. Torching (with hand capture)

Amphibians are most active at night so, with illumination from torches, visiting pools after dark permitted identification of the amphibian species that were active in each pool and selective hand capture of individuals that were required for the analytical programme. At each pool, the perimeter of the pool was walked slowly and any signs of movement investigated. Care was taken to avoid shining the torch beam directly at amphibians. Approximately 30 min per night were spent searching each pool. In order to minimise disturbance, pools were not visited for torching on nights when they were being used for bottle trapping. Torching was used for sampling the toad species (*B. bufo* and *B. calamita*).

3.1.3.2.2. Bird sampling

The British Association for Shooting and Conservation (BASC) were contacted in order to identify members that shoot in the vicinity of Drigg. Whilst there is no shooting permitted on the coastal sand dune site, the Egremont and District Wildfowlers Association were identified as having rights to shoot on the opposite side of the River Irt. This was the closest location to the dunes where shooting occurs and some species of wildfowl, especially resident *Anas platyrhynchos* (mallard), were thought likely to feed on the dune heath. Therefore, the Egremont and District Wildfowlers Association were asked if they would be willing to supply any of their 'bagged' birds for inclusion within the analytical programme. They agreed to donate one *A. platyrhynchos* and two *Anas crecca* (teal), which were collected in February 2006.

The wildfowlers confirmed that, in shot birds, death was assured according to the humane method given in Schedule 1 of the Animals (Scientific Procedures) Act 1986. The birds were supplied from the wildfowlers' freezers so the frozen birds were packed into a Thermos cool-box with ice packs for transport to the analytical laboratory.

3.1.3.2.3. Invertebrate sampling

There are many techniques that have been proposed for *Lumbricus terrestris* (earthworm) sampling. These include hand sorting of soil, the use of chemical expellants, the application of an electrical current and the use of a heat gradient (e.g. Coja et al., 2008; Eisenhauer et al., 2008; Smith et al., 2008). To avoid excessive on-site disturbance and in the absence of access to equipment required for electrical or heat expulsion, the chemical expellant technique was selected. Different researchers have trialled various chemical expellants and there is ongoing debate as to the relative efficacy of these expellants (e.g. Pelosi et al., 2009) so this study used a readily obtainable expellent, washing-up liquid,

which had been demonstrated previously to be effective in collecting worms for radioecological research (Beresford et al., 2007a). The washing-up liquid was diluted to 30% concentration and poured over the soil surface. As the solution percolated down through the soil, the washing-up liquid acted as an irritant and drove the worms to the surface where they were collected by hand. However, the worm density in sand dune soil is low so worm sampling was restricted to the most established dune heath area at the rear of Transect 1. At this location, it took more than 3 hours to collect a single worm sample so no further worm sampling was undertaken.

Sampling of caterpillars (*Arctiidae spp.*), slugs and snails (gastropoda) was opportunistic. Samples of these organisms were collected by hand.

All invertebrates were euthanised by immersion in 70% ethanol and this preserved them during transport to the analytical laboratory.

3.1.3.2.4. Mammal sampling

Small mammal sampling was undertaken using pre-fabricated live traps and following standard trapping procedures (e.g. Copplestone, 1996). Three types of trap were used: Longworth traps, Pipe traps and Trip traps. All three traps follow the same basic design. There is a chamber into which bedding and food (bait) are placed, an access tunnel leading to this chamber and a trip mechanism inside the access tunnel. When the trip mechanism is disturbed by an animal entering the main chamber, it closes a door over the tunnel entrance so that the animal cannot exit the trap.

Four trapping locations were used for small mammal sampling: two in the dune heath area of Transect 1 and two in the dune heath area of Transect 2. The trapping areas selected were chosen because they were the areas most likely to support small mammal populations at the dunes, as indicated by dense *F. rubra* cover (an important food source for *Microtus agrestis* (field vole) and *Apodemus sylvaticus* (field mouse) (Copplestone, 1996)) and the presence of small mammal burrows. The traps (64 per trapping location) were set out in a 70 m x 70 m grid, with approximately 10 m between traps.

Small mammals are most active during the spring and summer months so mammal trapping took place over the following periods: 3 nights in March 2006, 3 nights in May 2006, 2 nights in June 2006, 2 nights in May 2007 and 4 nights in July 2007. During each night of trapping, the traps were baited and set shortly before dusk, checked at 01:00 and again at

06:00. The check at 01:00 was to minimise the likelihood of unintended shrew deaths. However, even with this additional precaution in place, three shrew deaths occurred.

Time constraints prevented a pre-baiting period to allow the animals to become accustomed to the traps (Copplestone, 1996) and, possibly as a consequence of this, trapping success was low. In total 21 small mammals were trapped during the course of the study: *A. sylvaticus* (*n* = 15), *M. agrestis* (*n* = 3) and *Sorex araneus* (common shrew, *n* = 3). One specimen of *Talpa europaea* (European mole) was collected opportunistically.

Small mammals were euthanised immediately using the humane method given in Schedule 1 of the Animals (Scientific Procedures) Act 1986. The animals were then transferred to labelled plastic bags and packed into a Thermos cool-box, chilled with ice packs, for transport to the analytical laboratory.

3.1.3.2.5. Reptile sampling

Reptiles are only active for part of the year, hibernating during the months when the temperature is too low for them to thermally regulate. In Cumbria, their window of activity is between March and October. Therefore, the reptile sampling periods in the Drigg coastal sand dunes study were: 4 days in March 2006, 3 days in April 2006, 4 days in May 2006, 2 days in June 2006, 1 day in August 2006, 3 days in May 2007, 3 days in July 2007 and 3 days in October 2007. On each day, Reptile sampling was undertaken between 08:00 – 11:00 and 17:00 – 20:00, because these are the periods of the day when reptiles are most likely to be observed (Gent & Gibson, 1998).

Reptile sampling was conducted using standard methodologies (Gent & Gibson, 1998; Reading, 1996; Reading, 1997). The two approaches used were hand capture, using a Midwest Tongs Mini Hook™ in the case of *V. berus* capture, and the deployment of artificial refuges.

3.1.3.2.5.1. Artificial refuges

Reptiles are poikilotherms and are thus unable to raise their own body temperature through internal regulation (Pough et al., 2004). They require external heat sources and actively seek areas of direct sunlight where they can bask, or places that provide warmth. Artificial refuges are designed to act as a thermal sink and thus provide reptiles with a warm refuge under which they can elevate their body temperature (Gent & Gibson, 1998).

The artificial refuges used at the Drigg coastal sand dunes were constructed from sheets of corrugated iron cut into squares measuring 0.81 m x 0.75 m (Figure 3.10). Each square was an individual refuge and the upper surface of the square was painted black using a durable paint that would withstand long periods of exposure to environmental conditions. Two holes were drilled approximately 10 cm apart along one side of the square. A piece of rope was tied through these to form a handle. A hole was drilled at the opposite side of the square to the handle so that the refuge could be secured in position with a stainless steel U-shaped peg.

Artificial refuges were deployed in March 2006 and remained *in situ* until after the final sampling campaign in October 2007. The refuges were positioned in the field so that their black-painted surface was uppermost. This promoted heat absorption by the refuges, elevating their temperature over that of the surrounding environment. Temperature measurements made during refuge searches at Drigg showed that the temperature difference between the ground surface immediately next to the refuge and the area underneath the refuge could exceed 16^{o}C. The corrugated nature of the refuges helped to raise them up off the ground, facilitating reptile access to the warm area underneath the refuges.

Figure 3.10. Construction of an artificial refuge for reptile sampling

Three locations, each associated with one of the three main transects, were identified for the establishment of artificial refuge arrays (collections of artificial refuges). Each location was selected to ensure that it met the likely habitat requirements for reptiles, both in terms of the physical structure of the habitat and the presence of suitable foodstuffs. Each array consisted of 19 individual refuges which were set out in a hexagonal pattern with an inter-refuge distance (IRD) of 15 m. Thus the array had an area of 3360 m^2 and, when each refuge within an array was checked systematically following the order indicated in Figure 3.11, a transect length of 270 m.

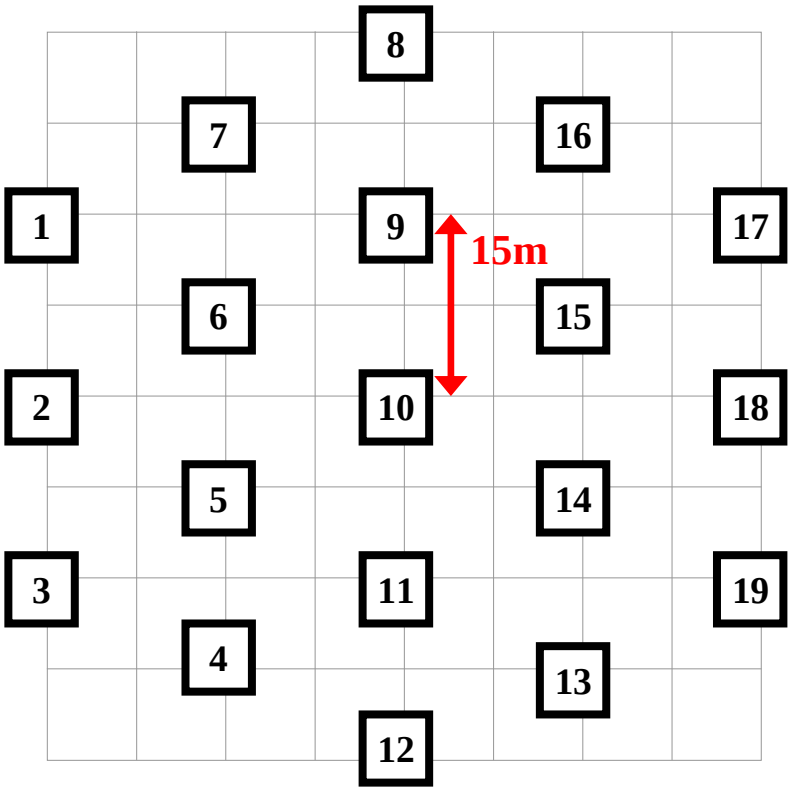

Figure 3.11. Standard layout for each refuge array used at Drigg. Each numbered box indicates the position of a refuge, the numbers corresponding to the order in which the refuges were checked during a transect walk.

Reading (1996) experimented with different IRDs and refuge numbers. He proposed that a standard survey method for reptiles should use a basic hexagonal array of 37 refuges with an IRD of 10 m. However, cost constraints prohibited the establishment of such arrays at Drigg and the 19 refuge array was determined to be an appropriate compromise.

During a sampling visit, each array was walked systematically by two field workers. One worker lifted the refuges while the other captured reptiles that were found underneath the refuges. All three arrays proved successful at attracting *L. vivipara*, which is abundant at Drigg. *A. fragilis* was also found under the refuges but appeared less abundant than *L. vivipara*. Only one of the refuges was found to be utilised by *V. berus* during the study so additional hand capture techniques had to be employed to collect specimens of this species.

3.1.3.2.5.2. Hand capture

The use of artificial refuges for reptile survey and sampling can be viewed as a passive technique. The reptiles are attracted to artificially created locations within their habitat and the field-worker targets those locations to collect the reptiles. However, as proved to be the case for *V. berus* at the Drigg dunes, artificial refuges are not necessarily effective ways to survey and collect all reptile species in a particular habitat. To enable *V. berus* to be collected it was necessary to undertake searches for signs of snake activity, such as skin sloughs, in areas of suitable habitat and then target those areas for intensive searches at times when the snakes were most likely to be basking. This approach is much more labour intensive than the use of artificial refuges and it was only possible to collect two snakes in this way. More were encountered but they were either too fast to catch in a terrain dominated by tufts of *A. arenaria* or were females, which had their basic details recorded (species, sex, length)[13] but were then released at the point of capture. This was in accordance with an agreement with the Herpetological Conservation Trust that the killing of female adders would be avoided where possible in order to minimise the impact of the study on the adder population at the Drigg dunes.

Animals to be taken for analysis were euthanised using the appropriate humane method given in Schedule 1 of the Animals (Scientific Procedures) Act 1986, transferred to labelled plastic bags and placed into a Thermos cool-box with ice packs for transport to the analytical laboratory.

[13] These data were provided to the Herpetological Conservation Trust

3.1.4. Measuring gamma air kerma rates

Gamma dose rates in air can be calculated from *in situ* measurements of gamma air kerma rates; air kerma rate being a measure of the radiation energy that is absorbed per unit mass of air over a given time period (μGy h^{-1}). This is the approach that has been used to determine gamma dose rates in the intertidal areas of the Esk Estuary (Emptage & Kelly, 1990; Wood et al., in press) and is the standard approach adopted for many routine monitoring and survey applications (e.g. RIFE, 2008).

3.1.4.1. Field measurements

Measurements of gamma ray air kerma rates were made *in situ* using a Mini-Instruments Environmental Monitor Type 6-80 fitted with an MC71 Geiger-Muller (G-M) tube, which is energy compensated for gamma radiation entering radially (Saint-Gobain Crystals & Detectors UK LTD, 2000).

The MC71 G-M tube was mounted vertically on a light-weight low attenuation tripod (to ensure rotational axis symmetry) and the G-M tube centre positioned at a height of 1 m (±0.2 m) above the sediment surface. This provides a field of view of approximately 8 m radius (200 m^2) at 662 keV for a typical exponential decrease in specific activity with depth (Tyler et al., 1996). A count time of 600 s was used, in order to ensure detection of a minimum of 700 counts (HMIP, 1995), and the total counts s^{-1} measured over the counting period were recorded. Measurements were not made during heavy rainfall, to reduce the likelihood of radon progeny washout influencing the results (HMIP, 1995), or after heavy rainfall when moisture in the surface sediments may attenuate the terrestrial gamma photons (Thompson et al., 1999).

To maximise the number of *in situ* measurements that could be made during a field visit, two Mini-Instruments Environmental Monitor Type 6-80s with MC71 G-M tubes were used. Both instruments were calibrated by VT Nuclear Services using a ^{226}Ra source to determine instrument-specific radium calibration factors (Table 3.5) at air kerma rates between 1 and 3 μGy h^{-1}. During calibration, a ^{137}Cs source was also used to derive a conversion coefficient for situations in which anthropogenic radionuclides are the dominant contributor to air kerma rate. However, previous work on the relative contribution of natural and anthropogenic radionuclides to measured external gamma dose rate in the intertidal areas of the Esk Estuary suggests that the anthropogenic radionuclide contribution is approximately 30% of the total dose rate measured (McDonald et al., 2005). Given that

the coastal sand dunes of west Cumbria are less contaminated by anthoropogenic radionuclides than intertidal areas of the Esk Estuary (Copplestone, 1996), the ^{226}Ra conversion coefficient was thought to be the most appropriate for the Drigg coastal sand dunes study.

To ensure that there was no significant difference in the performance of each instrument, duplicate measurements were made at 10 locations covering a total gamma dose rate range of 0.08 – 0.24 μGy h^{-1}. These locations included sand dune and intertidal saltmarsh areas in order to cover a wide dose rate range (discussed further in Chapter 8). A Shapiro-Wilk test confirmed normality of the measurement data ($P > 0.05$) and the Levene test confirmed homogeneity of variances ($P > 0.10$). A paired-sample t-test confirmed no significant difference ($P > 0.05$) between the means of the measurements from the two instruments and the linearity of comparative performance of the instruments across the dose rate range for the survey was confirmed by regression analysis ($r^2 = 0.93$). It was concluded that the response of the two instruments was comparable across the gamma dose rate range encountered within the survey and no systematic bias needed to be accounted for in processing the resultant survey data. Fixed point measurements were performed daily at a non-tidal location to check for instrument drift or meteorological influences but the measurements were stable throughout the survey period.

Table 3.5. Characterisation of instruments used for measuring gamma air kerma rates

Instrument	Mini-Instruments Environmental Monitor Type 6-80 (Serial No. FN 0000141) with an MC71 G-M tube (Serial No. 1736)	Mini-Instruments Environmental Monitor Type 6-80 (Serial No. FN 0000140) with an MC71 G-M tube (Serial No. 1738)
K^1 (^{226}Ra source)	18.6	18.7
K^1 (^{137}Cs source)	14.3	14.6
P^2 (counts s^{-1})	1.158 ± 0.066[3]	1.081 ± 0.043[4]
Intrinsic detector background (counts s^{-1})	0.2	0.2

[1] Instrument-specific calibration factor to convert counts s^{-1} to air kerma rate (μGy h^{-1}); [2] Sum of cosmic and intrinsic detector count rates (counts s^{-1}); [3] Mean ± standard deviation ($n = 5$); [4] Mean ± standard deviation ($n = 7$)

3.1.4.2. Calculation of gamma dose rates in air

Gamma dose rates can be reported in three ways:

1. Total gamma dose rate – the measured dose rate, including the cosmic radiation component.

2. Terrestrial gamma dose rate – the measured gamma dose rate with the cosmic radiation contribution subtracted, i.e. the dose rate due to both anthropogenic and natural radionuclides in the terrestrial environment.

3. Anthropogenic dose rate – the terrestrial dose rate with a natural radionuclide correction factor subtracted. For sandy substrates the correction factor is 0.05 μGy h^{-1} and for intertidal saltmarsh the correction factor is 0.07 μGy h^{-1} (RIFE, 2008).

Different studies adopt different reporting approaches so, to facilitate comparison with other surveys, all three quantities were reported in this study.

The following equation was used to calculate the terrestrial gamma dose rate:

$$D = \frac{N - P}{K}$$

Where D is the calculated air kerma rate (μGy h^{-1}); N is the measured count rate (counts s^{-1}); P is the sum of cosmic and intrinsic detector count rates (counts s^{-1}); and K is the instrument-specific calibration factor for converting counts s^{-1} to air kerma rate (μGy h^{-1}).

A typical value for P is 1.00 counts s^{-1}, comprising 0.2 counts s^{-1} due to the intrinsic detector background and 0.8 counts s^{-1} due to the contribution of cosmic radiation (HMIP, 1995; Thompson et al., 1999). Therefore, to calculate the total gamma dose rate, the assumed intrinsic detector background (0.2 counts s^{-1}) was used in place of P in the equation given above.

Although using 0.8 counts s^{-1} provides an approximate subtraction for cosmic background, the contribution of cosmic radiation to measurement results is both location and instrument specific. To more accurately quantify the value of P to use for each detector, measurements were performed over Esthwaite water (Ordnance Survey National Grid Reference: SD 359 969), a large water-body in Cumbria with a water depth in excess of 10 m and remote from surrounding high ground. Esthwaite water is approximately 65 m above sea-level. Whilst it is recognised that air kerma rate increases with altitude, the difference in the cosmic

contribution to measured air kerma rate between sea-level and 65 m elevation is negligible (Thompson et al., 1999).

Measurements were taken from a plastic boat positioned close to the middle of Esthwaite water to ensure that the majority of counts detected would be due to the intrinsic detector background and cosmic radiation contributions alone (Ambrosi, 2009). The *P* values determined at Esthwaite water are presented in Table 3.5. The mean cosmic and intrinsic detector background, based on readings from both detectors, was 0.059 ± 0.004 μGy h^{-1} (*n* = 12).

The results of the *in situ* measurements are presented and discussed in Chapter 8.

3.2. Sample preparation and property determination

To avoid issues associated with sample aging (Rudel et al., 2009), especially micro-organism activity in soil samples and tissue deterioration in biota samples, all samples were prepared for analysis as soon as possible after returning to the laboratory. In the interim, soil and water samples were stored in a cold room (< 3°C) and biota samples were stored frozen (– 20 °C).

3.2.1. Environmental media

3.2.1.1. Soil/sediment

3.2.1.1.1. Determination of soil moisture content

Soil samples were transferred to labelled aluminium foil trays, weighed to 0.01 g accuracy using a calibrated Oxford G41002 balance and placed in drying cabinets. The samples were dried to constant mass (± 0.1 % of the previous measurement) at 80°C, which took approximately 3 d. The final (constant) mass was subtracted from the fresh mass to determine the moisture content of the soil.

3.2.1.1.2. Bulk density determination

Soil bulk density, also known as apparent bulk density, describes the mass of soil relative to its volume (Allen, 1989). The volume of sample collected in 5 cm and 10 cm depth sections was calculated from the dimensions of the coring equipment. The volume of a 5 cm deep soil section was 332 cm^3 and the volume of a 10 cm deep section was 664 cm^3.

3.2.1.1.3. Particle size analysis

The dried soil samples were disaggregated using a polypropylene block. Following disaggregation, the samples were passed through a 2 mm sieve to remove stones and other extraneous material, which was discarded. A 150 – 250 g subsample, depending on the size of the original sample, was taken for particle size analysis (PSA) and the remainder of the sample was prepared for radiometric and chemical analysis (see Section 3.2.1.1.4. and Section 3.3.).

The dry sieving method was used for PSA. Although this method may result in underestimation of the fine particle fractions due to incomplete disaggregation of these particles, especially clays (Bihari & Dezso, 2008), the method is recognised as a suitable technique for sandy soil PSA (Rodriguez & Uriarte, 2009) and presented an efficient means for estimating the particle size distribution of the large number of soil samples collected from the Drigg sand dunes.

The soil was passed through a sieve stack, consisting of four sieves (2 mm, 600 µm, 212 µm and 63 µm) and a sample collection container, which were mechanically agitated for 600 s. After sieving, the mass of sample in each sieve was weighed to 0.01 g accuracy using a calibrated balance. This methodology enabled the following particle size fractions to be determined based on the Wentworth classification scheme (Wentworth, 1922): Coarse sand (600 µm – 2 mm), Medium sand (212 µm – 600 µm), Fine sand (63 µm – 212 µm) and Silt (< 63 µm).

3.2.1.1.4. Preparation of samples for gamma spectrometry analysis

With the > 2 mm fraction discarded, dried soil samples were ground using a Grinder La Minervia 11500 rotary mill to produce a homogenised uniform sample matrix. Up to 50 g of the homogenised sample was retained for determination of soil pH and organic matter content (see Sections 3.2.1.1.5. and 3.2.1.1.6. respectively). The remaining sample was then transferred into either a 150 ml pot or 330 ml marinelli beaker counting geometry, depending on the volume of sample material available. The lids were fitted to the counting geometries and a gas-tight seal formed by dipping in melted wax. The sealed samples were left for a minimum of 21 d to achieve secular equilibrium between ^{226}Ra and its daughters, ^{214}Bi and ^{214}Pb (Karangelos et al., 2004; Saidou et al., 2008).

3.2.1.1.5. Soil pH determination

Measurements of soil pH were made for surface soil (0 – 5 cm) samples from ten locations across the dunes (three locations on transect 1, three on transect 2 and four on transect 3).

Soil pH was determined using a standard methodology (Allen, 1989; Copplestone et al., 2007). A 5 ml volume of homogenised soil sample was transferred to a wide-mouth High-density polyethylene (HDPE) 60 ml bottle using a measuring spoon and 25 ml (± 0.5 ml) of deionised water added. The bottle was then capped, shaken on an orbital shaker for 5 min and then left for 2 h to reach pH equilibrium.

A calibrated Mettler-Toledo MPC227 pH meter fitted with an InLab®413 pH combination polymer electrode was used to measure the pH of the 1:5 (volume/volume) soil suspensions. After every 5 sample measurements the instrument calibration was checked using Merck Colourkey pH buffer solutions (pH 5.00 and pH 9.00). Later in the day, but not longer than 24 h after preparation of the suspensions, repeat measurements were made of the pH to ensure that pH equilibrium had been reached at the time of the first reading and that the readings were constant.

3.2.1.1.6. Determination of organic matter/organic carbon content

The soil organic matter/organic carbon content was measured in samples from the same locations used for pH determination, but determinations were made for all core sections (n = 71) rather than just the top 0 – 5 cm sections. Prior to determination of the organic matter/organic carbon content, the soils were dried (see section 3.2.1.1.1) and homogenised by grinding (see Section 3.2.1.1.4).

Two methods commonly used in the determination of soil organic matter are the wet oxidation method and the loss-on-ignition method (Allen, 1989). In both cases, the organic carbon content is estimated from the result using a conversion factor. Both methods have their limitations (see Schumacher, 2002) so ten samples (from the same locations used for pH determination) were analysed using both methods to determine which would be more appropriate for analysis of sand dune soil.

3.2.1.1.6.1. Wet oxidation method

This method is based on the Walkey-Black method (Allen, 1989; Walkley & Black, 1934). It uses a solution of potassium dichromate, sulphuric acid and orthophosphoric acid to oxidise soil organic matter. The quantity of potassium dichromate remaining at the end of

this oxidation process is determined by titration with ferrous sulphate and the soil organic matter content is calculated from this.

Soil (0.5 g ± 0.01 g) was transferred to a conical flask. 15 ml (± 0.1 ml) of potassium dichromate solution (M(Molar)/6) was added along with 20 ml (± 1 ml) of concentrated sulphuric acid (specific gravity (SG) 1.84) and the contents of the flask swirled for 1 minute. The flask was then left to stand for at least 30 min. After 30 min, 200 ml (± 10 ml) of deionised water was added followed by 10 ml (± 1 ml) of ~85% orthophosphoric acid (SG 1.75) and the flask swirled to mix the contents. Barium diphenylamine sulphonate reagent (2 ml ± 0.1 ml of 0.16% solution) was added to the flask and the contents mixed again.

A burette was filled with ferrous sulphate solution (M/2) and this was titrated against the potassium dichromate solution remaining in the flask. The colour changed from muddy brown to blue and the titration was stopped at the point when the solution turned green. The volume titrated was recorded to the nearest 0.05 ml. If the titre (volume titrated) was < 2 ml then the analysis was repeated with 0.25 g ± 0.01 g soil to ensure complete digestion of the organic matter.

A 'blank' sample was also prepared, following the procedure outlined above, but without the addition of soil to the flask. The ferrous sulphate solution was titrated against the blank for standardisation, to determine (to the nearest 0.05 ml) the ferrous sulphate titre required to oxidise the potassium dichromate alone.

The organic matter and organic carbon content were calculated as follows:

$$\%\ Organic\ Matter = \frac{15(1 - x/b) \times 0.67}{m}$$

$$\%\ Organic\ Carbon = \frac{15(1 - x/b) \times 0.67}{m \times 1.72}$$

Where *x* is the titre obtained during titration against the sample (ml), *b* is the titre obtained during titration against the blank (ml), *m* is the mass of soil sample used in the analysis (g) and 1.72 is the factor used to convert soil organic matter to organic carbon. This conversion factor is a generic value which is based on an assumption that soil organic matter is 58% carbon (Read & Ridgell, 1922).

3.2.1.1.6.2. Loss-on-ignition method

The loss on ignition (LOI) method determines the mass lost from a dried soil sample subjected to ignition temperatures in a muffle furnace. For determining the organic matter content in calcareous soils, such as sand dune soils, the temperature selected must be high enough to produce complete combustion of the organic material and low enough to ensure that inorganic carbonates are not destroyed (Schumacher, 2002). If this temperature can be identified for the soils to be analysed, there is the scope to undertake sequential LOI (Heiri et al., 2001). This allows both the organic carbon and the carbonate content of the soil to be estimated. Temperatures that have been proposed for organic matter combustion in sandy sediment, without destruction of inorganic carbonates, include 420^{o}C (Schumacher, 2002) and 550^{o}C (Heiri et al., 2001). To ensure complete destruction of inorganic carbonate, temperatures of 720^{o}C and 950^{o}C have been proposed (Heiri et al., 2001).

To determine the combustion temperatures that were suitable for the soils collected from the Drigg coastal sand dunes, temperature tests were carried out on five soil samples. The samples included soil from the yellow foredunes and more organic rich soil from the dune heath. Three replicates of each soil sample (sub-samples of the homogenised sample) were used to assess mass loss at each combustion temperature. The combustion temperatures used were 420^{o}C, 550^{o}C, 720^{o}C and 950^{o}C. Each sample was analysed using the method described below.

Clean crucibles (one for each soil sample to be analysed) were heated in an oven to 100^{o}C ± 5^{o}C for at least 15 minutes. The crucibles were then placed in a dessicator to cool to room temperature (~ 21^{o}C). Once at room temperature, each crucible was weighed on a calibrated Mettler AE50 balance to the nearest 0.0001 g and the masses recorded. 5 g ± 0.2 g of soil sample was placed in a prepared crucible and combined mass recorded to the nearest 0.0001 g. The filled crucible was placed in an oven at 100^{o}C ± 5^{o}C for 3 h, cooled to room temperature in a dessicator and re-weighed to the nearest 0.0001 g. The crucible was then placed in a Carbolite GLM 11/7 muffle furnace at the selected experimental ignition temperature (either 420^{o}C, 550^{o}C, 720^{o}C or 950^{o}C, all ± 25^{o}C) and left to combust for 3 h. The crucible was then removed, cooled to room temperature in a dessicator and re-weighed to the nearest 0.0001 g. The percentage mass loss was determined using the following equation:

$$\%\ Mass\ loss = \frac{(m_s - m_i) \times 100}{m_s - m_c}$$

Where m_s is the mass of the oven dried soil and crucible (g), m_i is the mass of the soil and crucible following ignition (g) and m_c is the mass of the empty crucible (g).

There was no notable difference between the mass loss of samples at 420°C and the samples at 550°C. Similarly, there was no notable difference between the mass loss at 720°C and the loss at 950°C. However, particularly for the foredune samples that had a lower organic matter and higher carbonate content than dune heath soils, there was a two-fold increase in mass loss at the higher temperatures compared to the lower temperatures. Therefore, for soil from the Drigg dunes, either of the lower temperatures and either of the higher temperatures could be used to ensure complete combustion of the organic and inorganic carbon respectively. However, to minimise any possibility of loss of inorganic carbon during the first stage of sequential LOI and to maximise the combustion of inorganic carbon during the second stage of sequential LOI, the lowest (420°C) and highest (950°C) temperatures were selected for use in further determinations on Drigg coastal sand dune soils.

3.2.1.1.6.3. A method for sand dune soil

There was very good agreement between the organic matter content determined by the Walkley-Black method and that determined by LOI at 420°C (Figure 3.12). The variability in the results of both methods increased by similar amounts with increasing organic matter content and the regression line suggests that LOI may underestimate at very low organic matter concentrations. However, for determining organic matter content in general sand dune soils, both methods were shown to be suitable.

The loss on ignition method was selected for analysing the organic matter content of other soil samples from the dunes. This method allowed faster processing of samples and was less labour intensive. It also presented the opportunity to undertake sequential LOI to provide an estimate of carbonate content as well as organic matter content. The % mass loss equation given in Section 3.2.1.1.6.2 was used to determine the organic matter content of the soil after ignition at 420°C. The organic carbon content was calculated from this using the organic matter to organic carbon conversion factor of 1.72:

$$\%\ Mass\ loss = \frac{(m_s - m_i) \times 100}{(m_s - m_c) \times 1.72}$$

This factor is the standard conversion factor used in most organic matter-organic carbon conversions (Allen, 1989), but may be too low to use as a general soil value (Howard,

1965). This is because LOI overestimates organic matter in many soils because it doesn't correct for the release of bound water from clay minerals (Howard & Howard, 1990). However, given that the clay mineral content of sand dune soils is low (see Chapter 8), the factor was deemed appropriate for use in this study.

After ignition at 420°C and calculation of the organic carbon content, the soils were returned to the muffle furnace for ignition at 950°C and the mass loss equation used to determine the percentage loss due to combustion of inorganic carbon (in this instance the quantity m_s in the above equation was the soil and crucible mass after ignition at 420°C). Multiplying the mass loss by 1.36 provided an estimate of the carbonate content of the soil (Heiri et al., 2001).

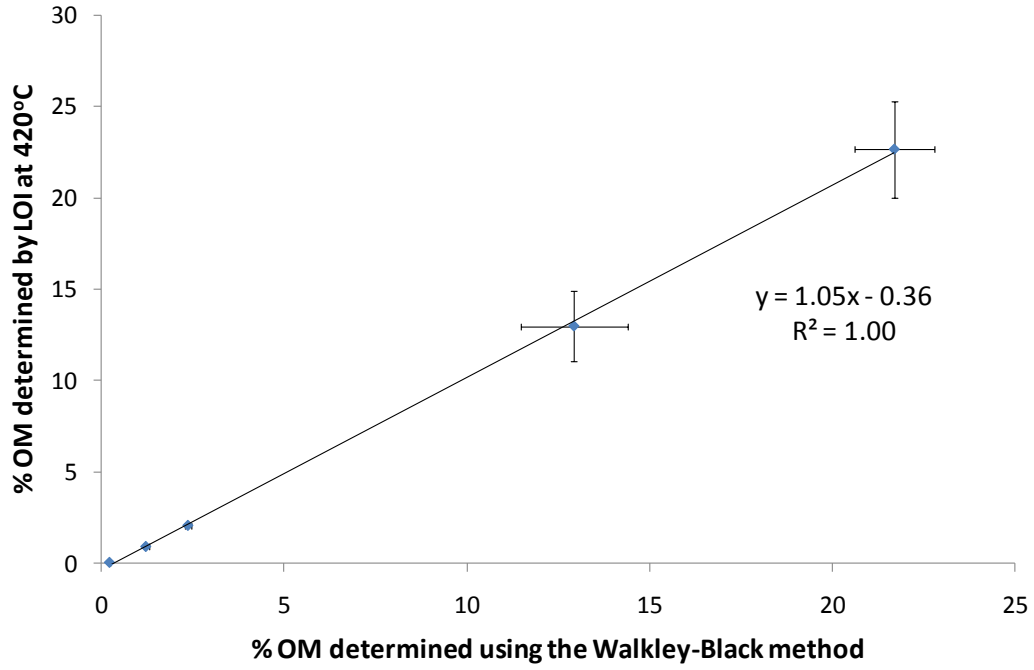

Figure 3.12. Comparison of the Walkley-Black and loss-on-ignition (LOI) methods for determining organic matter (OM) content in sand dune soil. Error bars show the standard deviation of 3 sub-sample results.

3.2.1.2. Water

The volume of the each water sample collected from the Drigg dunes was in the range 2 – 6 l but the calibrated geometry used for gamma analysis of water samples was 1.3 l. Therefore, each water sample was transferred to a measuring cylinder to determine its volume and then evaporated on a hotplate to reduce the sample volume to 1.3 l. The original sample volume measurements allowed the original radionuclide activity concentrations of the total deposition samples to be determined following gamma analysis. Each evaporated sample was transferred to a 1.3 l marinelli beaker for subsequent analysis by gamma spectrometry (see Section 3.3.1).

3.2.2. Biota

3.2.2.1. Vegetation

Vegetation samples, including shrub and lichen samples but excluding fungi, were placed into trays and hand sorted to ensure that only the target species was present in the sample. Any extraneous material was removed. The vegetation samples were then cut into small (1 – 2 cm long) pieces. The trays were weighed to 0.01 g accuracy using a calibrated Oxford G41002 balance and the vegetation was then air dried (20^{o}C) to constant mass (± 0.1 % of the previous measurement), which took approximately 4 d. The dried samples were ground in a Glen Creston vegetation mill using a 2 mm sieve to produce a uniform sample matrix and packed into 300 ml marinellis for gamma analysis.

The samples of fungi were hand sorted in trays to remove any unwanted material. Each sample was then cut into small (~ 1 cm^{2}) pieces, placed in a labelled plastic bag and weighed. The bag was transferred to an Edwards high-vacuum system E-C Supermodulyo freeze-drier and the sample dried to constant mass, which took between 24 h and 48 h. Dried samples of fungi were ground in a Glen Creston vegetation mill using a 2 mm sieve and packed into 150 ml pots for gamma analysis.

3.2.2.2. Animals

The methodology used for processing the animal samples was designed to ensure that the activity concentrations determined using the techniques described in Section 3.3 were as representative as possible of the whole-body tissue (or absorbed) activity concentrations, which is the parameter predicted and used by the models evaluated in Chapters 4 and 5.

With the exception of the invertebrates, all animals had their gastrointestinal tract (GIT) removed. Birds were plucked and the pelt was removed from small mammals. All animal samples, including the invertebrates, were washed prior to further processing.

Birds were ashed at 450^{o}C in a Carbolite GLM 11/7 muffle furnace. Other animal samples were freeze dried to constant mass in an Edwards high-vacuum system E-C Supermodulyo freeze-drier. All samples were ground in a dust extraction cupboard to produce a uniform sample matrix using either pestle and mortar or a coffee mill, depending on the resistance of the sample to grinding.

Newt, invertebrate, *L. vivipara* and *A. fragilis* samples were each bulked to provide sufficient material for analysis. Samples of other animals were retained as individual organisms for analysis. The homogenised samples were packed into either 25 ml Petri dishes or 150 ml pot, depending on the sample size.

3.3. Sample analysis

3.3.1. Gamma spectrometry

The gamma spectrometry analysis technique has been described in detail by other authors (e.g. Copplestone, 1996; Copplestone et al., 2007; Rudge, 1989) and is summarised here.

3.3.1.1. Soil and biota

Soil and biota sample gamma spectrometry was performed using EG&G Ortec high-purity germanium (HPGe) detectors, the specifications for which are given in Table 3.6. Soil and vegetation samples were analysed at the University of Liverpool on detectors calibrated for 330 ml marinelli and 150 ml pot geometries. Animal samples were analysed at the Centre for Ecology and Hydrology (CEH) radioanalytical laboratory at Lancaster on detectors calibrated for 150 ml pot and 25 ml Petri dish geometries.

Count times varied depending on the sample matrix and the counting geometry. Soil samples were counted for a minimum of 24 h. Vegetation and animal samples were counted for a minimum of 48 h.

Mixed radionuclide standards covering a broad energy range (59 keV – 1.8 MeV) were used to derive weekly energy and monthly efficiency calibrations for each detector. The efficiency calibrations were sample density and geometry specific. Background counts were performed on a monthly basis to derive a background correction for each detector.

Spectra files were analysed using EG&G Ortec GammaVision® software (v 5.10) for samples analysed at the University of Liverpool and Canberra Genie-ESP software for samples analysed at CEH. The photon energy library used for photopeak identification, quantification and reporting included the following radionuclides: ^{7}Be, ^{40}K, ^{85}Sr, ^{60}Co, ^{95}Nb, ^{95}Zr, ^{99m}Tc, ^{131}I, ^{103}Ru, ^{106}Ru/Rh, ^{125}Sb,^{134}Cs, ^{137}Cs, ^{144}Ce, ^{152}Eu, ^{154}Eu, ^{207}Bi, ^{208}Tl, ^{210}Pb, ^{212}Bi, ^{212}Pb, ^{214}Bi, ^{214}Pb, ^{224}Ra, ^{226}Ra, ^{227}Th, ^{228}Ac,^{228}Th, ^{230}Th, ^{231}Pa, ^{234}Pa, ^{234}Th, ^{235}U and ^{241}Am. The list of radionuclides was more extensive than the list expected to be measurable at the Drigg coastal sand dunes but reflected the range of anthropogenic gamma-emitting radionuclides that may have reached the dunes from various sources (see Section 2.4) as well as a suite of natural gamma-emitting radionuclides that were likely to be detectable.

Table 3.6. Specifications of detectors used for soil and biota gamma spectrometry

Parameter	**Specification**
Manufacturer	EG & G Ortec
Detector type	n-type HPGe coaxial
Relative efficiency	20% – 70%
FWHM at 1.33MeV	< 1.90 keV – 2.50 keV
Physical arrangement	Horizontal and vertical
Shielding	100 mm thick lead cylinder with inner rings of cadmium and copper (both 2 mm – 3mm thick)
Crystal cooling	Insulated Dewar with liquid nitrogen reservoir to maintain temperature at approximately 77K. Thermal contact between crystal and liquid nitrogen was maintained via a cryostat.

3.3.1.2. Water

Water samples were analysed at Westlakes Scientific Consulting Ltd. The samples were counted on an EG&G Ortec p-type HPGe detector with a 30 % relative efficiency. The minimum count time was 45 h. The resultant spectra were analysed using EG&G Ortec GammaVision® software (v 6.01).

3.3.2. Radiochemical analysis

After analysis by gamma spectrometry, twenty six samples were prioritised for radiochemical analysis to determine ^{90}Sr, ^{99}Tc, ^{239,240}Pu and ^{241}Am[14] activity concentrations (see Chapter 4) but sample sizes for animals were often < 10 g dry weight so not all of these samples could be analysed for all of the radionuclides. The radiochemical analysis was performed at the CEH radioanalytical laboratory at Lancaster using their standard methods, which are summarised below.

3.3.2.1. Analysis for ^{90}Sr

Depending upon sample size, 1 – 10 g of dried and homogenised sample was ashed at 450°C and leached with aqua regia to extract strontium. The strontium was concentrated from the sample solution by co-precipitation with calcium oxalate. After dissolution, strontium was isolated by extraction chromatography. The sample was left for a 2-week ingrowth period to establish secular equilibrium between the parent (^{90}Sr) and daughter (^{90}Y). Once secular equilibrium had been reached, ^{90}Y was separated from ^{90}Sr and measured by Cerenkov counting. Counting was performed using a Quantulus liquid scintillation counter and the count time was 1 h. The measured ^{90}Y concentration was used to derive the ^{90}Sr activity concentration. ^{85}Sr was used as the yield monitor.

3.3.2.2. Analysis for $^{239+240}$Pu and ^{241}Am

Dried and homogenised sample material (1 – 10 g depending on sample size) was spiked with two yield monitors (^{242}Pu and ^{243}Am) and then ashed at 450^{o}C. The ashed residue was leached with aqua regia to extract plutonium and americium. These actinides were concentrated by co-precipitation with iron (III) hydroxide and purified using ion exchange and extraction chromatography. The purified actinides were electrodeposited onto stainless-steel discs and the discs analysed by alpha spectrometry using PIPS detectors.

3.3.2.3. Analysis for ^{99}Tc

Sample material for ^{99}Tc analysis (1 – 10 g of dried and homogenised material) was spiked with ^{99m}Tc and gradually ignited in a muffle furnace until 550^{o}C was reached. The ^{99}Tc was

[14] Radiochemical determination of ^{241}Am can normally achieve a lower limit of detection (LOD) than that obtained when analysing for ^{241}Am using gamma spectrometry. By prioritising some samples for radiochemical determination of ^{241}Am this increased the likelihood of obtaining absolute activity concentrations rather than < LOD values.

purified using anion-exchange chromatography and solvent extraction. The recovery of ^{99}Tc in the purified fraction was determined by gamma spectrometric measurement of ^{99m}Tc. The activity of ^{99}Tc in the purified fraction was determined by low-level liquid scintillation counting after a two-week period to permit the decay of ^{99m}Tc. Counting was performed using Quantulus liquid scintillation counter and the count time was 1 h.

3.3.3. Cation analysis

Dried and homogenised soil samples (n = 71) from the 10 locations used for pH and organic matter/organic carbon determinations (see Sections 3.2.1.1.5. and 3.2.1.1.6. respectively) were used for cation analysis. The samples were analysed for Ca^{2+}, K^{+}, Mg^{2+} and Na^{+}; four cations which have been shown previously to be present in coastal sand dune soils at elevated concentrations that vary between the yellow dunes and the more stabilised dune areas (see Section 2.1.2).

The purpose of the cation analysis was to determine the concentrations of biologically available cations in the sand dune soil. Therefore, an extraction technique was required which would liberate readily available cations from the soil but not those in less available phases (such as calcium contained within shell fragments that comprise a component of coastal dune sand, especially in the foredune areas). The use of 1M ammonium acetate at pH 9 has been recommended for extraction of cations because minimal dissolution of calcium carbonate occurs at this pH (Allen, 1989). However, the high concentrations of ammonium ions can introduce an additional interference signal into the analysis.

There were two analytical options for cation analysis. The first was the use of a Dionex DX-120 Ion Chromatograph, which provides rapid analysis of multiple cations, and the second was to use a Unicam 929 flame atomic absorption spectrophotometer (FAAS), which is more labour intensive. Given the large number of samples to be processed (n = 71), it was preferable to use the Ion Chromatograph but the equipment was known to be sensitive to the noise signal introduced by the high concentrations of ammonium ions in 1M ammonium acetate.

To see if it was possible to successfully extract cations from the sand dune soil and perform the analysis using the Ion Chromatograph, two extraction techniques were tested; one in which the cations were extracted using 0.001M ammonium acetate and the second using 1M ammonium acetate, both at pH9. The samples (n = 11) used for this comparison were different depth sections of soil cores from the foredune and dune heath areas of transect 3. These samples were chosen to ensure that the comparison included samples which were

likely to reflect the expected concentration range for each of the four cations being analysed.

For each extraction, 2 g (± 0.01 g) of ground soil was transferred to a sample bottle along with 50 ml of extractant. The contents of the bottle were mixed on a rotary shaker for 1 h and centrifuged to provide the solution for analysis. The samples were analysed using the Ion Chromatograph in the first instance.

As expected, the interference from the ammonium ions in the 1M ammonium acetate extractions prevented the cation concentrations in these samples from being quantified using the Ion Chromatograph but quantification of the 0.001M ammonium acetate extraction samples was possible. Therefore, the 1M ammonium acetate extractions were analysed using the FAAS.

For analysis on the FAAS, 24.5 ml of the solution to be analysed was added to a test-tube containing 0.5 ml of 'chemical modifier solution' (a solution of 50 ml concentrated hydrochloric acid, 6.35 g of caesium chloride and 50 ml of 10% Fisher Scientific reagent grade lanthanum chloride solution). This was done to overcome two common sources of interference in FAAS, namely ionisation and stable refractory compound formation. Both Na and K are easily ionised within the air-acetylene flame of the FAAS, which is a problem because ionised atoms emit radiation at a different wavelength to that used for the analysis. Stable refractory compound formation affects Ca, and to a lesser extent Mg. The formation of these stable refractory compounds reduces the number of atoms available for excitation. By adding the 'chemical modifier solution' to the samples prior to analysis, the caesium acts as an ionisation suppressant[15] and the lanthanum acts as a releasing agent[16] to minimise the problem of stable refractory compound formation. The sample solutions were then analysed for each element sequentially.

Calibration standards were prepared by dilution of commercial stock solutions with ammonium acetate extractant and a 2 ml 'chemical modifier solution' spike. The commercial stock solutions used were Fisher chemicals Standard solution of 1000 parts-per-million (ppm) for K and Na and BDH Spectrosol grade standard solution of 1000 ppm for Ca and Mg. Five concentrations levels were prepared for each cation standard to enable

[15] A cation having a lower ionisation energy than the analyte. The first ionisation energy is the minimum energy (measured in kJ mol^{-1}) required to remove the most loosely bound electron from an isolated gaseous atom to form an ion with a 1+ charge (Whitten et al., 1988). Cs, K, Na have first ionisation energies of 376, 418 and 494 kJ mol^{-1} respectively (Stark & Wallace, 1982).

[16] A releasing agent is a cation that reacts preferentially with the anion of the stable refractory compound.

a multipoint calibration covering the spectrometers recommended working range for each element. Any samples for analysis which were found to have cation concentrations in excess of this working range were diluted with a fresh mixture of extractant and 'chemical modifier solution' to bring the concentrations within the calibrated range.

A comparison of the results from the Ion Chromatograph and FAAS demonstrated that the 0.001M ammonium acetate extraction was an insufficient extractant of the sand dune soil (Table 3.7), resulting in cation quantifications that were up to three orders of magnitude lower than those obtained from analysis of the 1M ammonium acetate extraction samples. Therefore, all 71 soil samples for cation analysis were subjected to 1M ammonium acetate extraction and analysed using the flame atomic absorption spectrophotometer.

The results of the cation analysis are presented and discussed in Chapter 8.

Table 3.7. Comparison of soil cation extractions performed using 0.001 M and 1M ammonium acetate

Location code[1]	Depth section (cm)	Cation concentration (mg kg^{-1})							
		Na^+		K^+		Mg^{2+}		Ca^{2+}	
		IC[2]	FAAS[3]	IC[2]	FAAS[3]	IC[2]	FAAS[3]	IC[2]	FAAS[3]
3.3	0 - 5	0.19	55.06	0.42	20.76	0.32	38.14	2.14	2077.57
3.3	10 - 15	0.17	56.91	0.35	18.26	0.28	34.22	1.71	1673.97
3.3	15 - 20	<0.15	46.61	0.34	16.47	0.31	32.95	1.58	1555.77
3.3	20 - 30	<0.15	53.51	0.29	16.24	0.37	44.42	2.12	2201.93
3.3	30 - 40	<0.15	49.63	0.33	18.00	0.38	39.44	2.77	1655.63
3.7	0 - 5	0.48	20.91	0.75	34.03	0.57	68.07	0.90	152.06
3.7	5 - 10	<0.15	12.04	0.20	10.92	0.30	17.38	0.57	35.42
3.7	10 - 15	<0.15	9.26	0.17	9.05	0.29	15.73	0.63	28.94
3.7	15 - 20	<0.15	9.48	0.23	9.55	0.31	15.64	0.59	28.87
3.7	20 - 30	<0.15	9.10	0.22	9.41	0.32	15.78	0.59	27.12
3.7	30 - 40	<0.15	8.77	0.33	8.08	0.33	16.08	0.63	30.51

[1] refer to Table 3.2 for explanation of location code; [2] sample extracted using 0.0001 M ammonium acetate and analysed on the Ion Chromatograph (IC); [3] sample extracted using 1 M ammonium acetate and analysed on the FAAS

3.4. Data presentation and statistical analysis

In the subsequent chapters of this thesis, summarised data present the arithmetic mean ($\bar{X}$) and standard deviation (*s*), which were derived using the following equations:

$$\bar{X} = \frac{\sum X}{n}$$

$$s = \sqrt{\frac{\sum (X - \bar{X})^2}{n-1}}$$

where X is the value of an observation and *n* is the total number of observations.

In summarising data from various sources, including sources that only report summarised data (e.g. some of the CR data for reptiles – see Chapter 7), the weighted arithmetic mean and standard deviation was calculated using the method described by Hosseini et al. (2008):

$$N = \sum_i n_i$$

$$M = \frac{\sum_i n_i CR_i}{N}$$

$$V_{combined} = \frac{V_W + V_B}{N-1} = \frac{\left(\sum_i (n_i - 1) E_i\right) + \left(\sum_i n_i CR_i^2 - NM^2\right)}{N-1}$$

$$s_{combined} = \sqrt{V_{combined}}$$

where N is the total number of observations in all studies; M is the weighted mean for all studies; n_i is the number of observations in study *i*; CR_i is the mean CR value in study *i*; $V_{combined}$ is the combined variance, which consists of both the variation within studies (V_W) and the variation between studies (V_B); E_i is the measure of error in study i, which can be the variance, standard deviation or standard error; and $s_{combined}$ is the weighted standard deviation for all studies.

If study *i* reported mean and standard deviation data for both biota and media activity concentrations and the mean data were used to calculate the CR for that study, E_i was calculated using the following equation (IAEA, in prep):

$$E_i = CR \times \sqrt{\left(\frac{\text{Biota mean}}{\text{Biota standard deviation}}\right)^2 \times \left(\frac{\text{Media mean}}{\text{Media standard deviation}}\right)^2}$$

For comparison with other published data compilations, the arithmetic mean is often appropriate. However, some data compilations report the geometric mean. The following equations (IAEA, in prep) can be used to estimate both the geometric mean ($\bar{X}_{geometric}$) and standard deviation ($s_{geometric}$) from the arithmetic summary statistics reported in this thesis:

$$\bar{X}_{geometric} = \exp\left(-0.5 \ln\left(\frac{s^2 + \bar{X}^2}{\bar{X}^4}\right)\right)$$

$$s_{geometric} = \exp\left(\sqrt{\ln\left(\frac{s^2 + \bar{X}^2}{\bar{X}^2}\right)}\right)$$

In some cases, the derivation of summary statistics involved the inclusion of limit of detection (LOD) values. The approach adopted for the treatment of LOD values depended on the intended use of the data. Therefore, the approach used is described on a chapter-specific basis. Details of the statistical analysis techniques used are also described in individual chapters.

(This page is left blank intentionally)

CHAPTER 4 – APPLICATION OF THE ERICA INTEGRATED APPROACH TO THE DRIGG COASTAL SAND DUNES

The material presented in this chapter has been published as:

Wood et al., 2008. Application of the ERICA Integrated Approach to the Drigg coastal sand dunes. Journal of Environmental Radioactivity, 99(9), 1484-1495.

4.1. Introduction

The EC EURATOM-funded project 'Environmental Risks from Ionising Contaminants: Assessment and Management' (ERICA) developed an 'Integrated Approach' to assessing the impact of ionising radiation on ecosystems (Larsson, 2008). The Integrated Approach provides guidance and practical support on scientific, managerial and societal issues relating to the effects of ionising radiation on biota and ecosystems. This guidance and support is delivered through consideration of factors including: Problem formulation; Impact assessment; Stakeholder interaction; and Decision making. The Integrated Approach is supported by a software programme (the ERICA Tool; (Brown et al., 2008)), a guidance document (referred to as D-ERICA; (Beresford et al., 2007b)), databases on radionuclide transfer (Beresford et al., 2008d; Hosseini et al., 2008), dose conversion coefficients (Ulanovsky et al., 2008) and radiation effects (Copplestone et al., 2008) and guidance on decision-making (Zinger et al., 2008a).

Using some of the initial soil and biota sample data from the Drigg coastal sand dunes sampling and analysis programme (see Chapter 3), this chapter presents the application of the Integrated Approach and the ERICA Tool to an assessment of ionising radiation impact at the Drigg coastal sand dunes. The assessment was undertaken based on the intuitive use of the ERICA Tool, supported by the information contained within the guidance document (Beresford et al., 2007b) and the integrated help function within the ERICA Tool. This simulated the application of the ERICA Integrated Approach by a user with no detailed prior knowledge of ERICA, allowing both the usability and technical capability of the ERICA Tool and associated documentation to be tested. Key elements of the Integrated

Approach are critically evaluated and the strengths and limitations for assessment of radiation impacts on coastal sand dune sites are highlighted.

4.2. Problem formulation

Problem formulation is the starting point for any assessment. It establishes the purpose, context and boundaries for the assessment. The ERICA Tool and documentation (e.g. D-ERICA) guide the assessor through the major steps in the problem formulation process including: characterisation of the ecosystem(s) and site(s) to be assessed; the requirement for, and scope of, stakeholder involvement; source characterisation; the legislative/regulatory framework that may need to be considered; and the evaluation criteria to be used within the assessment.

4. 2.1. Characterisation of the site

The ERICA Tool can run assessments for terrestrial, freshwater and marine ecosystems. The Drigg coastal sand dunes span all three ecosystem types but are predominantly terrestrial. The assessment described here was restricted to impacts on biota in the terrestrial dune environment.

4.2.2. Stakeholder engagement

Interaction with stakeholders played an important role in directing the emphasis of the assessment and provided the opportunity to evaluate the communication of the ERICA Integrated Approach methodology and assessment findings to a well-informed group of lay people. Stakeholder engagement within the ERICA Integrated Approach (and the Drigg coastal sand dunes assessment) is detailed elsewhere (Zinger et al., 2008b) but is discussed here briefly due to the influence of stakeholder engagement on the problem formulation phase of this assessment.

The level of public and institutional interest in the Drigg coastal sand dunes and the potential impacts of ionising radiation in the west Cumbrian environment made it important to engage a range of stakeholders from the outset of the assessment. These stakeholders included representatives from the nuclear industry, nuclear regulators, conservation groups, parish and district council (i.e. local government), landowners, the agricultural community and the general public. The stakeholders provided positive feedback on the comprehensive nature of the ERICA Integrated Approach. They felt it was important for the Drigg coastal sand dunes assessment to determine whether *B. calamita* and *T. cristatus* were impacted by

ionising radiation, recognising that the dunes support important populations (in the UK amphibian conservation context) of these two species. However, the stakeholders were concerned at the lack of data available on radionuclide transfer to these species and the assumptions that would need to be made. They were in favour of field sampling to address this data requirement.

4.2.3. Source identification and characterisation

There are a number of anthropogenic radionuclide sources that may have resulted in contamination of the Drigg coastal sand dunes site. These include the discharges into the marine environment from the Sellafield site and subsequent sea-to-land transfer, aerial discharges from the Sellafield emission stacks, discharges from the LLWR, global fallout from weapons testing, the 1957 Windscale accident and the 1986 Chernobyl accident (see Section 2.4). Sellafield and LLWR discharge data are available and a combination of models could be used to predict radionuclide transport to the dunes. However, there were few site-specific data against which predictions could be validated; data for the Drigg coastal sand dunes were limited to a few isolated measurements of radionuclides in *A. arenaria* (Nelis, 1990) and birds (Lowe, 1991). Therefore, there was limited scope to successfully characterise radionuclide activity concentrations in soil (the input data used for a terrestrial assessment within the ERICA Tool) at the dunes, based on existing data.

In the absence of comprehensive radionuclide activity concentration data for the dunes, and to address both the stakeholder requirement for amphibian data and the need for data to validate the ERICA Tool predictions, a field sampling campaign was undertaken. This field campaign aimed to develop a site-specific data set that would be applicable for validation of environmental radiation protection models. Full details of the sampling and analytical methodologies are given in Chapter 3. The data used in the ERICA Integrated Approach application presented here were for samples collected during 2005 and 2006. The sampling covered both biota and environmental media (Table 4.1) and the species targeted included those of direct interest to the stakeholders.

4.2.3.2. Radionuclide activity concentrations in samples collected from the Drigg coastal sand dunes

The radionuclide activity concentration data for soil and biota samples collected from the Drigg dunes are summarised in Tables 4.2 – 4.5. The mean and range are presented; the mean being calculated using Limit of Detection (LOD) values as absolute values (in

combination with values in excess of the LOD) to ensure that the impact assessment based on the mean activity concentrations is conservative (Wendelberger & Campbell, 1994). Where all values were below the LOD, the highest value is reported.

The ERICA Integrated Approach focuses on incremental (above natural background) dose rate. Naturally occurring radionuclide data are reported for completeness but do not contribute to the estimation of organism doses in the assessment. For biota, the only naturally occurring radionuclide reported is ^{40}K because previous work (Beresford et al., 2007a) has demonstrated high uncertainties in the determination, by gamma spectrometry, of natural radionuclides in biota.

Table 4.1. Samples collected from the Drigg coastal sand dunes during 2005 and 2006

Sample / Organism Group	**Common name**	**Latin name**
Amphibian	common toad	*Bufo bufo*
	common frog	*Rana temporaria*
	great crested newt	*Triturus cristatus*
	palmate newt	*Triturus helveticus*
	natterjack toad	*Bufo calamita*
Bird	mallard	*Anas platyrhynchos*
	teal	*Anas crecca*
Invertebrate	caterpillar	Non-specific
Mammal	field mouse	*Apodemus sylvaticus*
	field vole	*Microtus agrestis*
Reptile	common lizard	*Lacerta vivipara*
	adder	*Vipera berus*
	slow worm	*Anguis fragilis*
Plants	marram grass	*Ammophila arenaria*
	red fescue	*Festuca rubra*
	heather	*Calluna vulgaris*
	moss	*Racomitrium canescens*
	lichen	*Cladonia portentosa*
Soil/Sediment	Soil/sediment from foredunes	
	Soil/sediment from rear of the dunes	

Table 4.2. Activity concentrations (Bq kg^{-1} dry weight) in soil samples (0 – 10 cm depth) from the Drigg coastal sand dunes

Natural	***n***	**Mean[a]**	**Min**	**Max**	**Anthropogenic**	***n***	**Mean[a]**	**Min**	**Max**
^{7}Be	6	<7.3	<4.4	<7.3	^{60}Co	6	<0.7	<0.2	<0.7
^{40}K	6	281	254	308	^{90}Sr	6	13.1	<6.8	18.0
^{210}Pb	6	1.4	1	1.8	^{95}Nb	6	<1	<0.8	<1
^{212}Bi	6	12.7	11.7	13.7	^{95}Zr	6	<0.9	<0.7	<0.9
^{212}Pb	6	15.9	14.8	17.2	^{99}Tc	6	16.4	<6.9	34.5
^{214}Bi	6	12.1	11.4	12.4	^{103}Ru	6	<1	<0.7	<1
^{214}Pb	6	15.8	13.8	16.6	^{106}Ru	6	<2.7	<2.1	<2.7
^{224}Ra	6	24.6	22.4	26.2	^{125}Sb	6	<1.4	<0.8	<1.4
^{226}Ra	6	<12.7	<10.7	<12.7	^{134}Cs	6	<0.3	<0.3	<0.3
^{227}Th	6	59.9	56.7	64.0	^{137}Cs	6	136	109	178
^{228}Th	6	0.2	<0.1	0.3	^{144}Ce	6	<2.7	<2.3	<2.7
^{228}Ac	6	9.4	8.7	10.2	^{152}Eu	6	<0.1	<0.1	<0.1
^{230}Th	6	<61.4	<46.4	<61.4	^{154}Eu	6	0.7	<0.6	0.9
^{231}Pa	6	<13.4	<10.6	<13.4	^{238}Pu	6	5.1	<0.3	11.4
^{234}Pa	6	<1.1	<0.9	<1.1	$^{239+240}$Pu	6	27.8	1.00	63.8
^{234}Th	6	129	111	147	^{241}Am	6	49.2	7.1	102
^{235}U	6	<0.9	<0.8	<0.9					

[a] Where all values were <LOD the maximum LOD is given

Table 4.3. Whole body activity concentrations (Bq kg^{-1} fresh weight[b]) in dune vegetation

Nuclide	Mean[a] whole body activity concentrations, Bq kg^{-1} fresh weight (*n*, minimum, maximum)					
	marram grass (*Ammophila arenaria*)	heather (*Calluna vulgaris*)	red fescue (*Festuca rubra*)	lichen (*Cladonia portentosa*)	mixed herbage (Non-specific)	moss[b] (*Racomitrium canescens*)
^{40}K	88.7 (8, 43.2, 160)	37.9 (1, n/a, n/a)	109 (5, 85.6, 134)	34.3 (1, n/a, n/a)	51 (1, n/a, n/a)	357 (1, n/a, n/a)
^{60}Co	<0.7 (8, <0.1, <0.7)	<2.8 (1, n/a, n/a)	<1.3 (5, <0.1, <1.3)	<0.1 (1, n/a, n/a)	<0.1 (1, n/a, n/a)	<0.7 (1, n/a, n/a)
^{90}Sr	-	-	4.3 (3, 0.8, 9.2)	-	-	-
^{95}Nb	<1.3 (8, <0.2, <1.3)	<0.3 (1, n/a, n/a)	<8 (5, <0.2, <8)	<0.1 (1, n/a, n/a)	<0.1 (1, n/a, n/a)	<1.5 (1, n/a, n/a)
^{95}Zr	<1 (8, <0.3, <1)	0.5 (1, n/a, n/a)	<6 (5, <0.3, <5.8)	<0.2 (1, n/a, n/a)	<0.1 (1, n/a, n/a)	<2.1 (1, n/a, n/a)
^{99}Tc	-	-	1.4 (3, <1.3, 1.4)	-	-	-
^{103}Ru	<2.1 (8, <0.1, <2.1)	<0.4 (1, n/a, n/a)	<0.4 (2, <0.1, <0.4)	<0.1 (1, n/a, n/a)	<0.1 (1, n/a, n/a)	<1.1 (1, n/a, n/a)
^{106}Ru	<12.3 (8, <0.8, <12.3)	<1.4 (1, n/a, n/a)	<12.5 (5, <2.5, <12.5)	1.4 (1, n/a, n/a)	<0.2 (1, n/a, n/a)	24.5 (1, n/a, n/a)
^{110m}Ag	-	-	<1.4 (3, <0.8, <1.4)	-	-	-
^{125}Sb	<2.5 (8, <0.4, <2.5)	<0.9 (1, n/a, n/a)	<3.2 (5, <0.3, <3.2)	<0.2 (1, n/a, n/a)	<0.1 (1, n/a, n/a)	<2.4 (1, n/a, n/a)
^{134}Cs	<0.5 (8, <0.1, <0.5)	<0.3 (1, n/a, n/a)	<1.2 (5, <0.1, <1.2)	<0.2 (1, n/a, n/a)	<0.1 (1, n/a, n/a)	<1.1 (1, n/a, n/a)
^{137}Cs	3.8 (8, 0.7, 14.1)	25.3 (1, n/a, n/a)	3.9 (5, <1.3, 9.3)	12.8 (1, n/a, n/a)	1.9 (1, n/a, n/a)	21.1 (1, n/a, n/a)
^{144}Ce	<3.1 (8, <0.6, <3.1)	<1.7 (1, n/a, n/a)	<7.3 (5, <0.4, <7.3)	<0.436 (1, n/a, n/a)	0.324 (1, n/a, n/a)	<5.25 (1, n/a, n/a)
^{152}Eu	<1.4 (8, <0.3, <1.4)	<0.9 (1, n/a, n/a)	<1 (2, <0.7, <1)	3 (1, n/a, n/a)	0.3 (1, n/a, n/a)	<1.5 (1, n/a, n/a)
^{154}Eu	<0.7 (8, <0.1, <0.7)	<0.4 (1, n/a, n/a)	<0.4 (2, <0.1, <0.4)	<0.1 (1, n/a, n/a)	<0.1 (1, n/a, n/a)	<0.6 (1, n/a, n/a)
^{155}Eu	-	-	<2.3 (3, <1, <2.3)	-	-	-
^{238}Pu	-	-	<0.6 (2, <0.1, <0.6)	-	-	-
$^{239+240}Pu$	-	-	1.3 (3, 0.7, 2.4)	-	-	-
^{241}Am	9.3 (8, 3, 27.4)	1.9 (1, n/a, n/a)	2.5 (3, 1.3, 4.3)	5.2 (1, n/a, n/a)	4.7 (1, n/a, n/a)	5.9 (1, n/a, n/a)

[a] Where all values were <LOD the maximum LOD is given; [b] moss activity concentration data is reported as Bq kg^{-1} dry weight

Table 4.4. Whole body activity concentrations (Bq kg^{-1} fresh weight) in invertebrates and amphibians from the Drigg coastal sand dunes

Nuclide	Mean[a] whole body activity concentrations, Bq kg^{-1} fresh weight (*n*, minimum, maximum)					
	caterpillar (*Non-specific)*	**common toad (*Bufo bufo*)**	**natterjack toad (*Bufo calamita*)**	**common frog (*Rana temporaria*)**	**great crested newt (*Triturus cristatus*)**	**palmate newt (*Triturus helveticus*)**
^{40}K	<36.7 (3, <16.6, <36.7)	<22.5 (1, n/a, n/a)	41.0 (2, <28.0, 54.0)	38.6 (3, 28.8, 52.9)	79.2 (3, 51.3, 95.3)	57.9 (3, <17.5, 118)
^{60}Co	<3.7 (3, <2, <3.7)	<1.5 (1, n/a, n/a)	<2.9 (2, <1.7, <2.9)	<1.9 (3, <1.2, <1.9)	<2.3 (3, <1.8, <2.3)	<3.8 (3, <3, <3.8)
^{90}Sr	<1.2 (2, <0.8, <1.2)	-	1.9 (2, <1.2, 2.5)	8.3 (3, 6.7, 10.3)	7.7 (3, 7.3, 8.2)	11.9 (3, 5.2, 20.7)
^{95}Nb	<17.4 (3, <6.6, <17.4)	<53.2 (1, n/a, n/a)	<10.3 (2, <6.9, <10.3)	<5 (3, <4, <5)	<9.7 (3, <4.8, <9.7)	<15.7 (3, <9.1, <15.7)
^{95}Zr	<13.2 (3, <5.9, <13.2)	<16.3 (1, n/a, n/a)	<9 (2, <5.4, <9)	<4.4 (3, <3.5, <4.4)	<7.9 (3, <4.2, <7.9)	<13.1 (3, <7.2, <13.1)
^{99}Tc	<17.5 (1, <n/a, n/a)	-	8.3 (2, <4.8, 11.8)	<7.4 (3, <1.6, <7.4)	6.2 (3, <3.9, 8)	<10.2 (1, <n/a, n/a)
^{106}Ru	<29.2 (3, <14.8, <29.2)	<15.3 (1, n/a, n/a)	<22 (2, <12.3, <22)	<9.9 (3, <9, <9.9)	<18.9 (3, <9.9, <18.9)	<31.5 (3, <16.5, <31.5)
^{110m}Ag	<3.4 (3, <1.7, <3.4)	<2 (1, n/a, n/a)	<2.6 (2, <1.5, <2.6)	<1.2 (3, <1, <1.2)	<2.2 (3, <1.2, <2.2)	<3.6 (3, <1.9, <3.6)
^{125}Sb	<8 (3, <4, <8)	<3.8 (1, n/a, n/a)	<6.6 (2, <3.5, <6.6)	<2.8 (3, <2.4, <2.8)	<5.4 (3, <2.9, <5.4)	<9.1 (3, <4.6, <9.1)
^{134}Cs	<2.8 (3, <1.4, <2.8)	<1.4 (1, n/a, n/a)	<2.2 (2, <1.2, <2.2)	<1 (3, <0.9, <0.1)	<1.8 (3, <1, <1.8)	<3 (3, <1.5, <3)
^{137}Cs	2.8 (3, <1.6, 4.2)	2.3 (1, n/a, n/a)	<2.7 (2, <1.5, <2.7)	2.1 (3, <1, 2.7)	8 (3, 4.6, 12.8)	11.6 (3, 9, 13.3)
^{144}Ce	<20.6 (3, <10.2, <20.6)	<13.2 (1, n/a, n/a)	<15.8 (2, <8.9, <15.8)	<7.7 (3, <6.2, <7.7)	<13.6 (3, <7.4, <13.6)	<22.1 (3, <11.6, <22.1)
^{155}Eu	<5.8 (3, <2.9, <5.8)	<3.1 (1, n/a, n/a)	<4.1 (2, <2.5, <4.1)	<2.2 (3, <1.8, <2.2)	<3.8 (3, <2.1, <3.8)	<5.8 (3, <3.2, <5.8)
^{241}Am	3.5 (3, <2.7, 5.2)	<2.8 (1, n/a, n/a)	<4.4 (2, <2.2, <4.4)	2 (3, <1.7, 2.3)	<1.5 (3, <1.8, 4.9)	4.5 (3, <3, 6.2)

[a] Where all values were <LOD the maximum LOD is given

Table 4.5. Whole body activity concentrations (Bq kg^{-1} fresh weight) in reptiles, small mammals and birds from the Drigg coastal sand dunes

	Mean[a] whole body activity concentrations, Bq kg^{-1} fresh weight (*n*, minimum, maximum)						
Nuclide	**slow worm (*Anguis fragilis*)**	**common lizard (*Lacerta vivipara*)**	**European adder (*Vipera berus*)**	**teal (*Anas crecca*)**	**mallard (*Anas platyrhynchos*)**	**field mouse (*Apodemus sylvaticus*)**	**field vole (*Microtus agrestis*)**
^{40}K	78.2 (3, 57.6, 104)	49.8 (3, <22.5, 90.1)	85.8 (2, 66.6, 105)	74.0 (2, 63.9, 84.1)	111 (1, n/a, n/a)	124 (2, 110, 137)	83.5 (3, <63.2, 121)
^{60}Co	<2.1 (3, <1.6, <2.1)	<6.9 (3, <2.2, <6.9)	<2.2 (2, <1.8, <2.2)	<0.2 (2,<0.2,<0.2)	<0.2 (1, n/a, n/a)	<4 (2, <2.7, <4)	<11.5 (3, <4.4, <11.5)
^{90}Sr	12.8 (3, 4, 23.4)	<1.9 (3, <1.4, <1.9)	-	<0.9 (2,<0.2,<0.9)	0.8 (1, n/a, n/a)	-	-
^{95}Nb	<9.1 (3, <4.8, <9.1)	<18.7 (3, <8.1, <18.7)	<44.8 (2, <34.6, <44.8)	<1 (2,<1,<1)	<0.7 (1, n/a, n/a)	<87.8 (2, <80.1, <87.8)	<244 (3, <115, <244)
^{95}Zr	<7.4 (3, <4.2, <7.4)	<14.9 (3, <7.2, <14.9)	<14.2 (2, <11.4, <14.2)	<0.8 (2,<0.7,<0.8)	<0.6 (1, n/a, n/a)	<34.2 (2, <26.9, <34.2)	<77.1 (3, <40.9, <77.1)
^{99}Tc	<9.1 (3, <2.2, <9.1)	<12.7 (2, <10.1, <12.7)	-	2.7 (2,<0.6,4.9)	<0.5 (1, n/a, n/a)	-	-
^{106}Ru	<17.1 (3, <11.4, <17.1)	<35.4 (3, <16.5, <35.4)	<13.4 (2, <10.8, <13.4)	<1.9 (2, <1.6, <1.9)	<1.3 (1, n/a, n/a)	<39.1 (2, <26.0, <39.1)	<74.4 (3, <43.5, <74.4)
^{110m}Ag	<2 (3, <1.4, <2)	<4.1 (3, <2, <4.1)	<1.7 (2, <1.3, <1.7)	<0.2 (2,<0.2,<0.2)	<0.1 (1, n/a, n/a)	<5 (2, <3.6, <5)	<10 (3, <5.7, <10)
^{125}Sb	<4.8 (3, <3.3, <4.8)	<9.6 (3, <4.8, <9.6)	<3.1 (2, <2.6, <3.1)	<0.5 (2,<0.4,<0.5)	<0.1 (1, n/a, n/a)	<10 (2, <6.6, <10)	<18.6 (3, <11.0, <18.6)
^{134}Cs	<1.6 (3, <1.1, <1.6)	<3.3 (3, <1.7, <3.3)	<1.1 (2, <0.9, <1.1)	<0.2 (2,<0.1,<0.2)	<0.1 (1, n/a, n/a)	<3.9 (2, <2.4, <3.9)	<7 (3, <4.2, <7)
^{137}Cs	17.4 (3, 6.4, 30.9)	7.3 (3, <6.2, 8)	<1.6 (2, <1.1, <1.6)	2.1 (2, 2, 2.2)	3.2 (1, n/a, n/a)	3.8 (2, 3, 4.5)	8.2 (3, <5, 9.9)
^{144}Ce	<12.1 (3, <8, <12.1)	<25.8 (3, <12.1, <25.8)	<9.7 (2, <8.1, <9.7)	<0.9 (2,<0.8,<0.9)	<0.6 (1, n/a, n/a)	<33.8 (2, <22.8, <33.8)	<63.9 (3, <37.5, <63.9)
^{155}Eu	<3.1 (3, <2.3, <3.1)	<7.2 (3, <3.4, <7.2)	<2.1 (2, <1.8, <2.1)	<0.3 (2,<0.2,<0.3)	<0.2 (1, n/a, n/a)	<8.7 (2, <5.3, <8.7)	<14.9 (3, <9, <14.9)
^{238}Pu	0.1 (2, <0.1, 0.2)	-	0.1 (2, 0.1, 0.1)	0.1 (1, n/a, n/a)	0.1 (1, n/a, n/a)	-	-
$^{239+240}$Pu	0.6 (2, 0.5, 0.7)	-	0.2 (2, 0.2, 0.2)	0.4 (2, 0.4, 0.4)	0.2 (1, n/a, n/a)	-	-
^{241}Am	1.8 (2, 1.6, 1.9)	<6.4 (3, <3.1, <6.4)	1.6 (2, 1.6, 1.6)	0.7 (2, 0.5, 0.9)	0.3 (1, n/a, n/a)	<7.4 (2, <4.8, <7.4)	<13.4 (3, <8.1, <13.4)

[a] Where all values were <LOD the maximum LOD is given

4.2.4. Legislative framework and evaluation criteria

The Drigg coastal sand dunes and some of the biota inhabiting the dune system are protected under national and European legislation (EC, 1979; EC, 1992; UK Parliament, 1981; UK Parliament, 1994; see Section 2.3). However, there are no statutory evaluation criteria in the UK to determine radiation impacts on biota[17]. The Drigg assessment was carried out using the default 10 μGy h^{-1} screening incremental dose rate recommended in the ERICA Integrated Approach (Garnier-Laplace et al., 2006).

4.3. Impact assessment

The activity concentration and dose rate predictions presented in this chapter were derived using version 1.0 (August 2007) of the ERICA Tool[18]. This version of the ERICA Tool includes a transfer database and a database of Environmental Media Concentration Limits (EMCLs[19]). These databases have, in part, been parameterised with data from the early phases of the work presented in this thesis. Therefore, affected transfer parameters (Table 4.6) and EMCLs were re-set to values used in the preceding version of the ERICA Tool (Beresford et al., 2007f) for the purposes of this assessment, removing the potential for self-validation. Modifications to parameters, however minor, are included in Table 4.6 for completeness and to provide the opportunity for results to be replicated exactly.

[17] Although the Environment Agency (regulatory agency for England and Wales) use a screening value of 5 μGy h^{-1} and a management action level of 40 μGy h^{-1} (see Table 1.3). Above this management action level the Environment Agency would seek to reduce potential impacts (David Copplestone, Environment Agency, pers. comm.).

[18] The ERICA Tool and the accompanying documentation can be downloaded from **http://www.ceh.ac.uk/protect/ERICAdeliverables.html**, accessed 12th November 2009.

[19] The media activity concentrations for each radionuclide that would give rise to a dose rate equal to the selected screening dose rate.

Table 4.6. Radionuclide concentration ratios modified in the ERICA Tool transfer database to reflect those used prior to inclusion of data from the Drigg coastal sand dunes[1]. The values in the current version of the ERICA Tool (version 1.0 – August 2007) are shown in brackets.

Nuclide	Organism	Mean	Standard deviation	Min	Max	Probability distribution function
Cs	Mammal (Rat)	2.88E+00 (2.87E+00)	4.25E+00 (4.25E+00)	1.40E-02 (1.40E-02)	1.37E+02 (1.37E+02)	lognormal
	Mammal (Deer)	2.88E+00 (2.87E+00)	4.25E+00 (4.25E+00)	1.40E-02 (1.40E-02)	1.37E+02 (1.37E+02)	lognormal
	Bird	7.64E-01 (7.50E-01)	1.66E+00 (1.65E+00)	1.36E-03 (1.36E-03)	1.62E+01 (1.62E+01)	lognormal
	Bird egg	3.06E-02 (3.00E-02)	6.63E-02 (6.60E-02)			lognormal
	Reptile	8.64E+00 (3.59E+00)	1.27E+01 (9.91E+00)	(5.50E-02)	(2.81E+01)	lognormal
	Amphibian	5.81E-01 (5.37E-01)	9.25E-01 (8.97E-01)	6.70E-02 (1.74E-02)	2.08E+00 (2.08E+00)	lognormal
Sr	Bird	5.57E-01 (5.49E-01)	9.99E-01 (9.94E-01)	4.77E-03 (4.77E-03)	7.17E+00 (7.17E+00)	lognormal
	Bird egg	1.39E+00 (1.37E+00)	2.50E+00 (2.49E+00)			lognormal
	Reptile	4.70E+01 (1.18E+01)	(2.35E+01)	4.70E+01 (7.97E-03)	4.70E+01 (4.70E+01)	exponential
	Amphibian	1.08E+00 (8.25E-01)	1.65E+00 (1.22E+00)	2.88E-01 (1.69E-01)	2.49E+00 (2.49E+00)	lognormal
Tc	Bird	3.70E-01 (2.70E-01)				exponential
	Bird egg	3.70E+01 (2.70E+01)				exponential

[1] All other concentration ratios used were as per Beresford et al. (2008d)

4.3.1 Tier 1 assessment

The ERICA Tool assessment process is divided into three tiers, the functionality and data requirements becoming more extensive as one progresses through the tiers. The conservative screening assessment at Tier 1 provides a rapid method for evaluating media activity concentrations and, if certain criteria are met, enables the assessor to exit the assessment process and conclude with a high level of confidence that there are no significant radiation impacts on biota and that no further action is required (Brown et al., 2008). To retain a high degree of conservatism in this Tier, maximum measured activity concentrations were used as the input data (as recommended in the ERICA Tool and associated documentation). These activity concentrations were compared with EMCLs, which are the media activity concentrations for each radionuclide that would give rise to a dose rate equal to the selected screening dose rate, 10 μGy h^{-1} in the case of the ERICA default, for the limiting reference organism[20] in a given ecosystem (Beresford et al., 2007b). The terrestrial reference organisms that are predefined in the ERICA Tool are given in Table 4.7.

The ERICA Tool calculates risk quotients (RQs) (Table 4.8), the RQ being the ratio between the measured activity of a radionuclide and the nuclide's EMCL, and the assessment result is based on the summation of these RQs. The sum of the calculated RQs (ΣRQ) for the Drigg dunes is 0.4 and approximately half of this is from ^{241}Am for which 'flying insect' is the limiting reference organism. When ΣRQ is less than unity at Tier 1, it can be concluded that there is a very low probability that the absorbed dose rate to any organism will exceed the screening dose rate and the impact assessment may be terminated at that stage. However, the purpose of the case study was to validate the ERICA Integrated Approach so assessments were conducted at all Tiers.

[20] The ERICA project used the 'reference organism' definition developed in the earlier FASSET project (Brown et al., 2008). Reference organisms are "a series of entities that provide a basis for the estimation of radiation dose rate to a range of organisms which are typical, or representative, of a contaminated environment. These estimates, in turn, would provide a basis for assessing the likelihood and degree of radiation effects" (Larsson, 2004). The adoption of the reference organism approach is a pragmatic solution to the problem of modelling radionuclide transfer and radiation exposure in complex ecological systems. However, reference organisms may not always represent the most exposed organisms, for example, due to differences in the feeding ecology and habitat utilisation of particular organisms within an ecosystem. This should be considered when undertaking assessments that focus on reference organisms alone.

Table 4.7. ERICA terrestrial reference organisms and the proposed International Commission on Radiological Protection (ICRP) Reference animal and plant (RAP) geometries used to define them (after Beresford et al., 2007b).

Terrestrial ERICA RO	**ICRP RAP**
Amphibian	Frog
Bird	Duck
Bird egg	Duck egg
Detritivorous invertebrate	
Flying insects	Bee
Gastropod	
Grasses & Herbs	Wild grass
Lichen & bryophytes	
Mammal	Rat, Deer
Reptile	
Shrub	
Soil invertebrate (worm)	Earthworm
Tree	Pine tree

Table 4.8. Risk Quotients (RQs) calculated at Tier 1 for the Drigg coastal sand dunes assessment

Nuclide	**RQ**	**Limiting reference organism**
Co-60	9.45E-05	Mammal (Rat)
Sr-90	4.79E-02	Reptile
Nb-95	4.41E-05	Mammal (Rat)
Zr-95	3.60E-05	Detritivorous invertebrate, Soil invertebrate (worm)
Tc-99	1.63E-02	Bird egg
Ru-103	4.14E-04	Lichen & bryophytes
Ru-106	3.25E-03	Lichen & bryophytes
Sb-125	3.75E-05	Detritivorous invertebrate
Cs-134	1.97E-04	Mammal (Deer)
Cs-137	5.70E-02	Mammal (Deer)
Ce-144	3.20E-05	Tree
Eu-152	1.19E-06	Soil invertebrate (worm), Detritivorous invertebrate
Eu-154	5.82E-05	Detritivorous invertebrate
Pu-238	1.12E-02	Lichen & bryophytes
Pu-240	5.87E-02	Lichen & bryophytes
Am-241	1.63E-01	Flying insects
∑ Risk Quotients	3.58E-01	

4.3.2 Tier 2 assessment

Like Tier 1, this Tier provides a screening assessment but the assessor has access to additional functionality and the ERICA Tool supporting documentation recommends that expected or best estimate input data are used. The Drigg coastal sand dunes Tier 2 assessment was based on the mean measured anthropogenic radionuclide activity concentrations in soil (Table 4.2).

Tier 2 can be run with the default reference organisms (Table 4.7) alone but, to make the assessment more site-specific, the ERICA Tool 'create organism' wizard was used. This permits assessment for species which have different dimensions to those of the reference organisms. The assessor enters data to define the organism geometry, concentration ratios and occupancy factors. The concentration ratios (CRs) numerically relate the activity concentrations in biota to activity concentrations in environmental media (allowing the activity concentrations in one to be predicted from activity concentrations in the other). In the context of the ERICA Integrated Approach, the terrestrial CRs for the radionuclides discussed in this chapter can be defined as:

$$CR = \frac{Activity\ concentration\ in\ biota\ whole\ body\ (Bq\ kg^{-1}\ fresh\ weight)}{Activity\ concentration\ in\ soil\ (Bq\ kg^{-1}\ dry\ weight)}$$

The occupancy factors describe the proportion of time (as a fraction) that an organism spends in particular compartments of an ecosystem. For terrestrial ecosystems, the ERICA Tool accepts entry of values for time spent in the soil, on the soil surface and in the air.

Table 4.9 presents the parameters used to create organisms to represent the species of interest. Where appropriate, new organisms were parameterised using the default settings for the corresponding reference organism group. For example, *A. arenaria*, *F. rubra* and mixed herbage used the default physical dimensions, occupancy factors and CRs for the ERICA grasses & herbs reference organism. Default occupancy factors were modified as necessary based on literature review (e.g. to reflect the burrowing habits of *B. calamita*).

There appears to be a conceptual mismatch in the occupancy factors selected for birds and amphibians. Bird occupancy factors sum to less than 1 to reflect the fact that the birds spend time flying and at other terrestrial sites or in other types of ecosystem (marine or freshwater). Conversely, amphibians have a proportion of their life history associated with the aquatic environment but the sum of the occupancy factors remains at 1. This is because the amphibians, due to the physical location of the Drigg coastal sand dunes and the

surrounding land use (see Chapter 2), are not thought to undertake any significant off-site migration. In addition, although amphibian species present at the Drigg coastal sand dunes spend some time in the temporary freshwater pools that develop in the dune slacks, the wholly aquatic phase of their life history is relatively short and adult feeding is often terrestrial (Arnold, 2004; Gent & Gibson, 1998). The external dose rate predictions made during the assessment are likely to be slight over-estimates because they do not account for the period of time spent in the aquatic environment where the water will act as a shield; the activity concentrations for anthropogenic radionuclides in the water of these freshwater pools were at or below the LOD (see Chapter 8). However, this approach ensures that the amphibian dose rate predictions are as realistic as possible, without undertaking assessments for both the terrestrial and aquatic environments. It also errs on the side of conservatism, recognising the uncertainty in the assessment process and reflecting the specific interest of stakeholders in ensuring protection of amphibian species at the Drigg coastal sand dunes.

Whole-body absorbed dose rates were predicted for a suite of default reference organisms[21] and user-defined organisms. The calculated absorbed dose rates were weighted using the ERICA default radiation weighting factors[22] of 10 for alpha, 3 for low beta and 1 for beta/gamma (Brown et al., 2008) and an RQ calculated for each organism-nuclide combination; the RQ at Tier 2 being the ratio of predicted whole-body absorbed dose rate to the selected screening dose rate (10 μGy h^{-1}). This calculated RQ is termed the 'expected value RQ'. However, the purpose of Tier 2 is to identify and screen out situations where there is a very low probability that absorbed radiation doses are significantly impacting on biota at the site. To account for uncertainties in the input data and other parameters, an uncertainty factor (UF) is applied to generate a 'conservative RQ'. The UF selected is at the discretion of the assessor but the ERICA Integrated Approach proposes UFs of 3 or 5. Assuming that dose rates and RQs follow an exponential distribution and that the true means of these distributions equal the expected values, a UF of 3 would provide the dose rates and RQs at the 95th percentile (equivalent to a Tier 1 assessment) and a UF of 5 at the 99th percentile (Brown et al., 2008).

[21] The ERICA terrestrial reference organisms included in the assessment were those which were not represented by a user-defined organism. For example, the ERICA tree reference organism was included because no user-defined organism was parameterised using the default physical dimensions, occupancy factors and CRs for the ERICA tree.

[22] Radiation weighting factors reflect the assumed Relative Biological Effectiveness (RBE) of α, β, and γ radiation.

Table 4.9. Information used to parameterise organisms included within the Drigg coastal sand dunes assessment

Organism	Occupancy (fraction of time) In soil	At soil surface	In air	Dimension (m) A	B	C	Mass (kg)	Concentration ratios based on which ERICA default organism?
marram grass (*Ammophila arenaria*)	0	1	0	0.05[a]	0.01[a]	0.01[a]	0.00262[a]	Grasses & herbs
heather (*Calluna vulgaris*)	0	1	0	[b]	[b]	[b]	[b]	Shrub
red fescue (*Festuca rubra*)	0	1	0	0.05[a]	0.01[a]	0.01[a]	0.00262[a]	Grasses & herbs
lichen (*Cladonia portentosa*)	0	1	0	0.0401[c]	0.00229[c]	0.00229[c]	0.00011[c]	Lichen & bryophytes
mixed herbage (Non-specific)	0	1	0	0.05[a]	0.01[a]	0.01[a]	0.00262[a]	Grasses & herbs
moss (*Racomitrium canescens*)	0	1	0	0.0401[c]	0.00229[c]	0.00229[c]	0.00011[c]	Lichen & bryophytes
caterpillar (Non-specific)	0	1	0	0.02[d]	0.0075[d]	0.0075[d]	0.000589[d]	Gastropod
common toad (*Bufo bufo*)	0.25	0.75	0	0.0799[e]	0.03[e]	0.025[e]	0.0314[e]	Amphibian
natterjack toad (*Bufo calamita*)	0.6	0.4	0	0.06	0.03	0.04	0.02	Amphibian
common frog (*Rana temporaria*)	0.25	0.75	0	0.0799[e]	0.03[e]	0.025[e]	0.0314[e]	Amphibian
great crested newt (*Triturus cristatus*)	0	1	0	0.16	0.015	0.013	0.0085	Amphibian
palmate newt (*Triturus helveticus*)	0	1	0	0.09	0.012	0.0135	0.004238	Amphibian
slow worm (*Anguis fragilis*)	0.4	0.6	0	0.4	0.02	0.015	0.034	Reptile
common lizard (*Lacerta vivipara*)	0.4	0.6	0	0.14	0.01	0.02	0.01	Reptile
adder (*Vipera berus*)	0.75	0.25	0	0.65	0.02	0.02	0.0725	Reptile
teal (*Anas crecca*)	0	0.25	0.25	0.3[f]	0.1[f]	0.0802[f]	1.26[f]	Bird
mallard (*Anas platyrhynchos*)	0	0.3	0.25	0.3[f]	0.1[f]	0.0802[f]	1.26[f]	Bird
field mouse (*Apodemus sylvaticus*)	0.5	0.5	0	0.081	0.03	0.03	0.02	Mammal (rat)
field Vole (*Microtus agrestis*)	0.2	0.8	0	0.09	0.035	0.035	0.03	Mammal (rat)

Superscript suffix indicates default parameters for the following reference organism were used: [a] grasses & herbs, [b] shrub (this seems to have the same default geometry as 'grasses and herbs' within the ERICA Tool), [c] lichen & bryophytes, [d] flying insect, [e] amphibian, [f] bird

The Drigg coastal sand dunes Tier 2 assessment used a UF of 5 and no conservative RQ exceeded unity. The highest conservative RQ value was 0.3 for the reptile reference organism. This corresponded to a weighted absorbed dose rate of 0.7 μGy h^{-1}, the majority of which was attributable to internal exposure from ^{90}Sr. The highest dose received by a user-defined organism was 0.6 μGy h^{-1} to *V. berus*.

Calculated dose rates (Figure 4.1) were placed in context through reference to the radiation effects 'look-up' tables that have been generated for each reference organism from the FREDERICA radiation effects database (Copplestone et al., 2008), which provides chronic radiation effects data grouped by umbrella effect: morbidity, mortality, reproductive capacity and mutation (see Section 1.1.2.1). No chronic radiation effects data were reported for reptiles but acute lethal dose data suggested that they are less radiosensitive than mammals and birds (UNSCEAR, 1996). The look-up tables did not report any effects in mammals and birds at dose rates below 10 μGy h^{-1} and the lowest dose rate at which statistically significant reproduction effects were reported was 100 μGy h^{-1} in mammals (see Leonard et al., 1985).

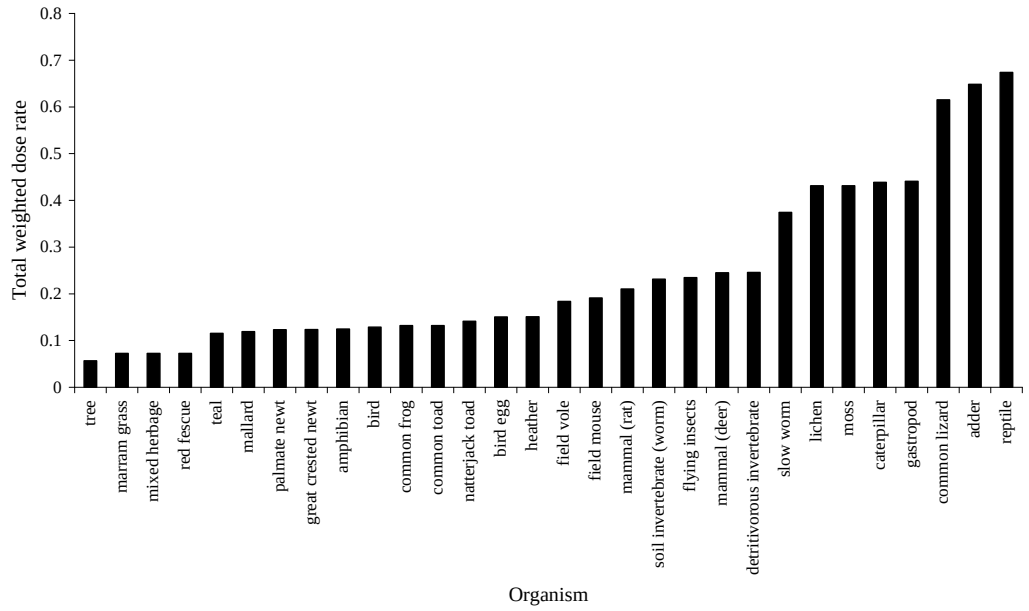

Figure 4.1. Total weighted absorbed dose rates (μGy h^{-1}) to organisms at the Drigg coastal sand dunes, calculated using Tier 2 of the ERICA Tool

In comparison with available radiation effects data, the Tier 2 calculated absorbed dose rates for biota at the Drigg coastal sand dunes were low. Adopting a UF of 5, there was thus less than a 1% probability that the absorbed dose rate to any organism exceeded the screening dose rate and it could be concluded that the risk to non-human biota at the site was negligible. If this was an assessment being undertaken for regulatory purposes at a site receiving minimal stakeholder interest, the assessment process could have been exited at this stage with a high degree of confidence.

4.3.3 Tier 3 assessment

Tier 3 assessments are not restricted to using the deterministic approach adopted in Tiers 1 and 2. The ERICA Tool has in-built probabilistic capability for Tier 3 assessments, allowing the input of probability distribution functions (pdfs) for activity concentration data and transfer parameters. This Tier does not incorporate a screening approach to justify exiting the assessment but provides full functionality for users to undertake complex site assessments and, with an understanding of the uncertainties associated with different elements of the assessment process, to make informed decisions to deal with any potential impact predicted by the ERICA Tool.

The screening assessments conducted at Tiers 1 and 2 demonstrated that there was a low probability of radiation impacts to biota at the Drigg coastal sand dunes. Therefore, Tier 3 was used to test the probabilistic treatment of the transfer component of the ERICA Tool by predicting activity concentrations in biota at the site against which the measured activity concentrations (Tables 4.3 – 4.5) could be compared. The comparison was restricted to four radionuclides for which the mean measured activity concentrations in media and biota were based on one or more values above the LOD, namely ^{90}Sr, ^{137}Cs, $^{239+240}$Pu and ^{241}Am. The input data for the assessment were mean measured activity concentrations in soil (Table 4.2) and the assessment was limited to the user-defined organisms, which had pdfs assigned as their transfer parameters based on their associated default reference organisms (Table 4.9).

The mean measured values and mean predicted values were compared graphically (Figures 4.2 and 4.3). The ERICA Tool either reasonably predicted or over-predicted the activity concentrations of ^{90}Sr, ^{137}Cs, $^{239+240}$Pu and ^{241}Am in the sand dune biota. The notable exception to this was the significant under-prediction ($p \leq 0.05$) of ^{241}Am in higher plants (*A. arenaria*, *Erica spp.*, *F. rubra* and mixed vegetation) and the marginal under-prediction of $^{239+240}$Pu in *F. rubra*. The most significant over-predictions ($p \leq 0.05$) were seen for

^{137}Cs, but the relative ^{137}Cs activity concentrations across the range of biota followed a similar pattern for both the measured and predicted data.

4.4. Discussion

The Tier 1 and Tier 2 assessments both demonstrated that ionising radiation from anthropogenic radionuclides was not impacting significantly on biota at the Drigg coastal sand dunes. Although some of the CRs in the versions of the ERICA Tool released between August 2007 and May 2009 included data from this thesis, in most cases the resultant changes in the CR values were minor and dose rate and activity concentration predictions made using the current ERICA Tool default CR values would be unlikely to differ markedly from those presented here.

In general, the inclusion of the Drigg coastal sand dunes data into the ERICA Tool CR database reduced the mean and standard deviation of the CRs for affected reference organism – radionuclide combinations (Table 4.6). The most notable change was in the reptile data, with CRs for Cs and Sr reducing by factors of 2 and 4 respectively. This reflects the lack of previous radioecological research that has been undertaken for reptiles relative to the other reference organism groups. For example, the original Cs mean CR for reptiles (which was used to generate the ERICA Tool reptile activity concentration predictions in this chapter) was derived from data for mammals. This derivation was based on data from a study undertaken in the Savannah River region of the United States (Brisbin et al., 1974a) which indicated that Cs transfer to reptiles may be a factor of 3 higher than transfer to mammals. The reptile Cs CR used in the August 2007 ERICA Tool transfer database was derived from 8 measurements for reptiles from the Drigg coastal sand dunes. Taking the ratio of reptile to mammal CRs for data from the sand dunes alone indicates that the relationship between transfer to mammals and transfer to reptiles for this ecosystem is closer to a factor of 1.6, almost half that proposed by Brisbin et al. (1974). It is clear that there is considerable uncertainty associated with both the old and the new CR for Cs transfer to reptiles and the applicability of the new CR to other terrestrial ecosystem types requires validation. This highlights a critical gap in knowledge for an important reference organism group that will be encountered in many environments requiring ionising radiation impact assessment and is an area that requires further research (see Chapters 7 and 8).

(a)

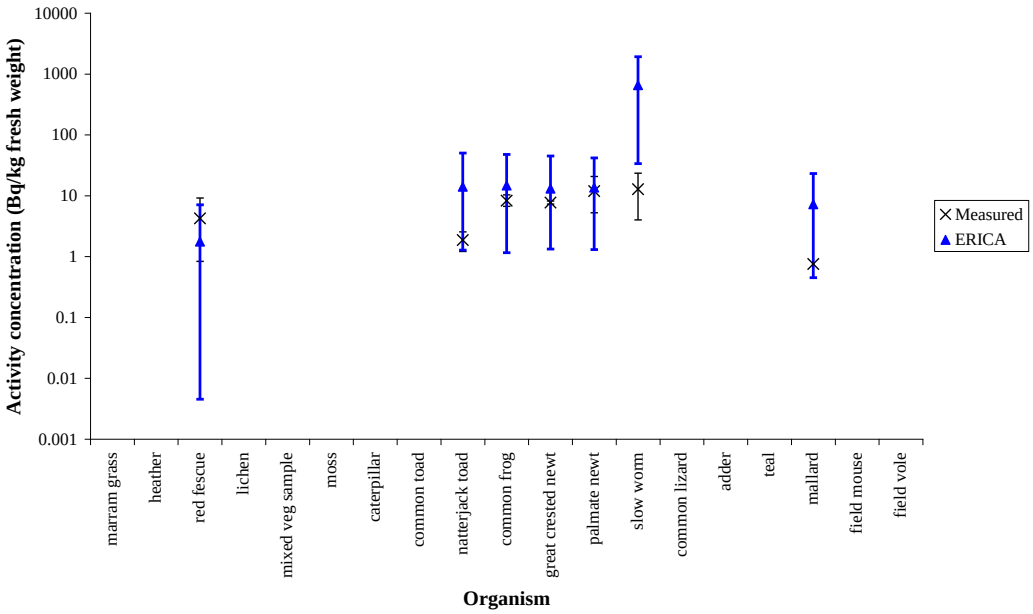

(b)

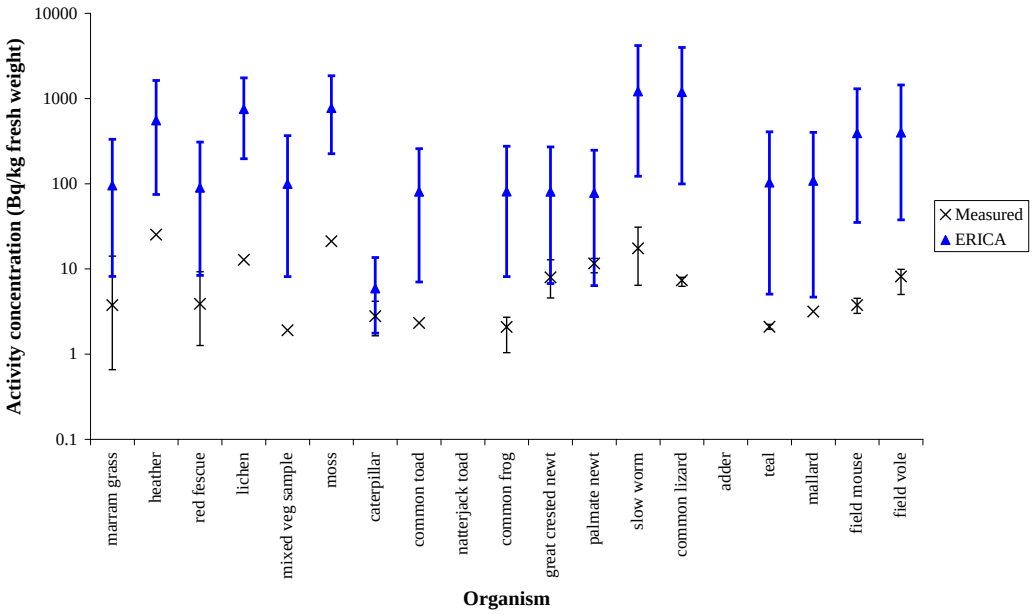

Figure 4.2. Measured and predicted activity concentrations in biota from the Drigg coastal sand dunes for (a) ^{90}Sr, (b) ^{137}Cs. Error bars indicate minimum and maximum values for measured data and 5th and 95th percentiles for predicted data.

(a)

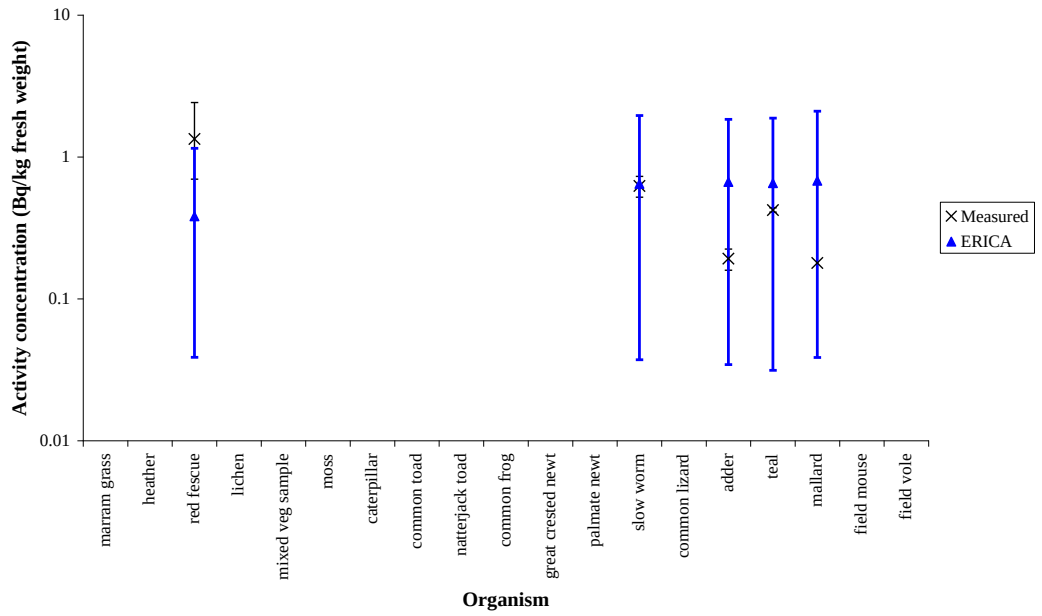

(b)

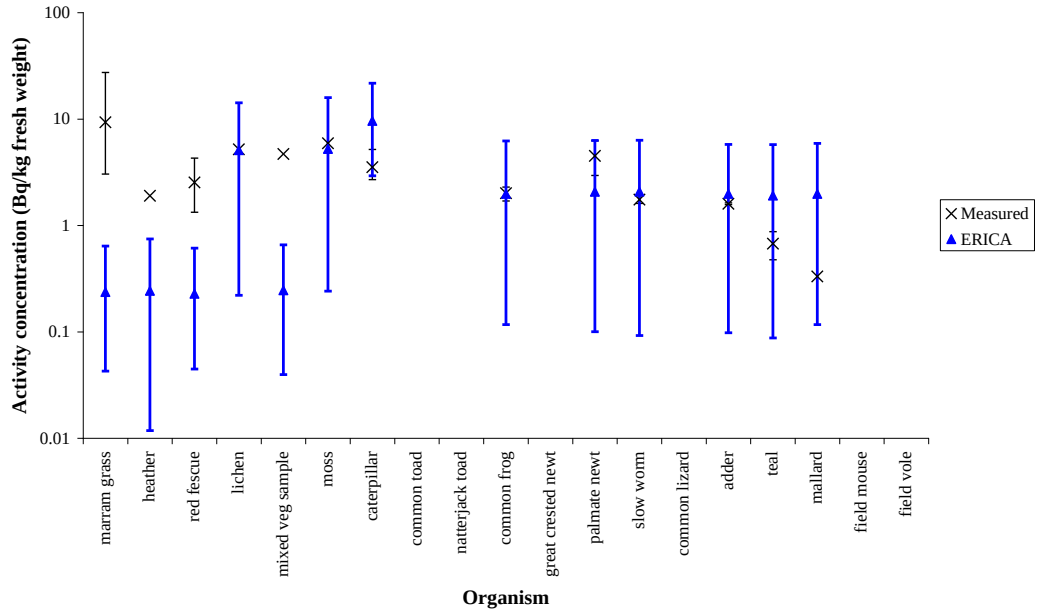

Figure 4.3. Measured and predicted activity concentrations in biota from the Drigg coastal sand dunes for (a) $^{239+240}$Pu and (b) ^{241}Am. Error bars indicate minimum and maximum values for measured data and 5th and 95th percentiles for predicted data.

At Tier 2, the calculated absorbed dose rates are compared to a screening dose rate to assess risks. ERICA proposed a screening dose rate of 10 μGy h^{-1} (Garnier-Laplace et al., 2008), which was derived following a review of radiation effects data. This was lower than the 40 μGy h^{-1} (chronic exposure) for terrestrial animals, below which it had previously been suggested that no measurable population effects would occur (IAEA, 1992; UNSCEAR, 1996), but was more transparently derived using methods commonly applied in chemical risk assessments. The calculated absorbed dose rates to biota from exposure to anthropogenic radionuclides at the Drigg dunes (0.7 μGy h^{-1} maximum) were more than an order of magnitude below the screening dose rate and it could be concluded that there was an extremely low probability of radiation impacts on sand dune biota.

The 0.7 μGy h^{-1} dose rate was calculated for the reptile reference organism and was largely due to internal irradiation from ^{90}Sr. The CR used to predict ^{90}Sr transfer to reptiles in this chapter (Table 4.6) was based on 1 measured value. The CR used in the August 2007 version of the ERICA Tool (Table 4.6) incorporated some data from this thesis (n = 4), which led to a four-fold reduction in the ^{90}Sr CR. Running the assessment with this revised CR would reduce the calculated absorbed dose rate for the reptile reference organism to 0.3 μGy h^{-1}, a reduction of over 50%. Again, this highlights the uncertainty associated with reptile radioecology due to the small number of studies that have been undertaken. This is an issue that is addressed, in part, in Chapters 7 and 8.

To put the estimated dose rates from anthropogenic radionuclides in context, the dose rates can be compared to natural radionuclides. Research on exposure of biota to natural radionuclides has demonstrated that ^{40}K is the principal contributor to background radiation (Beresford et al., 2008f). The Drigg coastal sand dunes assessment was repeated to estimate total dose rates from soil activity concentrations of ^{40}K alone. It was assumed that the CRs for K are the same as those for its chemical analogue, Cs. The highest estimated total dose rate from ^{40}K (> 0.7 μGy h^{-1}) was for the reptile reference organism and demonstrated that background radiation was the dominant contributor to the total radiation exposure for biota at the Drigg coastal sand dunes.

Although Tier 2 of the ERICA Tool predicted low dose rates to biota at the Drigg coastal sand dunes, the dose rates calculated may be atypical of the other terrestrial ecosystem types along the west Cumbrian coastline near to Sellafield. Given the free draining nature of the sand dune substrate, radionuclides deposited on the dunes either directly or via sea-to-land transfer may be expected to have a short residence time in the upper soil horizons compared to soils with a higher clay or organic matter content. This may lead to a

reduction in radionuclide transfer to sand dune biota via food chain uptake and a corresponding reduction in both the internal and external radiation exposure[23].

In the context of the Drigg coastal sand dunes assessment, the ERICA Tool appears somewhat inconsistent in its prediction of organism activity concentrations. The over-prediction of ^{137}Cs (Figure 4.2) is likely to be due to the data used to derive the ERICA Cs transfer factors being dominated by data from sites with a higher soil organic matter content. At such sites, radionuclide activity concentrations are often highest in the surface layers of the soil and decrease with depth. Retention of ^{137}Cs within the upper soil horizons (and within the rooting zone of higher plants at these sites) increases the opportunity for ^{137}Cs to be available for uptake by plants. Previous work (Copplestone et al., 2001b) suggests that sand dunes may have a different depth profile compared to many other terrestrial grassland sites, with radionuclide activity concentrations of ^{137}Cs and ^{241}Am being lower within the surface layers than at depths up to 12 cm below the soil surface (Figure 4.4). The water table is often many metres below the surface of a sand dune so rainfall percolating through the soil is the primary source of water for sand dune plants and the rooting structures of grasses like *A. arenaria* extend from the soil surface to approximately 1 m depth (Ranwell, 1972), maximising their opportunity to scavenge available water. As a result, compared to other terrestrial grassland sites, proportionally less of the sand dune plant root material is likely to fall within the zone of highest ^{137}Cs activity concentration and the resultant transfer of ^{137}Cs from soil to plant may be lower than in other terrestrial sites.

The over-prediction of ^{137}Cs activity concentrations in biota can be considered as introducing an element of conservatism into the assessment but an under-prediction, as seen in the case of ^{241}Am in higher plants (Figure 4.3), is of greater concern. The under-prediction of ^{241}Am may also be a function of the nature of the sand dune soil. It seems contradictory that the nature of the sand dune soil can be the cause of both an over-prediction of ^{137}Cs and an under-prediction of ^{241}Am but this can be explained by the difference in particle reactivity of these two radionuclides. Soil to plant transfer of ^{241}Am is lower than that of ^{137}Cs in fine-grained soils with high organic matter content. However, in large-grained sand dune soils where soil organic matter content is very low there are fewer binding opportunities for ^{241}Am and this may result in the ^{241}Am being more available for plant uptake. In addition, the relative increase in ^{241}Am activity concentration with depth

[23] For example, due to absorption of gamma photons within the medium (sand dune soil), gamma-emitting radionuclides at depth will contribute proportionally less to the measured gamma dose rates than gamma-emitting radionuclides in the surface soil

may be less pronounced than for ^{137}Cs (Figure 4.4). If ^{241}Am has a reduced tendency to accumulate at a particular depth within the sand dune soil profile this may result in a proportionally greater exposure of the roots to ^{241}Am throughout the rooting zone, which could lead to a higher root uptake than may be expected otherwise.

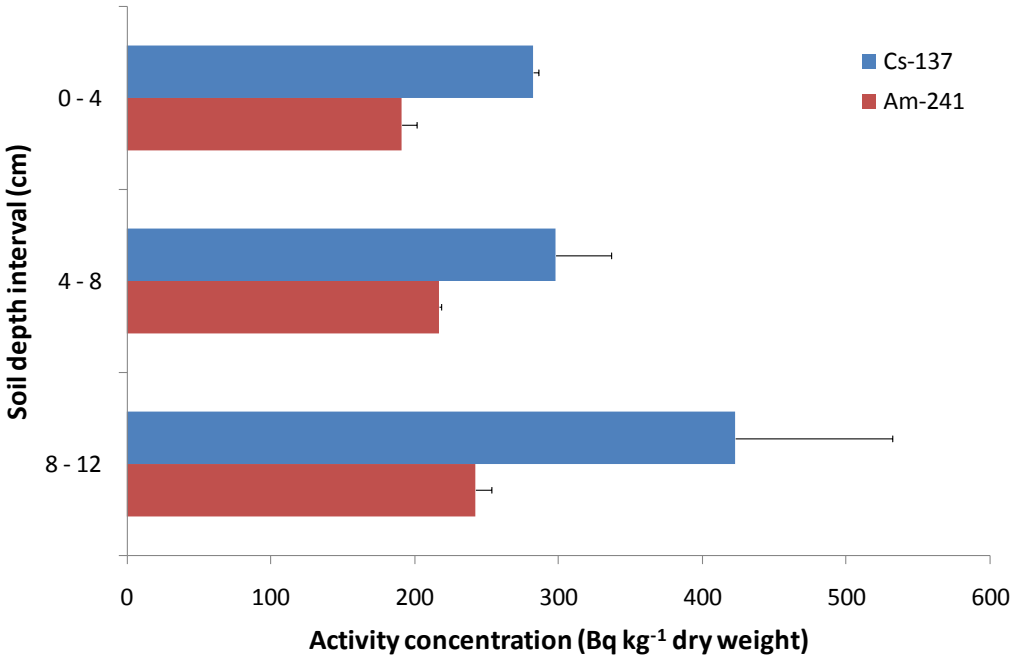

Figure 4.4. Distribution of radionuclide activity concentrations in the soil profile at the Sellafield coastal sand dunes (data from Copplestone et al., 2001b). Error bars show the standard deviation.

Whilst the nature of the soil may contribute to the observed over- and under-predictions, it is likely that the sea-to-land transfer mechanism is the dominant cause behind the inconsistency in predictions. This process is most effective for particle reactive radionuclides such as ^{241}Am and $^{239+240}$Pu, which were under-predicted in this assessment, and least effective for conservative radionuclides such as ^{137}Cs (see Section 2.4.1.1.3). Radionuclides deposited following sea-to-land transfer are likely to be intercepted by

surface vegetation and those that exhibit high particle reactivity may bind to the plant surface directly. Vegetation samples were not washed prior to analysis so the measured activity concentrations in higher plant samples collected from the site will reflect both the radionuclide uptake from the soil and surface-bound contamination, which has been shown in a previous study to dominate the activity concentration burden of coastal sand dune vegetation (Copplestone et al., 2001b).

However, this surface-bound contamination does not explain why $^{239+240}$Pu, which are also highly particle reactive, showed a more marginal under-prediction for $^{239+240}$Pu activity concentrations in *F. rubra*. There was approximately a two-fold difference in the ^{241}Am and $^{239+240}$Pu activity concentrations measured in both the soil and biota samples collected from the Drigg coastal sand dunes, the ^{241}Am being higher consistently. All measured values for these radionuclides were above the LOD so the difference in predictions from the ERICA Tool is not due to the inclusion of LOD values in the calculation of mean $^{239+240}$Pu activity concentrations. Reference to the transfer database within the ERICA Tool reveals the likely cause of the difference in the predictions, with ^{241}Am having a concentration ratio for 'grasses and herbs' of 4.96×10^{-3} and $^{239+240}$Pu a concentration ratio of 1.44×10^{-2}. This factor of three difference in the concentration ratios used to derive the mean predicted activity concentrations may account for the considerable under-prediction of ^{241}Am relative to $^{239+240}$Pu, but does not seem to reflect the fact that Am is generally assumed to be more mobile than Pu.

The ERICA Integrated Approach assumes an equilibrium state between the activity concentrations in biota and the activity concentrations in the soil and this may not be appropriate for sites such as the Drigg coastal sand dunes. To increase the accuracy of the predictions it may be necessary to use more site-specific transfer parameters (if sufficient data can be obtained). However, the ERICA Tool incorporates the functionality to input biota activity concentrations directly as part of the assessment process, thereby circumnavigating this issue of non-standard transfer relationships for those biota for which measured activity concentration data are available.

The comparisons between measured and predicted activity concentrations (Figures 4.2 & 4.3) also provided the opportunity to check one of the assumptions that forms part of the methodology adopted in ERICA for deriving CRs in the absence of published data for a specific reference organism-radionuclide combination, namely the use of the same CR for similar reference organism groups (Beresford et al., 2008d). For example, no Pu and Am CRs for amphibians, reptiles and birds were available so the CRs used in ERICA for

transfer of Pu and Am to these organisms were the CRs for mammals. However, the predicted $^{239+240}$Pu and ^{241}Am activity concentrations for these organisms were in reasonable agreement with measured values; mean predictions of activity concentrations by the ERICA Tool being comparable to, or in excess of, the measured values for all but ^{241}Am in the palmate newt (although the measured value was still lower than the 95th percentile prediction (Figure 4.3)). This gives some confidence that the methodology used for CR derivation within ERICA will generally result in conservative CRs being applied.

The data from the Drigg coastal sand dunes have allowed a detailed evaluation of the ERICA Tool to be undertaken and present an opportunity to test the application of other available tools and approaches for assessing the impact of ionising radiation on wildlife (e.g. Copplestone et al., 2001a; Copplestone et al., 2003; USDoE, 2002). However, small sample numbers for certain sample types (e.g. n = 6 for soil samples) introduce a degree of uncertainty into the assessment. This limitation is addressed in the following chapter, which draws on data from the full sampling and analysis programme undertaken at the Drigg coastal sand dunes to undertake an intercomparison of three publicly-available environmental radiation protection models (see Chapter 5).

4.5. Conclusions

The application of the ERICA Integrated Approach to the Drigg coastal sand dunes indicated that the radioactive discharges from the Sellafield site and the LLWR were not impacting significantly on biota inhabiting the dunes. Dose rates from natural radionuclides at the Drigg coastal sand dunes exceed those from anthropogenic radionuclides. However, this does not imply that biota at other locations are, or are not, impacted by discharges from these sites. The Drigg coastal sand dunes is just one of a wide range of ecosystem types that may be impacted.

Comparisons of measured and predicted activity concentrations have highlighted some areas of uncertainty, primarily associated with radionuclide transfer to reptiles. This reflects that lack of radioecological data for reptiles. The ERICA Tool consistently over-predicted activity concentrations of key radionuclides (^{90}Sr, ^{137}Cs, $^{239+240}$Pu and ^{241}Am) in reptiles so predictions made using the ERICA Tool may be considered conservative for this group of organisms. However, radionuclide transfer in the sand dune ecosystem may be atypical of other terrestrial environments due to the specific soil characteristics of the site. The transfer of radionuclides to reptiles is thus an area requiring further study and the

resulting data should be incorporated in future revisions of the ERICA CR database. This is discussed further in Chapters 7 and 8.

Using site-specific media activity concentrations as the input data, the ERICA Integrated Approach, in conjunction with the ERICA Tool and supporting documentation, provided an effective and accessible means for undertaking an assessment of the risks to non-human biota from ionising radiation at the Drigg coastal sand dunes, taking particular account of the interests and views of stakeholders. The functionality of the ERICA Tool, coupled with the insights provided by the guidance documentation into the issues and considerations associated with this type of assessment, lends confidence to the 'fitness-for-purpose' of the ERICA Integrated Approach. However, the overall merits of adopting the ERICA Integrated Approach and the degree of confidence in its applicability to the myriad of scenarios facing those wishing or needing to undertake impact assessments will be realised only through its continuing application and testing.

CHAPTER 5 – INTERCOMPARISON OF MODELS

This material presented in this chapter has been published as:

Wood et al., 2009. Assessing radiation impact at a protected coastal sand dune site: an intercomparison of models for estimating the radiological exposure of non-human biota. Journal of Environmental Radioactivity, 100(12), 1034-1052.

5.1. Introduction

Environmental legislation and policy decisions at national and regional levels have resulted in a requirement to assess the environmental impact of ionising radiation and a number of models have been proposed to address this requirement (see Chapter 1). Although the integration of these models into mainstream anthropocentric radiation protection is still debated (Brownless, 2007), some models are already being applied by regulators and industry for decision-making purposes (Allott & Copplestone, 2008; Beresford et al., 2008b; Copplestone et al., 2005b) and may thus have economic implications. There is likely to be a significant future requirement for such models as a consequence of recent ICRP Recommendations (ICRP, 2007b) and forthcoming revisions to the EC and International Safety Standards. To maximise both stakeholder acceptance of, and confidence in, assessment outcomes, there is a need to validate these models.

This chapter presents the application of three publicly available models to a terrestrial ecosystem assessment for the Drigg coastal sand dunes. The models critically evaluated were the United States Department of Energy (USDoE) RESRAD-BIOTA code (USDoE, 2002; USDoE, 2004), the England & Wales Environment Agency R&D 128/SP1a habitats assessment model (Copplestone et al., 2001a; Copplestone et al., 2003) and the EC-funded ERICA Integrated Approach and Tool (Beresford et al., 2007d; Brown et al., 2008; Larsson, 2008). Of the three models, only ERICA was developed to be openly available for use. R&D Publication 128 and RESRAD-BIOTA were developed for specific users but have subsequently been made publicly available, with training courses for the latter being marketed by the model developers. Thus, all three models are available to and are being applied by a variety of users. In addition to contributing to the developing knowledge-base on the relative performance of these models when applied to case study scenarios, this chapter aims to provide a more in-depth description and analysis of the decision-making

process for undertaking an assessment than has been presented in previous intercomparison exercises, especially with regard to the parameterisation of the models by the user.

5.2. Model intercomparison methodology: The 'informed user' concept

Intercomparisons and validations of biota dose assessment models are beginning to be published (Beresford et al., 2008f; Vives i Batlle et al., 2007; Wood et al., 2008), with authors assessing both the predictive capability and 'fitness for purpose' of the different models. Although there are various types of uncertainty that have been discussed in relation to ecological models (e.g. Loehle, 1987; Oughton et al., 2008), the uncertainty in predictions obtained using a particular model is essentially a function (f) of the combined uncertainties attributable to the assessment scenario and input data available (U_{DAT}), the algorithms used within the model (U_{MOD}) and the decisions made by the assessor (U_{ASS}). The total uncertainty (U_{TOT}) in the assessment outcome can therefore be defined by:

$$U_{TOT} = f(U_{DAT}, U_{MOD}, U_{ASS})$$

For a given scenario-model combination, U_{DAT} and U_{MOD} are constant so the key determinant of uncertainty in the assessment outcome is U_{ASS}. There is thus a need to consider the methodology used for running model intercomparison exercises and, in particular, the approach adopted for selecting the assessors to apply models to exercise scenarios. Although the significance of U_{ASS} has been alluded to previously (Kirchner et al., 1999; Kirchner & Steiner, 2008), the importance of assessor selection in the development of validation and intercomparison exercises for biota dose assessment models has received little attention to date, with model developers often applying their own models (e.g. Beresford et al., 2008f; Wood et al., 2008).

The decision about who should run particular models within a model intercomparison exercise should be guided by the aims and objectives of the exercise. Where the purpose of intercomparison is to determine the differences and commonalities between the algorithms and parameters used within different models (e.g. Vives i Batlle et al., 2007), intercomparison of applications by the model developers may be appropriate. However, where intercomparison exercises use an assessment scenario (e.g. a case study site) to determine the way in which models may be expected to perform in a decision-making context, the exercises should be 'informed user-led'. In this context, informed users would have a background in environmental radiation protection but not be a developer of the approach they are using for the intercomparison exercise.

Model application by informed users will become increasingly common as the requirement for undertaking biota dose assessments increases, due to evolving legislative frameworks and interest in the construction of new nuclear power plants (see Chapter 1). Informed user application of models is driven by both the available guidance documentation and the ease with which the models can be understood and applied. By conducting informed user-led model intercomparison exercises it could be anticipated that the results will provide a more realistic simulation of the way in which models may be expected to perform in practice. The findings of such exercises will help assessors to make evidence-based decisions as to which models to select for particular scenarios and facilitate model developers in refining the models and supporting documentation. The model intercomparison described in this chapter was developed in line with this informed user concept but it should be noted that the author has been involved with developing aspects of two of the three models discussed.

5.3. Data for the model intercomparison exercise

The data set used to provide both the input data for this model intercomparison exercise (soil activity concentrations) and measured biota activity concentration data against which model results could be compared was an expanded version of that used for the evaluation of the ERICA Integrated Approach (Chapter 4; Wood et al., 2008). It included data from the full range of samples collected from the Drigg coastal sand dunes between 2005 and 2007 (see Table 3.1). Samples were analysed for ^{137}Cs and ^{241}Am by gamma spectroscopy. A sub-set of samples (n = 26) were prioritised for ^{90}Sr, ^{99}Tc, ^{238}Pu, $^{239+240}$Pu analysis. Soil property determinations were undertaken using standard methods. The mean moisture content in the soil samples was 14% and the mean bulk density was 1.25 g cm^{-3}. Particle size analysis showed medium sand (212-600 µm) and fine sand (63-212 µm) to dominate within the sand dune soils, contributing 79% and 17% respectively to the soil dry weight. Detailed descriptions of the sampling and analysis methodologies are provided in Chapter 3.

For modelling exposure from ^{90}Sr, ^{99}Tc, ^{137}Cs, ^{238}Pu, $^{239+240}$Pu and ^{241}Am in the terrestrial environment, the three models considered in this intercomparison exercise can use radionuclide activity concentrations in sand dune soil (Table 5.1) to calculate external dose rates and predict whole-body activity concentrations in biota. These modelled biota activity concentrations can then be used to calculate internal dose rates. The models were applied using the available guidance documentation and intuitive use of the models (thereby simulating informed user application) to predict the following from the soil activity concentration data reported in Table 5.1:

1. Whole-body activity concentrations (Bq kg^{-1} fresh weight) for the biota listed in Table 3.1.
2. Internal unweighted absorbed dose rates (μGy h^{-1}) for the biota listed in Table 3.1.
3. External absorbed dose rates (μGy h^{-1}) for the biota listed in Table 3.1.

Table 5.1. Activity concentrations (Bq kg^{-1} dry weight) in soil samples (0 – 10 cm depth) from the Drigg coastal sand dunes, UK

		Activity concentration (Bq kg^{-1} dry weight)			
Radionuclide	*n*	mean	SD	min	max
^{90}Sr	6	13.1	4.7	<6.8	18
^{99}Tc	6	16.4	10.1	<6.9	34.5
^{137}Cs	48	59.4	45.9	1.5	213.2
^{238}Pu	6	5.1	5.2	<0.3	11.4
$^{239+240}Pu$	6	27.8	29.1	1	63.8
^{241}Am	54[1]	20.5	17.8	0.3	107.4

[1] Soil samples (*n* = 48) were analysed for ^{137}Cs and ^{241}Am by gamma spectrometry but an additional 6 samples were analysed for ^{90}Sr, ^{99}Tc, ^{238}Pu, $^{239+240}Pu$ and ^{241}Am using radiochemical techniques, hence the value of *n* reported for ^{241}Am is higher than for ^{137}Cs.

5.4. Applying the models

5.4.1. Generic aspects of model parameterisation

All three models have default organisms (Table 5.2) with pre-defined parameters which can be used to undertake generic assessments or used as a basis for modelling site-specific organisms. These default organisms are referred to as reference organisms in both the ERICA Tool and R&D128/SP1a. To model a site-specific organism it is necessary to assign parameters that define the organism geometry, the transfer of radionuclides to the organism and the behaviour of the organism within the environment. For the plants, lichen and fungi, the most appropriate default organism within each model was used to define these parameters (Table 5.3). The data used to guide the parameterisation of the animals

(organism dimensions, mass and ecology) were standardised across the three models. Although the mass and dimensions of the organisms sampled from the dunes were recorded, field sampling was undertaken specifically to provide activity concentration data with which to compare model predictions. Direct measurements of the dimensions and masses of site-specific organisms are often not available to an assessor. Therefore, in order to simulate the informed user application, these data were sourced from literature and web-based resources (Table 5.4).

Most literature sources only provide length measurements for individual organisms so images of the organisms were used to determine the proportional relationship between length and the other two axes (nominally width and height) of the organism as suggested in the ERICA Tool 'help' file. These three measurement axes are referred to as *x*, *y* and *z* within Table 5.4.

Multiple literature sources had to be used to compile the underpinning data sets for defining some organisms. As a result there are instances where mass data and dimension data do not reflect expected relationships. For example, *B. bufo* has body dimensions that are approximately twice those of *B. calamita* but the available references suggested the two species have similar masses. Whilst there is no reason to assume the density of *B. calamita* is significantly higher than that of *B. bufo*, the decision was taken to proceed using the available data for each species.

To calculate the radionuclide activity concentrations in an organism, the three models use transfer parameters; numerical multipliers that relate the activity concentration of a particular radionuclide in the environmental medium to the whole-body activity concentration of that radionuclide in the organism. These transfer parameters are referred to as concentration ratios (CRs) in the ERICA Tool, concentration factors (CFs) in R&D128/SP1a and bioaccumulation factors (B_{iv}s) in RESRAD-BIOTA. For the radionuclides (*R*) considered within this study, the transfer parameters are defined by:

$$CR, CF \text{ or } B_{iv} = \frac{Whole\text{-}body\ Activity\ concentration\ of\ R\ (Bq\ kg^{-1}\ fresh\ weight)}{Activity\ concentration\ of\ R\ in\ soil\ (Bq\ kg^{-1}\ dry\ weight)}$$

Table 5.2. Default organisms for terrestrial assessments in the three models used within this intercomparison exercise (the ERICA Tool, R&D128/SP1a and RESRAD-BIOTA)

The ERICA Tool	R&D128/SP1a	RESRAD-BIOTA
Amphibian	Ant	Terrestrial Animal
Bird	Bacteria	Terrestrial Plant
Bird egg	Bee	
Detritivorous invertebrate	Bird	
Flying insect	Bird egg	
Gastropod	Carnivorous mammal	
Grasses and herbs	Caterpillar	
Lichen and bryophytes	Earthworm	
Mammal	Fungi	
Reptile	Herb	
Shrub	Herbivorous mammal	
Soil invertebrate	Lichen	
Tree	Reptile	
	Rodent	
	Seed	
	Shrub	
	Tree	
	Woodlouse	

Table 5.3. Default organisms used to define the transfer, dosimetry and occupancy parameters for the sand dune plants, lichen and fungi within the ERICA Tool, R&D128/SP1a and RESRAD-BIOTA

Organism	R&D128/SP1a	The ERICA Tool	RESRAD
A. arenaria	Herb[a, b]	Grasses & herbs	Terrestrial plant
F. rubra	Herb[a, b]	Grasses & herbs	Terrestrial plant
C. vulgaris	Shrub[a]	Shrub[a, c, d]	Terrestrial plant
E. cinerea	Shrub[a]	Shrub[a, c, d]	Terrestrial plant
E. tetralix	Shrub[a]	Shrub[a, c, d]	Terrestrial plant
U. europaeus	Shrub[a]	Shrub[a, c, d]	Terrestrial plant
C. portentosa	Lichen[a, b, c]	Lichen & bryophyte[a, c, d]	Terrestrial plant
R. canescens	Lichen[a, b, c]	Lichen & bryophyte[a, c, d]	Terrestrial plant
Hygrophorous sp	Fungi[a, c, d]	Lichen & bryophyte[a, c, d]	Terrestrial plant
Lepiota sp	Fungi[a, c, d]	Lichen & bryophyte[a, c, d]	Terrestrial plant
Lycoperdon sp	Fungi[a, c, d]	Lichen & bryophyte[a, c, d]	Terrestrial plant
Marasmius sp	Fungi[a, c, d]	Lichen & bryophyte[a, c, d]	Terrestrial plant
Rhodophyllus sp	Fungi[a, c, d]	Lichen & bryophyte[a, c, d]	Terrestrial plant
Russula sp	Fungi[a, c, d]	Lichen & bryophyte[a, c, d]	Terrestrial plant

Transfer parameters for [a]Tc, [b]Sr, [c]Am and [d]Pu were derived using guidance given within the supporting documentation for the model.

Table 5.4. Parameters used to define the sand dune animals within the ERICA Tool, R&D128/SP1a and RESRAD-BIOTA

Organism	Dimension (mm)			Mass (kg)	R&D128/SP1a & ERICA Tool OFs			R&D128/SP1a reference organisms for		ERICA Tool reference organism	RESRAD-BIOTA			
	x	y	z		In soil	At soil surface	In air	DPUCs	CFs	for CRs	Geometry number	Generic BIVs	organism	AF	GF (soil)
Arctiidae spp	65 [a]	8 [a]	8 [a]	1.00E-03 [b]	0	0	1 [c]	Earthworm	Caterpillar [v, w, x, y, z]	Gastropod [v]	2	Terrestrial animal		1	0.5
Gastropoda	80 [d]	13 [d]	10 [d]	6.43E-04 [e]	0	0.25	0.75 [c]	Fungi	Caterpillar [v, w, x, y, z]	Gastropod [v]	3	Terrestrial animal		1	0.5
L. terrestris	80 [d]	6 [d]	6 [d]	8.78E-04 [e]	1	0	0	Caterpillar	Earthworm [v, w]	Soil invertebrate (worm) [v]	2	Terrestrial animal		1	1
B. bufo	150 [f]	85 [f]	75 [f]	4.45E-02 [g]	0.25	0.75	0	Reptile	Reptile [v, w, x, y, z]	Amphibian [x, y]	4	Terrestrial animal		1	0.625
B. calamita	80 [f]	40 [f]	30 [f]	5.07E-02 [h]	0.6	0.4	0	Reptile	Reptile [v, w, x, y, z]	Amphibian [x, y]	4	Terrestrial animal		1	0.8
R. temporaria	110 [f]	55 [f]	45 [f]	2.30E-02 [i]	0.25	0.75	0	Reptile	Reptile [v, w, x, y, z]	Amphibian [x, y]	4	Terrestrial animal		1	0.625
T. cristatus	150 [f]	19 [f]	14 [f]	7.00E-03 [j]	0	1	0	Rodent	Reptile [v, w, x, y, z]	Amphibian [x, y]	3	Terrestrial animal		1	0.5
T. helveticus	95 [f]	9 [f]	8 [f]	7.00E-03 [k]	0	1	0	Bee	Reptile [v, w, x, y, z]	Amphibian [x, y]	2	Terrestrial animal		1	0.5
T. vulgaris	110 [f]	13 [f]	10 [f]	7.00E-03 [k]	0	1	0	Fungi	Reptile [v, w, x, y, z]	Amphibian [x, y]	3	Terrestrial animal		1	0.5
A. fragilis	500 [f]	12 [f]	12 [f]	4.50E-02 [l]	0.4	0.6	0	Fungi	Reptile [v, w, x, y, z]	Reptile [v, x, y]	2	Terrestrial animal		1	0.7
L. vivipara	140 [f]	10 [f]	7 [f]	6.00E-03 [m]	0.4	0.6	0	Fungi	Reptile [v, w, x, y, z]	Reptile [v, x, y]	2	Terrestrial animal		1	0.7
V. berus	650 [f]	20 [f]	20 [f]	1.00E-01 [n]	0.75	0.25	0	Rodent	Reptile [v, w, x, y, z]	Reptile [v, x, y]	3	Terrestrial animal		1	0.875
A. crecca	360 [o]	175 [o]	160 [o]	3.64E-01 [p]	0	0.25	0.25 [q]	Carnivorous mammal	Bird [v, w, x, y]	Bird [x, y]	5	Terrestrial animal		0.5	0.5
A. platyrhynchos	580 [r]	250 [r]	200 [r]	1.08E+00 [s]	0	0.3	0.25 [q]	Carnivorous mammal	Bird [v, w, x, y]	Bird [x, y]	5	Terrestrial animal		0.55	0.5
A. sylvaticus	110 [t]	40 [t]	40 [t]	2.90E-02 [u]	0.5	0.5	0	Reptile	Rodent [v]	Mammal (rat) [v]	4	Terrestrial animal		1	0.75
M. agrestis	90 [t]	35 [t]	35 [t]	4.00E-02 [u]	0.2	0.8	0	Reptile	Rodent [v]	Mammal (rat) [v]	4	Terrestrial animal		1	0.6
S. araneus	85 [t]	30 [t]	30 [t]	1.20E-02 [u]	0.7	0.3	0	Bird egg	Rodent [v]	Mammal (rat) [v]	3	Terrestrial animal		1	0.85
T. europaea	140 [u]	60 [u]	50 [u]	9.50E-02 [u]	0.95	0.05	0	Reptile	Rodent [v]	Mammal (rat) [v]	4	Terrestrial animal		1	0.975

[a] http://ukmoths.org.uk/show.php?id=2069; [b] assumed same as *L. terrestris*; [c] the ERICA Tool can only model organisms 'in air' when organism mass >0.035kg so for the ERICA Tool assessment assumed 100% time at soil surface (OF at soil surface =1); [d] Catt, 1998; [e] Bradford et al., 2002; [f] Arnold, 2004; [g] Hoglund & Saterberg, 1989; [h] Miaud & Sanuy, 2005; [i] http://animaldiversity.ummz.umich.edu/site/accounts/information/Rana_temporaria.html; [j] Jehle & Arntzen, 2000; [k] assumed same mass as *T. cristatus*; [l] Gent & Gibson, 1998 & Platenberg & Griffiths, 1999; [m] Herczeg et al., 2008;
[n] http://animaldiversity.ummz.umich.edu/site/accounts/information/Vipera_berus.html.; [o] http://blx1.bto.org/birdfacts/results/bob1840.htm;
[p] http://animaldiversity.ummz.umich.edu/site/accounts/information/Anas_crecca.html; [q] height above ground set to 10m within ERICA Tool assessment;
[r] http://blx1.bto.org/birdfacts/results/bob1860.htm; [s] http://animaldiversity.ummz.umich.edu/site/accounts/information/Anas_platyrhynchos.html; [t] Hofmann, 1995;
[u] Burton, 1976. Transfer parameters for [v]Tc, [w]Sr, [x]Am, [y]Pu and [z]Cs were derived using guidance given within the supporting documentation for the model.

It should be noted that the authors had to assume that the RESRAD-BIOTA B_{iv}s were derived using the same fresh weight organism:dry weight soil relationship used to define the CRs and CFs because the RESRAD-BIOTA software and accompanying guidance documentation did not specify whether the units used within the model were dry weight or fresh weight. Subsequent discussions with RESRAD-BIOTA developers (Jing-Jy Cheng, Argonne National Laboratory, pers. comm.) have confirmed this assumption to be correct.

The ERICA Tool and RESRAD-BIOTA have additional functionality in relation to transfer. The ERICA Tool allows the use of a probability distribution function (instead of a single numeric value) to define radionuclide transfer for a particular radionuclide-organism combination and reports results based on the mean, 5^{th} and 95^{th} percentiles by default. RESRAD-BIOTA can also implement a kinetic-allometric approach to predict transfer using biological scaling relationships based on organism body mass (Higley et al., 2003), providing an alternative to the use of equilibrium transfer parameters and a method for predicting radionuclide transfer in the absence of measured transfer parameters for particular radionuclide-organism combinations.

The three models require organism geometries to be defined for the dosimetry component of the modelling process. Numerical multipliers that relate activity concentrations in soil and whole-body activity concentrations in biota to external and internal unweighted absorbed dose rates for each radionuclide-geometry combination are defined on the basis of these geometries (ellipsoids for most organisms). This parameter is referred to as a dose conversion coefficient (DCC) in the ERICA Tool, a dose per unit concentration factor (DPUC) in R&D128/SP1a and dose conversion factor (DCF) in RESRAD-BIOTA.

Calculated whole-body activity concentrations and absorbed dose rates are adjusted within the modelling process to account for differences in organism ecology (mainly habitat utilisation). Corrections are made to define the fraction of time an organism spends at a site under assessment and the organism's location within that site. For example, *A. platyrhynchos* is not permanently resident at the Drigg dunes whereas *L. terrestris* is. *L. terrestris* is located within the soil whereas *A. platyrhynchos* spends time on the soil surface and in the air above the site. The factors applied to correct for these differences are referred to as occupancy factors (OFs) in R&D128/SP1a and ERICA. These two models use three OFs for each organism, defining the fraction of time the organism spends in the soil, at the soil surface and in the air. If the OFs sum to less than 1, this implies that an organism is not permanently resident at the site and hence not permanently exposed to radionuclide contamination that may be present. RESRAD-BIOTA adopts a slightly different approach,

using an area factor (AF) to describe the fraction of time the organism spends at the site and a geometry factor (GF) to define the geometric relationship between the organism and the radionuclide source. The radionuclide source at a terrestrial site is assumed to be the soil so a GF of 0.5 implies a 2π geometry (organism on the soil surface) and a GF of 1 describes a 4π geometry (organism in the soil).

The following sections (5.4.2 to 5.4.4) describe the models and documentation used for this intercomparison exercise and the specific methods implemented for the parameterisation of each model.

5.4.2. R&D 128/SP1a

Designed for undertaking conservative assessments of regulated radioactive discharges, the model is provided in the form of three Microsoft® Office Excel workbooks (coastal aquatic, freshwater and terrestrial) with two supporting guidance documents: R&D Publication 128 (Copplestone et al., 2001a) and R&D Technical Report SP1a (Copplestone et al., 2003). The assessment for the Drigg dunes was conducted using version 1.20 of the terrestrial workbook (available from http://www.coger.org.uk/R&D128index.html).

CFs were assigned to each site-specific organism by using the default CFs for a corresponding reference organism. For example, *A. sylvaticus* was assigned the CFs for the 'rodent' reference organism and *A. crecca* was given the CFs for 'bird'. Where default CFs were missing for particular radionuclide-reference organism combinations (e.g. the CF for ^{137}Cs transfer to reptiles) these were assigned following the guidance recommended in R&D Technical Report SP1a (Copplestone et al., 2003). In the case of ^{137}Cs transfer to reptiles, the CF used was that for ^{137}Cs transfer to 'carnivorous mammal' (the highest default CF listed for ^{137}Cs transfer to a terrestrial reference organism). For some site-specific organisms, such as gastropoda, there was no directly comparable reference organism available so the CFs for a reference organism of similar ecology were selected (the caterpillar in the case of gastropoda).

Assessor-selected OFs were used for each site-specific organism when sufficient information was available on the ecology of the organisms to justify changing the default OFs.

Each reference organism within R&D128/Sp1a has a defined geometry. It is not possible to create new geometries within the model so the appropriate reference organism geometry must be assigned to each site-specific organism that the assessor wishes to model. Whilst

this process can be confusing due to the fact that the R&D128/Sp1a geometries are given the names of the reference organisms (e.g. 'bird egg', 'herbivorous mammal', 'reptile'), it should be noted that the reference organism is just a shape, an ellipsoid with generic dimensions for that organism group, which has been assigned CFs and generic OFs for the named organism group. The ellipsoid dimensions define the DPUCs for that reference organism geometry. The assessor must choose the appropriate ellipsoid for the site-specific organism they wish to model, irrespective of whether the name of the reference organism and the type of organism they wish to model are in agreement, and then assign the appropriate CFs and OFs to that ellipsoid. For example, for the purposes of deriving the DPUCs, *V. berus* was most accurately represented by the 'reptile' geometry but *T. vulgaris* was best represented by the 'bird egg' geometry and *A. platyrhynchos* by the 'carnivorous mammal' geometry (Table 5.4).

Copplestone et al. (2003) provided a method for assigning a reference organism geometry (and hence DPUCs) to a site-specific organism based on an identified linear relationship between the surface area:volume ratio of the ellipsoid and the DPUC for a particular radionuclide. However, Copplestone et al. (2003) did not provide the equations needed to calculate the surface area and volume of an ellipsoid. For this model intercomparison exercise, the equations given by Dieckmann (2003) were used to calculate the surface area and volume for an ellipsoid with semiaxes *a*, *b* and *c*. These semiaxes are the distances from the centre to the edges of the ellipsoid and are approximated by dividing each axis measurement quoted in Table 5.4 (*x*, *y* and *z*) by 2. The equation for the area of the ellipsoid is a suitable approximation assuming that $a > b \geq c$ (which is valid for all of the organism dimensions given in Table 5.4). The equations used were:

$$Volume = \frac{4}{3}\pi abc$$

$$Area = 2\pi\left(c^2 + abr + \frac{b^2 - c^2}{3ab}r^3\left(c^2 - \frac{a^2}{2} + \frac{a^4b^2 + 3a^4c^2 - 12a^2c^4 + 8b^2c^4}{40a^2b^2}r^2\right)\right)$$

Where $r = ArcCos\left[\frac{c}{a}\right] \Big/ \sqrt{1 - \frac{c^2}{a^2}}$

The surface area:volume ratio was calculated for each site-specific organism to be modelled. These ratios were compared to the ratios for each R&D128/Sp1a reference organism and the reference organism with the most numerically similar surface

area:volume ratio was selected to provide the reference organism geometry (and hence DPUCs) for each site-specific organism (Table 5.4).

As shown in Table 5.4, the same reference organism geometry was required to define the DPUCs for a number of site-specific organisms. For example, the 'reptile' geometry defined the DPUCs for *A. sylvaticus, B. bufo, B. calamita, M. agrestis, R. temporaria* and *T. europaea*. As a result, and because of how the model is structured in Microsoft® Office Excel, it was necessary to run the assessment multiple times to model each of these organisms.

5.4.3. RESRAD-BIOTA

RESRAD-BIOTA is the computer code that implements the USDoE's 'Graded Approach' (USDoE, 2002). The assessment used 'Level 3' of the RESRAD-BIOTA 1.22 Beta Tool and was applied with reference to the User Guide (USDoE, 2004), the technical guidance documentation (USDoE, 2002) and the database of bioaccumulation factors (available at http://homer.ornl.gov/nuclearsafety/nsea/oepa/bdac/database.html).

When modelling site-specific organisms in RESRAD-BIOTA the assessor must select one of the eight default organism geometries to provide the organism DCFs. The model lists example organisms to help the assessor select the appropriate geometry but the examples are often for organisms specific to the United States. Therefore, the method used for selecting the reference organism geometries in R&D128/SP1a (using the surface area:volume ratio of the ellipsoids) was applied and the nearest default RESRAD-BIOTA geometry selected (Table 5.4). This concept is less confusing within RESRAD-BIOTA because the geometries are identified by a numerical code (1 – 8) rather than being referred to by reference organism names.

The AFs and GFs used for the plants, lichen and fungi were those for the default 'terrestrial plant' (Table 5.3). For the animals, literature-derived information on the ecology of the organisms was used to define organism-specific AFs and GFs (Table 5.4). To ensure consistency in the approach used to parameterise the three models, the animal AFs were the sum of the OFs used for each organism in R&D128/SP1a and ERICA (e.g. *A. platyrhynchos* has OFs of 0 in the soil, 0.3 at the soil surface and 0.25 in air so the AF used for modelling *A. platyrhynchos* in RESRAD-BIOTA was 0.55). The GFs were also determined to be consistent with the parameterisation of the other models; the GF being calculated for this study as the fraction of time that an organism is exposed to a 2π (GF of 0.5) and 4π (GF of 1) source geometry. For example, the fraction of time that *B. bufo*

spends in the soil is 0.25 and the fraction of time it spends at the soil surface is 0.75 so the GF assigned to *B. bufo* was calculated as (0.25 x 1) + (0.75 x 0.5) = 0.625. This approach was adopted by the assessor because the RESRAD-BIOTA guidance does not describe fully the use of the GF.

RESRAD-BIOTA was run using the default B_{iv}s for 'terrestrial animal' and 'terrestrial plant'. However, these are generic B_{iv}s for the two organism groups and are intended to be used for simplistic conservative assessments. Therefore, the assessment was repeated for a selection of the animals (birds, mammals and reptiles) using RESRAD-BIOTA's kinetic-allometric function in an attempt to make more realistic, species-specific predictions. The allometric equations in RESRAD-BIOTA calculate radionuclide biological half-life, food intake rate, soil ingestion rate, maximum lifespan and inhalation rate. Organism mass is used in calculating the intake rates and maximum lifespan. The user can override the allometric calculations and change any of the parameters. However, this requires additional species-specific data and these data were rarely available. For this study, the parameters for which appropriate data were identified were organism mass (Table 5.4), maximum lifespan and diet (Table 5.5). Species-specific data on soil ingestion and inhalation rates could not be identified so the default allometric equations were used to derive values for these two parameters based on the organism mass.

Table 5.5. Parameters for allometric assessment in RESRAD-BIOTA 2, 3 & 4

Organism	Maximum lifespan (yr)	Fresh matter intake rate (FMI, g d^{-1})[a]	Dietary component (fraction of diet)
Anas crecca	3[b]	120	Invertebrate (0.5), Plant (0.5)[c]
Anas platyrhynchos	3[d]	254	Invertebrate (0.5), Plant (0.5)[e]
Anguis fragilis	15[f]	1.21	Invertebrate (1)[f]
Apodemus sylvaticus	2[g]	20.3	Plant (0.75), Invertebrate (0.25)[h]
Lacerta vivipara	12[f]	0.19	Invertebrate (1)[i,j]
Microtus agrestis	2[g]	23.6	Plant (1)[h]
Sorex araneus	1.25[g]	10.9	Invertebrate (1)[h]
Talpa europaea	3[g]	46.7	Invertebrate (1)[g,h]
Vipera berus	10[f]	1.37	*M. agrestis* (0.4), *A. sylvaticus* (0.4), *L. vivipara* (0.2)[f]

[a] Nagy, 2001; [b] http://blx1.bto.org/birdfacts/results/bob1840.htm;
[c] http://animaldiversity.ummz.umich.edu/site/accounts/information/Anas_crecca.html;
[d] http://blx1.bto.org/birdfacts/results/bob1860.htm;
[e] http://animaldiversity.ummz.umich.edu/site/accounts/information/Anas_platyrhynchos.html;
[f] Arnold, 2004; [g] Burton, 1976; [h] Hofmann, 1995;
[i] http://www.arkive.org/species/ARK/reptiles/Lacerta_vivipara/more_info.html?section=biology;
[j] http://www.uksafari.com/commonlizard.htm

To quantify radionuclide transfer for a site-specific organism using RESRAD-BIOTA's allometric functionality, the assessor must define dietary components for that organism, both in terms of the percentage composition of the diet (Table 5.5) and the B_{iv}s for each dietary component. RESRAD-BIOTA then uses allometry to calculate the site-specific organism's fresh matter intake rate (FMI) based on the body mass of the organism. For the invertebrate and plant dietary components, the default B_{iv}s for 'terrestrial animal' and 'terrestrial plant' were used. The B_{iv}s for other dietary components were calculated using repeat allometric runs of RESRAD-BIOTA, following the approach described in (Beresford et al., 2008a) to model trophic transfer up the food chain. For example, RESRAD-BIOTA was run allometrically using the default B_{iv}s for 'terrestrial animal' and 'terrestrial plant' to define the dietary components when calculating activity concentrations in *A. sylvaticus, L. vivipara* and *M. agrestis*. The calculated activity concentrations were then used to calculate the corresponding B_{iv}s for these three organisms and these B_{iv}s were entered into the allometric calculations to predict the activity concentrations in *V. berus*.

The use of calculated FMIs and generic B_{iv}s may result in highly conservative predictions. To investigate this, the allometric assessment was repeated using FMIs calculated from measured field metabolic rates in free-living animals (Nagy, 2001) that were representative of the organisms being modelled (Table 5.5) and more organism-specific literature-derived B_{iv}s (Table 5.6), the most comprehensive source available being the terrestrial transfer database from ERICA (Beresford et al., 2008d). In total, four assessments were undertaken using RESRAD-BIOTA to predict activity concentrations and dose rates for:

1. All site-specific organisms using RESRAD-BIOTA default B_{iv}s (hereafter this assessment is referred to as RESRAD-BIOTA 1);

And for sub-set of site-specific organisms (birds, mammals and reptiles) using:

2. RESRAD-BIOTA's allometric function to calculate FMIs and using default B_{iv}s for the invertebrate and plant dietary components (hereafter this assessment is referred to as RESRAD-BIOTA 2);
3. FMIs from Nagy (2001) and default B_{iv}s for the invertebrate and plant dietary components (hereafter this assessment is referred to as RESRAD-BIOTA 3); and
4. FMIs from Nagy (2001) and ERICA CRs for the invertebrate and plant dietary components (hereafter this assessment is referred to as RESRAD-BIOTA 4).

Table 5.6. Transfer parameters used to define transfer to dietary components for RESRAD-BIOTA allometric assessment

Radionuclide	Plant BIV[a]	ERICA Tool CR[b, c]	Invertebrate BIV[a]	ERICA Tool CR[b] Diet 1[d]	Diet 2[e]	Diet 3[f]
^{241}Am	7.64E-03	4.96E-03	4.00E-03	1.33E-01	1.01E-01	9.99E-02
^{137}Cs	9.50E+00	6.93E-01	1.10E+02	8.87E-02	1.34E-01	8.94E-02
^{238}Pu	1.00E-02	1.44E-02	3.25E-03	5.99E-02	3.88E-02	2.90E-02
^{239}Pu	1.47E-02	1.44E-02	3.00E-03	5.99E-02	3.88E-02	2.90E-02
^{90}Sr	3.84E+00	2.07E-01	7.58E+01	1.69E-01	4.07E-01	8.97E-03
^{99}Tc	8.00E+00	2.00E+01	3.48E+00	3.70E-01	3.70E-01	3.70E-01

[a] used in RESRAD-BIOTA 2 & 3; [b] used in RESRAD-BIOTA 4; [c] CR for 'grasses and herbs'; [d] mean of the ERICA Tool CRs for 'gastropod', 'soil invertebrate' and 'detritivorous invertebrate' to be representative of invertebrate dietary component for *A. crecca*, *A. fragilis*, *A. platyrhynchos*, *A. sylvaticus* and *S. araneus*; [e] ERICA Tool CR for 'detritivorous invertebrate' to represent dietary intake of *L. vivipara*; [f] ERICA Tool CR for 'soil invertebrate' to represent dietary intake of *T. europaea*.

5.4.4. ERICA

This is the most recently developed of the three models. It follows a tiered assessment structure (from conservative screening to probabilistic modelling assessments), which is supported by a software programme with a detailed help function (the ERICA Tool), a guidance document (Beresford et al., 2007d), and databases on radionuclide transfer, dose conversion coefficients and radiation effects. Case study testing (Beresford & Howard, 2005; Beresford et al., 2007f) and comments from potential future users were used during the development of the ERICA Tool to improve its' functionality and user friendliness (Zinger et al., 2008b) so, to an extent, this model benefitted from a process of 'informed user' engagement as it evolved.

The August 2007 release of the ERICA Tool was used to run a Tier 3 probabilistic assessment within this study. The ERICA Tool has a 'wizard' to guide the parameterisation of site-specific organisms. This includes a module to calculate the DCCs for new organisms based on user-defined dimensions, removing the need to align organisms to default geometries using the approach adopted for R&D128/Sp1a and RESRAD-BIOTA. Default CR values for appropriate organisms were allocated to the sampled species (see Tables 5.3 and 5.4); where appropriate default CRs were not available, analogous organisms were selected ('gastropod' for caterpillar and 'lichen and bryophyte' for fungi).

Full details of the approach used to parameterise the ERICA Tool for the Drigg dunes assessment are provided elsewhere (Chapter 4; Wood et al., 2008).

5.4.5. Input data for modelling

The models were run using the mean soil activity concentrations in Table 5.1 as the input data. However, although ^{239}Pu and ^{240}Pu were reported as a combined activity concentration in the soil, RESRAD-BIOTA and R&D128/Sp1a only include ^{239}Pu in their default lists of radionuclides. For these two models, the $^{239+240}$Pu soil data were entered as ^{239}Pu. The ERICA Tool includes both ^{239}Pu and ^{240}Pu in the default radionuclide list so it was necessary to decide how to enter the combined soil activity concentration reported. Reviewing the DCCs for the ERICA Tool default terrestrial reference organisms shows ^{240}Pu to have numerically higher DCCs so, in order to make an assessment conservative, it would be appropriate to input the combined activity concentrations as ^{240}Pu. However, for the purposes of this intercomparison exercise, it was decided to input the data as ^{239}Pu to allow direct comparison between the absorbed dose rate predictions made using the three models.

Two of the other radionuclides to be modelled (^{238}Pu and ^{99}Tc) were not in the R&D128/SP1a default list for the terrestrial ecosystem. For ^{238}Pu, the CFs and DPUCs for ^{239}Pu were used whilst for ^{99}Tc, ^{137}Cs was used as an analogue. This selection of radionuclide analogues is based on the guidance given by Copplestone et al. (2003) and is in agreement with the approach adopted by the model developers for an intercomparison exercise on activity concentration predictions (Beresford et al., 2008a).

5.5. Results

The data were analysed graphically (Figures 5.1 – 5.7), with model predictions being compared to measurement data where available. This approach is in line with that adopted in some other model intercomparison exercises (e.g. Davis et al., 1999).

5.5.1 Activity concentrations

The biota whole-body activity concentration data (measurements and model predictions) are presented by radionuclide in Figures 5.1 – 5.5. The measured mean activity concentrations presented were calculated using the methodology described in Chapter 4, with limit of detection (LOD) values being treated as absolute values for the purposes of calculation. In some instances the results of RESRAD-BIOTA 2 are not visible on the

figures. This occurred when the predicted activity concentration from RESRAD-BIOTA 2 was either numerically very close to or the same as the predicted activity concentration from RESRAD-BIOTA 3 for a particular radionuclide-organism combination.

Measured ^{241}Am activity concentrations were either accurately predicted (considered here to be within an order of magnitude) or under-predicted by all models (Figure 5.1). Under-predictions for ^{241}Am in the graminaceous species (*A. arenaria* and *F.rubra*) were particularly notable, especially the R&D128/Sp1a predictions which were three orders of magnitude lower than the mean measured data. RESRAD-BIOTA 1 – 4 generally under-predicted by one or more orders of magnitude the ^{241}Am activity concentrations in all organisms. The ERICA Tool and R&D128/Sp1a predicted activity concentrations that were closer to the measured activity concentrations in the animals, *C. portentosa*, *R. canescens* and fungi; the ERICA Tool tending to slightly under-predict (although the data were largely in the predicted 90th percentile range) and R&D128/SP1a tending to slightly over-predict. The data for rodents were an exception to this trend, with R&D128/Sp1a under-predicting the ^{241}Am activity concentrations by three and four orders of magnitude for *T. europaea* and *S. araneus* respectively.

RESRAD-BIOTA 1 – 3 consistently over-predicted the measured ^{137}Cs activity concentrations in all biota groups, with the predictions exceeding those of both ERICA and R&D128/SP1a for all but *V. berus* (Figure 5.2). RESRAD-BIOTA 4 predictions were in better agreement with the measured data, especially for *A. fragilis* and *S. araneus*. R&D128/SP1a predicted ^{137}Cs activity concentrations in plants, *C. portentosa* and fungi which most closely matched the measurement data. The R&D128/SP1a predictions for rodents were also in particularly good agreement with the measurement data but the activity concentrations for the other animals were over-estimated by approximately two orders of magnitude. ERICA predictions were in good agreement with measurement data for invertebrates, amphibians and the two species of fungi in which the highest ^{137}Cs activity concentrations were measured (175 Bq kg^{-1} fw in *Marasmius sp* and 159 Bq kg^{-1} fw in *Rhodophyllus sp*).

(a)

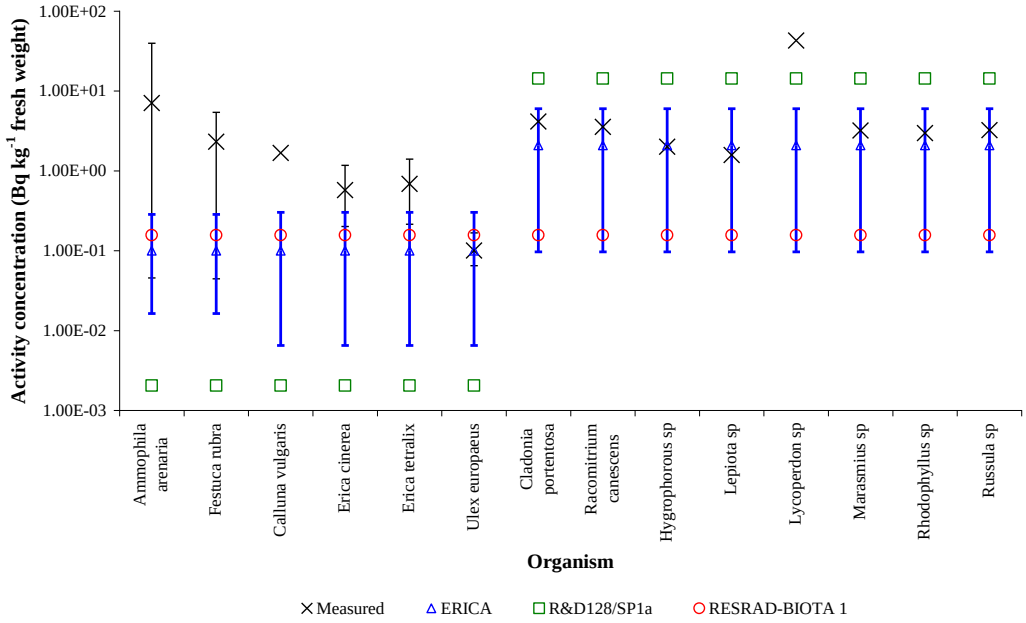

(b)

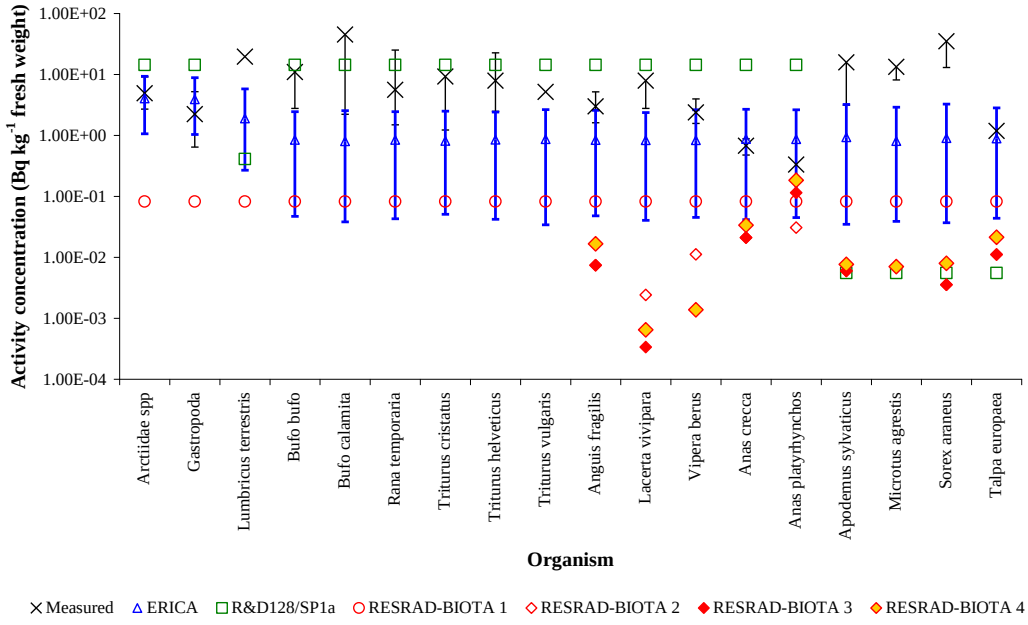

Figure 5.1. Measured and predicted ^{241}Am activity concentrations in (a) plants, lichen and fungi; and (b) animals from the Drigg coastal sand dunes. Error bars indicate minimum and maximum values for measured data (thin lines) and 5th and 95th percentiles for the ERICA Tool predictions (thick lines).

(a)

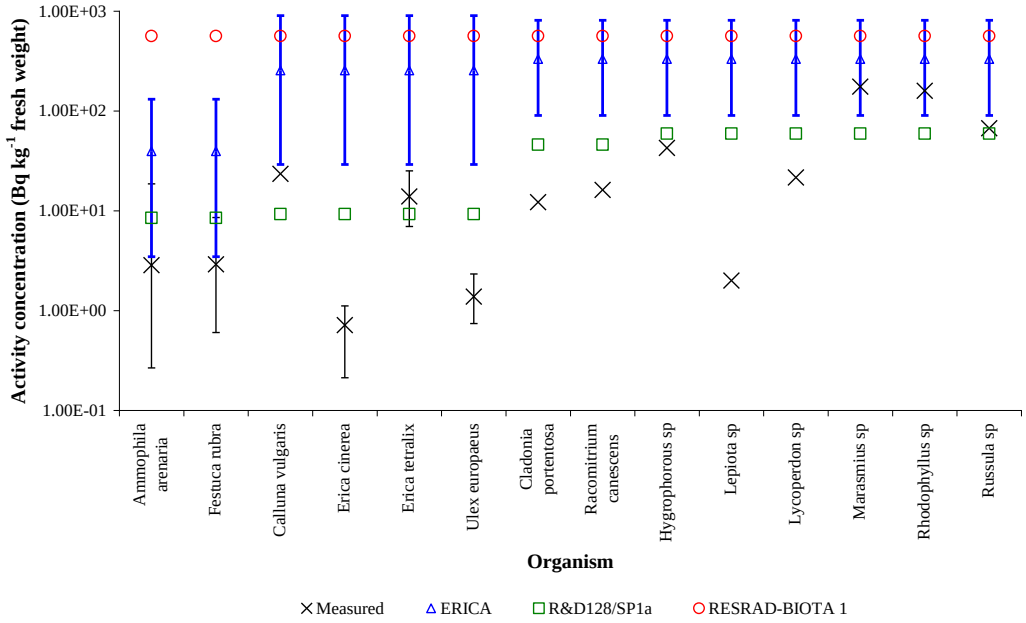

(b)

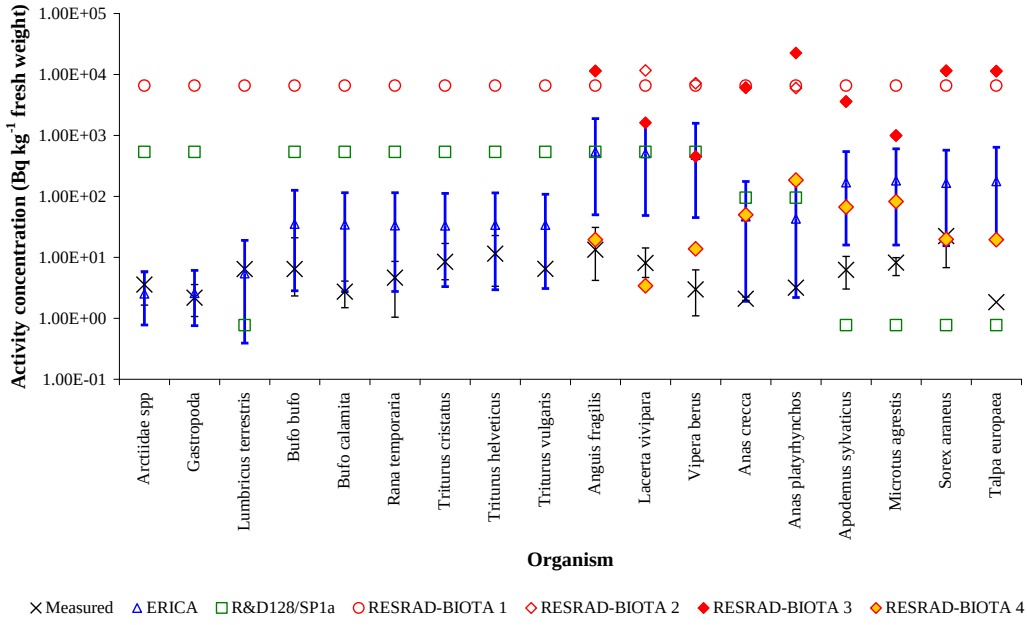

Figure 5.2. Measured and predicted ^{137}Cs activity concentrations in (a) plants, lichen and fungi; and (b) animals from the Drigg coastal sand dunes. Error bars indicate minimum and maximum values for measured data (thin lines) and 5th and 95th percentiles for the ERICA Tool predictions (thick lines).

(a)

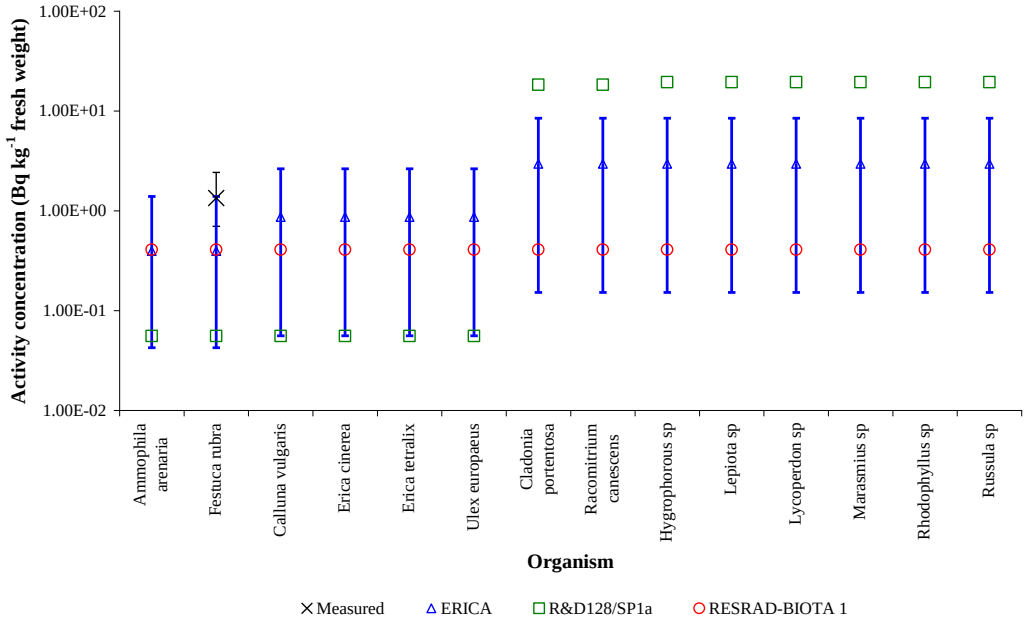

(b)

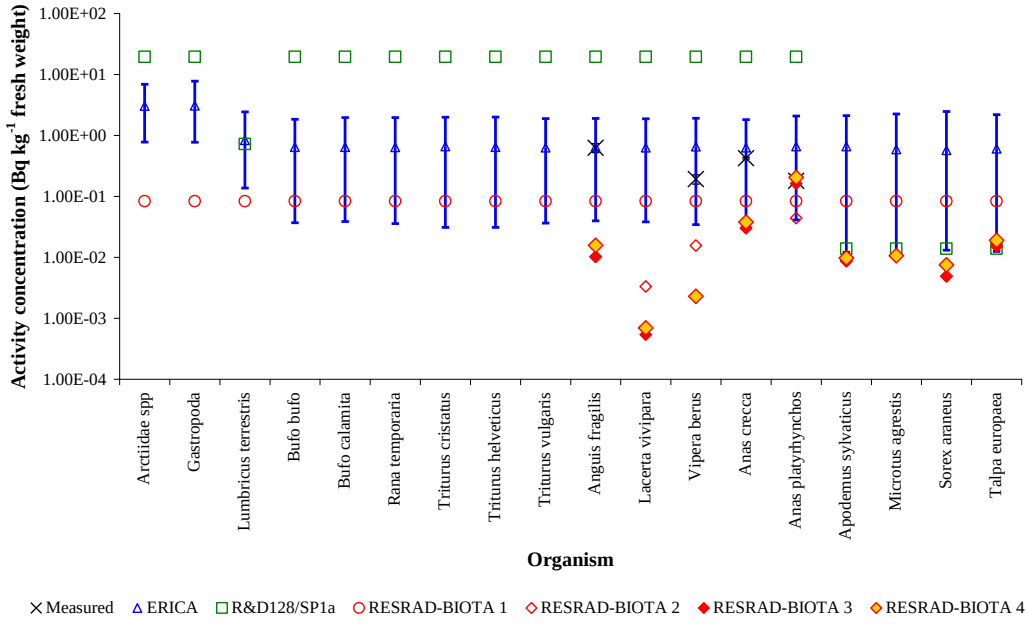

Figure 5.3. Measured and predicted $^{239+240}$Pu activity concentrations in (a) plants, lichen and fungi; and (b) animals from the Drigg coastal sand dunes. Error bars indicate minimum and maximum values for measured data (thin lines) and 5th and 95th percentiles for the ERICA Tool predictions (thick lines).

(a)

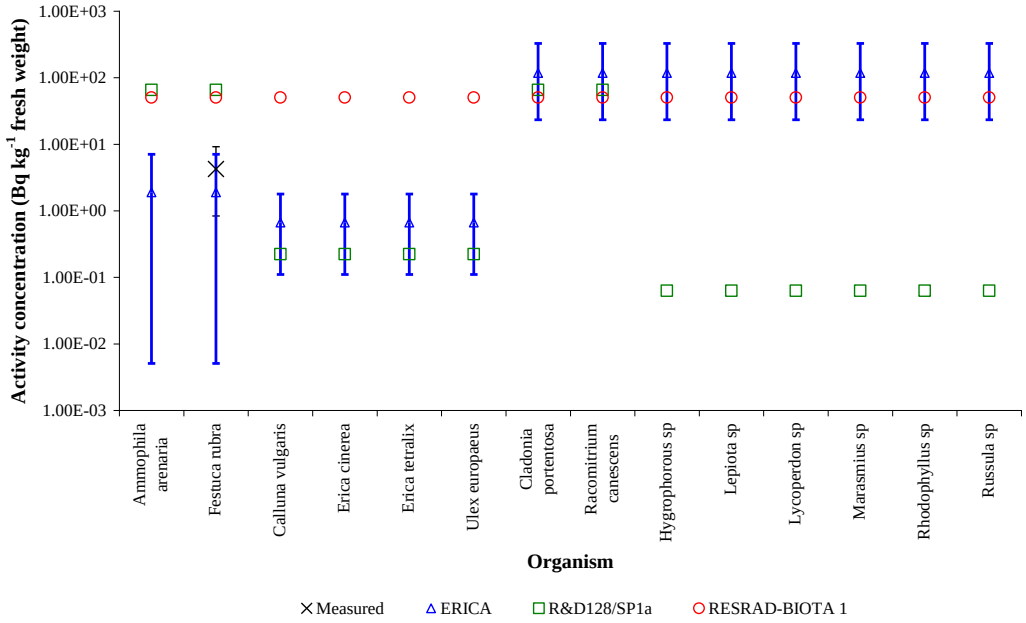

(b)

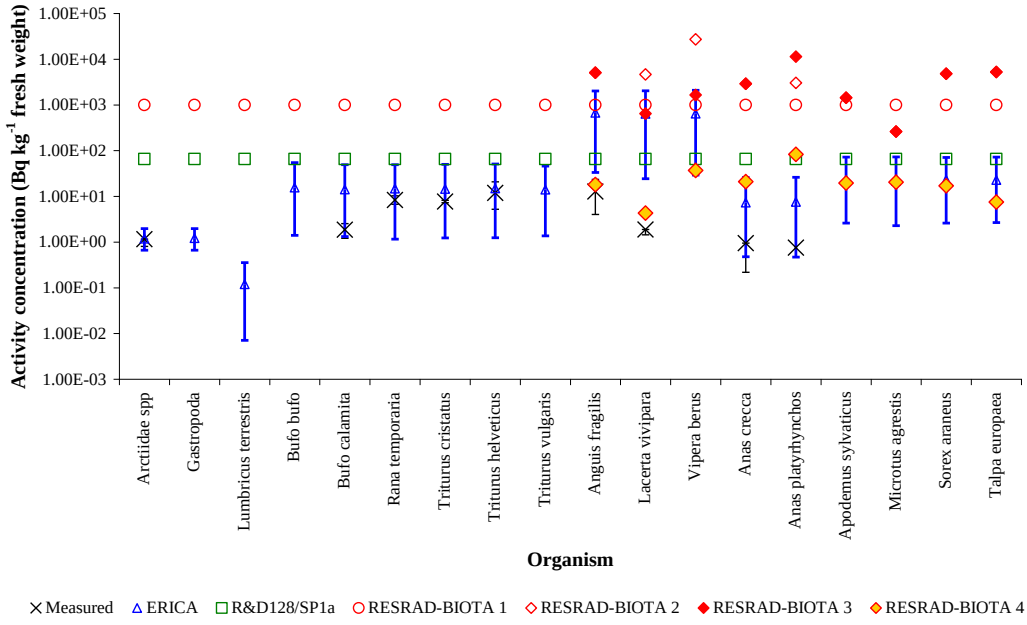

Figure 5.4. Measured and predicted ^{90}Sr activity concentrations in (a) plants, lichen and fungi; and (b) animals from the Drigg coastal sand dunes. Error bars indicate minimum and maximum values for measured data (thin lines) and 5th and 95th percentiles for the ERICA Tool predictions (thick lines).

(a)

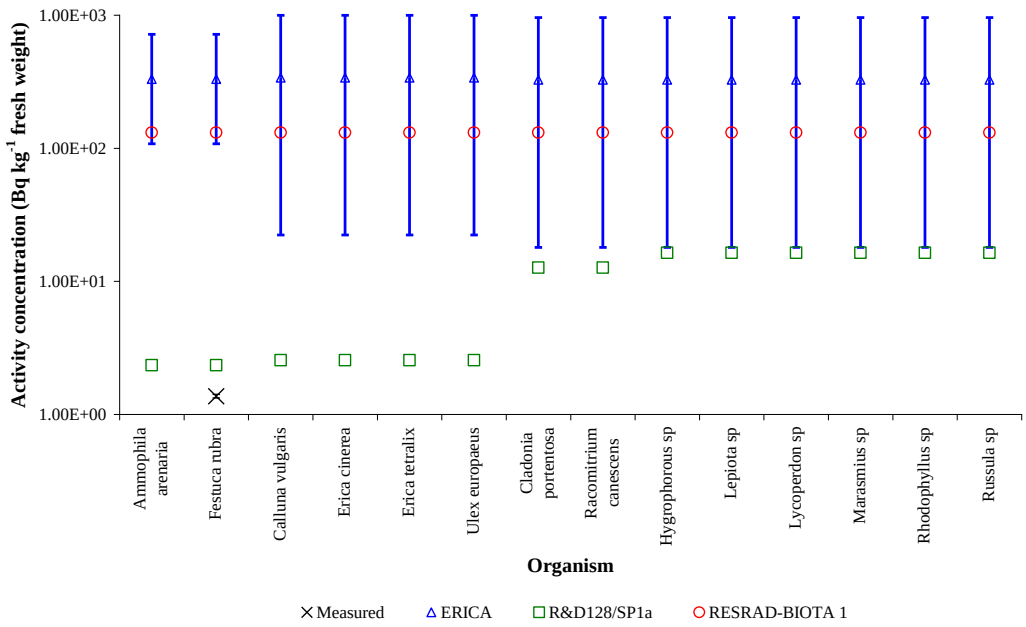

(b)

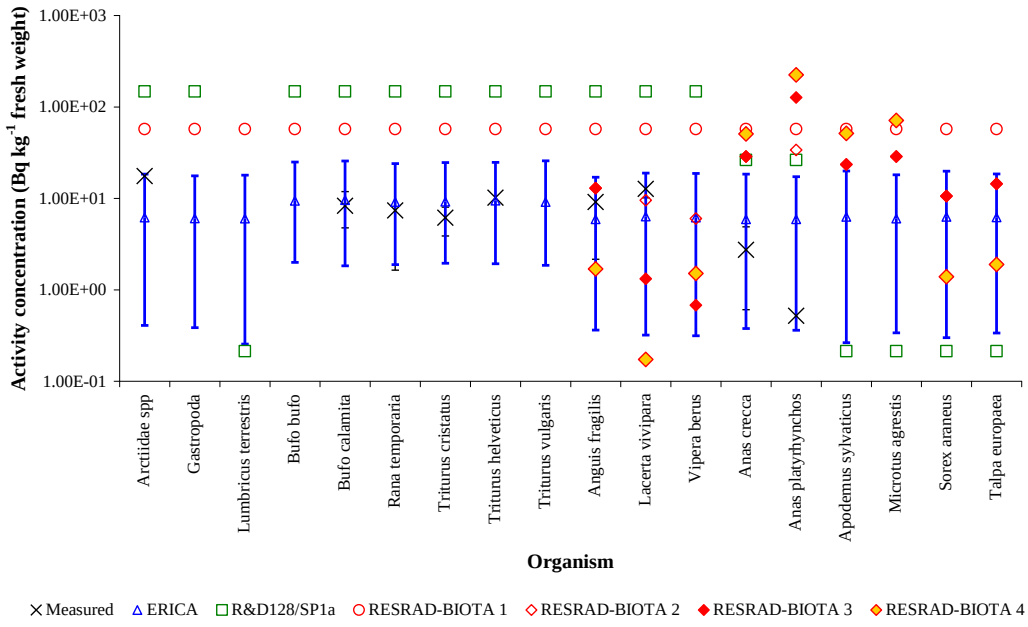

Figure 5.5. Measured and predicted ^{99}Tc activity concentrations in (a) plants, lichen and fungi; and (b) animals from the Drigg coastal sand dunes. Error bars indicate minimum and maximum values for measured data (thin lines) and 5th and 95th percentiles for the ERICA Tool predictions (thick lines).

(a)

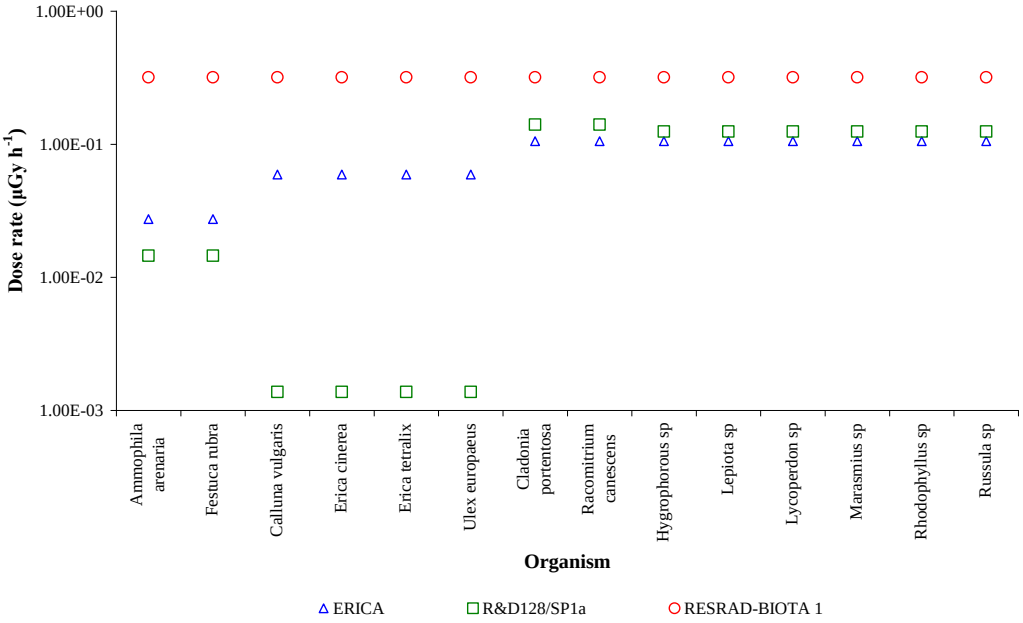

(b)

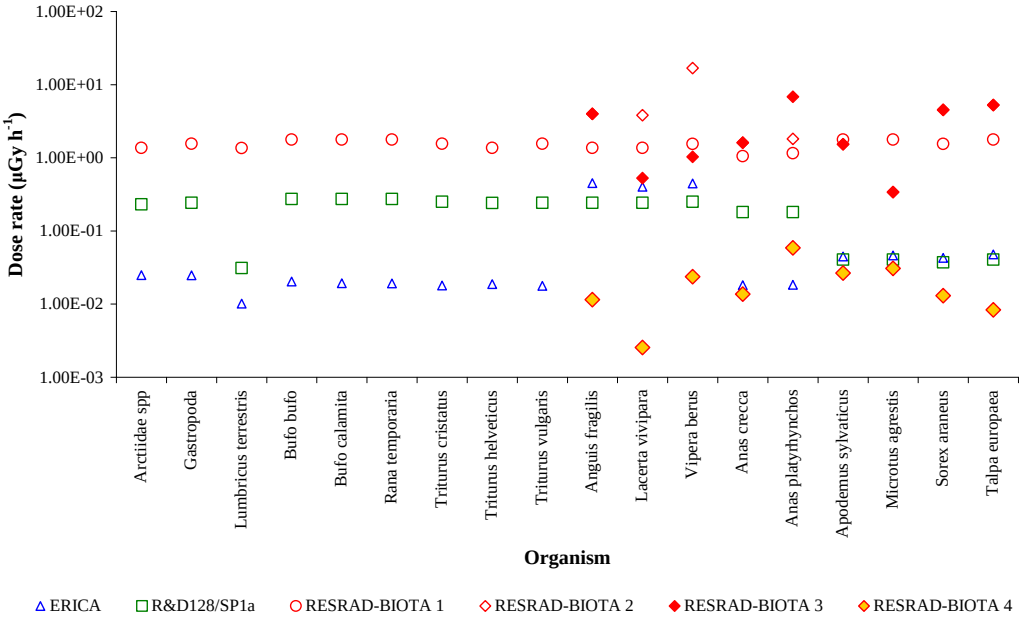

Figure 5.6. Predicted internal unweighted absorbed dose rates for (a) plants, lichen and fungi; and (b) animals from the Drigg coastal sand dunes.

(a)

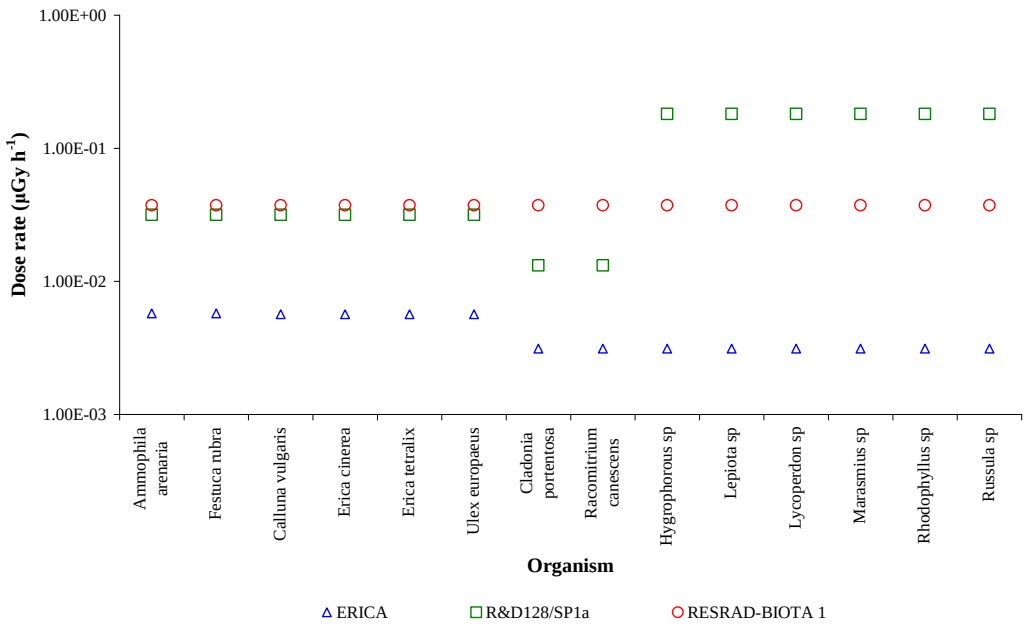

(b)

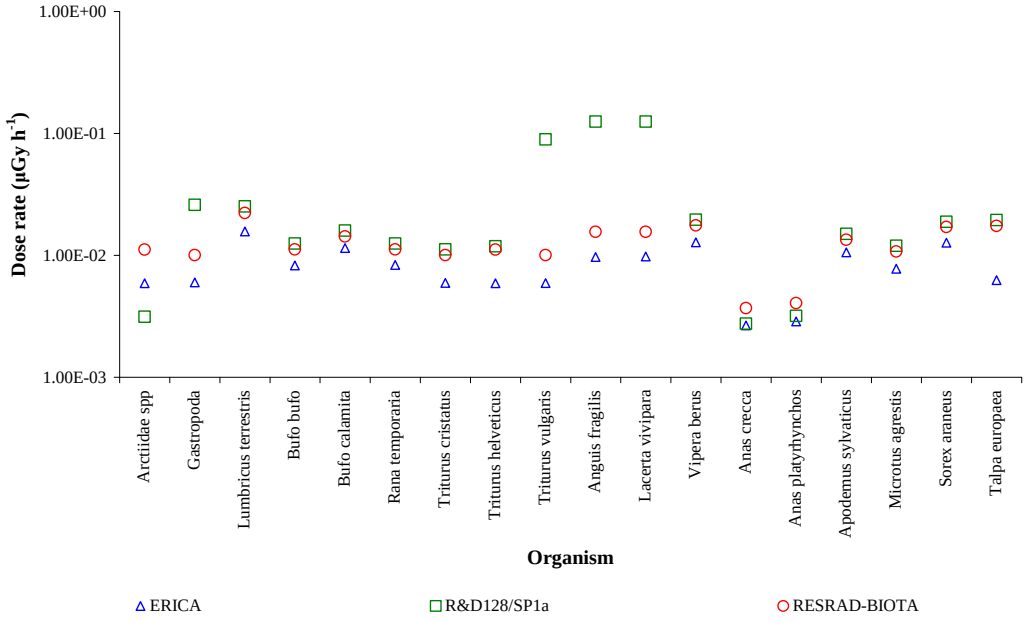

Figure 5.7. Predicted external absorbed dose rates for (a) plants, lichen and fungi; and (b) animals from the Drigg dunes. External dose rates were the same for all four RESRAD-BIOTA assessments so only one set of data for RESRAD-BIOTA is presented.

The ERICA Tool and R&D128/Sp1a used the same model-specific transfer parameters for ^{238}Pu as for $^{239+240}$Pu. RESRAD-BIOTA adopted B_{iv}s of 1.00 x 10^{-2} (^{238}Pu) and 1.47 x 10^{-2} (^{239}Pu) for Terrestrial Plant and 3.25 x 10^{-3} (^{238}Pu) and 3.00 x 10^{-3} (^{239}Pu) for Terrestrial Animal but the reason for the relative differences was unclear. The B_{iv} for ^{238}Pu was higher than ^{239}Pu for the Terrestrial Animal but lower for the Terrestrial Plant suggesting that the difference was not attributable to differences in half-life or some systematic decision taken by the model developers in the default B_{iv} database parameterisation. However, the differences in the B_{iv}s for the two isotopes are small so, on a model-by-model basis, the parameters used to define transfer of $^{239+240}$Pu to biota are a good approximation for those used to define the transfer of ^{238}Pu. As a result, the model predictions presented for $^{239+240}$Pu within Figure 5.3 are also representative of comparisons for ^{238}Pu.

Model predictions for the plutonium isotopes showed the same relative trends between the models as those noted for ^{241}Am, with RESRAD-BIOTA predicting the lowest activity concentrations and R&D128/SP1a the highest for all animals with the exception of rodents and *L. terrestris*. There were fewer measurement data for the plutonium isotopes than for ^{241}Am but the relationships between modelled and measured activity concentrations of ^{238}Pu and $^{239+240}$Pu were broadly comparable with those described for ^{241}Am. R&D128/SP1a notably under-predicted the activity concentration in the graminaceous species *F. rubra* but the magnitude of the under-prediction was lower than that seen for ^{241}Am (Figure 5.1).

Predicted ^{90}Sr activity concentrations (Figure 5.4) differed by up to four orders of magnitude in the animals (*L. terrestris*) and the fungi. In general, RESRAD-BIOTA 1 – 3 predicted the highest ^{90}Sr activity concentrations in animals and the ERICA Tool and RESRAD-BIOTA 4 predicted the lowest activity concentrations. For the plants and fungi, the trends in the relative predictions of the different models varied by organism group. R&D128/Sp1a and RESRAD-BIOTA 1 predicted similar activity concentrations in the graminaceous species but these were in excess of the predictions made by the ERICA Tool, which most closely matched the limited measurement data available. Shrub activity concentration predictions were comparable for ERICA and R&D128/SP1a but these were two orders of magnitude lower than the RESRAD-BIOTA 1 predictions. All three models predicted similar activity concentrations for the *C. portentosa* and *R. canescens*. Fungi activity concentration predictions were comparable for ERICA and RESRAD-BIOTA 1 but the R&D128/SP1a predictions for fungi were four orders of magnitude lower. In general, ERICA and RESRAD-BIOTA 4 predictions most closely matched the measurement data available with R&D128/Sp1a and RESRAD-BIOTA 1 – 3 predicting activity concentrations in excess of the measured values.

There was a consistent trend in the ^{99}Tc activity concentration predictions for plants *C. portentosa, R. canescens* and fungi, the ERICA Tool predicted activity concentrations approximately twice those of RESRAD-BIOTA 1 and the R&D128/SP1a predictions were one to two orders of magnitude below these (Figure 5.5). For invertebrates, amphibians and reptiles, R&D128/SP1a predicted the highest activity concentrations in general but for birds and small mammals the highest predictions were from RESRAD-BIOTA. Overall, the ERICA Tool predictions most closely matched the measured data for the animals and R&D128/Sp1a most closely predicted the *F. rubra* activity concentration.

5.5.2 Dose rates

Similar variability (two or more orders of magnitude) was seen in the internal and external dose rate predictions (Figures 5.6 & 5.7 respectively), with the greatest variation occurring in the internal dose rate predictions.

RESRAD-BIOTA 1 – 3 predicted the highest internal dose rates for all organisms. In general, the lowest internal dose rates were predicted by the ERICA Tool and RESRAD-BIOTA 4. A notable exception was the low internal dose rates for shrubs predicted by R&D128/SP1a but the shrub internal dose rate was dominated by the dose rate from ^{137}Cs and R&D128/SP1a predicted ^{137}Cs activity concentrations in shrubs that were two orders of magnitude below the activity concentrations predicted by the ERICA Tool and RESRAD-BIOTA.

The predicted external dose rates for almost all of the organisms within the Drigg coastal sand dunes assessment were dominated by ^{137}Cs. Differences in the dose rates predicted could therefore be attributed to differences in the dosimetry parameters (DCC/DPUC/DCF) being applied within each model for the animal predictions and differences in both the dosimetry and the default habitat utilisation parameters (OF, GF and AF) for the plant, *C. portentosa* and fungus predictions. The exceptions to this were the R&D128/SP1a external dose rate predictions for gastropoda, *T. vulgaris, A. fragilis* and *L. vivipara*. These dose rate predictions were dominated by $^{239+240}$Pu and ^{241}Am rather than ^{137}Cs. In general, there was a good agreement across models for most of the animal total external dose rate predictions. Predictions for plants, *C. portentosa* and fungi were more variable, especially those for fungi.

5.6. Discussion

5.6.1. Model predictions

5.6.1.1. Model predictions and 'fitness-for-purpose'

Models used in human radiation protection are known to produce differing results and there have been a number of internationally led exercises (e.g. Validation of Environmental Model Predictions (VAMP), Biospheric Model Validation Study (BIOMOVS) and Biosphere Modelling and Assessment (BIOMASS)) to understand the underlying reasons for these differences (Linsley & Torres, 2004). This work has now been extended into biota dose assessment models and similar variation has been observed (Beresford et al., 2008f). The orders of magnitude variation in activity concentration and dose rate predictions found in this study are consistent with the results reported for other intercomparison exercises on radionuclide transfer (e.g. Beresford et al., 2008a; Davis et al., 1999) and biota dosimetry (e.g. Vives i Batlle et al., 2007). Although this degree of variation has been reported in other studies, it is perhaps disconcerting that such variation exists. The international efforts to better understand the causes of this variation will hopefully improve the consistency[24] and/or better define the scope of application of each model.

The three publicly available models discussed in this chapter have the same basic objective, to predict radiation doses to biota. However, R&D128/Sp1a and RESRAD-BIOTA were developed to address specific national requirements, whereas the ERICA Tool was developed to be applicable within the European context. These differences in scale are reflected in the effort which was applied to the development of the individual models. As described above, the three models in this study have adopted slightly different approaches. R&D128/Sp1a, the first of the three models to be released into the public domain, provides a relatively simple tool that was intended to achieve a balance between realistic and conservative assessments. The ERICA Tool and RESRAD-BIOTA use a tiered (or graded) assessment approach, with lower tiers being conservative 'screening' tiers and higher tiers being used for more realistic assessment. Therefore, it is evident that, when selecting models and when evaluating the results of specific models relative to measured data and other model predictions, consideration must be given to the purposes for which the models

[24] For example, one of the working groups within the second phase of the International Atomic Energy Agency's Environmental Modelling for Radiation Safety programme is developing a handbook of generic radionuclide transfer parameters for wildlife.

were designed and are intended to be used and, in the case of the ERICA Tool and RESRAD-BIOTA, the assessment tier used.

For the model predictions presented in this chapter, R&D 128/SP1a and RESRAD-BIOTA 1 were expected to provide conservative predictions suitable for screening assessments because they use purposefully conservative transfer parameters. RESRAD-BIOTA 2 and RESRAD-BIOTA 3 were also expected to result in conservative predictions because, although they utilise the kinetic-allometric functionality of RESRAD-BIOTA, the food source activity concentrations which are used in the calculation of the ingested activity are based on the default B_{iv}s and should be highly conservative as a result. The ERICA Tool and RESRAD-BIOTA 4 were expected to result in the most realistic predictions because both incorporate mean measured organism-specific CRs from the ERICA Tool transfer database for terrestrial biota, although it is recognised that in some instances this database has been populated using a 'guidance' methodology where measurement data for specific radionuclide-organism combinations are lacking (see Beresford et al., 2008d).

As expected, R&D128/SP1a and RESRAD-BIOTA 1 were found to be generally conservative in their predictions when compared to the measured data. However, there were some anomalies, such as the very good agreement between the R&D128/SP1a predictions and the measured data for ^{137}Cs in rodents and the under-prediction of actinides in the graminaceous species.

The derivation of the R&D128/Sp1a CF for ^{137}Cs transfer to rodents has been commented on in another intercomparison exercise (Beresford et al., 2008a) in which it was noted that the R&D128/SP1a predictions for ^{137}Cs activity concentrations in rodents were much lower than those of other participating models (including the ERICA Tool and RESRAD-BIOTA). The reason for this is that the CF was derived from measured activity concentrations in specimens of *M. agrestis* that were collected from a small coastal sand dune system adjacent to the Sellafield site (see Chapter 6). Whilst this results in comparatively low predictions from R&D128/SP1a relative to other models, it also explains the good agreement of the R&D128/SP1a predictions with the measured rodent ^{137}Cs activity concentrations from the Drigg coastal sand dunes because the CF is specific to both this ecosystem type and geographical region.

The likely explanation for the under-prediction of ^{238}Pu, $^{239+240}$Pu and ^{241}Am in the graminaceous species is that the sea-to-land transfer mechanism, which is more efficient at transporting the highly particle-reactive actinides than other radionuclides such as ^{137}Cs

(Bryan et al., 2008), is causing an accumulation of actinides on the surface of sand dune vegetation and the sample analysis process does not discern between surface-bound activity and that within the plant tissues (Wood et al., 2008). The reason for the general under-prediction by all three models of ^{241}Am activity concentrations in rodents is less clear. This is not due to surface contamination or material within the gut because the rodents had their pelts and gastrointestinal tracts removed prior to analysis. It is possible that the elevated actinide activity concentrations on the surface of the vegetation, relative to the activity concentrations that may be expected from root uptake alone, are resulting in a higher than expected transfer of actinides up the food chain. However, given that the apparent ^{241}Am transfer to rodents may be lower in coastal sand dunes than in many other terrestrial ecosystems (Wood et al., 2009a), it is likely that this under-prediction is an artefact of the inclusion of a high number of LOD values in the calculation of the mean ^{241}Am activity concentrations in the rodent species collected from the Drigg sand dunes.

Observed under-predictions of radionuclide transfer may present a problem when trying to convince stakeholders that a model is 'fit-for-purpose' but the magnitude of some of the over-predictions is also of concern. This is particularly the case for the ^{137}Cs predictions because ^{137}Cs accounts for a major proportion of unweighted internal dose rates predicted for many of the organisms under assessment. Regulatory application of models and formulation of management decisions needs to be underpinned by confidence in the assessment process and results. Just as under-predictions can reduce stakeholder confidence in assessments through the possibility that sites requiring further assessment may not be identified, large over-predictions can also undermine the assessment process, fostering potential criticism regarding hyper-conservatism and resultant resource expenditure on site assessments and, potentially, regulation. A balance between conservatism and realism is required and the ^{137}Cs results suggest that RESRAD-BIOTA, and to an extent R&D128/SP1a, are not achieving that balance within the context of the sand dunes due to the default transfer parameters used. However, an experienced assessor should be able to identify a strategy for refining the assessment in step-wise manner to identify whether there is expected to be a real measurable impact on biota at the site in question and this information can be used as an input into the process of determining the appropriate actions to be taken to mitigate this impact.

With the exception of a few ^{241}Am results, the ERICA Tool either accurately predicted (within the 5th and 95th percentile range) or conservatively predicted the activity concentrations measured in biota. The most notable ERICA Tool over-predictions are for ^{137}Cs in plants, fungi and reptiles and ^{90}Sr in reptiles.

The over-prediction of ^{137}Cs and ^{90}Sr in reptiles is due to an error that the author has identified in one of the data sources used within the ERICA Tool to derive the CRs for this organism group. Correcting this error results in the ERICA Tool CRs which produce predictions that are similar to the measured data presented in this chapter. The corrected[25] Cs and Sr CRs for reptiles (4.23×10^{-1} and 3.38×10^{-1} respectively) will appear in the next release of the ERICA Tool transfer database and the derivation of these values is presented in Barnett et al.(2009).

The ERICA Tool predicted higher Cs concentrations in the fungi because this organism group does not have a corresponding reference organism within the ERICA Tool so the CRs for 'lichen and bryophyte' were used to represent fungi within the ERICA Tool assessment presented here. Lichen are known to be particularly effective at accumulating Cs (Machart et al., 2007) so the higher ERICA Tool predictions for fungi are to be expected.

The reason for the high ERICA ^{137}Cs predictions for plants compared to R&D128/Sp1a can be explained by the difference in the transfer parameters used within the two models due to the known low transfer of ^{137}Cs to vegetation from sand (IAEA, in press) and the geographical regions for which the models were developed. R&D128/SP1a was designed for use in England and Wales so, where possible, the model developers parameterised the model with measured data from that region, which included data from West Cumbria for sand dune biota. The ERICA Tool was designed for a much wider geographic application and, as a result, the selection of measurement data to include within the transfer parameter derivation was less constrained. The consequence of using this larger data set to derive the ERICA Tool transfer parameters is that higher mean transfer values have been calculated for Cs transfer to plants. Other work has shown that the apparent transfer of Cs in coastal sand dunes may be lower than at other terrestrial sites (Wood et al., 2009a) so it may be that the ERICA Tool CR for plants is derived from a dataset that includes more data from higher Cs transfer terrestrial sites than the database used to derive the R&D128/Sp1a CFs. Subsequent discussions have confirmed that there is a bias in the ERICA Tool database towards sites with organic soil due to the quantity of data available for these sites relative to other terrestrial sites (Nick Beresford, Centre for Ecology and Hydrology, pers. comm.). This potentially highlights the need for the future development of more ecosystem-specific transfer databases, providing separate transfer parameters for woodlands and grasslands for example, rather than combining the data into generic transfer parameters for terrestrial,

[25] The corrected values quoted include some additional reptile data from Chernobyl in their derivation.

freshwater and coastal/marine systems. However, this is likely to require substantial targeted field research to provide sufficient underpinning datasets to justify the calculation of more ecosystem-specific transfer values rather than generic values (Sheppard, 2005), especially when, for organism groups such as reptiles, the available data for constructing even a generic terrestrial transfer database are very limited (see Chapter 7).

When transfer parameters are lacking, the guidance given within the ERICA Tool and R&D128/SP1a supporting documentation for filling gaps in the transfer databases appears to be 'fit-for-purpose' in the context of the assessment presented in this chapter. Where guidance values are used they result in over rather than under-predictions. For example, for ^{99}Tc, all of the R&D128/SP1a predictions were based on the CFs for ^{137}Cs and the ERICA Tool predictions for reptiles were based on the ^{99}Tc CR for 'mammal' (although the ERICA Tool database now includes a CR for ^{99}Tc transfer to 'amphibian' (5.75×10^{-1}) which is higher than that for 'mammal' (3.70×10^{-1}) so, following the guidance given in Beresford et al. (2008b), future assessments should use this 'amphibian' value for reptiles). In the absence of data for certain radionuclide-organism combinations, these over-predictions increase confidence that assessments will not result in a decision to take no further action when further action may in fact be necessary.

Recognising the variability in activity concentration predictions by the models, it is perhaps surprising that there is relatively good agreement in the total internal absorbed dose rates predicted for many organisms, especially between R&D128/SP1a and the ERICA Tool. This phenomenon has been observed in other intercomparison exercises (Beresford et al., 2008f) and appears to be largely due to a 'balancing out' of under-predictions and over-predictions of the transfer of different radionuclides by the different models and to a lesser extent differences in the dosimetry parameters (DCCs, DCFs and DPUCs) applied to each organism.

The external dose rate predictions are generally in good agreement between the models but the notable differences in the R&D128/SP1a estimates for *T. vulgaris, A. fragilis, L. vivipara* and, to a lesser extent, gastropoda, require explanation. Investigating the proportional contribution of the different radionuclides to the total external dose rates predicted using R&D128/SP1a revealed that the external dose rates to these four organisms were dominated by ^{241}Am and $^{239+240}$Pu whereas for other animals the major contributor to external dose rate was ^{137}Cs. The reason for this is that these four organisms were aligned to the 'fungi' reference organism geometry for derivation of the DPUCs. The 'fungi' had default external alpha DPUCs of 2.97×10^{-3} for ^{239}Pu and 3.16×10^{-3} for ^{241}Am, whereas all

other R&D128/SP1a reference organisms that were used to provide DPUCs in this intercomparison exercise had external alpha DPUCs of zero. The author is aware that the DPUCs for 'fungi' are actually intended to conservatively predict the dose to the fungal mycelium based on the assumption that the small size of the hyphae allows alpha particles to be fully absorbed within the cells. However, the reported dimensions for 'fungi' in R&D128/Sp1a are for the fruiting body and consequently 'fungi' were included in the geometry alignment process. It was not clear within R&D128/SP1a that this would mean that the DPUCs for ^{239}Pu and ^{241}Am would not be zero (as would be expected). The gastropoda external dose rate prediction (which assumes the 'fungi' DPUC) is less affected than the predictions for *T. vulgaris, A. fragilis, L. vivipara* because of the lower soil OFs for gastropoda (Table 5.4).

It was noted that the ERICA Tool total external dose rate predictions for many of the animals (Figure 5.7) were lower than those from R&D128/SP1a and RESRAD-BIOTA. The reason for this is that the contribution of ^{90}Sr to the total external dose rate was lower in the ERICA Tool, probably due to shielding by skin/fur being considered in the derivation of the external DCCs within the ERICA Tool (Ulanovsky et al., 2008).

Overall, although there are some anomalies that have been highlighted and discussed when comparing both the relative performance of the models and the differences between measured data and model predictions, the three models appear to be generally 'fit-for-purpose'. Developing more comprehensive transfer databases which model users can access will serve to further strengthen that 'fitness-for-purpose' and help to reduce the uncertainty in the modelling process.

5.6.1.2. Decisions made by the assessor

Throughout this model intercomparison exercise there were a number of decisions that had to be made by the assessor which may be expected to affect the predictions obtained using the different models. Examples include the use of literature-derived mass data for parameterising site-specific organisms and the influence of decisions regarding the methods used for predicting transfer within RESRAD-BIOTA.

The use of different literature sources to derive the mass and dimension data for some organisms resulted in similar organisms appearing to have notably different densities (e.g. *B. bufo* and *B. calamita*). Mass data are not used within R&D128/SP1a but are used in RESRAD-BIOTA for deriving transfer predictions allometrically (Higley et al., 2003) and in the ERICA Tool for deriving the DCCs for site-specific organisms (Ulanovsky et al.,

2008). However, the inconsistencies in mass data used in this study are relatively small and the decisions made regarding the mass data to use within the intercomparison exercise presented here are not thought to significantly influence the predictions obtained from the different models, although this will contribute to the overall assessment uncertainty.

A more significant source of uncertainty within the model predictions is associated with the transfer parameters used and RESRAD-BIOTA 1-4 provide a demonstration of the extent to which assessor decisions regarding transfer can influence the assessment results. It is recognised that the default B_{iv}s used within RESRAD-BIOTA are for screening purposes and are intended to be conservative as a result so it is unsurprising that RESRAD-BIOTA 1 generally results in higher activity concentration predictions. The relatively minor changes to these predictions when the allometric functionality was invoked (RESRAD-BIOTA 2), even when FMI data from Nagy (2001) were used (RESRAD-BIOTA 3), demonstrate that the dominant influence on the predictions remains the transfer parameters used, which are the parameters to describe transfer to the organism food-source(s) in the case of the allometric assessments. Adopting organism-specific transfer parameters from the ERICA Tool to quantify transfer to the organism food-source(s) (RESRAD-BIOTA 4) generally resulted in predictions which were in better agreement with the measured data, especially for ^{137}Cs. However, if there is a suitable database of transfer parameters available, such as the database within the ERICA Tool, one might question whether an assessor would use the allometric function at all rather than using this database to parameterise all organisms within the assessment.

5.6.2. An informed user perspective on model application

In this intercomparison exercise, the assessment scenario interpretation was the same for all three models (the same assessor applied all three models) and there was consistency in the approach adopted by the assessor for making decisions regarding model parameterisation. Therefore, differences in the model predictions were largely due to differences in the default parameters used within the models (as discussed in section 5.6.1.) and the assessors' interpretation of the models and their accompanying guidance documentation.

From the perspective of an informed user, there were some notable differences in the ease with which the models could be understood and used. These include considerations of both the operation of the model and the model outputs.

The ERICA Tool was the most straightforward model to use because the software has a well-designed Graphical User Interface (GUI) that uses simple screens to guide the assessor

through each stage of the assessment and 'wizards' to enable more complex steps (such as creating a new organism) to be performed. The 'help' function within the ERICA Tool is comprehensive and, for the purposes of conducting the assessment presented here, largely removed the need to refer to the guidance documentation (Beresford et al., 2007d). This is likely to be a reflection of the extent to which informed users were involved in the development of the ERICA Tool.

RESRAD-BIOTA has a purpose-built GUI and integral 'help' function but the process of setting up and running the model was less intuitive than in the ERICA Tool and the 'help' function was relatively limited. As a result it was necessary to rely heavily on the supporting documentation (USDoE, 2004) to guide the assessment process. However, this documentation was written for an earlier version of RESRAD-BIOTA so there were some inconsistencies between the instructions in the documentation and the operation of the software. A potential issue in the operation of RESRAD-BIOTA is the lack of clarity over whether units are fresh weight or dry weight but, for the site considered in this assessment, the soil moisture content was 14% so the users' decision to treat the units as fresh weight or dry weight would have made a relatively small contribution to the uncertainty in model predictions. Although there were areas of ambiguity in the application of RESRAD-BIOTA to the assessment of the Drigg dunes, it should be noted that this is the only one of the three models for which training courses are available for users[26]. It is likely that this additional level of support for users would clarify the areas of ambiguity highlighted here.

R&D128/SP1a uses the familiar user interface of Microsoft® Office Excel but there is little information within the workbook to guide the assessment process and it was necessary to rely heavily on the supporting documentation (Copplestone et al., 2001a; Copplestone et al., 2003). The input sheet is relatively easy to follow and the units are clearly defined. However, the lack of equations for calculating the surface area and volume of ellipsoids is an important omission within the supporting documentation since the method for assigning DPUCs to user-defined organisms is dependent on the assessor calculating the surface area:volume ratio.

All three models produce assessment outputs that can be saved as separate files for future use. The R&D128/SP1a output is a Microsoft® Office Excel workbook for the assessment whereas the ERICA Tool and RESRAD-BIOTA output Hyper Text Markup Language

[26] In 2009, CEH (in association with the Institut de Radioprotection et du Sûreté Nucléaire (IRSN), the Environment Agency and Westlakes Scientific Consulting Ltd) was awarded a Natural Environment Research Council (NERC) knowledge exchange grant to develop and deliver a radiological environmental assessment training programme. This will include training in the use of the ERICA Tool.

(HTML) files. Although the HTML files are easier to print out and keep as a hardcopy record of the assessment, the manipulation of data into a form suitable for further data analysis is more time-consuming than working with the data outputs from R&D128/Sp1a. As with the input data, an important omission from the RESRAD-BIOTA output files is the clarification of whether the units quoted are for dry weight or fresh weight.

The model outputs can provide activity concentration, internal dose rate and external dose rate results for each organism under assessment but only the ERICA Tool and R&D128/SP1a do this by default. In RESRAD-BIOTA it is necessary to run the model twice, once with the ingestion pathway activated within the model (resulting in reported dose rates for each organism which are the total dose rate, i.e. external and internal dose rates combined) and once with the ingestion pathway deactivated (to obtain the external dose rates for each organism). The assessor must then calculate the internal dose rates for each organism by subtracting the external dose rates from the total dose rates. Whilst this is not a complicated procedure, it does detract from the usability of the model. However, it may be questionable as to if the intended users (USDoE site operators) would need to consider contributions to total dose rate.

5.6.3. Radioecological model intercomparison: a strategy for the future

The global community is potentially on the brink of a nuclear renaissance and those tasked with undertaking and evaluating the assessments of environmental impacts that may result from nuclear development need to understand and have confidence in the models used to undertake these assessments. Observations on the relative performance of the different models within this intercomparison exercise make a valuable contribution to the growing knowledge-base associated with this field of radioecological modelling. However, these observations require a caveat, namely that they are valid for the application of the assessment tools to the Drigg coastal sand dunes scenario by a specific assessor. The results obtained by a different assessor may be very different depending on the decisions made during the assessment process and this is demonstrated by the orders of magnitude difference in the results obtained using different parameters for the allometrically-derived predictions (RESRAD-BIOTA 2 – 4).

To improve the current knowledge-base further and provide constructive underpinning evidence to help guide assessors in the selection and application of models there is a need for a paradigm shift in the way in which intercomparison exercises for biota dose assessment models are conducted. The testing of biota dose assessment models undertaken

to date has largely been in the domain of the model developer, which may be appropriate if the model developer is the intended future user, but models, such as the ERICA Tool and RESRAD-BIOTA, have been developed for application by a broad range of users. This chapter has demonstrated that the insights gained through informed user application may provide a more realistic assessment of the way the models could be expected to perform when applied by the wider user community and, through an iterative process of testing and development, could make a significant contribution to improving the available models in addition to the improvements that result from developer-led applications. However, it is recognised that no further development of R&D128/Sp1a will take place because this was an interim approach awaiting the outputs of the EC-funded FASSET (Framework for Assessment of Environmental Impact (Larsson, 2004)) and ERICA projects. The outputs of these projects will be implemented shortly by the original users of R&D128/SP1a (David Copplestone, Environment Agency, pers. comm.).

There is a need to establish intercomparison exercises which focus on user application of models rather than the models *per se*. In these exercises a single model would be applied to a case study scenario by multiple informed users. By standardising both the scenario and the model used, such exercises would provide a more informative insight into the magnitude of the uncertainty introduced by assessor decisions and identify commonalities in 'errors' made by assessors. The findings of such exercises would complement those of other intercomparison exercises which investigate the technical aspects the models (e.g. Beresford et al., 2008a; Vives i Batlle et al., 2007).

The range of case study scenarios used for model intercomparison exercises needs to be expanded. This chapter presents a case study for an ecosystem with an unusual contamination pathway (the sea-to-land transfer mechanism) but there are many other interface ecosystems and ecosystems with unusual contamination pathways that assessors may need to consider. Furthermore, the model testing to date has examined a very limited range of radionuclides and there are many others which need to be considered in assessments of nuclear facilities.

Initiatives like the second phase of the IAEA's EMRAS programme[27] may provide one forum through which this model testing can be developed further.

[27] **http://www-ns.iaea.org/projects/emras/emras2/default.htm**, accessed 12th November 2009.

5.7. Conclusions

Intercomparison exercises are elucidating the commonalities, differences and relative merits of different models for assessing the impact of ionising radiation on biota but, in contrast to human dose assessment, this is a relatively new field of radiation protection. Despite this the models have already been applied successfully in a regulatory context (Allott et al., 2009; Beresford et al., 2008b). Therefore the three models examined in this study have all demonstrated their usefulness for the purpose for which they were developed but it is evident that, when selecting models and when evaluating the results of specific models relative to measured data and other model predictions, consideration must be given to the purposes for which the models were designed and are intended to be used.

This intercomparison exercise has highlighted the value of taking an informed user approach to investigate the way in which models may be expected to be applied in practice and a strategy has been proposed for the future development of intercomparison exercises.

The three models discussed here have been applied successfully to estimate radiation dose rates to biota inhabiting a coastal sand dune system but there is scope for refinement, especially in relation to transfer predictions. There is a need for the future development of more ecosystem-specific transfer databases, as well as transfer parameters for less-studied organisms such as reptiles, to help to reduce the uncertainty in the modelling process. Developing databases for temperate coastal sand dunes and for reptiles is the focus of Chapters 6 – 8 of this thesis.

Although RESRAD-BIOTA includes kinetic-allometric functionality, there are few data available to parameterise this for specific organisms and the biota activity concentration predictions obtained are dependent on the radionuclide transfer assumptions for the prey organisms. Therefore, this kinetic-allometric approach is of little use for undertaking assessments if transfer data are available for the biota groups to be modelled.

Where under-predictions for particular radionuclide-organism combinations have been identified, the relevance of the observed under-predictions should be evaluated in the context of different ecosystem types. Although there are some notable differences between the model predictions and measurement data presented in this study, there is no suggestion that the models are not 'fit-for-purpose'. The differences are a reflection of the idiosyncratic nature of ecosystems and, in this particular case, the atypical principal contamination pathway by which radionuclides are transferred to the coastal sand dunes. However, given the observed variability in predictions, it is recommended that assessors

should, wherever possible, compare assessment predictions with measured data for comparable sites and scenarios.

(This page is left blank intentionally)

CHAPTER 6 – RADIONUCLIDE TRANSFER AT SELLAFIELD COASTAL SAND DUNES

The material presented in this chapter has been published as:

Wood et al., 2009. Radionuclide transfer to invertebrates and small mammals in a coastal sand dune ecosystem. Science of the Total Environment, 407(13), 4062-4074.

6.1. Introduction

The relative performance of the different models available for undertaking radiation impact assessments for non-human biota across a range of ecosystem types and scenarios is being assessed through model validation and intercomparison exercises (e.g. Beresford et al., 2008a; Vives i Batlle et al., 2007; Wood et al., 2009b). The model intercomparison presented in Chapter 5 highlighted the fact that, when applying risk assessment models in the absence of site-specific biota activity concentration data, choices and assumptions made by the assessor regarding radionuclide transfer contribute significantly to the overall uncertainty and variability in the resultant biota activity concentration and dose rate predictions . This is particularly apparent in situations where literature-derived transfer parameters are lacking and the assessor selects transfer parameters using a 'guidance methodology', for example adopting transfer parameters for an organism of similar ecology (Copplestone et al., 2003) or taxonomy (Beresford et al., 2008d), or implementing a kinetic-allometric approach to predict transfer using biological scaling relationships based on organism body mass (Beresford et al., 2004; Higley et al., 2003). Therefore, there is a need to improve understanding of radionuclide transfer within ecosystems and to further develop the radionuclide transfer databases. Coastal sand dunes are one ecosystem for which radionuclide transfer data are lacking (Wood et al., 2008; Wood et al., 2009b). The availability of such data is especially important in the United Kingdom because some of the sites for which radiation impact assessments are required, due to national legislation, are sand dune ecosystems (see Chapter 2; Wood et al., 2008).

This chapter draws on a previously unpublished data set of radionuclide activity concentrations in coastal sand dune biota collected from Northwest England. The spatial and temporal variation in the food chain transfer of ^{137}Cs, ^{238}Pu, $^{239+240}$Pu and ^{241}Am within the coastal sand dune ecosystem are assessed based on a conceptual model of the principal

transfer pathways between the different ecosystem compartments (Figure 6.1). Soil and vegetation activity concentration data for the site have been discussed elsewhere (Copplestone, 1996; Copplestone et al., 2001b) and these data are used, in conjunction with the animal data presented in this chapter, to derive concentration ratios for invertebrates and small mammals inhabiting the coastal sand dune site.

6.2. Methods

6.2.1 Site description

The study site was a coastal sand dune system (Ordnance Survey National Grid Reference: NY016037) situated to the west of the Sellafield nuclear fuel reprocessing site in West Cumbria, England, near to the marine discharge pipeline that carries low-level liquid waste from the Sellafield complex. The Sellafield coastal sand dunes are located on a narrow (≤ 50 m wide) sand bank, which runs parallel to the coastline for approximately 2 km and is isolated from nearby agricultural land by the River Ehen (Figure 6.2). The home ranges of small mammals and ground dwelling invertebrates inhabiting the dunes are therefore restricted geographically, the organisms being confined to living and feeding within the study area. There is minimal direct human disturbance at the dunes and no livestock grazing so vegetation succession at the site is representative of a semi-natural to natural sand dune habitat. Due to the narrow nature of the sand bank and the erosion over time of the fore-dune zone, the coastal sand dunes near Sellafield have a relatively uniform topography compared to neighbouring dune systems such as the Drigg coastal sand dunes (Wood et al., 2008; Wood et al., 2009b).

The dunes are subject to historic and ongoing radionuclide contamination through atmospheric discharges and sea-to-land transfer via sea-spray (Eakins et al., 1982) of radionuclides discharged into the marine environment from the Sellafield site. Previous work at the study site has demonstrated spatial variation in ^{137}Cs and actinide (^{238}Pu, $^{239+240}$Pu and ^{241}Am) activity concentrations in the top 12 cm of soil, consistent with sea-to-land transfer being the dominant contamination pathway (Copplestone, 1996; Copplestone et al., 2001b). Activity concentrations, particularly for the actinides, decreased with increasing distance from the sea. Samples of *A. arenaria* and *F. rubra* displayed similar spatial variation in activity concentrations due to sea-to-land transfer. In addition, significant temporal differences were observed in the vegetation activity concentrations and these are thought to be related to climatic conditions prior to sampling (Copplestone et al., 2001b). Activity concentrations in soil and vegetation samples collected from the Sellafield

coastal sand dunes are summarised in Table 6.1 and these data are used in Section 6.3 for deriving invertebrate and small mammal concentration ratios.

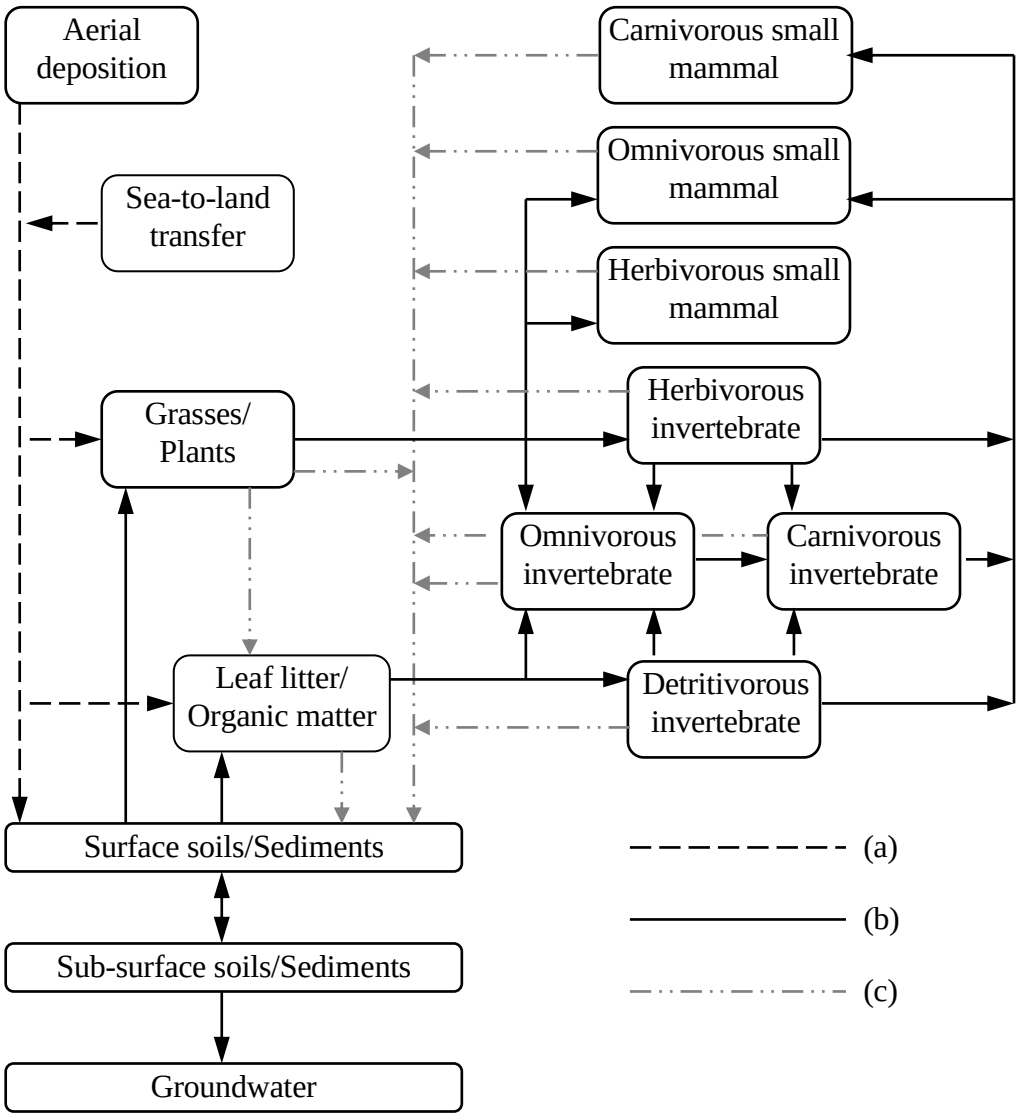

Figure 6.1. Conceptual model of the principal radionuclide fluxes within the sand dune ecosystem where: (a) represents routes by which anthropogenic radionuclides enter the sand dune ecosystem; (b) represents uptake by biota and processes such as (de)sorption, leaching and mass movement within the soils/sediments; (c) represents routes by which radionuclides are returned from the biota to the soils/sediments and includes excretion, mortality, moulting, decomposition and wash-off. The arrows indicate the direction of flow. Radioactive decay will occur in all compartments so has been excluded from the diagram.

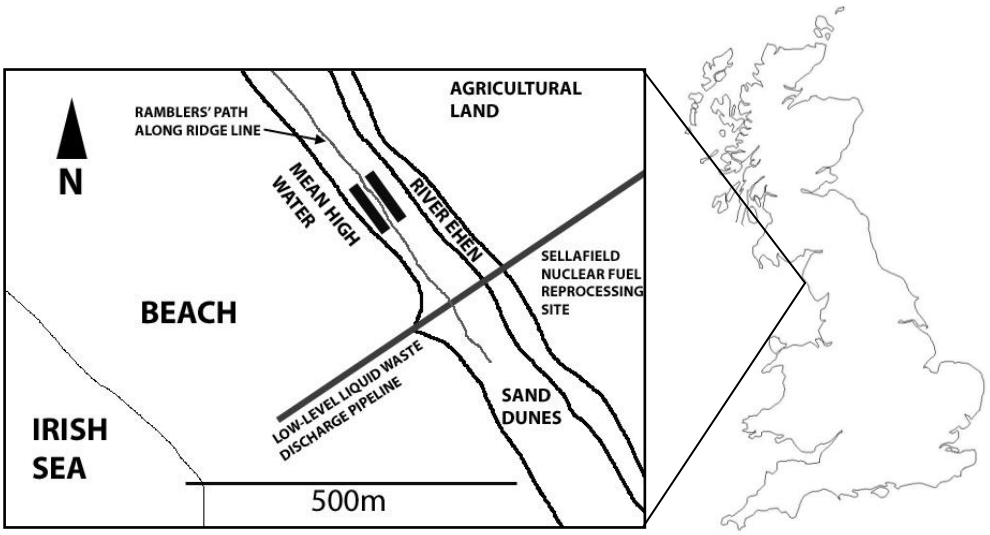

Figure 6.2. Location of the coastal sand dunes near Sellafield. Detailed map indicates the positions of the seaward and landward transects (black rectangles either side of the ramblers' path that runs along the ridge line of the sand dunes).

Table 6.1. Mean radionuclide activity concentrations for soil and vegetation samples collected from the Sellafield coastal sand dunes, Bq kg^{-1} dry weight ± SD (*n*, minimum, maximum)

Sample type	^{134}Cs	^{137}Cs	^{238}Pu	$^{239+240}$Pu	^{241}Am
Soil[a]					
Seaward transect	1.9 ± 0.8[b, c] (12, 0.7, 3.5)	320 ± 31 (12, 263, 380)	35 ± 8.7 (12, 31, 62)	179 ± 63 (12, 152, 379)	212 ± 16 (12, 191, 246)
Landward transect	3.0 ± 0.8[b, d] (12, 1.0, 4.2)	381 ± 70 (12, 295, 536)	31 ± 1.3 (11, 29, 34)	157 ± 6.5 (11, 148, 167)	205 ± 17 (12, 186, 236)
A. arenaria[e]	-	30 ± 14 (80, 8.6, 74)	2.5 ± 1.4 (19, 0.4, 5.3)	10 ± 5.0 (43, 3.3, 26)	32 ± 15 (80, 7.7, 76)
F. rubra[e]	-	31 ± 10 (93, 4.5, 77)	1.0 ± 0.9 (51, 0.2, 4.1)	3.5 ± 2.6 (51, 0.8, 12)	10 ± 8.0 (93, 0.2, 35)

[a] Soil samples collected between May 1993 and September 1994; [b] Limit of detection values treated as absolute values for calculating summary statistics; [c] Data used to calculate summary statistics include one value below the limit of detection; [d] Data used to calculate summary statistics include two values below the limit of detection; [e] Vegetation samples collected between May 1993 and February 1995

6.2.2 Field sampling

Sampling was undertaken between 1993 and 1995 by Dr David Copplestone (Environment Agency, UK). The sample site flora and habitat types were representative of those present on the seaward and landward facing slopes of the dunes. The site was located approximately 150 m north of the route of the marine discharge pipeline, at a point where the dunes were approximately 30 m wide. Two transects, each measuring 50 m x 4 m, were established running parallel to the shoreline, one each side of the primary ridge line and located approximately 5 m apart (Figure 6.2). The dominant grass species within the seaward transect and landward transects were *A. arenaria* and *F. rubra* respectively.

Invertebrates were sampled using pitfall traps, a well-established technique which has been used to collect invertebrates for radionuclide analysis in other studies (Copplestone et al., 1999; Rudge et al., 1993b; Toal et al., 2002). Although the size and composition of the pitfall trap catches is affected by a range of biophysical factors (Southwood, 1978), there appears to be a strong correlation between pitfall trap catches and the diet of carnivorous small mammals (Pernetta, 1976). Twelve pitfalls filled with 100 ml of 2% formalin solution were set along each transect in May 1993. The traps were changed at approximately monthly intervals until their removal in January 1995.

Baited Longworth live traps were used to collect specimens of three small mammal species (*A. sylvaticus*, *M. Agrestis* and *S. araneus*[28]). Live-trapping permitted targeted selection of specimens for analysis, minimising the number of animals culled. Four trapping campaigns, each utilising 30 – 50 traps, were undertaken between September 1993 and May 1995. Specimens retained for analysis were euthanised humanely and frozen to prevent tissue degradation.

6.2.3 Sample preparation

The combination of low invertebrate sample biomass and low activity concentrations necessitated the bulking of invertebrate taxa by transect for each time period. Bulk samples were rinsed with water to remove formalin and surface contaminants, sorted into taxonomic groupings (Table 6.2), oven-dried to constant mass at 85°C and homogenised using pestle and mortar.

[28] Under licence from English Nature (now Natural England).

A. sylvaticus specimens (n = 9) from the final trapping campaign were dissected to provide tissue samples (fur, gut, lungs, muscle, organs and skeleton) for the assessment of ^{137}Cs distribution within the body. All other small mammal specimens were used for the determination of whole-body activity concentrations and were washed in a 0.2% solution of Teepol® detergent to remove surface contamination (gut contents were not removed), dried to constant mass in an Edwards high-vacuum system E-C Supermodulyo freeze-drier and ground to 1 mm using a rotary knife grinder to produce a uniform sample matrix for radionuclide determination.

Table 6.2. Classification of invertebrates sampled at the Sellafield coastal sand dunes. Taxonomic groups highlighted in bold represent pooled units for analysis; where no species are listed or are not highlighted, then species were bulked into the higher Family or Order.

Class/ Subclass	**Order**	**Family**	**Genus/Species**
Arachnida	**Araneida**		
	Opiliones		
Crustacea	**Isopoda**		*Oniscus asellus*
			Philoscia muscorum
Diplopoda			
Insecta	**Collembola**		
	Coleoptera[a]	**Carabidae**	*Carabus violaceous*
			Feronia nigrita
		Cryptophagidae	
		Curculionidae	
		Elateridae	
		Scarabeidae	
		Staphylinidae	
	Diptera		
	Hymenoptera[b]		*Bombus spp.*
		Formicidae	
	Lepidoptera[b]		
Gastropoda			
Oligochaeta			*Lumbricus spp.*

[a] Adult and larval forms of Coleoptera were analysed separately; [b] Insufficient sample for analysis (<0.2 g dry weight).

6.2.4 Sample analysis

Invertebrate samples were transferred to 75 ml or 100 ml plastic pots (depending on sample size) and presented to an EG&G Ortec N-type high-purity germanium detector for determination of ^{137}Cs and ^{241}Am activity concentrations by gamma spectroscopy. The same procedure was used for small mammal samples but, due to the low activity concentrations, it was not possible to quantify ^{241}Am by gamma spectroscopy. Typical count times were 24 to 55 h for invertebrate samples and 70 to 110 h for small mammals.

Levels of ^{238}Pu, $^{239+240}$Pu and ^{241}Am in the small mammal samples were determined by radiochemical separation, based on an established method (Lovett et al., 1990), followed by alpha spectroscopy. To increase the efficiency of the radiochemical separation and reduce the count times required on the alpha detectors, species-specific bulking of small mammal samples from each trapping campaign was undertaken. Plutonium and americium were extracted from the samples using a nitric acid digest, co-precipitated using ammonium hydroxide, purified using ion exchange and electrodeposited onto stainless steel discs. The discs were counted on a Canberra QUAD-ALPHA spectrometer and count times typically ranged from 24 to 120 h. Yield recovery was quantified using ^{236}Pu and ^{243}Am. The peaks for both tracers were clearly resolved and mean yield recoveries (±1SD) were 87.7% ± 10.4% for ^{236}Pu and 59.4% ± 9.8% for ^{243}Am. Full details of the analytical methods are given in Copplestone (1996).

6.2.5 Statistical analysis

Statistical techniques were used, where possible, to test the null hypothesis that there was no statistically-significant difference between data sets. When activity concentration data were not normally distributed, logarithmic transformation of the data was performed and the Shapiro-Wilk test and Levene's test used to confirm normal distribution of the transformed data and equality of variances respectively. Data sets were then compared using either Student's *t*-test, for comparison between two sample groups, or one-way Analysis of Variance (ANOVA), for comparisons between three or more groups, to test for significant differences between the means. A 5% Least Significant Difference (LSD) test with Bonferroni adjustment was performed *post hoc* if a one-way ANOVA test identified significant differences between means.

If parametric test assumptions could not be validated, non-parametric statistical tests were used to test for statistically significant difference between the medians. For comparisons

between two sample groups the Mann-Whitney *U*-test was used. For comparisons between three or more sample groups the Kruskal-Wallis test was used.

Calculated test statistics were compared to tabulated critical values (Fowler & Cohen, 1990) to determine the statistical significance of each test statistic.

6.3. Results and discussion

6.3.1 Invertebrates

6.3.1.1 Activity concentrations in sand dune invertebrates

The whole-body radionuclide activity concentrations for each taxonomic group are presented in Tables 6.3 and 6.4. Samples that could not be analysed due to insufficient biomass, resulting from seasonal variability in the invertebrate assemblage, are indicated.

6.3.1.1.1 Inter-taxon variability in invertebrate whole-body activity concentrations

Inter-taxon variability in whole-body activity concentrations was seen for all radionuclides reported. The mean activity concentration data determined from all sampling periods (Tables 6.3 and 6.4) demonstrated consistently elevated activity concentrations in taxa such as Gastropoda (slugs and snails), Isopoda (woodlice) and Collembola (springtails) compared to taxa such as Diptera (true flies), Diplopoda (millipedes) and larval Coleoptera (carnivorous beetle larvae). The ranges in mean activity concentrations on the seaward transect were 6 to 284 Bq kg^{-1} dry wt ^{241}Am, 4 to 150 Bq kg^{-1} dry wt ^{137}Cs, 0.8 to 33 Bq kg^{-1} dry wt ^{238}Pu and 4 to 155 Bq kg^{-1} dry wt $^{239+240}Pu$. Activity concentration data for Diptera and Gastropoda always constituted the lowest and highest values respectively within these ranges. This 1 – 2 orders of magnitude inter-taxon variability was also apparent in the data for the landward transect, although the absolute activity concentrations were lower.

Table 6.3. Whole-body activity concentrations of ^{137}Cs and ^{241}Am (Bq kg^{-1} dry weight ± 2σ counting error) in coastal sand dune invertebrates.

Taxonomic group	^{137}Cs May 93-Aug 93	Sept 93-Feb 94	Mar 94-July 94	Aug 94-Jan 95	Mean (± SD)	^{241}Am May 93-Aug 93	Sept 93-Feb 94	Mar 94-July 94	Aug 94-Jan 95	Mean (± SD)
Seaward transect										
Araneida	5.6 ± 0.3	36.2 ± 5.2	69.0 ± 18.1	8.6 ± 1.4	29.9 ± 6.3	4.1 ± 0.3	68.9 ± 5.6	239 ± 12.1	11.8 ± 1.2	80.8 ± 109
Opiliones	54.9 ± 5.1	60.5 ± 7.2	4.6 ± 0.7	15.9 ± 2.9	34 ± 4.0	52.7 ± 4.8	79.0 ± 7.8	19.2 ± 0.5	24.2 ± 2.4	43.8 ± 27.7
Isopoda	154 ± 13.4	-	31.3 ± 8.3	8.4 ± 0.6	64.6 ± 7.4	165 ± 12.7	-	125 ± 5.6	5.4 ± 0.5	98.3 ± 82.9
Diplopoda	22 ± 2.1	-	7.2 ± 1.9	6.3 ± 1.2	11.8 ± 1.7	27.2 ± 1.9	-	25.6 ± 1.2	9.8 ± 1.0	20.9 ± 9.6
Collembola	n/a	-	75.0 ± 19.3	-	75 ± 19.3	n/a	-	266 ± 13.0	-	266
Coleoptera (adults)	43.4 ± 4.1	-	5.6 ± 1.4	24.8 ± 4.6	24.6 ± 3.4	49.6 ± 3.8	-	21.7 ± 1.0	38.7 ± 3.8	36.7 ± 14.1
Coleoptera (larvae)	-	-	6.2 ± 1.6	-	6.2 ± 1.6	-	-	21.9 ± 1.1	-	21.9
Carabidae	-	35.7 ± 4.2	8.2 ± 2.1	-	22.0 ± 3.2	-	51.6 ± 4.5	29.2 ± 1.4	-	40.4 ± 15.8
Diptera	6.0 ± 0.6	4.8 ± 0.6	1.2 ± 0.3	n/a	4.0 ± 0.5	6.9 ± 0.5	6.9 ± 0.6	4.2 ± 0.2	n/a	6.0 ± 1.6
Formicidae	42.2 ± 3.9	17.7 ± 2.1	-	7.3 ± 1.4	22.4 ± 2.5	48.2 ± 3.7	25.5 ± 2.2	-	11.3 ± 1.1	28.3 ± 18.6
Gastropoda	117 ± 10	148 ± 18.6	125 ± 32.8	209 ± 38.0	150 ± 24.9	132 ± 9.4	229 ± 20.1	457 ± 22.0	316 ± 31.4	284 ± 138
Oligochaeta	47.8 ± 4.5	6.0 ± 0.7	69.1 ± 17.8	9.5 ± 1.8	33.1 ± 6.2	54.6 ± 4.2	8.6 ± 0.8	245 ± 11.9	14.7 ± 1.5	80.8 ± 112
Landward transect										
Araneida	62.3 ± 4.2	15.7 ± 3.3	29.1 ± 3.2	8.0 ± 0.2	28.8 ± 2.7	27.3 ± 3.6	54.6 ± 3.1	17.4 ± 1.4	15.8 ± 0.2	28.8 ± 18.0
Opiliones	45.1 ± 5.6	21.6 ± 3.8	5.6 ± 0.6	6.5 ± 0.4	19.7 ± 2.6	36.1 ± 4.8	62.6 ± 3.6	3.0 ± 0.3	34.0 ± 0.5	33.9 ± 24.4
Isopoda	197 ± 12.7	35.8 ± 6.5	4.7 ± 0.5	7.2 ± 0.5	61.1 ± 5.1	92.1 ± 11.0	118 ± 6.2	2.5 ± 0.2	42.9 ± 0.6	63.8 ± 51,2
Diplopoda	26.7 ± 1.7	12.6 ± 2.1	12.9 ± 1.3	0.7 ± 0.1	13.2 ± 1.3	11.3 ± 1.5	34.8 ± 2.0	7.0 ± 0.6	3.5 ± 0.1	14.2 ± 14.1
Collembola	-	-	-	21.2 ± 1.4	21.2 ± 1.4	-	-	-	111 ± 1.5	111
Coleoptera (adults)	55.3 ± 3.6	24.8 ± 4.1	3.7 ± 0.4	4.2 ± 0.3	22 ± 2.1	28.4 ± 3.1	68.6 ± 4.0	2.0 ± 0.2	22.1 ± 0.3	30.3 ± 27.9
Coleoptera (larvae)	-	-	-	2.8 ± 0.2	2.8 ± 0.2	-	-	-	14.7 ± 0.2	14.7
Carabidae	-	-	-	4.9 ± 0.3	4.9 ± 0.3	-	-	-	25.8 ± 0.3	25.8
Diptera	8.7 ± 0.6	1.4 ± 0.2	0.4 ± 0.04	n/a	3.5 ± 0.3	3.7 ± 0.5	4.2 ± 0.2	0.2 ± 0.0	n/a	2.7 ± 2.2
Formicidae	103 ± 6.8	16.6 ± 2.8	-	3.5 ± 0.2	41.1 ± 3.3	48.8 ± 5.6	46.0 ± 2.7	-	18.1 ± 0.2	37.6 ± 17.0
Gastropoda	103 ± 7.4	121 ± 20.2	17.0 ± 1.9	41.2 ± 2.0	70.5 ± 7.9	47.8 ± 6.4	336 ± 19.3	10.3 ± 0.9	166 ± 2.2	140 ± 146
Oligochaeta	5.5 ± 0.4	45.1 ± 7.0	50.7 ± 5.0	5.4 ± 0.4	26.7 ± 3.2	4.3 ± 0.3	127 ± 6.7	27.0 ± 2.2	28.2 ± 0.4	46.5 ± 54.5

- Sample not obtained.
n/a Sample was not analysed due to limited biomass collected.

Table 6.4. Whole-body activity concentrations of ^{238}Pu and $^{239+240}Pu$ (Bq kg^{-1} dry weight ± 2σ counting error) in coastal sand dune invertebrates.

Taxonomic group	^{238}Pu May 93-Aug 93	Sept 93-Feb 94	Mar 94-July 94	Aug 94-Jan 95	Mean (± SD)	$^{239+240}Pu$ May 93-Aug 93	Sept 93-Feb 94	Mar 94-July 94	Aug 94-Jan 95	Mean (± SD)
Seaward transect										
Araneida	0.8 ± 0.1	5.9 ± 0.6	21.5 ± 1.85	1.8 ± 0.3	7.5 ± 9.6	3.7 ± 0.2	25.6 ± 0.9	102 ± 4.0	8.6 ± 0.6	35.0 ± 45.6
Opiliones	12.8 ± 1.1	8.2 ± 0.9	0.8 ± 0.1	3.7 ± 0.6	6.4 ± 5.2	56.7 ± 2.4	35.6 ± 1.3	3.8 ± 0.2	17.7 ± 1.3	28.5 ± 22.9
Isopoda	38.5 ± 2.9	-	7.9 ± 0.9	1.8 ± 0.1	16.1 ± 19.6	149 ± 6.2	-	46.9 ± 1.9	3.9 ± 0.3	66.5 ± 74.4
Diplopoda	5.1 ± 0.5	-	2.2 ± 0.2	1.5 ± 0.2	2.9 ± 1.9	22.7 ± 1.0	-	10.5 ± 0.4	7.2 ± 0.5	13.5 ± 8.2
Collembola	n/a	-	23.0 ± 2.0	-	23.0	n/a	-	109 ± 4.3	-	109
Coleoptera (adults)	10.1 ± 0.9	-	1.7 ± 0.2	6.0 ± 1.0	5.9 ± 4.2	44.8 ± 1.9	-	8.1 ± 0.3	28.3 ± 2.1	27.1 ± 18.4
Coleoptera (larvae)	-	-	1.9 ± 0.2	-	1.9	-	-	9.0 ± 0.4	-	9.0
Carabidae	-	4.7 ± 0.5	2.5 ± 0.2	-	3.6 ± 1.6	-	20.7 ± 0.8	12.0 ± 0.5	-	16.4 ± 6.2
Diptera	1.4 ± 0.1	0.6 ± 0.1	0.4 ± 0.0	n/a	0.8 ± 0.5	6.2 ± 0.3	2.8 ± 0.1	1.7 ± 0.1	n/a	3.6 ± 2.3
Formicidae	9.8 ± 0.9	2.3 ± 0.3	-	1.7 ± 0.3	4.6 ± 4.5	43.5 ± 1.8	10.2 ± 0.4	-	8.3 ± 0.6	20.7 ± 19.8
Gastropoda	24.9 ± 2.2	21.0 ± 2.2	39.0 ± 3.4	48.6 ± 7.8	33.3 ± 12.8	110 ± 4.6	91.5 ± 3.4	185 ± 7.3	231 ± 17.0	155 ± 65.2
Oligochaeta	11.1 ± 1.0	0.8 ± 0.1	21.2 ± 1.8	2.7 ± 0.4	8.8 ± 9.4	49.3 ± 2.1	3.5 ± 0.1	101 ± 4.0	10.8 ± 0.8	41.1 ± 44.5
Landward transect										
Araneida	2.3 ± 0.3	3.6 ± 0.5	4.0 ± 0.7	1.1 ± 0.2	2.8 ± 1.3	7.4 ± 0.6	14.7 ± 0.9	17.4 ± 1.4	4.5 ± 0.3	11.0 ± 6.1
Opiliones	3.0 ± 0.4	4.2 ± 0.5	0.7 ± 0.1	2.4 ± 0.3	2.6 ± 1.4	9.8 ± 0.8	16.9 ± 1.1	3.0 ± 0.3	9.7 ± 0.6	9.9 ± 5.7
Isopoda	7.8 ± 1.0	6.2 ± 0.9	2.6 ± 0.1	4.2 ± 0.4	5.2 ± 2.3	22.3 ± 1.8	29.0 ± 1.8	2.5 ± 0.2	12.3 ± 0.8	16.5 ± 11.6
Diplopoda	0.9 ± 0.1	2.3 ± 0.3	1.6 ± 0.3	0.3 ± 0.0	1.3 ± 0.9	3.1 ± 0.3	9.4 ± 0.6	7.0 ± 0.6	1.1 ± 0.1	5.2 ± 3.7
Collembola	-	-	-	7.9 ± 1.0	7.9	-	-	-	31.7 ± 2.1	31.7
Coleoptera (adults)	2.0 ± 0.3	4.6 ± 0.6	0.5 ± 0.1	1.6 ± 0.2	2.1 ± 1.7	6.4 ± 0.5	18.5 ± 1.2	2.0 ± 0.2	6.4 ± 0.4	8.3 ± 7.1
Coleoptera (larvae)	-	-	-	1.0 ± 0.1	1.0	-	-	-	4.2 ± 0.3	4.2
Carabidae	-	-	-	1.8 ± 0.2	1.8	-	-	-	7.4 ± 0.5	7.4
Diptera	0.3 ± 0.0	0.3 ± 0.0	0.1 ± 0.0	n/a	0.2 ± 0.1	1.0 ± 0.1	1.1 ± 0.1	0.2 ± 0.0	n/a	0.8 ± 0.5
Formicidae	3.7 ± 0.5	3.1 ± 0.4	-	1.3 ± 0.2	2.7 ± 1.2	11.9 ± 1.0	12.4 ± 0.8	-	5.2 ± 0.3	9.8 ± 4.0
Gastropoda	4.0 ± 0.6	22.3 ± 2.8	2.4 ± 0.4	11.6 ± 1.5	10.1 ± 9.1	13.0 ± 1.1	90.4 ± 5.6	10.3 ± 0.9	46.6 ± 3.0	40.1 ± 37.4
Oligochaeta	0.2 ± 0.0	7.8 ± 0.1	6.2 ± 1.1	2.0 ± 0.3	4.0 ± 3.5	0.6 ± 0.01	31.4 ± 2.0	27.0 ± 2.2	8.1 ± 0.5	16.8 ± 14.8

- Sample not obtained.
n/a Sample was not analysed due to limited biomass collected.

Similar inter-taxon variability has been noted in other studies on radionuclide burdens in terrestrial invertebrates from other sites in West Cumbria, including coniferous woodland (Copplestone et al., 1999) and grassland (Rudge et al., 1993b). However, at the woodland site, ^{137}Cs dominated the radionuclide activity profile of the invertebrates whereas the actinides, particularly ^{241}Am, dominated the activity profile in the sand dune invertebrates. This reflects the importance of the sea-to-land transfer mechanism for the sand dunes, a process that is particularly effective at transporting actinides onto coastal terrestrial sites (Bryan et al., 2008; Cambray & Eakins, 1980) due to the high particle reactivity of actinides and the elevated concentration of fine particulates in the sea surface microlayer from which sea spray is generated as a result of bubble bursting.

The sand dune invertebrate taxa can be divided into detritivore, herbivore, carnivore and omnivore (Table 6.5) based on the dominant feeding behaviours (Figure 6.1) of the species within each taxonomic group (Tilling, 1987). Detritivores, such as Collembola and Isopoda, had some of the highest activity concentrations of ^{137}Cs, ^{238}Pu, $^{239+240}$Pu and ^{241}Am whereas predatory groups, such as Coleoptera larvae, had particularly low activity concentrations by comparison. This trend was also evident in the woodland and grassland studies, the authors of these studies concluding that invertebrate whole-body activity concentrations were a function of invertebrate trophic status and the composition of their diet (Copplestone et al., 1999; Rudge et al., 1993b).

Table 6.5. Trophic status of the taxonomic groups collected from the Sellafield coastal sand dunes

Trophic status	Taxonomic groups
Carnivore	Araneida, Carabidae, Coleoptera (larvae), Opiliones
Detritivore	Collembola, Diplopoda, Isopoda, Oligochaeta
Herbivore	Gastropoda
Omnivore	Coleoptera (adults), Diptera, Formicidae

The relationship between feeding behaviour and radionuclide body-burden is to be expected and forms the basis for the conceptual model of radionuclide fluxes within the sand dune ecosystem (Figure 6.1). Radionuclides deposited onto a terrestrial site may reach the soil

surface directly or adhere to the surface of plant leaves before being transferred to soil by wash-off of the adhered nuclides or by death and decomposition of the leaves. After entering the soil, radionuclides often become associated with organic matter and fine particulates, especially clays, due to the larger surface area available for cation exchange and hence sorption (Bihari & Dezso, 2008). This partitioning of radionuclides within the soil is known to be particularly pronounced in sandy soils (Livens & Baxter, 1988a). Organic matter, and associated fine particulates, forms the principal food source for detritivorous invertebrates so ingestion of detritus by invertebrates is plausibly an important transfer pathway from soil into the food web along with other primary pathways including plant root uptake and surface contamination of plants. The activity concentrations in taxa at particular trophic levels and the transfer of radionuclides between trophic levels are therefore a function of the ecology and physiology of the different taxa and the environmental chemistry of the radionuclides involved. For example, in addition to being at a low trophic level in the food web, Isopoda, Collembola and Diplopoda are coprophagous (ingest their own faecal material) so their feeding ecology may serve to increase their uptake of elements from their food source (Dallinger & Wieser, 1977; Zimmer & Topp, 1998), especially when nutrients in the detritus are low (Kautz et al., 2002). In addition, these three taxa are known to accumulate metals in granules within the hepatopancreas (Isopoda) or mid-gut resorptive epithelial cells (Collembola and Diplopoda) (Kohler, 2002), which may contribute to the elevated activity concentrations of radionuclides determined in these taxa.

There was no evidence of biomagnification within the invertebrates examined from the sand dunes, lower trophic levels generally having higher activity concentrations for all four radionuclides (Tables 6.3 and 6.4). For actinides this is consistent with findings of mammalian studies that have demonstrated low gut transfer (e.g. Beresford et al., 2000) and partitioning of actinides into skeletal tissue (e.g. Beresford et al., 2007c) that is not readily digestible by consumers at higher trophic levels. However, there is evidence for the biomagnification of radiocaesium in both terrestrial and aquatic food webs (e.g. Palo, 2007; Sundbom et al., 2003). It may be that the ^{137}Cs bioavailability is lower at the sand dunes than at other terrestrial sites. This has been demonstrated to be the case for saltmarshes in West Cumbria that have been contaminated by marine discharges from the Sellafield site (Beresford et al., 2007c). Low bioavailability and the inclusion of gut contents in the analysis of invertebrate samples could be masking evidence of biomagnification within the invertebrate community. Alternatively other cations, such as sodium and potassium, which are continuously supplied to coastal dunes via sea spray (Ethering, 1967), may be

influencing the net rate of ^{137}Cs transfer through competition for soil cation exchange sites and root uptake (Smolders et al., 1997) and potential influences on invertebrate ionic regulation (Ramsay, 1949). Although elucidation of the relative importance of these mechanisms would require further research, the sand dune invertebrate data were consistent with other studies on terrestrial invertebrate food chain transfer in West Cumbria (Copplestone et al., 1999; Rudge et al., 1993b) suggesting that biomagnification of radiocaesium is not readily observed in terrestrial invertebrate communities.

There were notable differences in the whole-body activity concentrations of invertebrate groups at the same trophic level. In some instances this can be explained by specific differences in feeding behaviour. For example, Araneida (spiders) had the highest mean whole-body activity concentrations out of the predatory invertebrate groups present in the sand dune samples (29 Bq kg^{-1} dry wt ^{137}Cs, 5 Bq kg^{-1} dry wt ^{238}Pu, 23 Bq kg^{-1} dry wt $^{239+240}$Pu, 55 Bq kg^{-1} dry wt ^{241}Am). Rudge et al. (1993) and Copplestone et al. (1999) noted high activity concentrations in Araneida from the grassland and woodland sites and hypothesised that this was due to the feeding mechanism of this Order. Araneida feed by external digestion, introducing digestive enzymes from their venom glands into the soft tissues of their prey and subsequently ingesting the resulting liquefied material, leaving the exoskeleton of the prey behind. For ^{137}Cs especially, which concentrates in the soft tissues of organisms (Richmond, 1980), this effectively results in Araneida being exposed to a higher radionuclide activity concentration through consuming a prey item than other predatory organisms consuming the same prey type, such as Coleoptera larvae, as the latter consume skeletal as well as soft tissues. However, it is the radionuclide intake rather than the activity concentration in the material ingested that determines the tissue activity concentrations in the consumer. Given that the skeletal tissues aren't digested by these other predatory organisms and therefore do not contribute to the organisms' energy requirements, these predatory organisms may be expected to increase the mass of prey ingested in order to compensate for this. Therefore, it is more likely that the elevated activity concentrations in Araneida are due to the cellular degradation of the prey items' soft tissues prior to ingestion, which maximises the potential for gut transfer following ingestion because the radionuclides are contained within a largely liquid medium rather than incorporated in a solid matrix that must then be degraded as it passes through the digestive tract.

There were some notable differences between the invertebrate data for the sand dunes and the data reported for the woodland and grassland ecosystems. The latter studies found high activity concentrations in Oligochaeta (earthworms) compared to other invertebrates

sampled at these sites (Copplestone et al., 1999; Rudge et al., 1993b), a trend not seen in the sand dune data. Copplestone et al. (1999) concluded that the elevated activity concentrations determined in woodland Oligochaeta were due to the presence of soil in the gut, which contributes to between 22% and 55% of the earthworm dry weight (Brown, 1988). Unfortunately, the pitfall trapping technique used meant that, animals were killed upon contact with the formalin solution leaving no opportunity for depuration prior to sample analysis.

Rudge et al. (1993a) found that grassland Oligochaeta which had their gastrointestinal tracts removed had a mean whole body activity concentration of 225 Bq kg^{-1} dry wt whereas intact specimens revealed a three-fold increase in mean activity concentration of 793 Bq kg^{-1} dry wt. It is likely that a similar over-estimate of mean whole body activity concentration of woodland Oligochaeta was reported by Copplestone et al. (1999). The fact that this type of over-estimate was less apparent in the sand dune invertebrate data cannot be explained by any differences in sample collection and analysis procedures with similar methodologies being used in all three studies. However, the contribution of fine particulates to the soil composition in the sand dune ecosystem was considerably lower than that in the woodland ecosystem and the organic matter content was lower than in both the woodland and grassland ecosystems (Table 6.6). As many radionuclides become associated with organic matter and fine particulates, it is likely that the soil in the gut of organisms in the sand dune ecosystem had lower radionuclide activity concentrations than that of woodland and grassland Oligochaeta.

Table 6.6. Soil property data for sand dune, woodland and grassland sites in West Cumbria.

Ecosystem	Particle size distribution (%)			LOI (%)
	Sand (>20µm)	Silt (2-20µm)	Clay (<2µm)	
Sand dune[a]	98.0	1.0	1	1.45
Woodland[b]	43.2	42.2	14.6	13.7
Grassland[c]	98.5	1.3	0.2	5.4

[a]data from Copplestone et al. (2001b); [b]data from Copplestone et al. (1999); [c]data from Rudge (1989)

The highest invertebrate activity concentrations at the coastal sand dunes are found in the Gastropoda. When radionuclides are transferred from sea-to-land via sea spray, the spray droplets are intercepted by plants growing at the site and *A. arenaria* has been shown to be particularly effective in this regard (Copplestone et al., 2001b). Subsequent wash-off from *A. arenaria* onto other vegetation, such as *F. rubra*, leads to further surface contamination. The Gastropoda sampled at the dunes feed primarily by scraping the surface of vegetation, maximising the activity concentration of radionuclides that they ingest. However, as demonstrated for grassland Oligochaeta (Rudge et al., 1993b), it is likely that the majority of this ingested activity is not taken into the Gastropod's tissues hence depuration prior to analysis could reduce the whole-body activity concentrations determined, especially for the actinides.

6.3.1.1.2 Temporal variation in invertebrate whole-body activity concentrations

There was considerable seasonal variability in the total whole-body activity concentrations (the sum of the four radionuclides) and the activity concentrations of the individual radionuclides within the sand dune invertebrate taxa (Figures 6.3 – 6.5). However, with the exception of the Gastropoda, this temporal variation did not appear to be systematic between summer (May 1993 – August 1993, March 1994 – July 1994) and winter (September 1993 – February 1994, August 1994 – January 1995) periods. The Gastropoda data indicated a reduction in whole-body activity concentrations in the summer periods compared with that of winter periods. Climatic conditions are expected to result in higher levels of sea-to-land transfer of radionuclides during the winter months due to increased spray generation in the coastal surf zone. Vegetation activity concentration data for the site (Copplestone et al., 2001b) suggest that this may increase the surface radionuclide contamination on plants available for ingestion by Gastropoda. However, due to low sample numbers for the Gastropoda (n=8), it was not possible to determine whether this seasonal relationship was statistically significant.

For the majority of time periods, actinides contributed the largest component of the total whole-body activity concentrations of all taxa, with ^{241}Am contributing more to the total measured activity than the plutonium isotopes (Figures 6.3 – 6.5). In many instances, the largest single contributor to the total whole-body activity concentrations was ^{137}Cs. The isotopic ratios for a selection of invertebrate taxa (Table 6.7) differed significantly between time periods (Kruskal-Wallis test, $P<0.05$). The ^{137}Cs to actinide ratios in invertebrate taxa were high (i.e. exhibited a relative enrichment of ^{137}Cs compared to ^{241}Am and Pu isotopes) for invertebrate samples collected during the first sampling period (May to August 1993)

compared to the other sampling periods (Mann-Whitney *U*-test, P<0.05), particularly for Araneida, Isopoda and Coleoptera (adults). However, the reason for this is unclear and statistical analysis indicated no systematic variation in any of the invertebrate assemblage isotopic ratios between summer and winter periods (Mann-Whitney *U*-test, P>0.05).

6.3.1.1.3 Spatial variation in invertebrate whole-body activity concentrations

Actinide activity concentrations were significantly higher in invertebrate samples collected along the seaward transect (Student's *t*-test, P<0.01). The difference in activity concentrations was particularly apparent in the detritivorous and herbivorous taxa (Tables 6.3 and 6.4). Radiocaesium showed a more ambiguous relationship to distance from the shoreline, ^{137}Cs activity concentrations being higher for Gastropoda in the seaward transect but for many other taxa the activity concentrations were either similar between the transects or higher in the landward transect. Overall, the ^{137}Cs activity concentrations were not significantly different between transects (Student's *t*-test, P>0.10).

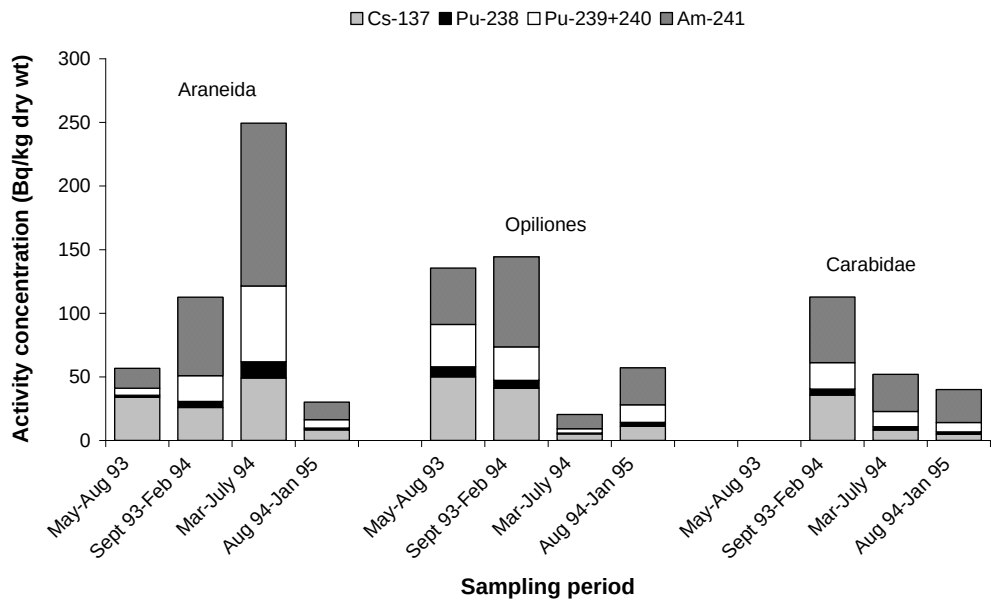

Figure 6.3. Temporal variation in ^{137}Cs, ^{238}Pu, $^{239+240}$Pu and ^{241}Am activity concentrations (Bq kg^{-1} dry weight) in carnivorous invertebrate taxa collected from the coastal sand dunes. Data presented are the mean of the seaward and landward transects.

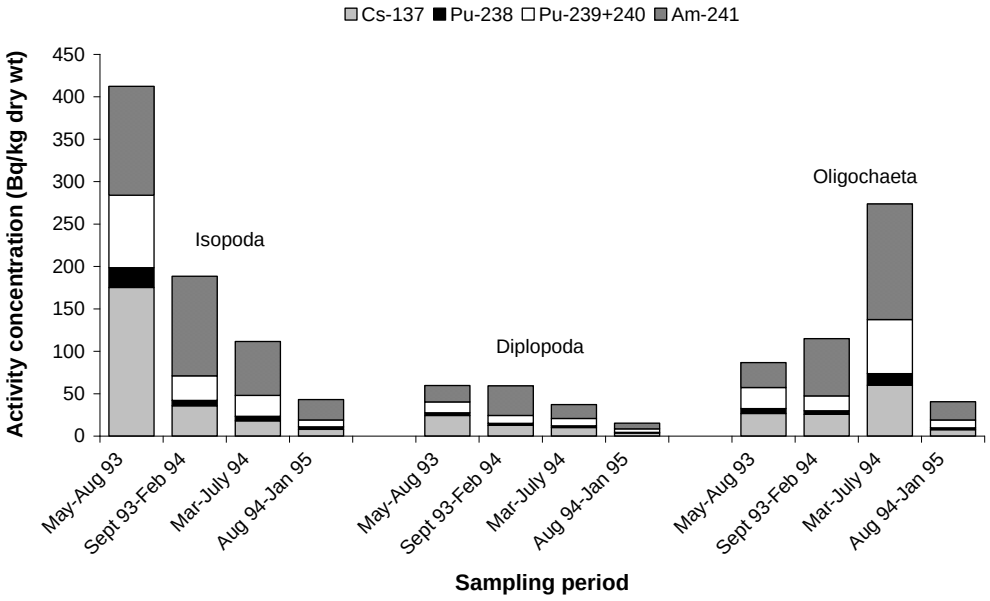

Figure 6.4. Temporal variation in ^{137}Cs, ^{238}Pu, $^{239+240}Pu$ and ^{241}Am activity concentrations (Bq kg^{-1} dry weight) in detritivorous invertebrate taxa collected from the coastal sand dunes. Data presented are the mean of the seaward and landward transects.

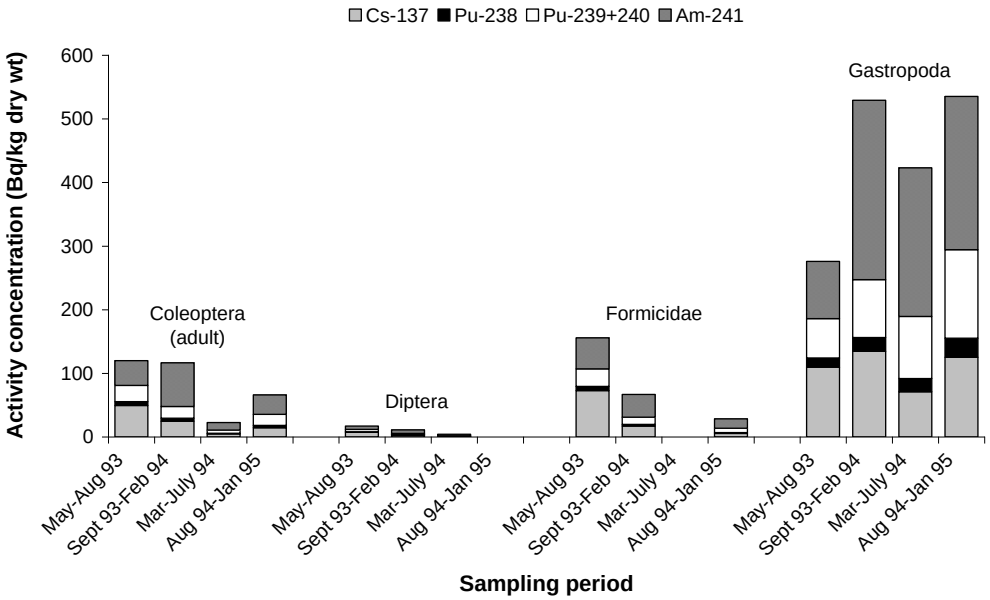

Figure 6.5. Temporal variation in ^{137}Cs, ^{238}Pu, $^{239+240}Pu$ and ^{241}Am activity concentrations (Bq kg^{-1} dry weight) in herbivorous and omnivorous invertebrate taxa collected from the coastal sand dunes. Data presented are the mean of the seaward and landward transects.

Table 6. 7. Mean isotopic ratios for selected invertebrate taxa collected from the Sellafield coastal sand dunes.

Radionuclides and taxon	May to August '93	September '93 to February '94	March to July '94	August to January '95
^{137}Cs:$^{239+240}$Pu				
Araneida	6.12	1.29	0.82	1.27
Opiliones	1.50	1.56	1.50	0.82
Isopoda	2.05	1.23	0.73	0.96
Carabidae	-	1.72	0.68	0.66
Coleoptera (adults)	1.93	1.34	0.92	0.84
^{137}Cs:^{241}Am				
Araneida	2.16	0.42	0.38	0.60
Opiliones	1.13	0.58	0.46	0.38
Isopoda	1.36	0.30	0.28	0.32
Carabidae	-	0.69	0.28	0.19
Coleoptera (adults)	1.27	0.36	0.39	0.48
^{238}Pu:$^{239+240}$Pu				
Araneida	0.28	0.24	0.21	0.22
Opiliones	0.24	0.23	0.22	0.22
Isopoda	0.27	0.21	0.21	0.37
Carabidae	-	0.23	0.21	0.25
Coleoptera (adults)	0.24	0.25	0.21	0.22
^{137}Cs:Actinides				
Araneida	1.49	0.30	0.24	0.38
Opiliones	0.58	0.40	0.33	0.24
Isopoda	0.74	0.23	0.19	0.22
Carabidae	-	0.46	0.19	0.14
Coleoptera (adults)	0.70	0.27	0.26	0.28

- Sample not obtained

Distance-dependent relationships have been established for the transfer of radionuclides from the coastal marine to the coastal terrestrial environment and models of varying complexity have been proposed (Hill et al., 2008; Howarth & Eggleton, 1988). However, at the closest point, the seaward and landward transects were only 5 m apart and these distance-dependent relationships do not predict notable changes in radionuclide deposition over such short distances. Attributing the variation in activity concentrations of the invertebrates collected from each transect to distance from the shoreline alone is thus questionable. Topography, and the associated changes in vegetation cover and soil characteristics, provides a more robust explanation for the spatial variation observed.

The coastal sand dunes have a highly uniform topography, consisting of a long sand bank with a seaward-facing slope and a landward-facing slope, and the transects were located either side of the apex of the dunes. The prevailing wind is south-westerly so the seaward-facing slope is subject to greater wind forces and sea-spray exposure than the more sheltered landward-facing slope. The resultant ecological zonation is manifested in the dominant vegetation cover of the two slopes, *A. arenaria* on the seaward slope and *F. rubra* on the landward slope. The differences in rooting structures, growth and decomposition of these two grass species will influence the organic matter content of the soil and the degree to which fine particulates are retained in the upper soil horizons. Soil property analysis indicated higher fine particulate and organic matter content in the landward transect (Copplestone, 1996).

Actinide contamination at the sand dunes is predominantly the result of sea-to-land transfer, via radionuclide-enriched sea-spray (Copplestone et al., 2001b) hence the seaward facing slope of the dunes receives a higher direct actinide input than on the landward slope. Deposited actinides are highly particle reactive and will bind strongly to soil particulates and adhere to plant surfaces. The invertebrate taxa analysed within this study are believed to have small home ranges at the dunes and significant migration between transects is not thought to occur. Therefore, although actinides have a low gut transfer coefficient, invertebrates feeding on the plant surfaces (e.g. Gastropoda) or detritus (e.g. Isopoda) of the seaward transect will be exposed to higher dietary actinide concentrations and consequently have higher actinide body-burdens than invertebrates on the landward transect. Invertebrates at higher trophic levels may also be expected to have elevated actinide activity concentrations in the seaward transect as a result of food chain transfer. The sand dune invertebrate data presented here support this hypothesis.

The ^{137}Cs contamination pathway for the dunes is predominantly via direct aerial deposition. Radiocaesium activity concentrations have been shown to have little or no correlation with distance (at distances > 50 m from the shoreline) at other sites in the Irish Sea coastal region (Bryan et al., 2008). However, there is some evidence that the sea-to-land transfer of ^{137}Cs is detectable within 50 m of the shoreline (Branford & Nelis, 1996). At the sand dune site, the seaward slope is < 50 m from the mean high water position, hence, ^{137}Cs deposition on the seaward transect was significantly higher than the landward transect (ANOVA, $P<0.05$) (Copplestone, 1996; Copplestone et al., 2001b).

Radiocaesium exhibits greater food chain mobility than actinides (Copplestone et al., 1999) so differences in the ecological structure and functioning of the seaward and landward

transects, which are also influenced by the topography of the site, are likely to result in differences in ^{137}Cs uptake. The elevated organic matter content in the soil of the landward transect would be expected to reduce the losses of ^{137}Cs due to leaching from the soil within this transect and may facilitate the retention of deposited radiocaesium within the food web. The lack of statistically significant differences in the invertebrate ^{137}Cs activity concentrations between the two transects could be due to the combined effects of increased ^{137}Cs deposition via sea-to-land transfer in the seaward transect and increased ^{137}Cs retention and cycling in the landward transect.

6.3.1.2 Radionuclide transfer parameters for sand dune invertebrates

The most widely used parameter for predicting radionuclide transfer to non-human biota is the concentration ratio (CR). The CR relates activity concentrations in environmental media (air, water or soil) to activity concentrations in an organism. For terrestrial ecosystems, the CR for the radionuclides considered within this chapter is defined as:

$$CR = \frac{Activity\ concentration\ in\ biota\ whole\ body\ (Bq\ kg^{-1}\ fresh\ weight)}{Activity\ concentration\ in\ soil\ (Bq\ kg^{-1}\ dry\ weight)}$$

The activity concentrations in the soil at the Sellafield sand dunes have been shown to exhibit some spatial but no temporal variation (Copplestone et al., 2001b). The invertebrates are not thought to undertake significant migration between transects so the CRs were derived using the mean soil activity concentrations for the soil in the seaward and landward transects respectively (Table 6.1). Tables 6.3 and 6.4 present invertebrate activity concentrations in Bq kg^{-1} dry weight so it was necessary to convert these data to fresh weight activity concentrations for the purposes of the CR calculation. This was done by applying the dry weight to fresh weight conversion factors (Table 6.8) used within the EC EURATOM-funded project 'Environmental Risks from Ionising Contaminants: Assessment and Management (ERICA)' (Beresford et al., 2008d). The CRs were calculated on a sample-by-sample basis and Table 6.9 presents the CR summary statistics for each taxonomic group.

One-way ANOVA confirmed that the mean trophic group CRs were significantly different ($P<0.05$). As expected, herbivorous and detritivorous invertebrates had higher CRs than carnivorous and omnivorous taxa. For all three elements, the general CR relationship between trophic groups was herbivores > detritivores > carnivores > omnivores. The statistical significance of this relationship for each element is presented in Table 6.9.

Table 6.8. Dry weight to fresh weight conversion factors applied to invertebrates and small mammals collected from the Sellafield coastal sand dunes. Based on the conversion factors used within the ERICA project (Beresford et al., 2008b).

Dry weight fraction	Biota group(s)
0.3	Small mammal
0.25	Araneida, Opiliones, Isopoda, Diplopoda, Collembola, Coleoptera (adults & larvae), Carabidae, Diptera, Formicidae
0.2	Gastropoda
0.17	Oligochaeta

That the lowest CRs calculated were for the omnivorous trophic group is surprising; intuitively this group would be expected to have CRs between those of the herbivores and carnivores based on the conceptual model of food chain transfer at the sand dunes (Figure 6.1). On examining the CRs for the individual omnivorous taxa it was apparent that the omnivorous taxonomic group CRs were being skewed by the Diptera. However, there may be increased measurement uncertainties in the Diptera whole-body activity concentration determinations, and consequently the CRs, as a result of the low Diptera biomass collected across all time periods. If Diptera were excluded from the calculation, the CRs for the omnivorous invertebrates were higher at 0.04, 0.02 and 0.03 for Am, Cs and Pu respectively, which were closer to the CRs for the carnivorous taxa.

The most comprehensive terrestrial CR database against which the sand dune CRs could be compared was the ERICA database (Beresford et al., 2008d). It should be noted that the data sets used to calculate the relevant ERICA generic terrestrial CRs (Table 6.10) included some data for sand dune invertebrates from the present study and consequently, the two sets of CRs (Table 6.9 and Table 6.10) were not entirely independent. However, only the 'Gastropod' actinide CRs and the 'Soil invertebrate' Pu CR were derived entirely from sand dune data. Other data used to derive the ERICA CRs were from other types of terrestrial site (e.g. woodland and grassland), so comparison between the CR data sets provided an indication of the extent to which sand dune-specific invertebrate CRs were comparable with those from other terrestrial ecosystems.

Table 6.9. Americium, caesium and plutonium CRs for invertebrates collected from the coastal sand dunes.

	Am					Cs					Pu [a]				
	n	**Mean**	**SD**	**Min**	**Max**	***n***	**Mean**	**SD**	**Min**	**Max**	***n***	**Mean**	**SD**	**Min**	**Max**
Taxon															
Araneida	8	6.52E-02	9.12E-02	4.83E-03	2.81E-01	8	2.11E-02	1.84E-02	4.38E-03	5.39E-02	16	3.55E-02	4.53E-02	5.17E-03	1.53E-01
Carabidae	3	4.22E-02	1.62E-02	3.15E-02	6.08E-02	3	1.25E-02	1.34E-02	3.22E-03	2.79E-02	6	2.07E-02	8.69E-03	1.18E-02	3.39E-02
Coleoptera (adults)	7	3.96E-02	2.61E-02	2.44E-03	8.37E-02	7	1.65E-02	1.44E-02	2.43E-03	3.63E-02	14	2.59E-02	2.19E-02	3.18E-03	7.21E-02
Coleoptera (larvae)	2	2.19E-02	5.59E-03	1.79E-02	2.58E-02	2	3.34E-03	2.13E-03	1.84E-03	4.84E-03	4	1.03E-02	3.29E-03	6.69E-03	1.36E-02
Collembola	2	2.24E-01	1.27E-01	1.35E-01	3.14E-01	2	3.63E-02	3.16E-02	1.39E-02	5.86E-02	4	1.08E-01	5.90E-02	5.05E-02	1.64E-01
Diplopoda	7	2.04E-02	1.44E-02	4.27E-03	4.24E-02	7	8.92E-03	6.34E-03	4.59E-04	1.75E-02	14	1.38E-02	9.99E-03	1.75E-03	3.66E-02
Diptera	6	5.18E-03	2.91E-03	2.44E-04	8.14E-03	6	2.71E-03	2.29E-03	2.62E-04	5.71E-03	12	3.38E-03	3.02E-03	3.18E-04	9.93E-03
Formicidae	6	3.97E-02	2.03E-02	1.33E-02	5.95E-02	6	2.22E-02	2.47E-02	2.30E-03	6.78E-02	12	2.48E-02	2.00E-02	8.28E-03	7.01E-02
Gastropoda	8	2.02E-01	1.45E-01	1.00E-02	4.31E-01	8	6.53E-02	3.87E-02	8.92E-03	1.31E-01	16	1.20E-01	8.61E-02	1.31E-02	2.78E-01
Isopoda	7	9.41E-02	7.45E-02	3.05E-03	1.94E-01	7	4.45E-02	5.55E-02	3.08E-03	1.29E-01	14	6.39E-02	7.89E-02	3.98E-03	2.75E-01
Oligochaeta	8	5.17E-02	6.71E-02	3.57E-03	1.97E-01	8	1.47E-02	1.32E-02	2.41E-03	3.67E-02	16	3.06E-02	3.20E-02	6.50E-04	1.03E-01
Opiliones	8	4.65E-02	2.95E-02	3.66E-03	9.32E-02	8	1.97E-02	1.79E-02	3.59E-03	4.73E-02	16	3.04E-02	2.63E-02	4.78E-03	9.11E-02
Trophic group															
Detritivore	24	6.93E-02[b]	8.18E-02	3.05E-03	3.14E-01	24	2.35E-02[b]	3.39E-02	4.59E-04	1.29E-01	48	4.18E-02[b,d]	5.56E-02	6.50E-04	2.75E-01
Herbivore	8	2.02E-01[c,d]	1.45E-01	1.00E-02	4.31E-01	8	6.53E-02[c,d,e]	3.87E-02	8.92E-03	1.31E-01	16	1.20E-01[c,d,e]	8.61E-02	1.31E-02	2.78E-01
Omnivore	19	2.88E-02[b]	2.48E-02	2.44E-04	8.37E-02	19	1.40E-02[b]	1.75E-02	2.62E-04	6.78E-02	38	1.84E-02[b,c]	2.00E-02	3.18E-04	7.21E-02
Carnivore	21	5.07E-02	5.86E-02	3.66E-03	2.81E-01	21	1.77E-02[b]	1.67E-02	1.84E-03	5.39E-02	42	2.90E-02[b]	3.28E-02	4.78E-03	1.53E-01

[a] Summary statistics derived from data for ^{238}Pu and $^{239+240}$Pu

CR significantly different to [b] herbivore CR, [c] detritivore CR, [d] omnivore CR, [e] carnivore CR (LSD with Bonferroni adjustment, P<0.05)

Table 6.10. ERICA CRs for terrestrial invertebrates and small mammals (Beresford et al., 2008b).

Organism	Am	Cs	Pu
Detritivorous invertebrate	1.01E-01[a]	1.34E-01[a]	3.88E-02[b]
Soil invertebrate (worm)	9.99E-02[a]	8.94E-02[a]	2.90E-02[a]
Gastropod	1.99E-01[b]	4.27E-02[a]	1.12E-01[b]
Flying insect	1.27E-01[a]	5.51E-02[a]	1.69E-02[a]
Mammal	4.08E-02	2.87E+00[a]	2.34E-02

[a] Some sand dune biota data used in the derivation of the CR; [b] CR derived entirely from sand dune biota data

The ERICA actinide CRs for 'Detritivorous invertebrate' and the Am CR for 'Soil invertebrate' were similar to those derived for the sand dune biota, although the Am CRs were lower for the sand dune biota. The Cs CRs for gastropods were comparable between the two data sets but, as for Am, the CRs derived from the sand dune data were lower than the ERICA CRs for detritivorous and soil invertebrates. The lower sand dune CRs for detritivorous and soil invertebrates are likely to be due to differences in the availability of the radionuclides in sand dune soil compared to more organic-rich soils. Some of the variation in invertebrate CRs may also be due to differences in the degree of gut depuration within different studies. Those studies in which little or no gut depuration has occurred could be expected to result in higher calculated CRs. Given that the trapping and collection techniques used for invertebrates within most field studies do not allow gut depuration, calculated CRs such as those used in ERICA may thus be significantly overestimating the actual transfer of radionuclides to invertebrates and hence result in over-estimation of internal dose rates. Although this is not a problem for screening assessments which are purposefully conservative (Beresford et al., 2007b), it does emphasise the need to consider the provenance of transfer parameters when undertaking assessments and potentially the

need to replace generic transfer parameters with values more appropriate for the type of ecosystem (e.g. woodland or sand dune) under assessment[29].

For all three elements, the sand dune-derived CRs for 'flying insects' (equated to Diptera) were markedly below those within the ERICA database but, as noted previously, there may be increased uncertainty in the sand dune CRs for Diptera as a result of the low biomass of each sample.

6.3.2 Small mammals

The three species of small mammal trapped at the sand dunes were *A. sylvaticus* (n = 18), *M. agrestis* (n = 12) and *S. araneus* (n = 8). Trapping efficiency varied between sampling periods. Large numbers of juveniles were caught in March and July 1994 but only adults were retained for analysis. Overall trapping efficiency was lower than that reported for other terrestrial ecosystems in West Cumbria, such as coniferous woodland (Copplestone et al., 1999), but this was expected due to the lower population densities of small mammals in sand dunes compared with woodlands (Gorman & Ahmad, 1993).

Analysis of the small mammal data revealed no significant difference between the radionuclide whole-body burdens of the two sexes (Mann-Whitney *U*-test, $P>0.05$). Therefore, the male and female activity concentration data were combined for the determination of mean species-specific activity concentrations (Figure 6.6) and for subsequent data analysis.

Small mammals inhabiting sand dunes have large home ranges compared with those inhabiting woodlands as a result of the lower food availability per unit area in sand dune habitats (Akbar & Gorman, 1993). Therefore the small mammals were not separated by transect and no analysis of spatial variation in small mammal activity concentrations was undertaken.

[29] If transfer parameters are derived from biota data that exclude gut contents, using these transfer paramters to estimate prey item activity concentrations in the RESRAD-BIOTA allometric approach described in Chapter 5 may result in an underestimate of radionuclide intake for the higher-trophic level organism being modelled allometrically. It may be necessary to modify the soil ingestion parameter used within the allometric equation (see Higley et al., 2003) to reflect soil within the gut-volume of prey items.

6.3.2.1 Activity concentrations in sand dune small mammals

6.3.2.1.1 Inter-species variability in small mammal whole-body activity concentrations

There were highly significant differences in the mean ^{137}Cs and ^{241}Am activity concentrations between the three small mammal species (One-way ANOVA, $P<0.01$). *S. araneus* had mean ^{137}Cs and ^{241}Am activity concentrations that were significantly higher than in both *A. sylvaticus* and *M. agrestis* (LSD with Bonferroni adjustment, $P<0.05$), but differences between *A. sylvaticus* and *M. agrestis* were not significant (LSD with Bonferroni adjustment, $P>0.05$). The plutonium isotope activity concentrations did not differ significantly between the three species (One-way ANOVA, $P>0.05$).

Differences in the whole-body activity concentrations of the three species of small mammal are expected due to diet (Figure 6.1). Activity concentrations in the herbivore *M. agrestis* (Ferns, 1976; Hofmann, 1995) should most closely reflect those in the sand dune vegetation whilst radionuclide transfer to *S. araneus*, a carnivore with a diet consisting of insects, spiders, slugs, snails, worms, young mice and carrion (Churchfield, 1984; Hofmann, 1995) should be related to activity concentrations in the sand dune invertebrates. Radionuclide transfer to *A. sylvaticus*, an omnivore feeding on seeds, vegetation, berries and fungi as well as invertebrates (Hofmann, 1995; Obrtel & Holisova, 1979) is expected to be a function of both the vegetation and the invertebrate activity concentrations.

The mean sand dune vegetation activity concentrations for ^{137}Cs and ^{241}Am were 31 and 20 Bq kg^{-1} dry wt respectively. For ground dwelling invertebrates, the mean activity concentrations were 39 Bq kg^{-1} dry wt ^{137}Cs and 69 Bq kg^{-1} dry wt ^{241}Am. Based on these data and the dietary composition of the three small mammal species, *M. agrestis* may be expected to have the lowest activity concentrations for these nuclides and *S. araneus* the highest, with the activity concentrations for *A. sylvaticus* being intermediary. The activity concentration data (Figure 6.6) support this hypothesis and the lack of significant difference in the *M. agrestis* and *A. sylvaticus* activity concentration data may be because *A. sylvaticus*, although omnivorous, predominantly feeds on vegetation rather than invertebrates (Hofmann, 1995). The similarity in whole-body activity concentrations of radiocaesium in *M. agrestis* and *A. sylvaticus*, due to commonalities in the composition of their diets, has also been reported by other authors (e.g. Rudge et al., 1993a).

The markedly higher activity concentrations in *S. araneus* are likely to be due to the specific food preferences of this species. *S. araneus* has a high metabolic rate (Rychlik & Jancewicz, 2002) and resultant high food intake rate relative to body mass. Food choice experiments (Rychlik & Jancewicz, 2002) and field studies (e.g. Pernetta, 1976) have demonstrated that *S. araneus* tends to select larger invertebrate prey items, especially earthworms and slugs. By comparison, field studies show that *A. sylvaticus* demonstrates a dietary preference for arthropods (e.g. Khammes & Aulagnier, 2007). Gastropoda and Oligochaeta collected from the sand dunes have higher whole-body activity concentrations than many of the arthropod groups (Tables 6.3 and 6.4) so *S. araneus* would be expected to have a higher dietary intake of radionuclides as a result.

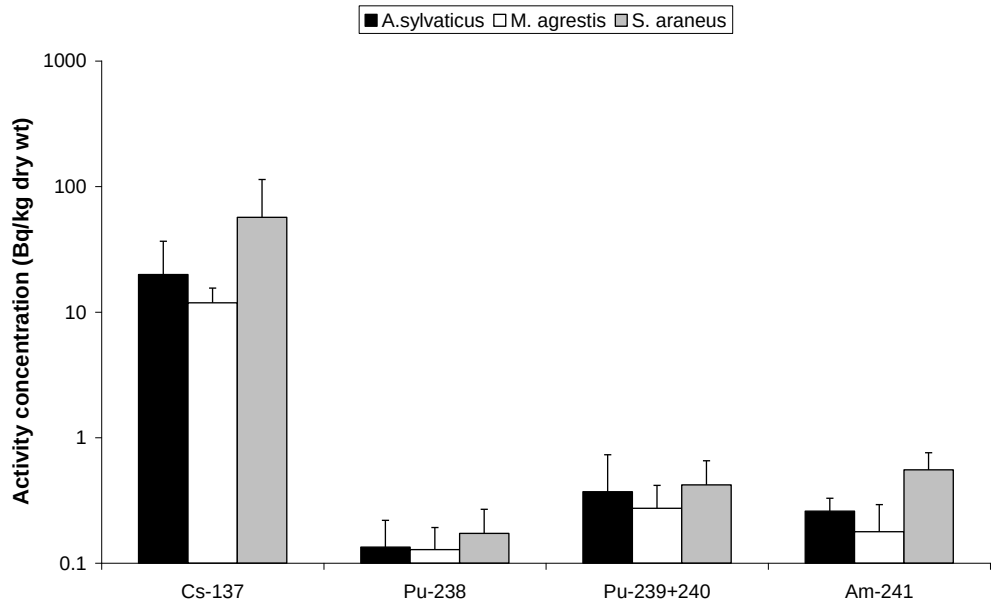

Figure 6.6. Mean ^{137}Cs, ^{238}Pu, $^{239+240}$Pu and ^{241}Am activity concentrations (Bq kg^{-1} dry weight) in small mammals from the Sellafield coastal sand dunes. Error bars represent the standard deviation.

6.3.2.1.2 Temporal variation in small mammal whole-body activity concentrations

The species-specific isotopic ratios for each sampling period indicated a possible elevation of ^{137}Cs relative to the actinides in *A. sylvaticus* during the summer months compared with the spring (Table 6.11). However, due to small sample sizes and large uncertainties, this trend could not be confirmed.

Table 6.11. Isotopic ratios for small mammals collected from the Sellafield coastal sand dunes. Data presented as mean ± SD (range when $n = 2$), n in parentheses.

Radionuclides and species	September 1993	March 1994	July 1994
^{137}Cs:$^{239+240}$Pu			
A. sylvaticus	94.0 ± 86.4 (3)	51.4 ± 19.0 (3)	76.6 ± 38.6 (3)
M. agrestis	-	44.8 – 52.8 (2)	34.7 ± 17.1 (4)
S. araneus	94.4 – 111 (2)	-	90.0 – 264 (2)
^{137}Cs:^{241}Am			
A. sylvaticus	122 ± 24.7 (3)	43.4 ± 15.9 (3)	69.9 ± 12.9 (3)
M. agrestis	-	35.7 – 48.4 (2)	74.6 ± 26.6 (4)
S. araneus	48.4 – 95.1 (2)	-	43.8 – 305
^{238}Pu:$^{239+240}$Pu			
A. sylvaticus	0.34 ± 0.14 (3)	0.43 ± 0.30 (3)	0.59 ± 0.09 (3)
M. agrestis	-	0.60 – 0.85 (2)	0.42 ± 0.30 (4)
S. araneus	0.40 – 0.44 (2)	-	0.09 – 1.67
^{137}Cs:Actinides			
A. sylvaticus	39.8 ± 27.6 (3)	19.7 ± 6.37 (3)	28.0 ± 10.3 (3)
M. agrestis	-	16.1 – 17.1 (2)	17.5 ± 8.36 (4)
S. araneus	27.8 – 43.3 (2)	-	19.1 – 135 (2)

- Sample not obtained

Although there was no statistically significant temporal trend in the ^{137}Cs whole-body activity concentrations of *A. sylvaticus*, (Kruskal-Wallis test, $P>0.05$), the observed trend in the isotopic ratios is consistent with the hypothesis formulated for Gastropoda: that the rate of sea-to-land transfer of actinides is highest during the winter period and reduces during the summer months. Furthermore, in West Cumbrian woodlands, fungi form a larger

proportion of the *A. sylvaticus* diet in late summer and Autumn (Toal et al., 2001). Seasonal changes in diet have been demonstrated to result in corresponding changes in whole-body activity concentrations in other small mammal populations (e.g. Rudge et al., 1993a) due to the high metabolic rates (and correspondingly short biological half-lives) of small mammals (Maklyuk et al., 2007). As fungi are known to accumulate ^{137}Cs (Barnett et al., 1999), a similar dietary shift at the sand dunes could also play a role but there are no dietary data available to confirm this. Statistical analysis of the temporal variation in the whole-body activity concentrations of other radionuclides could not be undertaken due to the small number of animals caught in each sampling period.

No statistically significant temporal variation could be determined for *M. agrestis* and *S. araneus* but, as for *A. sylvaticus*, this may be due to the low numbers of these species caught during each trapping campaign.

6.3.2.1.3 Tissue distribution of ^{137}Cs in A. sylvaticus

Analyses revealed the accumulation of ^{137}Cs in the soft tissue and muscle of *A. sylvaticus* with low activity concentrations in bone (Table 6.12), a finding consistent with other studies (Copplestone et al., 1999; Richmond, 1980).

Table 6.12. Distribution of ^{137}Cs in the tissues and organs of *A. sylvaticus* samples from the Sellafield coastal sand dunes.

Tissue	**^{137}Cs activity concentration Bq kg^{-1} fwt**
Body hair	32.1 ± 18.4
Gut (full)	64.7 ± 61.9
Lungs	203.9 ± 205.8
Muscle	212.6 ± 224.2
Organs	74.9 ± 53.5
Skeleton[a]	3.5 ± 1.3

[a] dry weight reported.

The low activity concentration of ^{137}Cs determined in the gut of *A. sylvaticus* is likely to be an artefact of the trapping and sample preparation procedures. In the period between an animal entering one of the baited Longworth traps and the trap being emptied, the animal tends to become engorged on the bait within the trap. Copplestone et al. (1999) noted that this promotes defaecation and hence elimination from the gut of the animals' normal dietary foodstuffs. The dissected gut tissues were analysed complete with their contents so the radionuclide activity concentration determined is likely to be artificially reduced due to the presence of bait within the gut.

It has been suggested that inhalation may be a secondary route of radiocaesium uptake in terrestrial ecosystems (Avery, 1996; Copplestone et al., 1999). However, due to high measurement uncertainties, it is not possible to determine whether inhalation of ^{137}Cs is contributing to the tissue distribution observed.

6.3.2.2 Radionuclide transfer parameters for sand dune small mammals

Radionuclides transferred via sea-to-land lead to significant surface contamination of vegetation (Copplestone et al., 2001b) causing higher actinide activity concentrations in vegetation than predicted using generic terrestrial plant CRs based on the measured soil activity concentrations (Wood et al., 2008; Wood et al., 2009b). Based on the conceptual model (Figure 6.1), herbivorous mammals at the dunes were therefore expected to have higher actinide body burdens than those predicted from activity concentrations in the soil alone. Similarly, ^{137}Cs at the dunes is thought to be associated with the thin (approximately 1 mm) layer of organic matter and fine particulates found on the surface of the sand dune soil. These particles are ingested by detritivorous invertebrates, which in turn are ingested by omnivorous and carnivorous small mammals (Figure 6.1). Therefore, a higher level of ^{137}Cs transfer to these small mammals was expected than may be predicted based on the mean activity concentration of the top 10 cm of soil (the standard depth used in ERICA for the calculation of CRs (Beresford et al., 2008d)). However, no evidence to support these scenarios was revealed and conversely, the calculated mean CRs for Am, Cs and Pu transfer to small mammals at the sand dunes (Table 6.13) were two orders of magnitude lower than the generic terrestrial ecosystem CRs used for small mammals in ERICA (Table 6.10). It is possible that other cations from the marine environment are influencing radionuclide transfer observed. For example, potassium may be reducing plant root uptake of caesium (Smolders et al., 1997) and sodium may be affecting the ionic regulation of the small mammals. However, there are no data against which this hypothesis can be tested.

Table 6.13. Americium, caesium and plutonium CRs for small mammals collected from the Sellafield coastal sand dunes.

Element	Species	*n*[a]	Mean	SD	Min	Max
Am	*Apodemus sylvaticus*	9	3.73E-04	9.89E-05	2.15E-04	4.88E-04
	Microtus agrestis	6	2.56E-04	1.64E-04	1.00E-04	5.31E-04
	Sorex araneus	4	7.97E-04	2.90E-04	5.31E-04	1.15E-03
	All species	19	4.25E-04	2.60E-04	1.00E-04	1.15E-03
Cs	*Apodemus sylvaticus*	18	1.71E-02	1.43E-02	1.37E-03	6.99E-02
	Microtus agrestis	12	1.02E-02	3.16E-03	4.11E-03	1.50E-02
	Sorex araneus	8	4.88E-02	4.87E-02	1.39E-02	1.68E-01
	All species	38	2.16E-02	2.75E-02	1.37E-03	1.68E-01
Pu[b]	*Apodemus sylvaticus*	18	9.24E-04	7.28E-04	2.14E-04	2.56E-03
	Microtus agrestis	12	8.10E-04	5.36E-04	2.68E-04	2.03E-03
	Sorex araneus	8	1.14E-03	7.45E-04	3.21E-04	2.65E-03
	All species	38	9.33E-04	6.69E-04	2.14E-04	2.65E-03

[a] *n* is the number of biota activity concentration determinations used to calculate the CR (from individual animals for Cs and bulk samples for Am and Pu); [b] Summary statistics derived from data for ^{238}Pu and $^{239+240}$Pu

6.4. Conclusions

This chapter and the associated paper (Wood et al., 2009a) present the first published study to derive radionuclide transfer parameters for animals within a coastal sand dune ecosystem. The sand dunes near Sellafield are subject to sea-to-land transfer of radionuclides and the influence of this unusual terrestrial contamination mechanism was reflected in the food chain transfer observed at the site. The activity concentration data for some biota (Gastropoda and *A. sylvaticus*) indicate temporal variation in radionuclide body burdens, which is attributed to climatic influences on the sea-to-land transfer mechanism and seasonal changes in diet.

There were significant differences in activity concentrations of ^{137}Cs and ^{241}Am, between different taxa of sand dune biota. These differences were primarily determined by trophic level, although variations in specific feeding ecology and physiology could have been responsible for differences between biota at the same trophic level.

The sand dune small mammal CRs were two orders of magnitude lower than the ERICA CRs for terrestrial ecosystems. This may be explained by the influence of other cations

from the marine environment (e.g. K and Na) on the net radionuclide transfer observed, but further research is required to test this hypothesis. In addition, effort needs to be directed towards determining the extent to which other sand dune biota groups, such as reptiles and amphibians, may demonstrate similarly suppressed CRs. These research questions are considered further in Chapters 7 and 8.

The difference in the sand dune CRs compared to other terrestrial sites highlights the need for appropriate ecosystem-specific transfer databases (e.g. for woodland, sand dune, grassland) to underpin the dose assessment models being used to assess the impact of ionising radiation on wildlife. There is an ongoing need to improve understanding of the differences in the behaviour and fate of radionuclides within these different ecosystems.

(This page is left blank intentionally)

CHAPTER 7 – RADIONUCLIDE TRANSFER TO REPTILES

The material presented in this chapter has been submitted, at the request of the journal editor, for publication in Radiation and Environmental Biophysics:

Wood et al., submitted. Radionuclide transfer to reptiles. Radiation and Environmental Biophysics.

7.1. Introduction

Reptiles are widespread throughout the world's terrestrial and aquatic ecosystems (Pough et al., 2004). Present on all continents except Antarctica (Shea, 2002), they are often a major contributor to the total faunal biomass of ecosystems, especially in arid regions (Campbell & Campbell, 2000). There are over 8000 species of extant reptile (Pough et al., 2004) and many play important roles in ecosystem functioning, such as the control of rodent populations (Liat, 1999). Reptile species may be considered keystone species (Davic, 2003; Paine, 1969) and a target for environmental protection.

Recognising both the ecological importance of reptiles and the significant global decline in reptile populations that is occurring due to multiple stressors, including habitat loss, environmental pollution, introduced invasive species and climate change (Gibbons et al., 2000; Irwin & Irwin, 2006), there is an increasing need to minimise those impacts that can be controlled through regulatory actions. Environmental pollution from regulated discharges is one such stressor. Due to the long life-spans and high trophic level of many reptile species, contaminants that bioaccumulate may pose a significant hazard to reptiles (Campbell & Campbell, 2001; Delany et al., 1988). Therefore, consideration of impacts on reptiles should be fully integrated into ecological risk assessments (ERA), but this has rarely been achieved (Campbell & Campbell, 2000).

The reason for the omission of reptiles from many ERA to date has been attributed to the paucity of data on the uptake and effects of contaminants in these poikilothermic vertebrates (Campbell & Campbell, 2002). They are the least studied of the vertebrate groups in the context of environmental contamination (Hopkins, 2000). Although there

have been attempts to synthesise available datasets to underpin the inclusion of reptiles within ERA (e.g. Campbell & Campbell, 2000; Campbell & Campbell, 2001), the available data remain limited.

One category of environmental pollutants for which few data exist is radionuclides (Beresford et al., 2008d; Campbell & Campbell, 2000; Campbell & Campbell, 2001). Due to the increasing recognition of the requirement to undertake specific assessments of the environmental impact of ionising radiation (ICRP, 2007a), there is a need to reappraise the available data on reptile radioecology with a focus on the applicability of these data to environmental radiation protection. Through analysis of both published and unpublished data, this chapter aims to define the current state-of-the-art in the prediction of radionuclide transfer to reptiles and provide a knowledge baseline to underpin the future development of radiation impact assessments for reptiles within ERA. The collated data on transfer to terrestrial reptiles at non-sand dune sites are compared with transfer data from the Drigg coastal sand dunes study to investigate the extent to which the differences between transfer to sand dune and non-sand dune small mammals (see Chapter 6; Wood et al., 2009a) are reflected in the transfer to reptiles.

7.2. Predicting radionuclide transfer

A number of models have been developed to assess the environmental impacts of ionising radiation (Beresford et al., 2008b; Beresford et al., 2008c). The models estimate absorbed radiation dose rates in biota from radionuclides in the surrounding environmental media (external dose rates) and radionuclides incorporated within the organisms tissues (internal dose rates). Evaluations of these models (see Chapter 5) have identified the parameters used to estimate the transfer of radionuclides to biota as a major source of uncertainty in model predictions (Beresford et al., 2009; Wood et al., 2009b). In particular, a need to develop appropriate transfer parameters for reptiles has been recognised (see Chapter 4; Chapter 5; Barnett et al., 2009; Wood et al., 2008; Wood et al., 2009b).

One method commonly applied within the available models to predict biota activity concentrations from activity concentrations in environmental media (soil/sediment, water and air) is the concentration ratio (CR) approach. The CR approach assumes radionuclide activity concentrations in biota are in biogeochemical equilibrium with the activity concentrations in environmental media. Therefore, the transfer of a specific radionuclide (R) to a specific organism can be defined by a numerical multiplier (the CR). For terrestrial

ecosystems, Beresford et al. (2008d) define the CR on an organism fresh weight (fwt) to soil dry weight (dwt) basis:

$$\mathrm{CR} = \frac{\text{Activity concentration of } R \text{ in biota whole-body (Bq kg}^{-1}\text{ fwt)}}{\text{Activity concentration of } R \text{ in soil (Bq kg}^{-1}\text{ dwt)}}$$

with the exception of chronic atmospheric releases of ^{3}H, ^{14}C, $^{32,33}P$ and ^{35}S, which are defined as:

$$\mathrm{CR} = \frac{\text{Activity concentration of } R \text{ in biota whole-body (Bq kg}^{-1}\text{ fwt)}}{\text{Activity concentration of } R \text{ in air (Bq m}^{-3}\text{)}}$$

For aquatic ecosystems, Hosseini et al. (2008) define the CR as:

$$\mathrm{CR} = \frac{\text{Activity concentration of } R \text{ in biota whole-body (Bq kg}^{-1}\text{ fwt)}}{\text{Activity concentration of } R \text{ in filtered water (Bq l}^{-1}\text{)}}$$

There are some potential limitations to the CR approach. These include the unrealistic assumption of instantaneous equilibrium between organism and medium (e.g. Mann et al., 2007), the lack of consideration of physico-chemical influences on uptake, such as the concentrations of chemical analogues (Jeffree, 1991; Whicker et al., 1990), the influence of temperature, which may be particularly relevant for reptiles due to their poikilothermic nature (Narayanan & Eapen, 1971; Peters & Brisbin, 1996), the influence of age on whole-body burden (Albrecht et al., 2007; Gochfeld & Burger, 1987; Sakai et al., 2000) and the effect of seasonal changes in both the endocrine cycle (Scott et al., 1986) and diet (Rudge et al., 1993a; Wood et al., 2009a). However, adopting a CR approach provides a useful means of estimating biota activity concentrations from media concentrations when undertaking impact assessments. It obviates the need for defining and quantifying the specific uptake (including transfer through gastrointestinal tract, skin and respiratory tissues) and elimination pathways that influence the net radionuclide transfer to an organism and, even with the limitations noted above, has been shown to produce good estimates of radionuclide body burdens across a range of organisms, radionuclides and ecosystems (e.g. Chapter 4; Chapter 5; Beresford et al., 2005; Wood et al., 2008).

7.3. Literature review and manipulation of data

The reptile CR data presented in this chapter were drawn from published literature, unpublished literature and in-house data sets. Although some review articles were available for specific reptile groups (e.g. Campbell & Campbell, 2000; Campbell & Campbell, 2001; Meyersschone & Walton, 1994), original data sources were consulted preferentially. The literature review covered both radioisotope and stable element data for the elements listed in Publication 38 of the International Commission on Radiological Protection (ICRP, 1983), which is the list of radionuclides for which dose rates can be calculated using one of the most recently developed models for biota dose assessment, the ERICA Tool (Brown et al., 2008). CRs were derived for elements rather than individual radioisotopes based on the assumption that all isotopes of an element will have the same CR (Beresford et al., 2008d; Hosseini et al., 2008). However, stable element data from heavily contaminated sites were omitted from the CR derivation because the kinetics of uptake may be dietary concentration, and hence media concentration, dependent (Mann et al., 2006). For example, the Pb and Zn CRs for the common lizard (*Lacerta vivipara*) at a site in the Mendip Hills, UK, which was heavily contaminated as a result of historic mining activities, were approximately two orders of magnitude lower than those for the same species at two other terrestrial grassland sites (Avery et al., 1983).

To derive CRs for use within biota dose assessment models, measured concentration data for the biota and environmental media of interest are required (ideally these data should be both spatially and temporally linked). However, in collating reptile CR data it was rarely possible to obtain all necessary information from a single source (publication, report or data set). Where biota data were for specific tissues rather than whole-body or where media data were lacking, spatially and temporally concurrent data from other sources were screened to fill these data gaps. If this process was unsuccessful, attempts were made to contact the original authors of the publications (or those who undertook the original sampling and analytical work) in order to access missing data. Despite these efforts, in most cases it was necessary to apply specific data manipulation techniques to obtain the estimates of whole-body CRs and associated summary statistics for each radionuclide-organism combination. Data manipulations included: (i) converting data from dry weight or ash weight to fresh weight; (ii) converting tissue data to whole-body data; (iii) converting radionuclide deposition data to soil activity concentrations; (iv) converting sediment data to water data when deriving aquatic CRs; (v) estimation of weighted means and standard deviations; and (vi) summarising data sets that included values below the limit of detection (LOD).

7.3.1. Converting dry, or ash, weight to fresh weight

The CR calculation requires fresh weight whole-body activity concentrations but data (whole-body or tissue) were often reported in the literature as dry weight or ash weight with no additional information to permit conversion to fresh weight. Therefore, reptile-specific conversion factors were sourced from reviewed literature and in-house data sets (Table 7.1).

Occasionally soil data were reported as ash weight rather than dry weight. To convert soil ash weight concentrations to dry weight, a dry weight:ash weight ratio of 1.15 was assumed (Noureddine et al., 1997).

Table 7.1. Dry weight (dwt) to fresh weight (fwt) ratios for reptile tissues

Tissue	***n***	**dwt:fwt**
Blood	1	0.21[1]
Bone[2]	3	0.71[3,4]
	59	0.24 (ash wt:fwt)[5]
Brain	4	0.24[3,4]
Carcass[6]	82	0.26[7]
Kidney	138	0.28[3,4,8,9,10,11,12,13,14]
Liver	98	0.27[3,4, 7,8,9,10,11,12,13,14,15,16]
Lung	12	0.27[13]
Muscle	201	0.22[3,4,8,9,10,12,13,14,15,17]
Scute[18]	57	0.42[4,14]
Spleen	1	0.25[4]
Whole-body	45	0.29[19]
	3	0.07 (ash wt:fwt)[20]
Egg	2	0.51[7]

[1] calculated from haematological parameters for a turtle (Withers, 1992) and in good agreement with generic value for human blood (Ohira et al., 1977); [2] bone includes shell (carapace and plastron) of turtles; [3] turtle data (Garcia-Fernandez et al., 2009); [4] crocodilian data (Jagoe et al., 1998); [5] crocodilian and turtle data (Pritchard & Bloodwell, 1986); [6] carcass is a composite of muscle and bone tissue (whole-body with organs removed); [7] snake data (Santos et al., 2007); [8] turtle data (Anan et al., 2001); [9] turtle data (Frias-Espericueta et al., 2006); [10] turtle data (Godley et al., 1999); [11] turtle data (Gordon et al., 1998); [12] turtle data (Maffucci et al., 2005); [13] turtle data (Storelli et al., 1998); [14] crocodilian data (Yanochko et al., 1997); [15] turtle data (Godley et al., 1998); [16] snake data (Ohlendorf et al., 1988); [17] crocodilian data (Jeffree et al., 2001); [18] scute is a composite of muscle, skin and bone; [19] snake data (Albrecht et al., 2007) and unpublished data for *A. fragilis*, *L. vivipara* and *V. berus* from the Drigg coastal sand dunes, UK (my data); [20] unpublished bird data from the Drigg Coastal sand dunes (my data); [21] egg is the whole egg (shell, shell membrane, albumen and yolk)

7.3.2. Converting tissue data to whole-body data

Few data sources provided whole-body data. In most cases data were reported for specific tissues and it was necessary to convert these tissue data to whole-body data for the purposes of CR calculation. Generally, the tissues for which data were reported were those that are recognised to be the major target tissues for particular elements and those which, on the basis of their mass relative to the whole-body, would be expected to contribute significantly to the whole-body burden for a particular element. These tissues were kidney, liver, muscle and bone in animals and albumen, eggshell and yolk in eggs. For a given radionuclide, the whole-body activity concentration was estimated from activity concentration in a specific tissue using a mass-balance approach, which is similar to that described in other studies (e.g. Yankovich & Beaton, 2000; Yankovich, 2009):

$$C_{WB} = \frac{C_T \times FM_T}{B_T}$$

where C_{WB} is the whole-body activity concentration (Bq kg^{-1} fwt); C_T is the activity concentration of tissue T (Bq kg^{-1} fwt); FM_T is the fractional fresh weight (fwt) mass of tissue T relative to the whole-body mass; and B_T is the fraction of the total body burden of the radionuclide in tissue T. By substituting C_T with 1 in the above equation, the whole-body: tissue concentration ratio can be estimated.

Data on the fractional mass of specific tissues and the fraction of the total body burden were sourced through literature review (Table 7.2). Muscle and eggshell were chosen as reference tissues for data on animal and egg contaminant distribution respectively. Data from references reporting either radionuclide or stable element data in both a reference tissue and at least one other tissue were entered into a database to derive reptile-specific data on tissue contaminant distributions. Recognising that data reported in different studies may be in incommensurable units, data were normalised to the reference tissue data on a study-by-study basis using the following equation:

$$R_{REF.T} = \frac{C_T}{C_{REF}}$$

where $R_{REF.T}$ is the fresh weight ratio between the contaminant burden in tissue T (C_T) and the concentration in the reference tissue (C_{REF}). Some references reported data as fresh weight (fwt) whereas other reported dry weight (dwt) so all data were standardised to fwt

prior to calculation of $R_{REF.T}$. If sample-specific fwt:dwt ratios were provided in the source reference then these were used to convert the data for that reference. However, this information was not normally provided, so the literature-derived reptile-specific fwt:dwt conversion factors were used (Table 7.1).

Table 7.2. FM_T and $M_{REF.T}$ values for reptiles

Tissue	Generic reptile (animal)[1]		Turtle (animal)		Tissue	Generic reptile (egg)	
(*T*)	FM_T[2]	$M_{REF.T}$[3]	FM_T[2]	$M_{REF.T}$[3]	(*T*)	FM_T[2]	$M_{REF.T}$[3]
Bone	7.22E-02[5]	8.23E-02	4.20E-01[6]	8.09E-01	Albumen	2.48E-01[7]	2.04E+00
Kidney	3.00E-03[6]	3.42E-03	3.00E-03[6]	5.78E-03	Eggshell[4]	1.22E-01[7]	1.00E+00
Liver	4.75E-02[8,9]	5.42E-02	5.80E-02[6]	1.12E-01	Yolk	6.31E-01[7]	5.19E+00
Muscle[4]	8.77E-01[5]	1.00E+00	5.19E-01[6]	1.00E+00	Yolk-Albumen[10]	8.78E-01	7.23E+00

[1] data applicable to crocodilians and squamate reptiles (snakes and lizards); [2] FM_T is the fractional fresh weight mass of tissue *T* relative to the whole-body mass; [3] $M_{REF.T}$ is the fresh weight ratio between the fractional mass of tissue *T* and the fractional mass of the reference tissue; [4] reference tissue; [5] crocodile data (Toop, 1988); [6] turtle data (Towns, 1987); [7] turtle data (Rie et al., 2001); [8] snake data (Santos et al., 2007); [9] snake data (Starck & Beese, 2002); [10] calculated values for yolk and albumen combined.

The calculated $R_{REF.T}$ values are summarised for animals (Table 7.3) and eggs (Table 7.4). Graphical evaluation of the data revealed no obvious differences between reptiles from different ecosystem types (terrestrial, freshwater and marine) and information on the sex of individual animals was rarely available so the $R_{REF.T}$ data presented in this chapter are generic values for reptiles, irrespective of ecosystem or sex. However, for presentation of FM_T, $M_{REF.T}$ and, for some elements, $R_{REF.T}$, turtles (including terrapins and tortoises) data are presented separately. For the mass data, this is because turtles have a shell (plastron and carapace), which markedly increases the proportional contribution of bone to the whole-body mass of these reptiles. For the $R_{REF.T}$ data, graphical examination of the data revealed elements for which there were some notable differences in $R_{REF.T}$ values between turtles and other reptiles, especially for Ca, Cd, Mn, Ni and Sr.

Table 7.3. Ratio of fresh weight tissue concentration to muscle concentration ($R_{REF.T}$) in reptilian animals. Values highlighted in grey are those which are based on assumptions rather than measured values (see footnotes for details).

	Bone			Kidney			Liver		
Element	***n***	**mean**	**SD**	***n***	**mean**	**SD**	***n***	**mean**	**SD**
Ag		3.23E+00[3]		44	8.02E+00[16]	2.87E+00	48	6.85E+02[16]	2.65E+01
Al	78	2.05E+01[17]	4.55E+00	90	5.65E-01[17,18]	7.56E-01	90	1.62E+00[17,18]	1.28E+00
As	78	1.69E+00[17]	1.31E+00	212	1.67E+00[17,19,20,21,22,23,24]	1.30E+00	316	2.32E+00[17,19,20,21,22,23,24,25,26,27,28,29]	1.52E+00
Ba	34	1.25E+02[30]	1.13E+01	46	1.55E+00[16,21]	1.26E+00	51	1.12E+00[16,21]	1.07E+00
Ca[1]	34	3.79E+03[30]	6.25E+01		1.48E+00[4]			1.17E+00[4]	
Ca[2]	1	2.80E+01[31]			3.35E+00[4]		10	7.32E-01[31]	4.67E-01
Cd[1]		1.19E+00[5]		96	2.30E+00[22,23,24]	1.53E+00	161	8.01E+00[22,23,24,25,27]	2.84E+00
Cd[2]	78	1.19E+00[17]	4.83E-01	287	9.01E+02[16,17,19,20,32,33,34,35,36,37,38,39]	9.02E+02	390	5.89E+01[16,17,19,20,21,26,28,29,32,33,34,35,36,37,38,39,40,41]	5.84E+01
Co	1	1.63E+00[42]		46	2.37E+02[16,21]	1.56E+01	52	2.50E+01[16,21,42]	5.05E+00
Cr	34	2.15E+00[30]	1.49E+00	190	1.39E+00[16,18,19,20,21,22,23,24]	1.18E+00	294	1.13E+00[16,18,19,20,21,22,23,24,25,26,27]	1.07E+00
Cs	19	2.66E-01[42,43]	5.30E-01	23	2.37E+00[21,43,44]	1.57E+00	53	7.38E-01[21,42,43,44,45,46]	8.68E-01
Cu	34	1.15E+01[30]	3.44E+00	220	1.59E+01[16,18,20,21,24,32,33,34,37,38,39,47]	4.00E+00	299	1.41E+02[16,18,20,21,24,28,29,32,33,34,36,37,38,39,40,47]	1.19E+01
Fe	112	8.86E-01[17,30]	9.46E-01	207	3.41E+00[17,18,20,24,34,37,38,39,47]	1.85E+00	286	3.07E+01[17,18,20,24,34,37,38,39,40,47]	5.55E+00
Hg		1.72E+00[6]		337	6.42E+00[16,19,21,22,23,24,35,36,37,38,39,46,48,49,50,51]	2.54E+00	473	7.35E+00[16,19,21,22,23,24,25,26,27,28,29,35,36,37,38,39,48,49,50,51]	2.71E+00
Mg	34	1.19E+01[30]	3.50E+00		1.48E+00[4]			1.17E+00[4]	
Mn[1]	34	2.11E+01[30]	4.66E+00	108	3.77E-01[18,22,23,24]	6.17E-01	178	4.53E+00[18,22,23,24,25,27]	2.13E+00
Mn[2]		5.75E-01[7]		108	2.51E+01[16,21,34,37,38,47]	2.47E+01	183	1.11E+01[16,21,26,34,37,38,40,47]	1.06E+01
Mo		1.57E+01[8]		46	6.86E+01[16]	8.37E+00	51	5.45E+01[16,21]	7.46E+00
Ni[1]	34	3.14E+01[30]	5.69E+00	10	1.16E+00[18]	1.14E+00	12	1.02E+00[18]	1.05E+00
Ni[2]	78	5.75E-01[17]	4.98E-01	136	6.39E+00[17,20,21,34]	5.89E+00	188	4.72E+00[17,20,21,28,34,40]	4.20E+00
Pb	115	1.17E+01[17,30,33,52]	3.44E+00	279	1.54E+00[17,18,19,20,21,22,23,24,32,33,34,35,39]	1.24E+00	369	1.92E+00[17,18,19,20,21,22,23,24,25,26,27,28,32,33,39,52]	1.39E+00
Po	1	4.00E+00[52]			3.72E+01[9]		2	3.72E+01[52]	8.62E+00
Ra	14	2.65E+01[31,52]	5.34E+00		2.26E+00[9]		15	2.26E+00[31,52]	1.56E+00
Rb		2.40E+00[10]		44	1.33E+00[16]	1.17E+00	48	1.02E+00[16]	1.02E+00
Sb		6.74E+01[11]		80	3.85E+00[16,20,21]	1.97E+00	51	2.25E+01[16,20]	4.79E+00
Se		1.00E+00[12]		216	1.98E+00[16,19,20,21,22,23,36,39]	1.41E+00	325	2.74E+00[16,19,20,21,22,23,25,26,27,28,29,36,39]	1.66E+00
Sn		4.58E+00[13]			2.29E+00[13]		31	2.29E+00[25]	1.54E+00
Sr[1]		3.79E+03[14]		12	1.48E+00[18]	1.27E+00	12	1.17E+00[18]	1.13E+00
Sr[2]		2.80E+01[14]		46	3.35E+00[16,21]	2.84E+00	51	7.21E-01[16,21]	4.53E-01

Table 7.3. cont. Ratio of fresh weight tissue concentration to muscle concentration ($R_{REF.T}$) in reptilian animals. Values highlighted in grey are those which are based on assumptions rather than measured values (see footnotes for details).

	Bone			Kidney			Liver		
Element	***n***	**mean**	**SD**	***n***	**mean**	**SD**	***n***	**mean**	**SD**
Th	1	1.10E+02[52]			2.55E+01[9]		3	2.55E+01[52]	6.18E+00
Tl		1.20E+01[15]		2	8.70E+00[21]	4.17E+00	3	1.11E+00[21]	1.29E+00
U	1	1.22E+01[52]			1.33E+01[9]		3	1.33E+01[52]	4.46E+00
V		6.00E+00[15]		46	1.10E+01[16,21]	3.36E+00	51	6.89E+00[16,21]	2.65E+00
Zn	114	5.31E+00[17,30,33]	2.32E+00	259	1.95E+00[16,17,18,2124,33,34,36,37,38,39,47]	1.40E+00	315	2.02E+00[16,17,18,2124,28,29,33,34,36,37,38,39,40,47]	1.42E+00
Zr		4.00E+00[15]		44	9.17E-01[16]	9.69E-01	48	2.47E+00[16]	1.59E+00

[1] excludes data for turtles; [2] data for turtles only; [3] 1:1 muscle:bone ratio (Saeki et al., 2001) using the fwt:dwt data for these tissues from Table 7.1; [4] same as Sr (Yankovich & Beaton, 2000; Yankovich, 2009); [5] turtle and generic reptile given same value; [6] 1:4 bone:kidney and bone:liver ratio (Jefferies & French, 1976; Sanchez-Chardi et al., 2007); [7] same as Ni (Yankovich & Beaton, 2000; Yankovich, 2009); [8] half Ni value (Yankovich & Beaton, 2000; Yankovich, 2009); [9] same as liver (Yankovich & Beaton, 2000); [10] 2.4:1 bone:muscle ratio (Yankovich & Beaton, 2000; Yankovich, 2009); [11] 3:1 bone:liver ratio (Yankovich, 2009); [12] 1:1 bone:muscle ratio (Yankovich & Beaton, 2000); [13] 1:1 liver:kidney ratio and 2:1 bone:liver ratio (Garcia et al., 2001); [14] same as Ca (Yankovich & Beaton, 2000; Yankovich, 2009); [15] bone:muscle ratios from Yankovich (2009); [16] turtle data (Anan et al., 2001); [17] turtle data (Torrent et al., 2004); [18] crocodile data (Swanepoel et al., 2000); [19] turtle data (Storelli et al., 1998); [20] turtle data (Kaska et al., 2004); [21] turtle data (Lam et al., 2004); [22] snake data (Campbell et al., 2005); [23] snake data (Burger et al., 2005); [24] crocodile data (Xu et al., 2006a); [25] crocodile data (Burger et al., 2000); [26] turtle data (Burger, 2002); [27] snake data (Burger et al., 2007); [28] turtle data (Davenport & Wrench, 1990); [29] turtle data (Godley et al., 1998); [30] crocodile data (Markich et al., 2002); [31] turtle data (Jeffree, 1991); [32] turtle data (Frias-Espericueta et al., 2006); [33] turtle data (Garcia-Fernandez et al., 2009); [34] turtle data (Gardner et al., 2006); [35] turtle data (Godley et al., 1999); [36] turtle data (Maffucci et al., 2005); [37] turtle data (Sakai et al., 1995); [38] turtle data (Sakai et al., 2000); [39] turtle data (Storelli et al., 2005); [40] turtle data (Franzellitti et al., 2004); [41] turtle data (Stone et al., 1980); [42] turtle data (Meyersschone & Walton, 1990); [43] turtle data (Towns, 1987); [44] lizard data (Narayanan & Eapen, 1971); [45] snake data (Copplestone et al., 2005a); [46] turtle data (Meyersschone et al., 1993); [47] turtle data (Andreani et al., 2008); [48] turtle data (Day et al., 2005); [49] crocodile data (HeatonJones et al., 1997); [50] crocodile data (Jagoe et al., 1998); [51] crocodile data (Yanochko et al., 1997); [52] crocodile and turtle data (Martin et al., 1998).

Table 7.4. Ratio of fresh weight tissue concentration to eggshell concentration ($R_{REF.T}$) in reptilian eggs.

	Albumen			Yolk			Yolk & Albumen		
Element	***n***	**mean**	**SD**	***n***	**mean**	**SD**	***n***	**mean**	**SD**
Ag	30	3.82E-02[3]	1.95E-01	30	7.94E-01[3]	4.11E-01		-	
Al		-			-		9	7.21E-02[4]	2.74E-01
As	30	7.73E-01[3]	4.26E-01	30	1.14E+01[3]	1.10E+01	10	6.29E-01[5]	5.09E-01
Ba	30	1.43E-01[3]	3.56E-01	30	2.49E+00[3]	1.95E+00		-	
Cd[1]		-			-		19	1.53E-01[4,5]	3.70E-01
Cd[2]		-			-		16	1.79E+00[6]	1.23E+00
Co	30	2.67E-03[3]	5.25E-02	30	9.09E-03[3]	9.65E-02	9	2.29E-01[4]	4.46E-01
Cr	30	1.15E-01[3]	3.24E-01	30	2.00E+00[3]	1.44E+00	35	1.00E-01[4,5,6]	3.05E-01
Cs	30	1.45E-01[3]	3.59E-01	30	2.00E-01[3]	4.07E-01		-	
Cu	35	4.48E-02[3,7]	2.10E-01	35	4.38E-01[3,7]	5.03E-01	19	2.00E-01[4,5]	4.11E-01
Fe	35	1.43E+00[3,7]	7.93E-01	35	1.71E+01[3,7]	1.68E+01	10	4.82E-01[5]	5.27E-01
Hg	35	1.44E-01[3,7]	3.57E-01	35	2.42E+00[3,7]	1.88E+00	19	8.74E-01[4,5]	3.41E-01
Mn[1]		-			-		10	4.11E-02[5]	2.09E-01
Mn[2]	35	1.85E-01[3,7]	3.94E-01	35	1.11E+00[3,7]	3.49E-01	16	4.46E-01[6]	5.13E-01
Mo	30	1.37E-01[3]	3.50E-01	30	2.55E-01[3]	4.43E-01	9	3.24E-02[4]	1.88E-01
Ni[1]		-			-		9	3.71E-02[4]	2.00E-01
Ni[2]	30	1.42E-03[3]	3.83E-02	30	1.58E-02[3]	1.27E-01		-	
Pb	30	4.27E-02[3]	2.06E-01	30	4.45E-01[3]	5.06E-01	35	5.86E-01[4,5,6]	5.00E-01
Rb	30	2.00E+00[3]	1.44E+00	30	3.52E+00[3]	3.03E+00		-	
Sb	30	1.89E-01[3]	3.98E-01	30	1.11E+00[3]	3.57E-01		-	
Se	30	1.08E-01[3]	3.16E-01	30	1.40E+00[3]	7.61E-01	16	4.03E+00[6]	3.61E+00
Sr[1]		-			-		9	3.00E-02[4]	1.81E-01
Sr[2]	30	6.27E+02[3]	6.37E+02	30	5.13E+01[3]	5.17E+01		-	
Tl	30	4.40E-02[3]	2.09E-01	30	1.32E-01[3]	3.44E-01		-	
V	30	1.39E+00[3]	7.52E-01	30	2.78E+00[3]	2.27E+00		-	
Zn	35	2.53E-01[3,7]	4.41E-01	35	3.25E+01[3,7]	3.24E+01	10	2.36E+00[5]	1.89E+00

- indicates no data available; [1] excludes data for turtles; [2] data for turtles only; [3] turtle data (Lam et al., 2006); [4] crocodile data (Stoneburner & Kushlan, 1984); [5] crocodile data (Xu et al., 2006a); [6] turtle data (Burger & Gibbons, 1998); [7] turtle data (Sakai et al., 1995).

The difference in Ca and Sr data between turtles and the other reptiles is probably due to the requirement for Ca (for which Sr is a chemical analogue) for shell development. Bone, including shell, accounts for 42% of body mass in turtles but only 7.2% in other reptiles (Table 7.2) so turtles have a high demand for Ca and it would appear that they have elevated blood Ca concentrations (and hence higher tissue concentrations) compared to other reptiles as a result. This is seen in both the animal and the egg data and results in lower animal $R_{REF.T}$ and higher egg $R_{REF.T}$ values for turtles compared to other reptile groups. The other elements for which marked differences were observed were Cd and Mn, both of which were found to concentrate more in the soft tissues of turtles (especially the kidney in the case of Cd) compared to other reptiles, and Ni, for which the turtle bone concentration was two orders of magnitude lower than for other reptiles. However, the reasons for these differences are unclear.

To develop generic B_T values that could be applied across studies, it was assumed that total whole-body burden of a given element was equivalent to the sum of the bone, kidney, liver and muscle burdens for that element. The R_{REF} data were used in conjunction with tissue mass data and an understanding of the element-specific tissue distribution in order to derive B_T. For each animal tissue, B_T was estimated from:

$$B_T = \frac{R_{REF.T} \times M_{REF.T}}{\sum\left(R_{REF.bo} \times M_{REF.bo}, R_{REF.k} \times M_{REF.k}, R_{REF.li} \times M_{REF.li}, R_{REF.m} \times M_{REF.m}\right)}$$

and

$$M_{REF.T} = \frac{FM_T}{FM_{REF}}$$

where $R_{REF.T}$ is the normalised tissue concentration of tissue T (bone, kidney, liver or muscle); $R_{REF.bo}$, $R_{REF.k}$, $R_{REF.li}$, $R_{REF.b}$ are the normalised tissue concentrations of bone, kidney, liver and muscle respectively; $M_{REF.T}$ is the ratio between the fractional mass of tissue T (FM_T) and the fractional mass of the reference tissue (FM_{REF}); and $M_{REF.bo}$, $M_{REF.k}$, $M_{REF.li}$ and $M_{REF.m}$ are the ratios of tissue to reference tissue fractional mass for bone, kidney, liver and muscle respectively. The same calculation procedure was used for egg tissues (albumen, eggshell and yolk). Some references reported data for combined yolk and albumen samples but these data were only used in the derivation of B_T when separate yolk and albumen data were unavailable. The derived B_T values are presented for animals (Table 7.5) and eggs (Table 7.6). These data were then used to derive whole-body (or whole-egg):tissue concentration ratios (Tables 7.7 & 7.8) for use in the development of the reptile CR database.

In some instances more than one reference was found to present variations of the same data set (e.g. Burger et al., 2005; Burger et al., 2007). To avoid biasing the summarised data on tissue distribution, only data from the most comprehensive reference (highest *n* and broadest tissue coverage) were collated. Where reptile-specific data were not available, mammal or bird data were used preferentially. If these data were not available, data on the proportional distribution between hard and soft tissues in fish were used. All data which are based on assumptions are highlighted in the tables.

Table 7.5. Estimated fraction of the total body-burden of elements in individual tissues (B_T) of reptilian animals and the percentage distribution between hard and soft tissues

	Generic reptile (excluding turtles)						Turtles					
	B_T				% of body-burden		B_T				% of body-burden	
Element	Bone	Kidney	Liver	Muscle	Hard tissues[1]	Soft tissues[2]	Bone	Kidney	Liver	Muscle	Hard tissues[1]	Soft tissues[2]
Ag	6.91E-03	7.14E-04	9.66E-01	2.60E-02	0.7	99.3	3.25E-02	5.78E-04	9.54E-01	1.25E-02	3.3	96.7
Al	6.07E-01	6.96E-04	3.16E-02	3.61E-01	60.7	39.3	9.33E-01	1.84E-04	1.02E-02	5.64E-02	93.3	6.7
As	1.10E-01	4.49E-03	9.88E-02	7.87E-01	11.0	89.0	5.19E-01	3.66E-03	9.81E-02	3.79E-01	51.9	48.1
Ba	9.06E-01	4.68E-04	5.35E-03	8.82E-02	90.6	9.4	9.89E-01	8.78E-05	1.23E-03	9.79E-03	98.9	1.1
Ca	9.97E-01	1.61E-05	2.02E-04	3.20E-03	99.7	0.3	9.54E-01	8.16E-04	3.44E-03	4.21E-02	95.4	4.6
Cd	6.37E-02	5.11E-03	2.82E-01	6.49E-01	6.4	93.6	7.02E-02	3.79E-01	4.78E-01	7.27E-02	7.0	93.0
Co	4.07E-02	2.46E-01	4.11E-01	3.03E-01	4.1	95.9	2.04E-01	2.11E-01	4.31E-01	1.54E-01	20.4	79.6
Cr	1.42E-01	3.84E-03	4.94E-02	8.05E-01	14.2	85.8	6.05E-01	2.81E-03	4.41E-02	3.48E-01	60.5	39.5
Cs	2.05E-02	7.56E-03	3.74E-02	9.35E-01	2.0	98.0	1.64E-01	1.04E-02	6.29E-02	7.63E-01	16.4	83.6
Cu	9.83E-02	5.64E-03	7.92E-01	1.04E-01	9.8	90.2	3.56E-01	3.51E-03	6.02E-01	3.82E-02	35.6	64.4
Fe	2.66E-02	4.25E-03	6.05E-01	3.64E-01	2.7	97.3	1.39E-01	3.82E-03	6.64E-01	1.94E-01	13.9	86.1
Hg	9.07E-02	1.41E-02	2.55E-01	6.40E-01	9.1	90.9	4.28E-01	1.14E-02	2.53E-01	3.08E-01	42.8	57.2
Mg	4.77E-01	2.47E-03	3.10E-02	4.89E-01	47.7	52.3	8.94E-01	7.95E-04	1.22E-02	9.31E-02	89.4	10.6
Mn	5.82E-01	4.32E-04	8.23E-02	3.36E-01	58.2	41.8	1.63E-01	5.09E-02	4.35E-01	3.51E-01	16.3	83.7
Mo	2.36E-01	4.28E-02	5.39E-01	1.82E-01	23.6	76.4	6.29E-01	1.96E-02	3.02E-01	4.95E-02	62.9	37.1
Ni	7.09E-01	1.09E-03	1.51E-02	2.74E-01	70.9	29.1	2.29E-01	1.82E-02	2.60E-01	4.93E-01	22.9	77.1
Pb	4.65E-01	2.54E-03	5.02E-02	4.82E-01	46.5	53.5	8.86E-01	8.32E-04	2.01E-02	9.35E-02	88.6	11.4
Po	9.48E-02	3.66E-02	5.80E-01	2.88E-01	9.5	90.5	3.76E-01	2.50E-02	4.83E-01	1.16E-01	37.6	62.4
Ra	6.58E-01	2.34E-03	3.70E-02	3.02E-01	65.8	34.2	9.44E-01	5.76E-04	1.11E-02	4.41E-02	94.4	5.6
Rb	1.57E-01	3.63E-03	4.40E-02	7.95E-01	15.7	84.3	6.34E-01	2.52E-03	3.73E-02	3.26E-01	63.4	36.6
Sb	7.13E-01	1.69E-03	1.56E-01	1.29E-01	71.3	28.7	9.39E-01	3.83E-04	4.32E-02	1.72E-02	93.9	6.1
Se	6.65E-02	5.48E-03	1.20E-01	8.08E-01	6.7	93.3	3.81E-01	5.39E-03	1.44E-01	4.70E-01	38.1	61.9
Sn	2.50E-01	5.19E-03	8.22E-02	6.63E-01	25.0	75.0	7.45E-01	2.66E-03	5.14E-02	2.01E-01	74.5	25.5
Sr	9.97E-01	1.61E-05	2.02E-04	3.20E-03	99.7	0.3	9.54E-01	8.16E-04	3.39E-03	4.21E-02	95.4	4.6
Th	7.86E-01	7.56E-03	1.20E-01	8.68E-02	78.6	21.4	9.57E-01	1.58E-03	3.06E-02	1.08E-02	95.7	4.3
Tl	4.75E-01	1.43E-02	2.88E-02	4.81E-01	47.5	52.5	8.92E-01	4.62E-03	1.13E-02	9.19E-02	89.2	10.8
U	3.63E-01	1.64E-02	2.60E-01	3.61E-01	36.3	63.7	7.94E-01	6.17E-03	1.19E-01	8.03E-02	79.4	20.6
V	2.59E-01	1.98E-02	1.96E-01	5.25E-01	25.9	74.1	7.26E-01	9.54E-03	1.15E-01	1.49E-01	72.6	27.4
Zn	2.82E-01	4.29E-03	7.04E-02	6.44E-01	28.2	71.8	7.77E-01	2.04E-03	4.08E-02	1.81E-01	77.7	22.3
Zr	2.25E-01	2.14E-03	9.11E-02	6.82E-01	22.5	77.5	7.16E-01	1.17E-03	6.10E-02	2.21E-01	71.6	28.4

[1] bone; [2] kidney liver and muscle combined

Table 7.6. Estimated fraction of the total body-burden of elements in individual tissues (B_T) of reptilian eggs and the percentage distribution between hard and soft tissues

	B_T				% of body-burden	
Element	**Albumen**	**Eggshell**	**Yolk**	**Yolk & Albumen**	**Hard tissues[3]**	**Soft tissues[4]**
Ag	1.50E-02	1.92E-01	7.93E-01	-	19.2	80.8
Al	-	6.57E-01	-	3.43E-01	65.7	34.3
As	2.56E-02	1.62E-02	9.58E-01	n.d.	1.6	98.4
Ba	2.05E-02	7.05E-02	9.09E-01	-	7.0	93.0
Cd[1]	-	4.76E-01	-	5.24E-01	47.6	52.4
Cd[2]	-	7.17E-02	-	9.28E-01	7.2	92.8
Co	5.16E-03	9.50E-01	4.48E-02	n.d.	95.0	5.0
Cr	2.01E-02	8.61E-02	8.94E-01	n.d.	8.6	91.4
Cs	1.27E-01	4.28E-01	4.45E-01	-	42.8	57.2
Cu	2.71E-02	2.97E-01	6.76E-01	n.d.	29.7	70.3
Fe	3.14E-02	1.08E-02	9.58E-01	n.d.	1.1	98.9
Hg	2.12E-02	7.21E-02	9.07E-01	n.d.	7.2	92.8
Mn[1]	-	7.71E-01	-	2.29E-01	77.1	22.9
Mn[2]	5.29E-02	1.40E-01	8.07E-01	n.d.	14.0	86.0
Mo	1.07E-01	3.84E-01	5.09E-01	n.d.	38.4	61.6
Ni[2]	-	7.89E-01	-	2.11E-01	78.9	21.1
Ni[3]	2.66E-03	9.22E-01	7.57E-02	-	92.2	7.8
Pb	2.56E-02	2.94E-01	6.80E-01	n.d.	29.4	70.6
Rb	1.74E-01	4.28E-02	7.83E-01	-	4.3	95.7
Sb	5.38E-02	1.40E-01	8.06E-01	-	14.0	86.0
Se	2.59E-02	1.18E-01	8.56E-01	n.d.	11.8	88.2
Sr[1]	-	8.22E-01	-	1.78E-01	82.2	17.8
Sr[2]	8.27E-01	6.48E-04	1.73E-01	-	0.1	99.9
Tl	5.04E-02	5.64E-01	3.86E-01	-	56.4	43.6
V	1.55E-01	5.47E-02	7.90E-01	-	5.5	94.5
Zn	3.03E-03	5.88E-03	9.91E-01	n.d.	0.6	99.4

[1] excludes data for turtles; [2] data for turtles only; [3] eggshell; [4] yolk and albumen; - indicates no literature data available; n.d. indicates that combined yolk & albumen ratios were not derived because separate yolk and albumen data were available.

Table 7.7. Estimated whole-body:tissue concentration ratios for reptilian animals

	Generic reptile (excluding turtles)				Turtles			
Element	**Bone**	**Kidney**	**Liver**	**Muscle**	**Bone**	**Kidney**	**Liver**	**Muscle**
Ag	1.04E+01	4.20E+00	4.92E-02	3.37E+01	2.22E+00	5.19E+00	4.98E-02	7.04E+01
Al	1.19E-01	4.31E+00	1.50E+00	2.43E+00	4.50E-01	1.63E+01	5.69E+00	9.21E+00
As	6.58E-01	6.68E-01	4.81E-01	1.11E+00	8.09E-01	8.21E-01	5.91E-01	1.37E+00
Ba	7.97E-02	6.41E+00	8.88E+00	9.95E+00	4.25E-01	3.42E+01	4.73E+01	5.30E+01
Ca	7.24E-02	1.86E+02	2.35E+02	2.74E+02	4.40E-01	3.68E+00	1.69E+01	1.23E+01
Cd	1.13E+00	5.87E-01	1.69E-01	1.35E+00	5.98E+00	7.92E-03	1.21E-01	7.14E+00
Co	1.77E+00	1.22E-02	1.16E-01	2.90E+00	2.06E+00	1.42E-02	1.35E-01	3.37E+00
Cr	5.08E-01	7.82E-01	9.63E-01	1.09E+00	6.94E-01	1.07E+00	1.32E+00	1.49E+00
Cs	3.53E+00	3.97E-01	1.27E+00	9.39E-01	2.56E+00	2.88E-01	9.22E-01	6.81E-01
Cu	7.34E-01	5.32E-01	6.00E-02	8.45E+00	1.18E+00	8.54E-01	9.63E-02	1.36E+01
Fe	2.72E+00	7.06E-01	7.85E-02	2.41E+00	3.02E+00	7.85E-01	8.74E-02	2.68E+00
Hg	7.96E-01	2.13E-01	1.86E-01	1.37E+00	9.80E-01	2.63E-01	2.30E-01	1.69E+00
Mg	1.51E-01	1.21E+00	1.53E+00	1.79E+00	4.70E-01	3.77E+00	4.77E+00	5.57E+00
Mn	1.24E-01	6.94E+00	5.77E-01	2.61E+00	2.57E+00	5.89E-02	1.33E-01	1.48E+00
Mo	3.06E-01	7.01E-02	8.82E-02	4.81E+00	6.67E-01	1.53E-01	1.92E-01	1.05E+01
Ni	1.02E-01	2.75E+00	3.15E+00	3.20E+00	1.83E+00	1.65E-01	2.23E-01	1.05E+00
Pb	1.55E-01	1.18E+00	9.47E-01	1.82E+00	4.74E-01	3.61E+00	2.89E+00	5.55E+00
Po	7.61E-01	8.19E-02	8.19E-02	3.04E+00	1.12E+00	1.20E-01	1.20E-01	4.47E+00
Ra	1.10E-01	1.28E+00	1.28E+00	2.90E+00	4.45E-01	5.20E+00	5.20E+00	1.18E+01
Rb	4.60E-01	8.27E-01	1.08E+00	1.10E+00	6.63E-01	1.19E+00	1.56E+00	1.59E+00
Sb	1.01E-01	1.77E+00	3.04E-01	6.82E+00	4.47E-01	7.84E+00	1.34E+00	3.02E+01
Se	1.09E+00	5.47E-01	3.97E-01	1.09E+00	1.10E+00	5.56E-01	4.03E-01	1.10E+00
Sn	2.89E-01	5.78E-01	5.78E-01	1.32E+00	5.64E-01	1.13E+00	1.13E+00	2.58E+00
Sr	7.24E-02	1.86E+02	2.35E+02	2.74E+02	4.40E-01	3.68E+00	1.71E+01	1.23E+01
Th	9.19E-02	3.97E-01	3.97E-01	1.01E+01	4.39E-01	1.90E+00	1.90E+00	4.83E+01
Tl	1.52E-01	2.09E-01	1.65E+00	1.82E+00	4.71E-01	6.49E-01	5.11E+00	5.65E+00
U	1.99E-01	1.83E-01	1.83E-01	2.43E+00	5.29E-01	4.86E-01	4.86E-01	6.46E+00
V	2.79E-01	1.51E-01	2.42E-01	1.67E+00	5.79E-01	3.14E-01	5.04E-01	3.47E+00
Zn	2.56E-01	6.99E-01	6.75E-01	1.36E+00	5.41E-01	1.47E+00	1.42E+00	2.87E+00
Zr	3.22E-01	1.40E+00	5.21E-01	1.29E+00	5.86E-01	2.56E+00	9.51E-01	2.34E+00

Table 7.8. Estimated whole-egg:tissue concentration ratios for reptilian eggs

Element	Albumen	Eggshell	Yolk	Yolk & Albumen
Ag	1.50E-02	1.92E-01	7.93E-01	-
Al	-	6.57E-01	-	3.43E-01
As	2.56E-02	1.62E-02	9.58E-01	n.d.
Ba	2.05E-02	7.05E-02	9.09E-01	-
Ca[1]	-	-	-	-
Ca[2]	-	-	-	-
Cd[1]	-	4.76E-01	-	5.24E-01
Cd[2]	-	7.17E-02	-	9.28E-01
Co	5.16E-03	9.50E-01	4.48E-02	n.d.
Cr	2.01E-02	8.61E-02	8.94E-01	n.d.
Cs	1.27E-01	4.28E-01	4.45E-01	-
Cu	2.71E-02	2.97E-01	6.76E-01	n.d.
Fe	3.14E-02	1.08E-02	9.58E-01	n.d.
Hg	2.12E-02	7.21E-02	9.07E-01	n.d.
Mg	-	-	-	-
Mn[1]	-	7.71E-01	-	2.29E-01
Mn[2]	5.29E-02	1.40E-01	8.07E-01	n.d.
Mo	1.07E-01	3.84E-01	5.09E-01	n.d.
Ni[2]	-	7.89E-01	-	2.11E-01
Ni[3]	2.66E-03	9.22E-01	7.57E-02	
Pb	2.56E-02	2.94E-01	6.80E-01	n.d.
Po	-	-	-	-
Ra	-	-	-	-
Rb	1.74E-01	4.28E-02	7.83E-01	-
Sb	5.38E-02	1.40E-01	8.06E-01	-
Se	2.59E-02	1.18E-01	8.56E-01	n.d.
Sn	-	-	-	-
Sr[1]	-	8.22E-01	-	1.78E-01
Sr[2]	8.27E-01	6.48E-04	1.73E-01	-
Th	-	-	-	-
Tl	5.04E-02	5.64E-01	3.86E-01	-
U	-	-	-	-
V	1.55E-01	5.47E-02	7.90E-01	-
Zn	3.03E-03	5.88E-03	9.91E-01	n.d.
Zr	-	-	-	-

[1] excludes data for turtles; [2] data for turtles only; - indicates no literature data available; n.d. indicates that combined yolk & albumen ratios were not derived because separate yolk and albumen data were available.

7.3.3. Converting radionuclide deposition data to soil activity concentrations

In some data sets, predominantly from the Russian-language literature, soil data were presented as deposition data (e.g. Bq m^{-2}) rather than activity concentration data (e.g. Bq kg^{-1}). A sampling depth of 10 cm and a soil bulk density of 1400 kg m^{-3} dwt were assumed where no further information was provided to enable conversion from Bq m^{-2} to Bq kg^{-1} (Beresford et al., 2008d).

7.3.4. Converting sediment data to water data when deriving aquatic CRs

Aquatic CRs were calculated relative to activity concentrations in water but in some cases media activity concentration data were only available for sediments. To convert the sediment activity concentrations to water concentrations, distribution coefficient (K_d) values were used. The distribution coefficient provides a measure of the degree of partitioning between sediment and water for a given element or radionuclide and can be defined as:

$$K_d\left(\mathrm{l\ kg^{-1}}\right) = \frac{\text{Activity concentration of } R \text{ in sediment (Bq kg}^{-1}\text{ dwt)}}{\text{Activity concentration of } R \text{ in filtered water (Bq l}^{-1}\text{)}}$$

The freshwater K_d values used in the study presented here were obtained from a database of K_d values held by Tamara Yankovich (AREVA Resources Canada Inc., Canada) and are presented in Table 7.9.

When activity concentration data in sediments were reported on a fresh weight rather than dry weight basis, moisture content values of 50% and 90% were assumed for sandy and organic sediments respectively (Tamara Yankovich, pers. comm.).

Table 7.9. Freshwater distribution coefficient (K_d, l kg^{-1}) values used in the development of the reptiles transfer database (Tamara Yankovich, AREVA Resources Canada Inc., pers. comm.).

Element	*n*	Mean	SD
As	44	3.6E+03	5.1E+03
Ca	95	3.2E+03	3.0E+03
Cd	14	1.4E+04	1.6E+04
Cr	83	7.6E+04	8.2E+04
Cu	14	1.4E+04	1.6E+05
Hg	10	7.0E+02	7.2E+02
Pb	95	1.5E+05	2.3E+05
Se	2	1.4E+03	1.6E+03
Zn	94	3.2E+04	4.5E+04

7.3.5. Estimation of weighted means and standard deviations

The CR data presented in Section 7.4 were weighted with respect to both sample numbers and standard deviations reported in the source data sets using the approach described in Section 3.4. The value of *n* reported is the total number of observations from all studies used in the estimation of the CR, the arithmetic mean was derived from the means for each individual study (weighted by *n* for each study) and the standard deviation comprised both the variance within studies and the variance between studies.

Where information was lacking in the source data sets used to derive the summary statistics, the assumptions described by Beresford et al. (2008d) were used: (i) if the number of observations and an error term (e.g. standard deviation) were not reported, $n = 1$ was assumed; (ii) if only a range was reported, $n = 2$ was assumed; and (iii) if an error term was reported without the number of observations being specified, $n = 3$ was assumed.

7.3.6. Summarising data sets that included LOD values

Some data sets included LOD data, also known as censored data (Helsel, 1990), so it was necessary to select an appropriate method to incorporate these data into the calculation of the CR summary statistics. One method is to substitute the LOD values with a value between 0 and the LOD; commonly the LOD value is replaced with a value equal to one-half of the LOD (e.g. Garcia-Fernandez et al., 2009; Tajimi et al., 2005). Although the LOD/2 substitution method is in line with the approach adopted for development of databases on radionuclide transfer to wildlife that have been compiled under European Commission (Beresford et al., 2008d; Hosseini et al., 2008) and International Atomic Energy Agency (Nick Beresford, Centre for Ecology and Hydrology, pers. comm.) initiatives, its use cannot be justified except on the grounds of simplicity. There is little, if any, statistical rationale behind the substitution method and the approach performs worst in situations where there are multiple detection limits (Helsel, 2005b), which is a situation often encountered in radioecological data sets and especially those obtained from gamma spectrometry.

Although some authors (Antweiler & Taylor, 2008) continue to support the use of substitution as an 'adequate' method for handling LOD values, there are many theoretical (e.g. Helsel, 1990; Helsel, 2005a; Helsel, 2006; Hornung & Reed, 1990) and empirical (e.g. Baccarelli et al., 2005; She, 1997) studies that demonstrate substitution to be inferior to methods adopted from medical statistics (known as survival analysis methods) and to non-

parametric survival analysis methods in particular (e.g. Zhang et al., 2009). Other fields of environmental science have been applying survival analysis techniques to handle datasets that include LOD values for the past two decades (e.g. Baccarelli et al., 2005; Millard & Deverel, 1988; She, 1997) so it is surprising that, given the regularity with which LOD values are encountered in radioecological datasets, these methods do not appear to have been widely adopted within radioecology.

The Kaplan-Meier method (Kaplan & Meier, 1958), a non-parametric technique, is the most widely applicable of these survival analysis methods (e.g. Antweiler & Taylor, 2008; Brady & Pratt, 2007) and was used to estimate the mean and standard deviation when summarising reptile CR datasets which included LOD values. The analysis was performed using Statistical Package for the Social Sciences (SPSS) 16.0 for Windows.

7.4. Transfer parameters for reptiles

Calculated CRs for reptiles in freshwater and terrestrial ecosystems are presented in Tables 7.10 – 7.13. No data were available on transfer to marine reptiles. In Tables 7.10 (freshwater reptiles) and 7.12 (terrestrial reptiles), the data are presented for each of the main groups within the Class Reptilia that may need to be considered when conducting assessments of ionising radiation impacts of biota, namely snakes (Order: Squamata, Suborder: Serpentes), lizards (Order: Squamata, Suborder: Sauria) including worm lizards (Order: Squamata, Suborder: Amphisbaenians), crocodilians (Order: Crocodylia) and turtles, terrapins and tortoises (Order: Testudinata). In Tables 7.11 (freshwater reptiles) and 7.13 (terrestrial reptiles), the available transfer data are summarised to provide generic reptile CRs for use in ERA applications.

Most biota dose assessments consider sites receiving regulated radionuclide discharges (Beresford et al., 2008b), which include sites receiving anthropogenic radionuclide inputs, for example from nuclear power plants and radioactive waste disposal sites, and those contaminated by natural radionuclides, due to activities such as uranium and phosphate mining. It is for this reason that Tuatara (Order: Sphenodontidae) are not considered within this chapter. There are only two species within this Order and both are endemic to New Zealand, which has been a nuclear-free zone since the establishment of the New Zealand Nuclear Free Zone, Disarmament, and Arms Control Act 1987.

To the best of the authors' knowledge, this chapter presents the most comprehensive meta-analysis of transfer to reptiles undertaken to date. There is scope for further detailed

analysis of these data but the purpose of this chapter is to establish a knowledge baseline to underpin the future development of radiation impact assessments for reptiles within ERA. Therefore, the remainder of the chapter considers: (i) an overview of the available data; (ii) a comparison of CRs across reptile groups and with CRs that were compiled for other aquatic and terrestrial vertebrates as part of the ERICA project (relevant aquatic and terrestrial ecosystem CRs for comparison are presented in Tables 7.14 and 7.15 respectively); and (iii) approaches to address some of the knowledge gaps in reptile transfer that have been highlighted by this study.

7.4.1 Data availability

Reptile CR data were available for 35 elements in freshwater ecosystems (Tables 7.10 and 7.11) and 15 elements in terrestrial ecosystems (Tables 7.12 and 7.13).

7.4.1.1. Aquatic reptile CR data

7.4.1.1.1. Animals

The majority of the aquatic reptile data available were for snakes and turtles (Table 7.10). There were data on the transfer of 14 elements to crocodilians but the number of measurements for each element was low (maximum $n = 3$). Few CR data were available for transfer to aquatic lizards. The differences in data availability are likely to be a reflection of the prevalence of different reptile groups in the aquatic ecosystems that have been used for measuring contaminant burdens in reptile tissues and the relative ease with which these reptiles can be studied.

Snakes and freshwater turtles are commonly encountered in the main locations that have been used for targeted research on reptiles; these locations are mainly in the United States. Working with snakes, particularly non-venomous species (most of the species for which data are presented in Table 7.10 are non-venomous), and turtles poses minimal risk to researchers compared with other reptiles commonly encountered in these locations, such as *Alligator mississippiensis* (American alligator), which present greater difficulties for researchers due to their physical size and the inherent dangers involved in working with these large predators.

Table 7.10. Concentration ratios for the four main groups of reptiles in freshwater ecosystems

	Crocodilian			Lizard		Snake			Turtle			Crocodilian egg		
Element	***n***	**mean**	**SD**	***n***	**mean**	***n***	**Mean**	**SD**	***n***	**mean**	**SD**	***n***	**mean**	**SD**
Am		-			-		-		1	3.22E+03[16]			-	
As	2	9.77E+01[1]	3.60E+01		-	6	3.05E+02[5,6]	5.70E+01	1	3.27E+02[17]		10	5.82E+02[1]	3.79E+01
B		-			-	1	2.04E+01[6]		1	1.07E+00[17]			-	
Ba		-			-	1	1.41E+02[6]			-			-	
Ca		-			-	1	9.89E+02[6]		1	1.23E+01[17]			-	
Cd	2	8.37E+00[1]	3.55E+00		-	5	2.36E+03[5]	8.81E+02		-		10	3.98E+01[1]	1.25E+01
Ce		-			-	1	6.02E+02[6]		1	6.50E+02[17]			-	
Cm		-			-		-		1	7.69E+01[16]			-	
Co		-			-		-		28	1.23E+01[18,19]	2.23E+01		-	
Cr	2	6.83E+00[1]	1.22E+00		-	6	1.92E+03[5,6]	9.42E+02	1	2.26E+02[17]		10	2.10E+01[1]	1.56E+00
Cs	3	6.43E+02[2]	9.32E+01		-	52	4.94E+03[7,8,19,10]	8.68E+03	38	2.87E+03[16,18,19]	1.41E+04		-	
Cu	2	2.88E+02[1]	6.76E+01		-	6	1.59E+03[5,6]	1.16E+03	1	3.33E+03[17]		10	5.45E+03[1]	4.55E+02
Fe	2	1.46E+02[1]	2.85E+01		-	1	2.83E+03[6]		1	9.29E+02[17]		10	4.87E+02[1]	6.27E+01
Hg	2	4.78E+01[1]	2.67E+01		-	20	1.30E+04[11]	3.70E-01	24	3.11E+01[20]	3.10E+01	10	1.00E+02[1]	1.01E+01
K		-			-	1	2.72E+03[6]		1	1.20E+03[17]			-	
La		-			-	1	2.64E+02[6]		1	2.14E+02[17]			-	
Mg		-			-	1	7.10E+01[6]		1	4.91E+01[17]			-	
Mn	2	1.15E+02[1]	5.06E+01		-	21	8.34E+02[6,12]	3.18E+03	1	5.68E+01[17]		10	2.64E+02[1]	5.24E+01
Mo		-			-	1	2.10E+01[6]		1	1.71E+03[17]			-	
Na		-			-	1	4.04E+02[6]			-			-	
Ni		-			-	1	1.89E+03[6]		1	2.20E+00[17]			-	
Pb	3	1.20E+02[1,3]	9.79E+01	1	8.15E+01[4]	6	4.39E+02[6,13,14]	7.65E+02	2	1.10E+03[21]	5.86E+01	10	1.90E+02[1]	2.64E+01
Po	1	7.31E+03[3]		1	4.72E+03[4]	3	1.49E+03[14]	6.22E+02	2	4.47E+03[21]	2.03E+02		-	
Pu		-			-		-		2	5.92E+03[16]	3.01E+03		-	
Ra	1	3.31E+03[3]		1	1.80E+02[4]	3	2.70E+02[14]	8.71E+01	13	7.75E+02[21,22]	1.62E+03		-	
Rb		-			-	1	3.40E+03[6]		1	1.59E+00[17]			-	

Table 7.10 cont. Concentration ratios for the four main groups of reptiles in freshwater ecosystems

	Crocodilian			Lizard		Snake			Turtle			Crocodilian egg		
Element	***n***	**mean**	**SD**	***n***	**mean**	***n***	**Mean**	**SD**	***n***	**Mean**	**SD**	***n***	**mean**	**SD**
Sb		-			-	1	5.66E+01[6]		1	4.50E+03[17]			-	
Se		-			-	11	2.65E+03[5,15]	2.46E+03		-			-	
Sr		-			-	1	4.07E+02[6]		39	1.21E+04[16,17,18,19,23]	4.94E+04		-	
Th	1	4.70E+02[3]		1	2.44E+02[4]	3	1.52E+03[14]	6.21E+02	2	9.62E+02[21]	9.51E+02		-	
U	1	4.54E+01[3]		1	5.03E+01[4]	3	9.24E+01[14]	8.02E+01	3	1.86E+02[17,21]	1.40E+02		-	
V		-			-	1	9.26E+02[6]		1	1.23E+03[17]			-	
Y		-			-		-		1	4.98E+02[17]				
Zn	2	2.80E+03[1]	1.62E+02		-	3	2.78E+04[6,13]	2.28E+04	1	4.95E+04[17]		10	4.13E+03[1]	5.91E+02
Zr		-			-	1	1.70E+03[6]		1	7.53E+02[17]			-	

[1] data for *Alligator sinensis* (Xu et al., 2006a); [2] data for *Alligator mississippiensis* (Brisbin, 1989) with linked media data (Whicker et al., 1990); [3] data for *Crocodylus johnstoni* (Martin et al., 1998); [4] data for *Varanus panoptes* (Martin et al., 1998); [5] data for *Nerodia fasciata* (Hopkins et al., 1999) with linked media data (Hopkins et al., 1998); [6] data for *Nerodia sipedon* (Tamara Yankovich, AREVA Resources Canada Inc., pers. comm.); [7] data for *Nerodia taxispilota* (Bagshaw & Brisbin, 1985) with linked media data (Risk Assessment Corporation, 2001); [8] data for mixed snake species (Brisbin et al., 1974b) with linked media data (Risk Assessment Corporation, 2001); [9] data for *Nerodia spp*. (Garten et al., 1975; Staton et al., 1974) with linked media data (Risk Assessment Corporation, 2001); [10] data for *Nerodia taxispilota* (Hinton & Scott, 1990); [11] data for *Nerodia sipedon* (Campbell et al., 2005) with linked media data (Campbell et al., 1998); [12] data for *Nerodia sipedon* (Campbell et al., 2005) with linked media data (Thompson, 2001); [13] data for *Nerodia sipedon* (Niethammer et al., 1985) with linked media data (Schmitt & Finger, 1982); [14] data for *Acrochordus arafurae* (Martin et al., 1998); [15] data for *Pituophis melanoleucus sayi* (Ohlendorf et al., 1988) with linked media data (Presser & Ohlendorf, 1987; Saiki & Lowe, 1987); [16] data for *Trachemys scripta scripta* (Whicker et al., 1990); [17] data for *Chelydra serpentina* (Tamara Yankovich, AREVA Resources Canada Inc., pers. comm.); [18] data for *Chelydra serpentina* and *Trachemys scripta* (Meyersschone et al., 1993) with linked media data (Oaks et al., 1987); [19] data for *Chelydra serpentina* and *Chrysemys picta* (Yankovich et al., in press); [20] data for *Chelydra serpentina* and *Trachemys scripta* (Meyersschone et al., 1993); [21] data for *Elseya dentata* (Martin et al., 1998); [22] data for *Chelydra serpentina* and *Pseudemys nelsoni* (Pritchard & Bloodwell, 1986); [23] data for *Trachemys scripta scripta* (Towns, 1987) with linked media data (Whicker et al., 1990)

Table 7.11. Summary of concentration ratios for reptiles (animals and eggs) in freshwater ecosystems[1].

	All reptiles			Reptiles excluding turtles			Turtles			Reptile eggs		
Element	***n***	**mean**	**SD**	***n***	**mean**	**SD**	***n***	**mean**	**SD**	***n***	**mean**	**SD**
Am	1	3.22E+03			-		1	3.22E+03			-	
As	9	2.61E+02	1.04E+02	8	2.53E+02	1.08E+02	1	3.27E+02		10	5.82E+02	3.79E+01
B	2	1.07E+01	1.37E+01	1	2.04E+01		1	1.07E+00			-	
Ba	1	1.41E+02		1	1.41E+02			-			-	
Ca	2	5.01E+02	6.91E+02	1	9.89E+02		1	1.23E+01			-	
Cd	7	1.69E+03	1.36E+03	7	1.69E+03	1.36E+03		-		10	3.98E+01	1.25E+01
Ce	2	6.26E+02	3.43E+01	1	6.02E+02		1	6.50E+02			-	
Cm	1	7.69E+01			-		1	7.69E+01			-	
Co	28	1.23E+01	2.23E+01		-		28	1.23E+01	2.23E+01		-	
Cr	9	1.30E+03	1.18E+03	8	1.44E+03	1.19E+03	1	2.26E+02		10	2.10E+01	1.56E+00
Cs	93	3.95E+03	1.11E+04	55	4.71E+03	8.49E+03	38	2.87E+03	1.41E+04		-	
Cu	9	1.50E+03	1.28E+03	8	1.27E+03	1.15E+03	1	3.33E+03		10	5.45E+03	4.55E+02
Fe	4	1.01E+03	1.27E+03	3	1.04E+03	1.55E+03	1	9.29E+02		10	4.87E+02	6.27E+01
Hg	46	5.66E+03	6.49E+03	22	1.18E+04	3.80E+03	24	3.11E+01	3.10E+01	10	1.00E+02	1.01E+01
K	2	1.96E+03	1.07E+03	1	2.72E+03		1	1.20E+03			-	
La	2	2.39E+02	3.51E+01	1	2.64E+02		1	2.14E+02			-	
Mg	2	6.01E+01	1.55E+01	1	7.10E+01		1	4.91E+01			-	
Mn	24	7.42E+02	2.98E+03	23	7.72E+02	3.04E+03	1	5.68E+01		10	2.64E+02	5.24E+01
Mo	2	8.63E+02	1.19E+03	1	2.10E+01		1	1.71E+03			-	
Na	1	4.04E+02		1	4.04E+02			-			-	
Ni	2	9.46E+02	1.33E+03	1	1.89E+03		1	2.20E+00				
Pb	12	4.40E+02	6.23E+02	10	3.07E+02	5.97E+02	2	1.10E+03	5.86E+01	10	1.90E+02	2.64E+01
Po	7	3.63E+03	2.26E+03	5	3.30E+03	2.68E+03	2	4.47E+03	2.03E+02		-	
Pu	2	5.92E+03	3.01E+03		-		2	5.92E+03	3.01E+03		-	
Ra	18	7.99E+02	1.52E+03	5	8.61E+02	1.37E+03	13	7.75E+02	1.62E+03		-	
Rb	2	1.70E+03	2.40E+03	1	3.40E+03		1	1.59E+00			-	

Table 7.11 cont. Summary of concentration ratios for reptiles (animals and eggs) in freshwater ecosystems[1].

	All reptiles			Reptiles excluding turtles			Turtles			Reptile eggs		
Element	***n***	**mean**	**SD**	***n***	**mean**	**SD**	***n***	**mean**	**SD**	***n***	**mean**	**SD**
Sb	2	2.28E+03	3.14E+03	1	5.66E+01		1	4.50E+03			-	
Se	11	2.65E+03	2.46E+03	11	2.65E+03	2.46E+03		-			-	
Sr	40	1.19E+04	4.88E+04	1	4.07E+02		39	1.21E+04	4.94E+04		-	
Th	7	1.03E+03	7.44E+02	5	1.05E+03	7.76E+02	2	9.62E+02	9.51E+02		-	
U	8	1.16E+02	1.05E+02	5	7.46E+01	6.17E+01	3	1.86E+02	1.40E+02		-	
V	2	1.08E+03	2.17E+02	1	9.26E+02		1	1.23E+03			-	
Y	1	4.98E+02			-		1	4.98E+02			-	
Zn	6	2.31E+04	2.29E+04	5	1.78E+04	2.11E+04	1	4.95E+04		10	4.13E+03	5.91E+02
Zr	2	1.22E+03	6.66E+02	1	1.70E+03		1	7.53E+02			-	

[1] For data provenance see Table 7.10.

Table 7.12. Concentration ratios for lizards, snakes and turtles in terrestrial ecosystems.

	Lizard			Snake			Turtle	
Element	***n***	**mean**	**SD**	***n***	**mean**	**SD**	***n***	**mean**
Am	21	7.01E-02[1,2]	4.19E-02	3	7.81E-02[11]	2.34E-03		-
C		-		6	1.72E+00[12]	1.83E+00		-
Cs	88	5.57E-01[1,2,3,4,5,6,7]	9.65E-01	51	6.24E-01[11,13,14,15,16,17,18]	1.10E+00	1	5.17E-02[22]
Cu	44	3.24E-02[8]	2.67E-02		-			-
K	17	2.76E-01[2]	1.56E-01	5	2.50E-01[11,19]	1.36E-01		-
Mn	1	1.04E-02[9]			-			-
Ni	1	3.02E-01[9]			-			
Pb	43	3.88E-01[8,10]	1.02E+00	1	7.03E-02[20]			-
Po	13	1.10E+01[10]	2.48E+01	1	1.28E-01[20]			-
Pu	29	3.41E-03[1,2,3]	7.14E-03	12	2.95E-03[11,13,21]	5.03E-03		-
Sr	50	5.99E-01[2,3,4,6,7]	6.47E-01	32	8.05E-02[13,17,18]	1.05E-01	1	2.30E-01[22]
Tc	5	< 7.74E-01[2]			-			-
Th	13	2.74E-01[10]	5.46E-01	2	2.17E-03[19]	2.94E-03		-
U	13	2.46E+00[10]	3.73E+00	4	4.81E-03[19]	5.41E-03		-
Zn	30	2.00E-01[8]	5.64E-02		-			-

[1] data for *Amphibolurus cristatus*, *Cetemphorous nuchates*, *Pogona minor* and *Varanus gouldi* (Giles et al., 1990); [2] data for *Anguis fragilis* and *Lacerta vivipara* (Wood et al., 2008; Wood et al., 2009b); [3] data for *Lacerta agilis* (Barnett et al., 2009); [4] data for *Lacerta agilis* (Carrington, 2003); [5] data for *Lacerta agilis* and *Lacerta vivipara* (Copplestone et al., 2005a); [6] data for *Lacerta vivipara* (Martjushov et al., 1999); [7] data for *Agama sanguinolenta*, *Anguis fragilis*, *Eremias grammica*, *Lacerta practicola*, *Lacerta viridis*, *Ophisaurus apodus* and *Phrynocephalus interscapularis* (Sokolov et al., 1989); [8] data for *Lacerta vivipara* (Avery et al., 1983); [9] data for *Lacerta taurica* (Sharygin et al., 1979); [10] data for *Ctenotus brooksi*, *Ctenophorus fordi*, *Ctenotus leae*, *Ctenophorus nuchalis*, *Ctenotus regius* and *Tiliqua rugosa* (Read & Pickering, 1999); [11] data for *Vipera berus* (Wood et al., 2008; Wood et al., 2009b); [12] CR data for *Thamnophis sirtalis* calculated relative to soil rather than air (Yankovich et al., 2007); [13] data for *Natrix natrix* (Barnett et al., 2009); [14] data for *Elaphe obsoleta* (Bagshaw & Brisbin, 1985) with linked media data (Brisbin et al., 1974b); [15] data for mixed snake species (Brisbin et al., 1974a) with linked media data (Brisbin et al., 1974b); [16] data for *Vipera berus* (Copplestone et al., 2005a); [17] data for *Natrix natrix* and *Vipera berus* (Iljenko, 1970); [18] data for *Coluber caspius*, *Natrix natrix* and *Vipera ursinii* (Sokolov et al., 1989); [19] data for *Natrix natrix* (Beresford et al., 2007a); [20] data for *Vipera berus* (Gjelsvik & Brown, 2009); [21] data for *Coluber constrictor flaviventris*, *Crotalus viridis viridis* and *Pituophis melanoleucus sayi* (Geiger & Winsor, 1977); [22] data for *Testudo horsfieldi* (Sokolov et al., 1989)

Table 7.13. Summary of concentration ratios for reptiles in terrestrial ecosystems[1].

	All reptiles			Reptiles excluding turtles			Turtles	
Element	***n***	**mean**	**SD**	***n***	**Mean**	**SD**	***n***	**mean**
Am	24	7.11E-02	3.92E-02	24	7.11E-02	3.92E-02		-
C[2]	6	1.72E+00	1.83E+00	6	1.72E+00	1.83E+00		-
Cs	140	5.78E-01	1.01E+00	139	5.81E-01	1.01E+00	1	5.17E-02
Cu	44	3.24E-02	2.67E-02	44	3.24E-02	2.67E-02		-
K	22	2.70E-01	1.49E-01	22	2.70E-01	1.49E-01		-
Mn	1	1.04E-02		1	1.04E-02			-
Ni	1	3.02E-01		1	3.02E-01			-
Pb	44	3.81E-01	1.00E+00	44	3.81E-01	1.00E+00		-
Po	14	1.02E+01	2.40E+01	14	1.02E+01	2.40E+01		-
Pu	41	3.27E-03	6.54E-03	41	3.27E-03	6.54E-03		-
Sr	83	3.95E-01	5.64E-01	82	3.97E-01	5.67E-01	1	2.30E-01
Tc	5	< 7.74E-01		5	< 7.74E-01			-
Th	15	2.38E-01	5.14E-01	15	2.38E-01	5.14E-01		-
U	17	1.88E+00	3.40E+00	17	1.88E+00	3.40E+00		-
Zn	30	2.00E-01	5.64E-02	30	2.00E-01	5.64E-02		-

[1] For data provenance see Table 7.12; [2] CR for C calculated relative to soil rather than air

Table 7.14. Default concentration ratios used in the ERICA Tool for freshwater organisms (Hosseini et al., 2008).

Element	Organism	*n*	Mean	SD	Element	Organism	*n*	Mean	SD
Am	Benthic fish	7	3.50E+02	3.90E+02	Po	Pelagic fish	13	2.40E+02	2.00E+02
	Bird	17	2.00E+00	1.00E+00	Pu	Benthic fish	45	6.00E+01	1.30E+02
	Pelagic fish	54	1.80E+00	1.00E+00		Pelagic fish	45	6.00E+01	1.30E+02
Cd	Benthic fish	4	2.30E+02	2.00E+02	Ra	Benthic fish	17	8.00E+01	1.20E+02
Ce	Pelagic fish	8	1.50E+01	1.30E+01		Pelagic fish	17	8.00E+01	1.20E+02
Cm	Amphibian	8	1.00E+01	1.20E+01	Sb	Benthic fish	7	2.90E+02	5.40E+02
	Pelagic fish	54	1.50E+02	2.00E+00		Pelagic fish	7	2.90E+02	5.40E+02
Co	Amphibian	2	1.40E+02	1.60E+02	Sr	Benthic fish	14	1.70E+01	2.30E+01
	Benthic fish	29	4.40E+02	1.51E+03		Pelagic fish	14	1.70E+01	2.30E+01
	Pelagic fish	29	4.40E+02	1.50E+03	Th	Benthic fish	8	1.10E+02	1.10E+02
Cs	Amphibian	3	9.30E+03	1.20E+03		Pelagic fish	5	1.10E+02	1.10E+02
	Benthic fish	100	5.00E+03	6.70E+03	U	Benthic fish	11	3.00E+01	6.00E+01
	Bird	72	3.00E+03	1.00E+00		Pelagic fish	11	3.00E+01	6.00E+01
	Pelagic fish	13	5.60E+03	4.70E+03					
Mn	Benthic fish	6	9.80E+02	2.00E+03					
	Pelagic fish	6	9.80E+02	2.00E+03					

Table 7.15. Default concentration ratios used in the ERICA Tool for terrestrial organisms (Beresford et al., 2008d).

Element	Organism	*n*	Mean	SD	Element	Organism	*n*	Mean	SD
Am	Mammal	121	4.08E-02	9.34E-02	Pu	Mammal	123	2.34E-02	8.13E-02
Cs	Amphibian	107	5.37E-01	8.97E-01	Sr	Amphibian	21	8.25E-01	1.22E+00
	Bird	158	7.50E-01	1.65E+00		Bird	69	5.49E-01	9.94E-01
	Mammal	1784	2.87E+00	4.25		Mammal	196	1.74E+00	2.35E+00
Mn	Mammal	4	2.49E-03	8.19E-04	Tc	Amphibian	2	5.75E-01	5.30E-01
Ni	Mammal	2	7.15E-02	9.92E-02		Bird	1	2.70E-01	
Pb	Amphibian	24	1.20E-01	5.20E-01	Th	Bird	-	3.89E-04	
	Bird	424	6.15E-02	1.73E-01		Mammal	18	1.22E-04	1.77E-04
	Mammal	502	3.88E-02	3.57E-02	U	Bird	-	5.41E-04	
Po	Mammal	36	2.78E-03	1.57E-03		Mammal	2	1.06E-04	1.29E-04

7.4.1.1.2. Eggs

The only data available for reptile egg CRs were for one species of crocodilian, *Alligator sinensis* (Chinese alligator), from one study undertaken in Zhejiang Province, China (Xu et al., 2006a). This study provided CR data for a total of 9 elements. However, given that these data are derived from 10 eggs of one crocodilian species collected from one location, the data should be used with caution when predicting transfer for other reptile species and/or sites.

7.4.1.1. Terrestrial reptile CR data

Lizards and snakes were the two main reptile groups for which data for terrestrial ecosystems were available (Table 7.12). CR values for Cs and Sr transfer to turtles were also located but these were based on measurements of one *Testudo horsfieldi* (Horsefield's tortoise) specimen from Turkmenistan (Sokolov et al., 1989) so should be used with caution. There were no data available on transfer to reptile eggs in the terrestrial environment.

7.4.1.3. Reptile CRs for use in ERA

It has been suggested that site-specific CRs based on a few measurements may not provide better transfer estimates than generic CRs (Sheppard, 2005). Similarly, given the small number of measurements and the small number of studies from which each CR value in Tables 7.10 and 7.12 were derived, there is limited justification for using CRs for different reptile types (rather than a generic reptile CR) for most of the elements reported. The most

likely difference in transfer between the reptile groups is the transfer to turtles compared with other reptiles for elements that partition between hard and soft tissues. This is because turtles have a markedly different fractional mass of hard (bone and shell) and soft tissues when compared with other reptiles (see Table 7.2).

Comparison of the Cs CR data for snakes and turtles in freshwater ecosystems (Table 7.10) supports this assertion. The CR for Cs transfer to turtles (2.87×10^3) is approximately 60% of that for snakes (4.94×10^3). Cs concentrates in soft tissues (Table 7.5). If the CR for turtles is estimated from the snake CR based on the fractional mass of soft tissues in snakes and turtles, the turtle CR would be 3.08×10^3. This is in good agreement with the measured value for turtles that is reported in Table 10 and suggests that the difference in Cs CR between snakes and turtles is due to a 'dilution' of the whole-body activity concentration in turtles due to the higher fractional mass of bone in these animals.

For use in ERA applications, the reptile CR values (Tables 7.10 and 7.12) are summarised in Tables 7.11 and 7.13 for 'All reptiles', 'Reptiles excluding turtles' and 'Turtles' in freshwater and terrestrial ecosystems respectively. Depending on the scenario and purpose of the assessment, those using these data can choose whether to use just the generic ('All reptiles') CR values or to distinguish between turtles and non-turtles.

7.4.2. CR comparisons

The derived CRs were compared across the reptile groups to look for differences between the CRs for these groups. To put the reptile CRs in context, the summarised CR data (Tables 7.11 and 7.13) were compared with CR data for other vertebrates in freshwater and terrestrial ecosystems. The most comprehensive CR data compilation available for comparison was that developed for the EC-funded project on Environmental Risk from Ionising Contaminants: Assessment and Management (ERICA) (Beresford et al., 2008d; Hosseini et al., 2008). Comparative vertebrate CR values used in ERICA are presented in Tables 7.14 and 7.15 for freshwater and terrestrial ecosystems respectively. In addition to the above comparisons, the extent to which reptile CRs may be habitat-specific was also assessed using radionuclides for which sufficient data were available.

7.4.2.1. CRs in freshwater ecosystems

There was generally good agreement between the reptile CRs (turtle and non-turtle) for As, Ce, Cs, Cu, Fe, K, La, Mg, Mn, V and Zr . There was also good agreement between reptile

CRs and the ERICA CR values for other aquatic vertebrates (amphibian, benthic fish, bird and pelagic fish) for Ce, Cs and Mn. However, the CRs for Ce, La and Mg were derived from single measurements so may not be representative.

For B, Ca, Mo and Rb there were differences in excess of one order of magnitude between the CRs for turtles and non-turtles. These CRs were all based on single values so the extent to which these values represent transfer to turtles and non-turtles is uncertain, especially given that the turtle Ca CR is approaching two orders of magnitude lower than the snake Ca CR value which is not what would be anticipated from the higher Ca requirement of turtles.

Both the Cs (2.87×10^3) and K (1.20×10^3) CRs for turtles were lower than the non-turtle CRs (4.71×10^3 and 2.72×10^3 for Cs and K respectively). This is likely to be due to the 'dilution' effect of the higher fractional mass of hard tissue in turtles. The turtle CR for Mn (5.68×10^1) was an order of magnitude lower than for non-turtles (7.72×10^2) and fish (9.80×10^2). However, this turtle CR was derived from a single specimen of *Chelydra serpentina* (snapping turtle) from Canada (Yankovich, pers. comm.) so may be site-specific and/or organism-specific. Similarly, the Sb CR for non-turtles (5.66×10^1) was an order of magnitude lower than the ERICA fish CR (2.90×10^2) whereas the turtle CR (4.50×10^3) was an order of magnitude higher than the fish CR, but these reptile CRs were also based on single measurements (Yankovich, pers. comm.).

The non-turtle CR for Cd (1.69×10^3) was an order of magnitude higher than the ERICA CR for benthic fish (2.30×10^2). However, the non-turtle CR was heavily skewed by data from one study of *Nerodia fasciata* (banded water snake, $n = 5$) in the US (Hopkins et al., 1999). Thus, the non-turtle CR may reflect site-specific conditions for that study rather than being suitable as a generic predictor of Cd transfer to freshwater reptiles. Further CR data from other study sites would be required in order to determine whether a generic reptile CR for Cd of 1.69×10^3 is appropriate.

The Hg CR for turtles (3.11×10^1) was three orders of magnitude lower than the CR for non-turtles (1.18×10^4). In this case, the non-turtle CR was heavily skewed by data from a study on *Nerodia sipedon* (water snake, $n = 20$) in the US (Campbell et al., 2005). The crocodilian CR (4.78×10^1) was in better agreement with the turtle data so the non-turtle CR presented in Table 7.11 may reflect a site-specific rather than generic transfer relationship.

The reptile CRs for Po and Pu were 1 – 2 orders of magnitude higher than the ERICA CRs for fish. The Po CRs were 4.47×10^3 for turtles, 3.30×10^3 for non-turtles and 2.40×10^2 for fish. The Pu CRs were 5.92×10^3 for turtles and 6.00×10^1 for fish. For both elements, the reptile data were derived from single studies (Martin et al., 1998; Whicker et al., 1990) so the measured CRs may be site-specific.

The turtle and non-turtle CRs for Ra (7.75×10^2 and 8.61×10^2 respectively) were an order of magnitude higher than the ERICA fish CR (8.00×10^1). However, there was good agreement in the reptile CR data across the different reptile groups and across study sites. This suggests that the Ra CR is higher for reptiles than for fish.

The Sr CRs for turtles (1.21×10^4) and non-turtles (4.07×10^2) are also higher than for fish (1.70×10^1). Although the non-turtle CR ($n = 1$) is based on one study from Canada (Yankovich, pers. comm.), the turtle CR is derived from turtle measurements ($n = 39$) reported from five studies (Meyersschone et al., 1993; Towns, 1987; Whicker et al., 1990; Yankovich, pers. comm.; Yankovich et al., in press). The high turtle CR for Sr (a Ca analogue) is likely to be due to the inclusion of turtle shell activity concentration data in the CR derivation.

7.4.2.2. CRs in terrestrial ecosystems

Although ERICA did not consider transfer to reptiles in aquatic ecosystems, it did present some CR values for reptiles in terrestrial ecosystems. Only the ERICA reptile CRs for Cs, Sr and Pu were based on measured data (Barnett et al., 2009; Beresford et al., 2008d) and the data sources for these were used in the development of the reptile CR database presented in this chapter. ERICA reptile CRs for other elements were derived using guidance that was developed for filling CR data gaps for the purposes of biota dose assessment (Beresford et al., 2008d; Copplestone et al., 2003). For terrestrial reptile – element combinations for which no measured data were available, ERICA reptile CR values were assumed to be the same as those for mammals with the exception of Pb, Ra, Th and U for which bird CR values were assumed (the bird CRs being higher than the mammal CRs for these elements).

The reptile CR for Am presented in Table 7.13 (7.11×10^{-2}) was similar to the ERICA CR for mammals (4.08×10^{-2}) whereas the Pu CR for reptiles (3.27×10^{-3}) was an order of magnitude lower than the mammal CR (2.34×10^{-2}). However, with the data from terrestrial coastal sand dune sites (Wood et al., 2008; Wood et al., 2009b) excluded, the

resultant reptile CRs for Am and Pu were 4.43×10^{-3} and 6.36×10^{-4} respectively (see Section 7.4.2.3). This suggests that actinide transfer to reptiles at generic terrestrial sites is lower (by 1 – 2 orders of magnitude) than transfer to mammals. These data also indicate that the ERICA 'guidance value' for predicting Am transfer to reptiles in the absence of measured data (assumed to be the CR for mammals) is conservative.

The non-turtle Cs CR (5.81×10^{-1}) was comparable to the ERICA amphibian and bird CRs (5.37×10^{-1} and 7.50×10^{-1} respectively) but an order of magnitude lower than the CR for mammal (2.87). It was also in good agreement with the revised CR proposed by Barnett et al. (2009) for use in ERICA (4.23×10^{-1}). The turtle CR (5.17×10^{-2}) was an order of magnitude lower than the non-turtle CR, a difference greater than expected due to differences in bone mass alone, but the turtle CR was based on a single measurement for a specimen of *Testudo horsfieldi* from the desert region of Turkmenistan (Sokolov et al., 1989) so may not be representative.

ERICA Pb CRs for mammal, bird and amphibian (3.88×10^{-2}, 6.15×10^{-2}, 1.20×10^{-1} respectively) were lower than the reptile CR (3.81×10^{-1}). The Po (1.02×10^{1}), Th (2.38×10^{-1}) and U (1.88) CRs for reptiles were also higher (by up to 4 orders of magnitude) than the CRs used in ERICA for other vertebrates (mammal CRs were 2.78×10^{-3} for Po, 1.22×10^{-4} for Th, 1.06×10^{-4} for U; bird CRs were 3.89×10^{-4} for Th, 5.41×10^{-4} for U). However, the reptile CRs were derived from data which included a study of reptiles in the Olympic Dam region of South Australia (Read & Pickering, 1999). The study reported data for reptiles from a site contaminated by windborne spray from wet acidic mine tailings and also from a control site, which was > 3 km from the tailings retention system. In comparing the CRs for the reptiles in the contaminated and control sites during the development of the reptile CR database, the CRs for U were found to be comparable for both the contaminated and control sites and the CRs for Pb, Th and Po at the contaminated site were found to be respectively three-fold, five-fold and ten-fold higher than the control site CRs. Whilst some skewing of the generic reptile CRs for Pb, Po and Th may be due to the inclusion of data from the site exposed to acidic spray from the mine tailings, especially in the case of Po, this does not explain the orders of magnitude differences between these data from South Australia and those from other regions (although there are few comparative data from other locations for these elements) and for other vertebrate groups. The reasons for these differences warrant further investigation. The revised reptile CRs would be 3.94×10^{-2} ($n = 31$) for Pb, 1.28×10^{-1} ($n = 1$) for Po, 2.17×10^{-3} ($n = 2$) for Th and 4.81×10^{-3} ($n = 4$) for U. These are in better agreement with the data for other vertebrates but, with the

exception of Pb, are still up to two orders of magnitude higher. This suggests that the ERICA 'guidance values' for reptiles (the mammal CR is used for Po and the bird CRs are used for Th and U) may be too low but, given the small number of measurements on which the revised reptile CRs are based, further measurements would be required to confirm this.

The Sr and Tc reptile CRs are in good agreement with the ERICA CRs for other vertebrates. Although the Tc reptile CR is an LOD CR ($< 7.74 \times 10^{-1}$), it suggests that the 'guidance value' recommended for use in ERICA (the Tc CR for mammal, 3.70×10^{-1}) is a suitable approximation. The reptile CR for Sr (3.97×10^{-1}) was in close agreement with the revised CR (see Barnett et al., 2009) that is currently recommended for use in ERICA (3.38×10^{-1}).

7.4.2.3. Habitat-specific transfer parameters

Small mammals inhabiting temperate coastal sand dunes have been shown to have actinide (Am and Pu in this case) and Cs CRs that were two orders of magnitude lower than the mammal CRs for these elements at other terrestrial sites (Chapter 6; Wood et al., 2009a). To determine whether similar habitat-specific differences could be observed in the reptile CRs, the summarised CRs for which there were sufficient sand dune and non-sand dune data (Am, Cs, Pu and Sr) were deconstructed to derive separate CRs for sand dune and non-sand dune reptiles. The sand dune data were all from a temperate coastal sand dune site in the United Kingdom (Chapter 4; Chapter 5; Wood et al., 2008; Wood et al., 2009b). The reptile data used were the non-turtle CR data because there were no turtle data available for the coastal sand dunes (the United Kingdom does not have wild populations of terrestrial turtles).

Two studies were used in the derivation of the Am CR for reptiles (7.11×10^{-2}), one was a study of the sub-tropical Maralinga test site in South Australia (Giles et al., 1990) and the other was the temperate coastal sand dune study (Chapter 4; Chapter 5; Wood et al., 2008; Wood et al., 2009b). The CR reported in Table 7.13 was dominated by data from the latter study. However, the two studies had very different mean CRs (8.19×10^{-2} for the coastal sand dunes and 4.43×10^{-3} for Maralinga).

There were also marked differences in the sand dune and non-sand dune CRs for Pu. The terrestrial reptile Pu CR (3.27×10^{-3}) was based on a larger number of studies than the Am CR (Barnett et al., 2009; Geiger & Winsor, 1977; Giles et al., 1990; Chapter 4; Chapter 5; Wood et al., 2008; Wood et al., 2009b) but, summarising the coastal sand dune CR data

separately from the CR data for other terrestrial sites, the Pu CRs were 1.34×10^{-2} for coastal sand dunes and 6.36×10^{-4} for other terrestrial sites.

The terrestrial reptile CR for Cs (5.81×10^{-1}) was derived from ten studies (Bagshaw & Brisbin, 1985; Barnett et al., 2009; Brisbin et al., 1974a; Carrington, 2003; Copplestone et al., 2005a; Giles et al., 1990; Iljenko, 1970; Martjushov et al., 1999; Sokolov et al., 1989; Chapter 4; Chapter 5; Wood et al., 2008; Wood et al., 2009b) . The CRs for sand dune and non-sand dune reptiles were 1.58×10^{-1} and 6.52×10^{-1} respectively. Therefore, unlike the actinide CRs, the Cs CR for sand dune reptiles was lower (by a factor of 4) than the non-sand dune reptile CR. However, the sand dune CR was still within the range of Cs CRs for non-sand dune biota.

The Sr CR (3.97×10^{-1}) for terrestrial reptiles was derived from six studies (Barnett et al., 2009; Carrington, 2003; Iljenko, 1970; Martjushov et al., 1999; Sokolov et al., 1989; Chapter 4; Chapter 5; Wood et al., 2008; Wood et al., 2009b). The sand dune reptile Sr CR was 5.42×10^{-1} and the non-sand dune CR was 3.85×10^{-1}. Taking measurement uncertainties into consideration, there was no evidence of a difference in Sr transfer between sand dune and non-sand dune habitats.

The available data suggest that generic reptile CRs for Cs and Sr are suitable for both sand dune and non-sand dune sites. However, for actinides, it may be appropriate to use separate CRs for sand dune and non-sand dune sites given that the sand dune CRs for Am and Pu are respectively 1 and 2 orders of magnitude higher than for other terrestrial sites. Due to the sea-to-land transfer mechanism, actinide concentrations are enhanced at the temperate coastal sand dune site from which the reptile data were derived (Chapter 5; Wood et al., 2009b). However, the reptile CRs show an opposite trend to that seen in sand dune mammals, for which the CRs are two orders of magnitude lower than at other terrestrial sites (Chapter 6; Wood et al., 2009a). Given that the sand dune reptiles (*Anguis fragilis*, *Vipera berus* and *Lacerta vivipara*) are at either the same or a higher trophic level than the sand dune small mammals, the reason for the high actinide CRs for reptiles is unclear and is an area for further research.

7.4.3. Approaches for addressing knowledge gaps

There are a number of approaches that could be used to address the knowledge gaps highlighted in this chapter. The ideal approach would be to undertake targeted field research to fill the data gaps with measured whole-body transfer values for the main reptile

types in both aquatic and terrestrial ecosystems. However, this is a resource intensive solution and, due to the fact that many reptiles are endangered and are protected under national and international conservation legislation (Chapter 4; Wood et al., 2008), alternatives to the standard destructive sampling approaches are desirable. Three approaches that may be used to fill some of the knowledge gaps are: (i) non-lethal sampling techniques; (ii) estimation of 'dilution' factors; and (iii) biological scaling relationships.

7.4.3.1. Non-lethal sampling approaches to determine contaminant burdens in adult reptiles

There is a growing demand for the development and refinement of non-lethal sampling strategies to determine contaminant burdens in reptiles (Hopkins et al., 2001). Live monitoring for gamma emitters has been used in some studies at radionuclide contaminated sites (e.g. Brisbin, 1989). However, given the low activity concentrations in reptiles at many study locations, this technique is unlikely to be practical in most research situations due to the long count times that would be required. Therefore, direct analysis of tissue samples is necessary and a selection of studies over the past decade have evaluated the effectiveness of using various tissues, harvested using non-lethal techniques, for estimating contaminant burdens in reptiles. Tissues considered include osteoderms, tail tissue, eggs, blood and skin.

Osteoderms[30] are found in turtles, crocodilians and many lizards (Pough et al., 2004). Sampling of these dermal bones in crocodilians has been successfully demonstrated as a non-lethal technique for estimating concentrations of Ca, Co, Pb, Mg and U in crocodiles (e.g. Markich et al., 2002; Twining et al., 1999), although it may be necessary to correct for age and snout-vent length (Jeffree et al., 2005). Turtle scutes[31] have also been shown to correlate with metal contamination in body tissues (Day et al., 2005) but the significance of these correlations may be species-specific (Schneider et al., 2009).

Work on *A. mississippiensis* has demonstrated that tail-tip samples (consisting of the distal 2 cm of the tail) are relatively easy to collect in the field and can be used to estimate the internal tissue concentrations, and hence whole-body burdens, of As, Cr and Cd (Burger et al., 2000). However, tail-tip sampling does not appear to have been used more widely in reptile contaminant burden analysis undertaken to date.

[30] Bony deposits in the dermal layers of the skin

[31] Scutes are bony plates on the external surface of a turtles and crocodilians

In oviparous species, egg laying is recognised route through which contaminants may be excreted by females (Burger, 1994; Godley et al., 1999; Xu et al., 2006a). Therefore, some studies have considered the extent to which egg contaminant burdens may be used to predict tissue and whole-body contaminant burdens in the female which laid the egg (e.g. Burger, 2002; Guirlet et al., 2008) and these have provided positive support for the use of this non-lethal sampling strategy. For example, analysis of stable element concentrations in the tissues and eggs of female sea turtles has demonstrated that concentrations in sea turtle eggs can be used to estimate concentrations in adult female turtles for elements such as Cd and Zn, which have adult whole-body to egg yolk ratios of 35 and 2.2 respectively (Sakai et al., 1995). Some eggs are infertile and fail to develop so these can be collected from nests as a non-lethal approach for determining element concentrations in adult reptile tissues. Analysing eggs, especially infertile eggs, is less damaging to the species than sampling body tissues (Godley et al., 1999) and this non-lethal technique is gaining general acceptance within the scientific community (Lam et al., 2006).

The relationships between element concentrations in reptile blood relative to concentrations in other tissues have been investigated by a number of authors (e.g. Burger et al., 2005; Burger et al., 2007; Day et al., 2005; Swanepoel et al., 2000; Towns, 1987). Positive correlations have been identified for particular blood, tissue and element combinations, such as mercury concentrations in blood and muscle of *Nerodia sipedon* (Burger et al., 2005), and blood sampling may therefore provide an alternative route to investigating element concentrations in adult reptiles. Although blood has been used exclusively by some authors for evaluating contaminant uptake in reptiles (Clark et al., 2000), blood generally reflects recent contaminant exposure (Burger et al., 2005) and the complex kinetics of elements within blood (Guirlet et al., 2008) are likely to result in high uncertainties.

There is also evidence to suggest that the physiological control of element levels in plasma may be different across the reptile groups and also between species within the same reptile group. For example, the activity of many enzymes in snake venom is dependent on the presence of various inorganic elements (Brisbin et al., 1974a). The haemorrhagic effectiveness of metalloproteases in venom from *Crotalus spp* (rattlesnake species) is dependent on the presence of Zn (LaportaFerreira et al., 1997) and the structural integrity of haemorrhagic and proteolytic enzymes and anti-coagulants in the venom of the *Agkistrodon acutus* (sharp-nosed viper) is maintained by Ca ions (Bjarnason & Fox, 1994). Although the extent of, and mechanisms for, concentration of these inorganic elements into snake

venom may not be fully understood (Xu et al., 2006b; Xu et al., 2009), this may indicate that snakes have an increased dietary uptake efficiency for particular elements and/or physiological mechanisms for increasing Zn concentrations in the venom glands. This is consistent with reptile haematology data which indicate that snakes have elevated blood concentrations of specific elements, such as Zn (Lance et al., 1995), compared to other reptiles. Therefore, estimating whole-body concentrations based on blood concentrations alone may require species-specific knowledge of the behaviour of certain elements.

An additional difficulty with using blood to estimate whole-body contaminant burdens is that, at least in the case of *Nerodia sipedon* (Northern Water Snake) studied by Burger et al. (2005), the blood sample ideally needs to be collected directly from the heart and cardiocentesis requires considerable expertise to achieve successful sample collection without injuring the snake. Whilst it is possible to sample blood from the caudal vein (Calle et al., 1994; Cuadrado et al., 2002; Hopkins et al., 2001), and this may reduce the risk of serious injury to the snake, the volume of sample that can be collected from this vein may be insufficient for performing a suite of haematological analyses (Burger et al., 2005; Cuadrado et al., 2003). Jugular venipuncture provides an alternative option for non-lethal sample collection (Cuadrado et al., 2003; Gottdenker & Jacobson, 1995). However, although available evidence indicates little difference in the blood chemistry of the different venipuncture sites (Cuadrado et al., 2003), jugular puncture does not appear to have been used in studies of contaminant uptake to date.

Analysis of contaminant residues in skin samples, which can be biopsied in the field under local anaesthetic, has also been investigated as a non-lethal technique for monitoring contaminant burdens in reptiles (e.g. Burger et al., 2007; Kaur, 1988) and for determining internal tissue concentrations (e.g. Burger et al., 2005). Skin shedding, or sloughing, happens on a regular basis in snakes and there is evidence to suggest that this may act provide a route for reducing contaminant burdens (Burger, 1992; Jones & Holladay, 2006). However, excretion of sequestered contaminants via the skin may not be as prevalent in other reptile groups. For example, laboratory-based research on Cd uptake in *Podarcis carbonelli* (Carbonell's wall lizard) demonstrated minimal loss of the Cd body-burden via skin shedding (Mann et al., 2006). Skin samples may thus show promise as a non-lethal technique but relationships between skin and internal tissue concentrations for different elements and reptile groups would need to be well-defined.

Overall, there is strong evidence to support the use of non-lethal techniques in future monitoring of contaminant burdens in reptile populations. These techniques may provide a useful means for furthering understanding of transfer to reptiles and enable CRs to be derived for many species with minimal impact (stress) to individual organisms and virtually no population impact. However, to fully utilise these techniques, there is a need to further develop the knowledge-base on the significance of the relationships, across a wider range of species, ecosystems and elements, between tissues that may be sampled non-lethally and whole-body contaminant burdens. One of the constraining factors may be the "correlational chaos" that has been observed between various tissues when contaminant concentrations are low (Gochfeld & Burger, 1987). Although there may be analytical and research challenges to be overcome, these non-lethal strategies remain a promising route to furthering understanding of contaminant transfer for protected species of reptile.

7.4.3.2. Estimating 'dilution factors'

As demonstrated in Section 7.4.1.3., for certain elements, data on the partitioning between hard and soft tissues and the fractional mass of these tissues in the organism make it possible to estimate reptile CR values for turtles from non-turtle data and vice versa. Where elements mainly concentrate in soft tissues (e.g. Cs) or hard tissues (e.g. Sr) a non-turtle to turtle 'dilution factor' can be applied. Assuming that turtles contain 58% soft tissue and non-turtles contain 93% soft tissue (on a whole-body fwt basis), the non-turtle to turtle 'dilution factor' would be 0.62 for elements that accumulate in soft tissue (the 'dilution factor' for elements that accumulate in hard tissues would be 6). For elements where partitioning between hard and soft tissues is less pronounced, the dilution factor could be modified to reflect this based on the B_T values presented in Table 7.5. However, it should be noted that there may be differences in the physiology of turtles compared to other reptiles which affect element uptake, such as the higher rate of uptake of Ca and analogous elements by turtles compared to other reptiles (Hinton & Whicker, 1985; Hinton & Scott, 1990), so using 'dilution factors' to estimate CRs should be done with caution.

7.4.3.3. Allometric approaches

Another method for filling data gaps on radionuclide transfer to reptiles is the use of allometric (or biological scaling) relationships, such as the kinetic-allometric approach presented by Higley et al. (2003), for which the major uptake and elimination pathways must be quantified to achieve a mechanistic prediction of radionuclide transfer. The

allometric approach is based on the observation that many physiological parameters relate to body mass via a power function (Higley et al., 2003), commonly scaling to quarter powers of the mass (West et al., 2000). Allometric relationships generally take the form:

$$Y = aM^b$$

where Y is the physiological parameter to be estimated, M is the organism mass and a and b are constants derived from measured data.

By estimating the uptake and elimination rates of radionuclides based on allometric scaling relationships for parameters such as food ingestion rate, life span and radionuclide biological half-life, it is possible to obtain radionuclide transfer predictions that are in good agreement with measured data (Beresford et al., 2004). Although initially developed for mammals (e.g. Adolph, 1949), the applicability of biological scaling to poikilotherms and ectotherms has also been demonstrated (Bennett & Dawson, 1976; Reichle et al., 1970). For example, Reichle et al. (1970) derived the following equation to predict the biological half-life of radiocaesium in poikilothermic vertebrates at 20^{o}C:

$$Y_{Cs} = 38.02M^{0.1390}$$

where Y_{Cs} is the biological half-life of radiocaesium and other terms have been defined previously.

An advantage of an allometric approach is that it provides a method for predicting transfer to species across a broad mass range (Higley et al., 2003), which for reptiles extends from 10^{-4} kg for species such as the *Sphaerodactylus ariasae* (dwarf gecko) (Hedges & Thomas, 2001) to 10^{3} kg for species such as the *Dermochelys coriacea* (leatherback turtle) (Arnold, 2004). Therefore, developing reptile-specific allometric relationships may provide an alternative to the use of CRs when predicting radionuclide transfer to reptiles.

7.5. Conclusions

To the best of the authors' knowledge, this chapter presents the most comprehensive databases available on transfer to reptiles and on resultant tissue partitioning. The data were originally collected to help support radiation dose assessments for biota but, because the data presented in this chapter are element rather than radionuclide specific, these data will also be useful to those undertaking assessments of stable-element transfer and impacts

on biota. In conjunction with the tissue distribution data, the whole-body CRs could also be used to estimate CRs to predict concentrations in specific tissues (e.g. muscle) from environmental media concentrations, thereby enabling the data to be used for modelling food chain transfer in human assessments where reptiles form an important component of the diet, such as in Australian aboriginal communities (Martin et al., 1998).

Although the overall number of measurements from which CR values were derived is generally low ($n < 10$), there are observations that lend confidence to the reptile CR data compilation presented, such as the good agreement between the CRs for Cs and K (a Cs analogue) and the comparable (within an order of magnitude) CR values for many elements across individual reptile groups. However, given the necessary use of assumptions and conversion factors in the development of the reptile CR database, the CR values presented in this chapter should be viewed as current best estimates.

For many elements, particularly in aquatic ecosystems, the CRs were derived from single studies. Although there may be numerous measurements reported within each of these studies, it is not possible to determine whether the resultant CRs are site-specific/ habitat-specific, as demonstrated for actinide CRs for temperate coastal sand dune reptiles, or suitable for more generic applications. Therefore, recognising the influence of transfer parameter selection on assessment results, there is a need to prioritise research to refine and expand the current reptile CR database. Where possible, this should be done using direct measurements of whole-body concentrations in the different reptile groups across a range of study sites. If whole-body measurements cannot be made, non-lethal techniques may be used to estimate the whole-body concentrations. As an interim approach, until sufficient field measurements can be made, data manipulations based on 'dilution factors' and allometric estimations of transfer may help to address knowledge gaps. In combination, the reptile CR data presented in this chapter and proposals for further development and refinement of the reptile CR database will help to ensure that the necessary underpinning data are available to allow this highly diverse and ecologically important group of vertebrates to be more fully considered within future environmental risk assessments.

CHAPTER 8 – RADIOECOLOGY OF TEMPERATE COASTAL SAND DUNES

8.1 Introduction

In the previous chapters, the trophic transfer of radionuclides in coastal sand dune ecosystems has been discussed in the context of environmental radiation protection modelling. Differences in transfer between sand dune and non-sand dune biota have been observed (see Chapters 6 & 7) and the need to derive concentration ratios (CRs) specific to coastal sand dunes has been highlighted.

This chapter draws on the data presented in Chapters 4 – 7 and additional data collected from the Drigg sand dunes (see Chapter 3 for details of the sampling and analytical methodologies). The chapter aims to determine the processes governing radionuclide activity concentrations in the soil profile of coastal sand dunes and further investigate why some sand dune biota (e.g. small mammals – see Chapter 6) may have lower CRs than comparable species at other terrestrial sites.

8.2. Radionuclide transport in temperate coastal sand dunes

The sources of radionuclide contamination at the Drigg coastal sand dunes have been discussed in Chapter 2. This section presents the radionuclide activity concentration data for soil and water samples collected from the Drigg coastal sand dunes and *in situ* measurements of gamma radiation dose rates. The spatial and depth distribution of radionuclides within the coastal sand dune ecosystem are investigated and discussed in the context of abiotic[32] transfer processes and radionuclide mobility within sand dune soils.

8.2.1. Sand dune soil profiles

The profiles of radionuclide activity concentrations (up to 40 cm depth) in cores collected from each of the three sampling transects at the Drigg coastal dunes (see Figure 3.1) are presented in Figures 8.1. – 8.7. In each figure, individual transects are represented by

[32] Bioturbation is not considered to be an important factor in the redistribution of radionuclides within the soil profile due to the low worm densities present at the Drigg coastal sand dunes (see Chapter 3).

separate horizontal rows of depth profile bar charts and each vertical column of bar charts corresponds to a particular distance from mean high water (MHW). The leftmost column of bar charts is the MHW sampling location at the seaward end of each sampling transect and subsequent columns are sampling locations at 100 m intervals from MHW. Bar charts that are coloured blue indicate locations which may be tidally inundated, such as the area upper beach and embryo dunes region at the seaward end of each transect and the beach and saltmarsh areas at the landward end of Transects 2 and 3. The bar charts presenting data for soils within the main sand dune complex are coloured red.

Data for seven radionuclides, four natural radionuclides (^{40}K, ^{208}Tl, ^{214}Bi and ^{228}Ac) and three anthropogenic radionuclides (^{60}Co, ^{137}Cs and ^{241}Am), are presented. The 0 – 10 cm soil activity concentrations and 0 – 10 cm and 0 – 40 cm deposition estimates for these radionuclides are summarised by sand dune zone in Tables 8.1 and 8.2 (see Section 2.1.3 and Table 3.2 for a the definition of the sand dune zones). The radionuclides reported include the six radionuclides (^{40}K, ^{208}Tl, ^{214}Bi, ^{228}Ac, ^{60}Co and ^{137}Cs) that have been shown, using the kerma rate per unit activity per unit mass (μGy h^{-1} per Bq kg^{-1}) values reported by the International Commission on Radiological Units and Measurements (ICRU, 1994), to dominate the gamma dose rates measured in air at 1 m above the surface of the intertidal areas of the neighbouring Esk Estuary (McDonald et al., 2005; Wood et al., in press). From the ^{232}Th series, ^{208}Tl and ^{228}Ac were the major contributors to dose rate and ^{214}Bi was the major dose rate contributor from the ^{238}U series.

8.2.1.1. Natural radionuclides in sand dune soils

Activity concentrations of ^{40}K, ^{208}Tl, ^{214}Bi and ^{228}Ac in soil are dependent on the parent material of the soil. The sand dunes and surrounding intertidal areas share a common parent material belonging to the Sandwich soil association (see Chapter 2) so the natural radionuclide activity concentration profiles (Figures 8.1 – 8.4) were relatively uniform both with depth and with distance from MHW. Mean activity concentrations (Bq kg^{-1} dry weight ± SD) were 274 ± 42, 3.00 ± 0.58, 6.70 ± 1.32 and 8.55 ± 1.87 for ^{40}K, ^{208}Tl, ^{214}Bi and ^{228}Ac respectively.

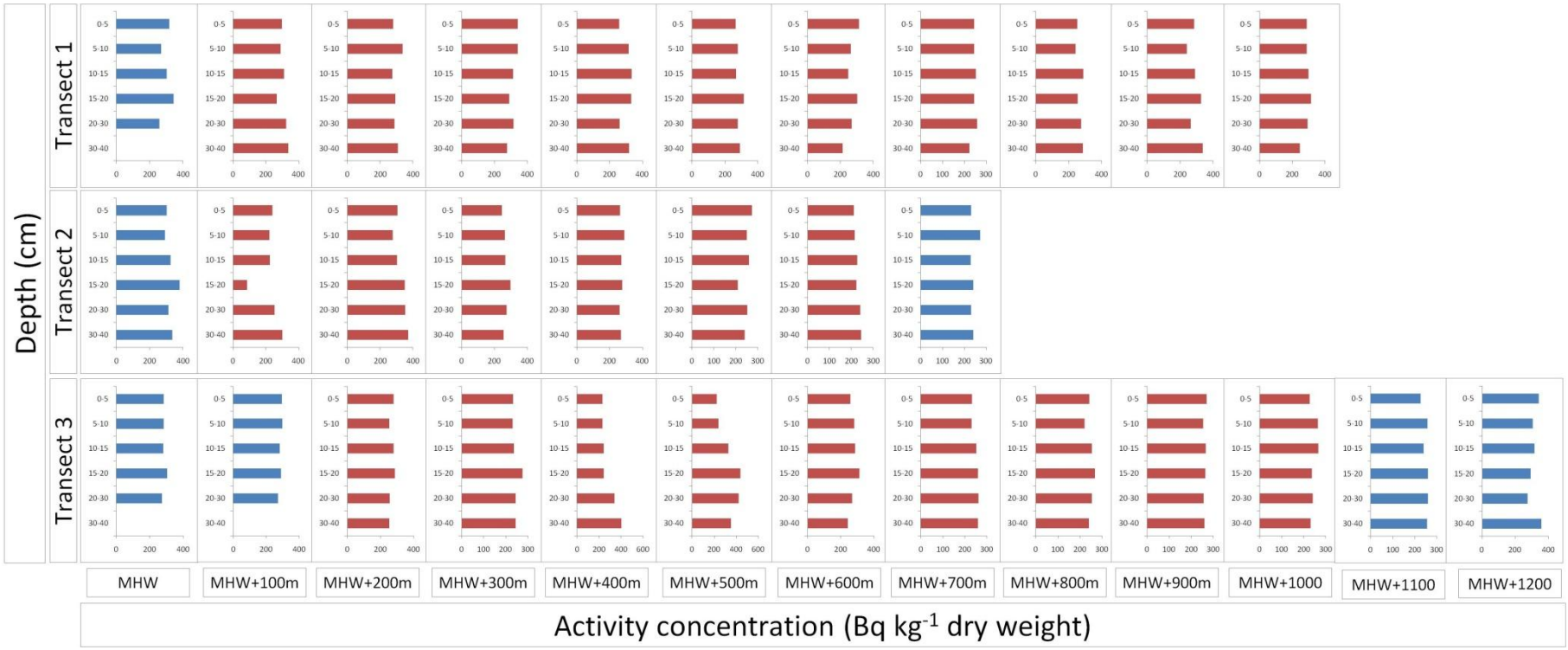

Figure 8.1. Depth profiles of ^{40}K activity concentrations (Bq kg^{-1} dry weight) in the upper 0 – 40 cm of soil along Transects 1 – 3 at the Drigg coastal sand dunes. The leftmost column of figures presents the soil activity concentration profiles at mean high water (MHW). Subsequent columns of figures present profiles at intervals of 100 m inland from MHW. Figures in blue indicate that the site may be tidally inundated. Figures in red indicate sites which are not tidally inundated.

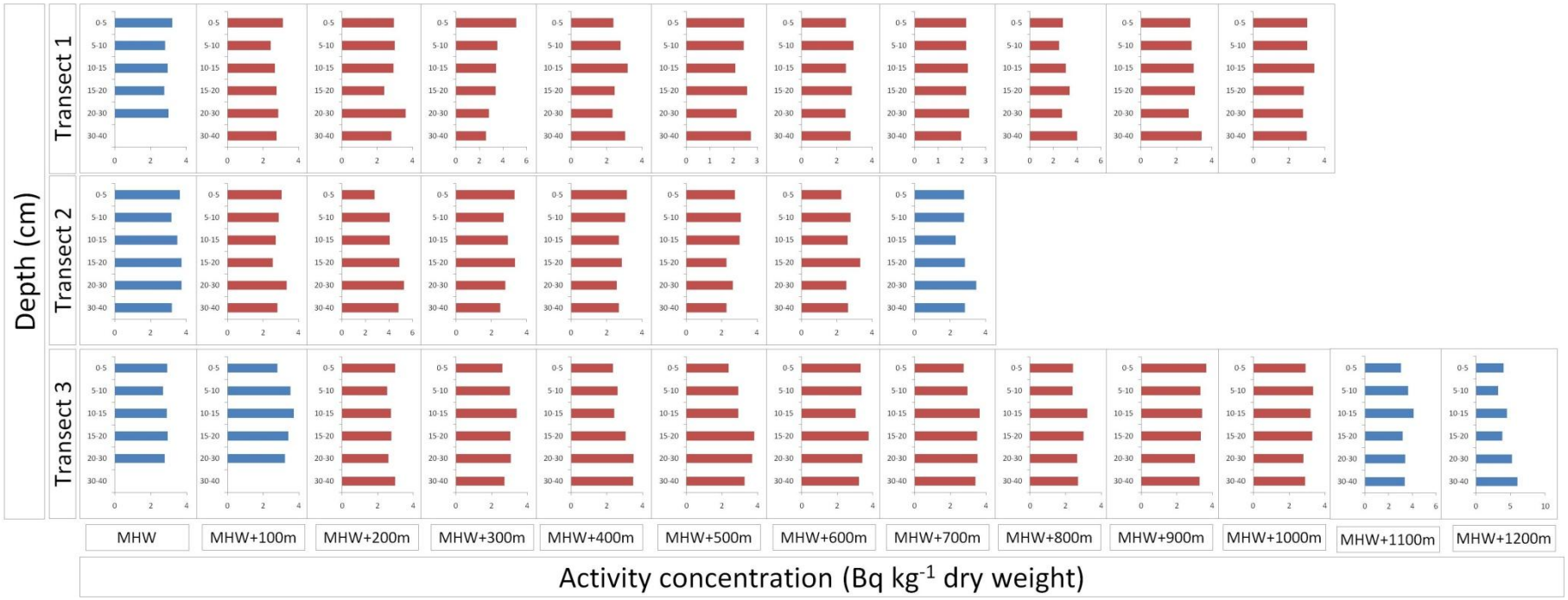

Figure 8.2. Depth profiles of ^{208}Tl activity concentrations (Bq kg^{-1} dry weight) in the upper 0 – 40 cm of soil along Transects 1 – 3 at the Drigg coastal sand dunes. The leftmost column of figures presents the soil activity concentration profiles at mean high water (MHW). Subsequent columns of figures present profiles at intervals of 100 m inland from MHW. Figures in blue indicate that the site may be tidally inundated. Figures in red indicate sites which are not tidally inundated.

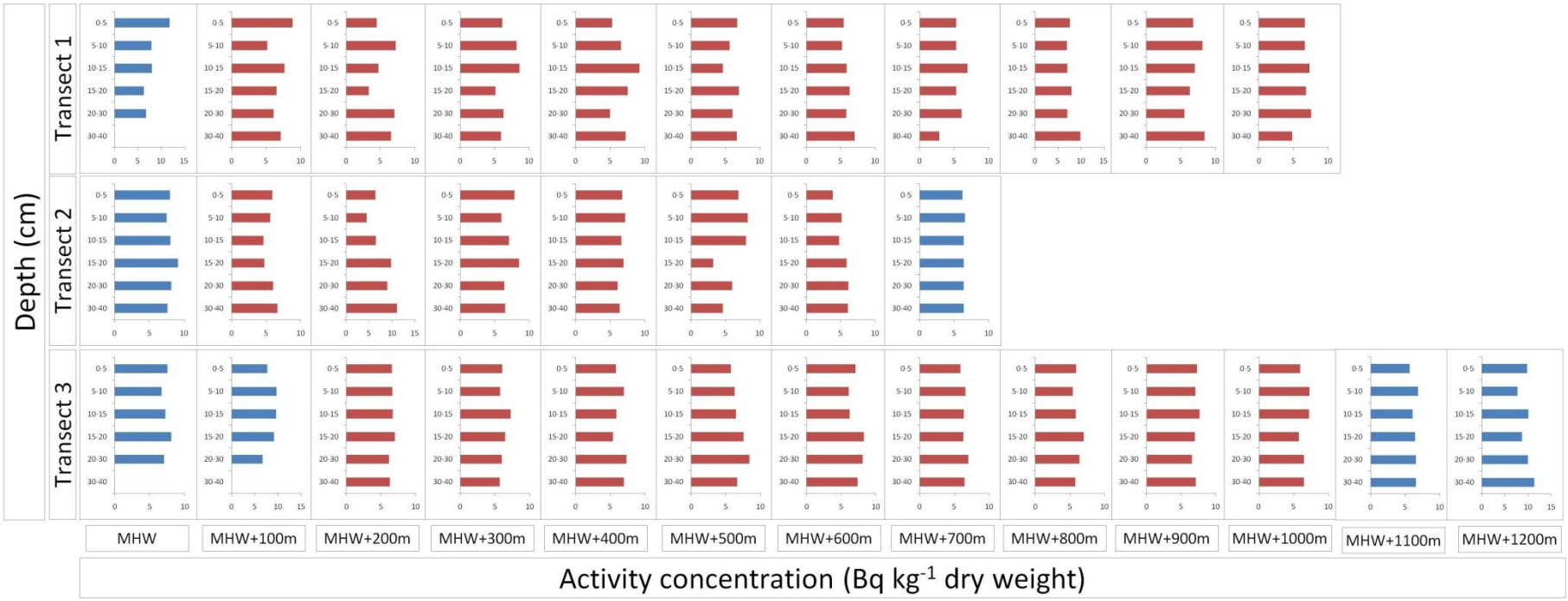

Figure 8.3. Depth profiles of ^{214}Bi activity concentrations (Bq kg^{-1} dry weight) in the upper 0 – 40 cm of soil along Transects 1 – 3 at the Drigg coastal sand dunes. The leftmost column of figures presents the soil activity concentration profiles at mean high water (MHW). Subsequent columns of figures present profiles at intervals of 100 m inland from MHW. Figures in blue indicate that the site may be tidally inundated. Figures in red indicate sites which are not tidally inundated.

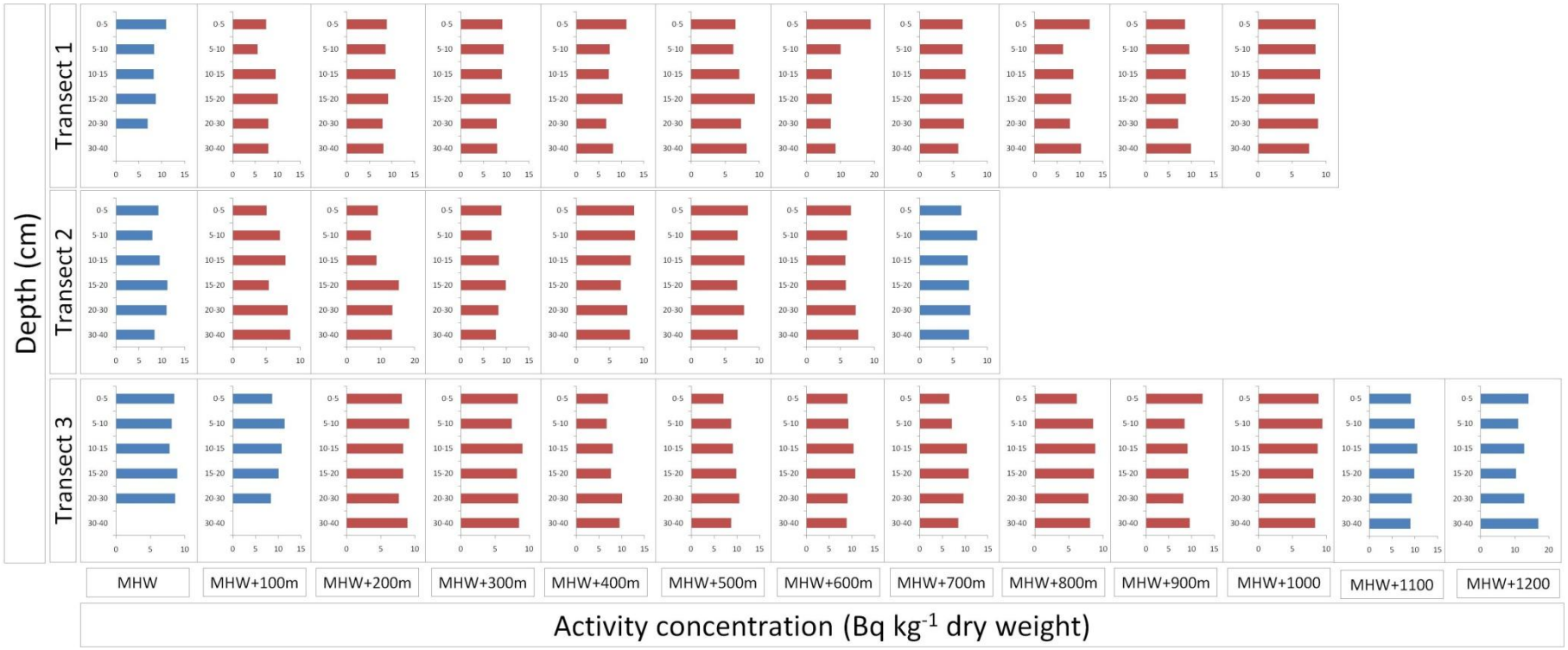

Figure 8.4. Depth profiles of ^{228}Ac activity concentrations (Bq kg^{-1} dry weight) in the upper 0 – 40 cm of soil along Transects 1 – 3 at the Drigg coastal sand dunes. The leftmost column of figures presents the soil activity concentration profiles at mean high water (MHW). Subsequent columns of figures present profiles at intervals of 100 m inland from MHW. Figures in blue indicate that the site may be tidally inundated. Figures in red indicate sites which are not tidally inundated.

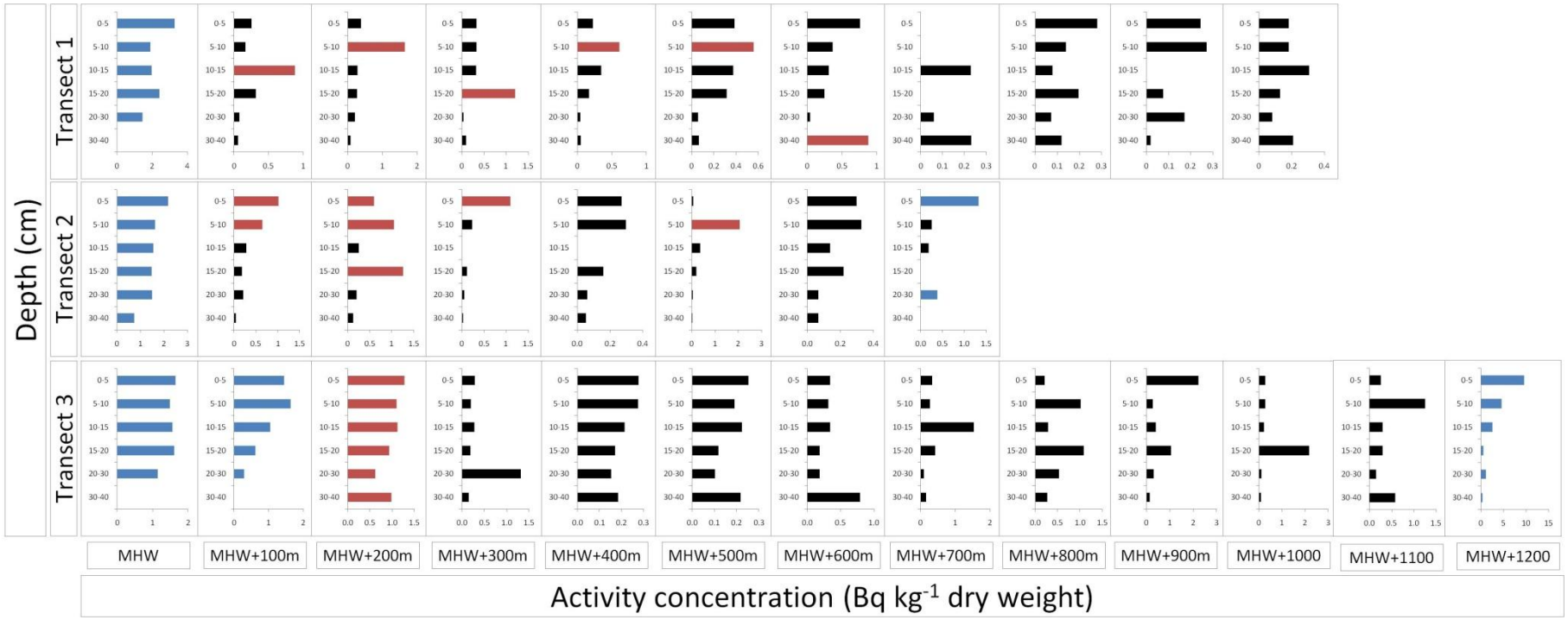

Figure 8.5. Depth profiles of ^{60}Co activity concentrations (Bq kg^{-1} dry weight) in the upper 0 – 40 cm of soil along Transects 1 – 3 at the Drigg coastal sand dunes. The leftmost column of figures presents the soil activity concentration profiles at mean high water (MHW). Subsequent columns of figures present profiles at intervals of 100 m inland from MHW. Figures in blue indicate that the site may be tidally inundated. Figures in red indicate sites which are not tidally inundated. Black bars indicate values below the LOD.

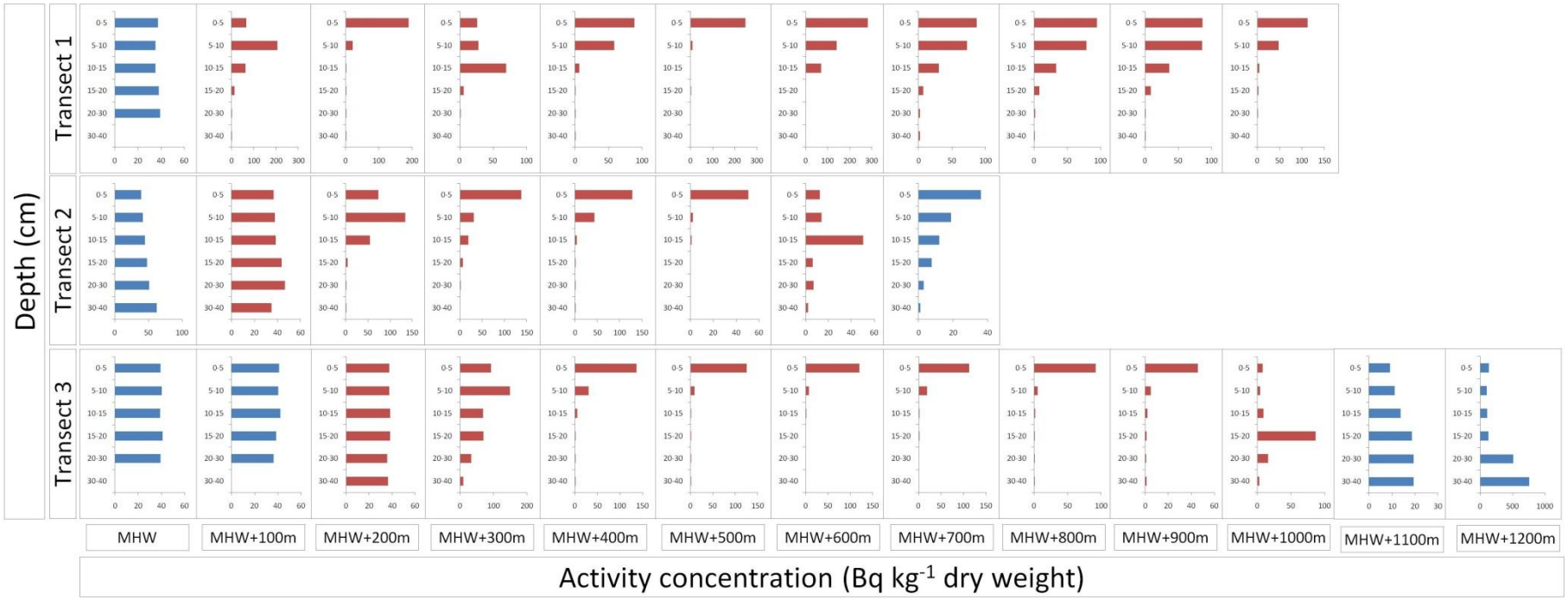

Figure 8.6. Depth profiles of ^{137}Cs activity concentrations (Bq kg^{-1} dry weight) in the upper 0 – 40 cm of soil along Transects 1 – 3 at the Drigg coastal sand dunes. The leftmost column of figures presents the soil activity concentration profiles at mean high water (MHW). Subsequent columns of figures present profiles at intervals of 100 m inland from MHW. Figures in blue indicate that the site may be tidally inundated. Figures in red indicate sites which are not tidally inundated.

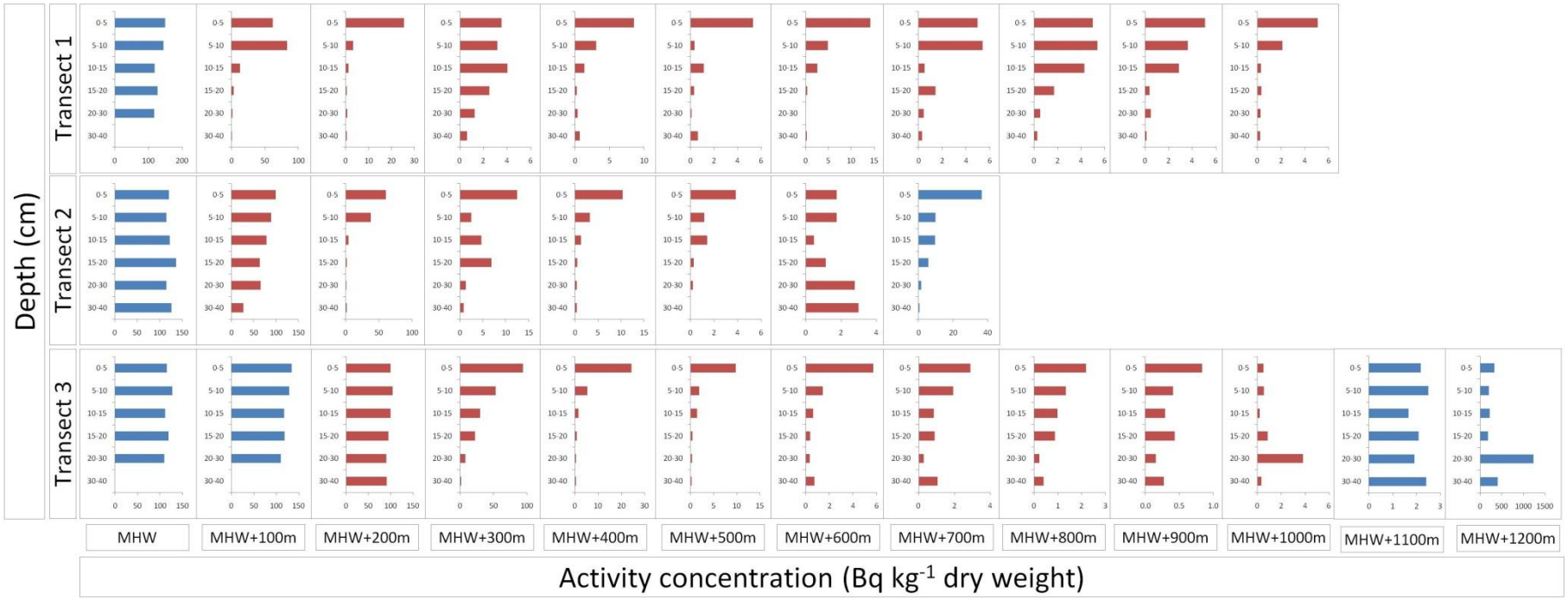

Figure 8.7. Depth profiles of ^{241}Am activity concentrations (Bq kg^{-1} dry weight) in the upper 0 – 40 cm of soil along Transects 1 – 3 at the Drigg coastal sand dunes. The leftmost column of figures presents the soil activity concentration profiles at mean high water (MHW). Subsequent columns of figures present profiles at intervals of 100 m inland from MHW. Figures in blue indicate that the site may be tidally inundated. Figures in red indicate sites which are not tidally inundated.

Table 8.1. Mean activity concentration (Bq kg^{-1} dry weight) for natural and anthropogenic radionuclides in the upper 0 – 10 cm of soil from different zones[1] of the Drigg coastal sand dunes.

		Activity concentration (Bq kg^{-1} dry weight)					
Radionuclide		**Zone 1**	**Zone 2**	**Zone 3**	**Zone 4**	**Saltmarsh**	**Slack**
Natural							
^{40}K	*n*	6	5	6	14	1	5
	mean	277.5	267.3	284.4	251.5	324.5	254.3
	SD	24.6	26.1	37.9	23.1		7.4
^{208}Tl	*n*	6	5	6	14	1	5
	mean	3.1	3.0	3.1	2.8	3.6	2.9
	SD	0.3	0.3	0.6	0.4		0.2
^{214}Bi	*n*	6	5	6	14	1	5
	mean	7.5	5.0	4.8	4.0	7.3	5.9
	SD	1.3	0.7	1.3	1.5		2.0
^{228}Ac	*n*	6	5	6	14	1	5
	mean	8.9	7.4	7.9	8.4	12.5	7.7
	SD	1.0	1.1	1.7	2.2		1.1
Anthropogenic							
^{60}Co	*n*	6	5	6	14	1	5
	mean	1.6	0.8	<1.6	<2.2	7.1	<1.5
	SD	0.6	0.4				
^{137}Cs	*n*	6	5	6	14	1	5
	mean	32.4	80.1	73.0	74.6	118.7	27.8
	SD	12.0	43.2	39.4	50.9		22.5
^{241}Am	*n*	6	5	6	14	1	5
	mean	90.4	64.9	17.7	4.4	269.4	6.5
	SD	61.3	38.2	27.7	3.8		8.5

[1] See Section 2.1.3 and Table 3.2 for details of zone classification

For comparison, mean activity concentrations (Bq kg^{-1} dry weight ± SD) estimated for soils in England and Wales from stable element data using specific activities of 31.6 Bq g^{-1} for ^{40}K, 4.07 Bq mg^{-1} for ^{232}Th and assuming equilibrium between ^{232}Th and its daughters are 514 ± 152 and 32 ± 9.5 for ^{40}K and ^{228}Ac respectively (Beresford et al., 2007a; Beresford et al., 2008e). These data were in good agreement with typical global values for soil (Gomez-Ros et al., 2004). The natural radionuclide activity concentrations determined in the soils from the Drigg coastal sand dunes were low by comparison and this was reflected in the low measurement values for *in situ* gamma dose rates in air at 1 m above the soil surface (see Section 8.2.5).

Table 8.2. Mean deposition (Bq m^{-2} dry weight) for anthropogenic radionuclides in the upper 0 – 10 cm and 0 – 40 cm of soil from different zones[1,2] of the Drigg coastal sand dunes.

Sampling depth (cm)	Radionuclide		Deposition (Bq m^{-2} dry weight) Zone 2	Zone 3	Zone 4	Slack
0 - 10	^{60}Co	*n*	5	6	14	5
		mean	103.0	<162.5	<270.3	<201.4
		SD	45.5			
	^{137}Cs	*n*	5	6	14	5
		mean	9538.8	7231.3	5402.1	2802.3
		SD	5192.7	4277.3	2811.7	2036.2
	^{241}Am	*n*	5	6	14	5
		mean	7931.9	1814.5	342.4	534.3
		SD	5162.1	3046.6	333.5	466.6
0 - 40	^{60}Co	*n*	5	6	14	-
		mean	450.5	<1101.5	<1205.9	
		SD				
	^{137}Cs	*n*	5	6	14	-
		mean	17800.9	11194.3	7614.3	
		SD	4615.9	10542.2	2947.5	
	^{241}Am	*n*	5	6	14	-
		mean	19973.3	2989.1	660.1	
		SD	19889.9	5196.6	424.7	

[1] See Section 2.1.3 and Table 3.2 for details of zone classification; [2] no data are presented for Zone 1 and saltmarsh because they are subject to tidal inundation so anthropogenic radionuclide activity concentrations at these locations would not be expected to reflect aerial deposition alone; - no 0 – 40 cm deposition data available for dune slack soils because the maximum core depth obtained from the dune slacks was 0 – 15 cm.

8.2.1.2. Anthropogenic radionuclides in sand dune soils

In contrast to the natural radionuclides, the depth profiles of anthropogenic radionuclide activity concentrations (Figures 8.5 – 8.7) demonstrated differences in activity concentration both with depth and with distance from MHW. Most of the main sand dune depth profiles (red bar charts) showed activity concentrations to be highest in the upper sections of the soil profile and to decrease with depth. The pattern is less clear for ^{60}Co

(Figure 8.5) than for ^{137}Cs and ^{241}Am but this is because many of the ^{60}Co values are limit of detection (LOD) values.

Sellafield discharges of ^{60}Co to the marine environment have led to accumulation of ^{60}Co in the intertidal sediments of the Esk Estuary (Emptage & Kelly, 1990; Kelly & Emptage, 1991; Kelly et al., 1991; Wood et al., in press) but there is no significant enhancement of ^{60}Co in the coastal terrestrial environment due to transfer from sea to land. This was reflected in the elevated ^{60}Co activity concentrations (up to 10 Bq kg^{-1} dry weight) measured in the core samples collected from the saltmarsh at the landward end of Transect 3 compared to the samples from other locations along the three transects (most of which were < 2 Bq kg^{-1} dry weight) and accounted for the below LOD values measured for most of the sand dune soil samples (Figure 8.5).

The observed decrease in the activity concentrations of ^{137}Cs and ^{241}Am with depth (Figures 8.6 and 8.7) was in agreement with measurements of five post-Chernobyl soil cores collected from the Drigg coastal sand dunes in June 1986 (Rudge, 1989). However, the Drigg sand dune soil data seemingly contradicted ^{137}Cs and ^{241}Am results for 0 – 12 cm cores collected from the Sellafield coastal sand dunes between April 1993 and September 1994 (Copplestone, 1996; Copplestone et al., 2001b). Over this depth range, there was an increase rather than decrease in activity concentration with depth, which was attributed to rapid leaching of radionuclides down through the soil (Copplestone et al., 2001b). Given that the deposition of ^{137}Cs would have been expected to peak in 1986 due to fallout from the Chernobyl plume as it passed over West Cumbria (see Section 2.4.2.2), this leaching explanation for the observed soil activity concentration profile at the Sellafield dunes implies that the ^{137}Cs peak moved down the soil profile at a rate of at least 1 cm y^{-1}.

The reason for the difference between the Sellafield and Drigg sand dune data may be due to differences in the spatial scale of the two dune systems. The Sellafield coastal sand dunes (see Figure 6.2) are located on a narrow (< 50 m wide sand bank) and all soil samples were collected within 100 m of MHW. In contrast, the Drigg dunes are up to 1 km wide (see Figure 3.1). Considering only the data for the Drigg dune sampling locations close to MHW which are stabilised by vegetation to the same extent as the Sellafield sand dunes (MHW+100 m on Transect 1, MHW+200 m on Transect 2 and MHW+300 m on Transect 3), there was some evidence of sub-surface maxima (peak activity concentrations at depths below the soil surface) in the ^{137}Cs activity concentration data.

These sub-surface maxima are likely to be due to a combination of leaching of historic deposition, such as that from Chernobyl, down the soil core and burial of less mobile deposits due to ongoing accumulation of less-contaminated aeolian sand from the backshore zone, which is the main source of sand supply for dune growth (see Section 2.1.1). The 0 – 5 cm activity concentration data for locations closer to MHW and further inland support this hypothesis and indicate that leaching rates of radionuclides in sand dune soil may not be as rapid as suggested by Copplestone et al. (2001c). The locations with subsurface maxima had 0 – 5 cm activity concentrations which were comparable to those of locations closer to MHW and the 'buried' activity peak was comparable to the 0 – 5 cm ^{137}Cs activity concentration of locations further inland. Given the short distance (< 100 m) between the Sellafield sand dune soil sampling locations and the back shore beach zone, it is plausible that the observed increase in activity concentration with depth was primarily due to a similar burial process rather than to leaching.

Further inland it appears to be leaching rather than burial which is the primary determinant of radionuclide concentration with depth and this is supported by the measurements of 100 cm core samples collected from the Drigg coastal sand dunes (Figure 8.8). It is also consistent with the activity concentration depth distributions in cores collected from sand dune slacks[33] (Figures 8.9 & 8.10) and with the changes in cation concentrations with depth (Figures 8.11 – 8.14).

[33] Sand dune slack data are presented for slacks 2, 3, 4, 5 and 7. No samples were collected from slack 1 because this slack was abandoned at an early stage of the sampling programme due to a low amphibian numbers. Although used for amphibian sampling, slack 6 was permanently filled with water so no soil cores could be collected.

(a)

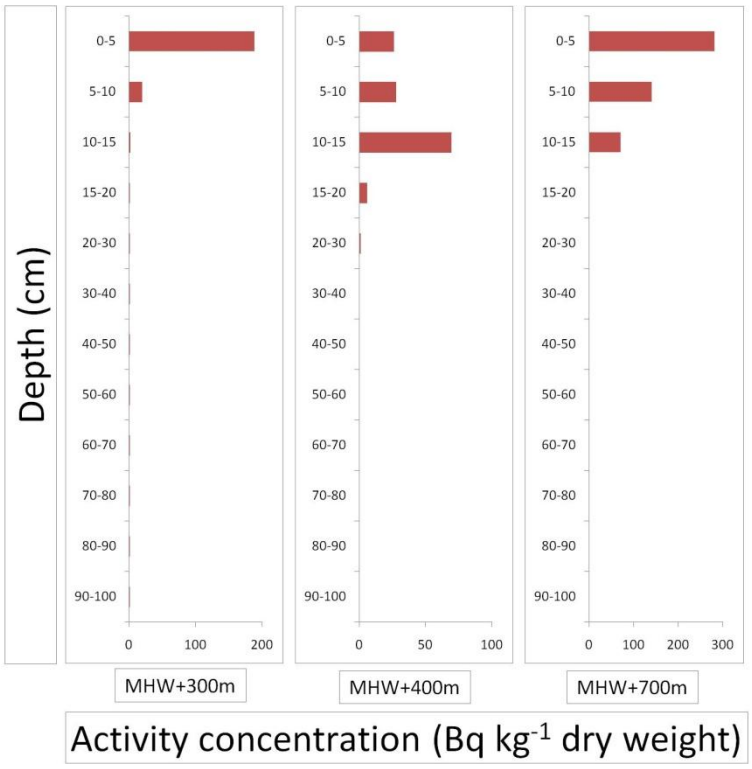

(b)

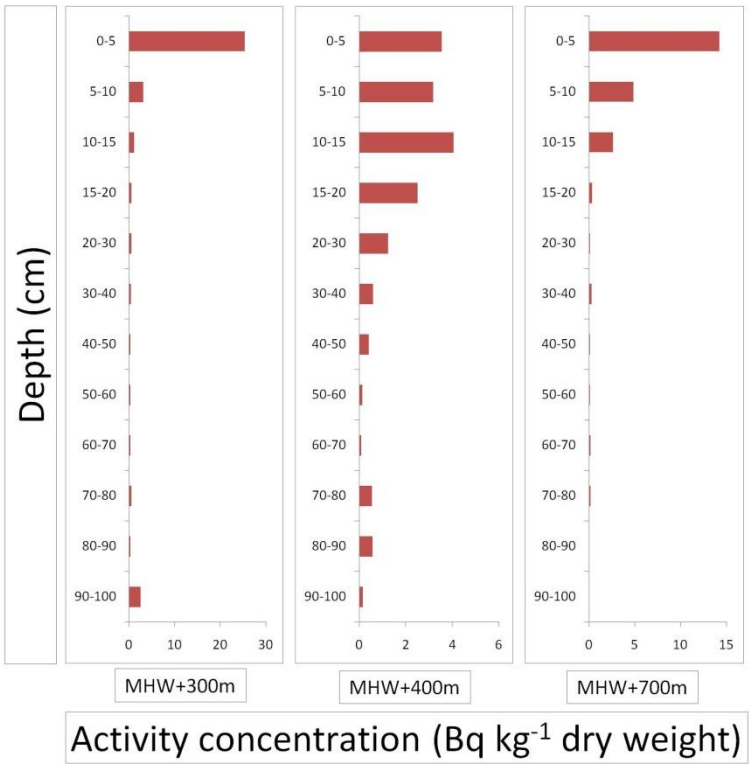

Figure 8.8. Depth profiles of (a) ^{137}Cs and (b) ^{241}Am activity concentrations (Bq kg^{-1} dry weight) from the three deep core (0 – 100 cm) sampling locations along Transect 1 at the Drigg coastal sand dunes.

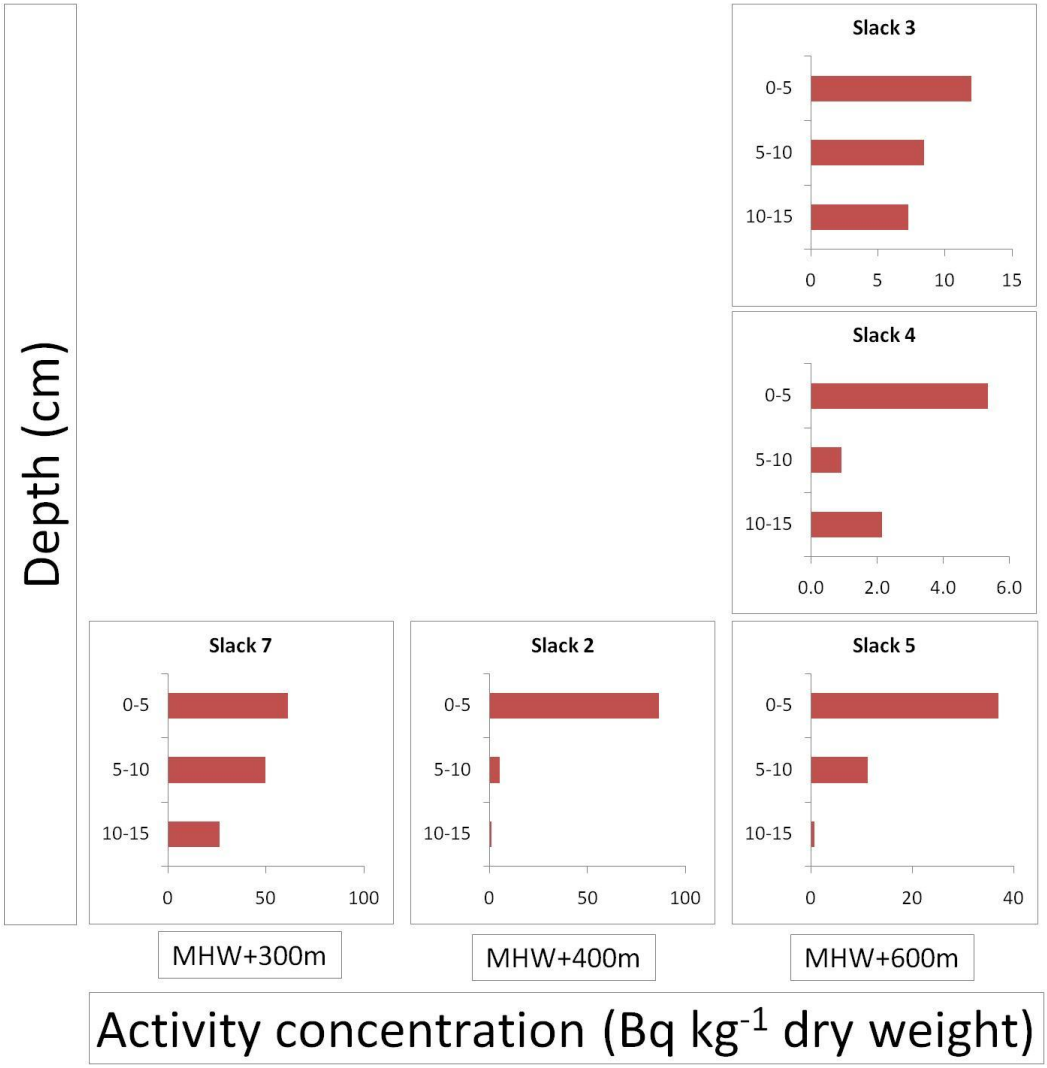

Figure 8.9. Depth profiles of ^{137}Cs activity concentrations (Bq kg^{-1} dry weight) in the upper 0 – 15 cm of soil from dune slack at the Drigg coastal sand dunes. All values were below the LOD so data presented are maximum LOD values. For slack location details see Table 3.3.

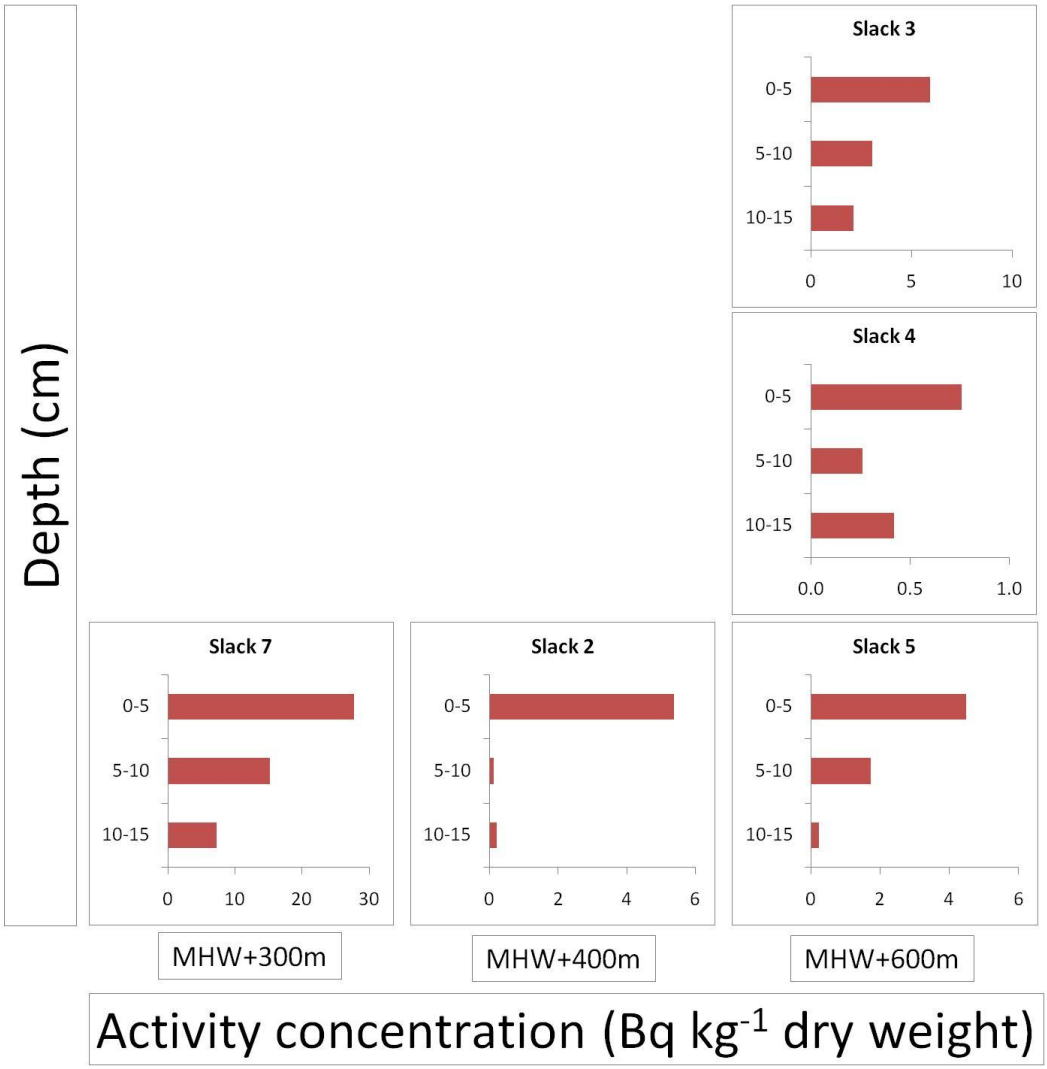

Figure 8.10. Depth profiles of ^{241}Am activity concentrations (Bq kg^{-1} dry weight) in the upper 0 – 15 cm of soil from dune slack at the Drigg coastal sand dunes. For slack location details see Table 3.3.

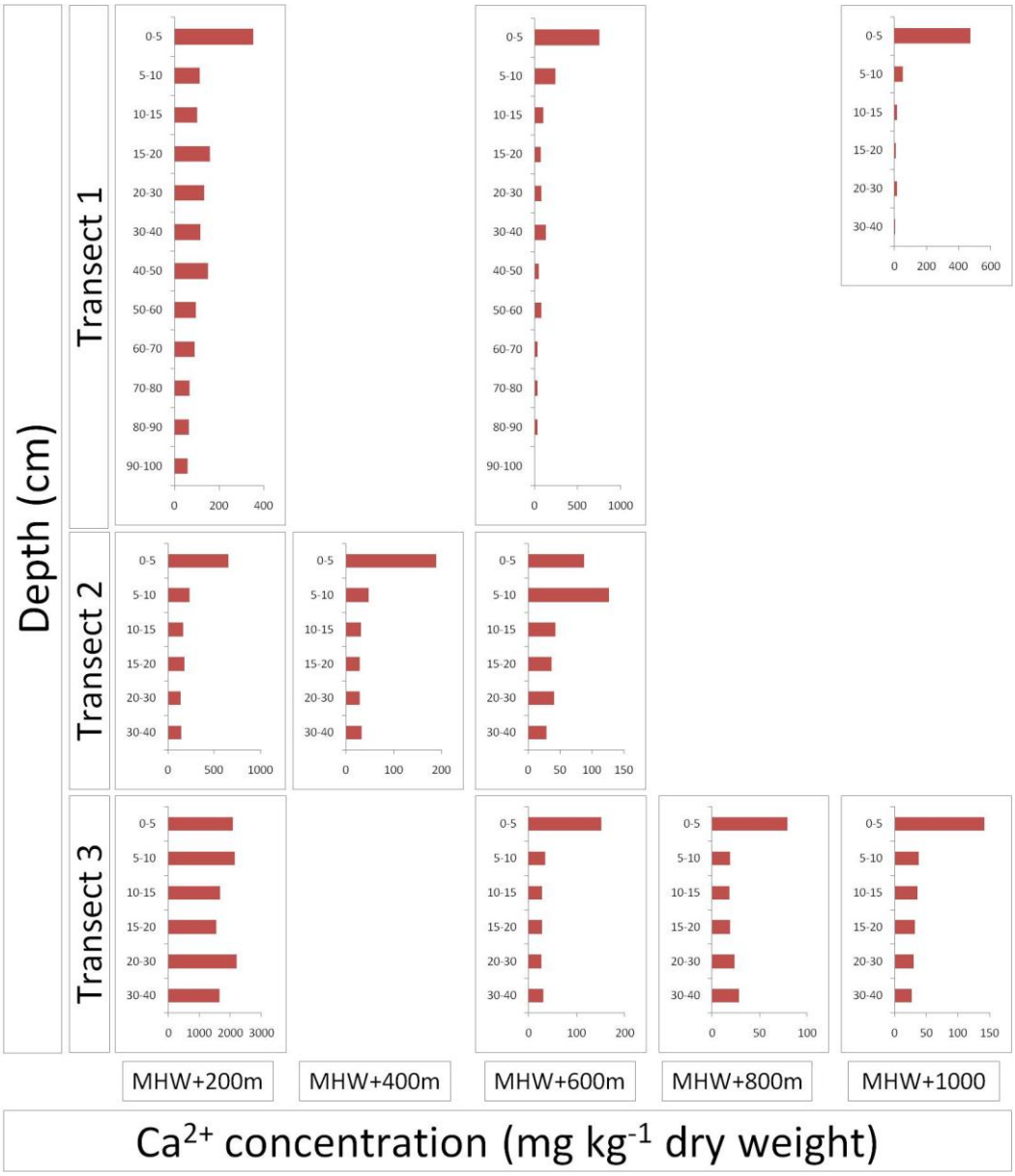

Figure 8.11. Depth profiles of Ca^{2+} concentrations (mg kg^{-1} dry weight) in soil from selected locations along Transects 1 – 3 at the Drigg coastal sand dunes.

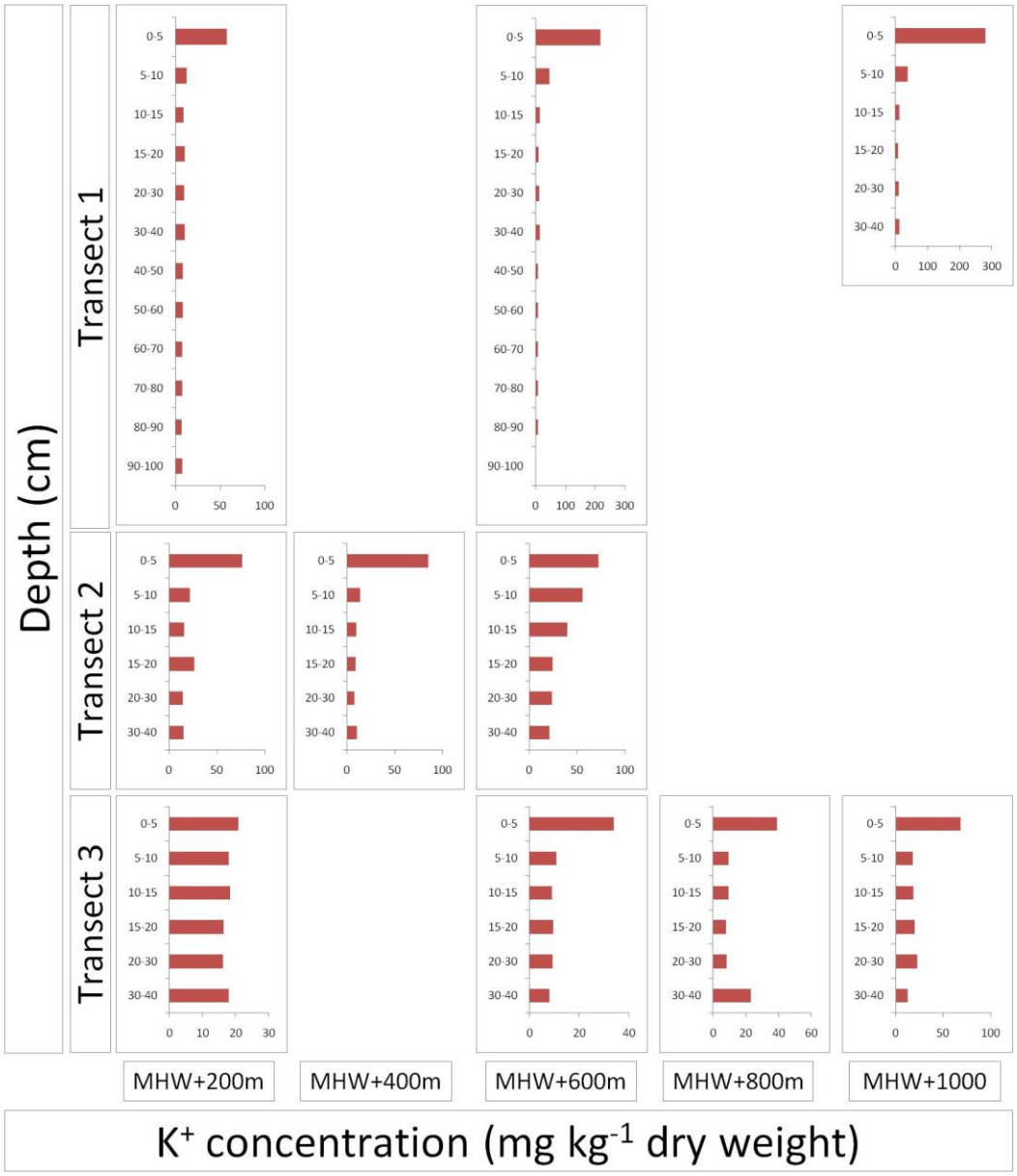

Figure 8.12. Depth profiles of K^+ concentrations (mg kg^{-1} dry weight) in soil from selected locations along Transects 1 – 3 at the Drigg coastal sand dunes.

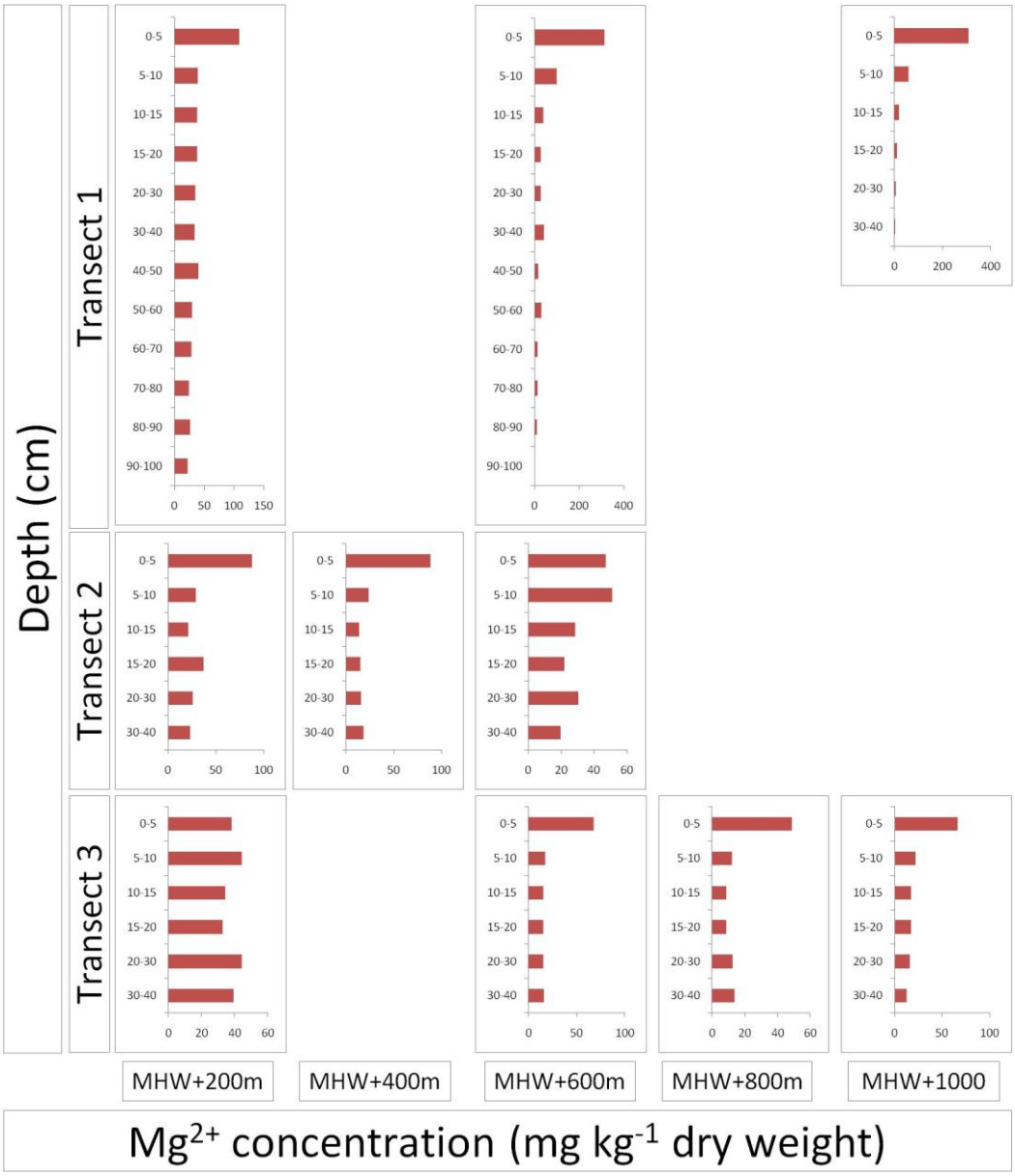

Figure 8.13. Depth profiles of Mg^{2+} concentrations (mg kg^{-1} dry weight) in soil from selected locations along Transects 1 – 3 at the Drigg coastal sand dunes.

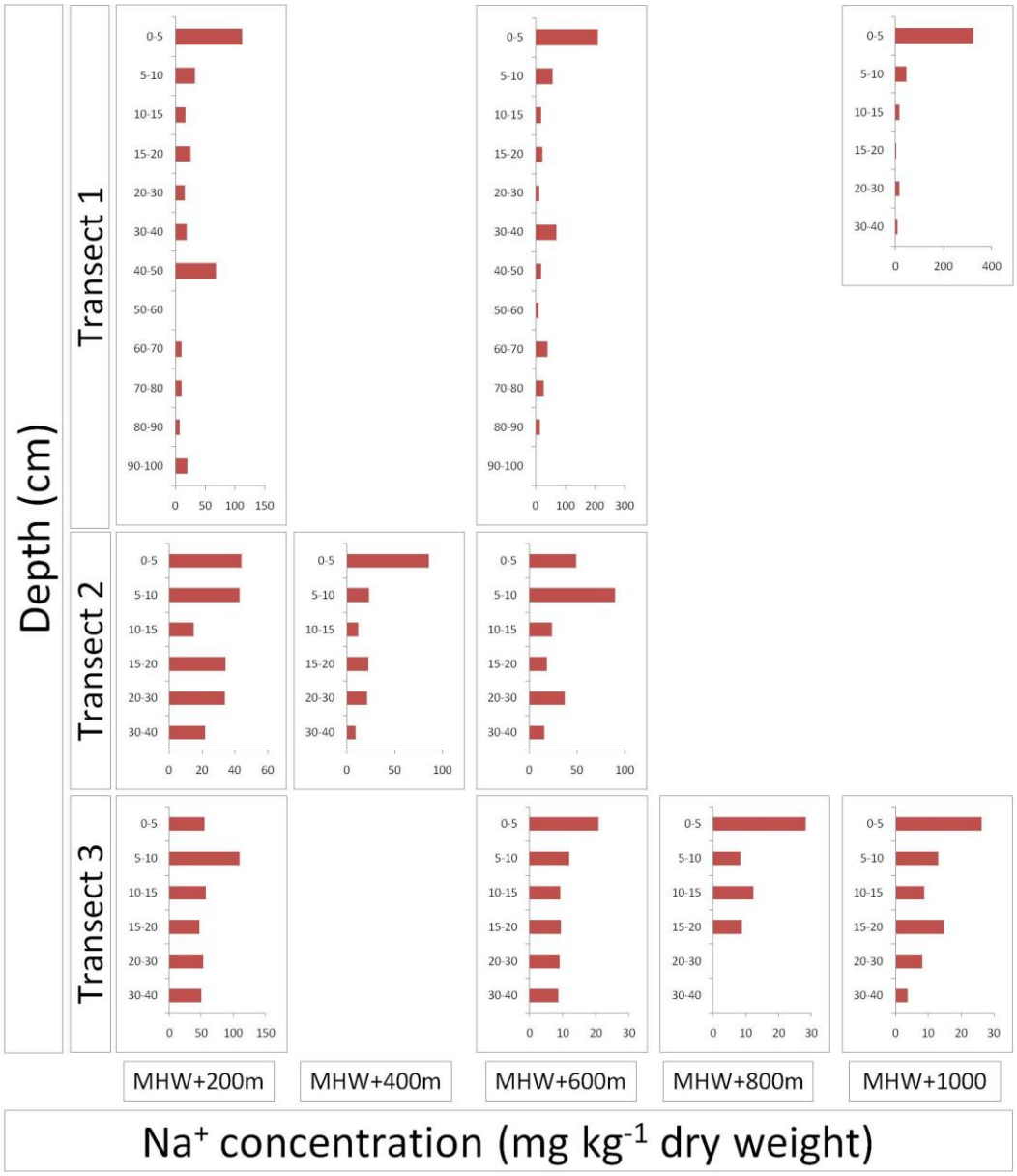

Figure 8.14. Depth profiles of Na^+ concentrations (mg kg^{-1} dry weight) in soil from selected locations along Transects 1 – 3 at the Drigg coastal sand dunes.

One anomaly in the ^{137}Cs and ^{241}Am activity concentration profiles was the MHW+1000 m profiles for Transect 3 (see Figures 8.6 & 8.7). This location was a re-vegetated blowout with a steep slope on the upwind side extending to a height of approximately 3 m above the lowest part of the blowout.

From the activity concentration profiles it appears that, after formation of the blowout, the blowout became an area of sand accretion rather than erosion (see Section 2.1.1). It is probable that the steep slope at the upwind side of the blowout resulted in a localised reduction in wind velocity, leading to sand accretion. The rate of sand accumulation in the base of the blowout is likely to have been increased by splash drift from the steep downwind slope (see Section 2.1.1). This would have resulted in sand from the surface soil being deposited on the base of the blowout and subsequently buried by sand from deeper within the soil profile.

The activity concentration data indicated that approximately 15 cm depth of sand had accumulated in the base of the blowout since the blowout occurred. Whilst it was not possible to establish when the blowout occurred from the data available, the organic matter and organic carbon data for this location demonstrated that the expected profile of decreasing organic matter/carbon concentration with depth had fully re-established (see Figures 8.15 & 8.16).

The ^{137}Cs and ^{241}Am activity concentration profiles for the MHW+600 m location on Transect 2 suggested that the soil profile at this location had also been disturbed, at least to a depth of 10 – 15 cm. Although re-vegetated, this disturbance is likely to be more recent than the blowout discussed previously because the organic matter/carbon and cation profiles at this location still showed signs of disturbance (see Figures 8.11 – 8.16).

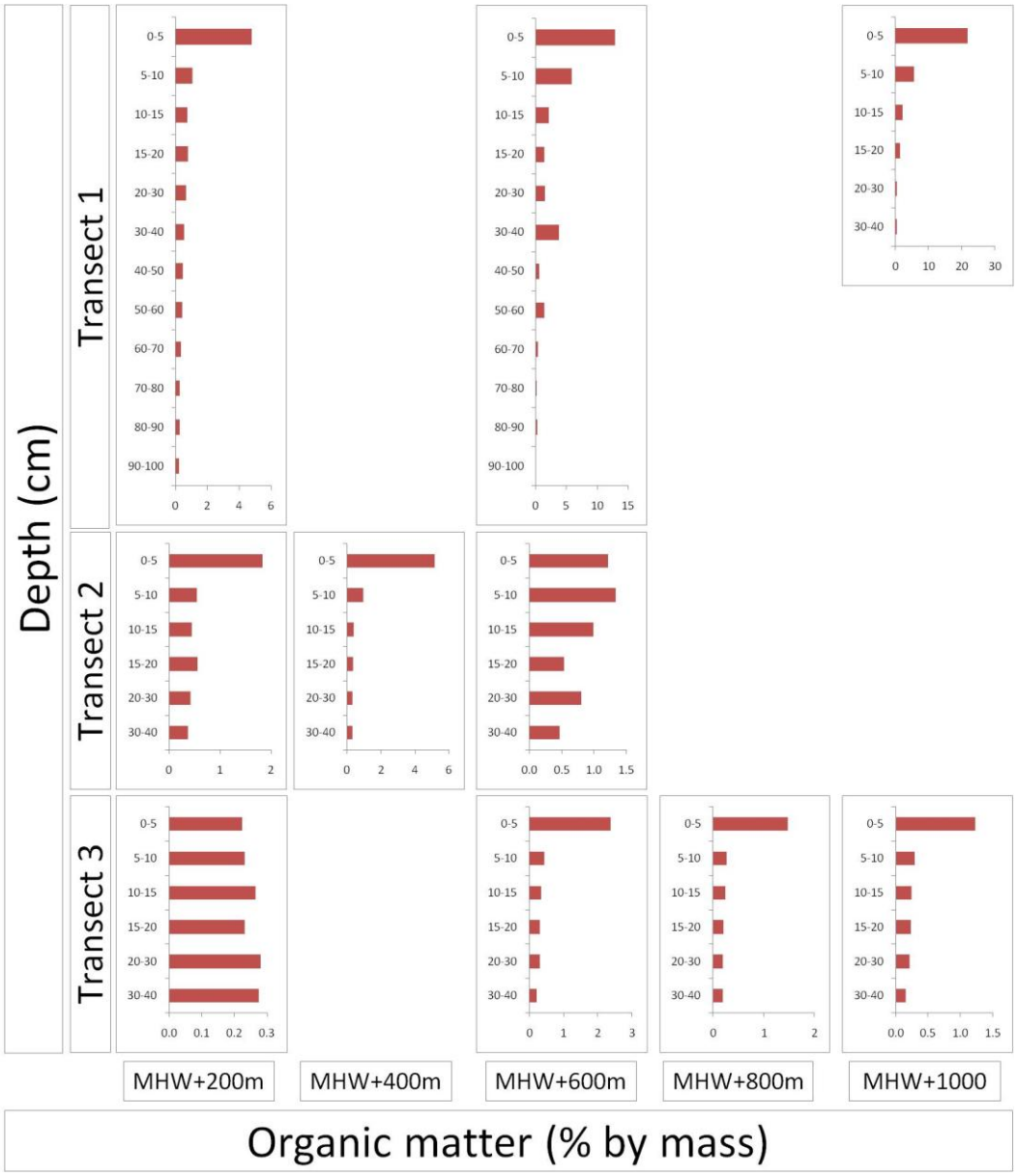

Figure 8.15. Depth profiles of estimated organic matter content (% by mass) in soil from selected locations along Transects 1 – 3 at the Drigg coastal sand dunes.

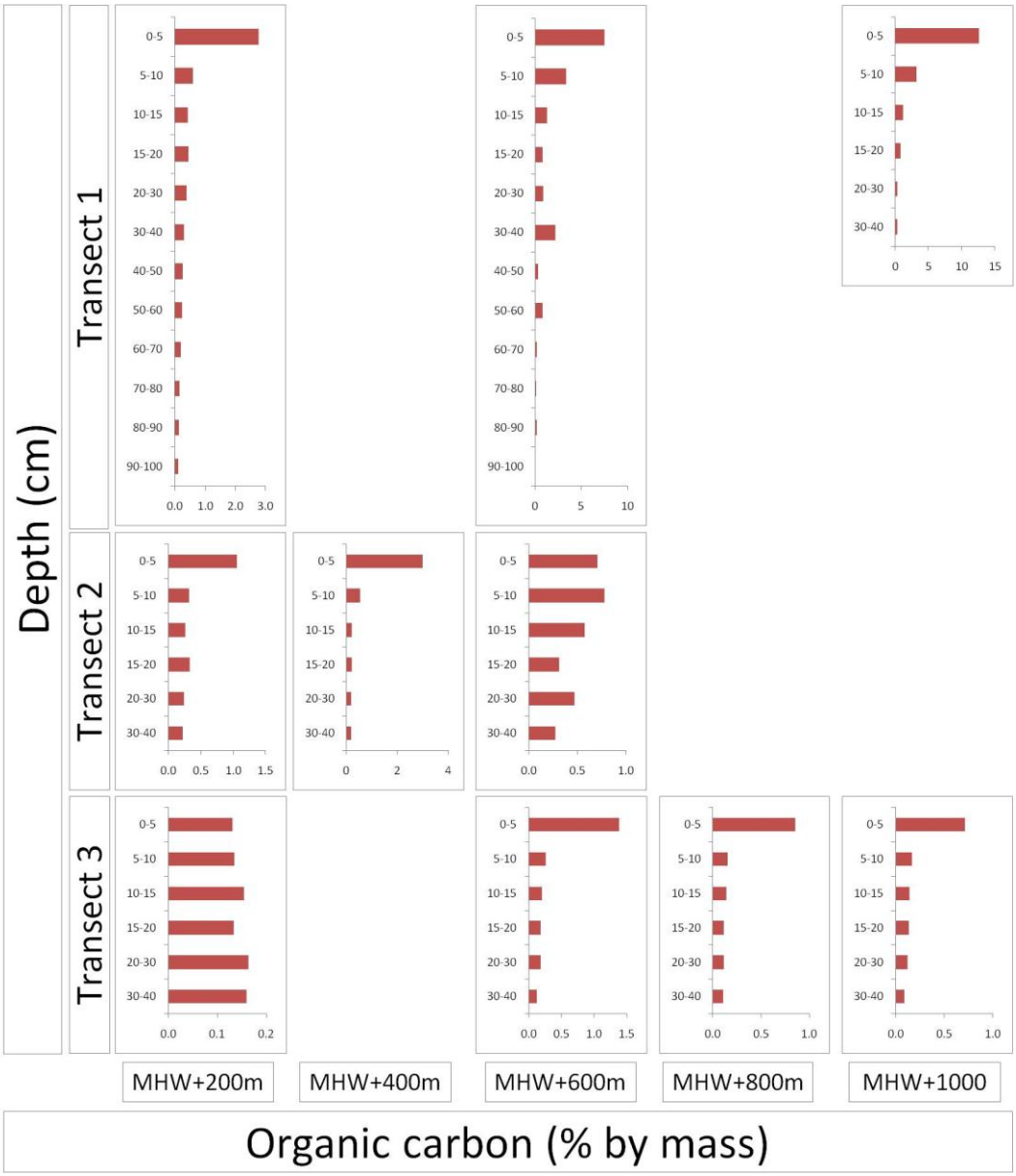

Figure 8.16. Depth profiles of estimated organic carbon content (% by mass) in soil from selected locations along Transects 1 – 3 at the Drigg coastal sand dunes.

8.2.1.3. Saltation versus sea-to-land transfer

The ^{241}Am activity concentration profiles (Figure 8.7) demonstrated a marked decrease in the ^{241}Am inventory in the upper 0 – 40 cm of the soil profile with increasing distance from

MHW. This was also observed in the ^{137}Cs depth profiles (Figure 8.6) but the reduction in ^{137}Cs activity with increasing distance from MHW occurred over a shorter distance than for ^{241}Am. There was no obvious difference in ^{137}Cs profiles beyond 200 m from the sites at the seaward end of each transect that had the potential to be tidally inundated. Furthermore, the absolute difference between the ^{137}Cs activity in soil at locations close to MHW compared to those further inland was lower than that observed for ^{241}Am.

These observations were to be expected based on previous research on the sea-to-land transfer of radionuclides, a process that results in increased actinide activity concentrations in coastal soils (see Section 2.4.1.1.3). It has been suggested that there may also be a detectable increase in ^{137}Cs activity concentrations within 50 m of the shoreline due to sea-to-land transfer (Branford & Nelis, 1996). However, the ^{137}Cs soil activity concentration profiles for the foredunes of Transect 2 (MHW+ 100 m) and Transect 3 (MHW+200 m) did not support this hypothesis (Figure 8.6). The activity concentrations for these foredunes were lower than for locations further inland and the ^{137}Cs activity concentrations were relatively uniform with depth. The ^{137}Cs activity concentrations were also notably similar to those of the locations at the front of Transects 2 and 3, which had the potential to be tidally inundated. This suggested that these foredunes were locations of rapid sand accretion. Although throughout most of the dune system, ^{137}Cs activity concentrations were more closely related to silt concentration than sand (Figure 8.17), the ^{137}Cs soil profile data suggested that the movement of ^{137}Cs contaminated sand particles in saltation (see Section 2.1.1), rather than sea-to-land transfer, was the dominant process determining ^{137}Cs activity concentrations in the foredunes.

The wind speed required to generate a friction velocity in excess of threshold velocity for saltaion has been calculated to be 6 m s^{-1} at 2 m above the sand surface (van Boxel et al., 1999; see Section 2.1.1). The mean wind speed at the Drigg coastal sand dunes is between 4.75 and 6.59 m s^{-1} depending on the season and seasonal wind speed maxima range from 14.92 to 19.03 m s^{-1} (George, 2006). Therefore, during all seasons, there are wind speeds that are high enough to initiate saltation.

The influence of sand transported in saltation was only observed in the upper 0 – 5 cm of the soil profile for the foredunes of Transect 1. This is because the Transect 1 foredune was highly stabilised by vegetation in comparison with the foredunes of Transects 2 and 3. Measurements of carbonate and pH in the soils of Transects 1 – 3 (Figures 8.18 and 8.19) indicated that the area of sand dunes covered by Transect 3 had formed more recently than

the dunes of Transect 1. As sand dunes stabilise and age, weathering of the shell fragments in the sand and the release of humic acids from accumulated organic matter results in the leaching of carbonates from the soil (see Section 2.1.1). The Transect 1 foredune had a lower carbonate content and lower pH than the foredunes of Transects 2 and 3, indicating that the Transect 1 foredune was older. This is in agreement with the cartographic records referred to in Section 2.2.2, which suggest that the length of the Drigg sand dune spit has increased in the last 300 – 400 y.

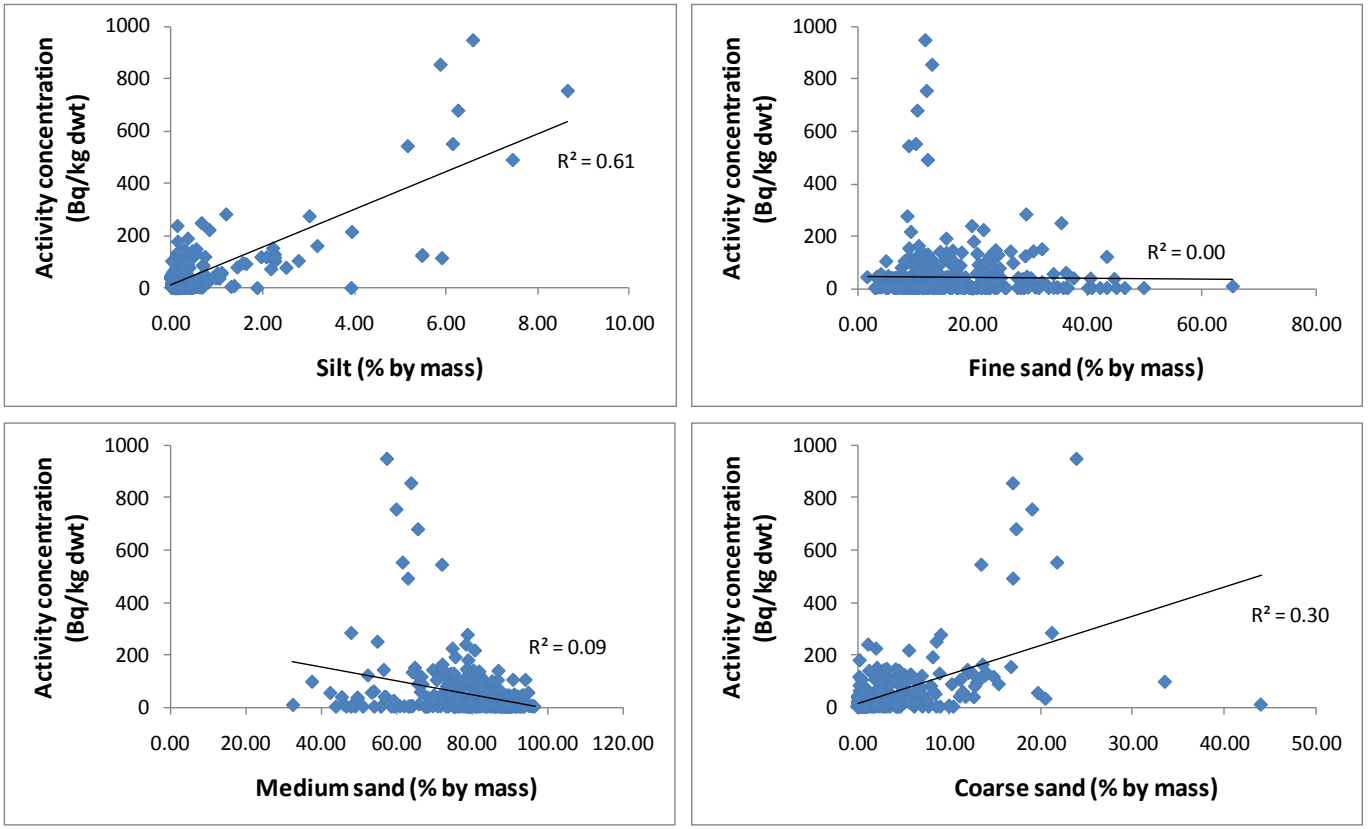

Figure 8.17. Relationship between ^{137}Cs activity concentration and particle size in soils from the Drigg coastal sand dunes. For definition of size classes see Section 3.2.1.

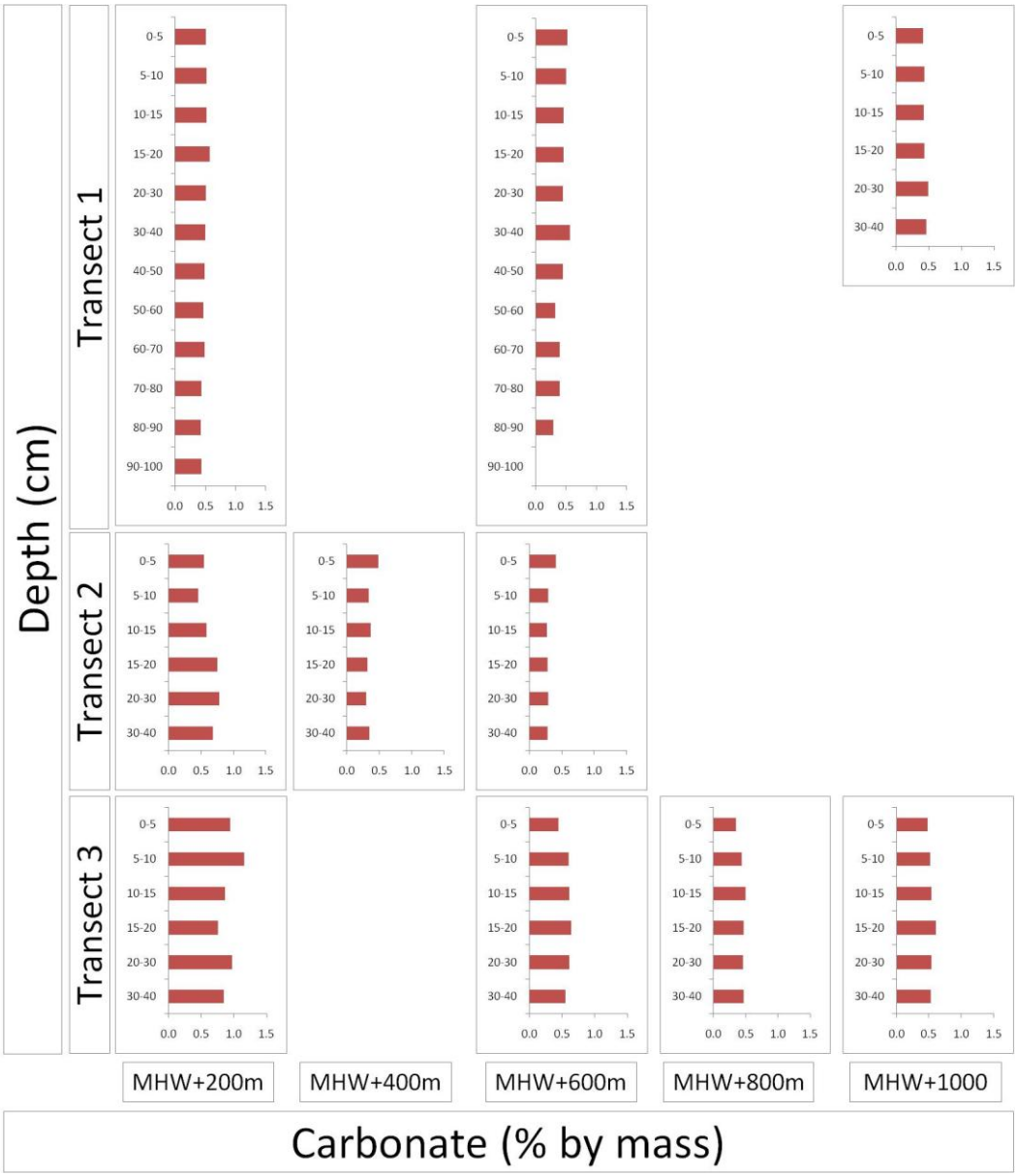

Figure 8.18. Depth profiles of estimated carbonate content (% by mass) in soil from selected locations along Transects 1 – 3 at the Drigg coastal sand dunes.

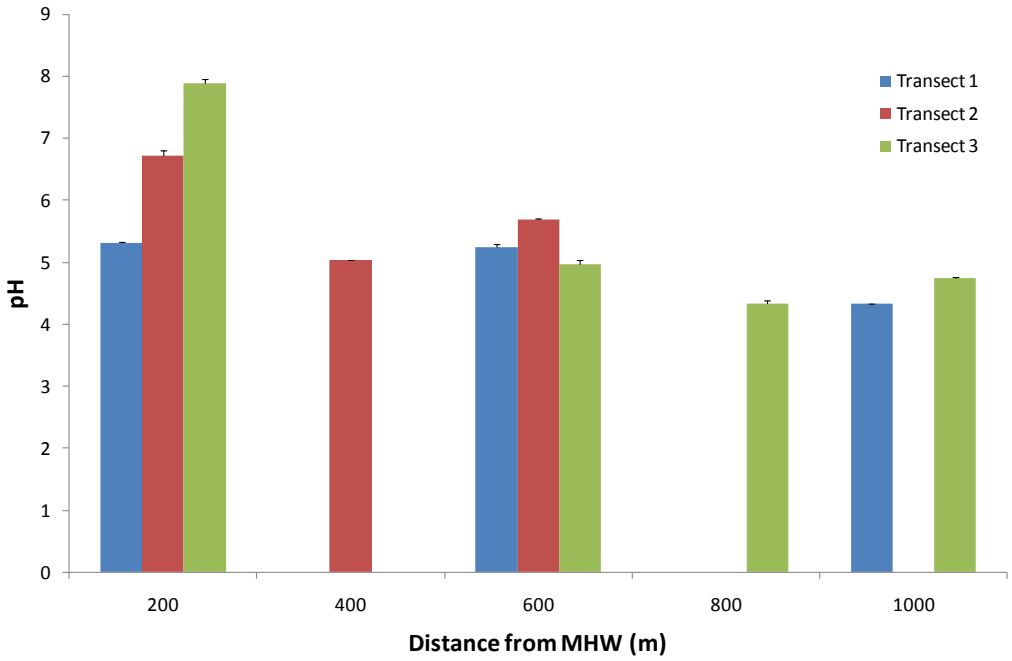

Figure 8.19. Change in pH of the top 0 – 5 cm of soil with increasing distance from mean high water along Transects 1 – 3.

8.2.2. Total deposition

The total deposition data from the Drigg coastal sand dunes (Table 8.3) further supported the hypothesis formulated in Section 8.2.1.2, namely that radionuclide leaching rates in sand dune soils may be lower than suggested by Copplestone et al. (2001c). In the samples collected from the foredune and dune heath areas, ^{137}Cs was only detectable in one sample from the foredune area of Transect 1. Using this value to predict annual deposition of ^{137}Cs at the Drigg coastal sand dunes resulted in an estimated annual deposition of 110 ± 33 Bq m^{-2}. This rate of deposition is too low to account for the measured ^{137}Cs activity concentrations in the surface soils at the Drigg sand dunes if the leaching rate is high.

Table 8.3. Activity concentrations in total deposition samples collected from the Drigg coastal sand dunes. For sampling location details see Table 3.4.

Transect	Location	Collector deployed	Sample collected	^{137}Cs (Bq l^{-1})	^{7}Be (Bq l^{-1})
1	Foredune	23/04/2006	17/05/2006	0.10 ± 0.03	2.43 ± 0.56
		16/06/2006	03/08/2006	<0.01	<0.11
1	Dune heath	31/03/2006	21/04/2006	<0.02	1.12 ± 0.34
		21/04/2006	17/05/2006	<0.02	1.64 ± 0.36
		17/05/2006	12/06/2006	<0.02	0.83 ± 0.23
		12/06/2006	03/08/2006	<0.01	0.14 ± 0.13
2	Foredune	31/03/2006	17/05/2006	<0.01	1.07 ± 0.23
		17/05/2006	13/06/2006	<0.02	<0.16
		13/06/2006	03/08/2006	<0.01	<0.08
2	Dune heath	31/03/2006	21/04/2006	<0.02	1.41 ± 0.36
		21/04/2006	17/05/2006	<0.02	2.09 ± 0.43
		16/06/2006	03/08/2006	<0.01	<0.08
3	Foredune	31/03/2006	21/04/2006	<0.02	0.77 ± 0.36
		21/04/2006	17/05/2006	<0.02	1.23 ± 0.35
		17/05/2006	13/06/2006	<0.02	<0.16
		13/06/2006	03/08/2006	<0.01	<0.09
3	Dune heath	31/03/2006	21/04/2006	<0.02	1.47 ± 0.36
		21/04/2006	17/05/2006	<0.01	1.28 ± 0.34
		17/05/2006	13/06/2006	<0.01	1.08 ± 0.23
		13/06/2006	03/08/2006	<0.01	<0.10

8.2.3. Nuclide and isotopic ratios

Soil samples from 6 locations, three foredune locations and three dune heath locations (one foredune and dune heath location per sampling transect), were analysed using alpha spectrometry (see Chapter 3) to determine the ^{90}Sr, ^{99}Tc, ^{238}Pu, $^{239+240}$Pu and ^{241}Am activity concentrations in the upper 0 – 10 cm of soil. There was good agreement across the activity concentration range between the ^{241}Am analytical results obtained using alpha spectrometry and those obtained using gamma spectrometry ($r^2 = 0.98$), confirming that gamma spectrometry was a suitable technique for determining ^{241}Am activity concentrations in the Drigg coastal sand dune soils.

The 0 – 10 cm soil depth data from the six locations were used to determine nuclide and isotopic ratios (Table 8.4). These ratios provided an indication of the main sources of anthropogenic radionuclide contamination at the dunes and difference in contamination sources for the foredunes and dune heath areas.

Table 8.4. Nuclide and isotopic activity concentration ratios for 0 – 10 cm depth soil samples from the Drigg coastal sand dunes

Nuclide / Isotopic Ratio	Foredune			Dune heath		
	n	mean	SD	n	mean	SD
^{90}Sr:^{99}Tc	3[1]	1.0	0.9	3[2]	1.2	0.9
^{137}Cs:^{90}Sr	3	5.5	3.4	3[2]	4.4	6.4
^{137}Cs:^{99}Tc	3[1]	3.6	1.2	3	2.9	2.9
^{137}Cs:$^{239+240}Pu$	3	1.6	1.7	3	12.2	6.9
^{137}Cs:^{241}Am	3	1.1	1.1	3	10.8	9.2
^{238}Pu:$^{239+240}Pu$	3	0.18	0.01	3[3]	0.27	0.005
$^{239+240}Pu$:^{241}Am	3	0.8	0.1	3	0.8	0.3
$^{239+240}Pu$:^{90}Sr	3	4.7	2.6	3[2]	0.3	0.3
$^{239+240}Pu$:^{99}Tc	3[1]	4.1	3.5	3	0.2	0.1
^{241}Am:^{90}Sr	3	5.9	2.8	3[2]	0.3	0.2
^{241}Am:^{99}Tc	3[2]	5.1	4.1	3	0.2	0.1

[1] includes one LOD value for ^{99}Tc; [2] includes two LOD values for ^{90}Sr; [3] includes one LOD value for ^{238}Pu.

The ratios of actinides to non-actinides demonstrated an enhancement of actinides in the foredunes due to the sea-to-land transfer process. The ratio of ^{238}Pu:$^{239+240}Pu$ can be used to distinguish between soils predominantly contaminated by Sellafield discharges and soils contaminated by weapons test fallout. The average ratio for Sellafield-derived Pu is 0.18 and the ratio for weapons test fallout is between 0.03 and 0.04 (Bryan et al., 2008). As expected, the ^{238}Pu:$^{239+240}Pu$ ratios in soil from the Drigg coastal sand dunes demonstrated that Sellafield discharges were the main source of actinide contamination at the site. The reason for the markedly higher ratio for the dune heath is unclear and cannot be explained by the inclusion of LOD data in the ratio derivation, but the ratio of 0.27 is comparable with the upper bound ratio values that have been reported for other coastal soils for which Sellafield discharges have been determined to be the principal contributor to Pu isotope activity concentrations (Bryan et al., 2008).

There was an indication from the ^{90}Sr:^{99}Tc ratios that ^{99}Tc activity concentrations may be slightly elevated in foredune soils, plausibly due to the transport of ^{99}Tc contaminated sand by saltation. However the use of LOD values in determining these ratios, coupled with the low sample numbers, may also explain this difference.

8.2.4. Dune slacks

Dune slacks are the most ecologically productive habitat within coastal sand dunes (see Section 2.1.3.). As a result, they may be expected to exhibit increased cycling, and hence retention, of radionuclides in the upper soil layers. In addition, leaching of radionuclides as water drains into the dune slacks from the surrounding dunes may be expected to lead to elevated activity concentrations in the dune slacks, similar to the 'valley floor' accumulation of ^{137}Cs that has been observed in upland catchments (Tyler & Heal, 2000). However, water activity concentrations for dune slack waters were all below the LOD for ^{137}Cs (Table 8.5). The ^{241}Am activity concentration depth profiles for dune slack soils (Figure 8.10) were similar to the profiles for non-slack soils at the same distances from MHW, whereas the ^{137}Cs soil activity concentrations (Figure 8.9) were generally lower in the dune slack soils. A plausible explanation for these observations is that both ^{137}Cs and ^{241}Am are relatively immobile in sand dune soils but, due to the high productivity of dune slacks, increased release of humic acids from accumulated organic matter results in a reduced pH in dune slack soils. An increase in hydrogen ions is known to displace Cs from binding sites (Livens & Baxter, 1988b) so, if this reduction in dune slack soil pH is occurring, this may lead to increased leaching of ^{137}Cs from soil of dune slacks in comparison with other sand dune soils.

Table 8.5. Activity concentrations in water samples collected from slacks at the Drigg coastal sand dunes. For slack location details see Table 3.3.

	Activity concentration (Bq l^{-1})			
	^{137}Cs		**^{7}Be**	
Slack No.	***n***	**Max**	***n***	**Max**
1	2	<0.03	2	<0.47
2	1	<0.03	1	<0.54
3	2	<0.03	2	<0.51
4	2	<0.03	2	<0.62
5	2	<0.03	2	<0.62
6	1	<0.03	1	<0.60
7	1	<0.03	1	<0.68

The lower ^{137}Cs activity concentrations in dune slack sediments and the < LOD ^{137}Cs activity concentrations in the water will result in amphibians receiveing a lower external dose rate during the time that they spend within the dune slacks compared with the time that they spend in other areas of the sand dunes. Therefore, when predicting external dose rates for sand dune amphibians, assuming that amphibians spend all of their time in areas other than the dune slacks will result in a conservative assessment.

8.2.5. Gamma dose rates

In situ measurement data for gamma dose rates in air at 1 m above the soil surface are presented in Table 8.6 and in Figure 8.20. The quantities reported are total gamma dose rate, which include the contribution from cosmic radiation, terrestrial gamma dose rate, for which the contribution of cosmic radiation is subtracted, and anthropogenic gamma dose rate, for which the contributions of both cosmic radiation and natural radionuclides in the soil are subtracted. The derivation of these quantities is explained in Section 3.1.4.2.

The high gamma dose rate at MHW+1200 m on Transect 3 was due to the high activity concentrations of ^{60}Co and ^{137}Cs in the saltmarsh sediments at this location compared to the activity concentrations of these radionuclides in the sand dune soils. Although the ^{241}Am activity concentrations were also high in these saltmarsh sediments, ^{241}Am was not a significant contributor to gamma dose rates in air, due to its low-energy gamma photons (59 keV).

For the other locations along each transect, the measured dose rates generally seemed to be related to ^{137}Cs activity concentrations in the soil. However, there was considerable variability in this relationship, especially beyond 300 m. This may be due to differences in the contribution of ^{137}Cs contamination to measured dose rates resulting from differences in the depth profile (due to absorption of gamma photons within the medium, ^{137}Cs at depth will contribute proportionally less to the measured gamma dose rates than ^{137}Cs in the surface soil). Another factor which may have influenced the *in situ* measurements is increased moisture retention in the soil profile at some of the grey dune and dune heath locations due to increased concentrations of organic matter in these soils (there was a positive correlation between soil moisture and organic matter concentrations measured in sand dune soils, $r^2 = 0.55$). Elevated moisture concentrations in surface soils are known to attenuate terrestrial gamma photons (Thompson et al., 1999).

Table 8.6. Summary of measured gamma dose rates and estimated exposure for the Drigg coastal sand dunes and adjoining areas of intertidal beach and saltmarsh

Location category		Gamma dose rate (nGy h^{-1})		
		Total	**Terrestrial**	**Anthropogenic**
Dune	n	25	25	25
	mean	67	19	-
	SD	6	6	-
	min	54	6	-
	max	80	33	-
Intertidal	n	112	112	112
	mean	105	56	9
	SD	33	33	18
	min	61	14	-
	max	227	175	105

- indicates that no anthropogenic contribution (and hence no exposure estimate) could be determined because the terrestrial gamma dose rate was lower than the correction factor for natural radionuclides (50 nGy h^{-1} for sandy substrates and 70 nGy $h^{-1}$for intertidal areas – see Section 3.1.4.).

(a)

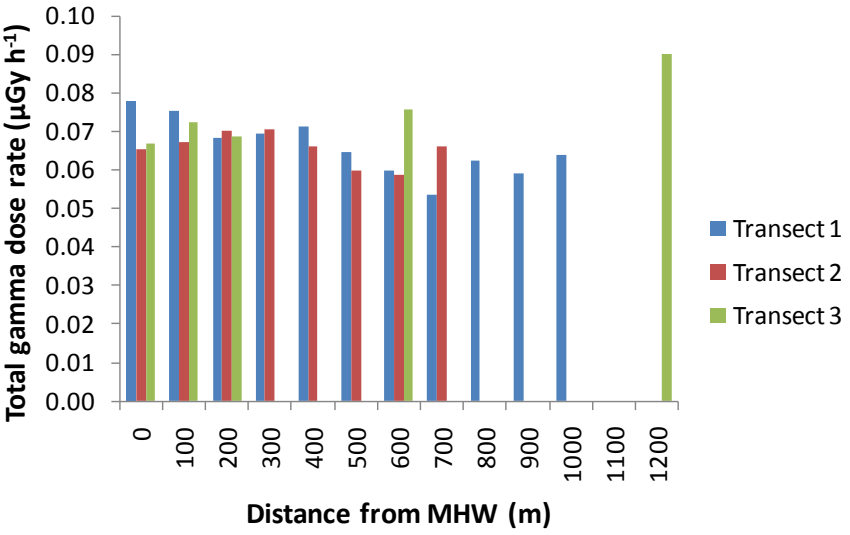

(b)

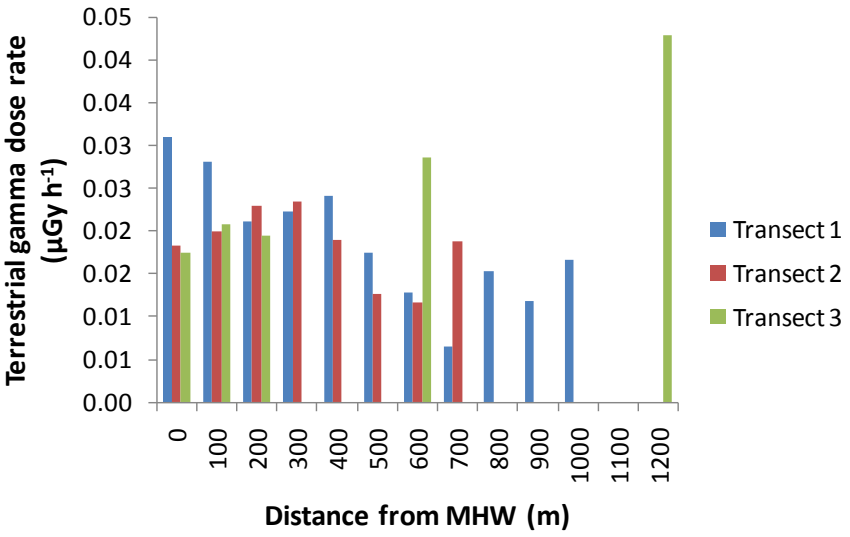

Figure 8.20. Measured (a) total and (b) terrestrial gamma dose rates (µGy h^{-1}) along Transects 1 – 3 at the Drigg coastal sand dunes

8.3. Concentration ratios for sand dune biota

In previous chapters, differences in the transfer of radionuclides to sand dune biota in comparison with similar species from other terrestrial sites have been observed. For example, the mean Am, Cs and Pu CRs for small mammals were 2 orders of magnitude lower for coastal sand dunes (see Chapter 6). One hypothesis proposed to explain this was the potential influence of other cations from the marine environment (e.g. K and Na) on the net transfer observed but, at the time of writing, there were no cation concentration data available for the Drigg coastal sand dune soils.

The cation concentrations that have been measured subsequently in soil samples collected from the Drigg coastal sand dunes are reported in Figures 8.11 – 8.14 and summarised in Table 8.7. The MHW + 200 m location of Transect 3 had a high cation concentration indicative of recently deposited sand from a tidally-inundated area. Therefore, summary values were also derived with this location omitted (Table 8.7). The cation concentrations in the soils of the Drigg coastal sand dunes were markedly higher than those reported for the sand dunes at Blakeney Point in Norfolk, UK (see Table 2.3) but were at the lower end of the concentration ranges that have been reported for various UK soils (Allen, 1989).

Based on these observations, it is unlikely that the cation concentrations in coastal sand dune soils account for the lower sand dune biota CRs. A more plausible explanation is that the radionuclides are in a less bioavailable form. As discussed in Sections 2.4.1.1.3 and 8.2.1.3, radionuclide transport from the marine environment, either by sea-to-land transfer or by saltation, results in deposition of particulate-bound activity on the coastal sand dunes. The core profile data (Section 8.2.1) and observations on the activity concentrations in the dune slacks suggest that this particulate-bound activity is not readily mobilised. Therefore, although activity concentrations in the surface soils may be high, the bioavailable fraction may be low. This is an area for future research.

Due to observed differences in radionuclide transfer to coastal sand dune biota in comparison with similar species from other terrestrial sites, a conclusion that is common to Chapters 4 – 7 is that there is a need to develop a database of transfer parameters which are specific to coastal sand dune ecosystems. The soil (0 – 10 cm) and biota activity concentration have therefore been used to derive CRs for biota at the Drigg coastal sand dunes. Where LOD values were included in the derivation of CR values, the approach

described for the derivation of reptile CRs was followed (see Section 7.3.6). Where all values were below the LOD, the maximum CR was reported.

Table 8.7. Cation concentrations (mg kg^{-1}) in the upper 0 – 10 cm of soil at the Drigg coastal sand dunes

	Cation concentration (mg kg^{-1})			
	Ca	**K**	**Mg**	**Na**
All locations (n = 10)				
Mean	400	60	79	69
SD	620	48	62	54
Excluding Transect 3 MHW+200 m (n = 9)				
Mean	210	64	83	68
SD	163	48	65	57

The CRs have been derived on a species-specific basis (Tables 8.8 & 8.9) and summarised by biota group (Table 8.10). The species-specific and summarised CRs for Cs transfer to small mammals at the Drigg coastal sand dunes were in good agreement with the CRs calculated using data from the Sellafield coastal sand dunes (see Table 6.13). Therefore, to provide a generic CR database that can be used in future assessments of the impacts of ionising radiation on biota at temperate coastal sand dune sites, the Drigg and Sellafield sand dune data were combined and the final CR database is presented in Table 8.11.

Table 8.8. Species-specific Am, Cs and K concentration ratios for Drigg coastal sand dune biota.

Species (latin)	Am			Cs			K		
	n	mean	SD	n	mean	SD	n	mean	SD
Bufo bufo	7	6.20E-01		7	8.11E-02	1.02E-01	7	2.01E-01	2.16E-01
Bufo calamita	3	2.55E+00		3	3.22E-02	1.67E-02	3	1.44E-01	5.60E-02
Rana temporaria	7	1.03E-01	2.59E-02	7	5.44E-02	2.93E-02	7	3.61E-01	4.60E-01
Triturus cristatus	7	5.23E-01		7	1.15E-01	6.36E-02	7	2.93E-01	1.14E-01
Triturus helveticus	15	1.49E-01	2.77E-02	15	1.33E-01	7.33E-02	15	4.39E-01	5.18E-01
Triturus vulgaris	1	2.92E-01		1	8.84E-02		1	5.22E-01	
Anas platyrhynchos	1	1.88E-02		1	4.33E-02		1	3.89E-01	
Anas crecca	2	3.81E-02	1.60E-02	2	2.86E-02	2.67E-03	2	2.60E-01	5.03E-02
Arctiidae spp	4	1.52E-01	0.00E+00	4	3.40E-02	1.88E-02	4	3.81E-01	
Gastropoda	5	5.13E-02	2.74E-02	5	2.75E-02	1.94E-02	5	1.79E-01	1.09E-01
Lumbricus terrestris	1	1.10E+00		1	8.78E-02		1	9.27E-01	
Apodemus sylvaticus	15	8.91E-01		15	7.54E-02	3.43E-02	15	5.10E-01	2.40E-01
Microtus agrestis	4	7.54E-01		4	1.17E-01	6.53E-02	4	3.10E-01	9.04E-02
Sorex araneus	3	1.98E+00		3	1.69E-01		3	1.12E+00	7.31E-01
Talpa europaea	1	6.68E-02		1	2.51E-02		1	3.08E-01	
Anguis fragilis	9	8.56E-02	2.13E-02	9	2.25E-01	1.45E-01	9	3.04E-01	1.69E-01
Lacerta vivipara	8	3.85E-01		8	1.28E-01	5.59E-02	8	2.16E-01	1.67E-01
Vipera berus	3	7.81E-02	2.34E-03	3	4.73E-02	4.08E-02	3	2.75E-01	8.60E-02
Ammophila arenaria	16	2.99E-01	5.01E-01	16	3.08E-02	5.40E-02	16	3.29E-01	2.67E-01
Festuca rubra	7	2.21E-01	2.59E-01	7	3.82E-02	3.31E-02	7	4.39E-01	2.16E-01
Mixed herbage	2	4.79E-02	1.88E-02	2	2.21E-02	1.62E-03	2	2.21E-02	1.62E-03
Calluna vulgaris	1	9.47E-02		1	3.21E-01		1	1.34E-01	
Erica cinerea	3	3.25E-02	2.95E-02	3	9.80E-03	6.30E-03	3	1.23E-01	4.61E-02
Erica tetralix	3	3.88E-02	3.57E-02	3	1.91E-01	1.34E-01	3	6.69E-02	3.03E-02
Ulex europaeus	3	5.59E-03	2.72E-03	3	1.89E-02	1.14E-02	3	3.95E-01	7.16E-02
Cladonia portentosa	1	2.34E-01		1	1.67E-01		1	2.02E-01	
Racomitrium canescens	1	2.01E-01		1	2.22E-01		1	1.02E+00	
Hygrophorus sp	1	1.13E-01		1	5.84E-01		1	4.39E-01	
Lepiota sp	1	8.93E-02		1	2.74E-02		1	5.69E-01	
Lycoperdon sp	2	2.42E+00		2	2.95E-01		2	1.37E+00	7.60E-01
Marasmius sp	6	1.81E-01		6	2.40E+00	1.30E+00	6	4.52E-01	8.82E-02
Rhodophyllus sp	2	1.68E-01		2	2.18E+00	3.01E+00	2	6.58E-01	3.53E-01
Russula sp	5	1.83E-01		5	7.53E-01	1.44E+00	5	4.20E-01	1.90E-02

Values highlighted in grey are those for which all CRs were LOD values so the maximum CR value was reported.

Table 8.9. Species-specific Pu, Sr and Tc concentration ratios for Drigg coastal sand dune biota.

Species (latin)	Pu			Sr			Tc		
	n	mean	SD	n	mean	SD	n	mean	SD
Bufo calamita	-			2	1.43E-01	7.20E-02	2	5.06E-01	3.05E-01
Rana temporaria	-			3	6.33E-01	1.41E-01	3	4.50E-01	
Triturus cristatus	-			3	5.88E-01	3.61E-02	3	3.18E-01	9.99E-02
Triturus helveticus	-			3	9.08E-01	6.07E-01	1	6.20E-01	
Anas platyrhynchos	2	6.06E-03	5.56E-04	1	5.75E-02		1	3.17E-02	
Anas crecca	3	1.46E-02	1.15E-03	2	7.22E-02		2	1.67E-01	1.84E-01
Arctiidae spp	-			2	8.82E-02		1	1.07E+00	
Anguis fragilis	4	1.96E-02	7.33E-03	3	9.74E-01	7.49E-01	3	5.56E-01	
Lacerta vivipara	-			3	1.43E-01		2	7.74E-01	
Vipera berus	4	8.72E-03	5.12E-03	-			-		
Festuca rubra	5	4.25E-02	3.55E-02	3	3.25E-01	3.33E-01	3	8.27E-02	2.54E-03

Values highlighted in grey are those for which all CRs were LOD values so the maximum CR value was reported; - indicates no CR data available.

8.4. Conclusions

There was little variation, both spatially and with depth, in soil natural radionuclide activity concentrations at the Drigg coastal sand dunes. This was to be expected because the sand dune soils share a common parent material. Anthropogenic radionuclides showed a general decrease in activity concentrations with increasing soil depth. However, there was evidence that foredune locations may exhibit an increase in activity concentrations with depth due to burial of historical deposition by less contaminated sand from the backshore beach zone.

Due to the influence of the sea-to-land transfer process, a decrease in the activity concentrations of Pu isotopes and ^{241}Am was observed with increasing distance from MHW. Isotopic ratios indicated that the primary source of actinide contamination at the Drigg coastal sand dunes was discharges from the Sellafield site.

Changes in soil radionuclide activity concentration data with increasing distance from MHW suggest that saltation, in addition to sea-to-land transfer, is an important process influencing measured activity concentrations in sand dune soil, especially for ^{137}Cs at locations within 200 m of the beach.

Blowout formation and splash drift may be important processes in determining depth profiles in sand dune soil on a localised scale. Therefore, blowouts and areas at the base of sand dunes should be avoided when sampling soils to determine activity concentrations for environmental assessment purposes.

Dune slack soils may have lower ^{137}Cs activity concentrations than soils in other sand dune habitats, plausibly due to higher organic matter accumulation leading to leaching of humic acids and a resultant reduction in soil pH. At lower pH, the mobility of ^{137}Cs increases and this may result in increased leaching rates in dune slack soils.

The measured cation data do not support the hypothesis that elevated concentrations of marine cations (e.g. K and Na) may explain the low Am, Cs and Pu CRs for sand dune biota. Although cation concentrations in the soils at the Drigg coastal sand dunes were markedly higher than those reported for the sand dunes at Blakeney Point, they were at the lower end of the concentration ranges reported for other UK soils. A more plausible explanation for the low sand dune small mammal CRs is that the radionuclides deposited, due to sea-to-land transfer or saltation, are in a particulate-bound form and are not readily mobilised. Therefore, although activity concentrations in surface soils may be high, the bioavailable fraction may be low.

Table 8.10. Concentration ratios for biota from the Drigg coastal sand dunes

Biota group	Am			Cs			K			Pu			Sr			Tc		
	n	mean	SD	n	mean	SD	n	mean	SD	n	mean	SD	n	mean	SD	n	mean	SD
Amphibian	40	9.13E-02	6.72E-02	40	9.37E-02	7.62E-02	40	3.44E-01	3.82E-01	-			11	6.07E-01	3.68E-01	9	2.11E-01	1.77E-01
Bird	3	3.17E-02	1.59E-02	3	3.35E-02	8.69E-03	3	3.03E-01	8.25E-02	5	1.12E-02	4.78E-03	3	3.71E-02	2.50E-02	3	1.20E-01	1.25E-01
Invertebrate (all)	10	7.14E-02	6.48E-02	10	2.80E-02	2.26E-02	10	2.09E-01	2.59E-01	-			2	8.82E-02		1	1.07E+00	
Invertebrate (detritivore)	1	1.10E+00		1	8.78E-02		1	9.27E-01		-			-			-		
Invertebrate (herbivore)	9	7.14E-02	6.15E-02	9	2.80E-02	2.14E-02	9	1.29E-01	1.05E-01	-			2	8.82E-02		1	1.07E+00	
Mammal (all)	23	1.98E+00		23	7.71E-02	4.89E-02	23	5.01E-01	3.60E-01	-			-			-		
Mammal (herbivore)	4	7.54E-01		4	1.17E-01	6.53E-02	4	3.10E-01	9.04E-02	-			-			-		
Mammal (omnivore)	15	8.91E-01		15	7.54E-02	3.43E-02	15	5.10E-01	2.40E-01	-			-			-		
Mammal (carnivore)	4	1.98E+00		4	2.51E-02	0.00E+00	4	7.78E-01	1.09E+00	-			-			-		
Reptile	20	8.19E-02	1.64E-02	20	1.58E-01	1.20E-01	20	2.77E-01	1.45E-01	8	1.34E-02	8.28E-03	6	5.42E-01	6.11E-01	5	7.74E-01	
Grass & herb	25	2.57E-01	4.26E-01	25	3.22E-02	4.64E-02	25	3.60E-01	2.45E-01	5	4.25E-02	3.55E-02	3	3.25E-01	3.33E-01	3	8.27E-02	2.54E-03
Shrub	10	3.25E-02	3.24E-02	7	1.32E-01	1.46E-01	10	1.89E-01	1.51E-01	-			-			-		
Lichen & moss	2	2.18E-01	2.33E-02	2	1.94E-01	3.83E-02	2	6.10E-01	5.77E-01	-			-			-		
Fungus	17	2.42E+00		17	1.36E+00	1.60E+00	17	5.81E-01	3.76E-01	-			-			-		

Values highlighted in grey are those for which all CRs were LOD values so the maximum CR value was reported; - indicates no CR data available.

Table 8.11. Concentration ratios for temperate coastal sand dune biota[1]

Biota group	Am			Cs			K			Pu			Sr			Tc		
	n	mean	SD	n	mean	SD	n	mean	SD	n	mean	SD	n	mean	SD	n	mean	SD
Amphibian	40	9.13E-02	6.72E-02	40	9.37E-02	7.62E-02	40	3.44E-01	3.82E-01	-			11	6.07E-01	3.68E-01	9	2.11E-01	1.77E-01
Bird	3	3.17E-02	1.59E-02	3	3.35E-02	8.69E-03	3	3.03E-01	8.25E-02	5	1.12E-02	4.78E-03	3	3.71E-02	2.50E-02	3	1.20E-01	1.25E-01
Invertebrate (all)	82	6.69E-02	8.78E-02	82	2.39E-02	2.94E-02	10	2.09E-01	2.59E-01	144	4.06E-02	5.55E-02	2	8.82E-02		1	1.07E+00	
Invertebrate (detritivore)	25	6.93E-02	8.35E-02	25	2.32E-02	3.35E-02	1	9.27E-01	0.00E+00	48	4.18E-02	5.56E-02	-			-		
Invertebrate (herbivore)	17	1.35E-01	1.40E-01	17	4.56E-02	3.63E-02	9	1.29E-01	1.05E-01	16	1.20E-01	8.61E-02	2	8.82E-02		1	1.07E+00	
Invertebrate (omnivore)	19	2.88E-02	2.48E-02	19	1.40E-02	1.75E-02	-			38	1.84E-02	2.00E-02	-			-		
Invertebrate (carnivore)	21	5.07E-02	5.86E-02	21	1.77E-02	1.67E-02	-			42	2.90E-02	3.28E-02	-			-		
Mammal (all)[2]	19	4.25E-04	2.60E-04	61	3.76E-02	4.47E-02	23	5.01E-01	3.60E-01	38	9.33E-04	6.69E-04	-			-		
Mammal (herbivore)[2]	6	2.56E-04	1.64E-04	16	3.36E-02	5.53E-02	4	3.10E-01	9.04E-02	12	8.10E-04	5.36E-04	-			-		
Mammal (omnivore)[2]	9	3.73E-04	9.89E-05	33	3.78E-02	3.96E-02	15	5.10E-01	2.40E-01	18	9.24E-04	7.28E-04	-			-		
Mammal (carnivore)[2]	4	7.97E-04	2.90E-04	12	4.34E-02	4.45E-02	4	7.78E-01	1.09E+00	8	1.14E-03	7.45E-04	-			-		
Reptile	20	8.19E-02	1.64E-02	20	1.58E-01	1.20E-01	20	2.77E-01	1.45E-01	8	1.34E-02	8.28E-03	6	5.42E-01	6.11E-01	5	7.74E-01	
Grass & herb	25	2.57E-01	4.26E-01	25	3.22E-02	4.64E-02	25	3.60E-01	2.45E-01	5	4.25E-02	3.55E-02	3	3.25E-01	3.33E-01	3	8.27E-02	2.54E-03
Shrub	10	3.25E-02	3.24E-02	7	1.32E-01	1.46E-01	10	1.89E-01	1.51E-01	-			-			-		
Lichen & moss	2	2.18E-01	2.33E-02	2	1.94E-01	3.83E-02	2	6.10E-01	5.77E-01	-			-			-		
Fungus	17	2.42E+00		17	1.36E+00	1.60E+00	17	5.81E-01	3.76E-01	-			-			-		

[1] CRs derived from data for biota at the Drigg and Sellafield coastal sand dunes in West Cumbria, UK; [2] All Drigg small mammal Am results were obtained using gamma spectrometry and were all high LOD values so have been excluded from the calculation of Am CRs; Values highlighted in grey are those for which all CRs were LOD values so the maximum CR value was reported; - indicates no CR data available.

(This page is left blank intentionally)

CHAPTER 9 – CONCLUSIONS

In each of the main chapters of this thesis (Chapters 4 – 8), detailed discussion has been presented and conclusions drawn. Therefore, this final chapter reviews the main outcomes and findings of this thesis, drawing on the information presented in Chapters 4 – 8, to conclude this 6-year research project on the radioecology of temperate coastal sand dunes.

9.1. Measurement

- Sampling was undertaken at the Drigg coastal sand dunes between February 2005 and October 2007 (see Chapter 3)
- A total of 617 samples of environmental media (n = 468) and biota (n = 149) were collected, focussing on three main sampling transects, and radiometric analyses performed (see Chapter 3).
- *In situ* dose rate measurements were recorded for most sampling locations (see Chapter 8)

9.1.1. Environmental media

- The media samples collected were soil, pool water (from temporary ponds within the humid dune slacks) and total deposition samples (see Chapter 3).
- Activity concentrations have been reported for a suite of natural radionuclides (^{40}K, ^{208}Tl, ^{214}Bi and ^{228}Ac) and anthropogenic (^{60}Co, ^{90}Sr, ^{99}Tc, ^{137}Cs, ^{238}Pu, $^{239+240}$Pu and ^{241}Am) radionuclides in sand dune soil (see Chapters 4 – 6 and 8).
- Total deposition and pool water samples have been analysed by gamma spectrometry and ^{137}Cs activity concentrations reported (see Chapter 8).
- Soil property determinations (bulk density, carbonate content, organic matter content, organic carbon content, pH and soil moisture) have been performed on sand dune soils and used in analysis of activity concentration depth profiles and of the spatial variation in radionuclide activity concentrations (see Chapter 8).

- Selected soil samples have been used to determine stable element concentrations for four cations of marine origin: Ca, K, Mg and Na (see Chapter 8).

9.1.2. Biota

- Biota samples collected included species of amphibian, bird, invertebrate, mammal, reptile, plant (including lichen and moss) and fungus (see Chapter 3).

- For biota samples, activity concentrations for ^{40}K, ^{90}Sr, ^{99}Tc, ^{137}Cs, ^{238}Pu, $^{239+240}Pu$ and ^{241}Am have been reported (see Chapters 4 – 7).

9.1.3. Treatment of LODs

- Recognising the importance of appropriate treatment (depending on the purpose) of limit of detection (LOD) values when data sets used to derive summary statistics include values below the LOD, two different methods have been used to handle these data. For the purposes of model comparison, where one of the aims was to ensure conservatism in model predictions, the LOD values were used (see Chapters 4 and 5). For the purposes of CR data derivation, where the purpose was to derive realistic CR estimates, a non-parametric statistical technique (Kaplan-Meier) from medical research (survival analysis) applications was used. The latter technique has gained acceptance in other fields of environmental science but does not appear to have been used in previous radioecological applications (see Chapters 7 & 8).

9.1.4. Processes influencing radionuclide activity concentrations in soil

- Activity concentrations of anthropogenic radionuclides in the coastal sand dunes of West Cumbria were low compared with neighbouring saltmarsh areas (see Chapter 8).

- The sea-to-land transfer process resulted in elevated actinide activity concentrations in sand dune soil. These activity concentrations decreased with increasing distance from mean high water (MHW) (see Chapters 4, 5, 6 and 8).

- Isotopic ratios indicated that the primary source of actinide contamination at the Drigg coastal sand dunes was discharges from the Sellafield site (see Chapter 8).

- In general, radionuclide depth profiles in sand dune soil demonstrated a reduction in activity concentration with depth (see Chapter 8).

- The soil profile at foredune locations close to MHW may show an increase in activity concentrations depth due to burial of historical deposition by less contaminated sand from the backshore zone of the beach (see Chapter 8).

- Changes in soil radionuclide activity concentration data with increasing distance from MHW suggest that saltation, in addition to sea-to-land transfer, is an important process influencing measured activity concentrations in sand dune soil, especially for ^{137}Cs at locations within 200 m of the beach (see Chapter 8).

- On a localised scale, blowout formation and splash drift may also be important processes in determining depth profiles in sand dune soil. Therefore, blowouts and locations at the base of sand dunes should be avoided when sampling soils to determine activity concentrations for environmental assessment purposes (see Chapter 8).

- Dune slack soils may have lower ^{137}Cs activity concentrations than soils in other sand dune habitats, plausibly due to higher organic matter accumulation leading to leaching of humic acids and a resultant reduction in soil pH. At lower pH, the mobility of ^{137}Cs increases and this may result in increased leaching rates in dune slack soils (see Chapter 8).

9.1.5. Activity concentrations in biota

- Significant differences in ^{137}Cs and ^{241}Am activity concentrations in different taxa of sand dune biota have been observed and these were related primarily to differences in trophic level (see Chapter 6)

- Differences between biota at the same trophic level can be explained by differences in feeding ecology and physiology (see Chapter 6).

9.2 Modelling

- Three publically available biota dose assessment models (ERICA, R&D128/SP1a and RESRAD-BIOTA) have been used to estimate absorbed radiation dose rates for biota at the Drigg coastal sand dunes (see Chapters 4 and 5).

- In undertaking this model intercomparison, the value of taking an 'informed user' approach was highlighted and the 'informed user' concept refined (see Chapter 5).

- The dose rates arising from anthropogenic radionuclide contamination at these coastal sand dunes are unlikely to have significant impacts on non-human biota based on the results of environmental radiation protection modelling presented in Chapters 4 & 5.

- Dose rates from natural radionuclides at the Drigg coastal sand dunes exceed those from anthropogenic radionuclides (see Chapter 4).

- Whilst the three models were suitable for undertaking an environmental radiation protection assessment for the Drigg coastal sand dunes, scope for refinement was identified, specifically with regard to radionuclide transfer (see Chapters 4 & 5).

- Although RESRAD-BIOTA includes kinetic-allometric functionality, there are few data available to parameterise this for specific organisms and the biota activity concentration predictions obtained are dependent on the radionuclide transfer assumptions for the prey organisms. Therefore, this kinetic-allometric approach is of little use for undertaking assessments if transfer data are available for the biota groups to be modelled (see Chapter 5).

- Am, Cs and Pu concentration ratios (CRs) for small mammals in temperate coastal sand dunes were found to be two orders of magnitude lower than at other terrestrial sites (see Chapters 4 – 6). This may be due to low bioavailability of these radionuclides in sand dune soils (see Chapter 8) and is an area for further research.

- Few CR data were available for predicting transfer to reptile species so there were limited data against which the Drigg coastal sand dune reptile data could be compared. Therefore, a comprehensive literature review was undertaken to develop a database of CR values for reptiles (see Chapter 7).

- A comparison of sand dune reptile CRs with CR data for reptiles at other terrestrial sites showed that the sand dune CRs for Am and Pu were 1 – 2 orders of magnitude higher (see Chapter 7). The reason for this is unclear and is an area for further research.

- Given the differences in CRs for temperate coastal sand dune biota compared with biota from other terrestrial sites, a specific CR database has been developed for use in future assessments of the impacts of ionising radiation on temperate coastal sand dune biota (see Chapter 8).

9.3. Communication of research findings

- In addition to communication of the research findings through this thesis, three papers have been published in international peer-reviewed journals (see Chapters 4 – 6).

- A fourth paper (to communicate the material presented in Chapter 7) has been submitted to an international peer-reviewed journal.

- Research results have also been communicated at national conferences (including Meetings of the Coordinating Group on Environmental Radioactivity (COGER)), international conferences (including the International Conference on Radioecology and Environmental Radioactivity) and international scientific meetings held at the International Atomic Energy Agency (IAEA) under the Environmental Modelling for Radiation Safety (EMRAS) programme.

The research presented in this thesis has advanced international scientific understanding of temperate coastal sand dune radioecology, reptile radioecology and radioecological modelling. Given that the global community appears to be on the verge of a nuclear renaissance, there will be an increasing requirement for personnel with expertise in environmental radioactivity, environmental radioprotection and radioecology to inform decision-making on the management of the environmental consequences of new nuclear build, the decommissioning of old reactors and the disposal of legacy wastes. It is hoped that this thesis and its associated outputs will be a valuable addition to the body of literature that will be used to inform future management decisions in the nuclear sector.

(This page is left blank intentionally)

REFERENCES

Aarkrog, A., 1989. Environmental radiation and radioactive releases. In 22nd Annual Meeting of the European Society for Radiation Biology (pp. 619-631). Brussels, Belgium: Taylor & Francis Ltd.

Adlys, G.A., Ryhanen, V., Kanapeckas, P., Adlys, G., Raila, S., Valinevicius, A., 2008. Formation of the nuclear energy ring in the Baltic Sea region. ECT - 2008: Proceedings of the 3rd International Conference on Electrical and Control Technologies, 172-175.

Adolph, E.F., 1949. Quantitative relations in the physiological constitutions of mammals. Science, 109(2841), 579-585.

Akbar, Z., Gorman, M.L., 1993. The effect of supplementary feeding upon the sizes of the home ranges of woodmice *Apodemus sylvaticus* living on a system of maritime sand dunes. Journal of Zoology, 231, 233-237.

Albrecht, J., Abalos, M., Rice, T.M., 2007. Heavy metal levels in ribbon snakes (*Thamnophis sauritus*) and anuran larvae from the Mobile-Tensaw River Delta, Alabama, USA. Archives of Environmental Contamination and Toxicology, 53(4), 647-654.

Alexakhin, R.M., Prister, B.S., 2008. Radioecology as a branch of natural science: some thoughts on the interesting past, intricate and vital present and future prospects. Radiatsionnaia biologiia radioecologiia, 48(6), 645-653.

Alexakhin, R.M., 2009. Radiation accidents - contribution to radioecological science and ecological lessons. Radioprotection, 44(5), 821-824.

Allen, S.E. (ed) (1989). Chemical analysis of ecological materials. Oxford: Blackwell Scientific Publishing.

Allisy-Roberts, P.J., 2005. Radiation quantities and units - understanding the sievert. Journal of Radiological Protection, 25(1), 97-100.

Allott, R., Copplestone, D., 2008. Paper 13-04: Update on Habitats assessments for England and Wales., in: Thirteenth Meeting of the National Dose Assessment Working Group, Barnwood, Gloucester. Available from: http://www.ndawg.org/documents/Paper13-04.pdf.

Allott, R., Copplestone, D., Merrill, P., Oliver, S., 2009. Habitats assessments for radioactive substances. Environment Agency, Bristol.

Ambrosi, P., 2009. Radiation protection and environmental standards. Metrologia, 46(2), S99-S111.

Anan, Y., Kunito, T., Watanabe, I., Sakai, H., Tanabe, S., 2001. Trace element accumulation in hawksbill turtles (*Eretmochelys imbricata*) and green turtles (*Chelonia mydas*) from Yaeyama Islands, Japan. Environmental Toxicology and Chemistry, 20(12), 2802-2814.

Andersson, P., Garnier-Laplace, J., Beresford, N.A., Copplestone, D., Howard, B.J., Howe, P., Oughton, D., Whitehouse, P., 2009. Protection of the environment from ionising radiation in a regulatory context (PROTECT): proposed numerical benchmark values. Journal of Environmental Radioactivity, 100(12), 1100-1108.

Andreani, G., Santoro, M., Cottignoli, S., Fabbri, M., Carpene, E., Isani, G., 2008. Metal distribution and metallothionein in loggerhead (*Caretta caretta*) and green (*Chelonia mydas*) sea turtles. Science of the Total Environment, 390(1), 287-294.

Andreotti, B., Fourriere, A., Ould-Kaddour, F., Murray, B., Claudin, P., 2009. Giant aeolian dune size determined by the average depth of the atmospheric boundary layer. Nature, 457(7233), 1120-1123.

Antweiler, R.C., Taylor, H.E., 2008. Evaluation of statistical treatments of left-censored environmental data using coincident uncensored data sets: I. Summary statistics. Environmental Science & Technology, 42(10), 3732-3738.

Aoyama, M., Hirose, K., Igarashi, Y., 2006. Re-construction and updating our understanding on the global weapons tests Cs-137 fallout. Journal of Environmental Monitoring, 8(4), 431-438.

Arens, S.M., Vankaampeters, H.M.E., Vanboxel, J.H., 1995. Air-flow over foredunes and implications for sand transport. Earth Surface Processes and Landforms, 20(4), 315-332.

Arnold, N., 2004. A field guide to the reptiles and amphibians of Britain and Europe. Collins, London.

Asher, W.E., Farley, P.J., 1995. Phase-doppler anemometer measurement of bubble concentrations in laboratory-simulated breaking waves. J. Geophys. Res.-Oceans, 100(C4), 7045-7056.

Avery, R.A., White, A.S., Martin, M.H., Hopkin, S.P., 1983. Concentrations of heavy metals in common lizards (*Lacerta vivipara*) and their food and environment. Amphibia-Reptilia, 4(4), 205-213.

Avery, S.V., 1996. Fate of caesium in the environment: Distribution between the abiotic and biotic components of aquatic and terrestrial ecosystems. Journal of Environmental Radioactivity, 30(2), 139-171.

Baccarelli, A., Pfeiffer, R., Consonni, D., Pesatori, A.C., Bonzini, M., Patterson, D.G., Bertazzi, P.A., Landi, M.T., 2005. Handling of dioxin measurement data in the presence of non-detectable values: Overview of available methods and their application in the Seveso chloracne study. Chemosphere, 60(7), 898-906.

Bagnold, R., 1954. The physics of blown sand and desert dunes. 2nd edn. Methuen & Co. Ltd., London.

Bagshaw, C., Brisbin, I.L., 1985. Long-term declines in radiocesium of two sympatric snake populations. Journal of Applied Ecology, 22(2), 407-413.

Barnett, C.L., Beresford, N.A., Self, P.L., Howard, B.J., Frankland, J.C., Fulker, M.J., Dodd, B.A., Marriott, J.V.R., 1999. Radiocaesium activity concentrations in the fruit-bodies of macrofungi in Great Britain and an assessment of dietary intake habits. Science of the Total Environment, 231(1), 67-83.

Barnett, C.L., Gaschak, S., Beresford, N.A., Howard, B.J., 2009. Radionuclide activity concentrations in two species of reptiles from the Chernobyl exclusion zone. Radioprotection, 44(5), 537-542.

Batlle, J.V.I., Balonov, M., Beaugelin-Seiller, K., Beresford, N.A., Brown, J., Cheng, J.J., Copplestone, D., Doi, M., Filistovic, V., Golikov, V., Horyna, J., Hosseini, A., Howard, B.J., Jones, S.R., Kamboj, S., Kryshev, A., Nedveckaite, T., Olyslaegers, G., Prohl, G., Sazykina, T., Ulanovsky, A., Lynch, S.V., Yankovich, T., Yu, C., 2007. Inter-comparison of absorbed dose rates for non-human biota. Radiation and Environmental Biophysics, 46, 349-373.

Bell, J.N.B., Shaw, G., 2005. Ecological lessons from the Chernobyl accident. Environment International, 31(6), 771-777.

Belot, Y., Caput, C., Gauthier, D., 1982. Transfer of americium from sea-water to atmosphere by bubble bursting. Atmospheric Environment, 16(6), 1463-1466.

Bennett, A.F., Dawson, W.R., 1976. Metabolism. In C. Gans & F.H. Pough, Biology of the Reptilia (pp. 127-223). New York: Academic Press.

Bennett, B.G., 2002. Worldwide dispersion and deposition of radionuclides produced in atmospheric tests. Health Physics, 82(5), 644-655.

Beresford, N.A., Mayes, R.W., Cooke, A.I., Barnett, C.L., Howard, B.J., Lamb, C.S., Naylor, G.P.L., 2000. The importance of source-dependent bioavailability in determining the transfer of ingested radionuclides to ruminant-derived food products. Environmental Science & Technology, 34(21), 4455-4462.

Beresford, N.A., Broadley, M.R., Howard, B.J., Barnett, C.L., White, P.J., 2004. Estimating radionuclide transfer to wild species - data requirements and availability for terrestrial ecosystems. Journal of Radiological Protection, 24(4A), A89-A103.

Beresford, N.A., Howard, B.J., 2005. Application of the FASSET framework at case study sites. Deliverable 9 of the ERICA project (FI6R-CT-2004-508847). Centre for Ecology & Hydrology, Lancaster. Available from: http://www.ceh.ac.uk/PROTECT/ERICAdeliverables.html.

Beresford, N.A., Wright, S.M., Barnett, C.L., Wood, M.D., Gaschak, S., Arkhipov, A., Sazykina, T.G., Howard, B.J., 2005. Predicting radionuclide transfer to wild animals: an application of a proposed environmental impact assessment framework to the Chernobyl exclusion zone. Radiation and Environmental Biophysics, 44(3), 161-168.

Beresford, N.A., Appleton, J.D., Barnett, C.L., Bescoby, M.W., Breward, N., Jones, D.G., MacKenzie, A.C., Scheib, C., Thørring, H., Wood, M.D., 2007a. Assessment of naturally occurring radionuclides in England and Wales. Environment Agency, Bristol. Available from: http://www.ceh.ac.uk/protect/pages/documents/AssessmentofnaturallyoccuringradionuclidesinEnglandandWales.pdf.

Beresford, N.A., Brown, J., Copplestone, D., Garnier-Laplace, J., Howard, B.J., Larsson, C.-M., Oughton, D., Pröhl, G., Zinger, I., 2007b. D-ERICA: An Integrated approach to the assessment and management of environmental risks from ionising radiation. Deliverable of the ERICA project (FI6R-CT-2004-508847). Swedish Radiation Protection Authority, Stockholm. Available from: http://www.ceh.ac.uk/PROTECT/ERICAdeliverables.html.

Beresford, N.A., Howard, B.J., Mayes, R.W., Lamb, C.S., 2007c. The transfer of radionuclides from saltmarsh vegetation to sheep tissues and milk. Journal of Environmental Radioactivity, 98, 36-49.

Beresford, N.A., Brown, J., Copplestone, D., Garnier-Laplace, J., Howard, B.J., Larsson, C.-M., Oughton, D., Pröhl, G., Zinger, I., 2007d. D-ERICA: An Integrated approach to the assessment and management of environmental risks from ionising radiation. Deliverable of the ERICA project (FI6R-CT-2004-508847). Swedish Radiation Protection Authority, Stockholm. Available from: http://www.ceh.ac.uk/PROTECT/ERICAdeliverables.html.

Beresford, N.A., Barnett, C.L., Wright, S.M., Howard, B.J., Crout, N.M.J., 2007e. Factors contributing to radiocaesium variability in upland sheep flocks in west Cumbria (United Kingdom). Journal of Environmental Radioactivity, 98(1-2), 50-68.

Beresford, N.A., Howard, B.J., Barnett, C.L., 2007f. Application of ERICA Integrated Approach at case study sites. Deliverable 10 of the ERICA project (FI6R-CT-2004-508847). Centre for Ecology & Hydrology, Lancaster. Available from: http://www.ceh.ac.uk/PROTECT/ERICAdeliverables.html.

Beresford, N.A., Barnett, C., Brown, J., Cheng, J., Copplestone, D., Filistovic, V., Hosseini, A., Howard, B., Jones, S., Kamboj, S., Kryshev, A., Nedveckaite, T., Olyslaegers, G., Saxén, R., Sazykina, T., Vives i Batlle, J., Vives-Lynch, S., Yankovich, T., Yu, C., 2008a. Inter-comparison of models to estimate radionuclide activity

concentrations in non-human biota. Radiation and Environmental Biophysics, 47(4), 491-514.

Beresford, N.A., Hosseini, A., Brown, J.E., Cailes, C., Copplestone, D., Barnett, C.L., Beaugelin-Seiller, K., 2008b. Evaluation of approaches for protecting the environment from ionising radiation in a regulatory context. Deliverable 4. Report for the PROTECT project. EC Contract Number:036425 (FI6R). Centre for Ecology and Hydrology, Lancaster. Available from: http://www.ceh.ac.uk/PROTECT/outputs/.

Beresford, N.A., Balonov, M., Beaugelin-Seiller, K., Brown, J., Copplestone, D., Hingston, J.L., Horyna, J., Hosseini, A., Howard, B.J., Kamboj, S., Nedveckaite, T., Olyslaegers, G., Sazykina, T., Batlle, J.V.I., Yankovich, T.L., Yu, C., 2008c. An international comparison of models and approaches for the estimation of the radiological exposure of non-human biota. Applied Radiation and Isotopes, 66(11), 1745-1749.

Beresford, N.A., Barnett, C.L., Howard, B.J., Scott, W.A., Brown, J.E., Copplestone, D., 2008d. Derivation of transfer parameters for use within the ERICA Tool and the default concentration ratios for terrestrial biota. Journal of Environmental Radioactivity, 99(9), 1393-1407.

Beresford, N.A., Barnett, C.L., Jones, D.G., Wood, M.D., Appleton, J.D., Breward, N., Copplestone, D., 2008e. Background exposure rates of terrestrial wildlife in England and Wales. Journal of Environmental Radioactivity, 99(9), 1430-1439.

Beresford, N.A., Barnett, C.L., Beaugelin-Seiller, K., Brown, J.E., Cheng, J.-J., Copplestone, D., Gaschak, S., Hingston, J.L., Horyna, J., Hosseini, A., Howard, B.J., Kamboj, S., Kryshev, A., Nedveckaite, T., Olyslaegers, G., Sazykina, T., Smith, J.T., Telleria, D., Vives i Batlle, J., Yankovich, T.L., Heling, R., Wood, M.D., Yu, C., 2008f. Findings and recommendations from an international comparison of models and approaches for the estimation of radiological exposure to non-human biota, in: International Conference on Radioecology and Environmental Radioactivity, Bergen.

Beresford, N.A., Barnett, C.L., Beaugelin-Seiller, K., Brown, J.E., Cheng, J.-J., Copplestone, D., Gaschak, S., Hingston, J.L., Horyna, J., Hosseini, A., Howard, B.J., Kamboj, S., Kryshev, A., Nedveckaite, T., Olyslaegers, G., Sazykina, T., Smith, J.T., Telleria, D., Vives i Batlle, J., Yankovich, T.L., Heling, R., Wood, M.D., Yu, C., 2009. Findings and recommendations from an international comparison of models and approaches for the estimation of radiological exposure to non-human biota. Radioprotection, 44(5), 565-570.

Bergan, T.D., 2002. Radioactive fallout in Norway from atmospheric nuclear weapons tests. Journal of Environmental Radioactivity, 60(1-2), 189-208.

Bihari, A., Dezso, Z., 2008. Examination of the effect of particle size on the radionuclide content of soils. Journal of Environmental Radioactivity, 99(7), 1083-1089.

Bjarnason, J.B., Fox, J.W., 1994. Hemorrhagic metallproteinases from snake-venoms. Pharmacology & Therapeutics, 62(3), 325-372.

Blanchard, D.C., 1955. Electrified droplets from the bursting of bubbles at an air-sea water interface. Nature, 175(4451), 334-336.

Blanchard, D.C., Woodcock, A.H., 1957. Bubble formation and modification in the sea and its meteorological significance. Tellus, 9(2), 145-158.

Blanchard, D.C., 1982. Transfer of americium from sea-water to atmosphere by bubble bursiting. Atmospheric Environment, 16(9), 2273-2273.

BNG Sellafield Ltd, 2007. Sellafield integrated waste strategy (Baseline version 1). British Nuclear Group Sellafield Ltd. Available from: http://sellafieldsites.co.uk/UserFiles/File/publications/stakeholder%20consultations/GEN-1792A%20Sellafield%20IWS%20Baseline%20Document%20May%202007.pdf.

Bradford, M.A., Jones, T.H., Bardgett, R.D., Black, H.I.J., Boag, B., Bonkowski, M., Cook, R., Eggers, T., Gange, A.C., Grayston, S.J., Kandeler, E., McCaig, A.E., Newington, J.E., Prosser, J.I., Setala, H., Staddon, P.L., Tordoff, G.M., Tscherko, D., Lawton, J.H., 2002. Impacts of soil faunal community composition on model grassland ecosystems. Science, 298(5593), 615-618.

Brady, D., Pratt, G.C., 2007. Volatile organic compound emissions from dry mill fuel ethanol production. Journal of the Air & Waste Management Association, 57(9), 1091-1102.

Branford, D., Nelis, P.M., 1996. Study of airborne radioactivity near to the high water mark at Drigg Point. Journal of Environmental Radioactivity, 31(3), 237-251.

Brechignac, F., Doi, M., 2009. Challenging the current strategy of radiological protection of the environment: arguments for an ecosystem approach. Journal of Environmental Radioactivity, 100(12), 1125-1134.

Brisbin, I.L., Staton, M.A., Pinder, J.E., Geiger, R.A., 1974a. Radiocesium concentrations of snakes from contaminated and non-contaminated habitats of AEC Savannah River Plant. Copeia, (2), 501-506.

Brisbin, I.L., Beyers, R.J., Dapson, R.W., Geiger, R.A., Gentry, J.B., Gibbons, J.W., Smith, M.H., Woods, S.K., 1974b. Patterns of radiocesium in sediments of a stream channel contaminated by Production Reactor Effluents. Health Physics, 27(1), 19-27.

Brisbin, I.L., 1989. Radiocesium levels in a population of American alligators: a model for the study of environmental contaminants in free-living crocodilians. In Proceedings of the 8th working meeting of the Crocodile Specialist Group of the Species

Survival Committee of the International Union for Conservation of Nature and Natural resources. Quito, Ecuador: IUCN.

Brown, J.E., Alfonso, B., Avila, R., Beresford, N.A., Copplestone, D., Prohl, G., Ulanovsky, A., 2008. The ERICA Tool. Journal of Environmental Radioactivity, 99(9), 1371-1383.

Brown, S.L., 1988. The effect of earthworms on caesium in the soil, with special reference to *Allolobophora longa*. In Imperial College of Science and Technology (pp. 109). University of London.

Brownless, G.P., 2007. Issues around radiological protection of the environment and its integration with protection of humans: promoting debate on the way forward. Journal of Radiological Protection, 27(4), 391-404.

Bryan, S., Hill, R., McDonald, P., Wilson, R.C., 2006. Sea to land transfer of anthropogenic radionuclides to the North Wales coast. Westlakes Scientific Consulting, Cumbria.

Bryan, S.E., McDonald, P., Hill, R., Wilson, R.C., 2008. Sea to land transfer of anthropogenic radionuclides to the North Wales coast, Part I: External gamma radiation and radionuclide concentrations in intertidal sediments, soil and air. Journal of Environmental Radioactivity, 99(1), 7-19.

Bunn, M., Wier, A., 2006. Terrorist nuclear weapon construction: How difficult? Annals of the American Academy of Political and Social Science, 607, 133-149.

Burger, J., 1992. Trace-element levels in pine snake hatchlings: tissue and temporal differences. Archives of Environmental Contamination and Toxicology, 22(2), 209-213.

Burger, J., 1994. Heavy metals in avian eggshells: another excretion method. Journal of Toxicology and Environmental Health, 41(2), 207-220.

Burger, J., Gibbons, J.W., 1998. Trace elements in egg contents and egg shells of slider turtles (*Trachemys scripta*) from the Savannah River Site. Archives of Environmental Contamination and Toxicology, 34(4), 382-386.

Burger, J., Gochfeld, M., Rooney, A.A., Orlando, E.F., Woodward, A.R., Guillette, L.J., 2000. Metals and metalloids in tissues of American alligators in three Florida lakes. Archives of Environmental Contamination and Toxicology, 38(4), 501-508.

Burger, J., 2002. Metals in tissues of diamondback terrapin from New Jersey. Environmental Monitoring and Assessment, 77(3), 255-263.

Burger, J., Campbell, K.R., Campbell, T.S., Shukla, T., Jeitner, C., Gochfeld, M., 2005. Use of skin and blood as nonlethal indicators of heavy metal contamination in northern

water snakes (*Nerodia sipedon*). Archives of Environmental Contamination and Toxicology, 49(2), 232-238.

Burger, J., Campbell, K.R., Murray, S., Campbell, T.S., Gaines, K.F., Jeitner, C., Shukla, T., Burke, S., Gochfeld, M., 2007. Metal levels in blood, muscle and liver of water snakes (*Nerodia spp.*) from New Jersey, Tennessee and South Carolina. Science of the Total Environment, 373(2-3), 556-563.

Burton, M., 1976. Guide to the mammals of Britain and Europe. Treasure Press, London.

Calle, P.P., Rivas, J., Munoz, M., Thorbjarnarson, J., Dierenfeld, E.S., Holmstrom, W., Braselton, W.E., Karesh, W.B., 1994. Health assessment of free-ranging anacondas (*Eunectes murinus*) in Venezuela. Journal of Zoo and Wildlife Medicine, 25(1), 53-62.

Cambray, R.S., Eakins, J.D., 1980. Studies of Environmental Radioactivity in Cumbria: Part 1. Concentrations of Plutonium and Caesium-137 in Environmental Samples from West Cumbria and a Possible Maritime Effect. United Kingdom Atomic Energy Authority Harwell Laboratory.

Cambray, R.S., Eakins, J.D., 1982. Pu, Am-241 and Cs-137 in soil in West Cumbria and a maritime effect. Nature, 300(5887), 46-48.

Cambray, R.S., Playford, K., Lewis, G.N.J., Carpenter, R.C., Gibson, J., 1989. Radiactive fallout in air and rain: results to the end of 1987. United Kingdom Atomic Energy Authority Harwell Laboratory.

Campbell, K.R., Ford, C.J., Levine, D.A., 1998. Mercury distribution in Poplar Creek, Oak Ridge, Tennessee, USA. Environmental Toxicology and Chemistry, 17(7), 1191-1198.

Campbell, K.R., Campbell, T.S., 2000. Lizard contaminant data for ecological risk assessment. Reviews of Environmental Contamination and Toxicology, Vol 165, 165, 39-116.

Campbell, K.R., Campbell, T.S., 2001. The accumulation and effects of environmental contaminants on snakes: A review. Environmental Monitoring and Assessment, 70(3), 253-301.

Campbell, K.R., Campbell, T.S., 2002. A logical starting point for developing priorities for lizard and snake ecotoxicology: A review of available data. Environmental Toxicology and Chemistry, 21(5), 894-898.

Campbell, K.R., Campbell, T.S., Burger, J., 2005. Heavy metal concentrations in northern water snakes (*Nerodia sipedon*) from East Fork Poplar Creek and the Little River, East Tennessee, USA. Archives of Environmental Contamination and Toxicology, 49(2), 239-248.

Carrington, R., 2003. The Effect of Chronic Radiation Dose on Individuals and Populations of Small Mammals in the Chernobyl Exclusion Zone. In School of Biological Sciences (pp. 79). Liverpool: University of Liverpool.

Carter, R.W.G., Hesp, P.A., Nordstrom, K.F., 1990. Erosional landforms in coastal dunes. In K.F. Nordstrom, N.P. Psuty & R.W.G. Carter, Coastal dunes: form and process (pp. 217-250). Chichester: John Wiley & Sons Ltd.

Catt, R., 1998. AA Book of Britain's Countryside. Midsummer Books Ltd, London.

Chamberlain, A.C., Dunster, H.J., 1958. Deposition of radioactivity in north-west England from the accident at Windscale. Nature, 182(4636), 629-630.

Chamberlain, A.C., 1996. Emissions from Sellafield and activities in soil. Science of the Total Environment, 177, 259-280.

Cherkashov, Y.M., Novosel'skii, O.Y., Checherov, K.P., 2006. Investigation of the development of the 1986 accident at the Chernobyl nuclear power plant. Atomic Energy, 100(4), 235-248.

Cherry, J., 1982. Sea cliff erosion at Drigg, Cumbria: evidence of prehistoric habitation Transactions of the Cumberland and Westmorland Antiquarian and Archaeological Society, 83, 1-6.

Churchfield, S., 1984. Dietary separation in three species of shrew inhabiting water-cress beds. Journal of Zoology, 204(OCT), 211-228.

Clark, D.R., Bickham, J.W., Baker, D.L., Cowman, D.F., 2000. Environmental contaminants in Texas, USA, wetland reptiles: Evaluation using blood samples. Environmental Toxicology and Chemistry, 19(9), 2259-2265.

Clark, M.J., Smith, F.B., 1988. Wet and dry deposition of Chernobyl releases. Nature, 332(6161), 245-249.

Coja, T., Zehetner, K., Bruckner, A., Watzinger, A., Meyer, E., 2008. Efficacy and side effects of five sampling methods for soil earthworms (Annelida, Lumbricidae). Ecotoxicology and Environmental Safety, 71(2), 552-565.

Cooper, A., McCann, T., Ballard, E., 2005. The effects of livestock grazing and recreation on Irish machair grassland vegetation. Plant Ecology, 181(2), 255-267.

Copplestone, D., 1996. The food chain transfer of radionuclides through semi-natural habitats. In School of Biological Sciences (pp. 369). Liverpool: University of Liverpool.

Copplestone, D., Johnson, M.S., Jones, S.R., Toal, M.E., Jackson, D., 1999. Radionuclide behaviour and transport in a coniferous woodland ecosystem: vegetation,

invertebrates and wood mice, Apodemus sylvaticus. Science of the Total Environment, 239(1-3), 95-109.

Copplestone, D., Bielby, S., Jones, S.R., Patton, D., Daniel, P., Gize, I., 2001a. Impact assessment of ionising radiation on wildlife. R&D Publication 128. Environment Agency, Bristol. Available from: http://www.coger.org.uk/RD128/R&DPublication128updated2002.PDF.

Copplestone, D., Johnson, M.S., Jones, S.R., 2001b. Behaviour and transport of radionuclides in soil and vegetation of a sand dune ecosystem. Journal of Environmental Radioactivity, 55(1), 93-108.

Copplestone, D., Wood, M.D., Bielby, S., Jones, S.R., Vives i Batlle, J., Beresford, N.A., 2003. Habitat regulations for Stage 3 assessments: radioactive substances authorisations. R&D Technical Report P3-101/Sp1a. Environment Agency, Bristol. Available from: http://www.ceh.ac.uk/PROTECT/pages/documents/Habitatsregulationsforstage3assessment.pdf.

Copplestone, D., Koulikov, A.O., Semenov, D.V., 2005a. Radionuclide concentrations in reptiles on some polluted territories of Russia. Russian Journal of Herpetology, 12(2), 83-86.

Copplestone, D., Wood, M.D., Merrill, P.C., Allott, R., Jones, S.R., Vives, J., Beresford, N.A., Zinger, I., 2005b. Impact Assessment of Ionising Radiation on Wildlife: meeting the requirements of the EU birds and habitat directives. Radioprotection, 40, S893-S898.

Copplestone, D., Wood, M.D., Tyler, A.N., Crook, P., 2007. UKSHS Report No. 4: Soil property and radiometric analytical methods. Environment Agency, Bristol. Available from: http://publications.environment-agency.gov.uk/pdf/SCHO0607BMSX-e-e.pdf?lang=_e.

Copplestone, D., Hingston, J., Real, A., 2008. The development and purpose of the FREDERICA radiation effects database. Journal of Environmental Radioactivity, 99(9), 1456-1463.

Copplestone, D., Andersson, P., Beresford, N., Brown, J., Dysvik, S., Garnier-Laplace, J., Hingston, J., Howard, B., Oughton, D., Whitehouse, P., 2009. Protection of the environment from ionising radiation in a regulatory context (PROTECT): Review of current regulatory approaches to both chemicals and radioactive substances. Radioprotection, 44(5), 881-886.

Costa-Font, J., Rudisill, C., Mossialos, E., 2008. Attitudes as an expression of knowledge and "political anchoring": The case of nuclear power in the United Kingdom. Risk Analysis, 28(5), 1273-1287.

Cowles, H.C., 1899. The ecological relations of the vegetation on the sand dunes of Lake Michigan. Botanical Gazette, 27, 95-117.

Cuadrado, M., Diaz-Paniagua, C., Quevedo, M.A., Aguilar, J.M., Prescott, I.M., 2002. Hematology and clinical chemistry in dystocic and healthy post-reproductive female chameleons. Journal of Wildlife Diseases, 38(2), 395-401.

Cuadrado, M., Molina-Prescott, I., Flores, L., 2003. Comparison between tail and jugular venipuncture techniques for blood sample collection in common chameleons (*Chamaeleo chamaeleon*). Veterinary Journal, 166(1), 93-97.

Dallinger, R., Wieser, W., 1977. Flow of copper through a terrestrial food-chain. 1. Copper and nutrition in Isopods. Oecologia, 30(3), 253-264.

Davenport, J., Wrench, J., 1990. Metal levels in a leatherback turtle. Marine Pollution Bulletin, 21(1), 40-41.

Davic, R.D., 2003. Linking keystone species and functional groups: A new operational definition of the keystone species concept - Response. Conservation Ecology, 7(1).

Davis, P.A., Avadhanula, M.R., Cancio, D., Carboneras, P., Coughtrey, P., Johansson, G., Little, R.H., Smith, G.M., Watkins, B.M., 1999. BIOMOVS II: An international test of the performance of environmental transfer models. Journal of Environmental Radioactivity, 42(2-3), 117-130.

Day, R.D., Christopher, S.J., Becker, P.R., Whitaker, D.W., 2005. Monitoring mercury in the loggerhead sea turtle, *Caretta caretta*. Environmental Science & Technology, 39(2), 437-446.

Dekker, L.W., Jungerius, P.D., 1990. Water repellency in the dunes, with special reference to the Netherlands. Catena Supplement, 18, 163-171.

Delany, M.F., Bell, J.U., Sundlof, S.F., 1988. Concentrations of contaminants in muscle of the American alligator in Florida. Journal of Wildlife Diseases, 24(1), 62-66.

Delbaere, B.C.W., 1998. Facts and figures on european biodiversity: state and trends 1998 - 1999. European Centre for Nature Conservation, Tilburg.

Dieckmann, A., 2003. The Surface Area Of An Ellipsoid, University of Bonn. Available from: http://pi.physik.uni-bonn.de/~dieckman/SurfaceEllipsoid/SurfEll.html.

Doody, P., 1989. Conservation and development of the coastal dunes in Great Britain. In F. van der Meulen, P.D. Jungerius & J.H. Visser, Perspectives in coastal dune management (pp. 53-67). The Hague: SPB Academic Publishing.

DTI, 2007. The future of nuclear power: the role of nuclear poser in a low carbon UK economy (consultation document). Department of Trade and Industry, London.

Duerden, S.L., Yearsley, R.A., Bennett, D.G., 2003. Drigg 2002 post-closure safety case review plan: assessment of the post-closure safety case for the Drigg low-level radioactive waste disposal site. Environment Agency, Reading.

Dunster, H.J., Howells, H., Templeton, W.L., 2007. District surveys following the windscale incident, October 1957. Journal of Radiological Protection, 27(3), 217-230.

Eakins, J.D., Pattenden, N.J., Cambray, R.S., Lally, A.E., Playford, K., 1981. Studies of environmental radioactiivity in Cumbria Part 2: Radionuclide deposits in soil in the coastal region of Cumbria. HMSO, London.

Eakins, J.D., Lally, A.E., Burton, P.J., Kilworth, D.R., Pratley, F.A., 1982. Studies of environmental radioactivity in Cumbria: Part 5. The magnitude and mechanism of enrichment of sea spray with actinides in West Cumbria. United Kingdom Atomic Energy Authority Harwell Laboratory.

Eakins, J.D., Morgan, A., Baston, G.M.N., Pratley, F.A., Yarnold, L.P., Burton, P.J., 1988. Studies of environmental radioactivity in Cumbria: Part 8. Plutonium and americium in the intertidal sands of north-west England. United Kingdom Atomic Energy Authority Harwell Laboratory.

EC, 1979. EC Birds Directive 79/409/EEC.

EC, 1992. EC Habitats Directive 92/43/EEC.

Edge, J.A., Walls, S.J., 1997. MOX fuel manufacture at Sellafield. Proceedings of the Topical Meeting on Criticality Safety Challenges in the Next Decade, 203-208.

Eisberg, R., Resnick, R., 1985. Quantumn physics of atoms, molecules, solids, nuclei and particles. 2nd edn. John Wiley & Sons, New York.

Eisenhauer, N., Straube, D., Scheu, S., 2008. Efficiency of two widespread non-destructive extraction methods under dry soil conditions for different ecological earthworm groups. European Journal of Soil Biology, 44(1), 141-145.

Emptage, M., Kelly, M., 1990. Gamma dose rates in the Esk Estuary. University of Lancaster, Lancaster.

Ethering, J.R., 1967. Studies of nutrient cycling and productivity in oligotrophic ecosystems. 1. Soil potassium and wind-blown sea-spray in a South Wales dune grassland. Journal of Ecology, 55(3), 743-752.

Ferns, P.N., 1976. Diet of a *Microtus agrestis* population in South West Britain. Oikos, 27(3), 506-511.

Fowler, J., Cohen, L., 1990. Practical statistics for field biology. John Wiley & Sons Ltd, Chichester.

Fox, J.R., Mortimer, R.J.G., Lear, G., Lloyd, J.R., Beadle, I., Morris, K., 2006. The biogeochemical behaviour of U(VI) in the simulated near-field of a low-level radioactive waste repository. Applied Geochemistry, 21(9), 1539-1550.

Franzellitti, S., Locatelli, C., Gerosa, G., Vallini, C., Fabbri, E., 2004. Heavy metals in tissues of loggerhead turtles (*Caretta caretta*) from the northwestern Adriatic Sea. Comparative Biochemistry and Physiology C-Toxicology & Pharmacology, 138(2), 187-194.

Frias-Espericueta, M.G., Osuna-Lopez, J.I., Ruiz-Telles, A., Quintero-Alvarez, J.M., Lopez-Lopez, G., Izaguirre-Fierro, G., Voltolina, D., 2006. Heavy metals in the tissues of the sea turtle *Lepidochelys olivacea* from a nesting site of the northwest coast of Mexico. Bulletin of Environmental Contamination and Toxicology, 77(2), 179-185.

Fry, F.A., 1983. Airborne radionuclides in the vicinity of a coastal nuclear-fuel reprocessing plant. Journal of Aerosol Science, 14(3), 452-455.

Fry, F.A., 1987. The Chernobyl reactor accident - the impact on the United Kingdom. British Journal of Radiology, 60(720), 1147-1158.

Gallie, P.R., 1996. Forty years of operation of Calder Hall. Atw-Internationale Zeitschrift Fur Kernenergie, 41(11), 719-723.

Garcia-Fernandez, A.J., Gomez-Ramirez, P., Martinez-Lopez, E., Hernandez-Garcia, A., Maria-Mojica, P., Romero, D., Jimenez, P., Castillo, J.J., Bellido, J.J., 2009. Heavy metals in tissues from loggerhead turtles (*Caretta caretta*) from the southwestern Mediterranean (Spain). Ecotoxicol Environ Saf, 72(2), 557-563.

Garcia, F., Ortega, A., Domingo, J.L., Corbella, J., 2001. Accumulation of metals in autopsy tissues of subjects living in Tarragona County, Spain. Journal of Environmental Science and Health Part a-Toxic/Hazardous Substances & Environmental Engineering, 36(9), 1767-1786.

Gardner, R., McLaren, S., 1999. Infiltration and moisture movement in coastal sand dunes, Studland, Dorset, UK: Preliminary results. Journal of Coastal Research, 15(4), 936-949.

Gardner, S.C., Fitzgerald, S.L., Vargas, B.A., Rodriguez, L.M., 2006. Heavy metal accumulation in four species of sea turtles from the Baja California Peninsula, Mexico. Biometals, 19(1), 91-99.

Garland, J.A., Wakeford, R., 2007. Atmospheric emissions from the Windscale accident of October 1957. Atmospheric Environment, 41(18), 3904-3920.

Garnier-Laplace, J., Della-Vedova, C., Gilbin, R., Copplestone, D., Hingston, J., Ciffroy, P., 2006. First derivation of predicted-no-effect values for freshwater and terrestrial ecosystems exposed to radioactive substances. Environmental Science & Technology, 40(20), 6498-6505.

Garnier-Laplace, J., Copplestone, D., Gilbin, R., Alonzo, F., Ciffroy, P., Gilek, M., Aguero, A., Bjork, M., Oughton, D.H., Jaworska, A., Larsson, C.M., Hingston, J.L., 2008. Issues and practices in the use of effects data from FREDERICA in the ERICA Integrated Approach. Journal of Environmental Radioactivity, 99(9), 1474-1483.

Garten, C.T., Gentry, J.B., Pinder, J.E., Sharitz, R.R., Smith, M.H., 1975. Radiocesium dynamics in a contaminated floodplain ecosystem in the southeastern United States, in: International Symposium on radiological impacts of releases from nuclear facilities into aquatic environments, IAEA, Otaniemi, Finland. International Atomic Energy Agency.

Geiger, R.A., Winsor, T.F., 1977. Pu-239 contamination in snakes inhabiting Rocky Flats Plant site. Health Physics, 33(2), 145-148.

Gent, A.H., Gibson, S.D., 1998. Herpetofauna Workers' Manual. Joint Nature Conservation Committee, Peterborough.

George, S., 2006. United Kingdom Windspeed: Measurement, Climatology, Predictability and Link to Tropical Atlantic Variability. In Department of Space and Climate Physics (pp. 164). London: University of London.

Gibbons, J.W., Scott, D.E., Ryan, T.J., Buhlmann, K.A., Tuberville, T.D., Metts, B.S., Greene, J.L., Mills, T., Leiden, Y., Poppy, S., Winne, C.T., 2000. The global decline of reptiles, Deja Vu amphibians. Bioscience, 50(8), 653-666.

Gilbertson, D.D., Schwenninger, J.L., Kemp, R.A., Rhodes, E.J., 1999. Sand-drift and soil formation along an exposed North Atlantic coastline: 14,000 years of diverse geomorphological, climatic and human impacts. Journal of Archaeological Science, 26(4), 439-469.

Giles, M.S., Twining, J.R., Williams, A.R., Jeffree, R.A., Domel, R.U., 1990. Final report to the Technical Assessment Group for the Maralinga Rehabilitation Project. Study No. 2. (Radioecology) in Technical Assessment Group Study Program Reports Volume 1. Department of Primary Industries and Energy, Canberra.

Gjelsvik, R., Brown, J., 2009. Po-210 and other radionuclides in terrestrial and freshwater environments. Nordisk kernesikkerhedsforskning, Roskilde.

Gochfeld, M., Burger, J., 1987. Factors affecting the distribution of heavy metals - age effects and the metal concentration patterns in common terns, *Sterna hirundo*. Biological Trace Element Research, 12, 389-399.

Godley, B.J., Gaywood, M.J., Law, R.J., McCarthy, C.J., McKenzie, C., Patterson, I.A.P., Penrose, R.S., Reid, R.J., Ross, H.M., 1998. Patterns of marine turtle mortality in British waters (1992-1996) with reference to tissue contaminant levels. Journal of the Marine Biological Association of the United Kingdom, 78(3), 973-984.

Godley, B.J., Thompson, D.R., Furness, R.W., 1999. Do heavy metal concentrations pose a threat to marine turtles from the Mediterranean sea? Marine Pollution Bulletin, 38(6), 497-502.

Gomez-Ros, J.M., Prohl, G., Taranenko, V., 2004. Estimation of internal and external exposures of terrestrial reference organisms to natural radionuclides in the environment. Journal of Radiological Protection, 24(4A), A79-A88.

Gordon, A.N., Pople, A.R., Ng, J., 1998. Trace metal concentrations in livers and kidneys of sea turtles from south-eastern Queensland, Australia. Marine and Freshwater Research, 49(5), 409-414.

Gorham, E., 1958. Soluble salts in dune sands from Blakeney Point in Norfolk. Journal of Ecology, 46(2), 373-379.

Gorham, E., 1961. The chemical-composition of some waters from dune slacks at Sandscale, North Lancashire. Journal of Ecology, 49(1), 79-82.

Gorman, M.L., Ahmad, Z.A.B., 1993. A comparative study of the ecology of woodmice *Apodemus sylvaticus* in two contrasting habitats - decicuous woodland and maritime sand dunes. Journal of Zoology, 229, 385-396.

Gottdenker, N.L., Jacobson, E.R., 1995. Effect of venipuncture on hematologic and clinical biochemical values in desert tortoises (*Gopherus agassizii*). American Journal of Veterinary Research, 56(1), 19-21.

Gray, J., Jones, S.R., Smith, A.D., 1995. Discharges to the environment from the Sellafield site, 1951-1992. Journal of Radiological Protection, 15(2), 99-131.

Greaver, T.L., Sternberg, L.S.L., 2007. Fluctuating deposition of ocean water drives plant function on coastal sand dunes. Global Change Biology, 13(1), 216-223.

Greenberg, M., 2009. Energy sources, public policy, and public preferences: Analysis of US national and site-specific data. Energy Policy, 37(8), 3242-3249.

Grootjans, A.P., Adema, E.B., Bekker, R.M., Lammerts, E.J., 2004. Why young coastal dune slacks sustain high biodiversity. In M.L. Martinez & N.P. Psuty, Coastal dunes: ecology and conservation (pp. 85-101). Berlin: Springer-Verlag.

Gualtieri, C., Mihailovic, D.T., 2008. Fluid mechanics of environmental interfaces. Taylor & Francis, London.

Guirlet, E., Das, K., Girondot, M., 2008. Maternal transfer of trace elements in leatherback turtles (*Dermochelys coriacea*) of French Guiana. Aquatic Toxicology, 88(4), 267-276.

Ham, G.J., 2009. The determination of Polonium-210 in urine following the Litvinenko incident. Radioprotection, 44(5), 41-46.

HeatonJones, T.G., Homer, B.L., HeatonJones, D.L., Sundlof, S.F., 1997. Mercury distribution in American alligators (*Alligator mississippiensis*) in Florida. Journal of Zoo and Wildlife Medicine, 28(1), 62-70.

Hedges, S.B., Thomas, R., 2001. At the lower size limit in amniote vertebrates: A new diminutive lizard from the West Indies. Caribbean Journal of Science, 37(3-4), 168-173.

Heiri, O., Lotter, A.F., Lemcke, G., 2001. Loss on ignition as a method for estimating organic and carbonate content in sediments: reproducibility and comparability of results. Journal of Paleolimnology, 25(1), 101-110.

Helsel, D.R., 1990. Less than obvious: statistical treatment of data below the detection limit. Environmental Science & Technology, 24(12), 1766-1774.

Helsel, D.R., 2005a. More than obvious: Better methods for interpreting nondetect data. Environmental Science & Technology, 39(20), 419A-423A.

Helsel, D.R., 2005b. Nondetects and data analysis: statistics for censored environmental data. John Wiley & Sons Inc., New Jersey.

Helsel, D.R., 2006. Fabricating data: How substituting values for nondetects can ruin results, and what can be done about it. Chemosphere, 65(11), 2434-2439.

Helsenfeld, P., Jungerius, P.D., Klijn, J.A., 2004. European coastal dunes: ecological values, threats, opportunities and policy development. In M.L. Martinez & N.P. Psuty, Coastal dunes: ecology and conservation (pp. 335-351). Berlin: Springer-Verlag.

Herczeg, G., Herrero, A., Saarikivi, J., Gonda, A., Jantti, M., Merila, J., 2008. Experimental support for the cost-benefit model of lizard thermoregulation: the effects of predation risk and food supply. Oecologia, 155(1), 1-10.

Higley, K.A., Domotor, S.L., Antonio, E.J., 2003. A kinetic-allometric approach to predicting tissue radionuclide concentrations for biota. Journal of Environmental Radioactivity, 66(1-2), 61-74.

Higley, K.A., Alexakhin, R.M., 2004. Dose limits for man do not adequately protect the ecosystem. Radiation Protection Dosimetry, 109(3), 257-264.

Hill, R., Bryan, S.E., McDonald, P., Wilson, R.C., Smith, A.D., 2008. Sea to land transfer of anthropogenic radionuclides to the North Wales coast, Part II: Aerial modelling and radiological assessment. Journal of Environmental Radioactivity, 99(1), 20-34.

Hinton, T.G., Whicker, F.W., 1985. The kinetics of radium and strontium in pond sliders *Pseudemys scripta* as a function of two temperature extremes. Savannah River Ecology Laboratory, Aiken.

Hinton, T.G., Scott, D.E., 1990. Radiecological techniques for herpetology, with an emphasis on freshwater turtles. In J.W. Gibbons, Life history and ecology of the slider turtle (pp. 267-287). Washington: Smithsonian Institute Press.

HMIP, 1995. Routine measurement of gamma ray air kerma rate in the environment. Technical Guidance Note (Monitoring) M5. Her Majesty's Inspectorate of Pollution, London.

Hofmann, H., 1995. Wild animals of Britain and Europe. Harper Collins Publishers, London.

Hoglund, J., Saterberg, L., 1989. Sexual selection in common toads - Correlates with age and body size. Journal of Evolutionary Biology, 2(5), 367-372.

Hopkins, W.A., Mendonca, M.T., Rowe, C.L., Congdon, J.D., 1998. Elevated trace element concentrations in southern toads, *Bufo terrestris*, exposed to coal combustion waste. Archives of Environmental Contamination and Toxicology, 35(2), 325-329.

Hopkins, W.A., Rowe, C.L., Congdon, J.D., 1999. Elevated trace element concentrations and standard metabolic rate in banded water snakes (*Nerodia fasciata*) exposed to coal combustion wastes. Environmental Toxicology and Chemistry, 18(6), 1258-1263.

Hopkins, W.A., 2000. Reptile toxicology: Challenges and opportunities on the last frontier in vertebrate ecotoxicology. Environmental Toxicology and Chemistry, 19(10), 2391-2393.

Hopkins, W.A., Roe, J.H., Snodgrass, J.W., Jackson, B.P., Kling, D.E., Rowe, C.L., Congdon, J.D., 2001. Nondestructive indices of trace element exposure in squamate reptiles. Environmental Pollution, 115(1), 1-7.

Hornung, R.W., Reed, L.D., 1990. Estimation of average concentration in the presence of nondetectable values. Applied Occupational and Environmental Hygiene, 5, 46-51.

Hosseini, A., Thorring, H., Brown, J.E., Saxen, R., Ilus, E., 2008. Transfer of radionuclides in aquatic ecosystems - Default concentration ratios for aquatic biota in the Erica Tool. Journal of Environmental Radioactivity, 99(9), 1408-1429.

Howard, P.J.A., 1965. Carbon-organic matter in various soil types. Oikos, 15(2), 229-236.

Howard, P.J.A., Howard, D.M., 1990. Use of organic-carbon and loss-on-ignition to estimate soil organic-matter in different soil types and horizons. Biology and Fertility of Soils, 9(4), 306-310.

Howarth, J.M., Eggleton, A.E.J., 1988. Studies of environmental radioactivity in Cumbria. Part 12: Modelling of the sea to land transfer of radionuclides and an assessment of the radiological consequences. HMSO.

HSE & EA, 2009. Generic design assessment progress report: Reporting period 1 April 2009 - 30 June 2009. Health and Safety Executive. Available from: http://www.hse.gov.uk/newreactors/reports/gda-q2-09.pdf.

IAEA, 1992. Effects of ionising radiation on plants and animals at levels implied by current radiation protection standards. International Atomic Energy Agency, Vienna.

IAEA, 2004. Sediment Distribution Coefficients and Concentration Factors for Biota in the Marine Environment International Atomic Energy Agency, Vienna.

IAEA, 2008. IAEA Generic Review for UK HSE of New Reactor Designs against IAEA Safety Standards: Review summary report. Health & Safety Executive. Available from: http://www.hse.gov.uk/newreactors/reports/iaeasummary.pdf.

IAEA, in prep. Handbook of parameter values for the prediction of radionuclide transfer to wildlife. International Atomic Energy Agency, Vienna.

IAEA, in press. Handbook of parameter values for the prediction of radionuclide transfer in terrestrial and freshwater environments. International Atomic Energy Agency, Vienna.

ICRP, 1977. Recommendations of the International Commission on Radiological Protection, Publication 26.

ICRP, 1983. Radionuclide transfromations - energy and intensity of transmissions, Publication 38. Annals of the ICRP, 11-13(1-2).

ICRP, 2007a. Recommendations of the International Commission on Radiological Protection, Publication 103. Annals of the ICRP, 37(2-4), 133-135.

ICRP, 2007b. Recommendations of the International Commission on Radiological Protection, Publication 103. Annals of the ICRP, 37(2-4).

ICRU, 1994. Gamma-ray spectrometry in the environment. ICRU Report 53. Bethesda.

Iljenko, A.I., 1970. Regularities of ^{90}Sr and ^{137}Cs in different links of food chains in zoocenosis. Journal of General Biology, 31(6), 698-709.

Irwin, L., Irwin, K., 2006. Global threats affecting the status of reptile populations. In S.C. Gardner & E. Oberdorster, Toxicology of reptiles (pp. 9-34). Boca Raton: Taylor & Francis Group.

Jackson, D., Lambers, B., Gray, J., 2000. Radiation doses to members of the public near to Sellafield, Cumbria, from liquid discharges 1952-98. Journal of Radiological Protection, 20(2), 139-167.

Jagoe, C.H., Arnold-Hill, B., Yanochko, G.M., Winger, P.V., Brisbin, I.L., 1998. Mercury in alligators (*Alligator mississippiensis*) in the southeastern United States. Science of the Total Environment, 213(1-3), 255-262.

Jefferies, D.J., French, M.C., 1976. Mercury, cadmium, zinc, copper and organochlorine insecticide levels in small mammals trapped in a wheat field. Environmental Pollution, 10(3), 175-182.

Jeffree, R.A., 1991. An experimental-study of ^{226}Ra and ^{45}Ca accumulation from the aquatic medium by fresh-water turtles (Family - Chelidae) under varying Ca and Mg water concentrations. Hydrobiologia, 218(3), 205-231.

Jeffree, R.A., Markich, S.J., Twining, J.R., 2001. Element concentrations in the flesh and osteoderms of estuarine crocodiles (*Crocodylus porosus*) from the Alligator Rivers Region, northern Australia: Biotic and geographic effects. Archives of Environmental Contamination and Toxicology, 40(2), 236-245.

Jeffree, R.A., Markich, S.J., Tucker, A.D., 2005. Patterns of metal accumulation in osteoderms of the Australian freshwater crocodile, *Crocodylus johnstoni*. Science of the Total Environment, 336(1-3), 71-80.

Jehle, R., Arntzen, J.W., 2000. Post-breeding migrations of newts (*Triturus cristatus* and *T. marmoratus*) with contrasting ecological requirements. Journal of Zoology, 251, 297-306.

JNCC, 2006. Drigg Coast Natura 2000 data form - Version 2.1. Joint Nature Conservation Committee. Available from: http://www.jncc.gov.uk/protectedsites/sacselection/n2kforms/UK0013031.pdf.

Johnson, C.A., Kitchen, K.P., Nelson, N., 2007. A study of the movement of radioactive material released during the Windscale fire in October 1957 using ERA40 data. Atmospheric Environment, 41(18), 3921-3937.

Jones, D.E., Holladay, S.D., 2006. Excretion of three heavy metals in the shed skin of exposed corn snakes (*Elaphe guttata*). Ecotoxicology and Environmental Safety, 64(2), 221-225.

Jones, M.L.M., Reynolds, B., Brittain, S.A., Norris, D.A., Rhind, P.M., Jones, R.E., 2006. Complex hydrological controls on wet dune slacks: The importance of local variability. Science of the Total Environment, 372(1), 266-277.

Jones, M.L.M., Sowerby, A., Williams, D.L., Jones, R.E., 2008. Factors controlling soil development in sand dunes: evidence from a coastal dune soil chronosequence. Plant and Soil, 307(1-2), 219-234.

Jones, S.R., Patton, D., Copplestone, D., Norris, S., O'Sullivan, P., 2003. Generic performance assessment for a deep repository for low and intermediate level waste in the UK--a case study in assessing radiological impacts on the natural environment. Journal of Environmental Radioactivity, 66(1-2), 89-119.

Jungerius, P.D., Vandermeulen, F., 1988. Erosion processes in a dune landscape along the Dutch coast. Catena, 15(3-4), 217-228.

Jungerius, P.D., 2008. Dune development and management, geomorphological and soil processes, responses to sea level rise and climate change. Baltica, 21(1-2), 13-23.

Kaplan, E.L., Meier, P., 1958. Nonparametric-estimation from incomplete observations. Journal of the American Statistical Association, 53(282), 457-481.

Karangelos, D.J., Anagnostakis, M.J., Hinis, E.P., Simopoulos, S.E., Zunic, Z.S., 2004. Determination of depleted uranium in environmental samples by gamma-spectroscopic techniques. Journal of Environmental Radioactivity, 76(3), 295-310.

Kashiwagi, T., Oda, T., 2008. Energy policy & New National Energy Strategy in Japan. Proceedings ICT 07: 26th International Conference on Thermoelectrics, 428-433.

Kaska, Y., Celik, A., Bag, H., Aureggi, M., Ozel, K., Elci, A., Kaska, A., Elca, L., 2004. Heavy metal monitoring in stranded sea turtles along the Mediterranean coast of Turkey. Fresenius Environmental Bulletin, 13(8), 769-776.

Kaur, S., 1988. Lead in the scales of cobras and wall lizards from rural and urban areas of Punjab, India. Science of the Total Environment, 77(2-3), 289-290.

Kautz, G., Zimmer, M., Topp, W., 2002. Does *Porcellio scaber* (Isopoda : Oniscidea) gain from coprophagy? Soil Biology & Biochemistry, 34(9), 1253-1259.

Kaygusuz, K., 2008. The Future of Nuclear Power and Renewable Energy Sources in the European Union. Energy Sources Part B-Economics Planning and Policy, 3(4), 348-361.

Kelly, M., Emptage, M., 1991. Distribution of radioactivity in the Esk estuary and its relationship to sedimentary processes. University of Lancaster, Lancaster.

Kelly, M., Emptage, M., Mudge, S., Bradshaw, K., Hamiltontaylor, J., 1991. The relationship between sediment and plutonium budgets in a small macrotidal estuary - Esk Estuary, Cumbria, UK. Journal of Environmental Radioactivity, 13(1), 55-74.

Kelly, M., Thorne, M., 2003. Radionuclides handbook. R&D Technical Report P3-101/Sp1b. Environment Agency, Bristol.

Kershaw, P.J., Woodhead, D.S., Lovett, M.B., Leonard, K.S., 1995. Plutonium from European reprocessing operations: its behaviour in the marine-environment. Applied Radiation and Isotopes, 46(11), 1121-1134.

Key, C.R., 1971. Delayed consequences of exposure to ionizing radiation: pathology studies at atomic bomb casualty commission, Hiroshima and Nagasaki, 1945-1970 - background and historical perspectives. Human Pathology, 2(4), 471-&.

Khammes, N., Aulagnier, S., 2007. Diet of the wood mouse, *Apodemus sylvaticus* in three biotopes of Kabylie of Djurdjura (Algeria). Folia Zoologica, 56(3), 243-252.

Kirchner, G., Peterson, S.R., Bergstrom, U., Bushell, S., Davis, P., Filistovic, V., Hinton, T.G., Krajewski, P., Riesen, T., de Haag, P.U., 1999. Effect of user interpretation on uncertainty estimates: examples from the air-to-milk transfer of radiocesium. Journal of Environmental Radioactivity, 42(2-3), 177-190.

Kirchner, G., Steiner, M., 2008. Uncertainties in radioecological assessment models - Their nature and approaches to reduce them. Applied Radiation and Isotopes, 66(11), 1750-1753.

Kohler, H.R., 2002. Localization of metals in cells of saprophagous soil arthropods (Isopoda, Diplopoda, Collembola). Microscopy Research and Technique, 56(5), 393-401.

Kondoh, K., 2009. The challenge of climate change and energy policies for building a sustainable society in Japan. Organization and Environment, 22(1), 52-74.

Krumbein, W., Slack, H., 1956. The relative efficiency of beach sampling methods. Tech. Memo. Beach Eros. Bd U.S., 90, 1-34.

Lam, J.C.W., Tanabe, S., Chan, S.K.F., Yuen, E.K.W., Lam, M.H.W., Lam, P.K.S., 2004. Trace element residues in tissues of green turtles (*Chelonia mydas*) from South China Waters. Mar. Pollut. Bull., 48(1-2), 174-182.

Lam, J.C.W., Tanabe, S., Chan, S.K.F., Lam, M.H.W., Martin, M., Lam, P.K.S., 2006. Levels of trace elements in green turtle eggs collected from Hong Kong: Evidence of risks due to selenium and nickel. Environmental Pollution, 144(3), 790-801.

Lance, V.A., Cort, T., Masuoka, J., Lawson, R., Saltman, P., 1995. Unusually high zinc concentrations in snake plasma, with observations on plasma zinc concentrations in lizards, turtles and alligators. Journal of Zoology, 235, 577-585.

LaportaFerreira, I.L., Santos, S.M.A., Santoro, M.L., Saiki, M., Vasconcelos, M.B.A., 1997. Comparative analyses of inorganic elements in venoms from three

subspecies of *Crotalus durissus* from Brazil. Journal of Natural Toxins, 6(1), 103-110.

Larsson, C.-M., 2008. An overview of the ERICA Integrated Approach to the assessment and management of environmental risks from ionising contaminants. Journal of Environmental Radioactivity, 99(9), 1364-1370.

Larsson, C.M., 2004. The FASSET framework for assessment of environmental impact of ionising radiation in European ecosystems - an overview. Journal of Radiological Protection, 24(4A), A1-A12.

Lee, Y.E., Jung, Y.B., 2008. Challenges of nuclear power for sustainable role in Korean energy policy. Energy Conversion and Management, 49(7), 1951-1959.

Leonard, A., Delpoux, M., Meyer, R., Decat, G., Leonard, E.D., 1985. Effect of an enhanced natural radioactivity on mammal fertility. Science of the Total Environment, 45(Oct), 535-542.

Liat, L.B., 1999. Reptiles as potential biocontrol agents of pest rodents in plantation areas. Biological Control in the Tropics, 82-84.

Linsley, G., Torres, C., 2004. The International Biosphere Modelling and Assessment Programme (BIOMASS): an overview. Journal of Environmental Radioactivity, 74(1-3), 279-283.

Livens, F.R., Baxter, M.S., 1988a. Particle-size and radionuclide levels in some West Cumbrian soils. Science of the Total Environment, 70, 1-17.

Livens, F.R., Baxter, M.S., 1988b. Chemical associations of artificial radionuclides in Cumbrian soils. Journal of Environmental Radioactivity, 7(1), 75-86.

Livingston, H.D., Povinec, P.P., 2000. Anthropogenic marine radioactivity. Ocean and Coastal Management, 43(8-9), 689-712.

Loehle, C., 1987. Errors of construction, evaluation and inference - A classification of sources of error in ecological models. Ecological Modelling, 36(3-4), 297-314.

Lovett, M.B., Boggis, S.J., Blowers, P., 1990. The determination of alpha-emitting nuclides of plutonium, americium and curium in environmental materials: Part 1. Sea Water Aquatic Environmental Protection: Analytical Methods. No. 7. Ministry of Agriculture, Fisheries and Food.

Lowe, V.P.W., 1991. Radionuclides and the birds at Ravenglass. Environmental Pollution, 70(1), 1-26.

Lutgens, F.K., Tarbuck, E.J., 1989. Essentials of geology. 3rd edn. Merrill Publishing Company, Columbus.

MA, 2003. Ecosystems and human well-being: a framework for assessment. Millenium Ecosystem Assessment. World Resources Institute, Washington DC.

MA, 2005. Millenium Ecosystem Assessment: findings of the condition and trend working group. Island Press, Washington D.C.

Macalister, T., 2009. 10-yr old Sellafield plant may be closed. In The Guardian. London.

Machart, P., Hofmann, W., Turk, R., Steger, F., 2007. Ecological half-life Of Cs-137 in lichens in an alpine region. Journal of Environmental Radioactivity, 97, 70-75.

Maffucci, F., Caurant, F., Bustamante, P., Bentivegna, F., 2005. Trace element (Cd, Cu, Hg, Se, Zn) accumulation and tissue distribution in loggerhead turtles (*Caretta caretta*) from the Western Mediterranean Sea (southern Italy). Chemosphere, 58(5), 535-542.

Maklyuk, Y.A., Maksimenko, A.M., Gashchak, S.P., Bondarkov, M.D., Chizhevskii, I.V., 2007. Long-term dynamics of radioactive ^{90}Sr and ^{137}Cs contamination of small mammals in the Chernobyl zone. Russian Journal of Ecology, 38(3), 181-189.

Malcolm, R., Soulsby, C., 2001. Hydrogeochemistry of groundwater in coastal wetlands: implications for coastal conservation in Scotland. Science of the Total Environment, 265(1-3), 269-280.

Mann, R.M., Serra, E.A., Soares, A., 2006. Assimilation of cadmium in a European lacertid lizard: is trophic transfer important? Environmental Toxicology and Chemistry, 25(12), 3199-3203.

Mann, R.M., Sanchez-Hernandez, J.C., Serra, E.A., Soares, A., 2007. Bioaccumulation of Cd by a European lacertid lizard after chronic exposure to Cd-contaminated food. Chemosphere, 68(8), 1525-1534.

Markich, S.J., Jeffree, R.A., Harch, B.D., 2002. Catchment-specific element signatures in estuarine crocodiles (*Crocodylus porosus*) from the Alligator Rivers Region, northern Australia. Science of the Total Environment, 287(1-2), 83-95.

Martin, P., Hancock, G.J., Johnston, A., Murray, A.S., 1998. Natural-series radionuclides in traditional North Australian aboriginal foods. Journal of Environmental Radioactivity, 40(1), 37-58.

Martinez, M.L., Maun, M.A., Psuty, N.P., 2004a. The fragility and conservation of the world's coastal dunes: geomorphological, ecological and socioeconomic perspectives. In M.L. Martinez & N.P. Psuty, Coastal dunes: ecology and conservation (pp. 355-369). Berlin: Springer-Verlag.

Martinez, M.L., Psuty, N.P., Lubke, R.A., 2004b. A perspective on coastal dunes. In M.L. Martinez & N.P. Psuty, Coastal dunes: ecology and conservation (pp. 3-10). Berlin: Springer-Verlag.

Martjushov, V.Z., Krivoluzky, D.A., Smirnov, E.G., Tarasov, O.V., 1999. Ecological consequences of radioactive pollution on South Ural. In D.A. Krivoluzky, Bioindication of radioactive pollution (pp. 49-85). Moscow: Nauka.

Mayall, A., 2005. A fine balance: multifunctional decision making and the regulation of Tc-99 discharges at Sellafield, in: Change and continuity in radiation protection, Cardiff, UK (pp. 291-297). Society for Radiological Protection.

McDonald, P., Bryan, S.E., Hunt, G.J., Baldwin, M., Parker, T.G., 2005. Field and model investigations of external gamma dose rates along the Cumbrian coast, NW England. Journal of Radiological Protection, 25(1), 67-82.

McHugh, J.O., Smith, B.D., Hunt, G.J., Thomas, R.E.G., 1986. The MAFF dry cloth collector programme for monitoring airborne radioactivity. Journal of the Society for Radiological Protection, 6(2), 63-67.

McKay, W.A., Walker, M.I., 1990. Plutonium and americium behaviour in Cumbrian near-shore waters. Journal of Environmental Radioactivity, 12(3), 267-283.

McKay, W.A., Pattenden, N.J., 1990. The transfer of radionuclides from sea to land via the air: a review. Journal of Environmental Radioactivity, 12(1), 49-77.

Meggitt, G., 2006. Fission, critical mass and safety - A historical review. Journal of Radiological Protection, 26(2), 141-159.

Meyersschone, L., Walton, B.T., 1990. Comparison of two freshwater turtle species as monitors of environmental contamination. Oak Ridge National Laboratory, Oak Ridge, Tennessee.

Meyersschone, L., Shugart, L.R., Beauchamp, J.J., Walton, B.T., 1993. Comparison of two freshwater turtle species as monitors of radionuclide and chemical contamination: DNA-damage and residue analysis. Environmental Toxicology and Chemistry, 12(8), 1487-1496.

Meyersschone, L., Walton, B.T., 1994. Turtles as monitors of chemical contaminants in the environment. Reviews of Environmental Contamination and Toxicology, 135, 93-153.

Miaud, C., Sanuy, D., 2005. Terrestrial habitat preferences of the natterjack toad during and after the breeding season in a landscape of intensive agricultural activity. Amphibia-Reptilia, 26(3), 359-366.

Michel, H., Barci-Funel, G., Barci, V., Ardisson, G., 2002. Input contribution and vertical migration of plutonium, americium and cesium in lake sediments (Belham Tarn, Cumbria, UK). Radiochimica Acta, 90(9-11), 747-752.

Millard, S.P., Deverel, S.J., 1988. Nonparametric statistical methods for comparing two sites based on data with multiple nondetect limits. Water Resources Research, 24(12), 2087-2098.

Miller, K.L., 1994. The nuclear-reactor accident at 3-mile Island. Radiographics, 14(1), 215-224.

Milstein, D., Cherp, A., 2007. Energy security and the environment in eastern Europe: the case study of Ukraine. In S. Stec & B. Baraj, NATO Advanced Research Workshop on Energy and Environmental Challenges to Security (pp. 237-249). Budapest, HUNGARY: Springer.

Mulkern, J., 1995. The thermal oxide reprocessing plant (Thorp). Atw-Internationale Zeitschrift Fur Kernenergie, 40(8-9), 564-566.

Nagy, K.A., 2001. Food requirements of wild animals: predictive equations for free-living mammals, reptiles and birds. Nutrition Abstracts and Reviews, Series B 71, 21R-31R.

Narayanan, N., Eapen, J., 1971. Caesium-137 in tissues of the lizard *Hemidactylus leschenaulti*. Journal of Animal Morphology and Physiology, 18(2), 171-175.

NDA, 2008. Low-level waste repository: Parent body agreement. Nuclear Decommissioning Authority, Cumbria.

Nelis, P.M., 1990. The transfer of radionuclides from sea-to-land in sea spray. In. Edinburgh: University of Edinburgh.

Nenot, J.C., 1990. Overview of the radiological accidents in the world, updated December 1989. International Journal of Radiation Biology, 57(6), 1073-1085.

Nield, J.M., Baas, A.C.W., 2008. The influence of different environmental and climatic conditions on vegetated aeolian dune landscape development and response. Global and Planetary Change, 64(1-2), 76-92.

Niethammer, K.R., Atkinson, R.D., Baskett, T.S., Samson, F.B., 1985. Metals in riparian wildlife of the lead mining district of southeastern Missouri. Archives of Environmental Contamination and Toxicology, 14(2), 213-223.

Norman, C., Dickson, D., 1986. The aftermath of Chernobyl. Science, 233(4769), 1141-1143.

Noureddine, A., Baggoura, B., Larosa, J.J., Vajda, N., 1997. Gamma and alpha emitting radionuclides in some Algerian soil samples. Applied Radiation and Isotopes, 48(8), 1145-1148.

Oaks, T.W., Kimborough, C.W., Pritz, P.M., Goodpasture, S.T., Huang, S.F., Gist, G.S., Weber, C.W., O'Hara, F.M., 1987. Environmental surveillance of the U.S. Department of Energy Oak Ridge reservation and surrounding environs during 1986. Oak Ridge National Laboratory, Oak Ridge.

Obrtel, R., Holisova, V., 1979. Food eaten by *Apodemus sylvaticus* in a spruce monoculture. Folia Zoologica, 28(4), 299-310.

Ochoa, P., van Ackere, A., 2009. Policy changes and the dynamics of capacity expansion in the Swiss electricity market. Energy Policy, 37(5), 1983-1998.

Ohira, Y., Ito, A., Ikawa, S., 1977. Correction of water-content and solute concentration in blood during hemoconcentration. Journal of Applied Physiology, 42(5), 739-743.

Ohlendorf, H.M., Hothem, R.L., Aldrich, T.W., 1988. Bioaccumulation of selenium by snakes and frogs in the San-Joaquin Valley, California. Copeia, (3), 704-710.

Olson, J.S., 1958. Rates of succession and soil changes on Southern Lake Michigan sand dunes. Botanical Gazette, 119, 125-170.

Oughton, D.H., Aguero, A., Avila, R., Brown, J.E., Copplestone, D., Gilek, M., 2008. Addressing uncertainties in the ERICA Integrated Approach. Journal of Environmental Radioactivity, 99(9), 1384-1392.

Paine, R.T., 1969. A note on trophic complexity and community stability. American Naturalist, 103(929), 91-93.

Palo, T.R., 2007. Variation in transfer factor of radiocaesium in bank voles (*Clethrionomys glareolus*) in clear cut and mature forest sites after the Chernobyl accident. Journal of Environmental Radioactivity, 92(2), 112-121.

Parker, C.A., Collingwood, W.G., 1926. The Gosforh district: its antiquities and places of interest. Titus Wilson & Son, Kendal.

Parker, J., 1977. Cumbria. 1st edn. John Bartholomew & Son Ltd, Edinburgh.

Parker, T.G., Mobbs, S.F., Kane, P., Thorne, M.C., 1989. Development of radiological impact assessments for the Drigg low level radioactive waste disposal site. British Nuclear Fuels Plc, Cumbria.

Pattenden, N.J., Cambray, R.S., Playford, K., 1987. Studies of environmental radioactivity in Cumbria: Part 15. The variation of radionuclide atmospheric deposition with

distance from the sea. United Kingdom Atomic Energy Authority Harwell Laboratory.

Pelosi, C., Bertrand, M., Capowiez, Y., Boizard, H., Roger-Estrade, J., 2009. Earthworm collection from agricultural fields: Comparisons of selected expellants in presence/absence of hand-sorting. European Journal of Soil Biology, 45(2), 176-183.

Pentreath, R.J., 1998. Radiological protection criteria for the natural environment. Radiation Protection Dosimetry, 75(1-4), 175-179.

Periáñez, R., Abril, J.M., García-Léon, M., 1996. Modelling the dispersion of non-conservative radionuclides in tidal waters--Part 1: Conceptual and mathematical model. Journal of Environmental Radioactivity, 31(2), 127-141.

Pernetta, J.C., 1976. Diets of shrews *Sorex araneus* L. and *Sorex minutus* L. in Wytham grassland. Journal of Animal Ecology, 45(3), 899-912.

Peters, E.L., Brisbin, I.L., 1996. Environmental influences on the ^{137}Cs kinetics of the yellow-bellied turtle (*Trachemys scripta*). Ecological Monographs, 66(1), 115-136.

Pielke, R.A., 2009. The British Climate Change Act: a critical evaluation and proposed alternative approach. Environmental Research Letters, 4(2), 7.

Platenberg, R.J., Griffiths, R.A., 1999. Translocation of slow-worms (Anguis fragilis) as a mitigation strategy: a case study from south-east England. Biological Conservation, 90(2), 125-132.

Pough, F.H., Andrews, R.M., Cadle, J.E., Crump, M.L., Savitzky, A.H., Wells, K.D., 2004. Herpetology. 3rd edn. Pearson Prentice Hall, New Jersey.

Presser, T.S., Ohlendorf, H.M., 1987. Biogeochemical cycling of selenium in the San-Joaquin Valley, California, USA. Environmental Management, 11(6), 805-821.

Pritchard, P.C.H., Bloodwell, J.M., 1986. Multidisciplinary study of radionuclides and heavy metal concentrations in wildlife on phosphate mined and reclaimed sites. Florida Audubon Society, Bartow.

Pye, K., 1990. Physical and human influences on coastal development between the Ribble and Mersey estuaries, northwest England. In K.F. Nordstrom, N.P. Psuty & R.W.G. Carter, Coastal dunes: form and process (pp. 339-359). Chichester: John Wiley & Sons Ltd.

Ramsay, J.A., 1949. The osmotic relations of the earthworm. Journal of Experimental Biology, 26(1), 46-56.

Ranwell, D.S., 1972. Ecology of saltmarshes and sand dunes. Chapman and Hall, London.

Read, J., Pickering, R., 1999. Ecological and toxicological effects of exposure to an acidic, radioactive tailings storage. Environmental Monitoring and Assessment, 54(1), 69-85.

Read, J.W., Ridgell, R.H., 1922. On the use of the conventional carbon factor in estimating soil organic matter. Soil Science, 13(1), 1-6.

Reading, C.J., 1996. Evaluation of reptile survey methodologies. English Nature, Peterborough.

Reading, C.J., 1997. A proposed standard method for surveying reptiles on dry lowland heath. Journal of Applied Ecology, 34(4), 1057-1069.

Real, A., Sundell-Bergman, S., Knowles, J.F., Woodhead, D.S., Zinger, I., 2004. Effects of ionising radiation exposure on plants, fish and mammals: relevant data for environmental radiation protection. Journal of Radiological Protection, 24(4A), A123-A137.

Reichle, D.E., Dunaway, P.B., Nelson, D.J., 1970. Turnover and concentration of radionuclides in food chains. Nuclear Safety, 11(1), 43-55.

Resch, F.J., Darrozes, J.S., Afeti, G.M., 1986. Marine liquid aerosol production from bursting of air bubbles. J. Geophys. Res.-Oceans, 91(C1), 1019-1029.

Rezk, M.R., 1970. Vegetation change from a sand dune community to a saltmarsh as related to soil characteristics in Mariut District, Egypt. Oikos, 21(2), 341-&.

Richmond, C.R., 1980. Retention and excretion of radionuclides of the alkali metals by five mammalian species. Health Physics, 38(6), 1111-1153.

Rie, M.T., Lendas, K.A., Callard, I.P., 2001. Cadmium: tissue distribution and binding protein induction in the painted turtle, *Chrysemys picta*. Comparative Biochemistry and Physiology C-Toxicology & Pharmacology, 130(1), 41-51.

RIFE, 1996. Radioactivity in Food in the Environment (RIFE-1). Available from: http://www.cefas.co.uk/publications/scientific-series/radioactivity-in-food-and-the-environment(rife).aspx.

RIFE, 1997. Radioactivity in Food in the Environment (RIFE-2). Available from: http://www.cefas.co.uk/publications/scientific-series/radioactivity-in-food-and-the-environment(rife).aspx.

RIFE, 1998. Radioactivity in Food in the Environment (RIFE-3). Available from: http://www.cefas.co.uk/publications/scientific-series/radioactivity-in-food-and-the-environment(rife).aspx.

RIFE, 1999. Radioactivity in Food in the Environment (RIFE-4). Available from: http://www.cefas.co.uk/publications/scientific-series/radioactivity-in-food-and-the-environment(rife).aspx.

RIFE, 2000. Radioactivity in Food in the Environment (RIFE-5). Available from: http://www.cefas.co.uk/publications/scientific-series/radioactivity-in-food-and-the-environment(rife).aspx.

RIFE, 2001. Radioactivity in Food in the Environment (RIFE-6). Available from: http://www.cefas.co.uk/publications/scientific-series/radioactivity-in-food-and-the-environment(rife).aspx.

RIFE, 2002. Radioactivity in Food in the Environment (RIFE-7). Available from: http://www.cefas.co.uk/publications/scientific-series/radioactivity-in-food-and-the-environment(rife).aspx.

RIFE, 2003. Radioactivity in Food in the Environment (RIFE-8). Available from: http://www.cefas.co.uk/publications/scientific-series/radioactivity-in-food-and-the-environment(rife).aspx.

RIFE, 2004. Radioactivity in Food in the Environment (RIFE-9). Available from: http://www.cefas.co.uk/publications/scientific-series/radioactivity-in-food-and-the-environment(rife).aspx.

RIFE, 2005. Radioactivity in Food in the Environment (RIFE-10). Available from: http://www.cefas.co.uk/publications/scientific-series/radioactivity-in-food-and-the-environment(rife).aspx.

RIFE, 2006. Radioactivity in Food in the Environment (RIFE-11). Available from: http://www.cefas.co.uk/publications/scientific-series/radioactivity-in-food-and-the-environment(rife).aspx.

RIFE, 2007. Radioactivity in Food in the Environment (RIFE-12). Available from: http://www.cefas.co.uk/publications/scientific-series/radioactivity-in-food-and-the-environment(rife).aspx.

RIFE, 2008. Radioactivity in Food in the Environment (RIFE-13). Available from: http://www.cefas.co.uk/publications/scientific-series/radioactivity-in-food-and-the-environment(rife).aspx.

Risk Assessment Corporation, 2001. Savannah River Site Environmental Dose Reconstruction Project: Phase II: Source term calculation and ingestion pathway data retrieval - evaluation of materials released from the Savannah River Site. Available from: http://www.cdc.gov/nceh/radiation/Savannah/.

Rodriguez, J.G., Uriarte, A., 2009. Laser diffraction and dry-sieving grain size analyses undertaken on fine- and medium-grained sandy marine sediments: a note. Journal of Coastal Research, 25(1), 257-264.

Roff, S.R., 2004. Establishing the possible radiogenicity of morbidity and mortality from participation in UK nuclear weapons development. Medicine, Conflict & Survival, 20(3), 218-241.

Rollinson, W., 1978. A history of Cumberland. Phillimore & Co. Ltd, London.

Rudel, H., Schroder, W., von der Trenck, K.T., Wiesmuller, G., 2009. Substance-related environmental monitoring. Environmental Science and Pollution Research, 16(5), 486-498.

Rudge, S.A., 1989. The biological transport of radionuclides in grassland and freshwater ecosystems. In Environmental & Evolutionary Biology (pp. 336). Liverpool: University of Liverpool.

Rudge, S.A., Johnson, M.S., Leah, R.T., Jones, S.R., 1993a. Biological Transport of Radiocesium in a Seminatural Grassland Ecosystem 2. Small Mammals. Journal of Environmental Radioactivity, 19(3), 199-212.

Rudge, S.A., Johnson, M.S., Leah, R.T., Jones, S.R., 1993b. Biological Transport of Radiocesium in a Seminatural Grassland Ecosystem 1. Soils, Vegetation and Invertebrates. Journal of Environmental Radioactivity, 19(3), 173-198.

Rychlik, L., Jancewicz, E., 2002. Prey size, prey nutrition, and food handling by shrews of different body sizes. Behavioral Ecology, 13(2), 216-223.

Saeki, K., Nakajima, M., Loughlin, T.R., Calkins, D.C., Baba, N., Kiyota, M., Tatsukawa, R., 2001. Accumulation of silver in the liver of three species of pinnipeds. Environmental Pollution, 112(1), 19-25.

Saidou, Bochud, F., Laedermann, J.-P., Kwato Njock, M.G., Froidevaux, P., 2008. A comparison of alpha and gamma spectrometry for environmental natural radioactivity surveys. Applied Radiation and Isotopes, 66(2), 215-222.

Saiki, M.K., Lowe, T.P., 1987. Selenium in aquatic organisms from subsurface agricultural drainage water, San-Joaquin Valley, California. Archives of Environmental Contamination and Toxicology, 16(6), 657-670.

Saint-Gobain Crystals & Detectors UK LTD, 2000. Mini-Instruments Environmental radiation Mater Type 6-80. Burnham-on-Crouch, UK.

Sakai, H., Ichihashi, H., Suganuma, H., Tatsukawa, R., 1995. Heavy-metal monitoring in sea-turtles using eggs. Marine Pollution Bulletin, 30(5), 347-353.

Sakai, H., Saeki, K., Ichihashi, H., Kamezaki, N., Tanabe, S., Tatsukawa, R., 2000. Growth-related changes in heavy metal accumulation in green turtle (*Chelonia mydas*) from Yaeyama Islands, Okinawa, Japan. Archives of Environmental Contamination and Toxicology, 39(3), 378-385.

Salge, M., Milling, P.M., 2006. Who is to blame, the operator or the designer? Two stages of human failure in the Chernobyl accident. System Dynamics Review, 22(2), 89-112.

Salisbury, E.J., 1922. The soils of Blakeney Point: A study of soil reaction and succession in relation to the plant covering. Annals of Botany, 36(143), 391-U397.

Salisbury, E.J., 1952. Downs and dunes. Bell, London.

Sanchez-Chardi, A., Lopez-Fuster, M.J., Nadal, J., 2007. Bioaccumulation of lead, mercury, and cadmium in the greater white-toothed shrew, *Crocidura russula*, from the Ebro Delta (NE Spain): sex- and age-dependent variation. Environmental Pollution, 145(1), 7-14.

Santos, X., Arenas, C., Llorente, G.A., Ruiz, X., 2007. Exploring the origin of egg protein in an oviparous water snake (*Natrix maura*). Comparative Biochemistry and Physiology a-Molecular & Integrative Physiology, 147(1), 165-172.

Schmitt, C., Finger, S., 1982. The dynamics of metals from past and present mining activities in the Big and Black river watersheds, southeastern Missouri. Final Report to US Army Corps of Engineers. National Fisheries Research Laboratory, US Fish and Wildlife Service, Columbia.

Schneider, L., Belger, L., Burger, J., Vogt, R.C., 2009. Mercury bioacumulation in four tissues of *Podocnemis erythrocephala* (Podocnemididae: Testudines) as a function of water parameters. Science of the Total Environment, 407(3), 1048-1054.

Schumacher, B.A., 2002. Methods for the determination of total organic carbon (TOC) in soils and sediments. United States Environmental Protection Agency, Las Vegas.

Scott, D.E., Whicker, F.W., Gibbons, J.W., 1986. Effect of season on the retention of ^{137}Cs and ^{90}Sr by the yellow-bellied slider turtle (*Pseudemys scripta*). Canadian Journal of Zoology-Revue Canadienne de Zoologie, 64(12), 2850-2853.

Sellegri, K., O'Dowd, C.D., Yoon, Y.J., Jennings, S.G., de Leeuw, G., 2006. Surfactants and submicron sea spray generation. Journal of Geophysical Research - Atmospheres, 111(D22).

Sexton, R.J., Asme, 2007. Windscale pile reactors: decommissioning progress on a fifty year legacy. In 11th International Conference on Environmental Remediation and Radioactive Waste Management (pp. 19-25). Bruges, Brazil: Amer Soc Mechanical Engineers.

Sharygin, S.A., Korzhenevskii, V.V., Firsov, S.L., 1979. Geochemical ecology of the Crimean lizard. Soviet Journal of Ecology, 10(5), 437-438.

She, N., 1997. Analyzing censored water quality data using a non-parametric approach. Journal of the American Water Resources Association, 33(3), 615-624.

Shea, G., 2002. Reptiles and amphibians. Fog City Press, San Francisco.

Sheppard, S.C., 2005. Transfer parameters - Are on-site date really better? Human and Ecological Risk Assessment, 11(5), 939-949.

Simpson, J., 1992. Windscale 1957: anatomy of a nuclear accident - Arnold, L. Nature, 356(6367), 297-298.

Smith, F.B., Clark, M.J., 1986. Radionuclide deposition from the Chernobyl cloud. Nature, 322(6081), 690-691.

Smith, J., 2005. Effects of ionising radiation on biota: do we need more regulation? Journal of Environmental Radioactivity, 82(1), 105-122.

Smith, J., Potts, S., Eggleton, P., 2008. Evaluating the efficiency of sampling methods in assessing soil macrofauna communities in arable systems. European Journal of Soil Biology, 44(3), 271-276.

Smith, J.T., 2007. Are passive smoking, air pollution and obesity a greater mortality risk than major radiation incidents? BMC Public Health, 7.

Smolders, E., Van den Brande, K., Merckx, R., 1997. Concentrations of ^{137}Cs and K in soil solution predict the plant availability of ^{137}Cs in soils. Environmental Science and Technology, 31(12), 3432-3438.

Soil Survey of England & Wales, 1983. Legend for the 1:250,000 soil map of England & Wales: a brief explanation of the consticuent soil associations. Rothamsted Experimental Station, Harpenden.

Sokolov, V.E., Krivoluzky, D.A., Usachev, V.L., 1989. Wild animals in the global radioecological monitoring. Nauka, Moscow.

Southwood, T.R.E., 1978. Ecological methods with particular reference to the study of insect populations. 2nd edn. Chapman and Hall, London.

Spiel, D.E., 1998. On the births of film drops from bubbles bursting on seawater surfaces. Journal of Geophysical Research - Oceans, 103(C11), 24907-24918.

Starck, J.M., Beese, K., 2002. Structural flexibility of the small intestine and liver of garter snakes in response to feeding and fasting. Journal of Experimental Biology, 205(10), 1377-1388.

Stark, J.G., Wallace, H.G., 1982. Chemistry data book. 2nd edn. John Murray (Publishers) Ltd, London.

Staton, M.A., Brisbin, I.L., Geiger, R.A., 1974. Some aspects of radiocesium retention in naturally contaminated captive snakes. Herpetologica, 30, 204-211.

Steers, J.A., 1946. The coastline of England and Wales. Cambridge University Press, Cambridge.

Stone, W.B., Kiviat, E., Butkas, S.A., 1980. Toxicants in snapping turtles. New York Fish and Game Journal, 27(1), 39-50.

Stoneburner, D.L., Kushlan, J.A., 1984. Heavy-metal burdens in American crocodile eggs from Florida Bay, Florida, USA. Journal of Herpetology, 18(2), 192-193.

Storelli, M.M., Ceci, E., Marcotrigiano, G.O., 1998. Distribution of heavy metal residues in some tissues of *Caretta caretta* (Linnaeus) specimen beached along the Adriatic Sea (Italy). Bulletin of Environmental Contamination and Toxicology, 60(4), 546-552.

Storelli, M.M., Storelli, A., D'Addabbo, R., Marano, C., Bruno, R., Marcotrigiano, G.O., 2005. Trace elements in loggerhead turtles (*Caretta caretta*) from the eastern Mediterranean Sea: overview and evaluation. Environmental Pollution, 135(1), 163-170.

Sundbom, M., Meili, M., Andersson, E., Ostlund, M., Broberg, A., 2003. Long-term dynamics of Chernobyl ^{137}Cs in freshwater fish: quantifying the effect of body size and trophic level. Journal of Applied Ecology, 40(2), 228-240.

Swanepoel, D., Boomker, J., Kriek, N.P.J., 2000. Selected chemical parameters in the blood and metals in the organs of the Nile crocodile, *Crocodylus niloticus*, in the Kruger National Park. Onderstepoort Journal of Veterinary Research, 67(2), 141-148.

Tajimi, M., Uehara, R., Watanabe, M., Oki, I., Ojima, T., Nakamura, Y., 2005. Correlation coefficients between the dioxin levels in mother's milk and the distances to the nearest waste incinerator which was the largest source of dioxins from each mother's place of residence in Tokyo, Japan. Chemosphere, 61(9), 1256-1262.

Thompson, I.M.G., Botter-Jensen, L., Deme, S., Pernicka, F., Saez-Vergara, J.C., 1999. Technical recommendations on measurements of external environmental gamma radiation doses. Radiation Protection 106. European Commission, Luxembourg.

Thompson, P.M., 1988. Environmental monitoring for radionuclides in maritime ecosystems: are species other than man protected adequately. Journal of Environmental Radioactivity, 7(3), 275-283.

Thompson, S.D., 2001. Environmental monitoring on the Oak Ridge reservation: 2001 results. Oak Ridge National Laboratory, Oak Ridge.

Tilling, S.M., 1987. A key to the major groups of British terrestrial invertebrates. Field Studies, 6, 695-766.

Toal, M.E., Copplestone, D., Johnson, M.S., Jackson, D., Jones, S.R., 2001. A dynamic compartmental food chain model of radiocaesium transfer to *Apodemus sylvaticus* in woodland ecosystems. Science of the Total Environment, 267(1-3), 53-65.

Toal, M.E., Copplestone, D., Johnson, M.S., Jackson, D., Jones, S.R., 2002. Quantifying Cs-137 aggregated transfer coefficients in a semi-natural woodland ecosystem adjacent to a nuclear reprocessing facility. Journal of Environmental Radioactivity, 63(1), 85-103.

Toop, C.M., 1988. The Alligator: Monarch of the Marsh. Florida National Parks and Monuments Association Inc., Homestead.

Torrent, A., Gonzalez-Diaz, O.M., Monagas, P., Oros, J., 2004. Tissue distribution of metals in loggerhead turtles (*Caretta caretta*) stranded in the Canary Islands, Spain. Mar. Pollut. Bull., 49(9-10), 854-860.

Towns, A.L., 1987. ^{137}Cs and ^{90}Sr in turtles: a whole-body measurement technique and tissue distribution. In Department of Radiology and Radiation Biology (pp. 39). Fort Collins: Colorado State University.

Twining, J.R., Markich, S.J., Prince, K.E., Jeffree, R.A., 1999. Osteoderms of estuarine crocodiles record their enhanced Pb exposure in Kakadu National Park. Environmental Science and Technology, 33(24), 4396-4400.

Tyler, A.N., Sanderson, D.C.W., Scott, E.M., Allyson, J.D., 1996. Accounting for spatial variability and fields of view in environmental gamma ray spectrometry. Journal of Environmental Radioactivity, 33(3), 213-235.

Tyler, A.N., Heal, K.V., 2000. Predicting areas of ^{137}Cs loss and accumulation in upland catchments. Water Air and Soil Pollution, 121(1-4), 271-288.

UK Biodiversity Group, 1999. Tranche 2 action plans: Maritime species and habitats. Available from: http://www.ukbap.org.uk/UKPlans.aspx?ID=28#1.

UK Parliament, 1981. Wildlife and Countryside Act.

UK Parliament, 1994. Conservation (Natural Habitats) Regulations.

Ulanovsky, A., Prohl, G., Gomez-Ros, J.M., 2008. Methods for calculating dose conversion coefficients for terrestrial and aquatic biota. Journal of Environmental Radioactivity, 99(9), 1440-1448.

UNSCEAR, 1996. Sources and effects of ionizing radiation. Report to the general assembly with scientific annex A/AC.82/R.54. United Nations Scientific Committee on the Effects of Atomic Radiation Vienna.

UNSCEAR, 2000. Sources and effects of ionizing radiation. Report to the general assembly with scientific annexes. United Nations Scientific Committee on the Effects of Atomic Radiation Vienna. Available from: http://www.unscear.org/unscear/en/publications/2000_1.html.

USDoE, 2002. A graded approach for evaluating radiation doses to aquatic and terrestrial biota Technical Standard DOE-STD-1153-2002. United States Department of the Environment, Washington D.C. Available from: http://www.hss.energy.gov/nuclearsafety/nsea/oepa/bdac/resrad.html.

USDoE, 2004. RESRAD-BIOTA: A Tool for Implementing a Graded Approach to Biota Dose Evaluation. ISCORS Techncal Report 2004-02 DOE/EH-0676. United States Department of the Environment, Washington D.C. Available from: http://web.ead.anl.gov/resrad/documents/RESRAD-BIOTA_Manual_Version_1.pdf.

van Boxel, J.H., Arens, S.M., Van Dijk, P.M., 1999. Aeolian processes across transverse dunes. I: Modelling the air flow. Earth Surface Processes and Landforms, 24(3), 255-270.

van den Ancker, J.A.M., Jungerius, P.D., Mur, L.R., 1985. The role of algae in the stabilisation of coastal dune blowouts. Earth Surface Processes and Landforms, 10, 189-192.

van der Hagen, H., Geelen, L., de Vries, C.N., 2008. Dune slack restoration in Dutch mainland coastal dunes. Journal for Nature Conservation, 16(1), 1-11.

Van der Meulen, F., Bakker, T.W.M., Houston, J.A., 2004. The costs of our coasts: examples of dynamc dune management from Western Europe. In M.L. Martinez & N.P. Psuty, Coastal dunes: ecology and conservation (pp. 259-277). Berlin: Springer-Verlag.

Viles, H.A., Spencer, T., 1995. Coastal problems: geomorphology, ecology and society at the coast. Edward Arnold, London.

Vincent, P., 1998. Particle size differentiation of some coastal sands: a multinomial logit regression approach. Journal of Coastal Research, 14(1), 331-336.

Vives i Batlle, J., Balonov, M., Beaugelin-Seiller, K., Beresford, N.A., Brown, J., Cheng, J.J., Copplestone, D., Doi, M., Filistovic, V., Golikov, V., Horyna, J., Hosseini, A., Howard, B.J., Jones, S.R., Kamboj, S., Kryshev, A., Nedveckaite, T., Olyslaegers, G., Prohl, G., Sazykina, T., Ulanovsky, A., Vives Lynch, S., Yankovich, T., Yu, C., 2007. Inter-comparison of absorbed dose rates for non-human biota. Radiation and Environmental Biophysics, 46(4), 349-373.

Wakeford, R., 2006. Chernobyl - 20 years on. Journal of Radiological Protection, 26(2), 125-126.

Walkley, A., Black, I.A., 1934. An examination of the Degtjareff method for determining soil organic matter, and a proposed modification of the chromic acid titration method. Soil Science, 37(1), 29-38.

Webb, G.A.M., Anderson, R.W., Gaffney, M.J.S., 2006. Classification of events with an off-site radiological impact at the Sellafield site between 1950 and 2000, using the International Nuclear Event Scale. Journal of Radiological Protection, 26(1), 33-49.

Webley, D.M., Eastwood, D.J., Gimingham, C.H., 1952. Development of a soil microflora in relation to plant succession on sand dunes, including the rhizosphere flora associated with colonizing species. Journal of Ecology, 40(1), 168-178.

Wendelberger, J., Campbell, K., 1994. Non-detect data in environmental investigations. American Statistical Association, Toronto.

Wentworth, C.K., 1922. A scale of grade and class terms for clastic sediments. Journal of Geology, 30, 377-392.

West, G.B., Brown, J.H., Enquist, B.J., 2000. The origin of universal scaling laws in biology. In J.H. Brown & G.B. West, Scaling Biology (pp. 87-112). New York: Oxford University Press.

Whicker, F.W., Pinder, J.E., Bowling, J.W., Alberts, J.J., Brisbin, I.L., 1990. Distribution of long-lived radionuclides in an abandoned reactor cooling reservoir. Ecological Monographs, 60(4), 471-496.

Whitfield, S.C., Rosa, E.A., Dan, A., Dietz, T., 2009. The future of nuclear power: value orientations and risk perception. Risk Analysis, 29(3), 425-437.

Whitten, K.W., Gailey, K.D., Davis, R.E., 1988. General chemistry. 3rd edn. Saunders College Publishing, Philadelphia.

Wilson, K., 1960. The time factor in the development of dune soils in South Haven Peninsula, Dorset. Journal of Ecology, 48(2), 341-359.

Withers, P.C., 1992. Comparative Animal Physiology. Saunders College Publishing, Fort Worth.

Wood, M.D., Knowles, J.D., Whittaker, J.H., Copplestone, D., Malcolm, H.M., Bielby, S., 2003. Developing experimental protocols for chronic irradiation studies on wildlife. R&D Technical Report P3-101/Sp2. Environment Agency, Bristol.

Wood, M.D., Copplestone, D., Crook, P., 2007. UKSHS Report No. 2: Chemical and Radiometric Sample Collection Methods. Environment Agency, Bristol.

Wood, M.D., Marshall, W.A., Beresford, N.A., Jones, S.R., Howard, B.J., Copplestone, D., Leah, R.T., 2008. Application of the ERICA Integrated Approach to the Drigg coastal sand dunes. Journal of Environmental Radioactivity, 99(9), 1484-1495.

Wood, M.D., Leah, R.T., Jones, S.R., Copplestone, D., 2009a. Radionuclide transfer to invertebrates and small mammals in a coastal sand dune ecosystem. Science of the Total Environment, 407(13), 4062-4074.

Wood, M.D., Beresford, N.A., Barnett, C.L., Copplestone, D., Leah, R.T., 2009b. Assessing radiation impact at a protected coastal sand dune site: an intercomparison of models for estimating the radiological exposure of non-human biota. Journal of Environmental Radioactivity, 100, 1034-1052.

Wood, M.D., Hall, P.J., Wittrick, S., Copplestone, D., Leah, R.T., in press. Survey of gamma dose rates in air around the Esk Estuary. Environment Agency, Bristol.

Woodhead, D.S., 1986. The radiation exposure of black-headed gulls (*Larus ridibundus*) in the Ravenglass Estuary, Cumbria, UK: a preliminary assessment. Science of the Total Environment, 58(3), 273-281.

Woolf, D.K., 1993. Bubbles and the air-sea transfer velocity of gases. Atmosphere-Ocean, 31(4), 517-540.

Woolven, S.C., Radley, G.P., Crawford, I.C., Waite, A.R., 1988. National sand dune vegetation: Drigg dunes 1987 - 1988. Nature Conservancy Council, Peterborough.

Wu, J., 1988. Bubbles in the near-surface ocean: a general description. Journal of Geophysical Research – Oceans, 93(C1), 587-590.

Xu, Q.H., Fang, S.G., Wang, Z.W., Wang, Z.P., 2006a. Heavy metal distribution in tissues and eggs of chinese alligator (*Alligator sinensis*). Archives of Environmental Contamination and Toxicology, 50(4), 580-586.

Xu, X.L., Liu, X.H., Zhang, L.Y., Chen, J.X., Liu, W.Q., Liu, Q.L., 2006b. Effects of metal ions on the conformation and activity of acutolysin D from *Agkistrodon acutus* venom. Protein Journal, 25(6), 423-430.

Xu, X.L., Zhang, L.Y., Shen, D.K., Wu, H., Peng, L.L., Li, J.H., 2009. Effect of metal ion substitutions in anticoagulation factor I from the venom of *Agkistrodon acutus* on the binding of activated coagulation factor X and on structural stability. Journal of Biological Inorganic Chemistry, 14(4), 559-571.

Yankovich, T., Beaton, D., 2000. Concentration ratios of stable elements measured in organs of terrestrial, freshwater and marine non-human biota for input into internal dose assessment: a literature review. Atomic Energy Canada Ltd, Ontario.

Yankovich, T.L., Sharp, K.J., Benz, M.L., Carr, J., Killey, R.W.D., 2007. Validation of the Carbon-14 Specific Activity Model in a Wetland Environment for Application in Biota Dose Assessment, in: American Nuclear Society (ANS) topical meeting on Decommissioning, Decontamination and Reutilization (DD&R), Chattanooga, Tennessee, 16-19 September 2007.

Yankovich, T.L., 2009. Mass balance approach to estimating radionuclide loads and concentrations in edible fish tissues using stable analogues. Journal of Environmental Radioactivity, 100(9), 795-801.

Yankovich, T.L., Vives i Batlle, J., Vives-Lynch, S., Beresford, N.A., Barnett, C.L., Beaugelin-Seffler, K., Brown, J.E., Cheng, J., Copplestone, D., Heling, R., Hosseini, A., Howard, B.J., Kamboj, S., Kryshev, A.I., Nedveckaite, T., Smith, J.T., Wood, M.D., in press. International model validation exercise on radionculide transfer and doses to freshwater biota. Journal of Radiological Protection.

Yanochko, G.M., Jagoe, C.H., Brisbin, I.L., 1997. Tissue mercury concentrations in alligators (*Alligator mississippiensis*) from the Florida Everglades and the Savannah River site, South Carolina. Archives of Environmental Contamination and Toxicology, 32(3), 323-328.

Yi-Chong, X., 2008. Nuclear energy in China: Contested regimes. Energy, 33(8), 1197-1205.

Zhang, D.H., Fan, C.P., Zhang, J., Zhang, C.H., 2009. Nonparametric methods for measurements below detection limit. Statistics in Medicine, 28(4), 700-715.

Zimmer, M., Topp, W., 1998. Nutritional biology of terrestrial isopods (Isopoda : Oniscidea): Copper revisited. Israel Journal of Zoology, 44(3-4), 453-462.

Zinger, I., Copplestone, D., Howard, B.J., 2008a. Decision-making in environmental radiation protection: using the ERICA Integrated Approach. Journal of Environmental Radioactivity, 99(9), 1510-1518.

Zinger, I., Oughton, D.H., Jones, S.R., 2008b. Stakeholder interaction within the ERICA Integrated Approach. Journal of Environmental Radioactivity, 99(9), 1503-1509.

APPENDIX 1

Temporal changes in topography and vegetation cover at specific locations on the Drigg coastal sand dunes have been documented through the use of fixed-point photography. The photographs presented in this appendix cover the period 1984 – 2005.

Photographs taken in 1984 and 1987 are credited to D. Simpson. Photographs taken in 1994 are credited to R.J. Cooper. Photographs taken from 2005 are credited to Ash Bennett.

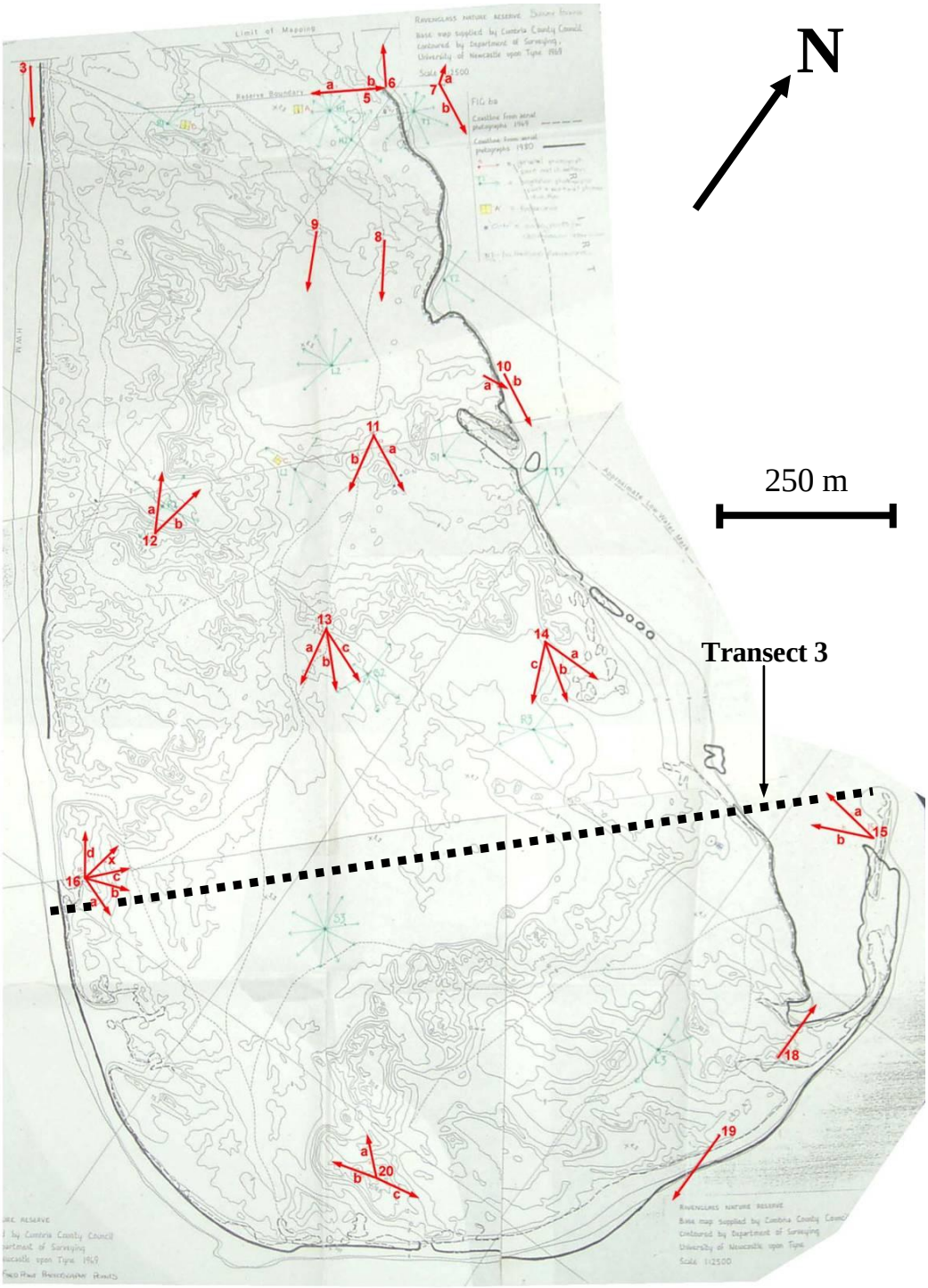

Plate A1.1. Fixed-point photography locations at the Drigg coastal sand dunes (Ash Bennett, private ecological consultant, pers. comm.). The path of sampling transect 3 (see Section 3.1.2) is indicated by the dashed black line. Transects 1 and 2 are outside of the area covered by the fixed-point photography.

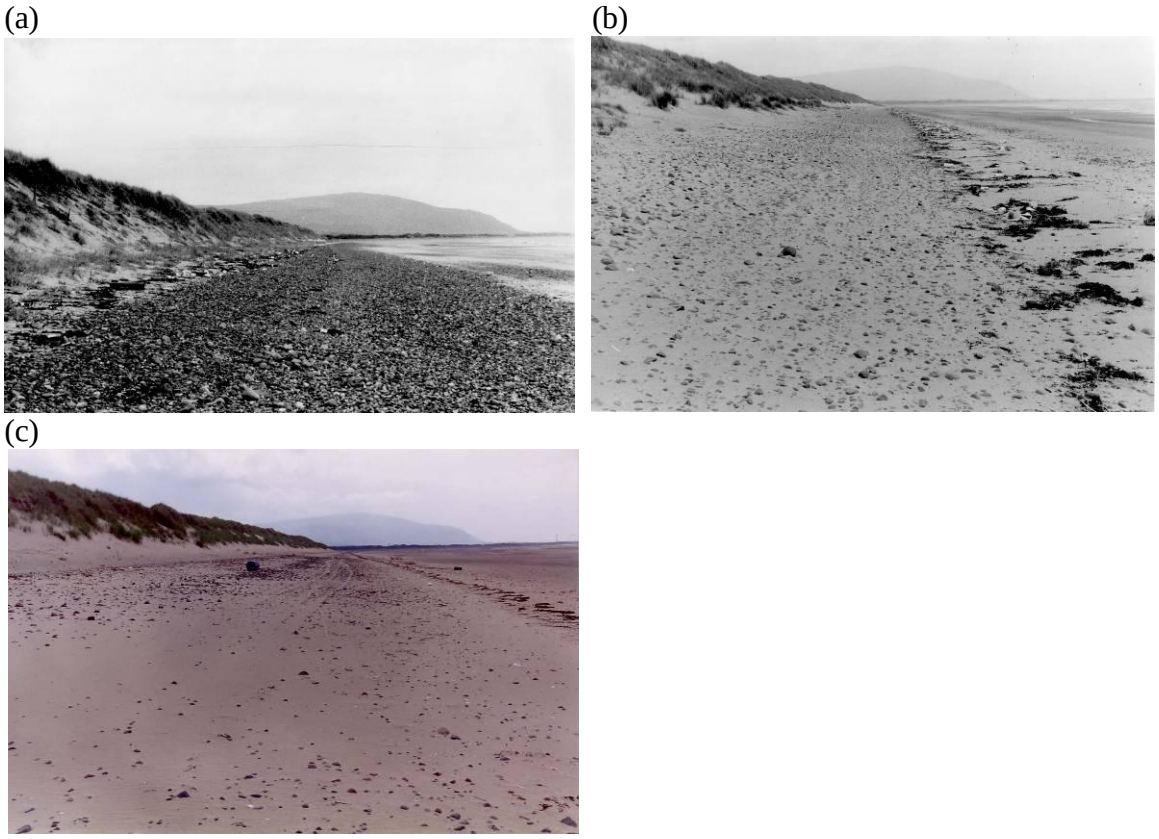

Plate A1.2. View from fixed-point photograph location 3 in (a) 1984, (b) 1987 and (c) 1994

(a)

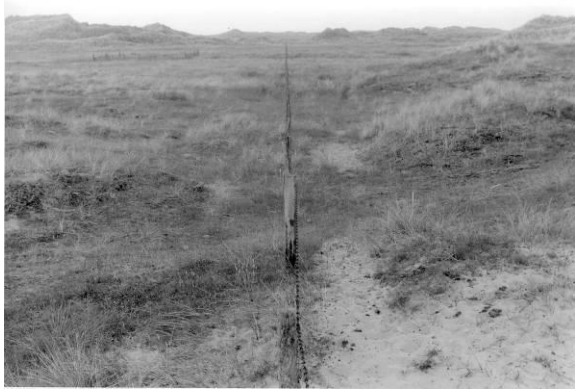

(b)

(c)

Plate A1.3. View from fixed-point photograph location 5a in (a) 1987, (b) 1994 and (c) 2005

(a)

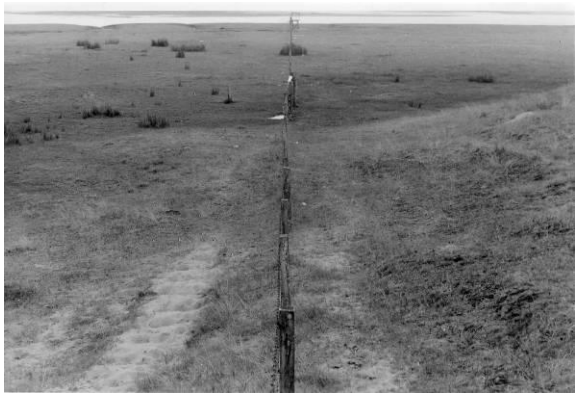

(b)

(c)

Plate A1.4. View from fixed-point photograph location 5b in (a) 1987, (b) 1994 and (c) 2005

(a)

(b)

(c)

Plate A1.5. View from fixed-point photograph location 6 in (a) 1987, (b) 1994 and (c) 2005

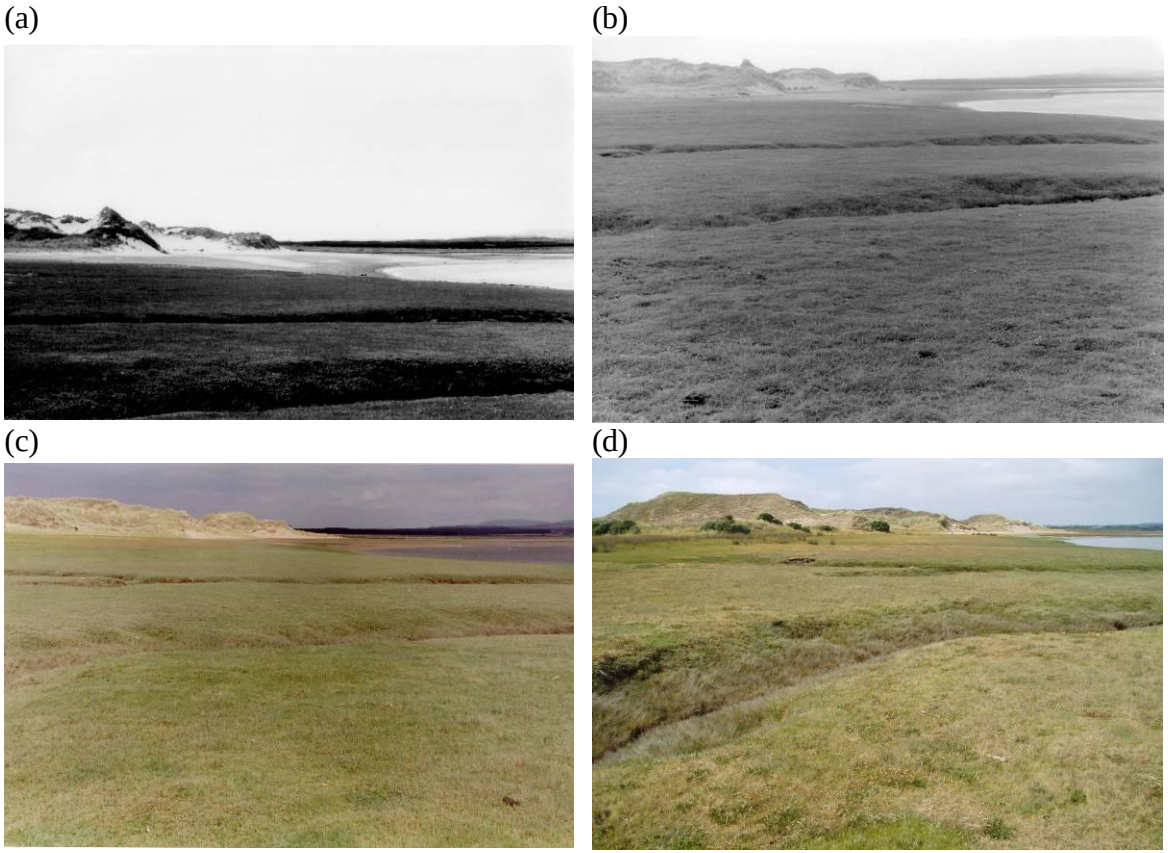

Plate A1.6. View from fixed-point photograph location 7a in (a) 1984, (b) 1987, (c) 1994 and (d) 2005

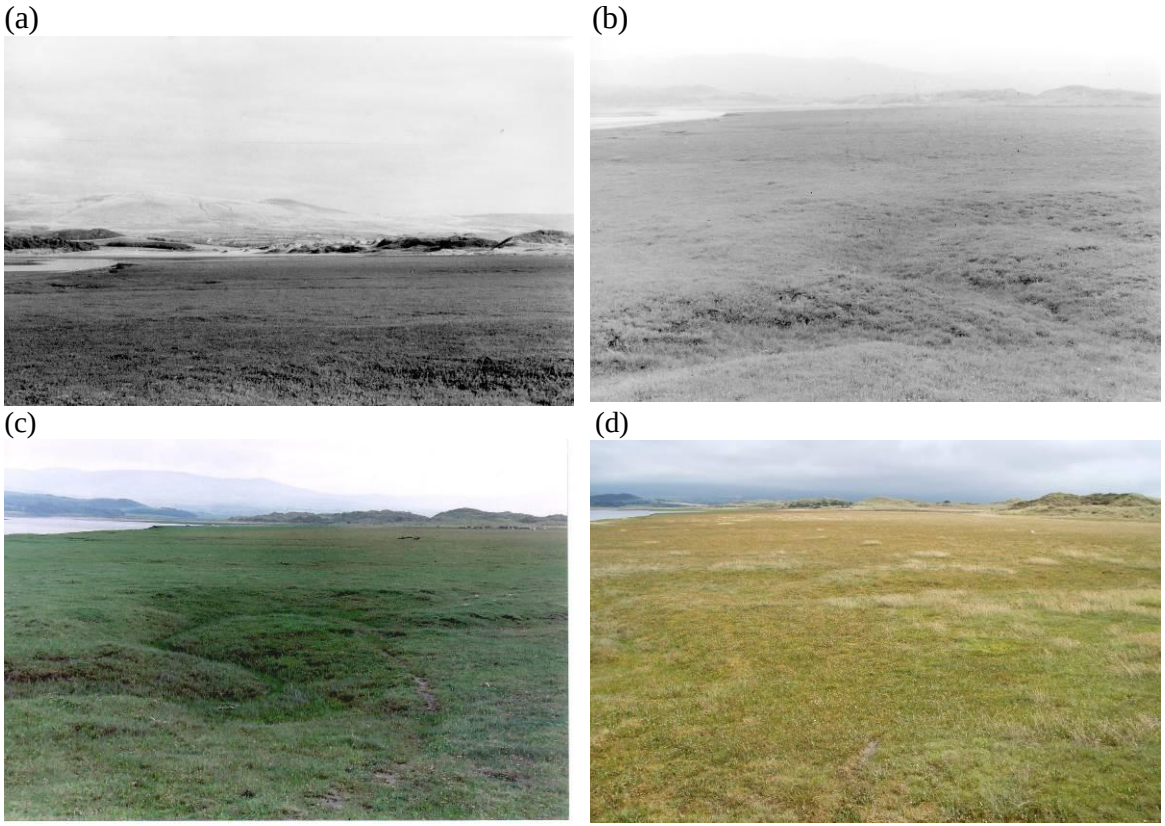

Plate A1.7. View from fixed-point photograph location 7b in (a) 1984, (b) 1987, (c) 1994 and (d) 2005

(a)

(b)

(c)

Plate A1.8. View from fixed-point photograph location 8 in (a) 1987, (b) 1994 and (c) 2005

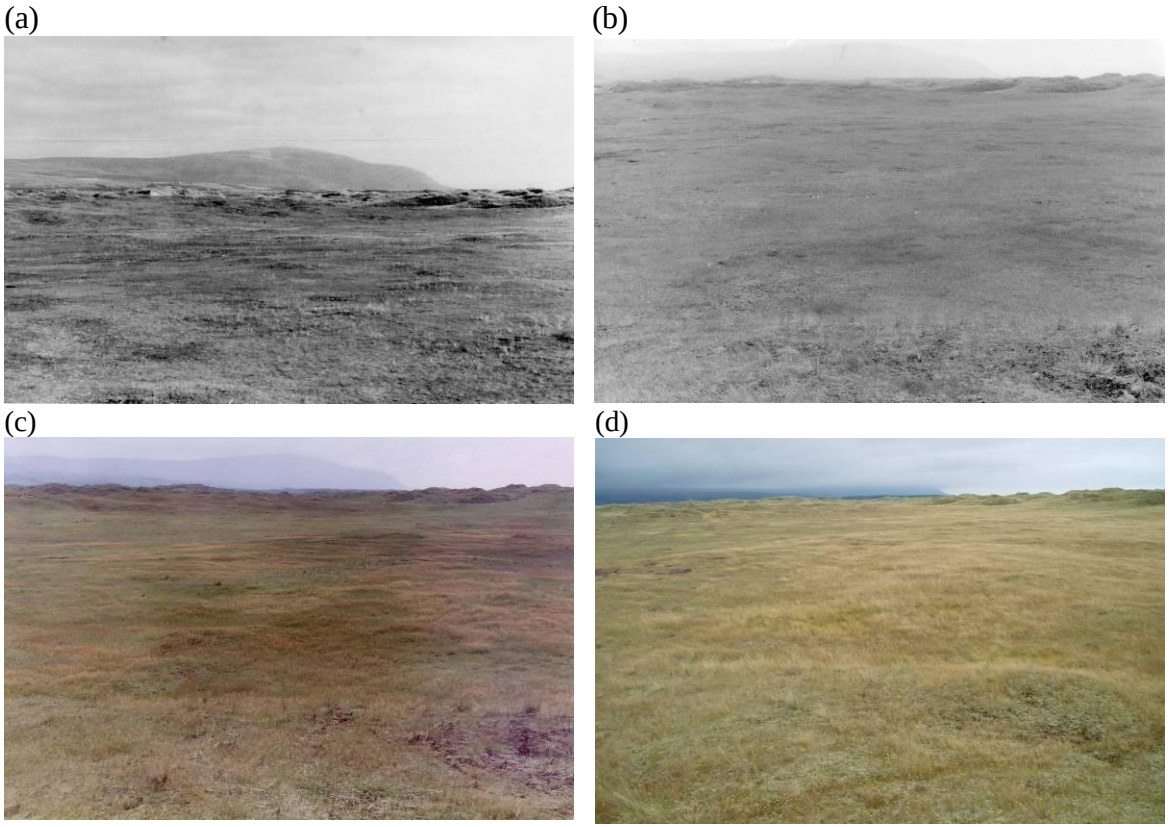

Plate A1.9. View from fixed-point photograph location 9 in (a) 1984, (b) 1987, (c) 1994 and (d) 2005

Plate A1.10. View from fixed-point photograph location 10a in (a) 1987, (b) 1994 and (c) 2005

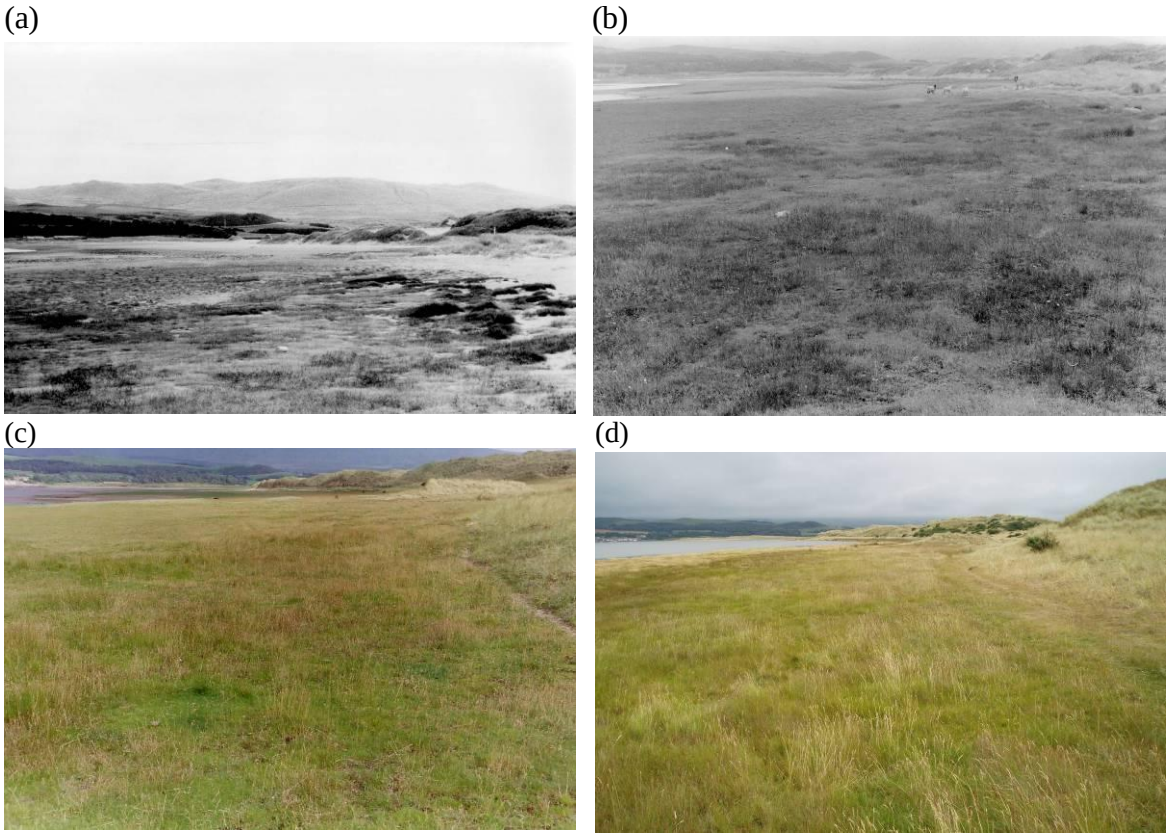

Plate A1.11. View from fixed-point photograph location 10b in (a) 1984, (b) 1987, (c) 1994 and (d) 2005

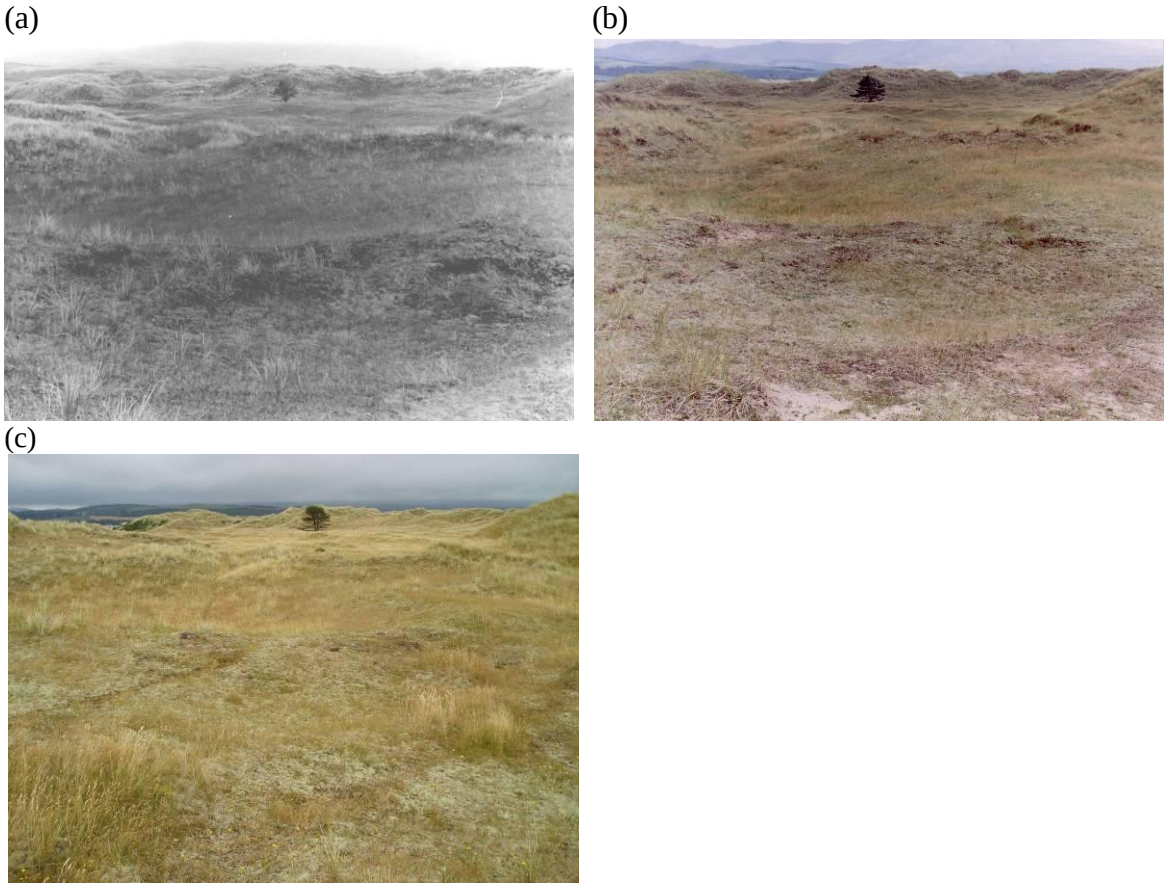

Plate A1.12. View from fixed-point photograph location 11a in (a) 1987, (b) 1994 and (c) 2005

(a)

(b)

(c)

Plate A1.13. View from fixed-point photograph location 11b in (a) 1987, (b) 1994 and (c) 2005

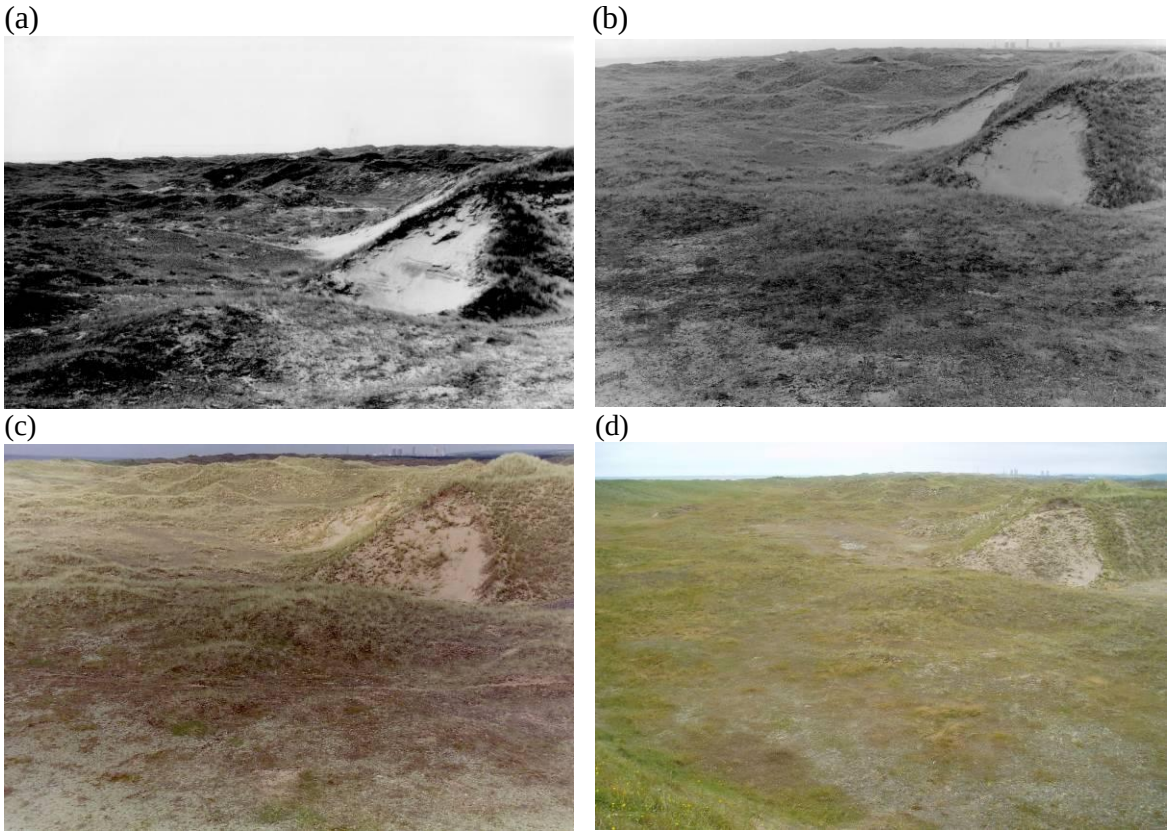

Plate A1.14. View from fixed-point photograph location 12a in (a) 1984, (b) 1987, (c) 1994 and (d) 2005

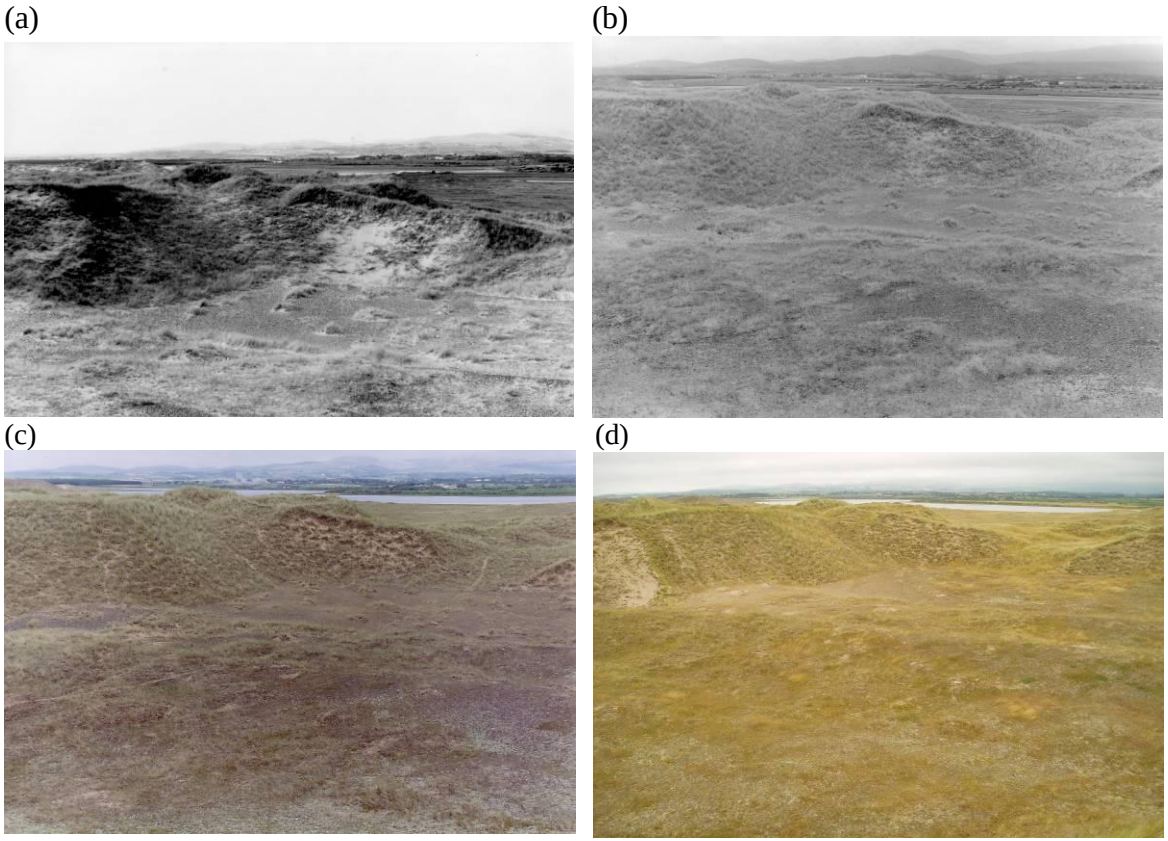

Plate A1.15. View from fixed-point photograph location 12b in (a) 1984, (b) 1987, (c) 1994 and (d) 2005

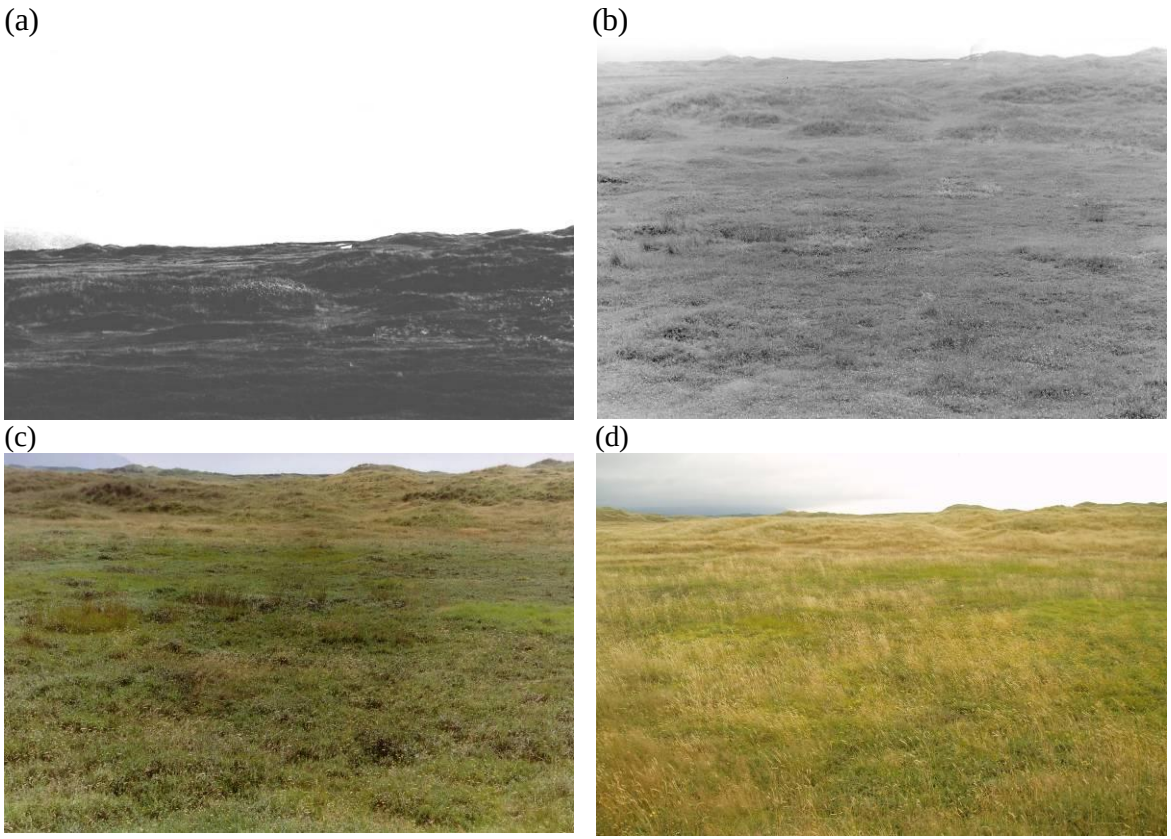

Plate A1.16. View from fixed-point photograph location 13a in (a) 1984, (b) 1987, (c) 1994 and (d) 2005

(a) (b)

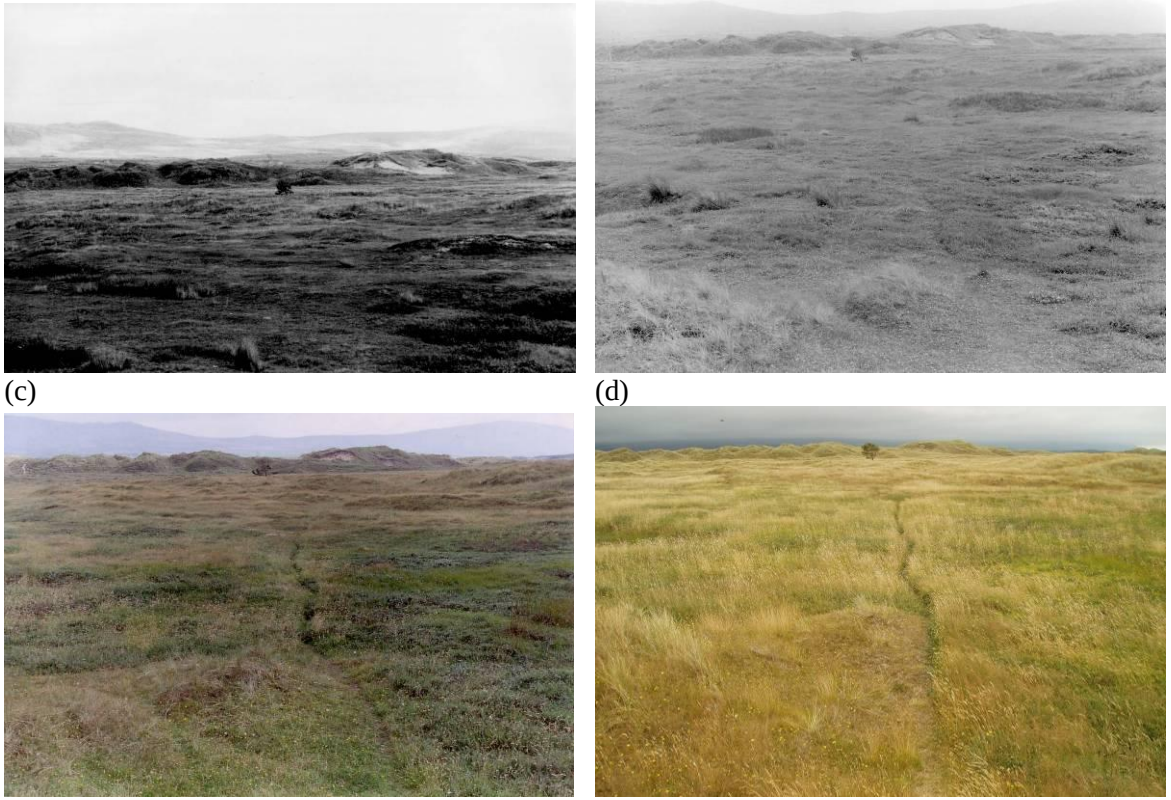

(c) (d)

Plate A1.17. View from fixed-point photograph location 13b in (a) 1984, (b) 1987, (c) 1994 and (d) 2005

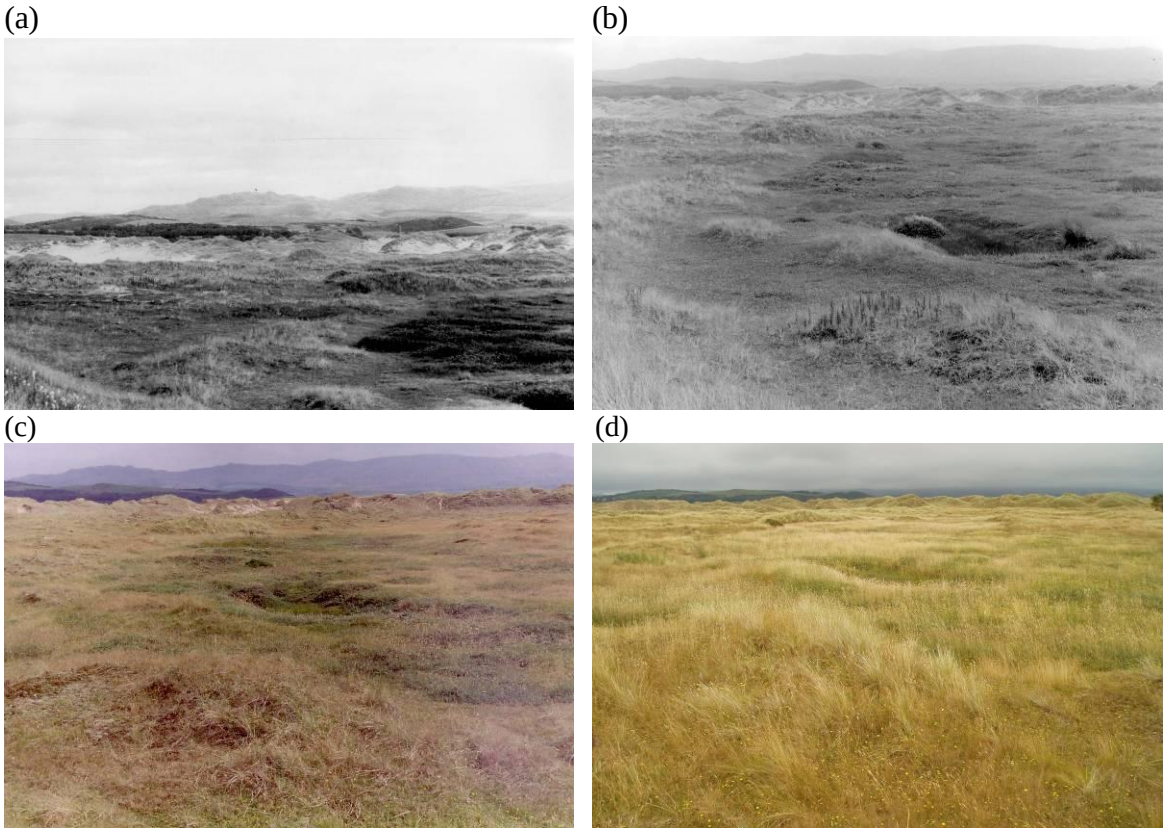

Plate A1.18. View from fixed-point photograph location 13c in (a) 1984, (b) 1987, (c) 1994 and (d) 2005

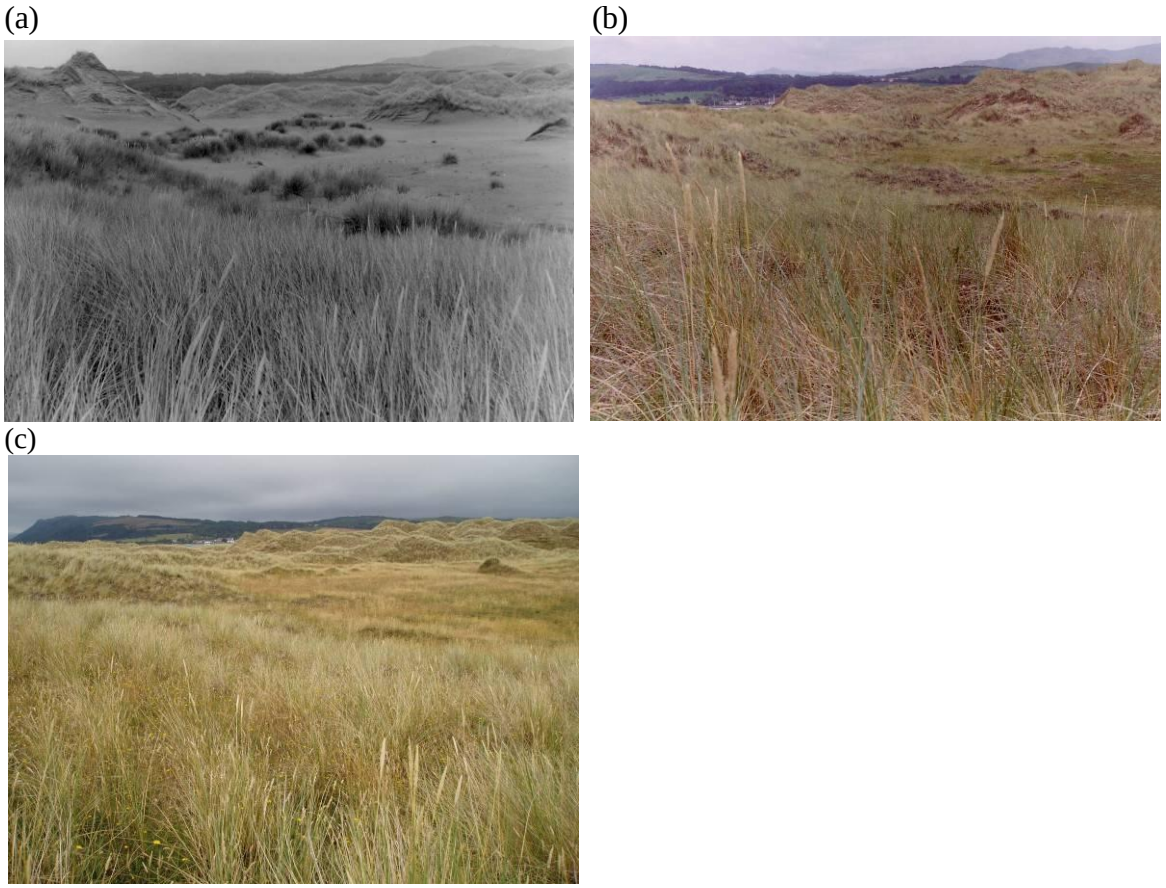

Plate A1.19. View from fixed-point photograph location 14a in (a) 1987, (b) 1994 and (c) 2005

(a)

(b)

(c)

Plate A1.20. View from fixed-point photograph location 14b in (a) 1987, (b) 1994 and (c) 2005

(a)

(b)

(c)

Plate A1.21. View from fixed-point photograph location 14c in (a) 1987, (b) 1994 and (c) 2005

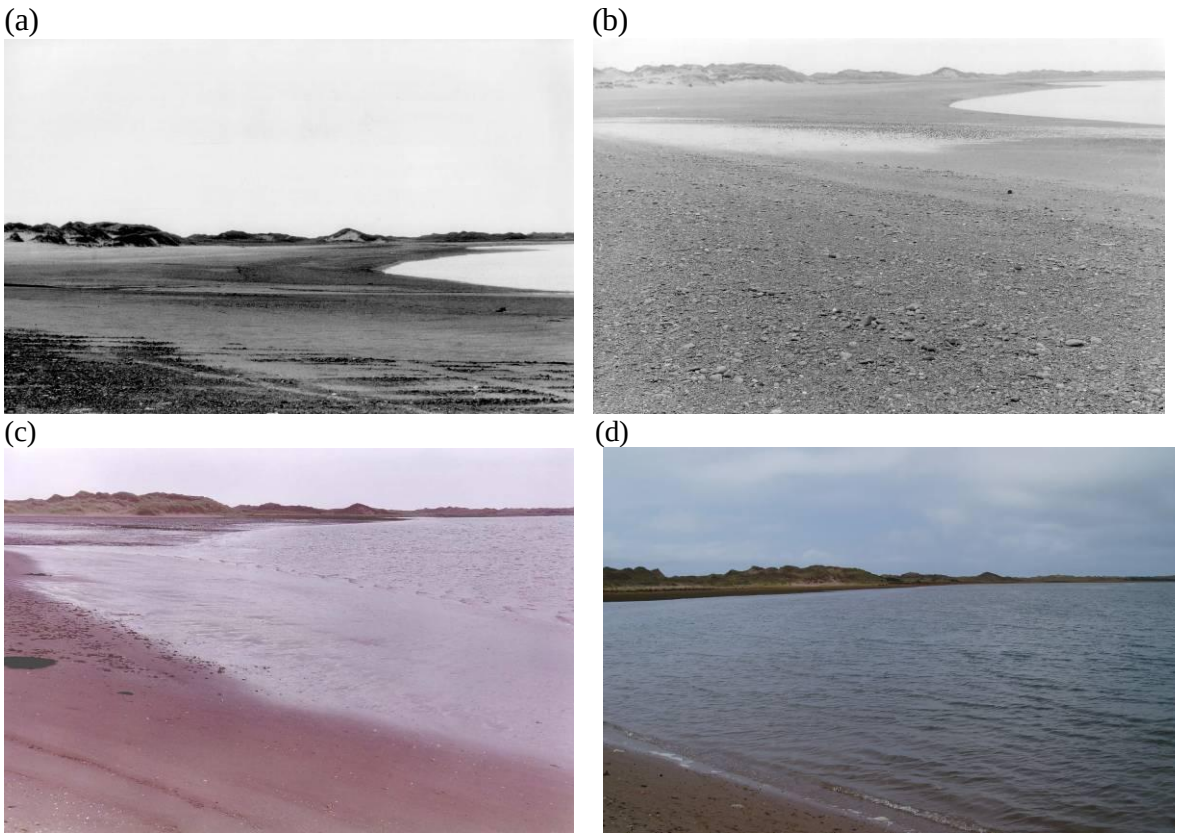

Plate A1.22. View from fixed-point photograph location 15a in (a) 1984, (b) 1987, (c) 1994 and (d) 2005

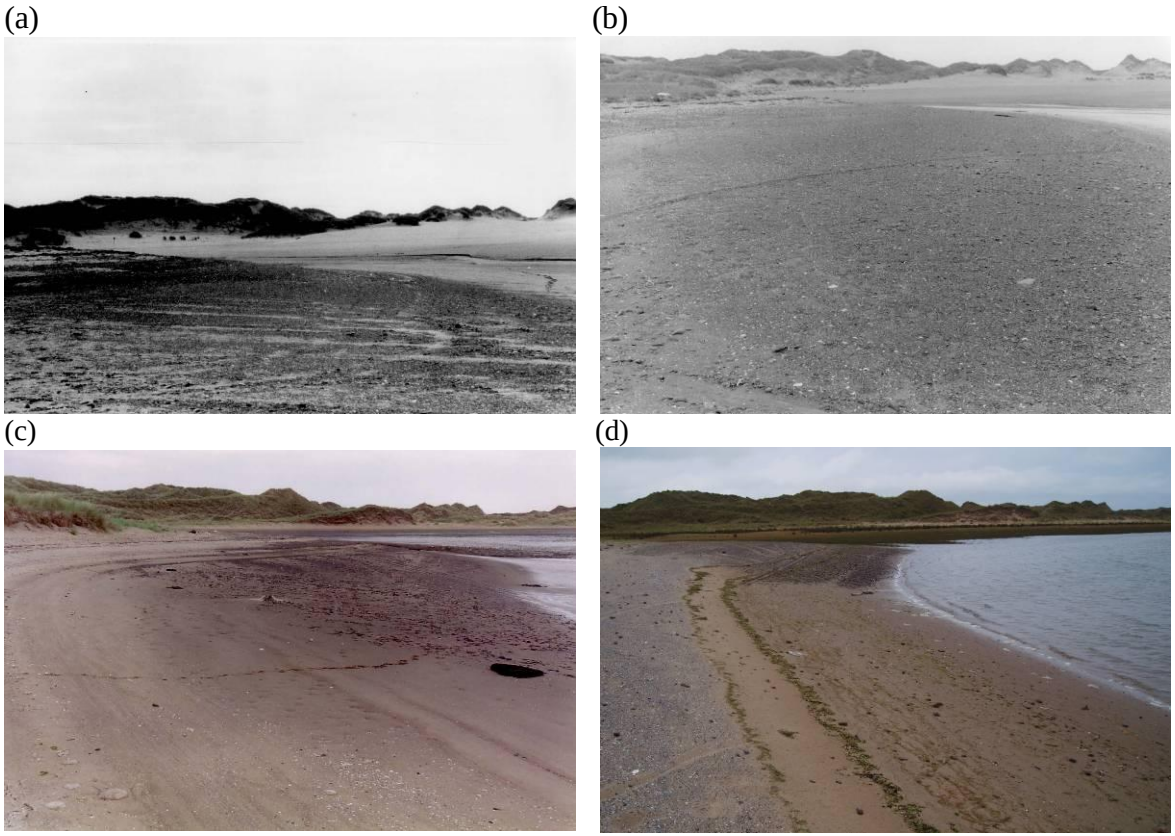

Plate A1.23. View from fixed-point photograph location 15b in (a) 1984, (b) 1987, (c) 1994 and (d) 2005

(a)

(b)

(c)

Plate A1.24. View from fixed-point photograph location 16a in (a) 1987, (b) 1994 and (c) 2005

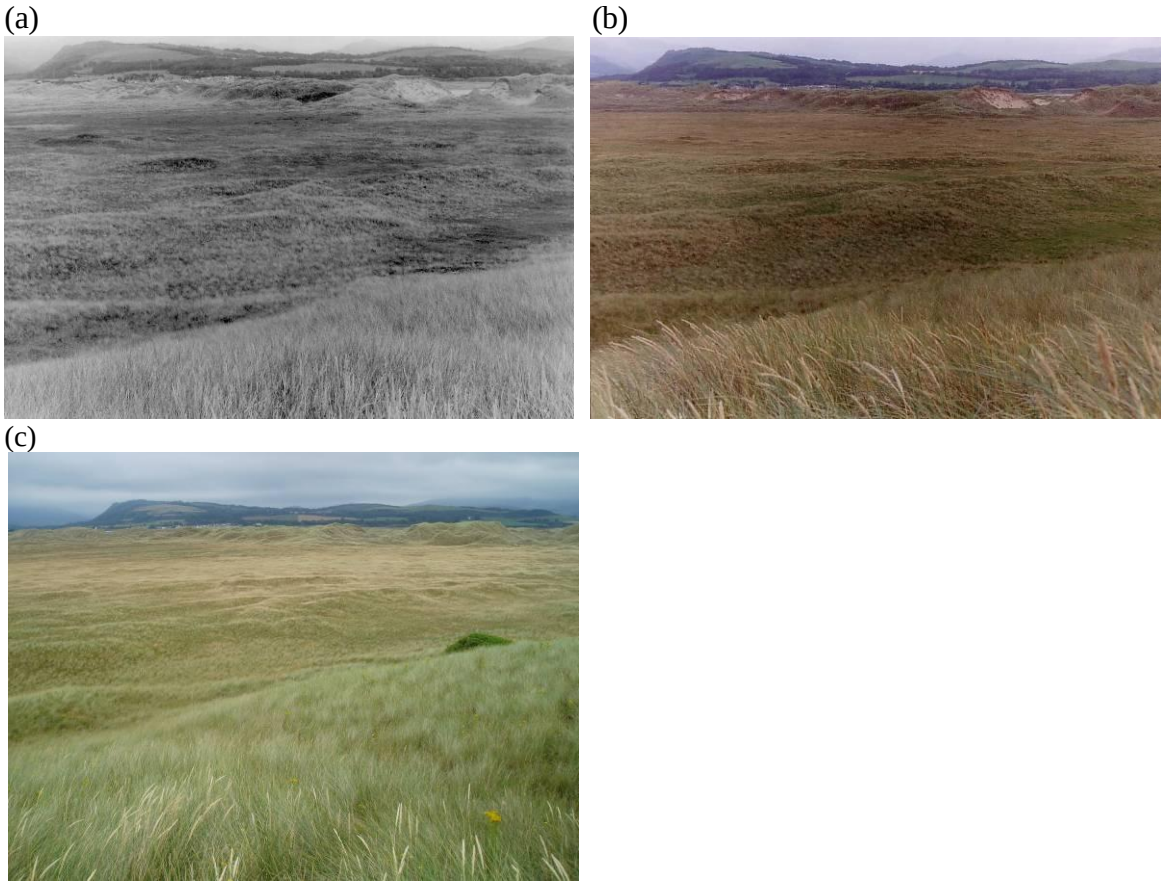

Plate A1.25. View from fixed-point photograph location 16b in (a) 1987, (b) 1994 and (c) 2005

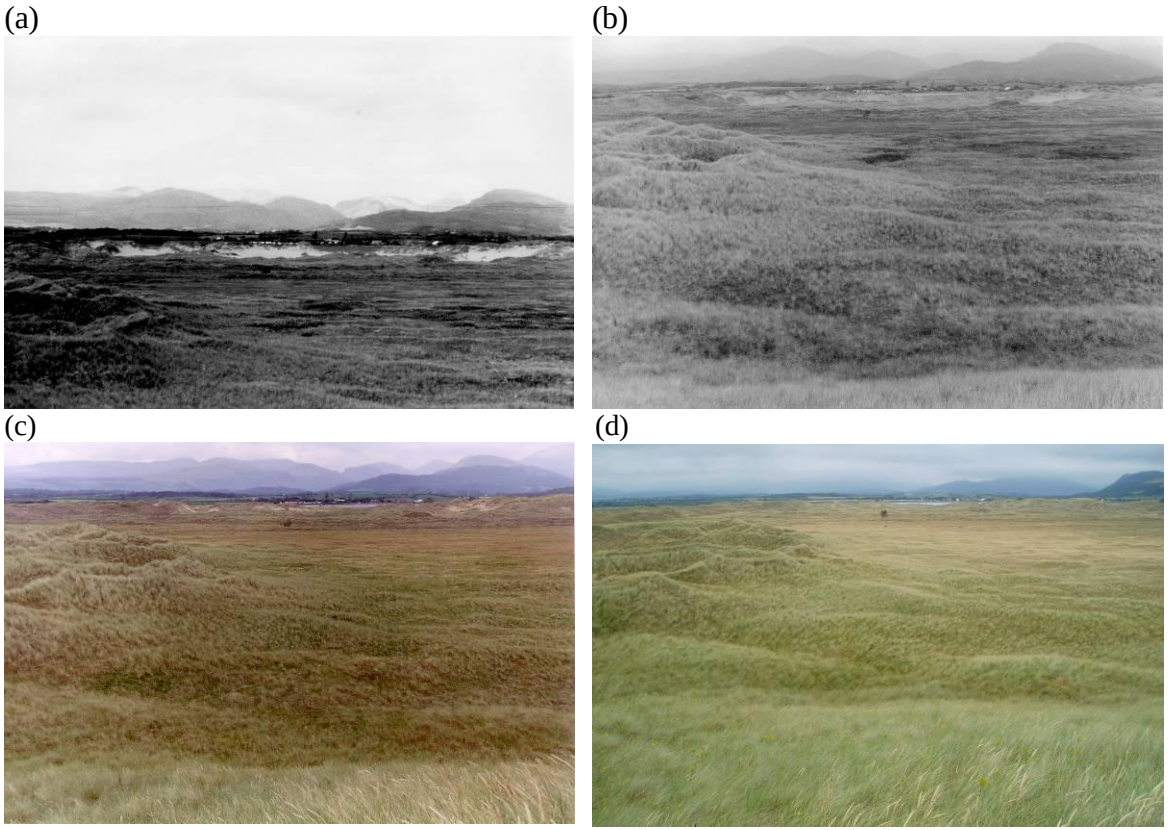

Plate A1.26. View from fixed-point photograph location 16c in (a) 1984, (b) 1987, (c) 1994 and (d) 2005

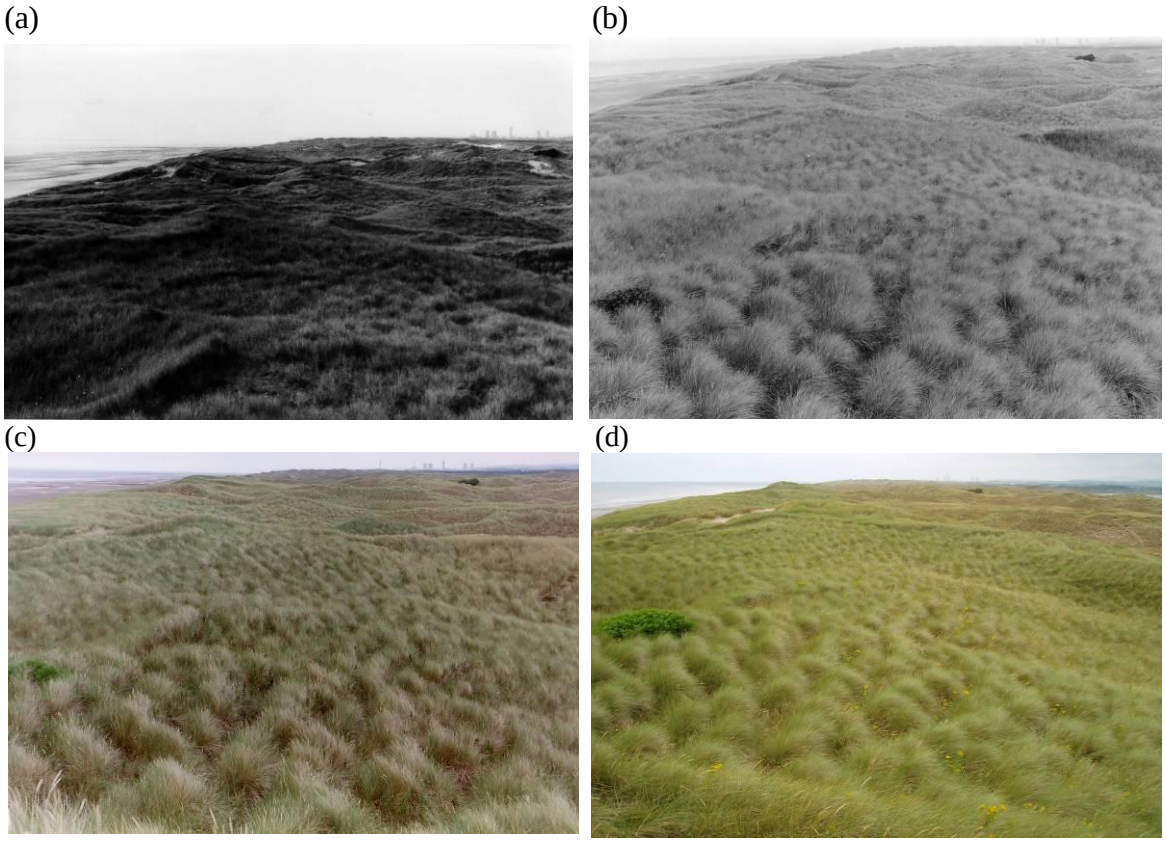

Plate A1.27. View from fixed-point photograph location 16d in (a) 1984, (b) 1987, (c) 1994 and (d) 2005

(a)

(b)

(c)

Plate A1.28. View from fixed-point photograph location 16x in (a) 1984, (b) 1994 and (c) 2005

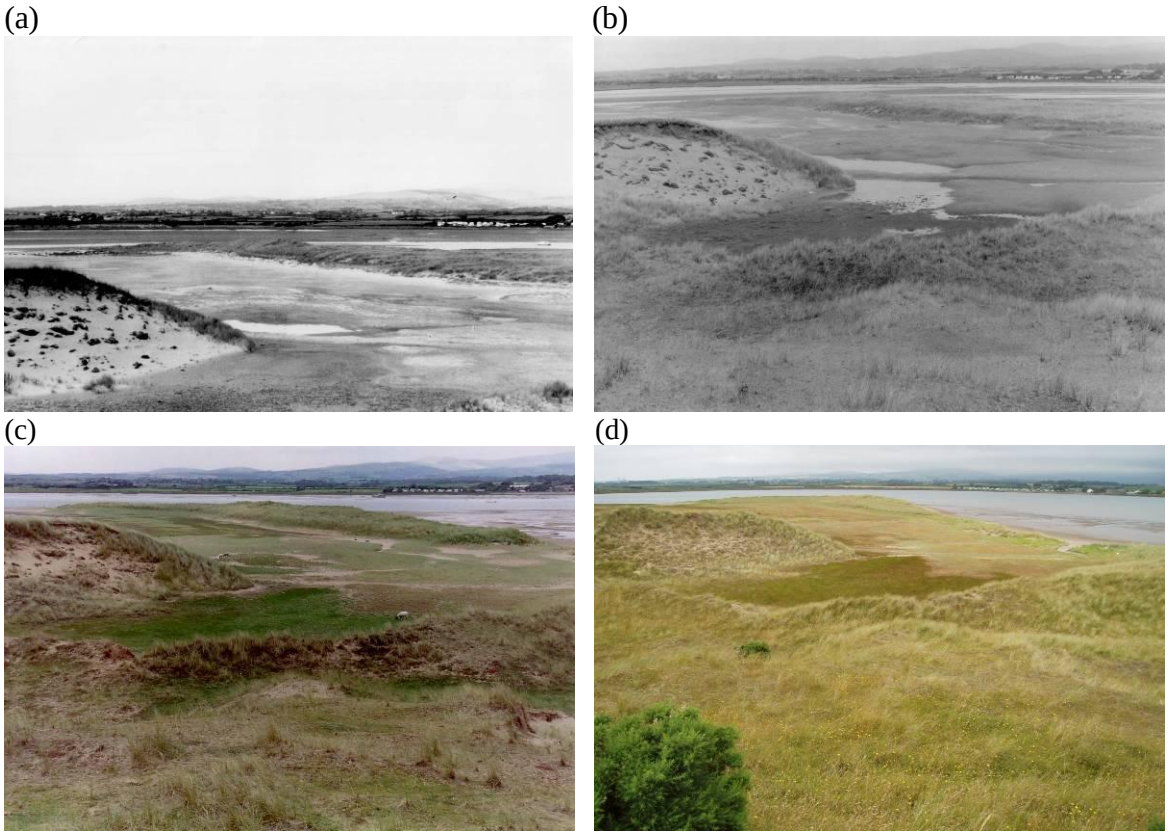

Plate A1.29. View from fixed-point photograph location 18 in (a) 1984, (b) 1987, (c) 1994 and (d) 2005

(a)

(b)

(c)

Plate A1.30. View from fixed-point photograph location 19 in (a) 1987, (b) 1994 and (c) 2005

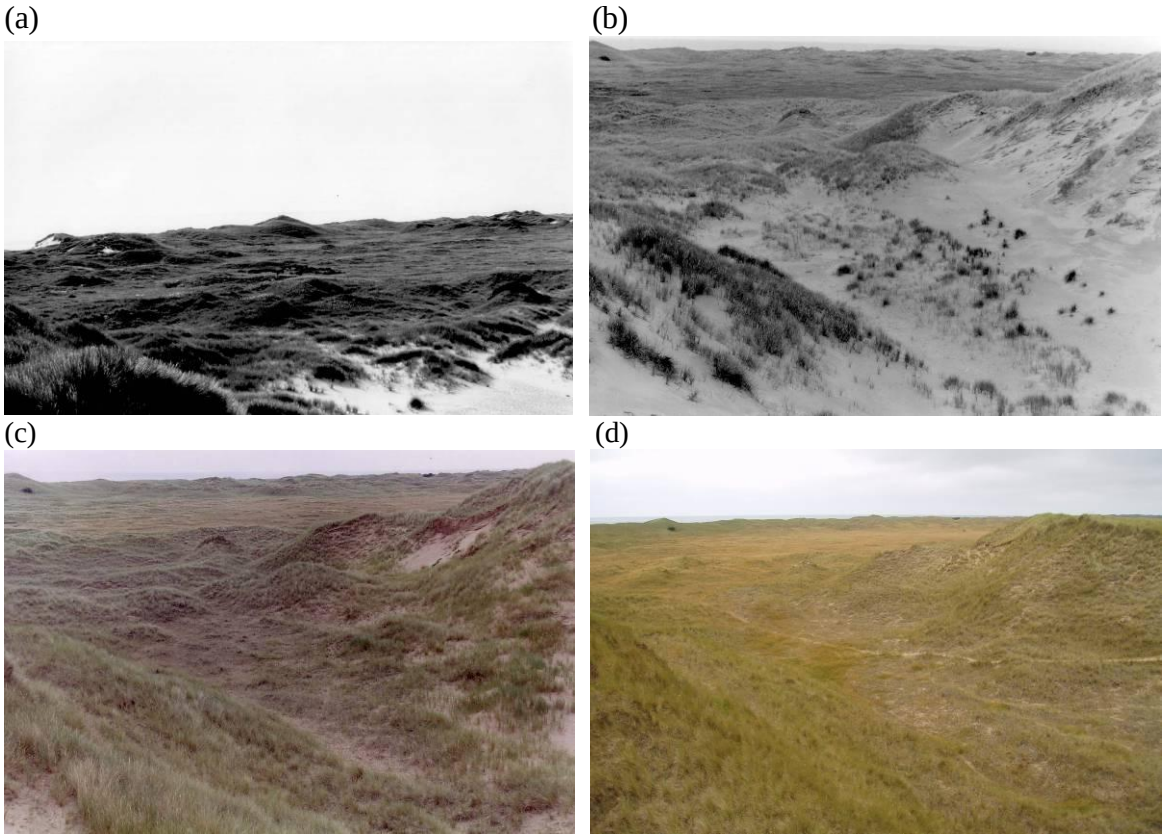

Plate A1.31. View from fixed-point photograph location 20a in (a) 1984, (b) 1987, (c) 1994 and (d) 2005

Plate A1.32. View from fixed-point photograph location 20bin (a) 1984, (b) 1987, (c) 1994 and (d) 2005

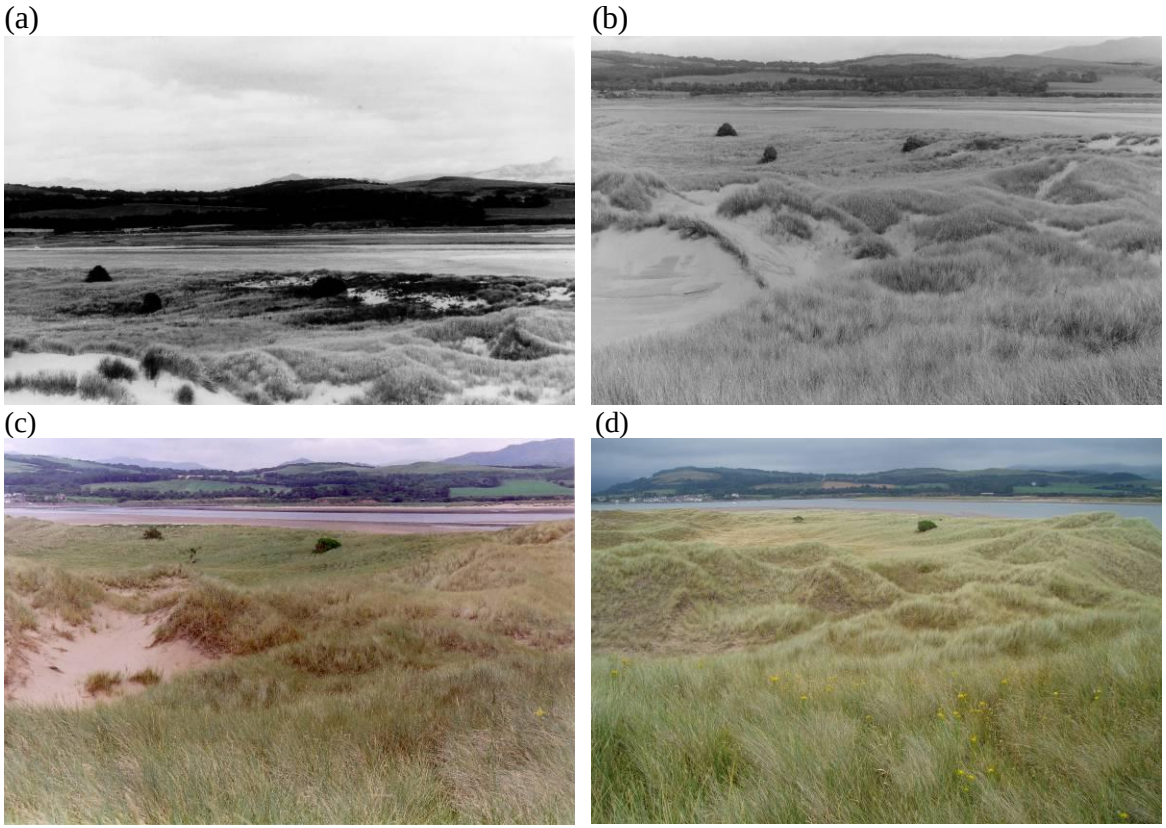

Plate A1.33. View from fixed-point photograph location 20c in (a) 1984, (b) 1987, (c) 1994 and (d) 2005